

1989

# The effect of water temperature and reactor geometry on turbulent flocculation

Adrian T. Hanson  
Iowa State University

Follow this and additional works at: <https://lib.dr.iastate.edu/rtd>

 Part of the [Civil and Environmental Engineering Commons](#)

## Recommended Citation

Hanson, Adrian T., "The effect of water temperature and reactor geometry on turbulent flocculation " (1989). *Retrospective Theses and Dissertations*. 9129.  
<https://lib.dr.iastate.edu/rtd/9129>

This Dissertation is brought to you for free and open access by the Iowa State University Capstones, Theses and Dissertations at Iowa State University Digital Repository. It has been accepted for inclusion in Retrospective Theses and Dissertations by an authorized administrator of Iowa State University Digital Repository. For more information, please contact [digirep@iastate.edu](mailto:digirep@iastate.edu).

## INFORMATION TO USERS

The most advanced technology has been used to photograph and reproduce this manuscript from the microfilm master. UMI films the text directly from the original or copy submitted. Thus, some thesis and dissertation copies are in typewriter face, while others may be from any type of computer printer.

The quality of this reproduction is dependent upon the quality of the copy submitted. Broken or indistinct print, colored or poor quality illustrations and photographs, print bleedthrough, substandard margins, and improper alignment can adversely affect reproduction.

In the unlikely event that the author did not send UMI a complete manuscript and there are missing pages, these will be noted. Also, if unauthorized copyright material had to be removed, a note will indicate the deletion.

Oversize materials (e.g., maps, drawings, charts) are reproduced by sectioning the original, beginning at the upper left-hand corner and continuing from left to right in equal sections with small overlaps. Each original is also photographed in one exposure and is included in reduced form at the back of the book. These are also available as one exposure on a standard 35mm slide or as a 17" x 23" black and white photographic print for an additional charge.

Photographs included in the original manuscript have been reproduced xerographically in this copy. Higher quality 6" x 9" black and white photographic prints are available for any photographs or illustrations appearing in this copy for an additional charge. Contact UMI directly to order.

# U·M·I

University Microfilms International  
A Bell & Howell Information Company  
300 North Zeeb Road, Ann Arbor, MI 48106-1346 USA  
313/761-4700 800/521-0600



**Order Number 9014904**

**The effect of water temperature and reactor geometry on  
turbulent flocculation**

**Hanson, Adrian T., Ph.D.**

**Iowa State University, 1989**

**U·M·I**

**300 N. Zeeb Rd.  
Ann Arbor, MI 48106**



**The effect of water temperature and reactor  
geometry on turbulent flocculation**

by

**Adrian T. Hanson**

**A Dissertation Submitted to the  
Graduate Faculty in Partial Fulfillment of the  
Requirements for the Degree of  
DOCTOR OF PHILOSOPHY**

**Department: Civil Engineering  
Major: Sanitary Engineering**

**Approved:**

Signature was redacted for privacy.

**~~In~~ Charge of Major ~~Work~~**

Signature was redacted for privacy.

**For the Major Department**

Signature was redacted for privacy.

**~~For~~ the Graduate College**

**Iowa State University  
Ames, Iowa**

1989

## TABLE OF CONTENTS

	Page
ACKNOWLEDGEMENTS . . . . .	iv
INTRODUCTION . . . . .	1
OBJECTIVES . . . . .	5
LITERATURE REVIEW . . . . .	7
Introduction . . . . .	7
Particle Suspension . . . . .	10
Fluid Phase - Water . . . . .	10
Solid Phase - Kaolinite Clay . . . . .	16
Intermolecular and Surface Forces . . . . .	22
Electrostatic repulsion . . . . .	23
Debye-Huckel approximation . . . . .	25
Gouy-Chapman theory . . . . .	27
Van der Waals attraction . . . . .	32
Solvation forces . . . . .	38
Born repulsion . . . . .	41
DLVO Theory . . . . .	41
Temperature effects . . . . .	48
Discussion . . . . .	49
Turbulence . . . . .	50
Production range . . . . .	54
Energy containing eddies . . . . .	56
Inertial subrange . . . . .	58
Universal equilibrium subrange . . . . .	58
Coagulants . . . . .	100
Metal coagulants . . . . .	101
Cationic organic polymers . . . . .	146
Particle Counting . . . . .	167
Turbidity . . . . .	168
Electronic particle counters . . . . .	170
Coulter type counter . . . . .	174
HIAC particle counter . . . . .	177
Automatic image analysis . . . . .	184
Results from Flocculation Modeling Studies . . . . .	201
Population balance models . . . . .	201
Breakup . . . . .	214
Models including breakup . . . . .	224
Flow field homogeneity . . . . .	226
Structural Models . . . . .	228
Early attempts . . . . .	229
Present Modeling Efforts . . . . .	231

<b>METHODS SECTION</b> . . . . .	247
<b>Introduction</b> . . . . .	247
<b>Materials Preparation</b> . . . . .	249
Clay . . . . .	249
Buffered dilution water . . . . .	254
Coagulant . . . . .	256
Acid . . . . .	257
<b>Equipment and Methods</b> . . . . .	257
pH adjustment and monitoring . . . . .	257
Sample collection . . . . .	265
Counting cell cleaning . . . . .	269
Reactor cleaning . . . . .	271
Turbidity measurement . . . . .	272
Zeta potential . . . . .	275
Jar test technique . . . . .	276
Temperature measurement . . . . .	278
Tachometer . . . . .	278
Motor controller . . . . .	282
Data acquisition and control . . . . .	282
Control of mixing intensity . . . . .	283
Reactor . . . . .	290
Lemont OASYS fully automatic image analysis . . . . .	292
<b>EXPERIMENTAL DESIGN</b> . . . . .	305
Particle Counter Evaluation . . . . .	305
Flocculation Experiments . . . . .	305
Changes in the flow field . . . . .	307
Changes in system chemistry . . . . .	312
<b>RESULTS AND DISCUSSION</b> . . . . .	316
Particle Counter Evaluation . . . . .	319
Effect of Temperature on Flocculation . . . . .	328
Turbulence results . . . . .	328
System chemistry results . . . . .	340
Breakup data . . . . .	347
Miscellaneous results . . . . .	359
Musings . . . . .	362
<b>CONCLUSIONS</b> . . . . .	372
<b>BIBLIOGRAPHY</b> . . . . .	376
<b>APPENDIX A</b> . . . . .	396
<b>APPENDIX B</b> . . . . .	408



## ACKNOWLEDGEMENTS

This project was supported financially by the National Science Foundation (NSF) under grant number ECE-86 13737, and the support has been greatly appreciated. The Iowa State University Engineering Research Institute (ERI) has also provided financial support.

I thank my major professor, Dr. Cleasby, for the time he has invested in guiding me. I also appreciate all of the time that Dr. Baumann has invested in me. It has truly been a privilege to work with these two men. The support of my other committee members is also acknowledged; Dr Oulman, Dr. Demirel, and Dr. Crumpton.

The technical assistance provided by the ERI analytical laboratory has been priceless. Particularly the assistance of Dave Schoeller in designing and constructing the experimental hardware, and the electronics. The instruction given by Glenn Oren on the use of the AIA was absolutely essential in the successful completion of this project. I have greatly enjoyed the able assistance of Mr. Ravindra Srivastava, and Mr. Soo-Ming Foo during the course of this project. Also many long discussions with Dr. J. Haarhoff were stimulating. Last but not least, the enduring support of my wife and children (all six of them) during the 5+ years that we have been involved in this endeavor.

## INTRODUCTION

One of the primary functions of the sanitary engineering profession is to provide society with safe, aesthetically pleasing drinking water. Surface water, which is the predominant source of drinking water in many areas, is usually contaminated with particulates. This is of interest to the sanitary engineer, because as Lawler et al. (1980) states,

"Most pollutants of concern to human health and environmental quality are solid particles or are associated with solid particles."

The size of these particles range from less than  $0.1 \mu\text{m}$  to greater than  $100 \mu\text{m}$ , however, because of the selection processes at work in a natural water, the majority of the particles are in the  $1 \mu\text{m}$  range. This causes problems because the two unit processes traditionally used to remove particulates from drinking water, sedimentation and filtration, are both least effective at removing particles approximately  $1 \mu\text{m}$  in diameter. The particles much smaller than  $1 \mu\text{m}$  will be transported to the filter media for removal by Brownian transport. Particles larger than  $1 \mu\text{m}$  will be transported to the filter media or to the bottom of a tank by gravity and/or inertial forces. The  $1 \mu\text{m}$  particles, however, fall into a window where neither of these mechanisms is effective for particle transport. This is illustrated graphically by Figure 1 (Yao et al., 1971). To remove these particles effectively, it is necessary to grow them from individual particles to larger aggregates. The exact aggregate

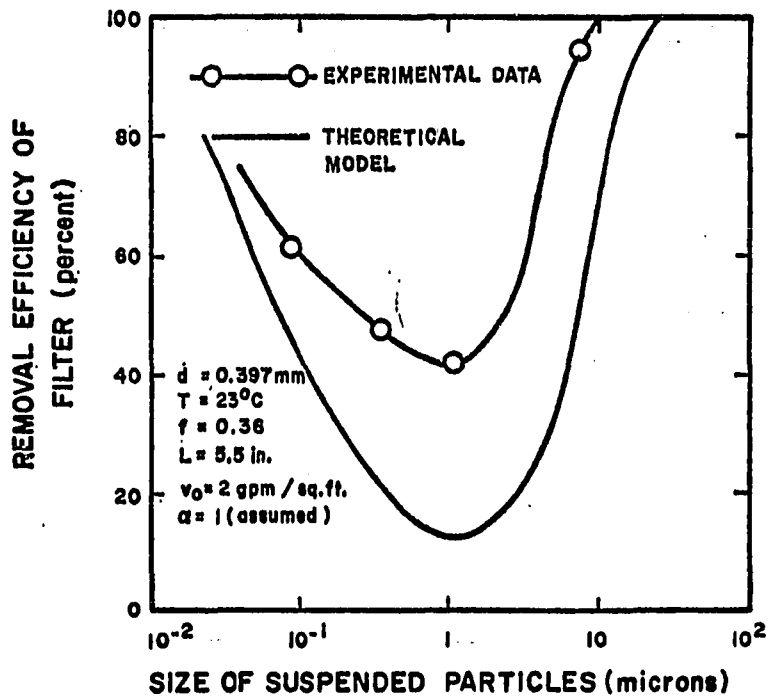


Figure 1. Comparison of theoretical model and experimental data for removal of colloids in a granular media filter

size desired will depend on the process to be used in removing the solids. Treweek (1979) noted that all particles larger than 10  $\mu\text{m}$  were removed by a deep bed sand filter. Obviously if the solids are to be removed in a sedimentation tank a larger size will be optimal.

Coagulation/flocculation is the process traditionally used to aggregate the small particles, and move them from the small size range to a size range which is amenable to removal by sedimentation and filtration. Coagulation is the chemical destabilization of the particulates, i.e., primary particles, so they will aggregate.

Flocculation is the formation of the aggregates, i.e., floc, by fluid transport of the particles to cause collision and growth.

A large body of research exists on coagulation/flocculation at 20 °C, and the industry has a fairly good working understanding of the process at warm temperature. Contrasted to this, there has been very little work done at low temperatures, i.e., less than 10 °C, and ironically the little work that has been performed frequently appears contradictory (Morris and Knocke, 1984; Camp et al. 1940).

It is a little surprising that so little work has been done at low temperature when one considers the amount of time each year that temperate zone surface waters are cold. The water temperature in a lake or reservoir can easily drop to 1 °C, and it is possible, in the north, to see 5 °C water temperatures for 5 or 6 months of the year

(Wetzel, 1975). The temperatures in a river will actually drop to 0 °C before ice cover (Hynes, 1970). Hutchinson (1974) reports that Lake Huron has 3.3 °C water 3 months of the year, and that these low temperatures are occasionally accompanied by high turbidities.

In light of the long time periods over which we must treat cold waters, and the fact that low temperature waters are capable of carrying more particulate matter than warm waters (Hynes, 1974), it is important to improve our understanding of the flocculation process at low temperatures. It is hoped that this work will help to clarify some of the questions which currently exist.

## OBJECTIVES

It is the objective of this study to experimentally investigate the effect of low temperature on flocculation in a turbulent flow field, and to establish a global view of the potential temperature effects. This was accomplished by first thoroughly reviewing the literature, and then performing a multiple temperature study in the laboratory. To do the experimental study in the laboratory, it is necessary to first select a water/particle system which:

- o mimics the systems encountered in full scale water treatment, as far as is practical,
- o is tightly controlled enough to be considered a constant in the experimental work.

Using the selected particle/water system the following points are addressed:

- o What turbulence intensity parameter best predicts the impact of the turbulent mixing regime on the flocculation process. Determine if maintaining a constant root mean square velocity gradient ( $G$ ), energy input per unit mass ( $\epsilon$ ), or Kolmogorov microscale ( $\eta$ ), will maintain the same level of treatment in the flocculation process at both high and low temperature.
- o What impact does changing the reactor geometry have on the flocculation process? It is well known that changing the reactor geometry will change the distribution of production scale turbulent eddies, and the isotropic-homogeneous characteristics of the turbulent flow field. Changing the reactor geometry and the temperature may provide insight into the actual mechanism of particle transport.

- o What parameter best predicts the impact of the system chemistry on the flocculation process. It is well established that system pH is the primary process control parameter for coagulation with metal salts. However, the metal salt precipitates involve hydroxides. Therefore, it is of interest to determine whether maintaining a constant pH or a constant pOH will better optimize the flocculation process when changing from high to low temperature.

This study made no attempt to address:

- o The sweep floc mechanism and the effect of temperature on sweep floc. Only the adsorption/destabilization mechanism is considered.
- o All of the work has been performed in the batch mode (comparable to plug flow), and the effects of temperature on flocculation in the continuous flow mode have not been addressed.
- o The mechanism by which the metal salts adsorb to the particle and destabilize it, is not considered.
- o The measurement of the turbulent flow field characteristics in the flocculation vessel was not performed as part of this study. This information was taken from the literature.

## LITERATURE REVIEW

### Introduction

It is hoped that the introduction will give the reader an overview of flocculation, and, in so doing, put the rest of the literature review into context. If the reader is familiar with the coagulation/flocculation process it is suggested that the reader go directly to the next section of the literature review.

First let's develop a mental picture of the flocculation process. We start with a suspension, in this case 25 mg/l kaolinite, of small particles, i.e., 0.1 to 10  $\mu\text{m}$ , which are distributed in the reactor homogeneously and isotopically. These small particles are stable in a colloidal sense, that is given a very long time they would not aggregate into larger particles. In general, this particle stability in a natural system is due to electrostatic repulsion induced by a negative charge on the particles. Note that, in this review of the literature the term "electrostatic repulsion" is used interchangeably with the term "double layer interaction".

The purpose of coagulation/flocculation is to destabilize these stable particles, and then cause the individual (primary) particles to stick together and form aggregates (floc). The primary particles are destabilized by adding a small amount of positively charged material to the suspension. This material, called the primary



coagulant, eliminates nearly all of the electrostatic repulsion between the particles by adsorbing onto the surface of the particles. To prevent an uneven distribution of the coagulant in the suspension, it is necessary to intensely mix the suspension as the coagulant is added. This is referred to as rapid mixing.

Once the electrostatic repulsion has been neutralized, van der Waals attraction can act to stick the particles together. However, for van der Waals attraction to operate it is necessary for the particles to come close together. In turbulent flocculation it is the turbulent flow field which moves the particles, and brings them close to each other, so that they can collide and stick to each other. If the particles are larger than the Kolmogorov microscale, they are moved, relative to each other, by turbulent eddies. Particles being moved by the turbulent eddies are only moved effectively by eddies which are approximately the same size as the particles. If the particles are smaller than the microscale, they are moved relative to each other by localized shear flows, which are induced by the stretching of the eddies in energy transfer.

Energy is put into the reactor by a paddle which creates large eddies or production scale eddies (2+ cm). This energy is transferred or cascaded down to the smaller eddies through a process called vortex stretching. Practically this is important because the energy is introduced into the system in a region where the flow field is

inertia controlled, and very little energy dissipation occurs. The energy must get from this large length scale region, down to a small length scale region. The Kolmogorov microscale, which represents the point at which viscous dissipation dominates the flow field, is at about 200  $\mu\text{m}$  in this system. The primary particles are about 2  $\mu\text{m}$ . If the mixing energy is very low, much of the energy will be dissipated as heat before it is transferred down to a size where it can effectively move the primary particles. As the energy into the reactor is increased the amount of energy in the small eddy size is increased. This, however, is a two-edged sword. As the energy which drives the flocculation is increased, the energy available for floc breakup due to shear stress is also increased.

The system under investigation is quite complex. It is necessary to understand the colloid chemistry and the fluid dynamics of the system if we are to interpret the temperature effect data intelligently. It is hoped that by reviewing the basic literature it will be possible to gain some insight into this specialized, applied problem.

Recall that the objective of this research is to establish a global view of flocculation in a turbulent flow field with regard to potential temperature effects. It is suggested that temperature changes, from 20 °C to near freezing, could affect the flocculation process in the following areas:

- o abrupt changes in the physical chemistry in water as the solid/liquid phase boundary is approached,
- o changes in the surface chemistry of clay,
- o changes in the Derjaguin, Landau, Verwey, and Overbeek (DLVO) forces which may effect particle-particle interactions,
- o changes in the structure of the turbulent flow field due to viscosity changes,
- o changes in the chemistry of the system, both the water and the coagulant.

The literature concerning each of these five areas will be discussed. In addition the literature on particle counting, as it relates to monitoring the flocculation process, and the literature on modeling of the flocculation process will be reviewed.

#### Particle Suspension

The particle suspension used in this study consists of kaolinite clay in water. Dispersions of clay in water are classified as lyophobic colloidal systems (van Olphen, 1987). A lyophobic colloid is one which does not readily hydrogen bond with water. In this section we will discuss the nature of the suspension, and how temperature effects the solvent and the clay.

#### Fluid Phase - Water

During the phase change from water to ice, there is a change in the nature of water. Morris and Knocke (1984) noted, in a case study of flocculation with alum, that flocculation efficiency dropped off

radically at temperatures less than 4.5°C. This would make one wonder if, perhaps, the properties of liquid water undergo some unusual changes as the system approaches the water/ice phase change. The coagulation-flocculation process, in a municipal setting, may be carried out right at 0°C, or even below. If one is to fully understand this work, and extrapolate the results of this work down to the practical limits of practice, it is necessary to understand the behavior of water near the solid/liquid phase transition boundary.

There is one main point the writer hopes to establish in this section. As long as water does not freeze, it's various properties can be described by a smooth well behaved function of temperature. Thus, data collected at 20, 5, and 2 °C can be extrapolated to 1 °C, or even lower, if the physical properties of water are the only important system variables.

The classical picture of the events preceding freezing are described by Davis and Day (1961) in the following manner. The density of water increases as the temperature drops, until 4 °C is reached. At this point the influence exerted by hydrogen bonding is stronger than the tendency to contract, and the water molecules begin to arrange themselves along the directional lines of the hydrogen bonds. Thus, the water expands and decreases in density until it reaches 0 °C. At

0 °C, it solidifies to ice. Let's look at how these events effect the properties of the liquid.

Wetzel (1975) notes that the unique properties of water depend upon the atomic structure, bonding, and association characteristics of the water molecules. It is not possible to directly observe how these change as the water approaches freezing, so it is necessary to measure secondary parameters and draw conclusions from these. We will look at, among other things, nuclear magnetic relaxation (NMR), x-ray scattering, conductivity, and viscosity data.

One thing which may change as the water approaches freezing is the connectivity of the water molecules. This connectivity is due to the water hydrogen bonding with itself, and determines such properties as viscosity and di-pole relaxation frequency (Nimtz, 1986). The di-pole relaxation frequency is measured using NMR. The random motions of a proton in the vicinity of another proton produces a time-dependent magnetic field through magnetic di-pole coupling (Franks, 1972). Measuring the relaxation of the magnetic field provides information on rotational diffusion, translational diffusion, and intermolecular exchange of the water molecules. Di-pole relaxation time and chemical potential values are both presented in graphical form by Nimtz (1986). These values, which extend into the super-cooled region, indicate a nice smooth change with no anomalies in the curve.

X-ray Scattering experiments and studies of infrared and Raman adsorption spectra, indicate that there is a considerable degree of short range order in water. These experiments also reveal the coordination characteristic of the tetrahedrally bonded structure in the liquid. X-ray scattering studies, reported by Kavanau (1964), indicate that the average number of nearest-neighbors is 4.4 to 4.6 in liquid water. This coordination number is 4 for ice and approaches 5 as boiling is approached (Franks, 1983). This indicates that water is a highly structured liquid over its entire liquid phase, and the degree of order reduces slowly as the liquid is heated toward boiling (Franks, 1983). The spectra from the x-ray scattering also indicate that any given molecule can "see" order only as far as three molecular diameters. Beyond that the molecular arrangement becomes uniform and random with no preferential intermolecular spacing. Thus one can see that, although water is highly structured for a liquid, that structure is local in nature. Turski (1986) states that local orientational order exists in a liquid, and that order undergoes a change to long range orientational order only when the liquid freezes. The change from short range to long range order is manifested in the volume change related to freezing. From Figure 2 (Turski, 1986), which shows a dimensionless order parameter plotted against temperature, we can see that the transition from short range order to long range order is abrupt, and corresponds to freezing.

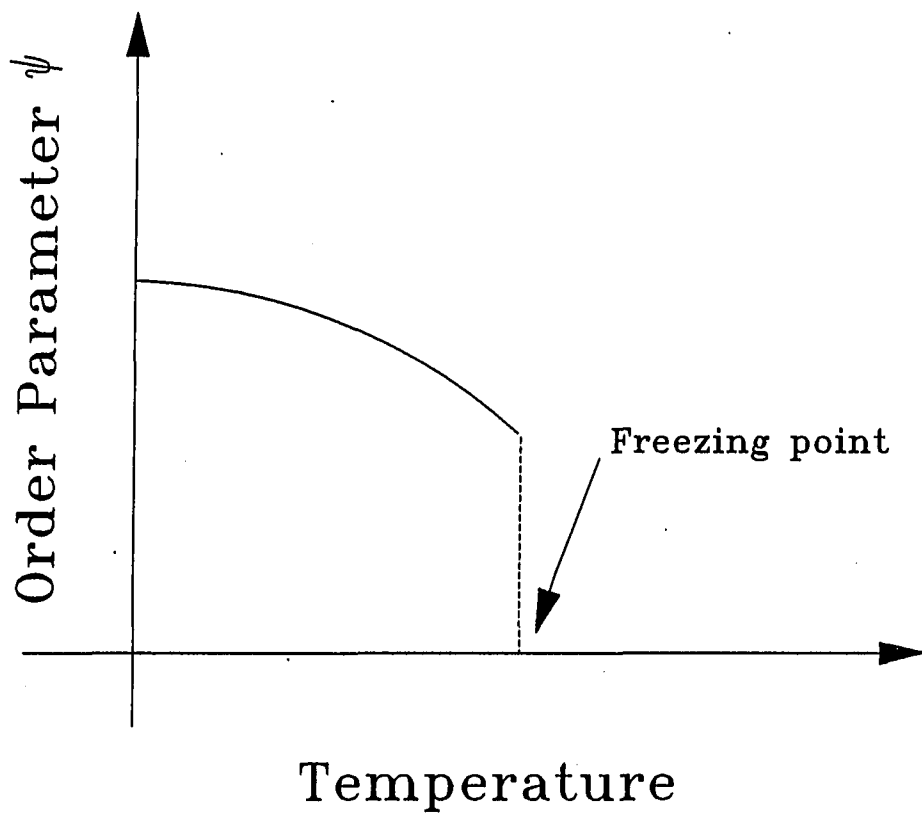


Figure 2. Schematic showing the temperature dependence of the order parameter  $\psi$

Rahman and Stillinger (1971) reported monte carlo simulation results for water super-cooled to  $-8.3^{\circ}\text{C}$ ., the liquid water showed no marked tendency to organize into ice nuclei. This indicates that the intrinsic structure of the water does not change until freezing occurs. Wetzal (1975) notes that liquid water at  $0^{\circ}\text{C}$  experiences  $10^{11}$  to  $10^{12}$  reorientation and translational movements per second. Ice molecules at  $0^{\circ}\text{C}$  experience only  $10^5$  to  $10^6$  reorientation and translational movements per second.

Franks (1972) reports that all of the major thermodynamic properties of water, including molar volume, compressibility, and specific heat all change smoothly with temperature right up to the point at which water freezes. The transport properties of water, including viscosity and thermal conductivity, also change smoothly up to the point of ice formation. In the case of viscosity the relationship is well behaved to a super-cooled temperature of  $-20^{\circ}\text{C}$ .

These computer simulations and laboratory measurements of fundamental properties of water reported in the literature make it obvious that no abrupt changes occur in the physical chemistry of water near the phase change prior to freezing. Thus, no abrupt changes in flocculation efficiency should occur at temperatures lower than  $4.5^{\circ}\text{C}$ .



### Solid Phase - Kaolinite Clay

The information presented here is intended as background, to assist in understanding how the particle system effects such things as interparticle forces, floc strength, particle counting, and coagulation/flocculation process in general. A number of particle systems were initially considered for the experimental study, including:

- o clay (kaolinite, Kentucky Ball Clay)
- o mono-dispersed iron particles (Matejevic et al. 1975; Matejevic and Scheiner 1978)
- o mono-dispersed aluminum particles (Brace and Matejevic, 1973)
- o mono-dispersed latex spheres.

Of these the clay was selected because:

- o It frequently represents a large fraction of the particulates present in the real system, and will thus make the experimental results more meaningful to the industry as a whole.
- o It has frequently been used in past research reported in the literature.
- o A clay was found which, for practical purposes, was mono-dispersed.
- o This clay was available in large quantities with consistent physical and chemical properties.

Of the primary particle systems evaluated, only the clay will be discussed here. Two main points will be stressed; the fundamental properties of clay which will effect our understanding of the

flocculation results, and the properties of clay which might be temperature sensitive. The discussion will center around the physical and chemical characteristics of kaolinite, and where practical it will be compared to montmorillonite and illite.

Clay minerals from the kaolinite group are probably the most common clays (Deer et al. 1966). Of the clay minerals in the kaolinite group, kaolinite is the most common member (Mitchell, 1976). Thus, it is a material which is representative of naturally occurring particulate contaminants. Kaolinite is referred to as a 1:1 mineral, because at a molecular level it consists of alternating sheets of molecules. One sheet has an octahedral structure, which consists of aluminum coordinated octahedrally with oxygen or hydroxide. The other sheet is a silica sheet, which consists of silica coordinated tetrahedrally with oxygen. The bonding between the successive layers is by van der Waals attraction and hydrogen bonding. This bonding is of sufficient strength so that there is no interstitial swelling. The average molecular formula for kaolinite is  $(OH)_8Si_4Al_4O_{10}$  (Mitchell, 1976).

It is fortunate that the chemical composition of kaolinite is subject to very little variation (Deer et al. 1986), and the structural composition is subject to very little variation (van Olphen, 1977). This means that the surface chemistry of kaolinite is fairly consistent from sample to sample.

The kaolinite particles possess a net negative charge which is probably the result of substitution (Mitchell, 1976). A number of studies reported by Bennett and Hulbert (1986) show that at near neutral pH, the faces of the kaolinite have a negative charge, and the edges have a neutral charge. This is also supported by Lyklema (1987) and Sonntag and Russel (1986). Table 1, from Sonntag and Russel, demonstrates the pH dependence of the faces and edges. Note that at all pH values the edge charge is almost trivial in comparison to the face charge.

Table 1. Electrokinetic potentials of the edges and faces of kaolinite particles, as a function of pH and NaCl concentration (in moles/dm<sup>3</sup>)

pH	Electrokinetic potential in mV			
	edge		face	
	10 <sup>-4</sup>	10 <sup>-1</sup>	10 <sup>-4</sup>	10 <sup>-1</sup>
6	14	4	-54	-26
7	4	1	-54	-26
8	-14	-4	-54	-26

The net charges on the faces of the clay may be accounted for by substitution of either Al<sup>+3</sup> for Si<sup>+4</sup> in the silica sheet, or substitution of a divalent cation for Al<sup>+3</sup> in the octahedral sheet. Replacement of only 1 in every 400 Si would account for the net negative charge in many kaolinite clays (Mitchell, 1976). This

indicates that a constant charge assumption may be appropriate for DLVO modeling of the interparticle forces.

Table 2 contains ranges of typical cation exchange capacity (CEC) and specific surface area (S) values for the most common clays.

Table 2. Ranges of typical clay mineral characteristics

Characteristic	Kaolinite	Montmorillonite	Illite
CEC(meq/100 gm)	3-15	80-150	10-40
S(m <sup>2</sup> /gm)	10-20	Primary 50-120 Secondary 700-840 (Interlayer)	65-100

From the CEC and S, it is possible to estimate the surface charge density in the following manner:

$$\sigma = \text{CEC}/S$$

The units on  $\sigma$  are coulombs per meter squared. CEC, which is usually expressed in terms of meq per gram, represents exchangeable cations per unit mass of suspended particles. The units meq per unit mass can be converted to coulombs per gram by multiplying by 96.5 coulomb/meq (Newman, 1987). Both Newman (1987) and van Olphen (1977) note that the CEC of kaolinite is low compared to the other clays, but the charge density is comparable to the charge density of montmorillonite. This is because the cations are exclusively located on the exterior surfaces of the kaolinite, and the particles are

rather thick, yielding a small exterior surface. The charge is concentrated on the surface because the basal spacing of the kaolinite does not leave room for interlayer cations. This means that all of the charge compensating cations must adsorb to the exterior surface of the clay (van Olphen, 1977). Thus, from a DLVO perspective, the system geometry of kaolinite is as simple as it could possibly be for a clay. Table 3 uses average values from Table 2 to estimate the surface charge density values for the clays.

Table 3. Average surface characteristics for common clays

Characteristic	Kaolinite	Montmorillonite	Illite
CEC(C/gm)	8.69	110.98	24.13
S(m <sup>2</sup> /gm)	15	770	82.5
$\sigma$ (C/m <sup>2</sup> )	0.58	0.14	0.29

Even though this table is based on the average of a range of values, it serves to illustrate a point. The surface charge density of kaolinite is comparable to that of other naturally occurring clays. van Olphen (1977) states that most data for kaolinite calculate a charge density of 0.15 to 0.2 C/m<sup>2</sup>, which is very similar to the values reported for montmorillonite and illite.

The size and shape of the primary particles in a flocculating system is important because they effect:

- o the fluid transport mechanism,
- o the particle capture efficiency,
- o the interparticle forces, and
- o our ability to measure the particles.

Kaolinite is usually a well formed six-sided plate. The dimension of the plates may range from 0.1 to 4  $\mu\text{m}$ , and the thickness may range from 0.05 to 2  $\mu\text{m}$  (Mitchell, 1976). Newman (1987) Notes that kaolinite particles are fairly large often having 50 percent or more greater than 0.5  $\mu\text{m}$ .

Another area of interest is the interaction of the clay water interface. Kavanau (1964) states that colloids in general are encased in a thin crust of bound water at least one molecule thick. Newman (1987), writing specifically about kaolinite says, "studies on the structure and energy status of water adjacent to kaolinite surfaces seem to agree that the range of influence of the surface extends to between two and four water molecule layers."

The temperature induced changes which might affect the behavior of the clay, would be system chemistry changes, which might alter the surface chemistry of the clay. As the  $\text{pK}_w$  of water changes, the surface ionizable sites may also change, if the system pH is held constant. However, it has been shown that the zeta potential of kaolinite is only mildly sensitive to pH changes in the pH range of 5

to 8 (Hall, 1965; Hong-Xiao and Stumm, 1987a). Based on this weak dependence of surface chemistry, i.e., surface charge, on pH it is expected that the surface chemistry of the clay will not be greatly affected by the normal temperature changes.

#### Intermolecular and Surface Forces

The term hydrophobic is frequently applied to clays, and implies that clay materials do not like to disperse in water. It is perhaps more accurate to say that water likes itself too much to tolerate the clay. The surface of the clay is incapable of hydrogen bonding with the water. This disrupts the water "lattice", and leads to a thermodynamically unstable situation (Israelachvili, 1985). If it is thermodynamically unfavorable for the colloidal clay to remain dispersed, why doesn't it aggregate? Is there an energy barrier, and if so what is its source? Once the energy barrier is removed and the clay begins to aggregate, what forces hold the aggregates together? In this section we will discuss the fundamental colloidal forces needed to understand the flocculation process. In addition, we will discuss the effect of temperature on the magnitude of these forces.

We will begin by discussing the following basic forces:

- o electrostatic repulsion (Double-layer forces),
- o van der Waals attraction,
- o structural forces
- o Born repulsion.

We will not discuss steric interactions because they are not pertinent to the system under discussion.

After we have been introduced to the basic forces we will discuss DLVO theory and net potential energy curves for the flocculating system.

### Electrostatic repulsion

From the previous section on clay we recall that kaolinite has a net negative surface charge of 0.15 to 0.2 C/m<sup>2</sup>. Because of this net surface charge, a layer of ions with an opposite charge is developed around the particle. If one considers both the surface charge on the particles, and the sum of the counter-ion atmosphere around the particle, the system is electrically neutral. The ions in the atmosphere around the particles, which are, for the most part, positively charged, interact, and cause the particles to repel each other. This is shown in Figure 3, and is referred to as electrostatic repulsion. The term double layer refers to early attempts to model the system as a simple parallel plate capacitor with one set of charges on the particle surface and the opposing charges in a layer at a fixed distance from the surface. This simple model is called the Helmholtz model (Bennett and Hulbert, 1986), and is shown in Figure 4. This model quickly gave way to models which recognized that the ions form a diffuse layer around the particle and not restricted to a plane.



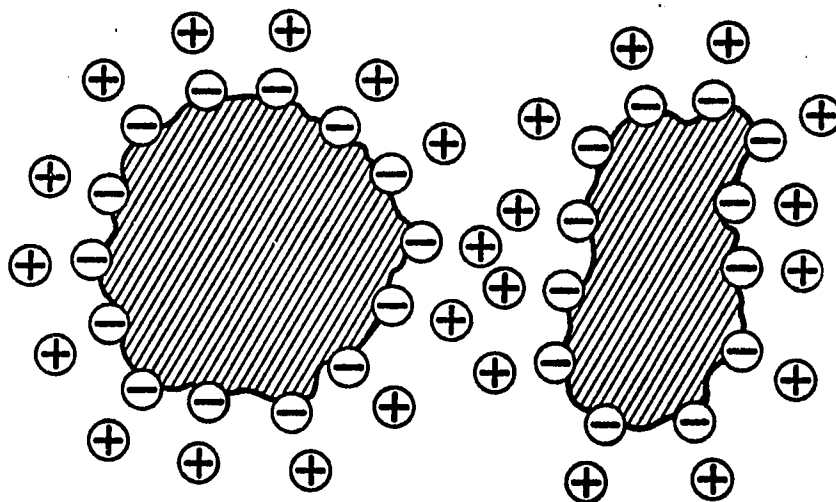


Figure 3. Electrostatic repulsion between the like-charged ion layers tends to prevent coalescence of particles in suspension

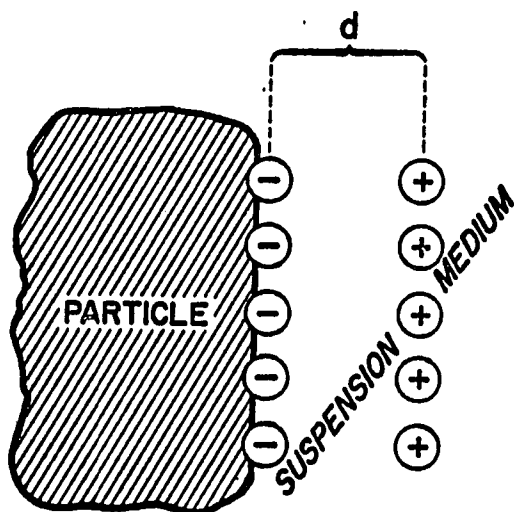


Figure 4. The Helmholtz model of a charged particle in suspension, in which oppositely charged layers of ions are separated by a distance  $d$

The diffuse layer is the result of a number of interacting physical phenomena including (van Olphen, 1977; Israelachvili, 1986):

- o the oppositely charged ions in solution are attracted to the particle surface,
- o the like charged ions are repelled from the surface of the particle,
- o and the action of thermal diffusion tends to evenly distribute the ions.

The final result is a distribution of counter-ions similar to the distribution shown in Figure 5 (Hirtzel and Rajagopalan, 1985). The diffuse layer model assumes that the ionic charge distribution can be described by the Poisson-Boltzman equation (Hiemenz, 1986). This equation does not have an explicit solution, but a number of limiting cases have been solved. We will briefly consider two of these limiting cases.

Debye-Huckel approximation This limiting case assumes that the potential across the diffuse layer is low. This model has very limited applicability, but one very important and frequently used quantity came out of this model; the Debye length. The Debye length is usually referred to using the greek letter  $\kappa$ . The quantity  $1/\kappa$  is sometimes referred to as the double-layer thickness, and is used as a yardstick for comparing all other distances to the double-layer. It should be noted that this is not actually the thickness of the diffuse layer, but is equal to the plate separation of an equivalent

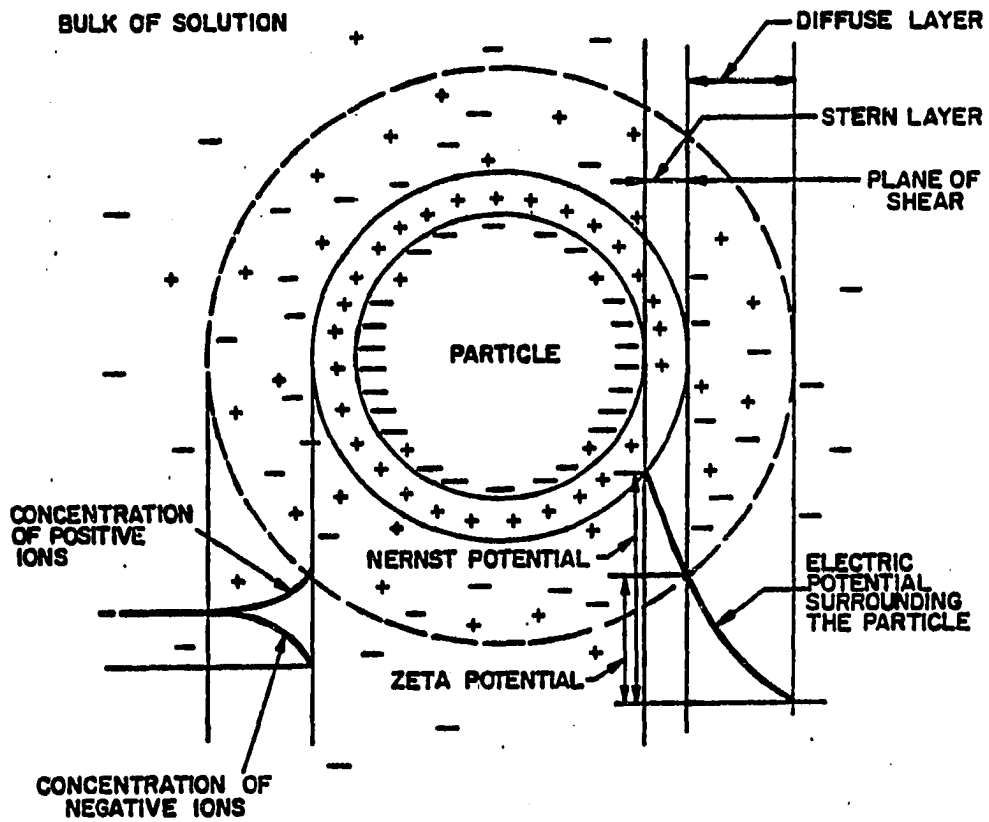


Figure 5. Theoretical representation of the ion structure around a charged particle based on the Stern model

capacitor. The following equation is the mathematical expression for the Debye length (Hiemenz, 1986).

$$\kappa^2 = \frac{e^2 \sum Z_i^2 n_{i0}}{\epsilon_0 \epsilon_r K T}$$

- $e$  -  $1.60 \times 10^{-19}$  C  
 $\epsilon_0$  -  $8.85 \times 10^{-12}$  C<sup>2</sup>/J-M  
 $\epsilon_r$  - 80 (strong function of temperature) = (relative dielectric constant)  
 $\epsilon$  -  $\epsilon_0 \epsilon_r = 7.08 \times 10^{-10}$  C<sup>2</sup>/J-M  
 $K$  - Boltzman's Constant =  $1.38 \times 10^{-23}$  J/degree K  
 $T$  - Temperature Kelvin =  $273.15 + \text{Degrees C}$   
 $n_i$  -  $1000 M_i N_A$   
 $M_i$  - Moles of ion with valence  $Z_i$   
 $N_A$  - Avogadro's Number =  $6.02 \times 10^{23}$   
 $\sum Z_i^2 n_{i0}$  -  $1000 N_A \sum Z_i^2 M_i$   
 $\sum Z_i^2 M_i$  -  $2I$   
 $I$  - Ionic Strength

Gouy-Chapman theory This theory also starts with the basic Poisson-Boltzman equation, however, the model developed using this theory is not restricted to low potential. The Gouy-Chapman theory is not without limitations. For instance, this model does not work well at the surface of the particle. This, however, is not a real concern in the context of turbulent flocculation. We are interested in particle-particle interactions in the suspension, and as we will see, the particle surfaces probably never touch in a real floc.

One last refinement of the double-layer model which is sometimes of interest is the Stern layer. If the magnitude of the surface charge is high enough, it is possible to form a saturated surface layer consisting of only oppositely charged ions next to the surface of the particle (Hiemenz, 1986). This is also seen in Figure 5.

In applying the double-layer model to the electrostatic repulsion interaction of the two surfaces approaching each other, it is necessary to assume that either the surface charge remains constant or the surface potential remains constant. Israelachvili (1985) notes that, in general, the interaction potential will be somewhere between these two limits. The repulsive energy is always larger with the constant charge assumption than with the constant potential assumption (Honig et al., 1971). The following equation is the mathematical expression for the electrostatic potential energy in the vicinity of the surface as the result of the diffuse double layer as based on the Gouy-Chapman model.

$$\phi = \frac{64 n_o K T r_o^2}{\kappa} e^{-\kappa d}$$

- $\phi$  - potential energy (J/m<sup>2</sup>)
- $d$  - separation distance (m)
- $T$  - Degrees Kelvin
- $K$  - Boltzman's Constant (J/Degree K)
- $\kappa$  - Debye Length (1/m)
- $n_o$  -  $1000 M_i N_A$  - number of charge determining ions
- $r$  -  $r_o e^{-\kappa x}$  ; where  $x$  is distance above the surface(m)
- $r_o$  -  $r$  at the surface,

$$e = 1.60 \times 10^{-19} \text{ (C)}$$

Table 4 (Rajagopalan and Kim, 1981) contains the relaxation times for the double-layer, the time of charge adjustment, and the time between Brownian collisions.

Table 4. Relaxation time for various processes

Process	Range of Values
Relaxation time of double layer (time for readjustment of the double layer)	$\sim 10^{-8}$ sec
Time for Brownian collision	$\sim 10^{-5} \sim 10^{-7}$ sec
Time for charge adjustment	$\sim 10^{-6} \sim 10^{-4}$ sec

The values in Table 4 are calculated values using the following approach (Rajagopalan and Kim, 1981). The relaxation time for the readjustment of the double layer and the relaxation time for Brownian collisions are taken as the average time needed for the displacement of the atoms or particles across the double layer. The relaxation time for charge adjustment is determined by the exchange current density, which is the rate of transport of charges across the double layer in either direction when the interface has reached its equilibrium potential difference. The relaxation time for charge adjustment depends on the detailed structure of the double layer, such as the concentrations and mobilities of ions on either side of the double layer.

The time scales involved make it clear that there may indeed be situations where the constant potential assumption is neither appropriate nor adequate (Rajagopalan and Kim, 1981). If the constant charge assumption is to be employed, a surface charge estimate for clean kaolinite is available from the literature (see previous section).

If one is to use the constant potential assumption, it is suggested that zeta potential is a useful estimate of surface potential. The zeta potential of a particle is the electric potential in the double-layer at the interface between a particle which moves in an electric field and the surrounding liquid. When a constant electric field is applied to charged particles in suspension, the particles will reach a limiting velocity when the viscous drag force equals the accelerating force (Bennett and Hulbert, 1986). The magnitude of the zeta potential is considered a measure of the particle's repulsion for like charged particles (van Olphen, 1977). The zeta potential ( $\zeta$ ) of a system of particles may be calculated from the experimentally measurement of the steady motion of particles under the influence of an electric field, and the following formula.

$$\zeta = 4\pi\mu v / \epsilon E$$

E	- electric field (V)
$\mu$	- liquid viscosity ( $\text{N m}^{-2} \text{ s}$ )
v	- particle velocity ( $\text{m s}^{-1}$ )
$\epsilon$	- medium dielectric constant ( $\text{C V}^{-1} \text{ m}^{-1}$ )
$\zeta$	- Zeta Potential (V)

Zeta potential has traditionally been used as a measure of surface potential, but there is now considerable disagreement in the literature over this practice. van Olphen (1977) states:

"It has been realized that the seat of the zeta potential is the shearing plane or slip plane between the bulk liquid and an envelope of water which moves with the particle. Since the position of the shearing plane is not known, the zeta potential represents the electric potential at an unknown location.... Because of the ill-defined character the zeta potential is not a useful quantitative criterion of stability....this parameter has lost its significance."

Others view the parameter in a more benevolent light. Bennett and Hulbert (1986) admit that the zeta potential allows some quantitative description of the properties of a clay suspension. Schenkel and Kitchener (1960) state that it seemed reasonable to employ experimentally determined zeta potential, assumed to be the potential drop in the diffuse part of the double-layer, as being roughly the same as the potential relevant in the theory of repulsion between interacting double-layers. He noted that any value taken for the surface potential would be uncertain. Ottweill (1987) found measured values of surface potential on clay surfaces agreed very well with zeta potentials.



Bennett and Hulbert (1986) have suggested that a zeta potential on the order of 20-30 mV is the "critical zeta potential", which needs to be exceeded in absolute value if the particle suspension is to be stable. Figure 6 is an indication of the relative stability of particles systems at different zeta potentials (Zeta Meter, Inc.). This figure presumes that if the zeta potential, and therefore the surface potential, is below a certain value the particles will approach each other close enough for van der Waals attraction to cause bonding.

#### Van der Waals attraction

If two like particles are brought close enough together, they will tend to adhere to each other due to strong, short range forces of the type that hold the particles together internally. These forces are referred to as the van der Waals-London forces (Bennett and Hulbert, 1986). The strength of these forces is small compared to the forces generated by a chemical bond, as seen in Table 5. These forces are strong enough, however, to cause irreversible flocculation under some conditions.

As noted by Russel (1987) with regard to van der Waals forces in flocculation "the possibility of irreversible flocculation caused by strong van der Waals-London forces has preoccupied colloid science for decades".

**What ZP values reflect stability? How about flocculation?**

-120	-70	-50	-30		-20	-10	-5	0 +3
excellent	good	moderate		transition		poor	fair	excellent
DISPERSION					AGGLOMERATION			

Figure 6. The effect of zeta potential on particle stability; ZP values are in millivolts

Table 5. Relative bond strength

Bond Type	Strength KJ/mole	
	(Israelachvili, 1985)	(Camp, 1968)
Co-valent	500	210-420
Hydrogen	10-40	12-42
Van der Waals	1	4-8

Although the forces are manifested at a macroscopic scale, they are generated at an atomic level. In general, the van der Waals forces can be thought of as an induced dipole-induced dipole interaction between atoms. The van der Waals interaction is essentially electrostatic, arising from the dipole field of an atom "reflected back" by a second atom that has been polarized by the field of the first atom (Israelachvili, 1985). Consideration of the Bohr atom will yield a qualitative understanding of these forces. In the simplest Bohr atom the electron orbits a proton, and there is no permanent dipole moment. However, at any instant there exists an instantaneous dipole of moment whose field will polarize a nearby neutral atom giving rise to an attractive interaction (Israelachvili, 1985).

The interactive energy between two identical atoms was derived by London in 1930 using quantum mechanical perturbation theory. London's expression for the interaction energy is as follows (Israelachvili, 1985):

$$w(r) = (-3/4 \alpha h \nu) / (4 \pi \epsilon_0)^2 r^6 \rightarrow - C/r^6$$

- $\alpha$  - electronic polarizability of second atom ( $C^2 m^2 J^{-1}$ )
- $h$  - Planck's constant;  $6.626 \times 10^{-34} J s$
- $\nu$  - orbiting frequency of the electron, which for the Bohr atom is  $3.3 \times 10^{15} sec^{-1}$
- $\epsilon_0$  - permittivity of freespace ( $C^2 J^{-1} m^{-1}$ )
- $r$  - separation distance of the atoms (m)
- $w(r)$  - London dispersion interaction free energy (J)

The attractive interaction of two atoms drops off as an inverse function of the separation distance to the sixth power. When dealing with a solid, which is a composite of many atoms, the interaction drops off as an inverse function of the separation distance squared (van Olphen, 1977). This increase in range is due to the geometric effects. Israelachvili (1985) notes that anything larger than 0.5 nm must be treated as a particle or its attractive interaction will be under-estimated. Many of the current attractive interaction models assume that the net attraction from a composite of molecules is the sum of all of the attractions, i.e., additivity. This is not true. The addition of pairwise potentials ignores the fact that the field being reflected back by other atoms in the area increase the attraction. The net effect is that the van der Waals force between the particles is enhanced and the attractive forces are higher than would be expected based on the two-body problem alone. The values

estimated using the two-body approach can be as much as 30 percent low (Israelachvili, 1985). The range of attractive forces between molecules is on the order of a few nanometers, but the range of the attractive forces between particles is up to 50 nanometers from the surface (Rigby et al. 1986).

The estimation of the attractive interaction potential between two bodies involves summing or integrating the interactive energies of all of the atoms in one body with all of the atoms in a second body. This summed interaction is material and geometry specific. Israelachvili (1985) and Hiemenz (1986) both contain tables of appropriate equations for various geometries. Parallel flat plates will be considered briefly, since clay has a plate structure. The following equation is for the flat plate geometry:

$$\phi = - \frac{A}{12\pi} \left\{ \frac{1}{d^2} + \frac{1}{(d + 2\delta)^2} - \frac{2}{(d + \delta)^2} \right\}$$

- $\phi$  - van der Waals attraction, infinite flat plate ( $J \text{ m}^{-2}$ )
- A - Hamakers constant (J)
- d - plate separation distance (m)
- $\delta$  - plate thickness (m)

The parameter "A", is referred to as Hamaker's constant, and is named after H.C. Hamaker, who did much of the original work in this area. The Hamaker's constant takes into account the effect the material has on the strength of the interaction. Frequently the constant will be written as "A<sub>123</sub>"; this means the Hamakers constant for material 1 and material 2 acting across material 3. Israelachvili (1985) gives the following formula for calculating the constant A for two identical materials interacting across a third:

$$A = \frac{3}{4} K T \left[ \frac{\epsilon_1 - \epsilon_3}{\epsilon_1 + \epsilon_3} \right] + \frac{3h\nu_e}{16(2)^{0.5}} * \frac{(n_1^2 - n_3^2)^2}{(n_1^2 + n_3^2)^{0.75}}$$

- $\nu_e$  - adsorption frequency (s<sup>-1</sup>)
- $n_i$  - refractive index of material i
- $\epsilon_i$  - dielectric permittivity of material i

The other variables as previously defined.

This is the Hamakers constant calculated based on the Lifshitz theory. It is seen that to calculate A one must have the dielectric constant ( $\epsilon_i$ ), and the refractive index (n) for each material. This information is widely available for water, but is less available for kaolinite. The dielectric constants are readily available for mica and quartz. Since all three of these minerals are silica

tetrahedrons (Mitchell, 1976), it seems reasonable to estimate A for kaolinite based on the values for mica and quartz. Table 6 contains values calculated using the formula given above, and values reported by Rigby et al. (1986).

Table 6. Hamakers constants; calculated values based on Lifshitz theory, and measured values

Solid	Hamakers constant(A); Solid-Water-Solid (J)		
	Israelachvili(1985)	Rigby et al. (1986)	
	20 °C	5 °C	
Mica	$2.00 \times 10^{-20}$	$1.99 \times 10^{-20}$	-----
Quartz	$6.04 \times 10^{-21}$	$5.91 \times 10^{-21}$	$1.70 \times 10^{-20}$
Fused Silica	-----	-----	$0.85 \times 10^{-20}$

From this table it is seen that the value of A is not highly sensitive to temperature change.

#### Solvation forces

Solvation forces are very short range forces related to the structure of the liquid water adjacent to the solid-liquid interface.

Israelachvili (1985) notes that, between macroscopic particles, the electrostatic repulsion and van der Waals-London forces are the two most important forces, but at short distances, i.e., under 1 to 3 nm, the solvation forces dominate over both of these. One must wonder, what role, if any, will these solvation forces play in determining the strength of the floc which are formed.

As noted earlier, the water adjacent to a solid surface is structurally different than the water in the bulk liquid, but within a distance of four molecular layers, these differences have disappeared. Figure 7 shows how solvation forces vary as two surfaces approach. Sigma ( $\sigma$ ) in Figure 7 is the incremental change in the separation distance between two surfaces corresponding to the period exhibited by the force oscillation shown in Figure 7(b) as two surfaces approach each other. Measurements which have been performed on the water mica system have found a sigma ( $\sigma$ ) of 0.25 nm for water (Israelachvili, 1985). This correlates quite well with the diameter of a water molecule. From this sigma, and the four layers of structured water at a solid surface, it appears that the structure of the water is indeed responsible for these solvation forces. However, it is not the simple fact that the water molecules tend to lie in semi-ordered layers at the surface which causes these forces. It is the fact that it takes energy to re-arrange the hydrogen bonds between the water molecules and disrupt the ordering as the two surfaces approach each other (Israelachvili, 1985). Recall that for a simple ideal liquid, the liquid interacts with its twelve nearest neighbors. Water is a highly structured hydrogen bonding liquid, which interacts with only its 4-5 nearest neighbors. If the surface is incapable of hydrogen bonding, the water will arrange itself to



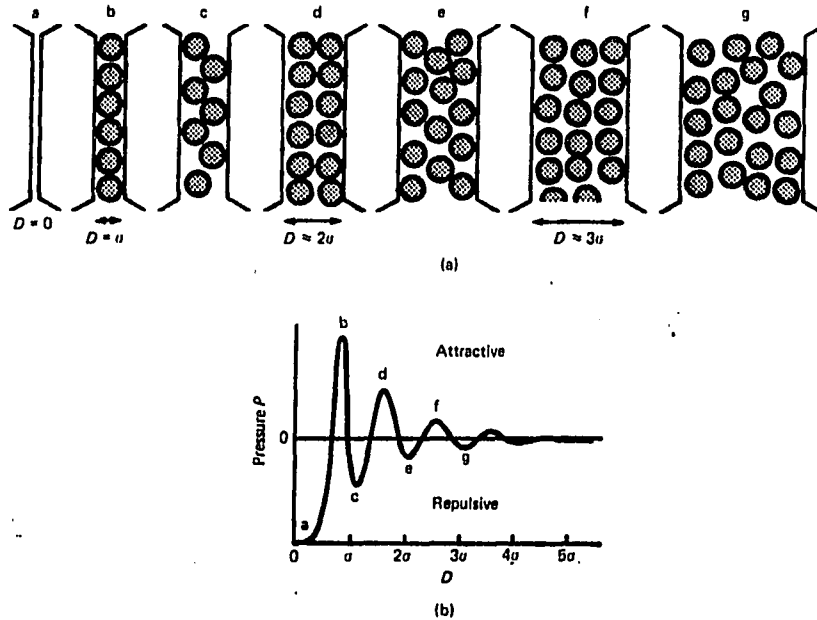


Figure 7. Structural changes in a liquid as two surfaces approach; (a) The molecular ordering of water at the surface changes as the separation distance  $D$  changes. Note that the density of the liquid molecules in contact with the surfaces varies between maxima and minima.  $\sigma = 0.25$  nm for water. (b) Corresponding solvation pressure (schematic)

minimize the number of unsatisfied hydrogen bonds near the surface. This is the liquid structure which is being disrupted during the close approach of two solid surfaces. Note from Figure 7(a) that once the solvation interactions become important, as seen from the pressure changes in Figure 7(b), the density of the liquid changes from that of the bulk liquid. Both  $\epsilon$  and  $n$  of the Hamakers constant depend on  $\rho$ . Because of the interaction between A and the solvation interaction we must conclude that van der Waals and oscillatory solvation forces are not additive. Indeed, it is more correct to think of the oscillatory solvation forces as van der Waals force at small separation distances with the molecular properties of the liquid taken into account.

### Born repulsion

Born repulsion is commonly cited as one of the main forces in particle -particle interaction, along with electrostatic repulsion and van der Waals-London interaction. It is the repulsion caused by the overlapping of electron clouds as the particles approach each other on a molecular scale. Because of the solvation forces in an aqueous system, it is unlikely that Born repulsion will be active.

### DLVO Theory

DLVO theory combines the aforementioned individual forces into a single net particle-particle interaction potential. The theory is named after the four researchers who developed it simultaneously in

the early 1940's; Derjaguin, London, Verwey, and Overbeck (DLVO) (van Olphen, 1987). This net particle-particle interaction potential allows us to predict in a semi-quantitative manner whether or not a system will flocculate. Historically the DLVO theory included only electrostatic repulsion ( $V_R$ ) and van der Waals attraction ( $V_A$ ) (van Olphen, 1987). Current literature frequently adds solvation interactions and Born repulsion. For the purpose here, which is to consider primary minimum versus secondary minimum flocculation, it is only necessary to consider  $V_R$  and  $V_A$ . The total interaction potential is defined as:

$$V_T = V_R + V_A$$

The form of  $V_T$  is seen in Figure 8. This is a typical potential energy curve showing the interaction between two particles at varying separation distances. On this curve a positive value indicates repulsion and a negative value indicates attraction. The greater that magnitude of the negative value the stronger the bond. Notice that there are two minimums, corresponding to two separation distances at which particles would bond to each other. The deep minimum at the shortest separation distance is called the Primary minimum. The second shallower minimum is called the secondary minimum and produces a much weaker bond. The hump in the curve between the two minimums is called the flocculation barrier. The location, depth, and width of these two minimums is a function of  $V_R$  and  $V_A$ . There is nothing which can be done to increase the

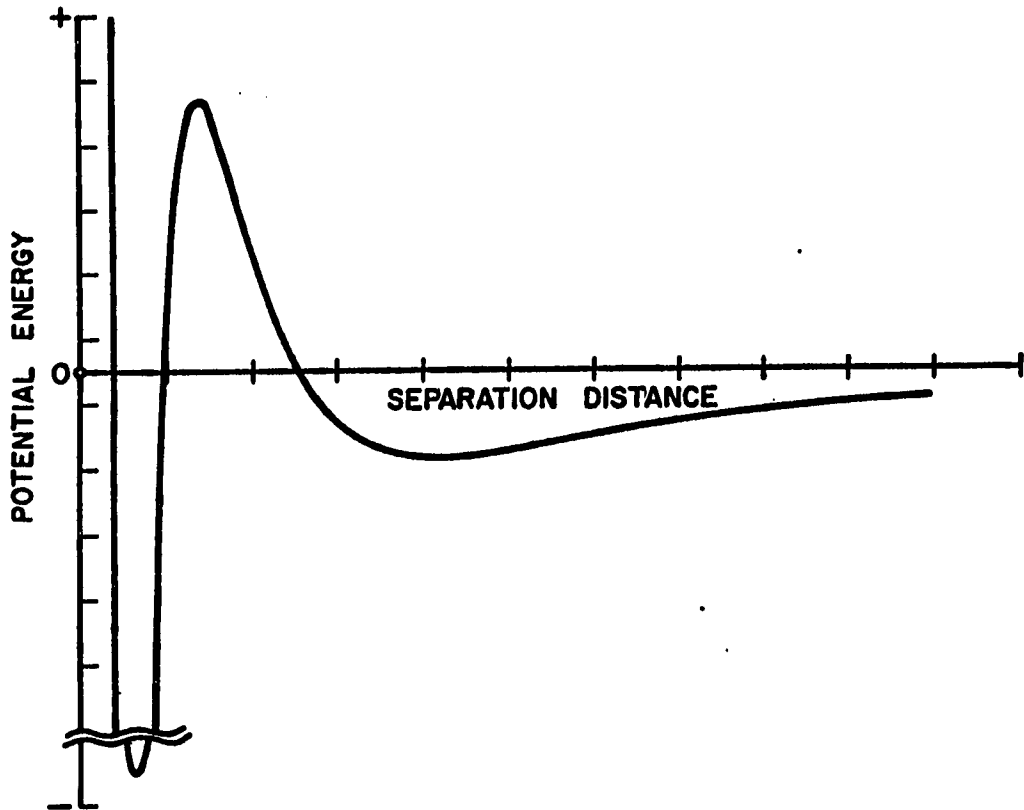


Figure 8. Potential energy versus interparticle distance for two particles in suspension; there are two minimas in potential energy

attractive potential of a system. Thus, if one desires to decrease the stability of a colloidal suspension, it is necessary to reduce the repulsive forces. The repulsion portion of the curve is a function of surface charge and solution chemistry. In the context of water treatment, the surface charge is usually modified. If we reduce or eliminate the surface charge the barrier to flocculation is reduced or removed.

With some materials secondary minimum flocculation is possible. Schenkel and Kitchener (1960) point out the possibility of flocculation in a secondary minimum which may lie at a separation distance as great as 100 to 200 nm. It must be realized that floc formed in the secondary minimum can be broken up by gentle agitation, but floc formed in the primary minimum is much more difficult to breakup (Bennett and Hulbert, 1986). For this reason flocculation in the primary minimum is often referred to as irreversible flocculation (Bennett and Hulbert, 1986). Schenkel and Kitchener (1960) used gentle mixing as a test for primary minimum flocculation versus secondary minimum flocculation. Based on this it is apparent that the practical objective in water treatment must be to achieve flocculation in the primary minimum, by removing the repulsion barrier.

Everything presented so far has been conceptually correct, but has ignored the non-ideality of the system. In a real systems things are

much more complex than in the system presented here. Bennett and Hulbert (1986) presents a discussion of the DLVO model, and has the following to say about the limitations placed on the model by the assumptions which are used:

"Of these (assumptions) the most restrictive is that the particles are perfect parallel infinite planes. Real particles are three dimensional and may have any orientation. Also the potential is not necessarily the same on all of the particles or on all of the faces of a single particle. So instead of a two dimensional curve showing the relationship between separation distance and potential energy for two particles, a four dimensional representation would be required. The potential at each point in space is determined by the effects of all of the particles in the vicinity and all of the particles are free to move. One can see that the theoretical treatment of a system of clay becomes very difficult."

Figures 9 and 10 are presented by Bennett and Hulbert (1986) as examples of a clay water system with some of the non-ideality accounted for. Note that although the particles are still ideal plates, they are free to rotate with respect to each other and there are multiple particles interacting. Figure 9 is a graph of the potential energy relative to another particle as a function of position, this figure is analogous to an ordinary topographic contour map. Figure 10 is the same system presented in Figure 9, with a higher solution electrolyte concentration, which has the same effect as lowering the surface charge on the clay. The negative numbers represent area of lowest potential energy, and the particles will tend toward those minimum points. Both of these figures represent flocculation in the primary minimum, but the particles in Figure 10

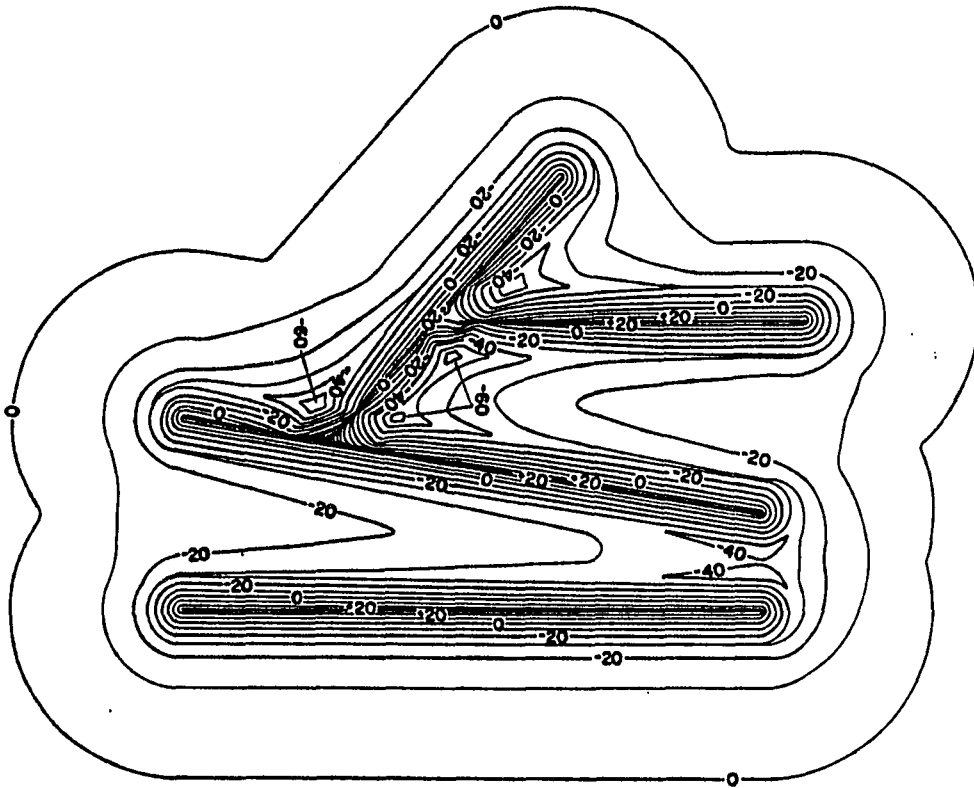
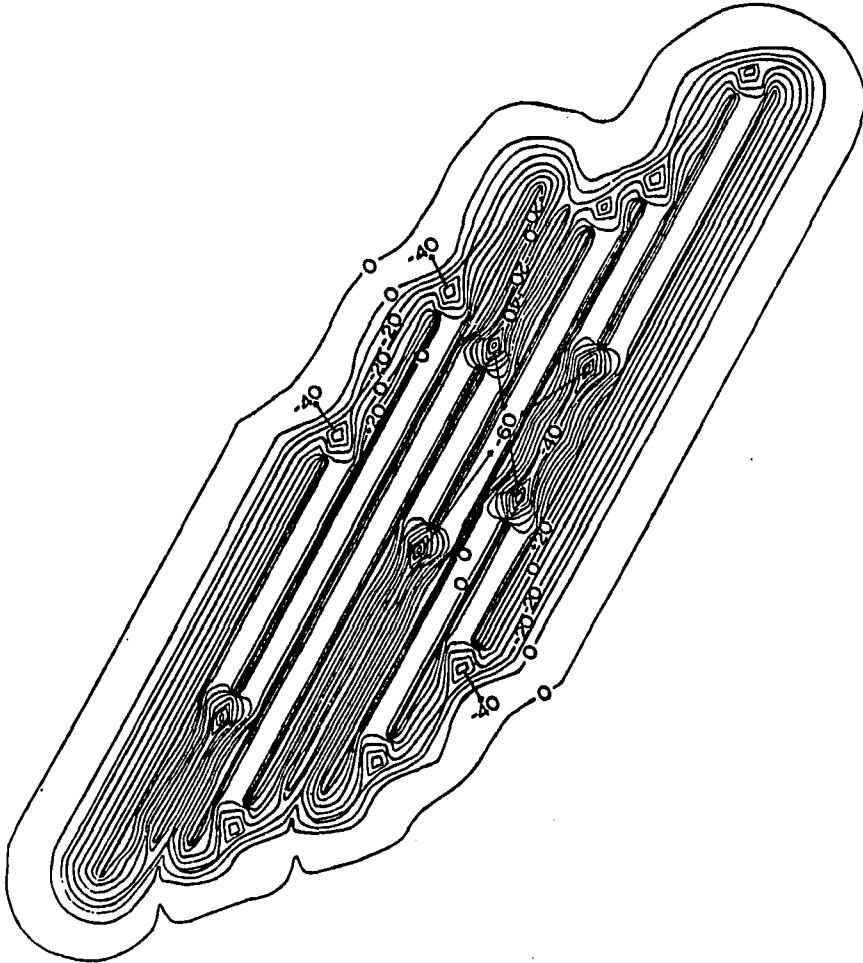


Figure 9. Potential energy in the vicinity of clay particles as felt by another particle that is free to translate in a plane



**Figure 10. Potential energy in the vicinity of clay particles in a system possessing greater electrolyte concentration than depicted in Figure 9. Contours represent potential energies as felt by another particle that is free to translate in a plane**



are more completely destabilized than the particles in Figure 9. Thomas and McCorkel (1971), in working with a mono-dispersed system of spheres, also found that the degree of destabilization affected the shape of the floc formed. He found that if the particles were well destabilized the floc were isotropic. However, if the particles were not well destabilized 50x times more particles had enough energy to stick to the end of a chain than had energy to stick to the middle.

Van Olphen (1977) described the many ways that clay platlets can associate with each other. He states that, in a real clay system, one must be concerned with two double-layers interacting in three modes; face-to-face, edge-to-edge, and face-to-edge. Again, the point being made is that the system is very complex, and the best we can hope for from the DLVO model is a crude qualitative understanding of the system.

#### Temperature effects

Of the forces which have been discussed, electrostatic repulsion is the only one which is noticeably temperature dependent. As noted by Bennett and Hulbert (1986), repulsion increases with a decrease in temperature, but such a change has almost no impact on London or Born interaction energies. Looking back at Table 6, one can see how little Hamakers constant changes over the temperature range of this work. Thus one would expect that, if temperature reduction has a

measurable effect, that effect would be to increase the energy barrier and reduce the flocculation efficiency. It is anticipated, based on the equation for  $V_R$ , that any increase in the repulsion will be very small, since the change in temperature experienced in this work is relatively small on the kelvin scale.

### Discussion

All of the forces discussed in this section are significant in determining particle interactions at a very small scale, and each force will be dominant at some separation distance and surface charge. Under the conditions which are of interest in water treatment flocculation, electrostatic repulsion is the naturally dominant force. If the electrostatic repulsion is partially suppressed and flocculation occurs in the secondary minimum (separation distances of 20 to 50 nm between particles), the floc will be extremely fragile. In this flocculation mode gentle agitation will disperse the floc back to primary particles. When the energy barrier is sufficiently suppressed, flocculation will occur in the primary minimum (separation distances of 3 to 5 nm between particles). In this mode a robust floc is formed, and the process is often referred to as irreversible flocculation. Structural or solvation forces are active from the surface out to 1 to 2 nm. It is expected that these forces will not act to prevent flocculation, but once flocculation occurs they may act to reduce the bond strength. If the particle surfaces are not allowed to approach each other any

closer than 4 to 8 molecular diameters ( $4 \text{ to } 8 * 0.25 \text{ nm} = 1 \text{ to } 2 \text{ nm}$ ), the van der Waals attraction will be much weaker than it would be if the surfaces approached each other until Born repulsion became dominant.

### Turbulence

In the last section we discussed the forces involved in colloid stabilization and destabilization. Once the colloid is destabilized it is necessary to bring the particles close enough to each other for van der Waals attraction to take over. The act of bringing the particles together is often referred to as particle transport. If the particles are small and destabilized, simple Brownian motion will cause flocculation given enough time. However, because of the economics involved in municipal water treatment, it is desirable to increase the rate of flocculation. This is done by carrying out the flocculation in a turbulent flow field. In this section we will discuss how the turbulent flow field relates to the flocculation process.

To understand turbulent transport it is first necessary to understand the phenomena of turbulence. Hinze (1975) gives the following definition of turbulence:

"Turbulent fluid motion is an irregular condition of flow in which the various quantities show a random variation with time and space coordinates, so that statistically distinct average values can be discerned."

Although this definition may be concise it does little to provide us with an intuitive understanding of turbulence and the basic underlying processes which drive turbulence.

Turbulence is frequently described as an energy cascade (or eddy cascade); where energy is put into the system at large length scales. It then cascades down to small length scales through the mechanism of vortex stretching, and finally leaves the system through viscous dissipation. L.F. Richardson said it this way (Reynolds, 1974):

"Big whirls have little whirls,  
that feed on their velocity;  
and little whirls have lesser whirls,  
and so on to viscosity."

Hinze (1975) says that turbulence can be thought of as a superpositioning of ever smaller periodic motions or eddies. Voke (1983) says:

"The turbulent flow of viscous fluid is one of the most complex and beautiful macroscopic phenomena found in nature. It is essentially four dimensional, involving the time dependent interchange of energy and momentum between vortices of different sizes and lifetimes, ..., with respect to each other in three dimensional space."

Perhaps the best way to gain an intuitive understanding of the turbulent flow field is to start with a simple model of turbulence, i.e., the Kolmogorov energy spectrum, and build a mental image from there. Figure 11 represents a typical energy spectrum for a high Reynolds number flow. This form of the energy spectrum, is frequently called the Kolmogorov spectrum law, because Kolmogorov was

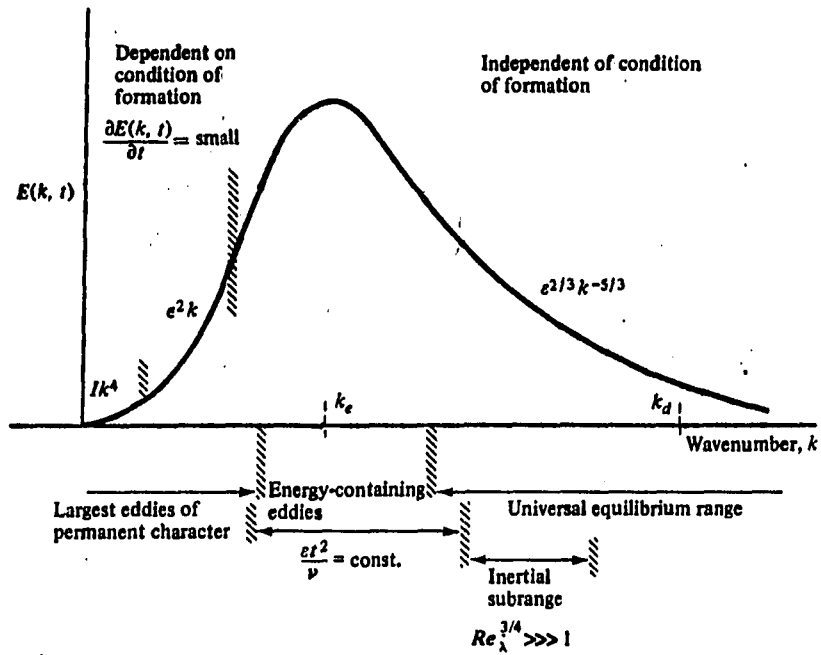


Figure 11. Form of the three dimensional spectrum  $E(k, t)$  in the various wave number ranges

the first to arrive at this result (Hinze, 1975). The graph represents the relationship between eddy size and the energy contained in each eddy size (Hinze, 1975). Various aspects of this energy spectrum will be discussed in the following paragraphs. The purpose of this discussion is to identify the major components of the turbulent flow field and the specific characteristics which will have an impact on orthokinetic flocculation.

The y-axis on Figure 11 is the kinetic energy ( $E(k,t)$ ) contained in a specific eddy size at a fixed point in time. If the turbulence is steady state the average spectrum will be constant over time. The x-axis is the wave number, which is the inverse of the vortex size ( $1/d$ ). Thus a large wave number corresponds to a small eddy. The variables  $k_e$  and  $k_d$  represent the eddy sizes which contain the majority of the energy, and dissipate the majority of the energy respectively.

The largest turbulent eddies in the turbulent flow field represent the length scale at which energy is being fed into the system. These large eddies are inertia controlled and are very little effected by viscous dissipation. The length scale of the large eddies become smaller through the mechanism of vortex stretching, and the energy of the large eddies is cascaded to smaller and smaller eddies (Frost and Moulden, 1977). Note that the words eddy and vortex are used interchangeably in the turbulence literature, although vortex is

probably the more correct of the two. The stretching process does not go on indefinitely. Eventually, an eddy size is reached where the system becomes viscosity dominated rather than inertia dominated. At this point the vortex is no longer a free vortex, i.e., it becomes bound by viscous forces, and the energy cascade is stopped. Once the vortices reach this length scale, their energy is quickly dissipated to heat, and below this length scale we no longer have a turbulent flow field.

#### Production range

Frost and Moulden (1977) refers to this range as the "energy bearing anisotropic eddies". This range is most frequently referred to, however, as the "production scale eddies". The reason for this is easily seen in Figures 12 and 13 (Corrsin, 1961). The eddies in this size range represent the spectral location of the kinetic energy inflow. Vortices in this size range are produced directly by the velocity gradients induced by the mixing equipment.

This introduction of kinetic energy into the system is shown schematically in Figure 12. The box furthest to the left represents the kinetic energy in the bulk flow. This bulk flow kinetic energy is responsible for direct production of the largest eddies in the second box. Figure 13 shows this same concept in the wave number space reference frame. In Figure 13 we see that the majority of the energy goes into the system in the small wave number region, which

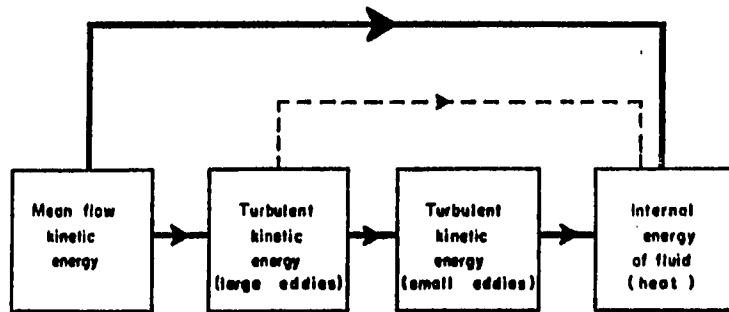


Figure 12. Crude representation of average energy degradation path

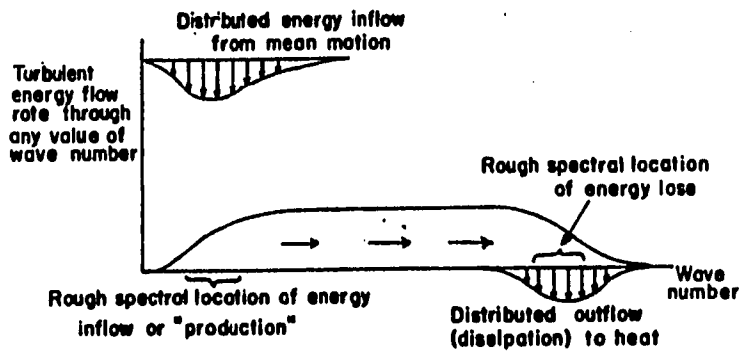


Figure 13. Schematic representation of average turbulent kinetic energy path in wave number space



corresponds to the large eddy sizes. This large eddy range can be divided into two sections (Hinze, 1975). The first section consists of the very largest eddy sizes which are strictly a function of reactor geometry, and exist under all turbulent flow conditions. These are the eddies which are largely responsible for the convective diffusion in the turbulent flow field. This convective diffusion is sometimes referred to as eddy diffusivity. The second, and smaller, range of eddies in this region are a function of the energy per unit mass of liquid-time ( $\epsilon$ ). This size range only exists if there is enough energy being put into the system to stay ahead of the downward cascade of energy to the smaller size eddies. None of the eddies in the production range are sensitive to viscosity effects, and therefore temperature effects. Placek and Tavlarides (1985) reported that these production scale eddies in a mixed reactor equipped with a Rushton impeller, are 1/2 to 1 times the blade height.

#### Energy containing eddies

In the low-wave-number range of the energy spectrum, a peak occurs at the wave number value  $k_e$ . The range of wave-numbers around  $k_e$ , where the eddies containing the majority of the turbulent flow field total kinetic energy are found, is called the range of energy containing eddies (Frost and Moulden, 1977). The variable  $k_e$ , in Figure 11, is the wave number of the average size energy containing eddy. If the diameter of the eddy, i.e., the eddy length scale, is  $d$ , then  $k_e$  is

1/d. The structure of the turbulence in this region is determined by (Hinze, 1975):

- o  $\epsilon$  energy/unit mass-time
- o  $t$  time
- o  $\nu$  kinematic viscosity.

The first of these,  $\epsilon$ , is important because the energy dissipated at high wave numbers is the same energy supplied by the large eddies (Frost and Moulden, 1977). Since the energy must pass through the energy containing eddy range, it effects the shape of this range. Time is important because the relative rate of change of the total kinetic energy is the same order as the time scale of the large eddies. Viscosity is important to the shape of this portion of the spectrum unless  $Re \gg 1$ . If the Reynolds number of an eddy of size  $l$  is greater than  $10^5$ , the structure of this region is independent of viscosity (Frost and Moulden, 1977). The following definition for Reynolds number is used here:

$$Re = u'd/\nu$$

where  $d$  is the length scale for the eddy associated with  $k_e$ ,  $\nu$  is kinematic viscosity, and  $u'$  is the root mean square velocity in the flow field, i.e.,  $u' = ((\text{ave } u^2))^{0.5}$ . Argaman and Kaufman (1968) report a volume weighted  $u'$ , at various  $G$  values, for the reactor selected for use in this study. If we use the  $u'$  given by Argaman and Kaufman and assume that  $d$  is of the same order of magnitude as the impeller blade height, i.e., the size of the largest eddies present, we will establish an upper bound for the  $Re$  number in the

reactor used in this study under the operating conditions that were used. Note that this will overestimate  $d$  and thus will overestimate the Reynolds number. Figures 14 and 15 are the estimated eddy  $Re$  associated with  $k_e$  for the turbine geometry and the stator & stator geometry used in this research respectively. These geometries will be discussed later. The important thing to note here is that in neither case is the  $Re$  even close to  $10^5$ . Thus for this system one would expect the energy containing range to be viscosity dependent.

#### Inertial subrange

The inertial subrange only exists in turbulent flows with an eddy  $Re$  greater than  $10^5$  (Frost and Moulden, 1977). Since this is not the case in this work, it is very unlikely that a viscosity independent inertial subrange exists in the reactor conditions employed in this research.

#### Universal equilibrium subrange

This is the eddy size range in which the majority of the energy dissipation takes place. In fact this range is frequently called the "dissipation subrange". In Figure 12, the second box from the right would represent this eddy size range. Figure 12 shows that the kinetic energy moves from the small eddies directly to the internal energy of the fluid (Corrsin, 1961). Figure 13, once again, shows this same information in a wave number space reference frame. In Figure 13 energy is put into the system at the large eddies, cascaded

**APPROX. EDDY REYNOLDS NUMBER  
TURBINE IMPELLER @ VARIOUS TEMPERATURES**

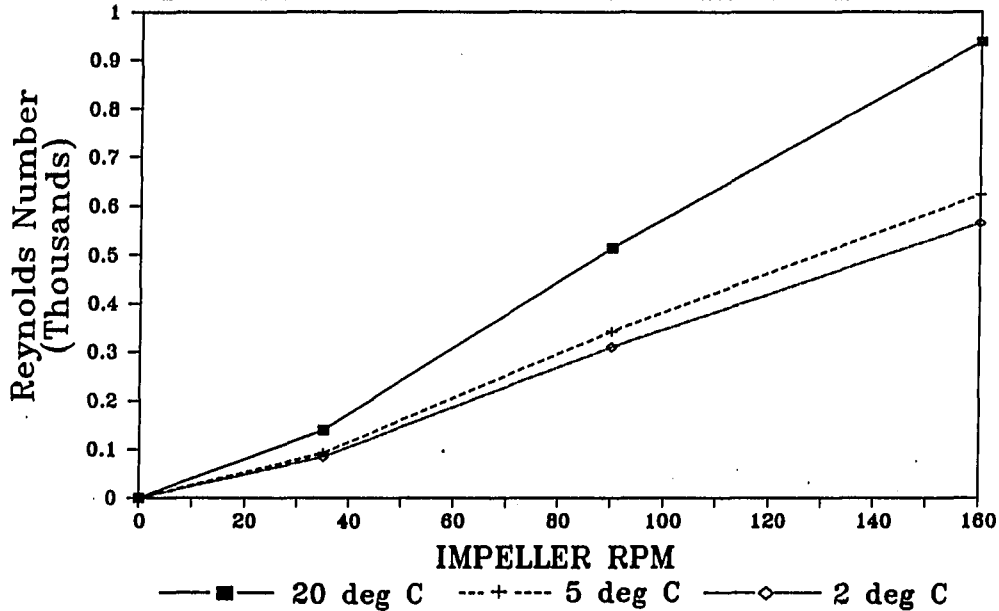


Figure 14. Approximate eddy Reynolds number for the turbine impeller at various temperatures

**APPROX. EDDY REYNOLDS NUMBER  
STAKE & STATOR IMPELLER @ VARIOUS TEMPERATURES**

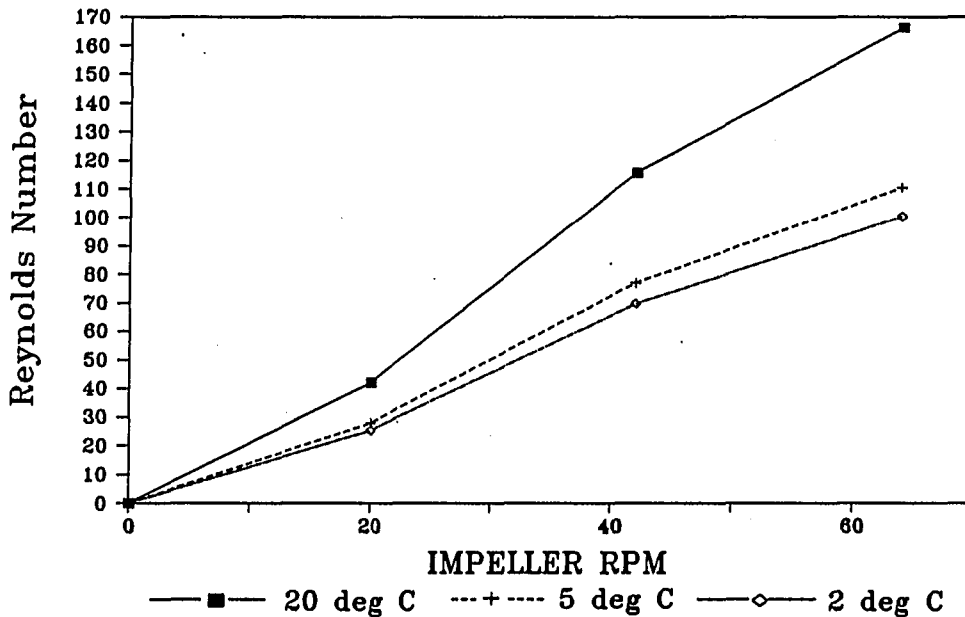


Figure 15. Approximate eddy Reynolds number for the stake and stator impeller at various temperatures

down to the small eddies, and then leaves the system at the small eddies through viscous dissipation. Kolmogorov speculated that small scale eddies, in a homogeneous turbulent flow, lose the preferred orientation of the mean rate of strain, taking on a universal structure or isotropy. This was referred to as local isotropy by Kolmogorov (Frost and Moulden, 1977). For this universal structure to exist the eddy Re number referred to earlier must be on the order of 100 (Frost and Moulden, 1977). In the part of the energy spectrum where the universal structure might exist, the time scales are much shorter than the time scales in the mean flow. Thus the small scales react quickly enough to be considered at equilibrium with the mean flow at all times. Thus the name "universal equilibrium range" (Frost and Moulden, 1977). Hinze (1975) also states that even if the large scales of turbulence are strongly anisotropic, the small scale turbulence will tend to be isotropic. The reason for this is illustrated nicely by Figure 16 (Bradshaw, 1971). If one starts at the top of the energy cascade and assumes stretching in only 1 direction (Z), the stretching is nearly isotropic in only four generations.

Since the naturally occurring colloids are less than 10  $\mu\text{m}$  in size, it is likely that if any eddy size will be important in flocculation, it will be the universal equilibrium range. This leads us to ask how can we characterize this smallest scale of turbulence. The  $k_d$  in Figure 11 is the wave number associated with the size of eddies that

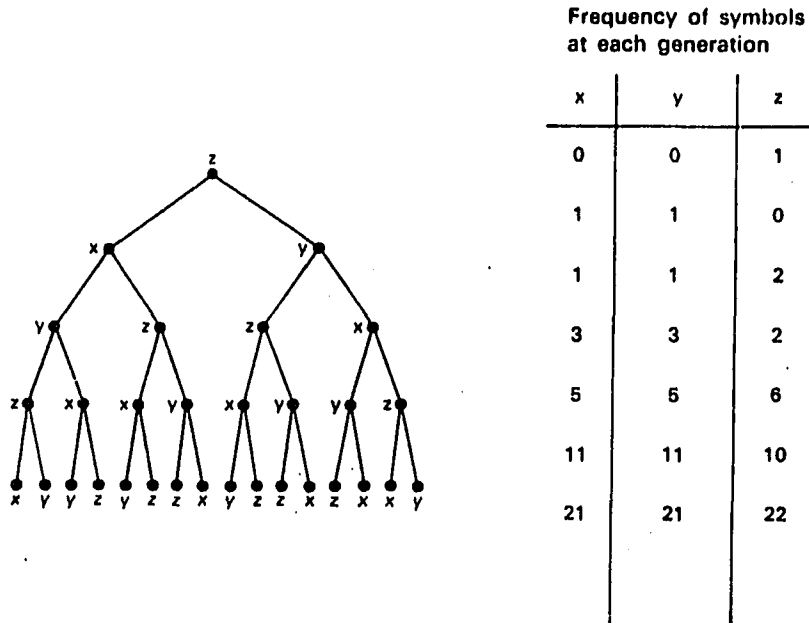


Figure 16. "Family Tree" showing how vortex stretching produces small-scale isotropy. The labels are the directions of stretching in each "generation": the length scale decreases from one generation to the next

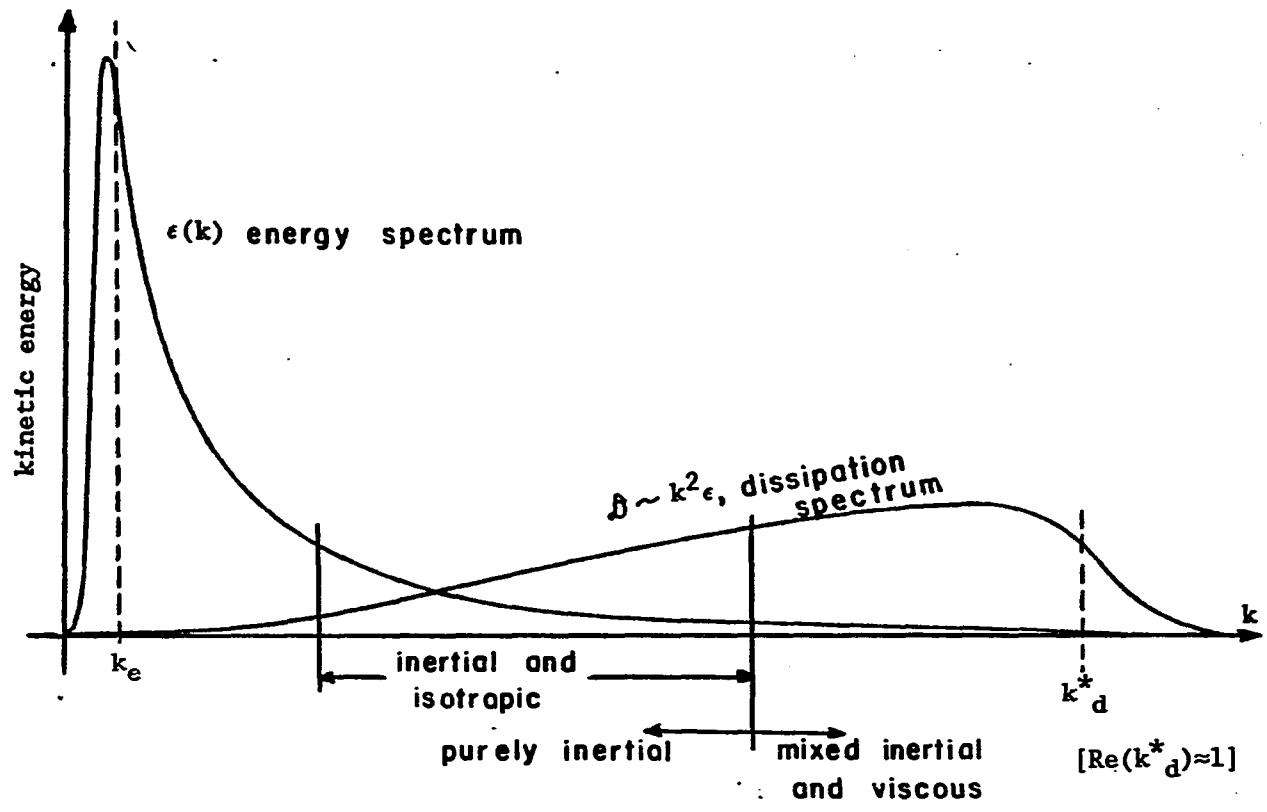


Figure 17. Spectral ranges in turbulence of moderate Reynolds number

provide the main contribution to the total energy dissipation (Hinze, 1975). It should be noted that at moderate Reynolds numbers, viscous dissipation affects the turbulent flow structure over the entire eddy size range, except the very largest eddies. Figure 17 shows the relationship between the energy spectrum and the dissipation spectrum in wave number space (Corrsin, 1959). Kolmogorov used dimensional reasoning to derive the length scale ( $\eta$ ) which corresponds to  $k_d$ , i.e.,  $k_d = 1/\eta$ . This special length scale is referred to as the Kolmogorov microscale, and is defined as:

$$\eta = \left[ \frac{\nu^3}{\epsilon} \right]^{1/4}$$

- $\nu$      - kinematic viscosity
- $\epsilon$      - energy/unit mass-time

Following Kolmogorov's development of  $\eta$ , one notes that this length scale represents an eddy whose Reynolds number is equal to 1. By definition, a Reynolds number of 1 indicates that the inertial and viscous forces are equal at this length scale. This implies that viscous dissipation will peak at a wave number greater than or equal to  $k_d$ . Based on this line of reasoning, it is common to define  $k_d = 1/\eta$ , which is to say  $k_d\eta = 1$  (Hinze, 1975). However, various



researchers have shown both experimentally and theoretically that the dissipation peak is actually at a smaller wave number (larger eddy size) than  $1/\eta$ . Hinze (1975) reports values of  $k_d\eta$  which range from 0.5 to 0.09. What this means in the context of flocculation is that much of the energy put into the reactor at the production range, is not available for particle transport at and below the Kolmogorov microscale. Looking at the energy dissipation spectrum in Figure 17 we can see that the turbulent energy dissipation does not reach far below the Kolmogorov microscale. This is because, as we cross the  $k_d$  boundary, viscous forces soon become dominant and a free vortex cannot exist. This means that the mechanism driving the energy cascade is no longer present, and therefore the lower scale of turbulence has been reached. Below this scale, all particle transport is caused by localized shear fields. It is also noted that below the Kolmogorov microscale, the rate of energy dissipation is none linear and the rate is decreasing. Figure 18, which is based on Argaman and Kaufman's (1968) work, contains calculated values for Kolmogorov's microscale at various G-values, and temperatures. Since Figure 18 shows the relationship between G based on the volume averaged  $\epsilon$  and  $\eta$  based on the volume averaged  $\epsilon$ , it is the same for all impeller geometries. It is interesting to note that the primary particles used in this work had an equivalent circular diameter of 1.8  $\mu\text{m}$ . This would place the primary particles well below the length scale of the smallest turbulent eddies.

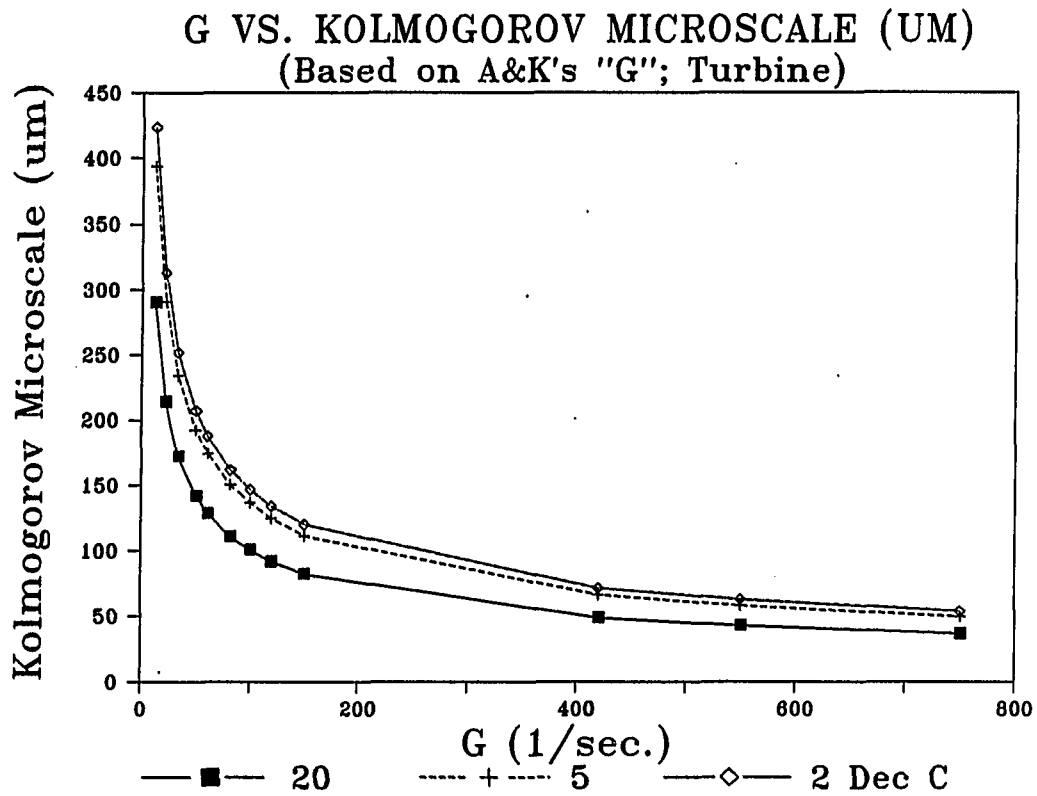


Figure 18. G versus the Kolmogorov microscale of turbulence  $\eta$  at various temperatures. G is from Argaman and Kaufman (1968),  $\eta$  is calculated based on G

To understand what is happening at scales smaller than the microscale, it is necessary to consider the mechanism involved in vortex stretching. Sanitary engineering literature has typically illustrated vortexes as small 2-dimensional spirals (Amirtharajah, 1981). This leaves us with little appreciation of the true complexity of vortex stretching in a turbulent flow field. Figure 19 is a sample of the traditional fluid mechanics imagery used to illustrate vortex stretching (Tennekes and Lumley, 1972). Again, this communicates none of the true 3-dimensional complexity. It is only recently that it has become possible, through computer simulation, to visualize 3-dimensional vortex stretching. Figure 20 represents two isolated vortex tubes interacting (Zabrusky, 1987). Although Figure 20 begins to hint at the complexity of this process, it still involves only two vortex tubes. In reality there are many vortex lines interacting simultaneously. Frost and Moulden (1977) refer to the turbulent flow field as a tangle of vortex lines. Figure 21 shows six vortex rings arranged as the faces of a cube, and then allowed to interact over time (Glaberson and Schwarz, 1987). The tangle of vortex lines in the last frame looks like a pile of spaghetti, and this is the result of starting with only 6 vortex lines. Note that the two tubes in Figure 20 are identical in size. This is in fact a realistic situation. Frost and Moulden (1977) point out that only eddies of a comparable size can interact with each other. The cascade of energy takes place from neighboring size to neighboring size, there are no short cuts (Frost and Moulden,

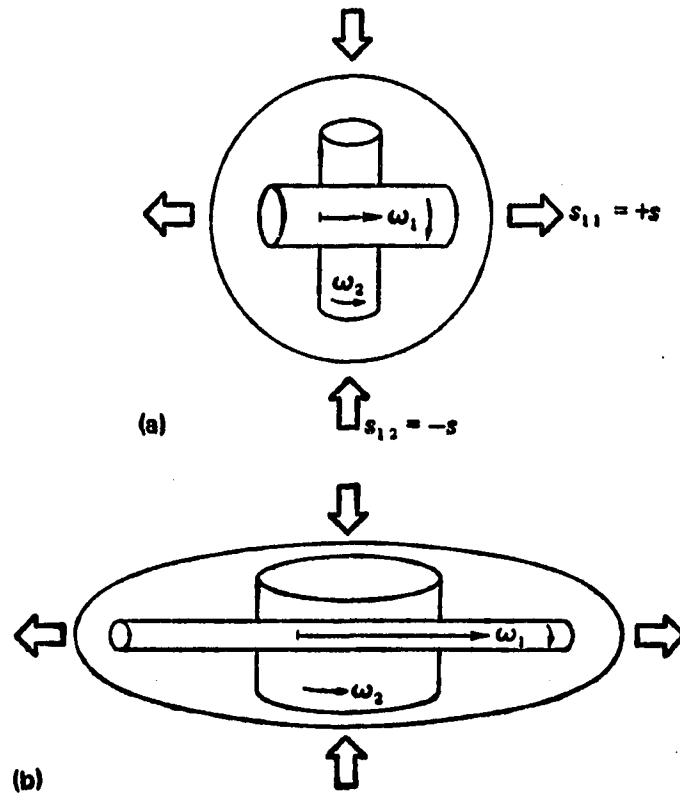


Figure 19. Vorticity stretching in a strain field: (a) before stretching, (b) after stretching

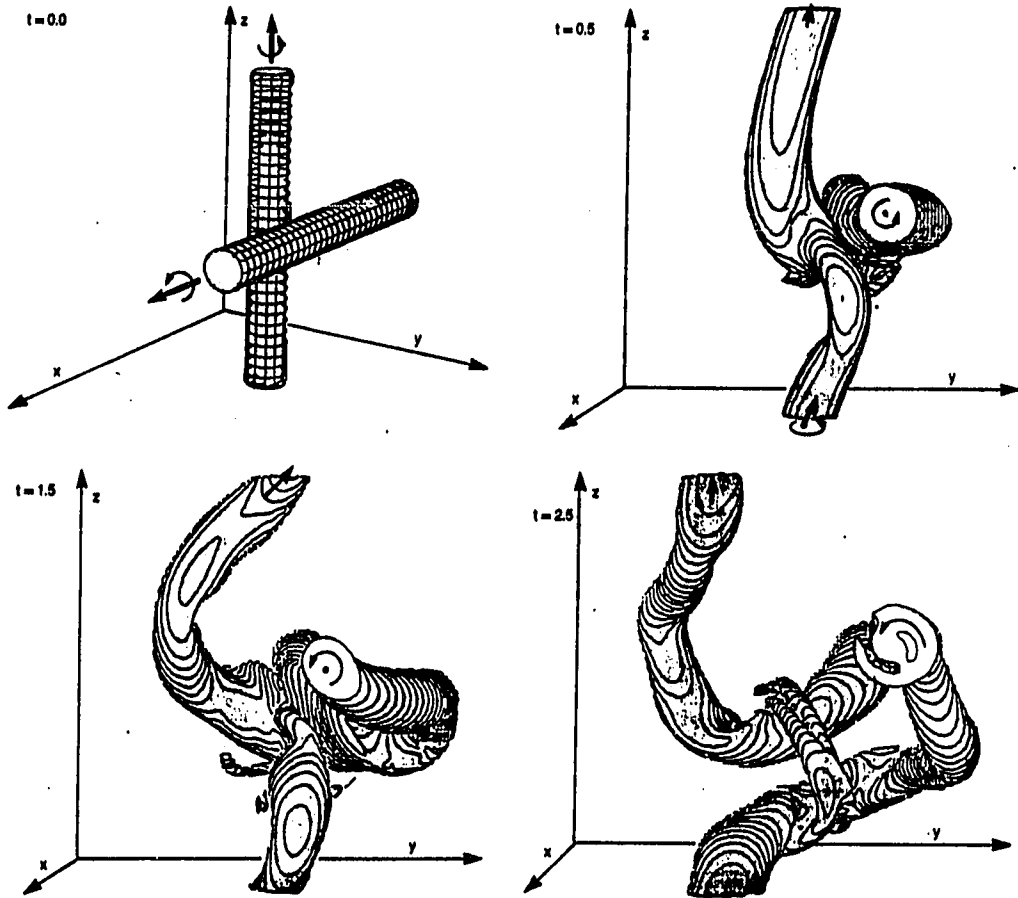
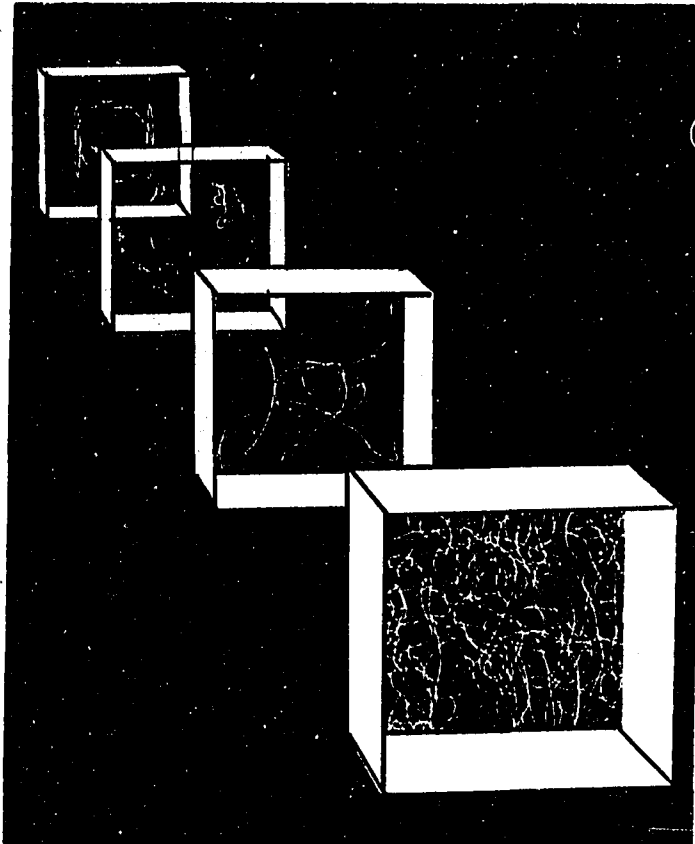


Figure 20. Computer simulation: evolution with time of two identical circular tubes of vorticity located in three dimensional space



**Figure 21. Computer simulation: evolution of a vortex tangle from six vortex rings interacting**

1977). It is also interesting that viscosity does not play an important role in vortex stretching. It is the fluid strain field which drives the stretching.

What does all of this mean with respect to turbulent flocculation? Particles, like eddies, are only moved efficiently relative to each other by eddies which are similar in size to the particles. Therefore, it is unlikely that even the smallest turbulent eddies will play a direct role in turbulent flocculation until the floc have grown very large (Koh, Andrews, and Uhlherr, 1984). However, one can see that the turbulent vortex tubes are space filling, and the process of stretching will create a myriad of localized shear fields. It is these localized shear fields which drive the flocculation.

Assume the following:

- o the primary particles are smaller than the Kolmogorov microscale,
- o the primary particles are homogeneously dispersed throughout liquid volume.

We can think of the mechanism for turbulent flocculation in the following way. For simplicity, consider the image of vortex stretching presented in Figure 19. In (a) there are two vortices of equal size. In accord with our previous assumptions, these vortices each represent a volume of fluid containing a homogeneous distribution of particles. Before stretching the particles are moving relative to the bulk flow, but are stationary with respect to

each other. As the vortex undergoes stretching, a localized velocity gradient (i.e., shear gradient) is induced in the fluid contained in the vortex, and this localized velocity gradient induces particle collisions. Thus, the vortices in the turbulent flow field are responsible for causing the collisions which result in floc growth, but not in the direct sense. The magnitude of the localized velocity gradient will be dictated by the diameter at which the vortex tube stops stretching. This is determined by the size at which the vortex tube ceases to be a free vortex and becomes bound by viscous forces. The Kolmogorov microscale of turbulence is an approximate indicator of this eddy diameter.

The entire discussion of turbulence to this point has dealt with idealized turbulence. That is turbulence which is homogeneous and isotropic, with no average bulk flow present. Specifically we have been discussing the model proposed by Kolmogorov. From this model of turbulence we have established the following information regarding homogeneous isotropic turbulent flows:

- o The largest eddies are strictly a function of reactor geometry, and only the largest eddies are a function of reactor geometry.
- o In a homogeneous turbulent flow field the smallest eddies will tend to be isotropic even if the larger eddies are anisotropic.
- o At the energy input typical of flocculation, the inertial subrange probably does not exist.



- o Turbulent eddies only interact effectively with features in the flow field of nearly equal size, therefore even the smallest turbulent eddies do not interact with the primary particles.
- o Localized shear fields formed by the turbulent eddies do interact with the primary particles, and will cause flocculation.
- o The smaller the Kolmogorov microscale of turbulence the more intense the localized velocity gradient.
- o The energy dissipation spectrum is non-linear, and below the microscale of turbulence ( $\eta$ ), the rate of dissipation is decreasing.

This picture of turbulence, although simple and idealized, is qualitatively sound. Even recent turbulence work based on dynamical system theory, i.e., chaos theory, relies on the intuitive picture of turbulence developed by Kolmogorov, as well as many of his original assumptions (Schertzer and Lovejoy, 1986; Paladin and Vulpiani, 1986). This is encouraging because it indicates that, at least for intuitive purposes, this simple picture developed here is not too far from the mainstream of turbulence research.

In addition to having a simple mental picture of turbulence, it is also necessary to understand that what has been discussed so far is more of a metaphor than a model (Leibovich and Lumley, 1986). If we would use this metaphor to interpret data, it is important that we consider how far we have stretched the assumptions upon which the metaphor is based. It is possible that the stretching of our assumptions may make the metaphor useless. For instance, in a mixed

tank reactor the turbulence is not isotropic, or homogeneous, nor is bulk flow absent. Corrsin (1959) notes that the mean strain rate in all shear flows must tend to make the structure of the flow anisotropic in all parts of the spectrum. Fortunately, perhaps because of its inherent simplicity, the model is fairly robust. With a few qualifiers we will find it quite useful.

In our idealized model, see Figure 12 (Corrsin, 1961), the large scale turbulence simply existed uniformly distributed throughout space, and drove the energy cascade. In an actual mixed tank reactor the energy balance is better represented by the block diagram in Figure 22 (Placek et al. 1986), than by Figure 12. The fact that there are multiple pathways of varying degrees of importance in different regions of the flow leads to a situation in which the flow field can be extremely non-homogeneous. Looking at an example is perhaps the best way to see how this might impact the flocculation process.

Figure 23 shows a Rushton impeller and the flow field near the impeller. The Rushton impeller is an impeller geometry similar to the turbine used in this study, and it has been the subject of extensive experimental and theoretical work. From the Rushton impeller we can, perhaps, gain some insight into the complexities inherent in the flow field of a stirred tank reactor. The first thing to notice is that not all of the energy put into the impeller

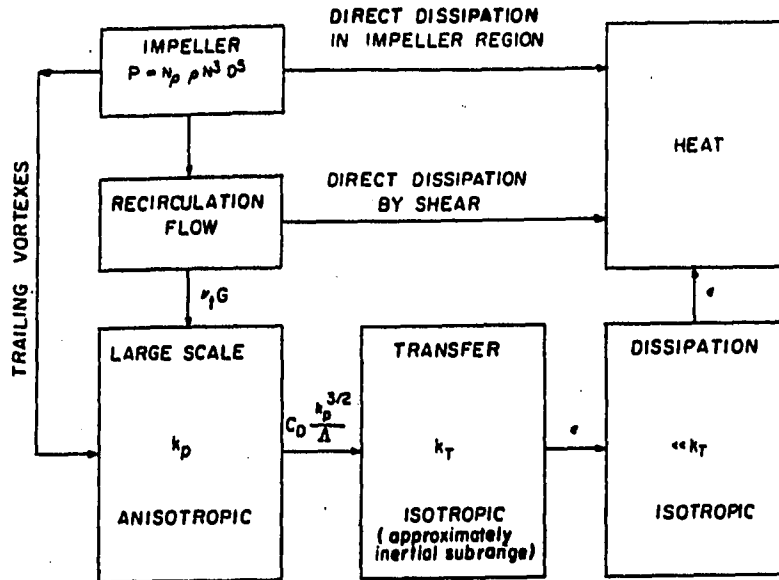


Figure 22. Model of dissipation of mechanical energy in an agitated vessel

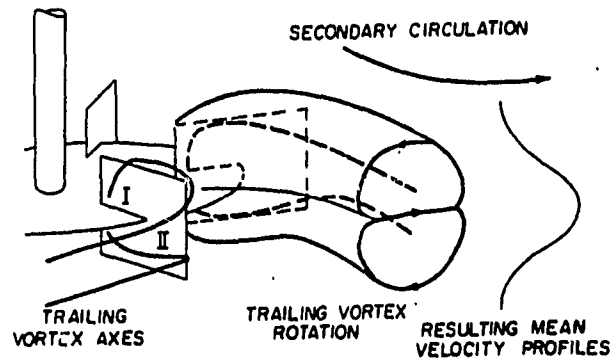


Figure 23. Trailing vortices behind a Rushton-type turbine impeller and resulting mean velocity profile

generates turbulence. Some of the energy is dissipated directly by the impeller, and some is dissipated directly in the fluid shear. This means that only a fraction of the energy per unit mass ( $\epsilon$ ) put into the reactor actually generates turbulence. Clark (1985b) indicates that as much as 30 percent of the total energy put into the reactor can be lost without producing any turbulence.

It is interesting that the impeller does not generate turbulence directly. The impeller generates pseudo-turbulent flows, i.e., trailing vortices, impeller discharge flows, and recirculating flows, and these flows generate the turbulence. Although these flows generated by the impeller exhibit intense fluctuations, they are non-random, and thus are referred to as non-random pseudo-turbulent flows (Van't Reit et al. 1976). The two major regions of interest are the recirculation flow in the majority of the vessel, and the flow in the impeller discharge region (Placek et al., 1986). The secondary flows in the recirculation region are induced by the impeller discharge flows. The flow in the impeller discharge region can be divided into two distinct flows. The radial discharge flow from the Rushton impeller, and the pair of trailing vortices. All three of these flows are shown in Figure 23.

The accepted view of the turbulent structure around the Rushton impeller has changed radically in the last decade as our ability to measure turbulent structure has improved. The early work showed an

extremely non-homogeneous flow field, and the turbulence was reported to be generated by the impeller and the zone associated with the impeller (Cutter, 1966; and Rao and Brodkey, 1972). It was also reported that the turbulence generated in these areas was dissipated where it was generated. Cutter (1966) published the following:

- o 5/10 of the total dissipation was in the impeller stream,
- o 2/10 of the dissipation was in the impeller itself,
- o 3/10 of the energy was dissipated in the rest of the tank volume.

Rao and Brodkey (1972) and others published work which appeared to confirm Cutter's work. However, all of this early work was based on the assumption that:

- o the velocity fluctuations caused by pseudo-turbulence was turbulence,
- o turbulent energy was dissipated where it was created.

In the vigorously recirculating flow field of the Rushton impeller neither of these assumptions is true.

Recent work (Van't Reit and Smith, 1975; Van't Reit et al. 1976; Gunkel and Weber, 1975; Placek and Tavlarides, 1985; and Calbrese and Stoots, 1989) has taken a more sophisticated approach to analyzing this flow field. This recent work has not only recognized the non-homogeneous nature of the flow field, but it also accounts for the existence of pseudo-turbulent flow structures and corrects for the

anisotropic character of the turbulence. This has been important in understanding the structure of the flow field around the impeller.

The following are some of the major points which have been established (Gunkel and Weber, 1975):

- o The pseudo-turbulent flows, associated with the trailing vortices, and the impeller flow stream, are transported out of the impeller zone.
- o Because the pseudo-turbulence is transported out of the impeller zone, much of the turbulence is produced out away from the impeller zone.
- o There is a time lag between the production of turbulence, and its dissipation. This time lag may give the turbulence an opportunity to leave the impeller zone before it is dissipated.

It is universally agreed that the flow in the impeller discharge region is more energetic than the flow in the recirculation region. The questions of interest are; how much more energetic is it?, and how much of the energy reaches a scale which will effect objects the size of floc and primary particles? If the energy is generated and dissipated in an extremely energetic atmosphere, the energy will affect very small size scales. That is, the local microscale of turbulence will be very small. This will tend to enhance the early stages of flocculation, because the increased energy at small length scales will increase primary particle collisions. This is, however, a two-edged sword. As the floc grow, the intense energy in the impeller region will break the floc up. Van't Reit and Smith (1975) estimates that 10 percent of the recirculation flow actually passes through the high energy portion of the impeller region. This means

that 90 percent of the flow is not subjected to these stresses, and may grow floc large enough to be damaged by the high energy environment if it passes through the impeller.

Because of the recent work, we have also come to understand that the flow field around the Rushton turbine impeller is much more homogeneous than once thought. Van't Reit et al. (1976) note that the localized energy dissipation found by Rao and Brodkey (1972) and Cutter (1966), of 100x the average, was certainly too large. Van't Reit et al. speculate that 10x the average might be more reasonable. Okamoto et al. (1981) indicated that the rate of dissipation in the impeller discharge region was 6x greater than the bulk mean value, and that 70 percent of the energy was dissipated in the bulk flow. Placek and Tavlarides (1985) drew the same conclusions from the data of Gunkel and Weber (1975). Glasgow and Kim (1986) report that a 40  $\mu\text{m}$  floc will experience a rate of strain 4.6x larger than the average energy input would lead one to anticipate.

The velocity gradients in the recirculation region far from the reactor walls are smaller, and therefore the production rate of large vortices in this region is also small (Placek et al. 1986). Figures 24 and 25 show visually how the energy is dissipated in the vessel (Placek et al. 1986). Figure 24 shows calculated kinetic energy profiles for the upper right quadrant of the vessel. Figure 25 shows the energy dissipation profile for the same region. What is

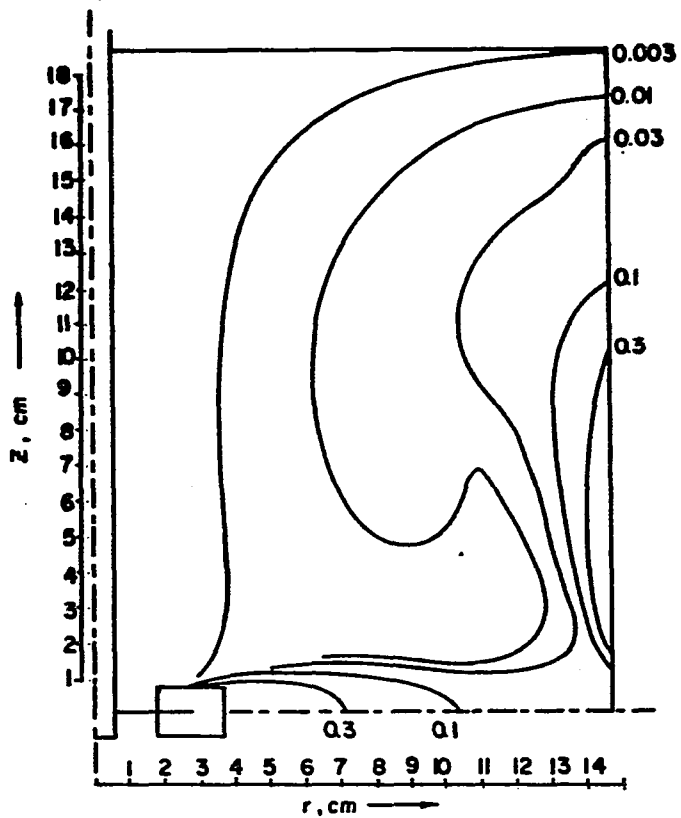


Figure 24. Calculated profiles of overall kinetic energy of turbulence for flow field around a Rushton-type impeller

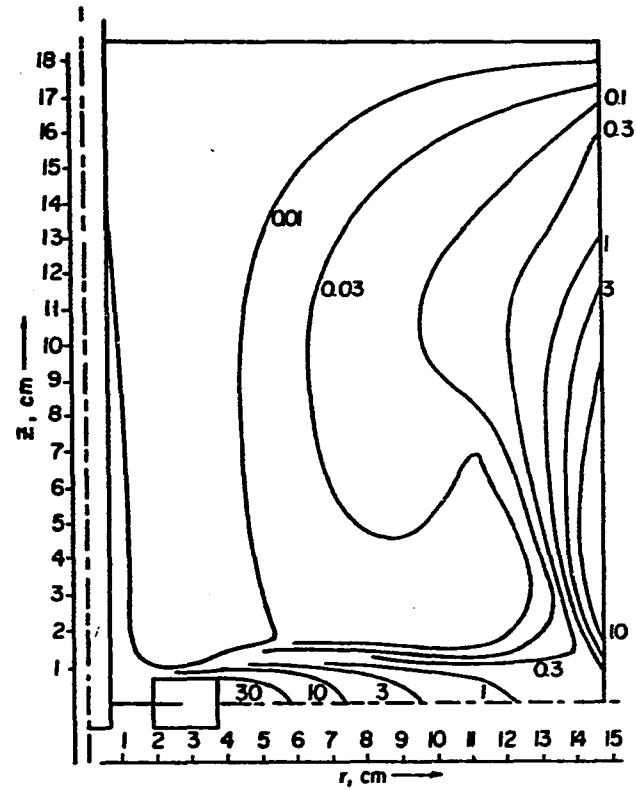


Figure 25. Calculated profiles of the dissipation rate of turbulence for flow field around a Rushton-type impeller



important in these figures is not the absolute values shown, but the pattern illustrating the areas of high and low energy dissipation, and the fact that high kinetic energy and high dissipation are a one to one mapping. The profiles in Figures 24 and 25, make it obvious that the system geometry is important in a mixed reactor. From these figures one can see that:

- o The areas of low energy in the recirculation region are areas which are less likely to be efficient in flocculation of small particles, and also less prone to causing floc breakup.
- o The high energy regions are likely to efficiently flocculate small particles, and also breakup the floc which are formed in the less energetic regions.

Figure 26 shows an interesting characteristic of the Rushton impeller recirculation region. Note that the particle concentration in the less energetic area is lower. This is because the particles used in this simulation tended to settle out of these areas. This figure is based on a computer simulation, and does not directly address the colloidal particles used in this work. However, it does point out that the flow field, under certain circumstances, may effect not only the energy available for inducing collisions, but also the number concentration of particles in the different flow regions.

The Rushton impeller example prompts the following observations:

- o It seems reasonable that mixer geometry may be an important variable in flocculator efficiency.

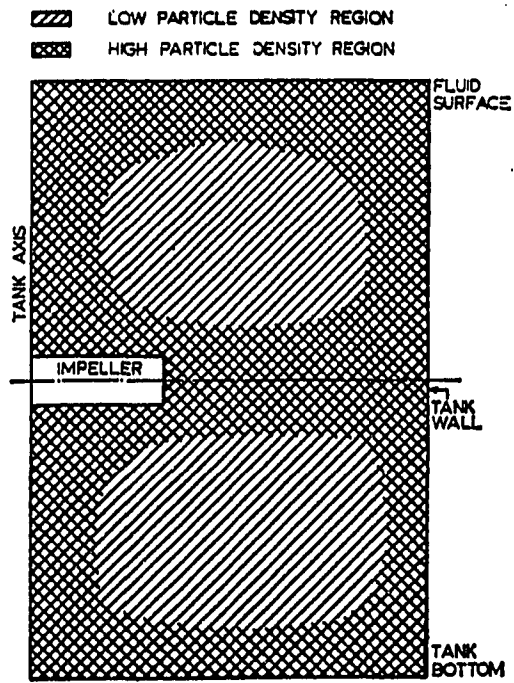


Figure 26. Computer Simulation: particle spatial variation through out a vessel agitated by a Rushton-type impeller

- o It also seems that a mixer geometry which distributes the energy uniformly throughout the reactor vessel may have some advantages in flocculation where both growth and breakup are of concern.
- o One must wonder if  $\text{ave } \epsilon$  or  $G$ , which is based on  $\text{ave } \epsilon$ , is a reasonable parameter to use in quantifying a turbulent flow field which is obviously non-homogeneous.

It is appropriate at this point to look at the information available on the effect of geometry on flocculation efficiency. In reviewing this literature it is important to bear in mind a number of things. First, there have been a large number of parameters used to measure flocculation efficiency. Researchers have used settled turbidity, filtered turbidity, filtration number, and relative turbidity. It is not easy to directly compare these various techniques, and none of them actually measure the ability of the system to remove primary particles by flocculation. Settled and filtered turbidity represent an attempt to measure primary particles remaining after a subsequent unit process. This approach has two flaws. First, it is impossible to separate the efficiency of the two unit processes, i.e., flocculation and filtration, or flocculation and settling. Second, turbidity may be correlated to the number concentration of primary particles remaining, but it still does not measure the number concentration and size distribution of the remaining particles. Let's consider these criticisms. Flocculation, by itself, is an extremely complex process, and there is large uncertainty in scaling bench scale results up to design scale. The same is true of both sedimentation and filtration. In performing basic research it is

important that the indicators used to measure flocculation efficiency not be tied to a second complex process with potentially unmeasurable biases. For instance, in sedimentation, flocculation will occur due to differential settling, and floc with a dense structure will be removed in preference to floc with an open structure. Both of these phenomena will tend to bias the results, but neither of them is easily quantified.

It is well known that the particles which are very small and very large relative to the wavelength of light, are less efficient at scattering light than particles which are close in size to the wavelength of light (Friedlander, 1977). Since the turbidity measure is based on light scattered at 90 degrees, turbidity measurements will also exhibit this same bias. If the particle count is high the raw water particle concentration is usually well correlated with turbidity. However, turbidity is not sensitive enough to shifts in the particle size distribution to be a good measure of flocculation efficiency. Thus, if one is attempting to compare the efficiency of a number of impellers using turbidity as a parameter, it has been necessary to measure settled or filtered turbidity. It would be better to compare shifts in the particle size distribution than to compare shifts in turbidity. If one is to understand what aspects of an impellers geometry are important in flocculation, it is important to be able to track the changes in the particle size distribution induced by the impellers. As stated previously, the structure of the

flow field and the size of the particles in the flow field interact. Thus, different impellers may be optimal under different conditions.

It is also very likely that the mode of flocculation (i.e., mechanism) will influence the measured efficiency of the impellers. In the adsorption/destabilization mode (A/D), the primary particles are destabilized, and begin to flocculate during rapid mixing, but the size distribution of the particles does not change appreciably prior to the flocculation basin. In the sweep floc mode, a chemical precipitate is formed during rapid mix. This precipitate is generally much larger than the primary particles which were originally present. This large precipitate then proceeds to sweep up the primary particles. It is easy to see that an impeller which is optimal in one situation may not be optimal in another.

The impeller geometry and flocculation mode will also impact the floc structure, and floc structure affects the ability of filtration and sedimentation to effectively remove the particles. Thus, rather than simply speaking of flocculation efficiency, one should perhaps speak of flocculation efficiency with respect to flocculation mode and the succeeding unit process.

Because of the difficulty in interpreting and comparing the literature results, each of the studies will be presented in

chronological order. Major trends will be discussed, but no real attempt will be made to fully integrate this literature.

Drobny (1963) Compared 30 variations of an impeller similar to the turbine used in this work. Alum floc nucleated by a small amount of Fullers earth was flocculated at a pH between 6 and 7. The alum dose used in forming the floc was not reported, but based on the information presented, the flocculation mode was probably sweep floc. Flocculation efficiency was based on relative turbidity, i.e., the increase in turbidity due to alum precipitation during flocculation. The comparison was based on a constant power per unit volume for all of the impellers. Drobny concluded:

"It appears definite that the flocculation process may be made more efficient with respect to power input by simple variations in the paddle design."

Argaman and Kaufman (1968) studied the two impeller designs shown in Figure 27, namely a turbine impeller and a stake and stator impeller. Note that these same impellers were selected for use in the present work because they appear to represent the extremes of practical impeller geometry. Argaman and Kaufman flocculated a 25 mg/l kaolinite suspension using 25 mg/l of alum as  $Al_2(SO_4)_3 \cdot 14H_2O$ . Their work was performed at an unspecified pH, but it is assumed, based on the dose, that they were utilizing the sweep floc mode. The flocculation efficiency was based on a type of relative turbidity. A sample of the flocculated material was taken and shaken vigorously.

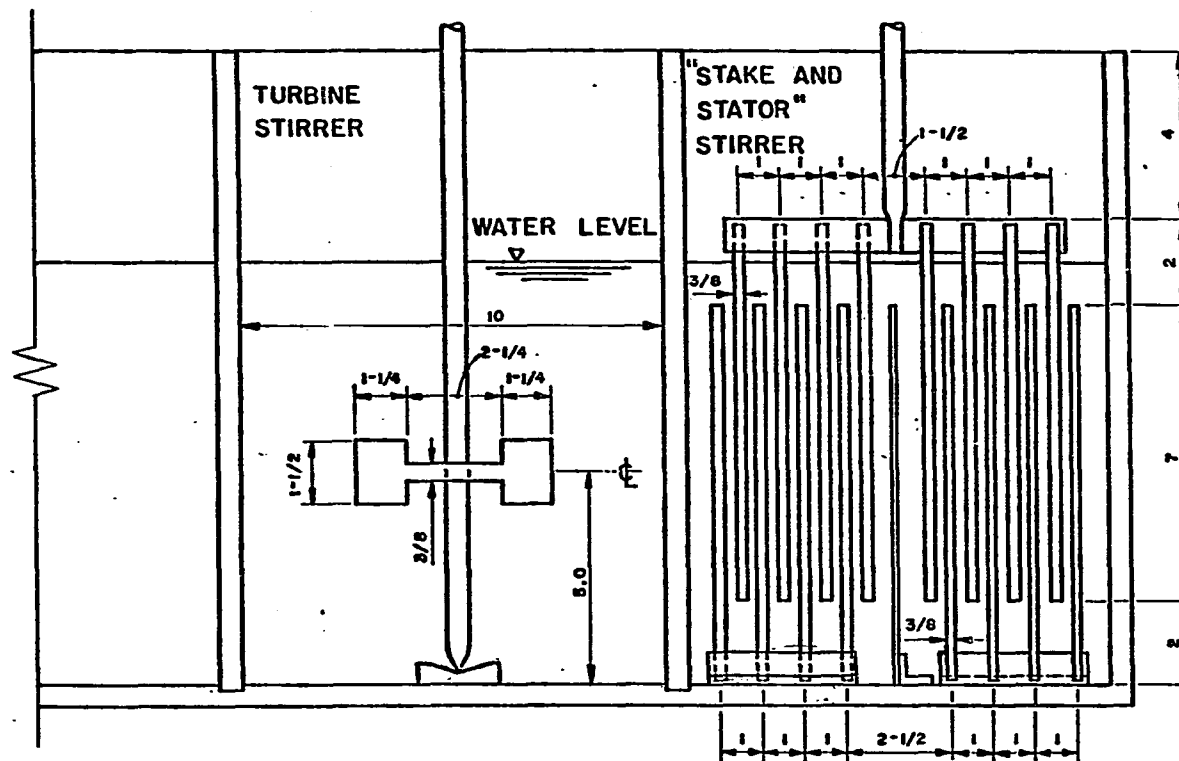


Figure 27. The turbine and stake and stator impellers used by Argaman and Kaufman (1968); all dimensions are in inches

It was assumed that this shaking would reduce the floc to primary particles. The turbidity of the shaken sample was measured, and assumed to represent the original primary particle concentrations. Turbidity was then measured on a second sample which had been settled for 30 minutes prior to being shaken. The percent difference between these two was considered the reduction in primary particles. It is very likely that the assumption that the floc were reduced to primary particles by shaking was in serious error. It is expected, however, that the errors induced by this faulty assumption did not invalidate their conclusions with respect to impeller efficiency. They concluded that, in the region in which they were working, the performance of the stake and stator impeller was superior to the turbine impeller. The work was performed at approximately 21 °C.

Patwardham and Mirajgaonkar (1970) compared 6 paddle geometries, flocculating clay using alum at a pH of 7.6. Based on this pH it is probable that the work was performed in the sweep floc mode. Figure 28 shows the basic impeller geometry, experimental conditions, and results. It is not explicitly stated, but it appears that settled turbidity was used as the measure of flocculation efficiency. The impeller geometries were compared at constant impeller speed. The conclusion was again drawn that there was a geometry effect.

Bhole and Limaye (1977) conducted experiments with 5 vessel geometries and 5 impeller geometries. The experiments were conducted



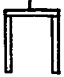
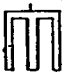




Depth of water 11.8 cms Surface Area 127 sq.in Cross Area 157.5 sq.in. Volume 1500 cc.			PADDLE DETAILS										Speed 40 r.p.m. Stirring time 20 mins Temp. 24 Deg. C pH 7.6	
S. No.	Paddle	$A_r^3$ cm <sup>4</sup>	$\frac{A \times 100}{A_c} = P$	Paddle edge length cms	Theoretical S'	Theoretical 1-k	Theoretical GM	Flocculation Number F <sub>N</sub>	Settling velocity cm/min	Turbidity RESIDUAL p.p.m.	Width of blades Width of opening	Efficiency of turbidity removal		
1		1845	20 13.2	42	7.4	0.815	69.5	283	.3816	20	.25	82		
2		1845	39.6 26.1	64	7.35	0.798	67	379	.4572	17	.6491	85		
3		1845	39.2 25.9	84	9.45	0.764	64	570	.4826	16	.6485	85.5		
4		1845	50 33	185	10.32	0.746	61.5	1103	.635	10	1.00	91		
5		1841	52 34.3	234	12.5	0.686	57.5	1519	.762	7	1.082	94		
6		1815	73.3 48.5	54	13.3	0.666	51.5	600	.635	11	1.987	90		

Figure 28. Geometry of the paddles used by Patwardham and Mirajgaonkar (1970)

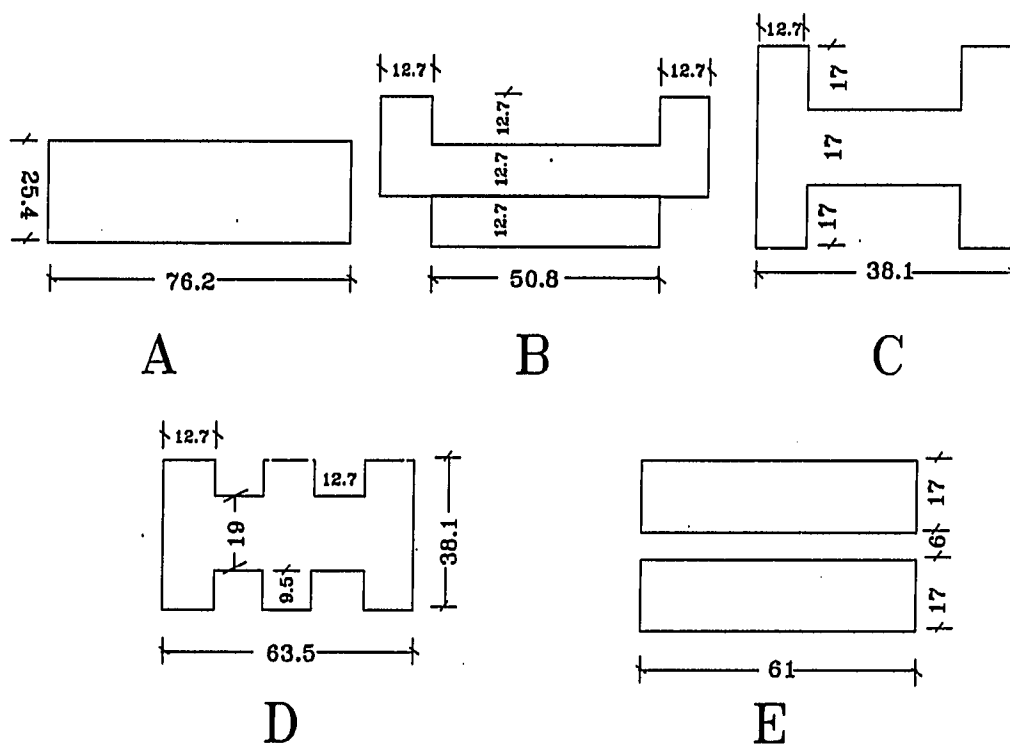


Figure 29. Geometry of paddles used by Bhole and Limaye (1977)

flocculating 25 to 100 mg/l of Fullers earth with 1 to 20 mg/l of alum at a pH of 7. This work may have been in either the sweep floc mode or in A/D mode, but it was probably in the A/D region. Again, the exact measure of flocculation efficiency was not stated. It appears that settled turbidity divided by initial turbidity was used as the measure of flocculation efficiency. Again, it was concluded that geometry had a significant impact. Shapes D and C from Figure 29 gave optimal removal.

Oldshue (1983) and Oldshue and Mady (1978, 1979) report on a plant scale comparison of an axial flow impeller and a dangling plate flocculator. This work was performed at 4 degrees Celsius. A low turbidity (8 NTU) lake water was flocculated with an unspecified amount of alum and caustic. The initial raw water pH was 5.1 to 5.4. It is assumed that the caustic was used to raise the pH and provide some alkalinity, but no information is given by the author with regard to these details. However, with an initial turbidity of 8 NTU it is likely that the flocculation was in the sweep floc mode. The author concluded that when compared to the dangling plate flocculator the axial flow impeller gave the same flocculation with less energy input.

Some preliminary comparisons were also made at a bench scale involving a rake, a Rushton impeller, and an axial flow impeller. In the bench scale portion of the work, 5 minutes of flocculation was

found sufficient for removal of color and turbidity. This short time requirement would indicate the sweep floc mode. Removal of turbidity and color were used as indicators of flocculation efficiency. The following conclusions were drawn. The axial flow impeller gave optimal flocculation at a lower energy. The rake performed as well as the axial flow, but the energy requirements were higher. The Rushton impeller was less energy efficient than either the axial flow impeller or the rake, and it did not flocculate as well as either of the other geometries at their respective optimum energy levels. It should be noted that data collected in this work was extremely sketchy, especially when one considers the sweeping conclusions drawn. In spite of this weakness, the data indicates a geometry effect.

Ives (1984), working in a 1 liter reactor, compared the 9 impeller geometries shown in Figure 30. A 16.7 mg/l kaolinite suspension was flocculated with  $\text{Al}_2(\text{SO}_4)_3 \cdot 16\text{H}_2\text{O}$  at an unspecified pH. Based on the information provided it is likely that the work was performed in the sweep floc mode. The author states that all of the impellers were tested under the same conditions. However, it is not clear what this means. It could mean constant G, constant  $\epsilon$ , or constant rpm. Under the circumstances it is assumed that the author meant constant G. Two measures of flocculation efficiency were used to evaluate the 9 impellers; settled turbidity and the filtration number. The settled turbidity was based on a sample drawn from 30 mm below the surface 10

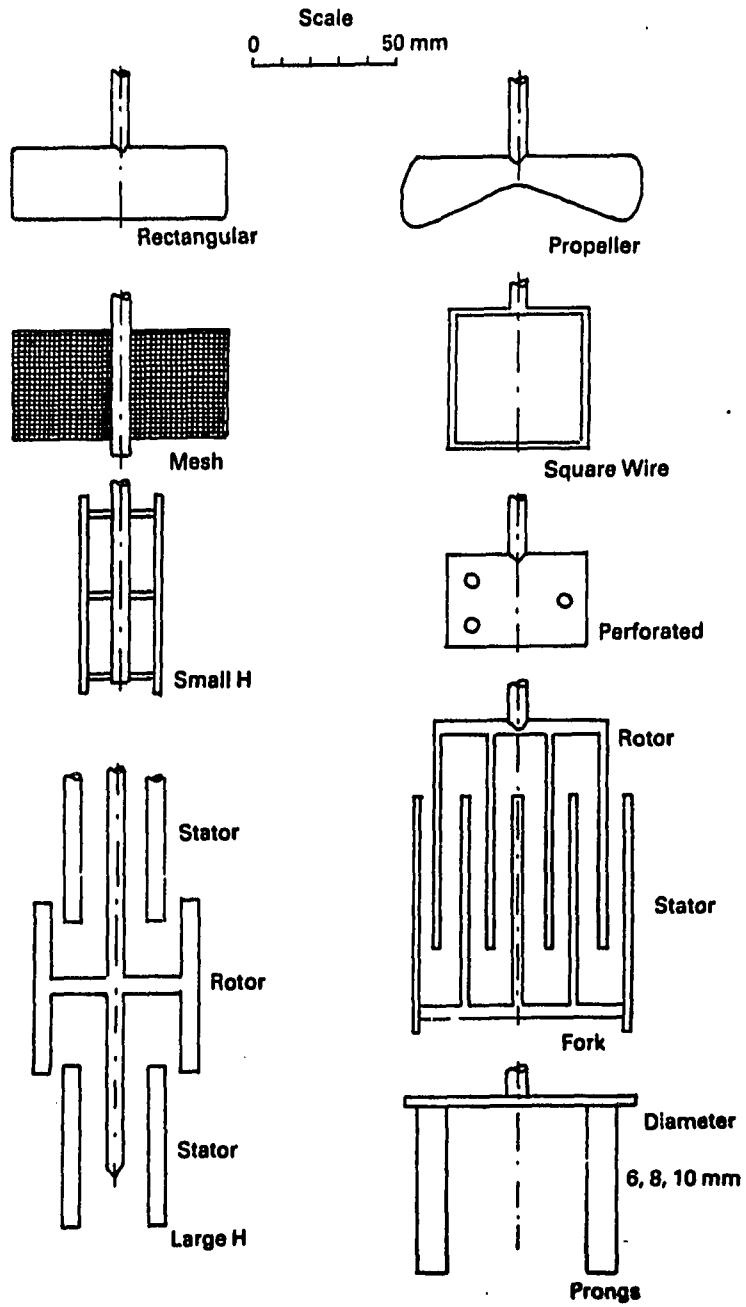


Figure 30. Geometry of paddles used by Ives (1984)

minutes after the paddle rotation had ceased. The filterability number is equal to:

$$F = \frac{H C_F}{V_a C_o t}$$

- H - headloss  
 V<sub>a</sub> - approach velocity  
 t - time  
 C<sub>o</sub> - inlet turbidity  
 C<sub>F</sub> - outlet turbidity

The lower the filterability number the better the performance. An optimum coagulant dosage was determined using each test parameter; settled turbidity, and filterability number. The 9 impellers were then compared using the optimum dosage for the parameter being used in measuring efficiency. Figures 31 and 32 show the results. There are a number of things to be noted in comparing the results:

- o The only impeller which showed a consistent performance, was the axial flow impeller (propeller). It was consistently bad.
- o There appear to be different geometry effects, but there are so many variables which are either unknown (coagulant dose, pH, ions in solution, mixing intensity), or changing at the same time that it is impossible to deduce why the impellers behave differently.

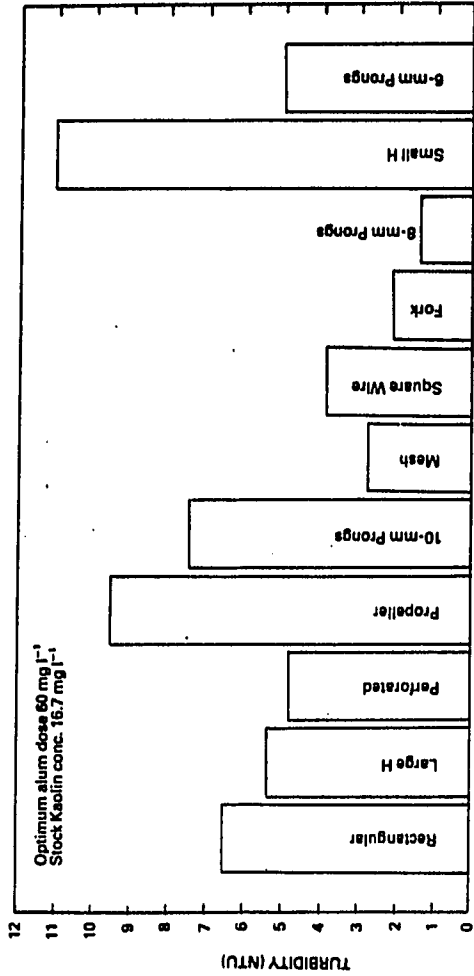


Figure 31. Turbidity after sedimentation for various paddle geometries

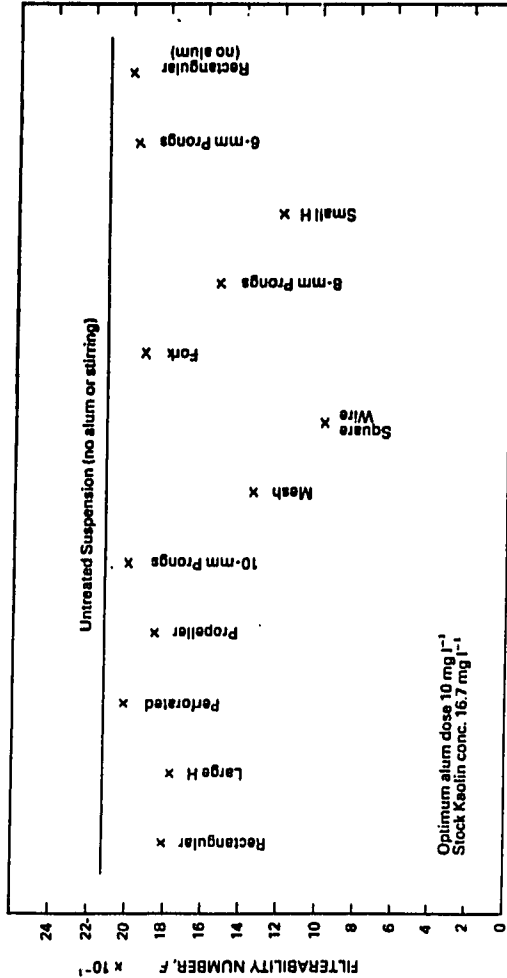


Figure 32. Filterability numbers for various paddle geometries

Ives concluded that, in the alum/clay/tap water system flocculated in a jar tester,  $G$  is not a sufficient criterion to choose among several impeller designs.

It is seen from the foregoing references that impeller geometry does affect flocculation. It is not clear at this point how the mode of flocculation, the flocculation efficiency measurement parameter, and the size of the particles present all interact in the selection of an optimal impeller geometry for a given system. We may speculate on this later based on the data collected in this study.

One last thing before we leave the general topic of turbulence. Let's look at  $G$ , the root-mean-square-velocity-gradient, and its usefulness, or lack of usefulness, in flocculation.

$G$  was developed in 1943 by Camp and Stein, to address a specific need. Engineers needed a means of quantifying the work which could be performed by a turbulent flow field. It is interesting that, in a practical sense, no one has yet proposed a usable parameter which is easily measurable, and does a better job than  $G$ . As a predictor of the work done by a turbulent flow field  $G$  is still a "good" parameter for design.  $G$  is used in sanitary engineering for many things including scale up of jar test results to full scale plant operation, estimation of optimal operating conditions in plant start-up, and as a means of correcting energy input into the flocculation process for



changes in water temperature.  $G$  is frequently seen in the following form:

$$G = \sqrt{\frac{P}{\mu V}} = \sqrt{\frac{\epsilon}{\nu}}$$

- P - power input
- V - unit volume
- $\mu$  - liquid viscosity.
- $\epsilon$  - energy input/unit mass of water
- $\nu$  - kinematic viscosity

$G$  has shown itself to be a useful tool. The real question here is not with regard to the usefulness of  $G$ . The real question is, what are the limitations of  $G$ . Is it a real measure of the physical situation in the reactor, or is it simply correlated to what is happening in the reactor. It is necessary to establish the limitations of  $G$  if we are to use it intelligently.

From Camp and Stein (1943), it is seen that the total work done by fluid shear per unit volume per unit time is equal to  $\epsilon$ .  $\epsilon$  can be expressed in terms of  $G$  using the following relationship:

$$\epsilon = \nu * G^2$$

- $G$  - absolute velocity gradient  
 $\nu$  - kinematic viscosity

This relationship is fundamentally sound, there are no major theoretical flaws in the development of the relationship between  $\epsilon$  and  $G$  at a point (vanishingly small unit volume) in the fluid flow. Unfortunately it is not convenient to measure  $G$  at a point. Camp and Stein (1943) proceeded from this point to develop a relationship between  $\epsilon_m$  and  $G_m$ .  $\epsilon_m$  is the mean value of the work input per unit mass of water per unit time, where  $\epsilon_m$  is calculated by dividing the total work input by the total mass of water in the reactor.  $G_m$  is the root mean square velocity gradient. It was in going from the relationship between  $G$  and  $\epsilon$  at a point, to the relationship in the entire reactor that Camp and Stein stretched their assumptions to the point of breaking them. They made a number of theoretical errors, as pointed out by Clark (1985b) and Saatci (1987). Fortunately, these errors, while academically interesting, appear to have little real bearing on the usefulness of  $G$  as a practical tool. The flaw which is of most concern, perhaps an unavoidable flaw, is the assumption that the velocity gradient throughout the vessel is homogeneous, which corresponds to an assumption the  $\epsilon$  is also homogeneous throughout the vessel. We have already seen in our discussion of turbulence that  $\epsilon$  varies significantly in a stirred tank, and that the small scale turbulence variations are important to localized

transport. A number of researchers have voiced concern over the non-homogeneity of  $\epsilon$ , and the effect this has on the usefulness of  $G$ .

Patwardham and Mirajgaonkar (1970) concluded that  $G_m$  is inadequate for deciding upon the best flow pattern to achieve effective flocculation, and that  $G_m$  needed to be supplemented by other suitable design criteria. He went on to suggest that the impeller which provided the highest pumping rate for the same  $G_m$  seemed to be more beneficial. From this point on, unless stated otherwise,  $G$  will refer to  $G_m$ .

Argaman and Kaufman (1968) noted that the performance differences they observed in comparing two paddle types was sufficient evidence that  $G$  alone was not adequate for characterizing the flow field. The theory they developed identified  $u^2$  and its spectrum as the only energy parameters directly effecting the flocculation process.

Oldshue and Mady (1979) state that the  $G$  factor is inadequate, because the shear rate distribution in the tank is not constant from impeller geometry to impeller geometry, at the same  $G$  value. The  $G$  factor in Oldshue's opinion "is too simplistic to be the single correlating parameter over a wide variety of mixing variables".

There have been a number of papers in the past eight years suggesting alternatives to  $G$ . Cleasby (1984), Clark (1985b), and Glasgow and

Kim (1986) all voiced specific criticisms of  $G$ . Cleasby (1984) suggested the use of  $\epsilon^{2/3}$  as a more appropriate energy parameter. It is suggested, however, that this quantity will be subject to the same spatial variation problems which plague  $G$ . Clark (1985b) and Glasgow and Kim (1986) suggest that the flow field variability might be overcome by compartmentalizing the reactor, and this has in fact been done (Koh, 1984). Compartmentalizing the reactor implies a need to know the detailed flow field in the mixed vessel. Some researchers such as Glasgow (1985) feel quite strongly about this matter:

"The inhomogeneity of turbulence in stirred baffled tanks and flocculation basins renders the velocity gradient,  $G$ , meaningless. It should be mandatory that all research in flocculation incorporate measurement of the spatial variation of the dissipation rate as part of the experimental plan"

Glasgow, probably goes too far here, since, although it has been shown that impeller geometry effects are measurable, it has not been shown that they are an overriding practical concern.

This brings us back to a comment made some pages ago.  $G$  is a useful tool, but we must realize its limitations. From a design and operations point of view there is nothing available which can replace  $G$  at this time. From a research point of view, we must be careful not to expect more of  $G$  than it has to offer. Any modelling or data interpretation based solely on  $G$  will have built into it all of the errors inherent in the parameter  $G$  because of the spatial variation of  $\epsilon$  in the reactor.

### Coagulants

So far we have considered the following major aspects of the flocculating system:

- o the liquid phase (water),
- o the solid phase (kaolinite primary particles),
- o the attractive-repulsive forces effecting particle-particle interactions in a liquid medium,
- o the particle transport mechanism in the liquid (turbulence).

In this section we will consider the last major component of this system which needs to be discussed, the coagulants which destabilize the particles.

A coagulant is a substance which is added to a colloidal suspension to cause or enhance the destabilization of the particles in the suspension, so that the particles may be flocculated. There are two major classes of primary coagulants being used in the water treatment industry: metal salts, and organic polymers.

The metal salts, particularly aluminum sulfate (alum), are the most commonly used coagulants (Sricharoenchaikit and Letterman, 1987). Synthetic organic cationic polymers are gaining popularity, and will very likely continue to do so as we come to understand them better.

In the following pages the two classes of coagulants will be considered individually, first the metal salts and then the polymers.

### Metal coagulants

Metal coagulants are available in a number of chemical forms, all of which are salts of aluminum or iron. The following are the metal coagulants in common use:

- o aluminum sulfate or alum ( $\text{Al}_2(\text{SO}_4)_3 \cdot \text{NH}_2\text{O}$ )
- o polyaluminum chloride ( $\text{Al}(\text{OH})_x\text{Cl}_y$ )
- o ferric sulfate ( $\text{Fe}_2(\text{SO}_4)_3$ )
- o ferrous sulfate ( $\text{FeSO}_4$ )
- o ferric chloride ( $\text{FeCl}_3$ )

Most of the discussion will be centered around alum, since the majority of the work in this project was performed using alum. Ferric sulfate was used for a lesser portion of the work, and it will also be discussed.

It is interesting to note that many researchers, in discussing metal salts, deal with aluminum and iron salts simultaneously, because their chemistry is similar. This format will be also followed here, but along with the similarities there are some distinct differences. These differences are, perhaps, very important, and an effort will be made to highlight the differences. The general mechanism of particle

destabilization are the same for both metals. However, because of differences in solution speciation, electron structure, and time scales in reaction kinetics, the two types of salts may respond differently to temperature changes.

Figures 33 and 34 represent turbidity coagulation diagrams for aluminum and iron respectively (Amirtharajah, 1984; and Johnson and Amirtharajah, 1983). The basic coagulation diagram is simply a solubility diagram for the particular metal system. Super-imposed on the solubility diagram are empirically determined regions of flocculation. We will discuss these figures in detail a little later, but they are presented at this point so the reader has an overall mental picture of the relationship between metal salt chemistry and flocculation. Before we discuss the details of Figures 33 and 34, it is important to consider the nature of the coagulant. The character of the coagulants and the changes that take place will be discussed starting from the coagulant in the stock solution tank, and following it through until it precipitates and/or adsorbs on the particle surface.

Figures 35, 36, and 37 (O'Melia, 1978) are speciation curves for the metal salts and water in equilibrium. Figure 35 represents aluminum sulfate, and Figure 36 and 37 represent ferric chloride, and ferric sulfate. The percent of metal speciation is read on the left vertical axis, and the pH is read on the right vertical axis. There

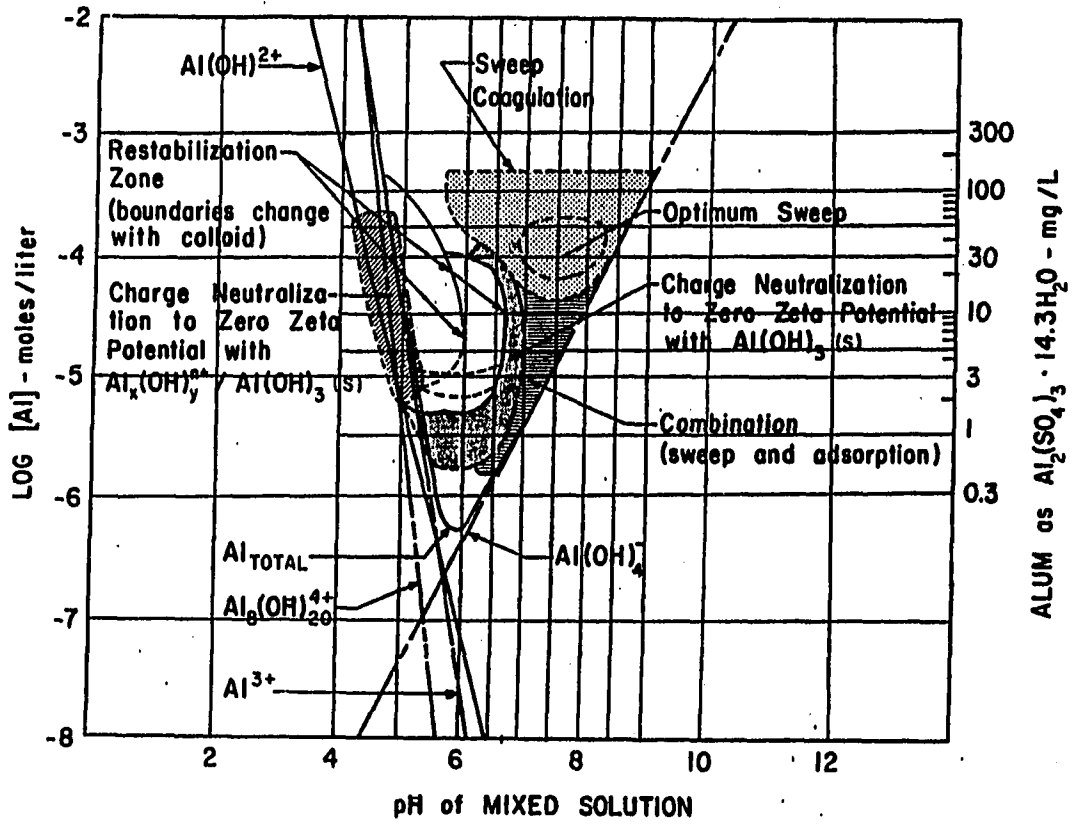


Figure 33. The alum coagulation diagram for turbidity removal



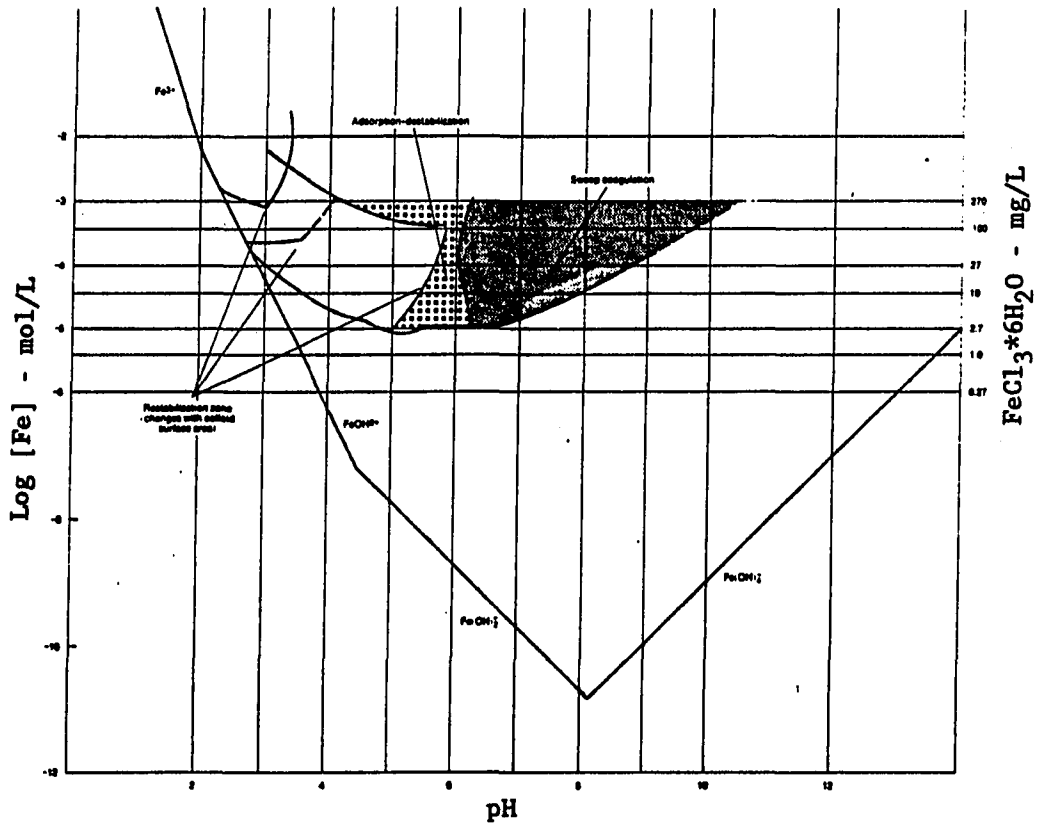


Figure 34. The ferric chloride coagulation diagram for turbidity removal

are two important features to note on these two figures. First the metal speciation is very sensitive to the concentration of the stock solution. Second the speciation for the aluminum sulfate is quite different from the speciation for the ferric sulfate. O'Melia notes that the stock solution of 1 mg/mL is commonly used in laboratory jar testing, and corresponds to a  $pAl_T$  of 2.52, and a  $pFe(III)_T$  of 2.31. This concentration will be used to contrast some of the speciation differences between these two metals. For the alum the  $pAl_T$  of 2.52 corresponds to the peak of the  $Al(H_2O)_6^{+3}$  curve, and the  $Al(H_2O)_6^{+3}$  represents 75 percent of the aluminum species. If the concentration is increased the sulfato complexes increase, and if the concentration is decreased the hydroxo complexes increase. At the same metal concentration, less than 2 percent of the Fe(III) present, is present as the free aquometal ions  $[Fe(H_2O)_6^{+3}]$ . Table 7 compares the speciation of the three coagulants when the concentration is 1 mg/mL. The information in Table 7 is taken from Figures 35, 36, and 37.

O'Melia (1978) in discussing the iron salts presented in Table 7 notes that, it is plausible that identical concentrations of iron stock solutions may produce different destabilizing species. It appears that this is even more likely when comparing the aluminum with the iron.

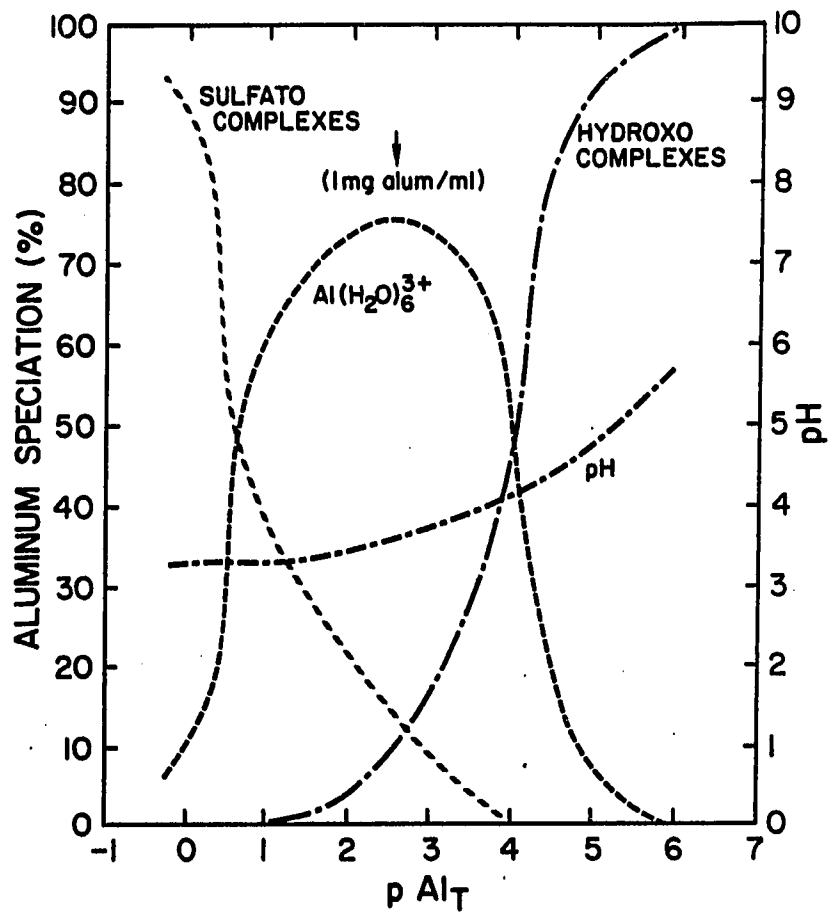


Figure 35. Species composition of aluminum sulfate solutions

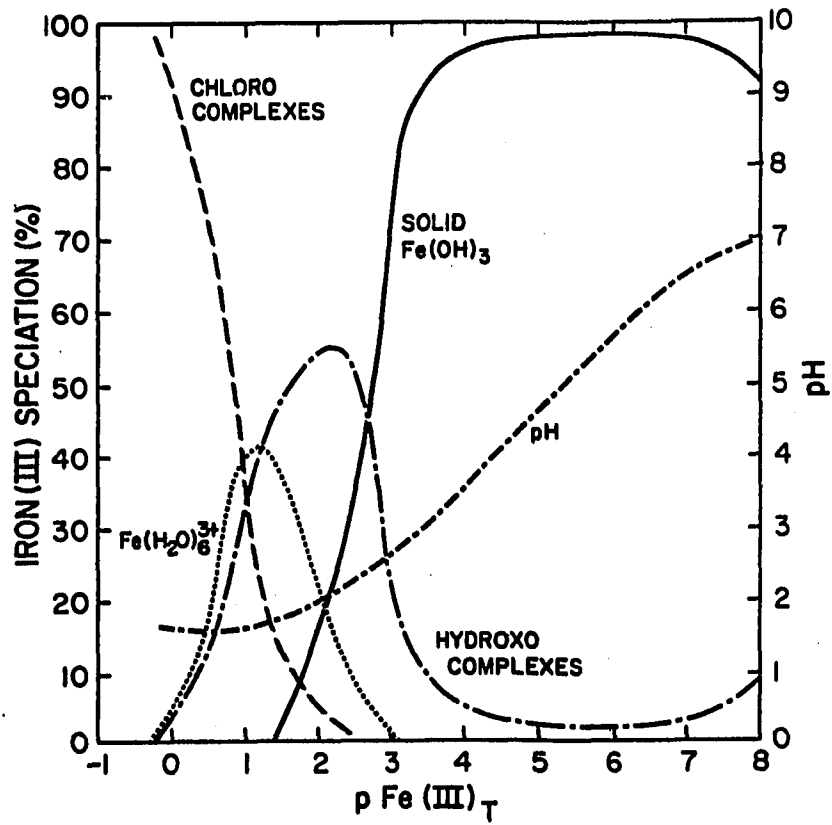


Figure 36. Species composition of ferric chloride solutions

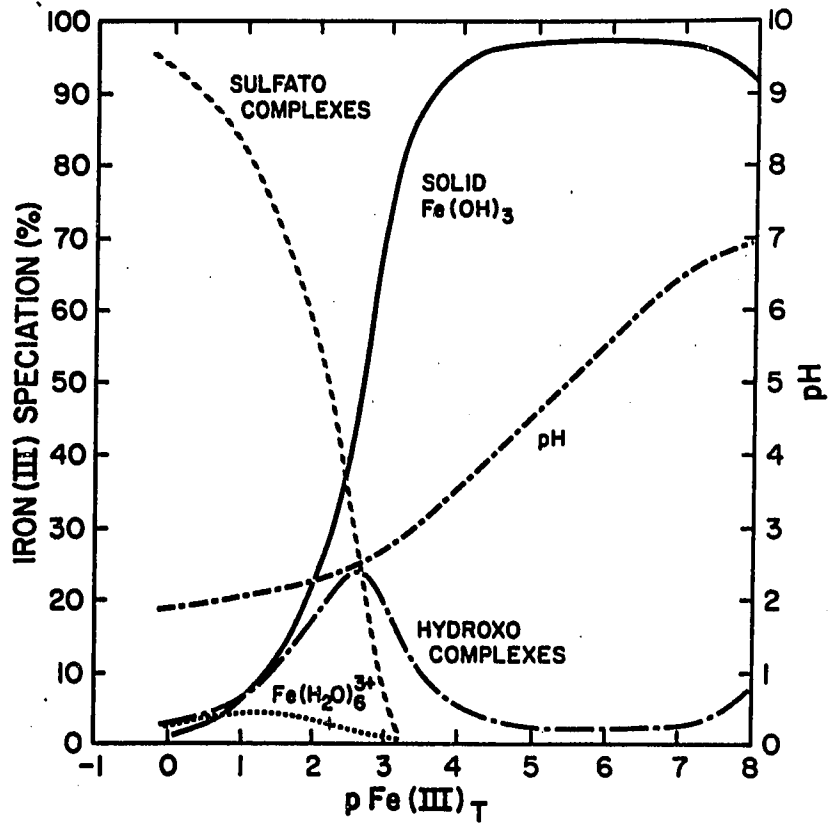


Figure 37. Species composition of ferric sulfate solutions

Table 7. Speciation comparison for 1 mg/mL Fe and Al solutions, based on percent of total

Coagulant	$\text{Al}_2(\text{SO}_4)_3$	$\text{Fe}_2(\text{SO}_4)_3$	$\text{FeCl}_3$
Species	percent of total present		
Free aqua metal ion $\text{M}(\text{H}_2\text{O})_6^{+3}$	85	2	18
Sulfato Complexes or Chloro Complexes	16	47	3
Hydroxo Complexes	9	21	56
Solid $\text{M}(\text{OH})_3$	-----	30	23

The speciation of the metal salts in solution is not only concentration dependent, it is also pH dependent. Figure 38 and 39 (Baes and Mesmer, 1976) demonstrate the complexity of the metal speciation with regard to both concentration and pH. The dashed lines in the figure represent the percent of metal present as a specific species. The number label in the lines (x,y) indicates the number of aluminum atoms in the species (x), and the number of hydroxides present in the species (y). Similar information on the pH dependence of aluminum speciation is shown in Figure 40 (Hayden and Rubin, 1974). The examples presented in these figures have been calculated and are based on an assumption of equilibrium in pure water. These figures are probably not too unrealistic. Weber and Stumm (1963) note that under the conditions normally found in

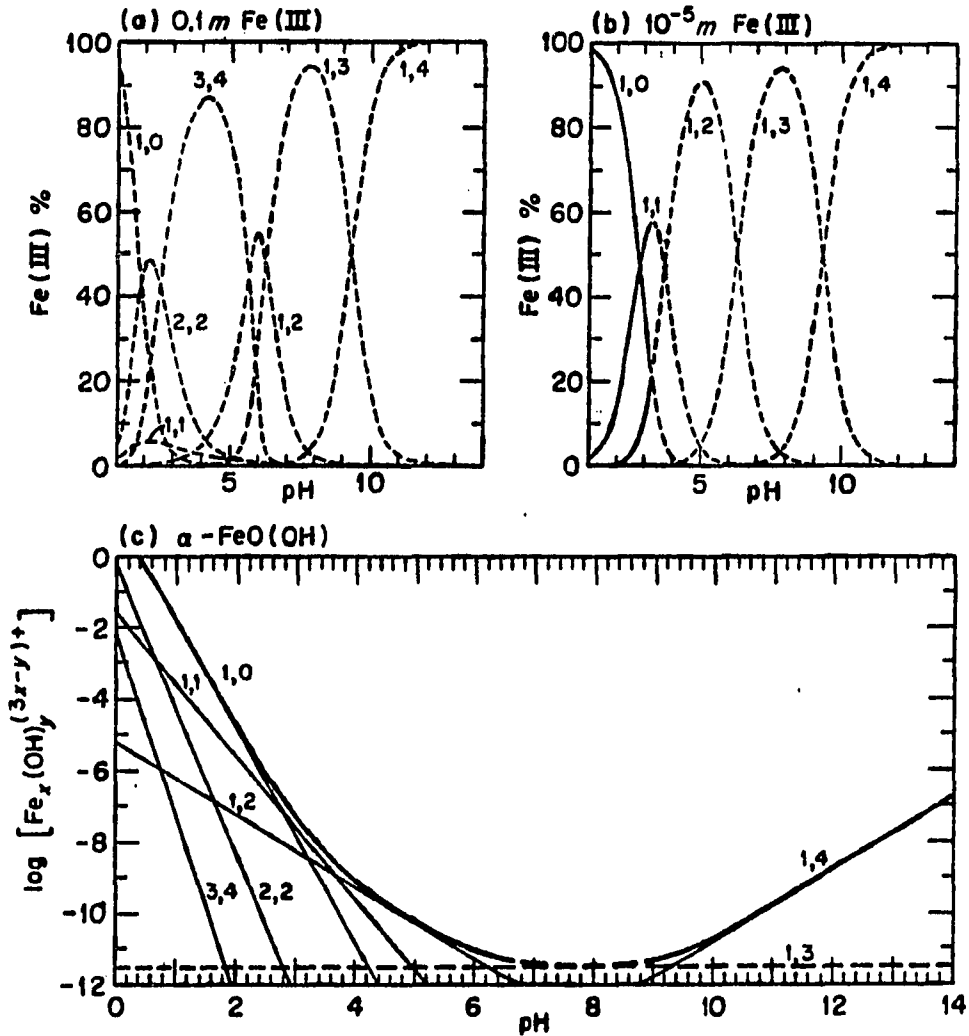


Figure 38. Distribution of hydrolysis products (x,y) at  $I = 1$  m and  $25^\circ\text{C}$  in (a)  $0.1$  m Fe(III), (b)  $10^{-5}$  m Fe(III), and (c) solutions saturated with  $\alpha$ -FeO(OH). The dashed curves in (a) and (b) denote regions supersaturated with respect to  $\alpha$ -FeO(OH); the heavy curve in c is total concentration of Fe(III)

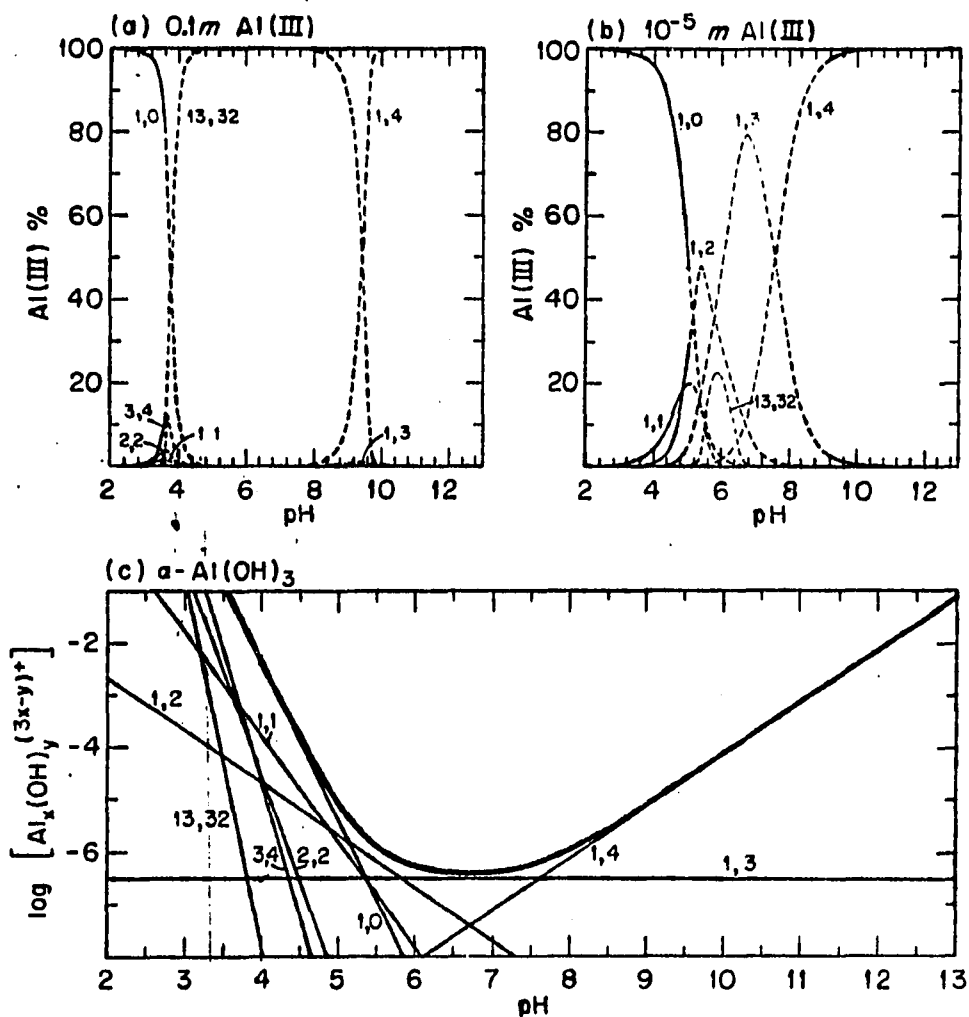


Figure 39. Distribution of hydrolysis products  $(x,y)$  at  $I = 1$  m and  $25^\circ\text{C}$  in (a)  $0.1$  m Al(III), (b)  $10^{-5}$  m Al(III), and (c) solutions saturated with  $\alpha\text{-Al(OH)}_3$ . The dashed curves in (a) and (b) denote regions supersaturated with respect to  $\alpha\text{-Al(OH)}_3$ ; the heavy curve in c is total concentration of Al(III)



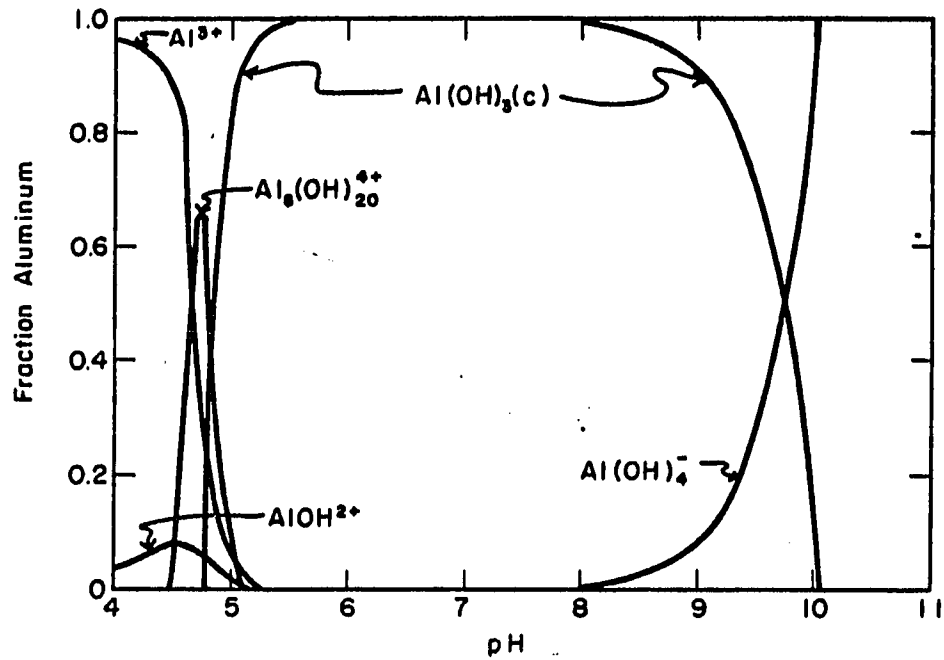


Figure 40. Distribution of  $5.0 \times 10^{-4}$  M hydrolyzed aluminum(III) as a function of pH

most natural waters, the solubility of Fe (III) and Al (III) are controlled by the solubility products of the corresponding hydroxides.

Most alum stock solutions will be fairly concentrated and have a pH between three and four. Consider Figure 39 (part a) which represents an aluminum concentration equal to 59.4 g/l as alum (with a molecular weight of 594 g/mole). From Figure 35, the equilibrium pH under these conditions would be about 3.3. This is the pH in the coagulant. The coagulant will be injected into the suspension to be coagulated, rapid mixed for a relatively short time (0.5-5 minutes), and then slow mixed or flocculated for a longer period of time (10-45 minutes). If a relatively high dosage of coagulant is injected, the final equilibrium speciation in the rapid mix tank may look similar to that shown in Figure 40, which represents an alum dosage of 294 mg/l. If the dosage is low the final speciation may be similar to the speciation shown in Figure 39 (part b), which represents 5.94 mg/l as alum (with a molecular weight of 594 g/mole). Describing these as the final equilibrium speciation assumes of course that equilibrium occurs before any of the material is adsorbed out of the system by the solids present. As the coagulant is injected into the suspension to be destabilized, the chemical speciation will be undergoing changes as it responds to the altering of both its pH and concentration. The rate at which the coagulant comes to its new equilibrium state and the rate at which the material

is adsorbed out of solution at the solid/liquid interfaces are obviously going to be interconnected. At this point we will ignore the adsorption time scales and only consider the equilibrium chemistry, but later we will return to the effect of adsorption rate versus precipitation rate.

Aqueous metal species in general are associated with water and in order for the metal to interact with another chemical species, the reactive species must penetrate the water sheath associated with the metal molecule. This is an area where the chemistry of aluminum and iron are quite different. Iron (III) is a d-block element. Aluminum, on the other hand, is an sp-block element. As a result, their electron structure is quite different, causing iron to undergo associative solvent exchange, while aluminum undergoes dissociative solvent exchange. That is, the iron (III) is capable of temporarily associating with an additional molecule, while the water molecule which is leaving finds its way out. Aluminum (III) is not capable of this, and as a result the water being displaced must leave before the aluminum (III) can interact with another molecule. The result of this is illustrated in Figure 41 (Burgess, 1988). We see from the right hand axis that the mean residence time for a water molecule in the primary hydration shell for iron (III) is in the  $\mu$ sec range, while for aluminum (III) it is in the sec range. Based on these time scales it appears reasonable that the iron (III) will come to equilibrium much quicker than aluminum (III).

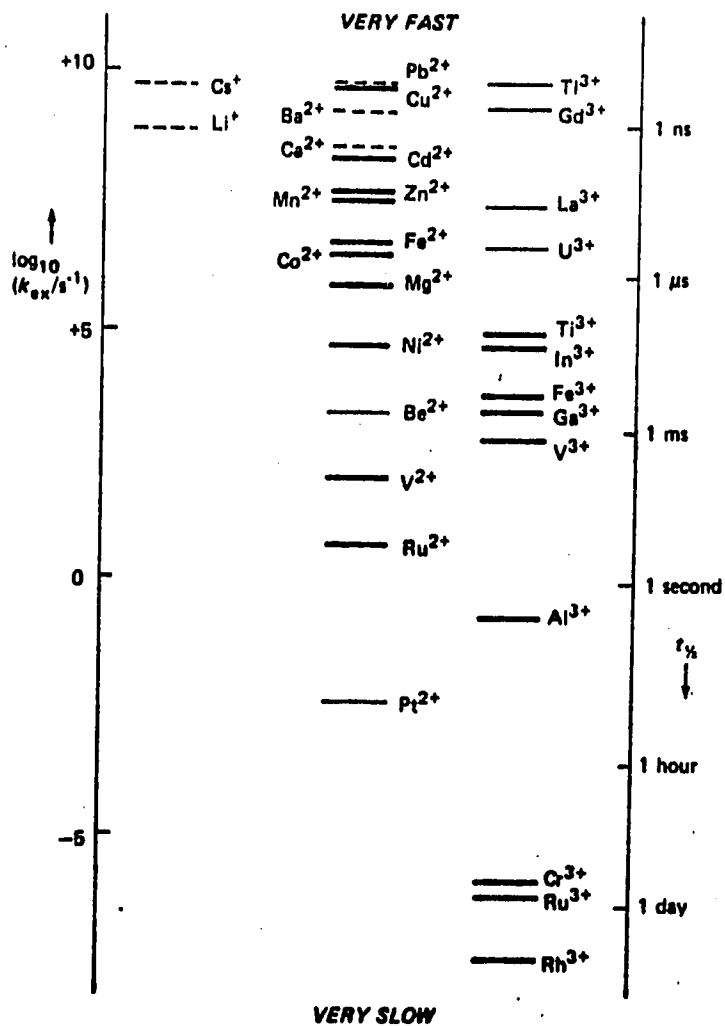


Figure 41. Rate constants for water exchange, and mean residence times for water molecules in primary hydration shells, for 2+ and 3+ metal ions, at 298 °K. Octahedral species are indicated by thick lines, non-octahedral species by thin lines. Dashed lines denote estimates arrived from rate constants for complex formation

Another characteristic of metal salt solutions which must be considered in diluting a stock solution is the effect of aging on speciation. Hong-Xiao (1987a), Stumm and Morgan (1962), and Johnson and Amithirajah (1983) note the aging effect on iron solutions. Hayden and Rubin (1974), Stumm and Morgan (1962), Matijevic and Tezak (1953), John Gregory (1978), Sullivan and Singly (1968) all discuss aging in alum solutions. Matijevic and Tezak (1953), and Sullivan and Singly (1968) both state that aging effects are more pronounced in solutions of lower concentration. If the concentration is high enough the pH will be lowered so that only the free aqua-metal ions are in existence. Thus, aging is mainly a concern in the more dilute solutions which will be used directly to dose the colloidal suspension. From Hayden's work (1974), the changes in the aluminum speciation occur rapidly for the first hour, and after 24 hours the change is gradual. From this one would conclude that it may be easier to obtain consistent results if the dilute stock solution is aged a few hours.

In the next few paragraphs we will return to Figures 33 and 34, and explore the coagulation diagrams. It is hoped that this discussion will illustrate the utility of these diagrams in understanding the flocculation process, i.e., how the system will react at different coagulant dosages and pH conditions. Two examples will be presented with the intent of demonstrating:

- o the complexity of the metal salt system, and
- o the difference between the adsorption/destabilization and sweep floc mechanism, and
- o the importance of coagulant precipitation kinetics in determining the flocculation mode, and thus, the potential importance of temperature.

For the sake of simplicity only alum will be considered, and the speciation presented in Figure 40 will be assumed to apply. The first example will be a high dose of alum (30 mg/l as alum). This is an optimal sweep floc dosage. The second example will be a low dosage (5 mg/l as alum), typical of A/D flocculation.

Recall the following information from Figure 40. In the stock alum solution the pH is less than four, so all of the aluminum is in the  $Al^{+3}(H_2O)_6$  state. It is only after the coagulant is injected into the raw water that the pH is raised and the species present start to change. There is only a narrow range, between pH of 4.5 to 5.2, where the complex aluminum polymers exist. From pH of 5.2 to 9 the aluminum species exist predominately as  $Al(OH)_3$  precipitate (Hayden, 1974).

Now let's consider what happens in Figure 33 if a dose of 30 mg/l is selected, and the pH is changed over a range of 4 to 9. Remember, these conditions represent the final coagulant concentration and pH in the reactor. As we start at a pH of 4 we are outside the

precipitation boundary in a region where all of the aluminum exists in a soluble  $Al^{+3}$  state. At a pH of 4.5 two things happen:

- o the solubility limit is reached,
- o the soluble species are dominated by the hydrolyzed polymeric aluminum species  $(Al_xOH_y)^{+n}$ ;  $(Al_8(OH)_{20})^{+4}$ , as seen in Figure 40)

The hydrolyzed polymeric species actually becomes the dominant species just prior to precipitation, and are only present in appreciable amounts over a narrow pH range (Hayden and Rubin, 1974). The narrow pH range in which these polymeric species dominate, appears to coincide with the first charge neutralization range in Figure 33. Small hydroxy complexes are reasonably soluble and easily adsorbed on to the colloid particles, making these complexes extremely effective coagulants (Eilbeck and Mattock, 1987).

As we continue across the diagram to a pH of 5, the hydrolyzed polymeric species disappear, and are replaced by  $Al(OH)_3$  as the dominant species. This is the restabilization range. The surface charge of the solid  $Al(OH)_3$  is pH dependent (Stumm and Morgan, 1981). At a low pH it is very positive, and as the pH increases the, the charge decreases. At the zero point of charge (ZPC), or the iso-electric point, the surface charge of the aluminum hydroxide precipitate is zero. Table 8 list representative values for the ZPC for the  $Al(OH)_3$  and  $Fe(OH)_3$  systems.

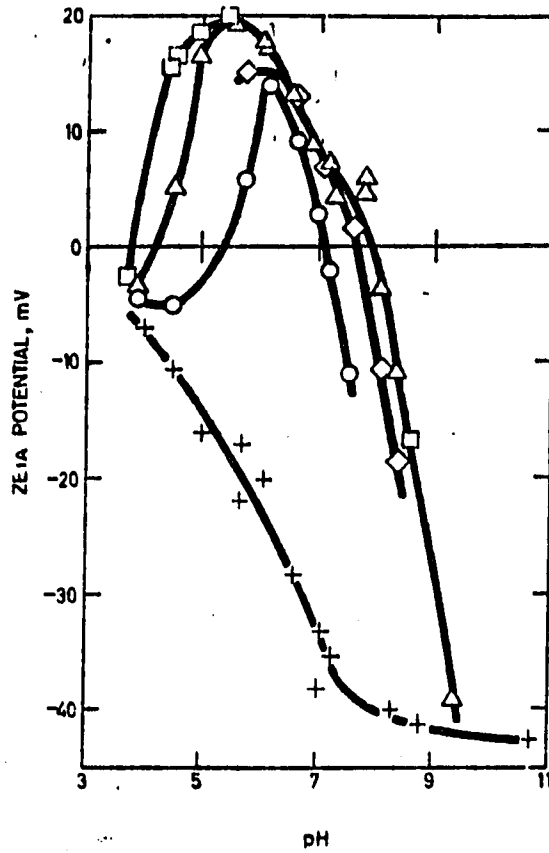
Table 8. Typical pH values resulting in the zero point of charge (ZPC) for hydroxide precipitates

Aluminum Hydroxide	Ferric Hydroxide	Source
	6.7	Stumm and Morgan, 1962
	8.0	O'Melia, 1978
	6.8	Hong-Xiao and Stumm, 1987a
7.0		Hayden and Rubin, 1974
9.0		Letterman and Vanderbrook, 1983
8.0		Amitharajah, 1984
8.0		Hall, 1965

In the restabilization area the surface charge on the precipitate is so high that the particles with adsorbed precipitate experience charge reversal, and become positively charged. It is noted that if the primary particle concentration is high enough, the restabilization zone may disappear entirely, because there will not be enough precipitate to reverse the original surface charge.

As the pH is raised the surface charge of the aluminum precipitate becomes lower and lower, and somewhere near pH of 6.0, the typical water is once more destabilized and will coagulate. Figure 42 (Hall, 1965) and Figure 43 (Hong-Xia and Stumm, 1987a) illustrate the zeta potential-pH relationship for alum and iron respectively. Figure 44 (Trace Inorganic Substances Committee, 1988) shows the anion adsorbtion-pH relationship for aluminum hydroxide and iron hydroxide.





(Concentration as  $10^{-4}M-Al$ )

+ nil. ○ 0.15 ◇ 0.60 △ 1.50 □ 6.0

Figure 42. Zeta potential of kaolinite in aluminum sulphate solutions

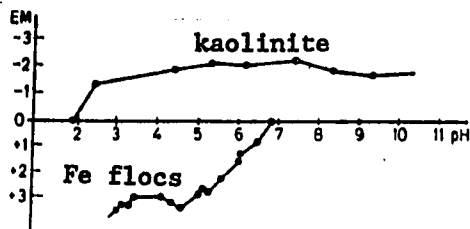


Figure 43. Microelectrophoresis mobility of kaolinite and Fe flocs

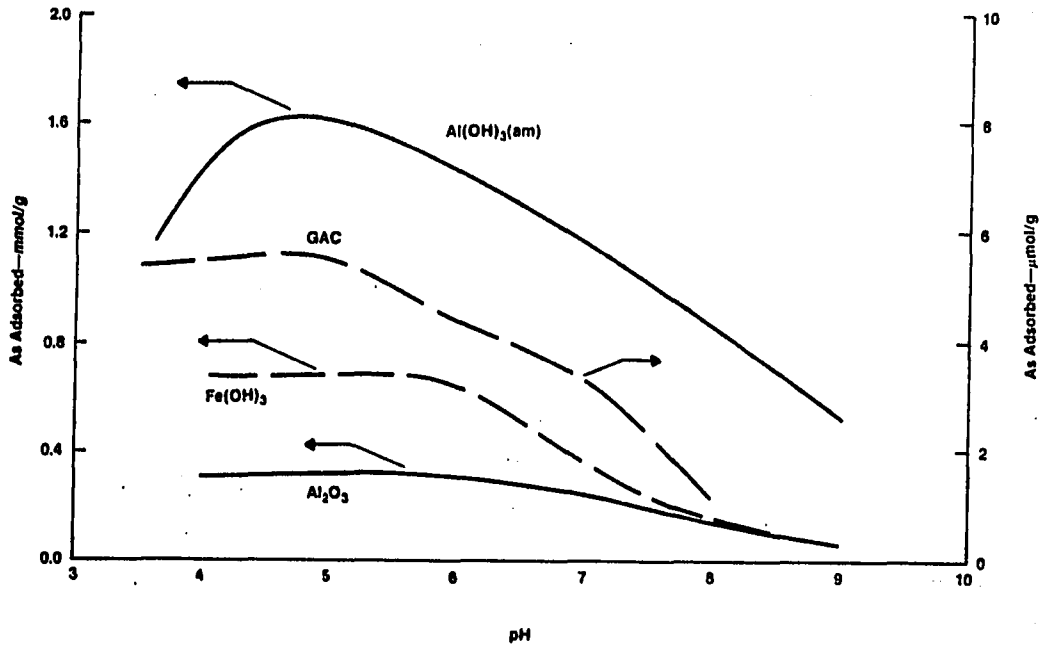
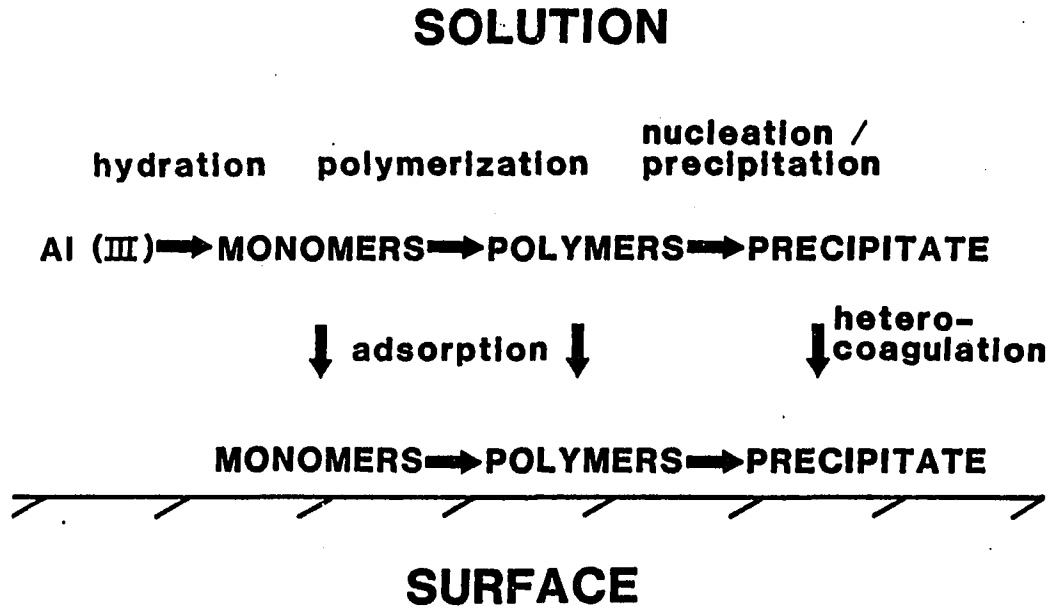


Figure 44. Adsorption fronts for arsenic(V) on four adsorbents (the decreasing extent of adsorption with increasing pH is typical for the removal of anions)

Again, note how sensitive the surface chemistry of these hydroxide precipitates is to shifts in pH. At a pH of 6.5 the adsorption/destabilization mechanism ceases to dominate the flocculation and sweep floc becomes the dominant mechanism. In sweep floc large quantities of aluminum hydroxide precipitate are formed. These precipitates sweep up the primary particles as they move through the water.

Interaction between the two mechanisms and the metal salts is shown schematically in Figure 45 (Dentel, 1987). Insight into this shift from one mechanism to another can be gained by considering the time scales involved in the various process steps (See Table 9, page 123), and the change in surface charge with pH.

When the pH is low enough so that adsorption followed by precipitation on the surface is favored, there will not be sufficient aluminum in solution to form the large quantities of precipitate needed for sweep floc to occur. However, as the adsorption step becomes less and less favorable, the soluble aluminum is in solution long enough for the sweep floc to form. Sweep floc dominates from pH of 6.5 to 8.4. At a pH of 8.4 the hydroxide species once more become more soluble.



**Figure 45.** Schematic representation of the various pathways followed by aluminum hydroxide species in solution or at a surface in contact with the solution

Table 9. Reaction type versus time scale (Amirtharajah, 1987)

Reaction	Time Scale (seconds)
Al (III) monomer adsorption	< 0.1
Al (III) polymer formation and adsorption	0.1 to 1
Formation of sweep floc aluminum hydroxide precipitate	1 to 7

Once again consider Figure 33, and assume a coagulant dose of 5 mg/l as alum. This is 1/6th of the dose discussed on the prior pages, and we will see a few changes. The first change evident in Figure 33 at the lower coagulant dose is that all of the regions previously mentioned shift to the right. The other significant difference is the disappearance of the sweep floc region. With the low dose of alum the A/D mechanism will be effective, but there is not enough aluminum added to the system to form a good sweep floc even if the pH is favorable.

Similar reasoning can be applied to the iron (III) system shown in Figure 34 (Johnson and Amirtharajah, 1984). There is evidence in the literature that sweep floc formed with iron (III) is denser and perhaps stronger than the floc formed with aluminum (III) (Morris, 1983; Dann, 1988).

The chemical makeup of the dilution water in which colloidal solids are suspended can also have a significant impact on the effectiveness of the metal salt coagulant. Letterman and Vanderbrook (1983) showed rather dramatically the importance of pH in the flocculation process, by flocculating a colloid suspension at a pH of 6 and 8 with alum. At pH = 8, the aluminum concentration required for charge neutralization was almost 10x greater than the concentration needed at a pH = 6.

Because the pH of the system is important it is desirable to work with a buffered system in flocculation research. Certain ions in solution either enhance or inhibit flocculation, thus it is important that a buffer be selected which does not inhibit flocculation.

An example will demonstrate the importance of the buffer. If Ames, Iowa tap water is allowed to sit overnight in an open beaker the final pH will be approximately 8.0. If 15 mg/l of alum is added to the unbuffered tap water, the pH will drop to 6.7. From Figure 33 we see this pH shift is enough to move from the sweep floc region to the A/D region. If one intends to work in the A/D region, it is obviously best to control the system so that the entire experiment takes place in that region. From Figure 33, one can see that the A/D region is very close to a pH of 7. This immediately suggests the carbonate system as the buffer of choice since its buffer intensity

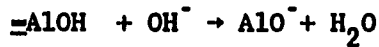
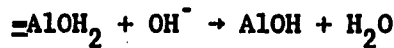
shows a peak between pH 5 to 8. Work by Miller (1925) and Letterman et al. (1979) indicate that adding a carbonate buffer to the system will not only stabilize the pH, but will broaden the window for good flocculation. In addition, Letterman et al. (1979), in reporting a frequency distribution for anions in natural waters, lists the carbonate concentration of an average water as 200 mg/l. This makes the carbonate buffer particularly attractive since it tends to mimic many commonly found natural waters.

The one other multivalent anion which is present in significant quantities in the water used in this study is sulfate. In general, when the concentration of sulfate in the system is low, the pH and aluminum concentration which yield charge neutralization are narrow. The effect of the sulfate anion appears to be similar to the effect of the carbonate anion, but the enhancement is more pronounced. The effects of the sulfate anion have been documented by many researchers (Miller, 1925; Letterman et al., 1983 and 1979; Packham, 1965; Hayden and Rubin, 1974; Sricharoenchaikit and Letterman, 1987; Dentel and Gossett, 1988; Hahn and Stumm, 1968a and 1968b; and Snodgrass, Clark and O'Melia, 1982). This work has uniformly indicated that the presence of the sulfate ion broadens the pH range and coagulant dose over which the A/D mechanism is effective. The work by Letterman et al. (1983) indicated that the sulfate concentration had two effects. First, it widened the window of optimal coagulation, and improved the residual turbidity which was achievable. Second, the increased

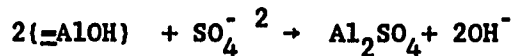
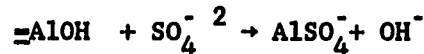
sulfate stabilized the electrophoretic mobility at very close to zero after the zero point of charge had been reached.

It is noted that the anion effect is likely to be unimportant in the sweep floc region, since we are dealing with the enmeshment of the primary particles in precipitate. Letterman et al. (1982) confirms this by stating that the critical anion concentration becomes negligible, and the restabilization region disappears above a pH of 7.5. In the pH range between 4.5 and 7.5 the anion concentration appears to have a significant impact on the efficiency of alum as a coagulant. It is in the region where charge reversal is most likely that the anion effect is most noticeable.

Letterman et al. (1982) explain the action of the anion effect based on modification of the hydroxide precipitate attached to the particles surface sites. The sulfate complexes with the aluminum hydroxide and reduces the charge on the hydroxide. The following equations have been suggested for this process:



and





The three parallel bars to the left of the Al atoms indicate a bond with a surface site. It is seen from these reactions that increasing the pH, or the sulfate concentration, increases the number of neutral and negative surface groups, which decreases the charge on the aluminum hydroxide surface. Keep this pH effect in mind, because it will come up again when we discuss temperature effects. Either low pH values or small amounts of adsorbable anion (sulfate) favors highly positive precipitate. This makes the precipitate very effective at neutralizing the negative charge on the clay, but also increases the possibility of restabilizing the suspension if overdosed.

It is unfortunate that the literature cited earlier for the bicarbonate anion, did not contain any electrophoretic mobility versus alum dose information. Without this information it is difficult to draw any conclusion with regard to the similarity between the mechanism in the sulfate system and the mechanism in the carbonate system. Letterman et al. (1982) does give information on the nitrate anion, and it appears to behave as the sulfate anion does, although it is less effective by a factor of 1000 on a molar basis. Letterman notes that the nitrate ion, in addition to having a lower charge, seems to have a lower affinity for the hydroxide precipitate. It seems reasonable that the same may be true of the bicarbonate anion. Letterman et al. (1979) states that the bicarbonate anion has 6 times the impact on turbidity removal that

nitrate does. This may indicate that the bicarbonate has a lower affinity for the hydroxide than the sulfate, but a higher affinity than the nitrate. He also notes that the effects of the sulfate and bicarbonate are not additive.

There has been limited work in which the investigators have dealt specifically with the impact of temperature on the flocculation process. The work which has been done using metal salts will be discussed here.

Liepold (1934) used alum, at pH of 8, to flocculate Lake Michigan water with turbidities in the range of 12 to 20 Jackson Turbidity Units (JTU). He used an alum dose of 17 mg/l at temperatures of 2.2, 7.2, 12.8, 18.3, and 24 °C. Leipold noted "No preventative or retarding effect on alum floc formation in 30 minutes of mixing". At the high temperature condition, the flocculation conditions reported here will be in the optimal sweep floc range. Assume the flocculation regions remain fixed relative to the boundaries of the solubility diagram, and that the diagram shifts with temperature as shown in Figure 46 (Dempsey, 1987). Based on these assumptions the flocculation at pH of 8 and 17 mg/l of alum will still be in sweep floc at a temperature of 2.2 °C.

Velze (1934) worked with alum coagulating a natural colored water in Northeastern New Jersey. The water contained 34-38 ppm color. The

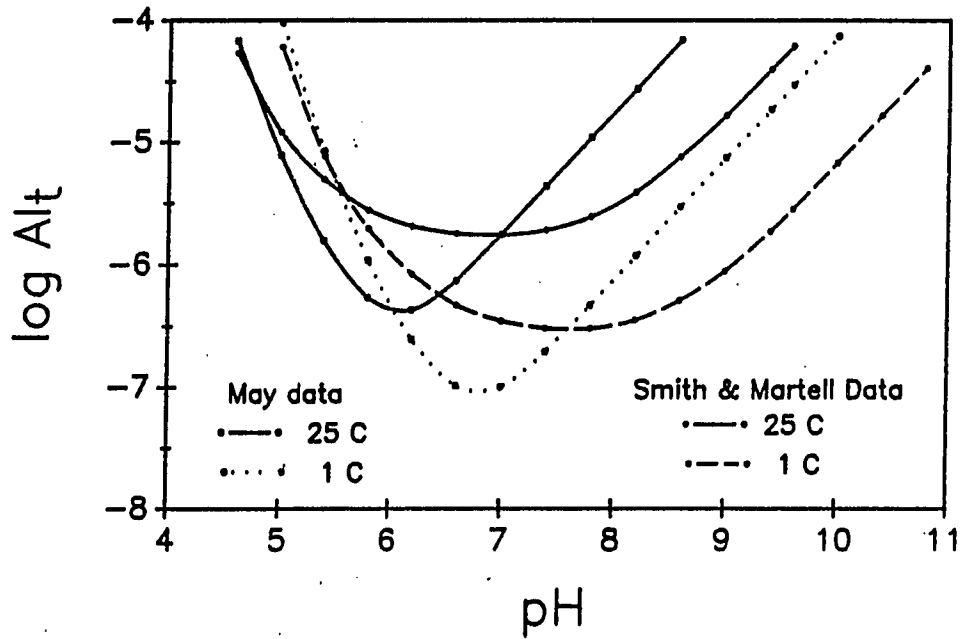


Figure 46. Calculated monomeric Al versus pH for two temperatures and using alternative reported values for the hydrolysis constants

alum dose was varied from 10.9 to 47 mg/l as alum, and the pH for most of the work was between 5 and 7. Velz observed some very interesting things. First, if the pH was held constant, the minimum alum dose to achieve good color removal dropped as the temperature dropped. The summer dose was 1.6 to 2.2 times as great as the winter dose. Second, if the dose was held constant and the pH was adjusted for optimal color removal, the detrimental effects of temperature could be practically eliminated. At 20-25 °C the optimum pH is 5.8, while at 8-14 °C, the optimum pH is 6.7. This represents a 0.9 pH unit shift over 11.5 °C. It should be noted that this phenomena was only observed when the minimum economical dose was used. As the dose was increased above this minimum, the effect of temperature disappeared. For a high surface area/volume system, like color, flocculation was probably occurring in the A/D flocculation region. Camp et al. (1940) set out to reconcile the apparent contradictions between Velz's (1934) results, Leipolds (1934) results, and the experience of plant operators flocculating particulates in cold water. Camp et al. assumed that iron and alum would behave identically, and elected to use ferric sulfate instead of alum. At that time it was easier to measure the residual iron than the residual aluminum. Ferric sulfate doses of 2, 3.15, 4.3, and 5.7 mg/l as Fe (9.1 to 25.8 mg/l as ferric sulfate) were applied to particle free water. Each of the coagulant doses was tested at 1-5, 15.1-15.3, and 28.3 °C. The shift in optimum pH seen by Velz using alum was once again seen with the iron, and as with Velz's work with

alum, the effect was most pronounced with the lowest dose. At doses of 5.7, 4.3, 3.15 mg/L as Fe, the optimum pH was 6.8, and did not shift a great deal as the temperature changed. However, at 2.0 mg/l as Fe, (9.1 mg/l as  $\text{Fe}(\text{SO}_4)_3$ ) the shift was substantial. The optimum pH values at the various temperatures were:

Temperature pH	
28.3	7.0
15.3	7.21
3.6	7.33

This represents a 0.33 pH unit shift over 24.7 °C. Significant, but much smaller than the shift seen with alum. Near pH=7, and with no particulate present in the system, the floc formed would be entirely sweep floc.

Camp noted that many investigators have shown that the time of formation of floc increases rapidly with increased variation in pH on either side of the optimum pH. Camp noted two other interesting things. First, the rate at which the floc formed seemed nearly independent of temperature. At the high dose, the floc started to form within 6 seconds at high temperature, and within 10 seconds at the low temperature. Camp measured the onset of floc formation by the disappearance of the tyndall effect. Second, all of the coagulant doses produced a better "quality" floc at high temperature, with little difference in floc "quality" between 15.3 and 3.6 °C. The exact meaning of the word quality, as used in this context, was

not defined. However, it is assumed that the author was referring to the appearant size of the floc.

Hannah et al. (1967) used 20 to 130 mg/l of alum (as alum), to flocculate 0.35 to 8.8 NTU water. Tests were performed at 0, 5, and 15 °C. These researchers noted that the settling and filtration deteriorated as the temperature decreased, with the differences most pronounced at temperatures below 5 °C and high alum dosages.

Unfortunately, no pH information was given, so it is impossible to know what was going on in a mechanistic sense. The dosage range given indicates probable sweep floc mechanism, but some of the data also indicates a sensitivity to the amount of surface area present, which would lead one to suspect charge neutralization (i.e., A/D mechanism). Not knowing any pH or alkalinity data, it is not possible to make much use of this data. It should also be noted that the authors apparently did not correct settling times for the change in liquid viscosity with temperature. This makes it impossible to distinguish between a reduction in flocculation efficiency and a reduction in sedimentation velocity due to higher viscosity at cold temperatures.

Hutchison and Foley (1974) treated a natural water containing 10-50 FTU of turbidity, with 10 to 25 mg/l of alum (as alum). The water was taken from the Great Lakes, probably Lake Huron. The study was prompted by the fact that the Port Elgin, Ontario water treatment

plant had severe after filter floc development when flocculation times were less than 3.5 minutes and the filtration rate was 5.6 gpm/ft<sup>2</sup>. Once again, the alkalinity and pH used in the study were not given. There is a hint that a pH of 7.3 was high, thus the entire study may have been in the A/D region, or it may have been in combination sweep floc and A/D region. There is no way to know without the pH information. The authors noted that at a temperature of 3.3 °C, 15 minutes of flocculation was sufficient to overcome all slow flocculation problems.

It is interesting to note that slow flocculation problems have not been mentioned with respect to iron. Perhaps the problem is related to the  $t_{1/2}$  of H<sub>2</sub>O coordination with the metal ion (as shown in Figure 40), which we saw was much longer for aluminum than for iron.

Treweek (1979) used a combination of 3 mg/l as alum and 0.25 mg/l of Cat-Floc T to treat a reservoir water. The turbidity of the reservoir water ranged from 1 to 3 NTU. The flocculation in this work was pretreatment for direct filtration, so the mixing intensity was relatively high ( $G = 100 \text{ sec}^{-1}$ ) and the mixing duration was relatively short (15 minutes). The temperature was varied from 19 to 4.5 °C, and no temperature effect was observed. Once again, no pH data was provided. It is obvious, from the alum dose, that the mechanism was either A/D, or a combination of the sweep floc and A/D mechanisms. However, without knowing the pH it is impossible to know

how far the aluminum hydroxide floc was from its ZPC. If the aluminum hydroxide is close to its ZPC, it may be simply adding additional particles, and the polymer may be responsible for the destabilization of the particles. If this is the case, one would not expect to see a temperature effect due to the alum.

Morris (1983) and Morris and Knocke (1984) investigated the effect of temperature (1, 5, 23 °C) and primary particle concentration on the flocculation of kaolinite with metal salts. Alum dosages of 0.01 to 10 mg/l as  $Al^{+3}$  (0.11 to 110 mg/l as alum with 14 waters) were used at a pH of 7.0. Iron dosages of 0.01 to 10 mg/l as  $Fe^{+3}$  (0.05 to 48.3 mg/l as  $FeCl_3 \cdot 6H_2O$ ) were used at a pH of 8. The pH was not considered a variable in this study, but neither was an effort made to hold it constant through most of the study. The pH drop caused by the coagulant addition was typically less than 0.6 pH units. The water used was a buffered tap water with a minimum alkalinity of 50 mg/l as  $CaCO_3$ . The tests were carried out in square mixing jars (Gator Jars), on a Phipps and Bird Jar test mixer. Each sample was treated as follows:

1 minute	rapid mix	intensity unknown
20 minute	slow mix	$G = 40 \text{ sec}^{-1}$
60 minute	settling	no temperature correction.

The following conclusions of interest came out of this work:



- o A decrease in temperature had a significant adverse effect on the removal of turbidity. The effect was most severe with aluminum sulfate, but significant with ferric chloride.
- o The reduction in turbidity removal at low temperature was caused by a change in the floc characteristic. A reduction in the apparent floc size at the lower temperature was noted.
- o The low temperature conditions did not inhibit the rate of aluminum or ferric hydroxide precipitation.

It is interesting that Morris and Knocke (1984) felt that these conclusions contradicted the results of Camp et al. (1940). However, if one reviews Camp's paper one finds substantial agreement.

Morris (1983) and Morris and Knocke (1984) represents a substantial effort along the same line which the work reported herein, and as such deserves some additional comment.

Morris and Knocke used settled turbidity to measure flocculation efficiency. Using settled turbidity as a measure of flocculation has inherent problems. These problems are compounded when, as in this case, the settling times are not corrected for the changes in water viscosity and density with temperature. Thus one must be very careful in interpreting the jar test data presented in Morris's work.

The authors also present particle counting data which needs to be considered carefully. The data were collected using a HIAC particle

counter with a 300  $\mu\text{m}$  sensor. It is noted that none of the 20 °C samples, alum or iron, contained any floc larger than 50  $\mu\text{m}$ . The 1 °C sample flocculated with iron contained no floc larger than 40  $\mu\text{m}$ , and those flocculated with alum contained no floc larger than 20-40  $\mu\text{m}$ , depending on the sample. The text (Morris and Knocke, 1984), however, states: "Thus, iron appeared to function more efficiently under low temperature conditions, owing to the formation of large flocs that settled more efficiently". This would lead one to believe that the authors could first, see the large floc, and then see visual differences in the floc. This is important because the resolution limit of the human eye is approximately 50  $\mu\text{m}$ . It is suggested that the particle counting data the authors have reported are really more indicative of the strength of second level aggregates than it is of the size of the floc, because the floc are probably ruptured in the counting procedure.

Morris and Knocke (1984) state: "Low-temperature conditions did not inhibit the rate of aluminum or ferric precipitation". This is in agreement with other work which has been done, and may very well be true. However, the first sample that the authors analyzed was collected 1 minute after the coagulant was injected. Camp et al. (1940) indicated, based on the Tyndall effect, that the precipitation was substantially complete in the first 3-6 seconds. Moffett (1968) indicated that the reaction time for the alum in the rapid mixing process is less than 0.1 seconds. Table 9 presented earlier in this

chapter indicates adsorption of the metal takes place in time scales of less than a second, and sweep floc forms in 1-7 seconds. Based on this, one must conclude that, it is not possible to rule out a temperature induced kinetic effect which could have a significant adverse impact on the flocculation process based on samples taken at 1 minute intervals.

One last thing to note is the pH selected for the testing of each of the coagulants. The iron was tested at a pH of 8 and the alum at a pH of 7. As we have already noted, the flocculation mode of metal coagulants is extremely sensitive to the system pH. Consider Figure 47 in light of Figures 33 and 34. Figure 47 represents the flocculation of a relatively low concentration of particles using varying doses of alum and ferric chloride at 1 °C. At 23 °C, both coagulants provided removal similar to the removal provided by the ferric chloride at 1 °C. The flocculation diagram, Figure 33, represents experimental conditions very close to the experimental conditions at 23 °C. Let's use this diagram to track what is happening in the data of Figure 47. First at 23 degrees. If we start at the low alum concentration on Figure 33 and move up the pH 7 line we see that once sufficient alum has been added, the conditions will always provide good flocculation. Morris (1983) states that the maximum pH depression experienced was 0.6 pH units. If it is assumed that this maximum pH depression corresponds to the maximum coagulant

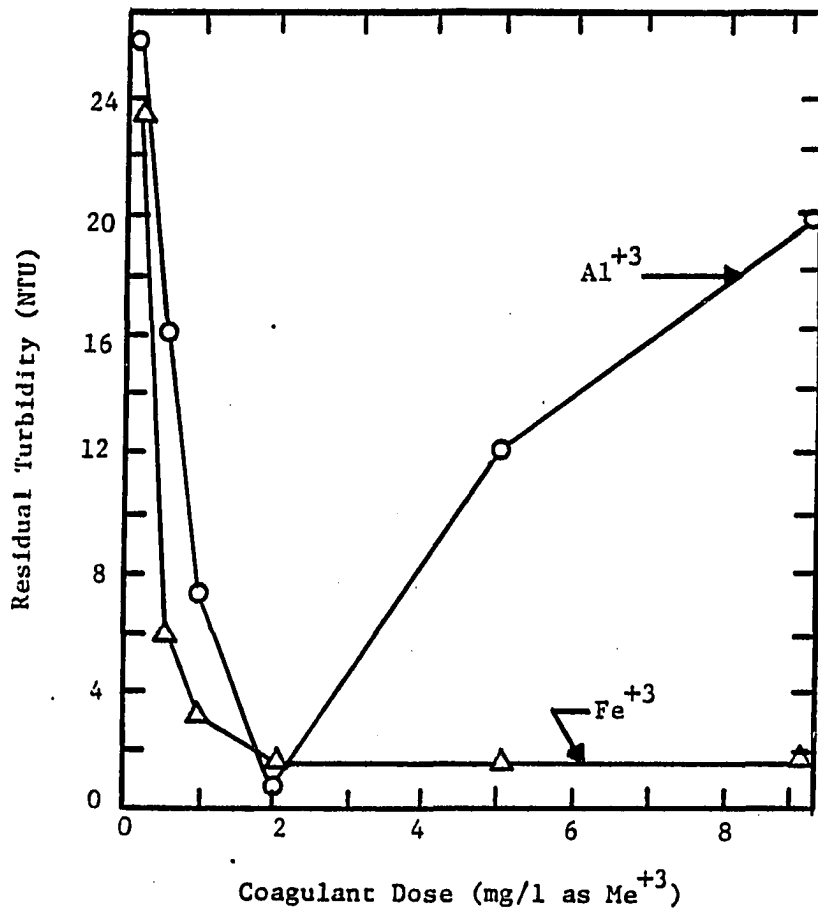


Figure 47. Comparison of turbidity removal efficiency under low temperature conditions by the use of alum and ferric chloride; 1 °C; alum @ pH=7; ferric chloride @ pH=8

dose, then at 110 mg/l as alum, the pH will drop 0.6 units. This will still be in the sweep floc region.

What happens at 1 °C? The previous interpretation of Velz (1934) indicated that the solubility diagram shifted 0.9 pH units with a 23 °C change in temperature. Dempsey (1987) shows the solubility diagram shifting 0.6 to 0.8 pH units with a 24 °C shift in temperature. If one simply corrects the diagram to hold the pOH constant as the temperature drops, a 0.74 pH unit shift of the diagram to the right is anticipated over a 20 °C temperature change. This evidence might lead one to hypothesis that as the temperature drops and the  $pK_w$  of water changes, the pH of the system must be adjusted to maintain a constant pOH. Common sense would also support this, because the species of importance in flocculation with metal salts are various hydroxide polymeric species or precipitates. The net effect of this hypothesis is to suggest that the entire coagulation diagram will be shifted to the right on the pH scale at cold temperature. Without redrawing the figure, one could read the expected coagulation behavior by entering the figure at a lower pH corresponding to the cold temperature pH shift of interest. Entering the diagram at a pH of 6.1 would be equivalent to the constant pOH condition at 1 °C for an experiment conducted at pH of 7.

One can use this hypothesis to interpret the observations in Figure 47. Entering the alum coagulation diagram at pH = 6.1, sweep

coagulation would be expected at an alum dosage of about 40 mg/L as alum, somewhat higher than the 2 mg/L Al (20 mg/L alum) observed in Figure 47. At the higher dosage used, the pH was depressed by the alum causing the operating point to fall well outside the sweep coagulation region with the consequent loss of coagulation evident at higher dosages in Figure 47. Again, assume that at the maximum dosage of alum, 110 mg/L as alum, a pH depression of 0.6 was experienced. Then the pH of 6.4 would be represented by a pH of 5.5 on Figure 33. This pH represents flocculation conditions well outside of the sweep floc region for reasons discussed earlier. Assuming that 1/2 the maximum dose of coagulant will yield 1/2 the maximum pH depression, a 50 mg/l dose at 1 °C would require entering Figure 33 at a pH of about 5.8. This is just outside the edge of good sweep floc. This scenario agrees with the  $Al^{+3}$  data in Figure 47.

Morris and Knocke (1984) ran the iron tests at a pH of 8.0. If one looks at the iron diagram, Figure 34, it is seen that this is in the middle of the very broad sweep floc region, and near the ZPC for iron hydroxide floc. The pOH can shift 2 full units, due to the cold temperature, at any dose and still not yield really poor flocculation. Thus, based on the pH at which the tests were run it is reasonable to expect that alum would have been effected more strongly by the temperature change than the iron.

Morris (1983) presents iron solubility diagrams calculated for 25 and 0 °C, and shows no significant differences in the diagrams. It appears, however, that the  $pK_w$  for 25 °C was used in the calculations for 0 °C. Thus any shift which might have been induced by the changing  $pK_w$  was not accounted for.

Knocke et al. (1986) investigated the impact of temperature on flocculation with aluminum and iron salts. Two natural waters containing turbidity and color, were flocculated at pH levels of 5.5 and 7.0, using 20, 40, 60, 80, and 100 mg/l of coagulant as the salt. The temperatures used were 2 and 22 °C. The following conclusion was drawn:

Low temperature will have the greatest impact on the removal of suspended solids or turbidity by coagulation and sedimentation. Removal of soluble organic compounds by coagulation, sedimentation, and filtration is not as significantly affected by low temperatures...organics removal is accomplished by incorporating these compounds into metal ion precipitates or floc."

This comparison highlights the problems inherent in attempting to evaluate temperature effects using secondary parameters such as filtration and sedimentation. Since flocculation, sedimentation, and filtration are all effected differently by changes in water temperature one must be careful in making comparisons.

The data in Figure 48 (Duluth Water Utility, 1987) show the effect of water temperature on optimal pH of flocculation. This figure

### Treatment Plant Operating pH vs. Temperature Duluth, Minn.

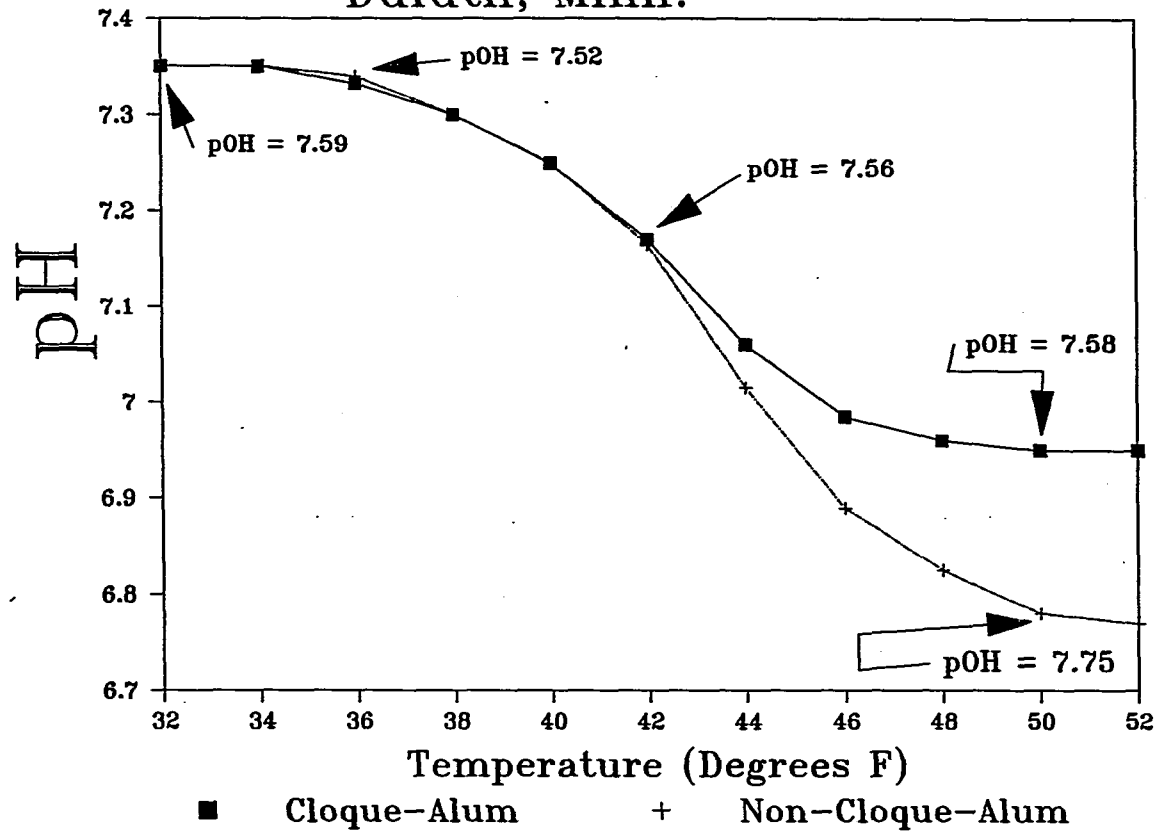


Figure 48. Full scale treatment plant operating curves showing pH goal versus temperature relationship for the Duluth, Minnesota water treatment plant



contains data from a full scale plant in Duluth Minnesota, which is treating Lake Superior water. These are operating curves for the treatment plant showing optimum treatment pH versus water temperature, for alum from two different sources. Note that with the Cloque alum, the pOH is very nearly constant at the temperatures which have been calculated. The pOH is also fairly constant for the non-Cloque alum, except at the higher temperatures. In light of the fact that this is full plant scale data, the agreement seen here is exceptional.

Brink et al. (1988) used combined alum (0-25 mg/l as alum) and polymer (0-8 mg/l Cat-Floc T) to flocculate a very low turbidity water. Filtered turbidity versus dose curves were generated at 3 and 19 °C, with all other conditions held constant. The curves produced were nearly identical, showing no discernible temperature effect. Al-Layla et al. (1974) studied the effect of temperature when using alum to flocculate live algal cultures. These researchers worked in the sweep floc region using 20 mg/l or more of alum, at a pH of 8.0 +/- 0.3, to flocculate algae at 10, 20 and 35 °C. They concluded that cold temperatures enhanced flocculation. This, however must be taken in context. At the warmer temperatures, the live algae produced gas bubbles which disrupted the floc. Because of this interesting phenomena it is difficult to draw any correlation between these results and the flocculation of inorganic materials at varying temperature.

Al-Ani et al. (1985) used a combination of alum and polymer to treat a very low turbidity water at different temperatures. Testing at 3 and 17 °C using the optimal alum and polymer dose showed no temperature effect. Turbidity removals, standard plate counts of bacteria, and total coliform removal were all used to measure flocculation efficiency at 18 and 5 °C under four different conditions of chemical pretreatment. No difference in the performance parameters was measured for the two temperatures. It appears that this work was done in sweep floc, but the pH was not reported.

Haarhoff and Cleasby (1988) studied the use of alum and ferric chloride to treat 3 °C water with a turbidity of less than 2 NTU. It appears from the discussion in this paper that the filter deposits at lower temperature, and therefore the floc formed at lower temperatures, are weaker than those formed at higher temperature. They found a number of interesting things. The ferric chloride was more effective at removing turbidity than the alum. At a molar dosage ratio of Fe-to-Al of 3:5.6, the headloss build up and turbidity removal for the two coagulants was identical. This indicates that at low temperatures there is a ratio of the ferric salt to the aluminum salt where they act identically. Based on their work the authors found no reason to reject alum as a low temperature coagulant.

Earlier an approximate temperature correction of the flocculation diagram was performed, and some of the data presented by Morris and Knocke (1984) were reevaluated. The re-interpretation assumed that the buffer intensity associated with a specific pH remained constant as the temperature dropped. Figures 49 and 50 illustrate the shift in the speciation of the carbonic acid system and buffer intensity induced by a 15 °C temperature drop. These curves are calculated based on the equations and constants presented in Stumm and Morgan (1981) and are corrected for the change in  $pK_w$  with temperature. It is seen that over the temperature range of interest, the equilibrium state of the carbonic acid system must be considered constant at constant pH. The kinetics of the system are a little more complex, and these will be discussed in the results section.

#### Cationic organic polymers

Edzwald (1981) notes that the use of synthetic organic polymers to improve solid-liquid separation has been one of the most significant developments in water treatment in the last 25 years. By 1981 the U.S. E.P.A. listed over 450 polymer products approved for use in potable water treatment (Mangravite, 1983). The majority of these 450 are intended for use as flocculant aids, and not as primary coagulants. In this section we are interested only in the cationic

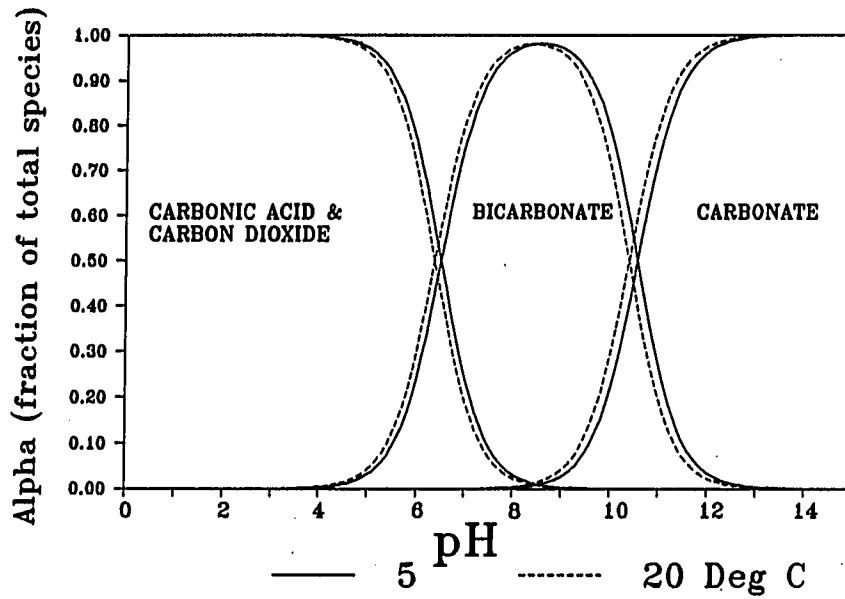


Figure 49. The Effect of temperature on the speciation of the carbonic acid system

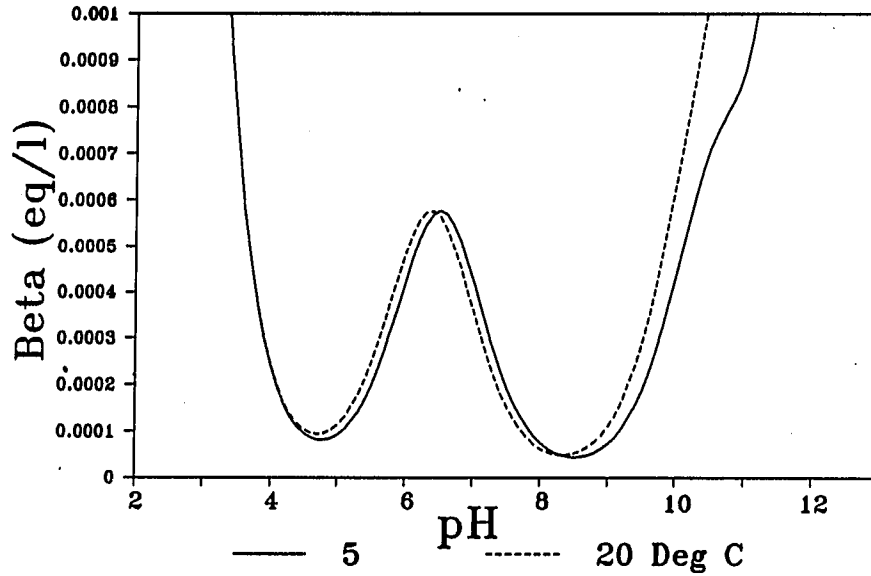


Figure 50. The effect of temperature on the buffer intensity of the carbonate system, based on Stumm and Morgan (1981)

polymers, which are capable of replacing the hydrolyzing metal salts as the primary coagulants (Edzwald, 1981; Mangravite, 1983).

Gregory (1978b) points out that polymers effect colloidal stability in various ways. It will be assumed in this literature review that only the lowest concentration of polymer capable of destabilizing the suspension is of interest. Based on this many of the more exotic polymer stability considerations, i.e., steric interactions, multilayering, etc., can be ignored.

There is universal agreement that the high density of positively charged sites on the cationic polymers are responsible for destabilizing negatively charged colloids. There is less agreement on the specific mechanics of the destabilization. The "patch" model proposed by Gregory seems to have the widest acceptance, and we will assume here that it is valid. Other models will be mentioned only as they influence our acceptance of the patch mechanism.

The patch model applies to high molecular weight cationic polymers with a high charge density. This model was developed by considering the distribution of charge densities on the polymers and on the surface of the particle to be destabilized. It is obvious that in many cases it is impossible for each of the charge sites on the surface to be neutralized individually by a charged polymer segment. When enough polymer has been adsorbed to neutralize the net negative

charge on the surface, a patchwork of "+" and "-" charged areas results. If, in a collision between two particles, a "+" and a "-" area collide the electrical interaction will not only allow them to come together, but will actually pull them together. This acceleration effect is actually measurable. Gregory (1978b) notes that this causes flocculation at an appreciably greater rate than predicted by the Smulochowski theory. As the ionic strength of the solution increases, the electrical enhancement of the flocculation process due to the patch effect decreases, just as one would expect.

This model also explains another phenomenon that simple uniform charge neutralization does not explain. When using a high molecular weight cationic polymer, one can get measurable flocculation with a negative zeta potential as large as -30 mv. This is appreciably more negative than the +/- 12 mv band usually considered acceptable (Gregory, 1978b). This enhanced flocculation has been attributed to bridging by some investigators. However, it is generally accepted that a polymer with a high density of "+" charges will lie fairly flat on a negative surface, and will not be subject to appreciable bridging (Gregory, 1978b). This is particularly true of highly branched polymers. It is primarily because of the increased flocculation rate and increased breadth of charges which will yield acceptable flocculation, that the patch model is seeing increased acceptance.

Poly (diallyldimethylammonium chloride) or poly DADMAC polymers and the poly quaternary amines or PQA polymers are the two types of cationic polymers most commonly used in the water treatment industry as primary coagulants for turbidity removal. Cat Flocc T and MagniFloc 573C are examples of the poly DADMAC and PQA polymers respectively. The poly DADMAC is linear and the high molecular weight PQA polymers are branched (Mangravite, 1983). Neither of these polymers is sensitive to pH changes over the range of pH values normally experienced in water treatment (Mangravite, 1983). The structure of the PQA base unit is shown in Figure 51 (Haarhoff, 1988; Mangravite, 1983). Cationic polymers are sold as concentrated aqueous solution (Mangravite, 1983). This concentrated polymer is diluted from 25-50 percent down to 1-5 percent for metering to the water to be treated. Both the concentrated and the dilute solutions are quite stable (Mangravite, 1983). Table 10 (Haarhoff, 1988) illustrates the charge stability of 3 cationic polymers which have been diluted to 1 mg/mL.

There is very little literature available with regard to the use of cationic polymers as primary coagulants. The majority of the work available deals with the use of polymers as coagulant aids. Much of the work available which does discuss cationic polymers as a primary coagulant, deals with direct filtration applications, and not with conventional flocculation.

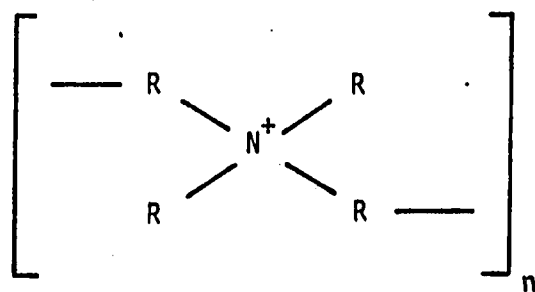
Table 10. Characteristics of the cationic polymer used

	CATFLOC T	MAGNIFLOC 572C	MAGNIFLOC 573C
Manufacturer	Calgon	Cyanamid	Cyanamid
Type	DADMAC <sup>a</sup>	PQA <sup>b</sup>	PQA
Molecular weight	high	medium	high
Form	viscous liquid	viscous liquid	viscous liquid
Charge Concentration after dilution to 1 mg/mL ( $\mu$ eq/mg)			
immediately after	1.6	4.2	3.9
after 1 day	1.6	4.2	3.9
after 3 days	1.4	4.2	4.0
after 8 days	1.4	4.1	4.0
average	1.5	4.2	4.0
Edzwald et al. (1987) - pH 7		4.1	4.2
NPOC (mg NPOC/mg polymer) (Non-Purgable Organic Carbon)			0.21

<sup>a</sup>Poly (diallyldimethyl ammonium chloride).

<sup>b</sup>Polyquaternary amine.





polyquaternary amine

Figure 51. The basic structural unit for poly-quaternary amine cationic polymers

There are indications in the literature that polymers are not sensitive to rapid mixing conditions (Dentel et al. 1986; Eilbeck and Mattock, 1987). However, one must be very careful to note the type of polymer and the application. If the polymer is not sensitive to rapid mixing conditions it is probably not being used as a primary coagulant, it is being used as a coagulant aid or flocculation aid. Mixing conditions are important when using cationic polymers as the primary coagulant (Mangravite, 1983; Birkner and Morgan, 1968; Leu and Ghosh, 1988; Ghosh et al., 1985; Stump and Novak, 1976; Yeh and Ghosh, 1981; and Morrow and Rausch, 1974).

Not only is mixing intensity important, but mixing time may also be important for the dispersion of the polymer. Gregory (1978b) showed, from theoretical considerations, that, even if one assumes instant and uniform polymer dispersion, the adsorption step may be sufficiently slow to effect the flocculation process. The assumption of instant and uniform polymer dispersion is very questionable. In a semi-dilute polymer solution, with a "good" solvent, and no fluid motion, polymer dissolution is a two step process (Brochard and DiGennes, 1983). The first step is a swelling of the transient network. The transient network refers to the tangle of polymer molecules in solution. All of the polymer chains will tend to spread out from regions of high concentration to regions of low concentration. In the second stage, viscous yield of the network, the polymer knots are slowly undone under the action of osmotic

forces. Brochard and DiGennes (1983) note that the super-imposed effects of shear flow on the dissolution process are probably quite complex. Skyluk and Stow (1969) also discussed the activation energy associated with physical disentanglement of a polymer molecule from a crowded area to an uncrowded area. At this point, it is not possible to speculate on how disentanglement impacts the rapid mixing of polymers, and therefore, flocculation with polymers. However, one thing is obvious, the situation with high weight organic cationic polymers is much different than the situation involving the use of metal salts as primary coagulants.

Yeh and Ghosh (1981) notes that "very little attention has been given to developing a rational procedure for the selection of the "right" polymer for a specific Job". Ghosh et al. (1985), Yeh and Ghosh (1981), and Leu and Ghosh (1988) have attempted to fill the void by categorizing polymers by molecular weight, charge density, and the monomer from which the polymer is synthesized. The various categories of polymers are then tested under various treatment conditions. Although this is an improvement it still leaves much to be desired. As Yeh and Ghosh (1981) note, the use of polymers could be vastly improved if the polymer manufacturers would take a more enlightened attitude toward providing needed information. According to Yeh and Ghosh, the type of information needed from the manufacturer for the selection of cationic polymers for direct filtration includes:

- o type of polymer or copolymer,
- o concentration of active ingredient,
- o concentration of free monomer,
- o proportion of ionizable groups,
- o molecular weight or intrinsic viscosity under specified conditions.

This information, with the extent of mixing required to disperse polymers effectively in the water, would begin to make intelligent decisions possible (Yeh and Ghosh, 1981).

Mangravite (1983) points out that even when molecular weights are provided by the manufacturer, one is never sure what the number really means. Different manufacturers define the average molecular weight differently, i.e., weight average, number average, etc. There are also problems with using the intrinsic viscosity to estimate molecular weight and size. Rabin (1988) says that the intrinsic viscosity relationship is much more complex than once thought. He goes on to show that one of the widely used relationships does not even provide qualitative agreement with actual behavior of the polymer in dilute solution. In addition, the hydrodynamic volume of a highly branched polymer will be very different from that of a linear polymer. Thus, comparisons of molecular weight based on intrinsic viscosity can be very misleading (Mangravite, 1983).

All of this is to say that we do not fully understand the rapid mixing of polymers, and how that rapid mixing will affect the flocculation process. With these qualifying remarks in mind, let's compare our expectations with the experience in the literature.

Birkner and Morgan (1968) flocculated 1.3  $\mu\text{m}$  polystyrene latex particles using poly(ethylenimine) (PEI), a low molecular weight cationic polymer ( $3.5 \times 10^4$  g/mole). PEI polymers are a highly branched primary coagulant. This polymer has been used extensively in laboratory studies, but is not used in water treatment, because it is expensive and relatively inefficient (Mangravite, 1983). The rapid mix conditions used by Birkner and Morgan were not specified. The flocculation conditions were varied from a G of 11 to 120  $\text{sec}^{-1}$ , and time from 6 to 424 minutes. Starting with  $2 \times 10^8$  particles/mL, flocculation at optimum polymer dosage, mixing intensity, and mixing time was carried out. This resulted in a 20 percent reduction in the total particle concentration after 25 minutes. The following trend in optimum mixing intensity with time was noted:

Time (minutes)	Optimum Mixing Intensity (G; $\text{sec}^{-1}$ )
6	93
25	47
92	11
424	11

The authors concluded that the value of G which provided the maximum reduction in primary particles, decreases as the elapsed time

increases. This was taken as evidence that mixing intensity is a very important factor in floc breakup in latter stages of flocculation. Temperature effects were not discussed. The positive charge density of PEI is pH sensitive (Mangravite, 1983). Without knowing the rapid mixing conditions and the pH conditions it is not possible to use this data in attempting to develop a global view of cationic polymer flocculation.

Morrow and Rausch (1974) found that cationic polymers can replace inorganic salts by applying a mixing intensity of  $400 \text{ sec}^{-1}$  or greater during rapid mixing. The authors used a pilot scale plant at three locations to compare conventional rapid mixing to high intensity rapid mixing. Conventional rapid mixing was defined as a G of  $300 \text{ sec}^{-1}$  for 10-60 seconds. The field results showed that a rapid mixing intensity of  $300 \text{ sec}^{-1}$  was not always effective with cationic polymers. This was attributed to the non-uniform distribution of polyelectrolyte, due to the low energy and short duration of the mixing period. In preliminary laboratory scale batch studies using Ohio river water, velocity gradients of greater than  $400 \text{ sec}^{-1}$  with rapid mix times of less than 2 minutes were optimal for use of an unspecified cationic polymer. As the velocity gradients were increased the rapid mix time needed was decreased until at a G of  $1000 \text{ sec}^{-1}$  only several seconds were necessary.

The first pilot scale study, by these authors, involved treating natural river water from the Beaver River at New Brighton. In this study a quaternary ammonium polymer (a modified poly DMDAAC; Cat Flocc B) was used. Two polymer dosages were evaluated at G values of 730, 600, 425, and 250  $\text{sec}^{-1}$ . The rapid mix time was varied from 30 seconds at a G of 750  $\text{sec}^{-1}$  to 3 minutes at a G of 250  $\text{sec}^{-1}$ . At 1 mg/l of polymer the optimum rapid mix was a G of 750  $\text{sec}^{-1}$  for 30 seconds. At a dose of 2 mg/l, 425 and 600  $\text{sec}^{-1}$  appeared optimal, with a noticeable decline in efficiency at a G of 750  $\text{sec}^{-1}$ . Temperature data were not provided, however, the comment was made that temperature changes had no impact on the use of cationic polymers.

The second study involved treating Missouri river water in St Louis County. This water has an annual turbidity range from 40-2,500 JTU. Both the poly DMDAAC (Cat Flocc) and a modified poly (DMDAAC) were tested. With the Missouri water it was concluded that the cationic polymer functioned most efficiently in a rapid mixing G range of 500 to 1,000  $\text{sec}^{-1}$ . The duration of the rapid mix was not specified.

The third study involved treating Mississippi river water in East St. Louis. Turbidity ranged from 100 to 300 JTU. The polymers used were poly (DMDAAC) and a modified poly (DMDAAC). Both polymers performed well when rapid mixed at G values of 450 and 600  $\text{sec}^{-1}$ . Alum, tested at the same time, performed well when rapid mixed at a G of 300

$\text{sec}^{-1}$ , but performed poorly when rapid mixed at a G of  $600 \text{ sec}^{-1}$ . The duration of the rapid mix was not specified.

Stump and Novak (1976) studied the effect of rapid mixing time, rapid mixing intensity, and flocculation time on direct filtration. A synthetic water with 300 mg/l of hardness as  $\text{CaCO}_3$  was used in the study. 100 mg/l (80 ftu) of kaolinite was used to provide the primary particles. Nine polymers, 8 cationic and 1 non-ionic, and alum were evaluated in this study. The default rapid mix time was 2 minutes. The flocculation conditions were not explicitly stated, but it appears that the mixing intensity was constant at a G of 20  $\text{sec}^{-1}$ , and the flocculation time was varied from 0 to 60 minutes. Both settled turbidities and direct filtration efficiency were used as a measure of flocculation effectiveness.

Five of the low molecular weight polymers were PEI polymers (MW of  $6 \times 10^2$  to  $1 \times 10^5$  g/mole). A few of the general characteristics of PEI polymers were given previously. The other low molecular weight polymer was a polyamine ( $5 \times 10^4$  g/mole). The polyamine is a branched polymer, and its charge density is pH dependent (Mangravite, 1983). The high molecular weight cationic polymers ( $2 \times 10^6$  and  $3 \times 10^6$  g/mole) both appear to be poly quaternary amines. These are slightly branched and pH has little effect on their charge density (Mangravite, 1983). The following conclusions were drawn based on the settled turbidity studies.



Alum, anionic polymer and low molecular weight cationic polymer all provided the best turbidity removal at the lowest rapid mixing intensity;  $G=100 \text{ sec}^{-1}$ . In general, as the molecular weight of the cationic polymer decreased the advantage of intense rapid mixing also decreased. The effect of the rapid mixing duration on the effectiveness of the low molecular weight polymers was found to be negligible when tested at 0.5 and 2 minutes.

For the higher molecular weight cationic polymers, both mixing intensity and duration were important. Both of the high molecular weight polymers improved from 25 percent turbidity removal to 90 percent turbidity removal when rapid mixing intensified from  $100 \text{ sec}^{-1}$  to  $350 \text{ sec}^{-1}$  for 2 minutes. The optimum rapid mix for the turbidity removal using the highest molecular weight polymer was  $750 \text{ sec}^{-1}$  for 4 minutes. There was, however, not a large difference between the 1, 2, and 4 minute values. At rapid mixing intensities of  $950 \text{ sec}^{-1}$  and  $1250 \text{ sec}^{-1}$  for 1 minute, the turbidity removal was impaired, but still better than what it was at  $100 \text{ sec}^{-1}$ . The 2 and 4 minute duration rapid mixing also showed a decrease in effectiveness at intensities of  $950$  and  $1250 \text{ sec}^{-1}$ , but the decrease in effectiveness was not as substantial as observed for the 1 minute duration.

Sedimentation studies showed that flocculation times in excess of 10 minutes are required with both low and high molecular weight cationic polymers. Twenty minutes of flocculation appears optimal in terms of increased turbidity removal/increased flocculation time.

Stump and Novak (1976) also investigated the effect of rapid mixing and flocculation time on direct filtration. Two polymers were used in this portion of the study; the  $5 \times 10^4$  g/mole polyamine, and the  $3 \times 10^6$  g/mole poly quaternary amine. Rapid mixing was for 2 minutes at a G of 100, 350, and 950  $\text{sec}^{-1}$ . Flocculation was for 0, 10, and 20 minutes at a G of 20  $\text{sec}^{-1}$ . Filtration was at 5  $\text{gpm/ft}^2$ . The measure of success was gallons of water filtered per  $\text{ft}^2$ , prior to run termination. The runs were stopped when headloss exceeded 10 inches of water, or the turbidity exceeded 1 FTU.

The optimal conditions for the polyamine were; rapid mix for 2 minutes at a G of 350  $\text{sec}^{-1}$ , and flocculate for 20 minutes at a G of 20  $\text{sec}^{-1}$ . These conditions provided twice the filtered water capacity of the next best condition. The optimal conditions for the poly quaternary amine were; rapid mix at a G of 950  $\text{sec}^{-1}$  for 2 minutes, and then flocculate at a G of 20  $\text{sec}^{-1}$  for 20 minutes. These conditions provided three times the filter capacity of the next best conditions. Using the low molecular weight polymer at optimal conditions produced 2.6x as much water as the high molecular weight polymer at optimal conditions. It is not known how changing the

flocculation intensity would have affected this result. It is also not known if the filtration runs were terminated due to turbidity breakthrough or due to excessive headloss.

Yeh and Ghosh (1981) studied the effect of polymer characteristics and mixing energy on direct filtration. The test suspension was 75 mg/l (20 NTU) bentonite clay suspension. The author found that for cationic polymers, with molecular weights less than 100,000 g/mole, the dominant coagulation/flocculation mechanism was charge neutralization, not bridging. The high molecular weight poly quaternary amine ( $3 \times 10^6$  g/mole) used in this study was the same polymer used by Stump and Novak (1976). Rapid mixing at  $100 \text{ sec}^{-1}$  was not adequate for this polymer regardless of subsequent slow mix conditions, because the low intensity rapid mixing did not disperse the polymer sufficiently. The optimum rapid mix for this polymer appeared to be at a G of  $650 \text{ sec}^{-1}$  for 3 minutes. The following general conclusion was drawn for low to medium weight polymer (10,000 to 100,000 g/mole); rapid mixing at a G in the range of 300 to  $650 \text{ sec}^{-1}$  for a period of 3 to 8 minutes was necessary.

Ghosh et al. (1985) studied 12 commercially available polymers; 4 PEIs, 3 with an amine type structure, and 7 poly (DADMAC)s. The effect of mixing on the efficiency of the polymer was studied using a 25 NTU bentonite suspension and the optimal dosage of the respective

polymer. The G of the rapid mix was varied while the following were held constant:

- o rapid mix 2 minutes
- o flocculation time 10 minutes
- o flocculation intensity  $G=25 \text{ sec}^{-1}$ .

The molecular weight of the polymer varied from  $2.2 \times 10^4$  to  $1.1 \times 10^7$  g/mole. Rapid mixing was considered optimal when the mean particle diameter,  $D_{NV}$ , was maximized. The  $D_{NV}$  is the number-volume mean diameter, and can be calculated from the following formula:

$$D_{NV} = \left[ \frac{\sum D^3 N}{\sum N} \right]^{1/3}$$

- D - mean particle size in a given size range
- N - number of particles in a given size range.

The optimum rapid mixing intensity was  $800 \text{ sec}^{-1}$ . When a rapid mixing intensity  $>800 \text{ sec}^{-1}$  was employed there was no significant increase in the  $D_{NV}$  of the floc produced. Only one of the polymers, a PEI (MW of  $2 \times 10^5$  g/mole), experienced a decrease in  $D_{NV}$  when rapid mixing intensities between 800 to  $1400 \text{ sec}^{-1}$  were employed.

Leu and Ghosh (1988) in studying cationic polymers as a primary coagulant noted that the complex effect of flocculation variables, suspension properties, polymer properties, and mixing conditions make

the literature appear somewhat inconsistent. They drew the following conclusions:

- o Although the initial periods of both rapid and slow mix seem to be important in flocculation with polymers, rapid mixing is more critical.
- o Good flocculation was obtained by using a high G value for a short time in rapid mixing.
- o To a large extent rapid mixing conditions (G and t) rather than the characteristics of the polymer determine the shape of the particle size distribution.

The second conclusion listed above may be misleading at first appearance. From the text it becomes obvious that a high G value for a short time refers to a G values in the range of 850 to 1250  $\text{sec}^{-1}$ . The authors specify the rapid mix Gt as  $2 \times 10^5$ . Therefore, the authors are recommending mixing times of 2.5 to 4 minutes. This recommendation appears to stem from the floc breakup which the authors observed if rapid mixing at a G of 850  $\text{sec}^{-1}$  extended beyond 4-5 minutes. The third conclusion also warrants some clarification. The authors data make it clear that structure and molecular weight are both significant. However, if the rapid mixing is intense enough and long enough to disperse the polymer properly, but not so long and intense that floc breakup occurs, all the polymers tested did a good job. No testing was performed at multiple temperatures.

MagniFloc 573C was selected for the work performed in this study. This is a poly quaternary amine (PQA), with a molecular weight of

approximately  $0.5 \times 10^5$  to  $1 \times 10^5$  g/mole. Haarhoff (1988) reported the following ultrafiltration separation information for this polymer.

Table 11. Molecular weight fractions of a dilute suspension of MagniFloc 573C

	Recovery after ultrafiltration	Molecular weight fraction		
		<10K <sup>a</sup>	10-100K	>100K
% of NPOC	102%	15	3	84
% of charge concentration	95%	0	0	95

<sup>a</sup>KiloDalton.

A dalton equals  $1.66024 \times 10^{-24}$  grams. The molecular weight fractions given in the preceding table refer to the weight of a molecule of standard protein. If one assumes that the standard protein and the polymer are geometrically similar, this table indicates that the majority of the charge is associated with the  $1 \times 10^5$  g/mole fraction of the polymeric mixture.

The polymer was separated into three different molecular weight fractions by ultra filtration. The charge concentration before separation was  $4.0 \mu\text{eq/mg}$  of polymer in a  $16.7 \text{ mg/l}$  polymer solution. The charge concentration found in the >100K fraction after ultrafiltration accounts for  $3.8 \mu\text{eq/mg}$  in the original solution. Thus, we can feel comfortable in assuming that the molecular weight

of the organic polymer being used to destabilize the particles is  $-1 \times 10^5$  g/mole.

Farinato (1988) indicated that in a "Good" solvent the radius of gyration for MagniFloc 573C should not be strongly temperature dependent. Water is a good solvent for this polymer, and there should be very little change in the radius of gyration between 20 and 5 °C. If the radius of gyration were a strong function of temperature, one would also expect the diffusion rate of the polymer, at infinite dilution, to be a strong function of temperature. However, it appears that the diffusion rate of the polymer should be insensitive to temperature effects.

Based on the literature reviewed here, one would expect that:

- o if the appropriate mixing time, mixing intensity, and system chemistry are selected,
- o and if the structure of the turbulent flow field is unimportant,

then one should be able to produce identical flocculation results at low and high temperature using cationic polymers. This of course assumes that floc breakup does not dominate. If the results are not identical, it will be necessary to determine whether the differences in response are due to inadequate rapid mixing, changing system chemistry, or a variation in the turbulent flow field structure.

### Particle Counting

Traditional flocculation research has been based on indirect measures of flocculation efficiency, such as settled water turbidity or filtered water turbidity (Lawler, 1987). This created an environment where phase separation was equated with flocculation. Treweek and Morgan (1977) noted that this measurement of physical separation biased investigators toward improvement of the physical separation processes, at the expense of possible chemical alterations which would enhance the destabilization phase of coagulation. Measuring the aggregate size distribution and number concentration allow the investigator to study directly the destabilization and aggregation of the colloids, rather than measuring the end result of the entire process, i.e., phase separation.

The current trend is toward the use of electronic particle counters. Lawler (1987) notes that the direct measure of changes in the particle size distribution brought about by flocculation allows a better focus on the effect of changing variables related to the flocculation process alone. The motivation in monitoring changes in the particle size distribution is to optimize the growth of particles out of the 1-10  $\mu\text{m}$  range, which are difficult to remove, and into the 10+  $\mu\text{m}$  range. The desired final floc size will depend on the unit process to be used to remove the floc from the water.



In this work turbidity has been used as a quality control parameter, and electronic particle counters and automatic image analysis (AIA) were considered for sample analysis. These three measures of particle number concentration will be discussed briefly.

### Turbidity

The turbidity of a sample is a measure the amount of light the sample scatters at an angle of 90 degrees from the incident beam measured in a standardized instrument. The water treatment industry as a whole makes extensive use of turbidity as an indicator of particle number concentration. The basic assumption is this; if there are more particles present, then there will be more light scattered. It turns out that this is true within certain limits, there is a correlation between turbidity and particle concentration. However, the relationship is neither simple, nor consistent for all particle systems. Turbidity will provide an indication of what is happening, but it does not provide detailed information. The following literature will illustrate some of the frustrations involved in trying to use turbidity as a primary measurement in flocculation work.

Beard II and Tanaka (1977) reported that many investigators have found it difficult to obtain accurate, consistent results with simple turbidity measurements. This probably isn't surprising since turbidity is a colligative property which depends upon particle

shape, refractive index, wavelength of the light source, particle size, and particle concentration. These authors found, using a HIAC particle counter, that turbidity measurements underestimated the concentrations of 2.5 to 10  $\mu\text{m}$  particles.

Treweek (1979) pointed out that a major limitation of turbidity as a measure of flocculation is that: "while the PSD may change significantly, this change may not be reflected in a corresponding turbidity change... Particle counts in contrast to turbidity measurements, provide a direct measure of particulate matter in the water and its size distribution". Kavanaugh et al. (1980) indicated that turbidity correlates poorly with particle number concentration measured using particle counting instruments.

Friedlander (1977) stated that most of the light scattered in turbidity is scattered by particles less than 10  $\mu\text{m}$  and the majority of the light is scattered by 0.01 to 1.0  $\mu\text{m}$  particles. Hudson (1965) stated that the most of the turbidity is caused by particles smaller than 10  $\mu\text{m}$ , with the majority being caused by particles smaller than 1.5  $\mu\text{m}$  in diameter. Thus, one would expect turbidity to correlate well with particle number concentration in the small particle sizes.

Dentel et al. (1986), found that turbidity correlated well with particle counts. Cleasby et al. (1988) presented data from a survey

of filtration plants producing low turbidity finished waters. In these data both the raw and finished water turbidity versus particle count data were presented. For turbidities above 0.3 ntu, the turbidity correlated well with HIAC (60  $\mu\text{m}$  sensor) total particle count. Below that point the correlation was poor. Previous work (McTigue and Berman, 1988) using particle counters at Tulsa, Oklahoma, confirmed work by Cleasby (1988) indicating that at turbidities less than 0.3 ntu, particle counts could not be correlated with turbidities.

Since turbidity is a colligative property, one might expect that as the number concentration of particles approaches some lower limit, the quality of the data, and therefore, the correlation will become poor.

#### Electronic particle counters

Kavanaugh et al. (1980) and Lawler et al. (1980) both agree that the use of particle size distribution information in process design, process selection, and operations decisions, provides a great improvement over secondary measures, such as simple turbidity. If one accepts this one must still select a method for measuring the particle size distribution. The technical literature contains very little solid data on how various particle counting instruments compare. There have been a number of publications which included reviews of currently available particle counting instruments's

(Allen, 1981; Treweek & Morgan, 1977; Kavanaugh, et al. 1980; Dentel et al. 1986; Groves, 1980). Unfortunately, none of them was a side by side comparison of the hardware. The majority of the information appears to have come from available literature, and personal experience in which the instruments were used under experimental conditions which may have been very different. Groves (1980) points out that in selection of particle counting instruments "it is essential for the analyst to realize the practical limitations which are inherent in any method of analysis which is available."

Lawler (1987) states that the two most common particle size distribution measuring instruments are the Coulter counter type and the HIAC type instruments. Akers (1978) maintains that the two most commonly used counting techniques are the Coulter type counters and the microscope.

The Coulter type counter and the HIAC have been the two most commonly used particle counting instruments in the water treatment literature. Tekippe and Ham (1970), Birkner and Morgan (1968), Lawler et al. (1983), Hannah et al. (1967a), Ives and Dibouni (1979), Leu and Ghosh (1988), Snodgrass et al. (1984), Ghosh et al. (1985), etc., have used the Coulter type counter in investigations dealing with particle size change and flocculation. Pandya and Speilman (1983), Reed and Mery (1986), Treweek (1979), Beard II and Tanaka (1977), Sricharoenchaikit and Letterman (1987), Yeh and Ghosh (1981), etc., have used the HIAC

in investigations tracking particles and flocculation. It is widely admitted by the investigators above, and by others (Gibbs, 1982; Kavanaugh et al., 1980; Sonntag and Russel, 1986; Lawler, 1987; Mathews and Rhodes, 1968; Grasso and Webber, 1988; and Camp, 1968) that, while these instruments are useful, they also have limitations.

The results presented by McTigue et al. (in press) in Table 12, indicate that the measurements from six different types of particle counters counting the same sample are not directly comparable to each other, either in determination of total numbers of particles, or in their size.

Electronic particle counters have been the heart of a debate which has been continuing for many years. The primary question has been how accurate is particle counter data and exactly how reproducible are the results? This is an especially troublesome issue when one is dealing with a suspension which has been flocculated. It is universally agreed that each technique has strengths and weaknesses.

Regardless of the particle counter used, sample handling is one of the largest sources of potential error. Lawler (1987) has published some general guidelines for sample handling developed specifically around the Coulter Counter. In general, the guidelines can be reduced to one sentence. Sampling of process flow streams, and subsequent sample handling and dilution must be carried out with

Table 12. Particle counter comparison

Instrument Name	Type	Range ( $\mu\text{m}$ )	Raw Water (#/ml)	Finished (#/ml)	Researcher
HIAC PC-320 60 $\mu\text{m}$ Sensor	Light Blockage	1-60	204,618	1,160	Cleasby, ISU
Spectrex SPC-410 Sensor 1 Sensor 2	Laser Light Scattering	17-100 1-17	16,000 140,000	418 378	#1 Burman, Tulsa #2 McTigue
Elzone	Electrical Resistance	.3-1,200	2,282,564	---	Factory
Coulter	Electrical Resistance	.5-900	1,500,000	4,200	Lawler, Tex. A&M
Brinkman	Laser Light Blockage	.3-300	700,000	8,300	Amitharajah G. I of T

extreme care (Lawler, 1987). Floc breakup is the largest concern. PSD measurement is complicated by the fact that the PSD may change during the course of the analysis (Kavanaugh et al. 1980). These changes are usually attributed to aggregate breakup during sampling, sample preparation, or in passing through the instruments sensing zone (Kavanaugh et al. 1980).

Work by Gallegos and Menzel (1987) has indicated that the effect of holding time is largely suspension dependent. Using a Malvern Autosizer II (PSD instrument), they measured particle size distribution changes over time for a number of natural samples. They found that an undiluted sample of water from a turbid creek carrying storm water began to flocculate after 2.5-6 hours, but particles from a turbid impoundment remained stable for 10 days. It is not possible to make a general statement with regard to the absolute effect of sample storage on the analysis provided by various instruments.

Coulter type counter      The Coulter principle is the basis for the Coulter counter and other electro-zone particle counting instruments (Groves, 1980). This principle is based on the fact that when a particle passes through a small orifice, which is submerged in an electrolyte solution, with electrodes on either side of the orifice, the resistance between the two electrodes is increased momentarily. The increase in resistance is caused by displacement of electrolyte, and is known to be a function of the particle volume.

According to Groves (1980), there are no flaws in the basic theory associated with this instrument, and it is capable of making a valuable contribution in the measurement of PSDs of fine powders. There are, however, a number of concerns when using the instrument with floc.

Tekippe and Ham (1970), discussed the potential for floc breakage using this instrument, and concluded that Coulter counter samples should be periodically inspected with a microscope, to guard against erroneous results due to floc breakage. Tekippe and Ham also recommend calibrating the Coulter counter using actual floc and a light microscope.

Kavanaugh et al. (1980) expresses concern over breakup of floc, and states that it will probably be necessary to use two or three different orifice sizes in sequence to avoid the breakup of larger floc. It is not clear how the large floc are removed from the sample prior to measurement with the smaller orifice. Or, if they are not removed, how their breakup during measurement with the smaller orifice will impact the results.

Snodgrass et al. (1984) noticed breakup of floc when using a 30  $\mu\text{m}$  orifice as opposed to a 90  $\mu\text{m}$  orifice. This breakup was evident even though the Reynolds number which had been 550 in the 90  $\mu\text{m}$  sensor,



had been reduced to 60 in the 30  $\mu\text{m}$  sensor. It is assumed that the Reynolds number has been based on the aperture diameter.

Floc breakup is only one concern. Another concern is particles growing into a sensors resolution range. A Coulter sensor is reliable from 2 to 40 percent of the aperture diameter. Thus a 90  $\mu\text{m}$  sensor can measure over a 2  $\mu\text{m}$  to 36  $\mu\text{m}$  range. Particles smaller than 2  $\mu\text{m}$  will grow into the useful range of the instrument, and may cause the researcher some difficulty (Treweek and Morgan, 1977).

A basic premise of the Coulter counter is that there is only one particle in the orifice at a time. If there is more than one particle in the sensing zone at a time they will be counted as one larger particle. This is referred to as coincident counts. To prevent coincident counts, it is necessary to dilute the samples to some predetermined particle concentration. Coincident counts are a potential source of very large error (Mathews and Rhodes, 1968; TeKippe and Ham, 1970; Kavanaugh et al. 1980).

TeKippe and Ham (1970) discuss the impact of adding electrolyte , and conclude that it is probably not a concern.

Treweek and Morgan (1977), Ghosh et al. (1985), and Mathews and Rhodes (1968) all express concern over the fact that aggregates may have a length which exceeds the thickness of the sensing zone. This

will cause a pulse which has width as well as height. The electronics in the Coulter is not capable of dealing with a two dimensional peak. This may be a source of significant error.

Treweek and Morgan (1977), and TeKippe and Ham (1970) discussed the effect of floc porosity on the Coulter counter. Treweek and Morgan gave a method for correcting for the errors caused by the floc porosity.

The Coulter counter has a practical range of 0.5 to 900  $\mu\text{m}$  (Treweek and Morgan, 1977; Groves, 1980).

HIAC particle counter      The HIAC is a light blockage particle counter. The particles to be counted are suspended in a fluid which has a refractive index different than the particles. The suspension is then passed through the sensing area. The sensing area consists of a small rectangular cell with windows on opposing sides. A collimated beam of light from a high intensity quartz halogen lamp is directed through the stream of liquid from one side of the cell. The beam of light is detected by a photodiode on the other side of the cell. As a particle passes through the sensing zone, the light intensity drops proportional to the cross-sectional area of the particle. The geometry of the sensor is such that the flow in the sensor is turbulent causing the particles to tumble as they pass through the sensing zone. The tumbling causes the amplitude of the

peak produced to be proportional to the greatest projected area of the particle (Allen, 1981).

A number of items which were of concern with the Coulter counter are not concerns with the HIAC, including:

- o electrolyte effect, since no electrolyte is needed (Groves, 1980; Kavanaugh et al. 1980),
- o porosity concerns, and
- o floc geometry effecting the pulse height, since the pulse is maximized by the particle tumbling (Allen, 1981).

The two main concerns with the HIAC appear to be sample dilution and floc breakage.

Beard II and Tanaka (1977) in comparing the HIAC particle counts with turbidity measurements say that the HIAC is relatively unaffected by particle shape, particle refractive index, and the wavelength of the light source, but it does require dilution of the sample. Beard used a 1-60  $\mu\text{m}$  sensor to analyze filter effluent and found the turbidimeter was measuring 85.1 % removal of total solids while the HIAC measured a 98.2 % removal. The authors went on to recommend the use of the 60  $\mu\text{m}$  sensor on all filter effluent samples, because of its sensitivity in the 1-2.5  $\mu\text{m}$  range. It is worth noting that they did not check their results with the light microscope. The investigators concluded that the HIAC would readily and reliably provide particle size and concentration on a real time basis. Groves

(1980) and Kavanaugh et al. (1980) also state that the HIAC is suitable for on line measurement of particles down to 1  $\mu\text{m}$ , but may require considerable dilution of the sample. Kavanaugh et al. (1980) expressed concern over monitoring filter influent with the HIAC, and recommended that the filter effluent be monitored to prevent problems with sensor blockage, coincident counts, and floc breakup.

Sricharoenchaikit and Letterman (1987) used a 60  $\mu\text{m}$  sensor, and assumed that all particles larger than 2  $\mu\text{m}$  would be counted. These investigators recognized the possibility of floc breakage, but asserted that it was negligible, since no aggregates with an equivalent circular diameter of larger than 20  $\mu\text{m}$  were measured. The authors assertion that breakup was negligible was based on a statement by Gibbs (1982) regarding the breakup of floc which exceeded 40 percent of the sensor aperture. Gibbs (1982) compared PSDs for a number of naturally flocculated materials and a number of laboratory produced floc. The size distributions were measured using a HIAC particle counter and light microscope. Gibbs found that any floc larger than 40 percent of the sensor aperture width experienced severe breakup. He recommended that an independent method be used to check for floc breakage before a HIAC be used to measure PSDs of any flocculated material. Figure 52 illustrates the breakup observed by Gibbs. It should be noted that although Sricharoenchaikit and Letterman asserted that breakup was negligible, they did not verify this microscopically. Reed and Mery (1986) compared HIAC particle

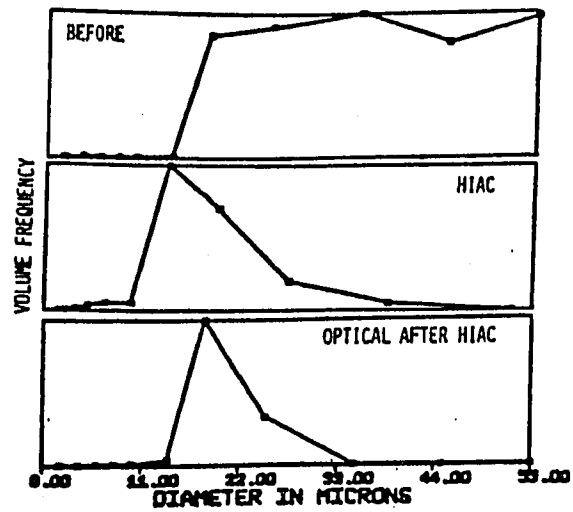


Figure 52. Size distribution for kaolinite flocs measured by using a microscope before HIAC analysis (top), by HIAC (middle), and by using a microscope after the floc had passed through the HIAC sensor (bottom)

size distribution data with data generated using a photographic technique (see Figure 53). The sensor used was the 600  $\mu\text{m}$  sensor. Two things in Figure 53 are noteworthy. The first is that the HIAC severely broke the flocculated material. The second is that the floc being counted were significantly larger than the rating on the sensor. One would have anticipated significant floc breakage.

Morris (1983) used a HIAC to measure size characteristics of flocculated kaolinite. The sensor used was reportedly capable of measuring particles from 1 to 300  $\mu\text{m}$ . There was apparently no effort made to check microscopically for breakup. This is interesting because the largest floc measured were less than 50  $\mu\text{m}$  in size. Morris and Knocke (1984) in discussing this work state that, at low temperature, the iron appeared to function more efficiently as a coagulant than alum because it formed large floc which settled more efficiently.

The work by Reed and Mery (1986), and the work by Morris and Knocke (1984) both highlight the fact that the researcher must be aware of the instruments limitations. One measuring device which is available to the researcher for quality control monitoring, which is apparently seldom used, is the human eye. Let's consider the capabilities of the eye as a quality control device. Table 13 lists the resolution limit of the human eye at a standard 250 mm (10 inches), as given by a number of sources.

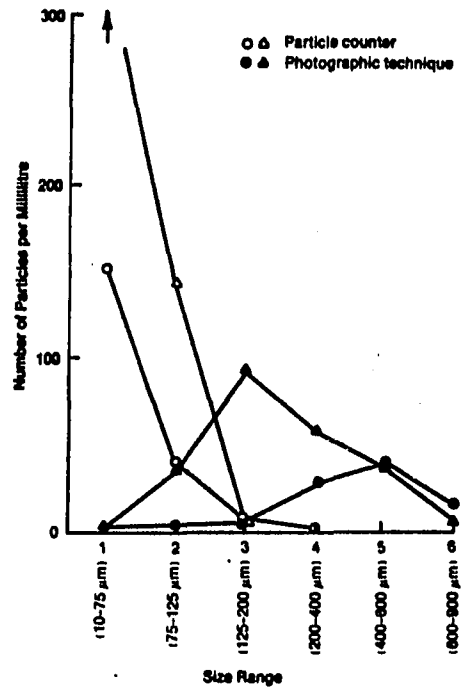


Figure 53. Comparison of floc size distributions as measured by an electronic particle counter and by a photographic technique

Table 13. Resolution limit of the human eye

Source	Resolution limit ( $\mu\text{m}$ )
Beck, 1924	169
Needham, 1958	127
Slayter, 1970	100
James, 1976	70
Rossauer, 1981	101
British Standard, 1984	75

James (1976) explains that under ideal conditions the resolution limit of the human eye at 250 mm is 70  $\mu\text{m}$ . This is usually reported as 100 to 200  $\mu\text{m}$  to account for non-ideality. If one can focus on an object closer to the eye than 250 mm, the resolution is improved. Under ideal conditions a myopic teenager can resolve 20  $\mu\text{m}$  at 50 mm, but this is extremely unusual. The average point of nearest focus for a human changes as a person ages. Average values are; 70 mm at 10 years old, 200 mm at 40 years old, and exceeding 250 mm between 40 and 50 years old. Based on this a maximum floc size of 50  $\mu\text{m}$  would not be visible for most people, and would certainly not be called large by anyone. This, for instance, would lead one to suspect that Morris (1983) may have been experiencing floc breakup without being aware of it. It is very possible that the data presented by Morris (1983) and Morris and Knocke (1984) were more indicative of floc strength, than of the equilibrium size distribution.



Automatic image analysis

It is clear that breakup is a serious concern when using an electronic particle counter, and yet it appears that few investigators verify their results optically. It is interesting that Treweek (1979), after recognizing the potential for floc breakup in an electronic particle counter, verified his results with another electronic particle counter, stating:

"Despite these recognized limitations the resulting particle counts and sizes were comparable to those achieved electronic particle counting and sizing, which unfortunately suffers from similar defects"

It is obvious that the electronic particle counters which are commonly used to count and size flocculated material should be evaluated for floc breakup. If one is to evaluate particle counting instruments, one must have a standard against which to measure their performance. It is widely recognized in fine particle literature that the microscope is the yardstick by which all particle measuring systems should be measured (Murphy, 1984; Herdan and Smith, 1963; Allen, 1981; Yamate and Stockham, 1977; British Standard 3406, 1984; ASTM E 20-85, 1985; Kavanaugh et al., 1980). Kavanaugh et al. (1980) called the optical microscope an "essential technique" for the calibration of other methods. Groves (1980) said: "sizing particles with the microscope must be considered the only absolute method because the operator is directly involved". A number of researchers have reported using the microscope to calibrate particle counting instruments or to check for floc breakage (Pandya and Speilman, 1983;

Swift and Friedlander, 1964; Tekippe and Ham, 1970; Birkner and Morgan, 1968; etc.). Other researchers (Hahn and Stumm, 1968b; Camp, 1968) have simply elected to put up with the tedium of using the microscope to gain the added confidence in their data.

Particle counting and measuring techniques using the optical microscope also have limitations. The techniques main strength, operator involvement, is frequently also its main weakness. Problems which may arise due to operator involvement stem from:

- o judgement errors in estimating size,
- o operator fatigue and boredom,
- o operator confusion when a large number of particles are present in a field of view,
- o time requirements.

Because of these potential problems a number of fairly detailed standards have been developed for doing microscopic counting, e.g., British Standard 3406:Part 4, 1984; ASTM E 20-85, 1985; ASTM F 312-69, 1986. These standards, in large part focus on minimizing the human error involved in counting and measuring particles.

An option which has recently become available due to technological advances is fully automated image analysis (AIA) coupled with the light microscope. In AIA the operator selects the field to be counted, adjusts the image focus and contrast, and the instrument

then does all of the counting and categorizing without further operator interference. Through the use of AIA the first three problems listed above are eliminated (Graf, 1977), and the fourth is greatly reduced as a concern. Kavanaugh et al. (1980) estimated 4 to 8 hours per sample for optical microscope analysis. Through the use of the AIA this is reduced to approximately 0.5 to 1 hour per sample. This compares to 10-45 minutes per sample with an electronic particle counter, depending on the sample preparation involved (Kavanaugh et al. 1980).

Like electronic particle counting, light microscopy has its limitations. As noted by Kavanaugh et al. (1980), because the samples analyzed are small there must be a certain minimum concentration of particles per ml in the original sample for this technique to be practical. Kavanaugh does not give a specific lower limit. Table 14 contains sampling guidelines which have been extracted from the literature.

Allen (1981) gives the percentage standard error of the mean size in a number distribution as  $100/(n)^{0.5}$ , where n is the number of particles measured. He states further that for particles containing a narrow range of sizes, this equation may be quite conservative. Murphy (1984) states that if 10 percent of the particles are in a single size class, and 0.5 percent accuracy is desired, 400 counts will probably be required. ASTM E 20-85 (1985)

Table 14. Light microscope sample size requirements

Source	Counts required	Accuracy specified
Lieberman, 1984	100	+/- 10 %
	1000	+/- 3 %
Allen, 1981	600	statistically accurate
British Standard 3406:Part 4, 1984	Minimum 625	2%
ASTM F312, 1986	100 total	
Murphy, 1984	100 in mode 10 in each class important to the shape of the PSD	
Yamate and Stockham, 1977	Minimum 100 25 in mode 10 in each class	
Harwood, 1977	300-500	quantitative

suggests the standard uncorrected 95 percent confidence interval shown in the following formula, for n less than 30.

$$\ln \bar{D} - 1.96 \ln \sigma/(n)^{0.5} < \ln \bar{D} < \ln \bar{D} + 1.96 \ln \sigma/(n)^{0.5}$$

- D - mean size in a log normal distribution
- $\sigma$  - standard deviation about the log mean
- n - number of particles measured

The guidelines from ASTM F312 (1986) given in the previous table, state explicitly that the guidelines are applicable to both size distribution and number concentration. The other guidelines do not state explicitly that they are valid for determining number concentration.

The sample cell used to hold the sample being counted, usually has a depth which is deeper than the microscope objectives depth of field. It is important to allow the small particles time to settle to the bottom of the cell (a uniform focal plane), before one counts the particles. Hahn and Stumm (1968b) reported loading sample cells, and then immediately taking photographs of the samples. The photographs

were then analyzed. This technique has potential to seriously undercount the small particles.

Another limitation which must be considered is the resolution limit of the measuring system, which in this case includes the light microscope and the AIA. The following table, Table 15, represents suggested practical ranges of application for the light microscope. The guidelines in Table 15 are based on a large number of practical considerations, and do not necessarily represent an absolute limitation of the hardware.

Table 15. Suggested range of usefulness for the light microscope in measuring particle size distributions

Source	Range ( $\mu\text{m}$ )	Practical limitation ( $\mu\text{m}$ )
Groves, 1980	1-1000	2
Treweek and Morgan, 1977	0.2-400	
Allen, 1981	0.8-150 <sup>a</sup>	
Murphy, 1984	0.8-20 <sup>a</sup>	
Harwood, 1976	0.5-100	

<sup>a</sup> Above this size limit the authors recommended use of a magnifying glass.

There is, however, a real lower limit to the resolving power of the optical light microscope. This lower limit is set by the size of the Airy disk produced by a given lens (Rossauer, 1981; Abramowitz, 1985; British Standard 3406, 1984). As light from a point on an object being imaged, is passed through a lens it is diffracted, and a spot

(or disk) is formed on the other side of the lens (Rossauer, 1981; Abramowitz, 1985). This is called point to spot imaging (Rossauer, 1981). The higher the numerical aperture of a lens, the shorter the wavelength of the light passing through the lens; and, the more highly corrected the lens is the smaller the Airy disc produced. The diameter of the Airy disc can be calculated as follows (Rossauer, 1981; Abramowitz, 1985):

$$d = \frac{0.61 \lambda}{\text{N.A.}}$$

Where:

- d - Airy disc diameter in  $\mu\text{m}$
- $\lambda$  - wavelength of light in A
- N.A. - Numerical Aperture of the lens or system

The diameter of the Airy disc produced, very closely approximates the optical resolution of the system. This is sometimes called the systems resolving power. The optical resolution of the system has been defined as the ability of an objective to separate clearly two points which are close to each other on a specimen (Abramowitz, 1985). The numerical aperture referred to above may be either the N.A. of the objective or the N.A. of the combined optics of the microscope system. The lens aperture is used to calculate the N.A., unless the system aperture is smaller. The numerical aperture for the system depends on both the aperture (N.A.) of the objective and

the aperture (N.A.) of the substage condenser, and can be estimated using the following formula (Abramowitz, 1985):

$$\text{N.A. system} = \frac{\text{N.A. objective} + \text{N.A. condenser}}{2}$$

The following table is intended to give the reader an appreciation for the physical limitation of the light microscope. The Table 16 contains calculated values for the system resolution of the microscope used in this work, as well as the numbers given by Olympus for the same instrument.

British Standard 3406 (1984) specifies that the diameter of the smallest particle examined with any objective should not be smaller than

$$d = 1.5/\text{N.A.}$$

This criteria insures that the diameter of the smallest particle examined will be 5 times the diameter of the Airy disc. It must be recognized that, if a particle smaller than this size is measured, there is a loss of accuracy, and the measurements eventually become more qualitative than quantitative. For a typical 20x objective, British Standard 3406 (1984) recommends a minimum particle size of 3



$\mu\text{m}$ , and a minimum system magnification of 500x.

Table 16. Optical microscope resolving power

Lens Mag.	Lens N.A.	Condenser N.A.	System N.A.	Lambda ( $\lambda$ , $\mu\text{m}$ )	Calc. Res. ( $\mu\text{m}$ )	Olympus Res. <sup>a</sup> ( $\mu\text{m}$ )
4	0.13	0.8	0.46	0.55	2.58	2.58
10	0.30	0.8	0.55	0.55	1.12	1.12
20	0.46	0.8	0.63	0.55	0.73	0.73
40	0.70	0.8	0.75	0.55	0.48	0.48

<sup>a</sup> Olympus's resolution comes from page 16 of the Olympus BHS instruction manual. The above calculations assume that a green monochromatic filter is used.

Another area of concern, in working with a light microscope, is the microscopes limited depth of focus, sometimes called the focal depth. This is the vertical distance between the upper and lower limits of sharpness in the observed image. Some typical values are given in Table 17 (Olympus, 1985).

This limitation can lead to a significant loss of accuracy when performing quantitative measurements on irregular objects whose vertical dimension is larger than the depth of focus.

Table 17. Depth of focus as a function of magnification

Objective lens Magnification	Depth of Focus ( $\mu\text{m}$ )
4	125.4
10	22.1
20	7.6
40	2.7

The last area which impacts the reliability of the measurements is the resolution of the image analyzer. This is obviously going to vary with the hardware and software of a specific system. It should be noted however, that the AIA should have, as a minimum, a resolving power equal to that of the microscope being used as a primary sensor. Figure 54 shows the resolution of the Lemont OASYS AIA as a function of system magnification (Lemont Scientific Inc., 1984).

The basic components of the AIA system are shown in Figure 55. A light microscope is fitted with a video camera. The computer system contains a hardware board called a "frame grabber" which takes the image from the video camera and digitizes it. The digitized image can then be edited from the keyboard, using various additions, subtractions, inversions, and filters. The final edited digitized image is analyzed by the computer system, and the information is stored to magnetic disk for future retrieval.

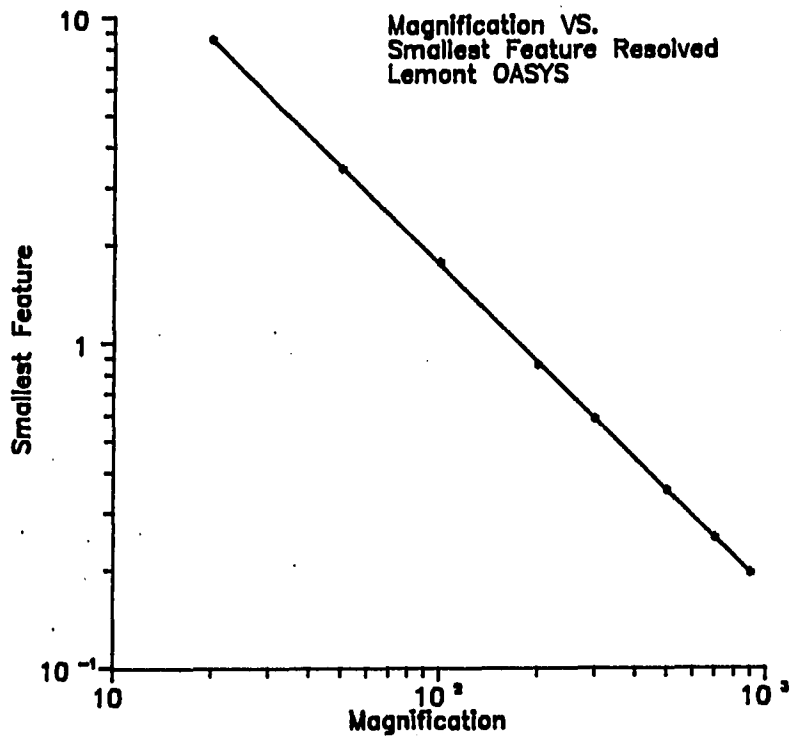


Figure 54. Magnification versus the smallest increment the Lemont AIA can measure, which is roughly equivalent to the smallest feature resolved; log-log plot

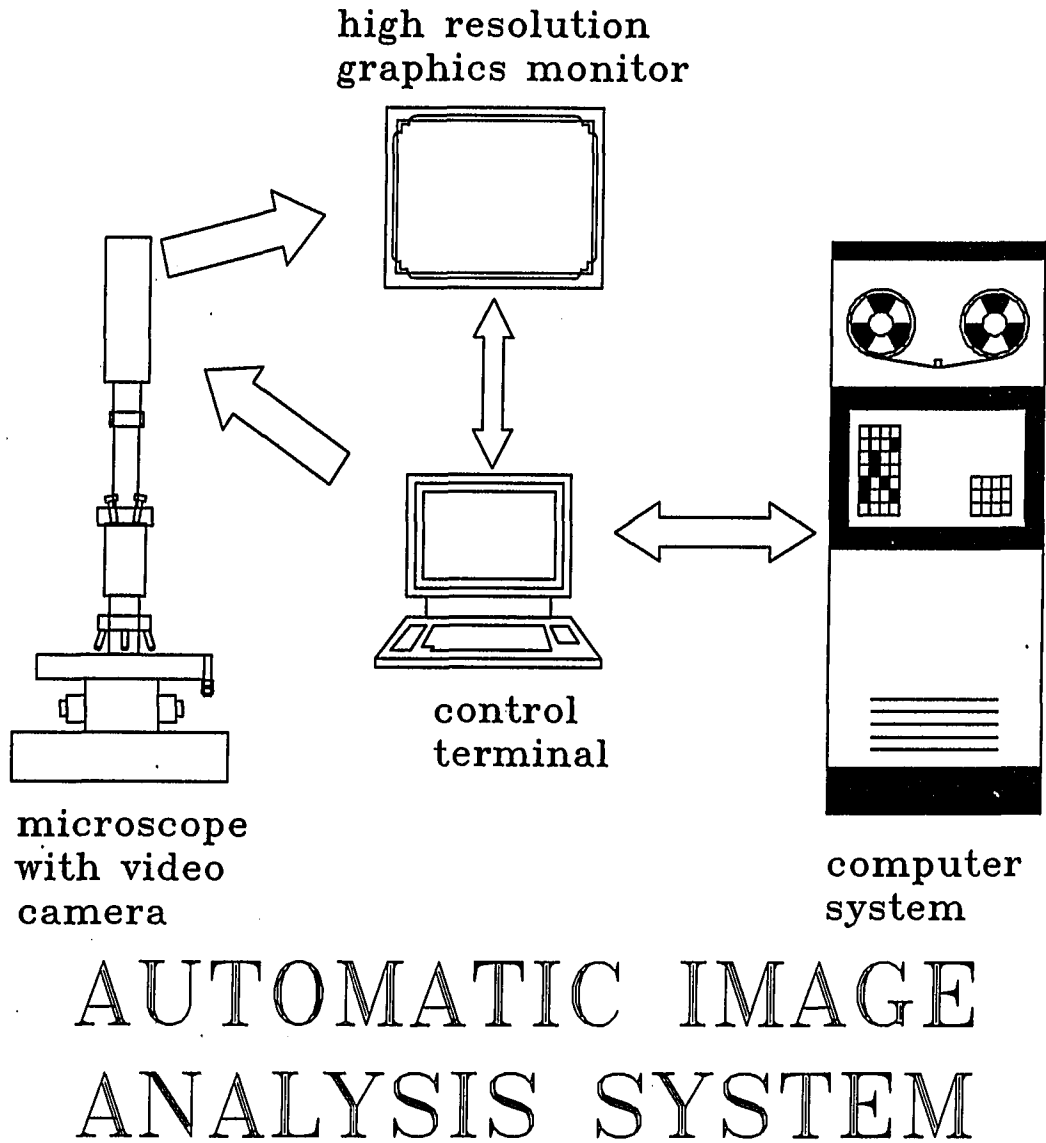


Figure 55. Schematic of the fully automatic image analysis system (AIA)

The computer is only capable of differentiating between intensities of gray. It identifies and measures objects based on the contrast between the object and the background. Typically there are 256 levels of gray, from black at level zero, to white at level 256. Figure 56 illustrates how the image detection operates (Graf, 1977). The height of the pulse is proportional to the gray level, and the width of the pulse is proportional to the object size. The ideal signal, from a contrast point of view, would be a white background, a black object, or vice versa, and distinct edges on the object. This is almost never the case. Usually the background is dark gray, the object is light gray and there is a transition zone of varying shades of gray at the objects boundary, making the edges fuzzy. The operator must select and set a threshold grey level for the image which is representative of the actual object boundary. Once this threshold level is set the AIA perceives a crisp image, and can continue with the analysis of the image.

The analysis is shown schematically in Figure 57. The computer scans the digitized image one line at a time, keeping track of detected points. When a detected point is found on a line the computer looks back at the proceeding line, to see if the point belongs to a previously detected object. This is referred to as "look-back logic". A summary of the object information is placed in the computer file on the line after the last detect point on an object. This summary contains all of the key information for all of the scan

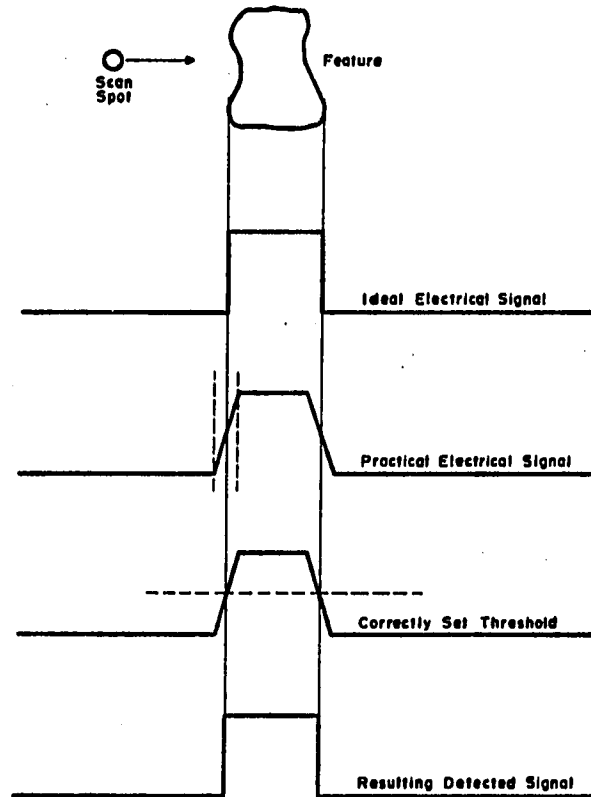


Figure 56. Computer detection of a feature in the digitized image

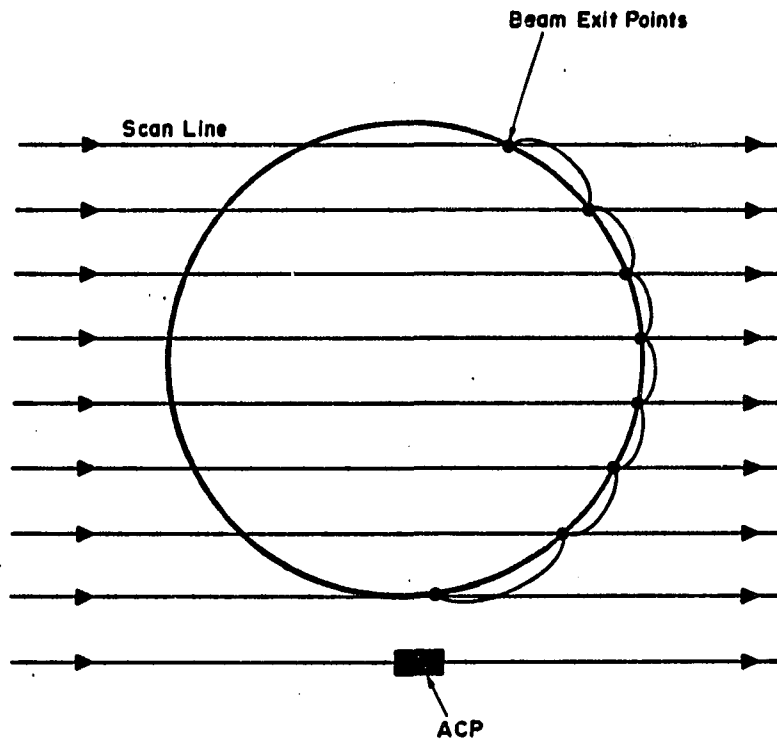


Figure 57. Computer measurement of a feature in the digitized image

lines intersecting the object (Graf, 1977). Based on this information the image analysis software can estimate the projected area, perimeter, angle of repose, length to width ratio, etc., and can divide the particles into classes based on this information. When the physical limitations have been considered, and determined to be acceptable, a number of practical considerations must be dealt with. It is necessary to select a systematic means of randomizing the sample cell to eliminate possible biases in the measuring processes (British Standard 3406, 1984; Murphy, 1984; ASTM E 20-85, 1985; ASTM F312-69, 1986). It is also necessary to consider how the data will be reported. A specific measure of particle size must be selected from the many parameters available, e.g., Feret's diameter, Martin's diameter, Maximum linear diameter, minimum linear diameter, projected area diameter, projected perimeter diameter. The most frequently used diameter is the projected area diameter (Stockham, 1977; Allen, 1981). Allen (1981) notes that the projected area diameter is the diameter most representative of the actual size of the particle. The projected area diameter is the diameter of a circle whose area is equal to the projected area of the particle. This is also called the equivalent circular diameter.

Once the ground rules for collecting the data have been established, one must decide how to best present the data. As pointed out by a number of authors, notably Lawler (1987), and Reed and Mery (1986), the usefulness of the data can be maximized by presenting it in a



format which yields the maximum information with the minimum of effort. If one is interested in the rate at which primary particles are being removed from the size range of inefficient removal (1-10  $\mu\text{m}$ ), the number concentration may be the best way to present the information. If one is interested in maximizing the operation of the sedimentation tanks, or optimizing the length of filter run by producing a specific size of floc, the volume or mass distribution may be the best way to present the data.

Dentel et al. (1986) performed a literature evaluation of the Coulter-type counter, the HIAC counter, and the light microscope. Based on this literature survey it was suggested that neither the Coulter-type counter, nor the light microscope were suitable for routine use in the water treatment process evaluation, but they felt that the HIAC deserved further consideration, based on:

- o Dentel et al. (1986) recommendation,
- o the availability of the HIAC in the laboratory,
- o the recommendation, cited earlier, of the light microscope as the only direct particle measurement technique.

The HIAC and the light microscope coupled with the AIA were both evaluated for use in this work.

## Results from Flocculation Modeling Studies

### Population balance models

Any discussion of flocculation modeling must start with the work of Smoluchowski in 1917. This work dealt with flocculation of micron-sized particles by Brownian motion and laminar shear flow, and did not consider turbulent flocculation. The work of Smoluchowski is still the basis for all population balance flocculation modeling. Many of the assumptions Smoluchowski found necessary are also common to the population balance models currently in use. The following assumptions apply to all of the population balance models discussed unless otherwise stated:

- o the initial particle size distribution is mono-dispersed
- o all particles and aggregates are assumed to be hard spheres
- o aggregates of size  $k$  are formed by the collision of particles of the size  $i$  and  $j$ ,  $(i+j=k)$ , and aggregates of size  $i$  are destroyed by collisions with particles or aggregates of any size
- o a single particle or aggregate is assumed to be the fixed collector and the other particles approach the collector particle and upon contact become permanently attached to the collector
- o During aggregation volume is conserved, so a particle of radius  $i$  and a particle of radius  $j$  form a particle with radius  $k$ . The particle with radius  $k$  will have a volume  $V_k = V_i + V_j$ . This implies that the aggregate density is not a function of radius.
- o no allowance is made for interaction between the particles before contact of the particles

Ernst (1986) gives the Smoluchowski coagulation equation, describing the time evolution of the number concentration, in the following form

$$c_k = 1/2 \sum_{i+j=k} K_{ij} c_i c_j - c_k \sum_{j=1}^{\infty} K_{kj} c_j$$

The variable "c" represents number concentration of particles.  $K_{ij}$  is referred to as the collision kernel. The kernel contains all of the actual physics in the population balance model (Racz, 1986; Jullien and Botet, 1987). This takes care of details such as:

- o how the collision cross section depends on the size and mobility of the aggregating material,
- o the type of flow field driving the flocculation process,
- o and as our understanding grows we may also be able to include information on floc structure in this term (more about this a little later).

Smoluchowski developed equations which represented aggregation driven by two different mechanisms. The first process he investigated is coagulation when the transport due to bulk flow mechanisms is unimportant. This is coagulation due to Brownian motion. If the particles are compact and the driving mechanism is Brownian motion the kernel is

$$K_{ij} = 4\pi D_{ij} (a_i + a_j)$$

$D_{ij} = (D_i + D_j)$ , which is the combined diffusion coefficient for particles i and j. The variables  $a_i$ ,  $a_j$  are the radii of the colliding spheres.

Upon substitution of the kernel into the original equation, the following discrete form of the equation results:

$$dc_k/dt = [kT/3\mu] \sum_{\substack{i=1 \\ j=k-i}}^{i=k-1} c_i c_j (R_{ij}) - [2kT/3\mu] c_k \sum_{i=1}^{\infty} c_i (R_{ik})$$

The first term represents particles growing out of the  $i$  and  $j$  classes and into the  $k$  class. The second term represents particles growing out of the  $k$  class into some other class. The term

$$R_{ij} = (a_i + a_j)(1/a_i + 1/a_j)$$

represents the collision sphere of the interacting particles.

The second process Smoluchowski investigated was coagulation due to bulk flow only. In addition to the previous assumptions this model also assumed that the particles followed the streamlines of the flow field. Smoluchowski assumed a laminar shear field with the form  $\underline{v} = (0, 0, \gamma z)$ . If the particles are compact and the driving mechanism is a laminar shear field the kernel is expressed as:

$$K_{ij} = 4/3(du/dz) A_{ij}^3.$$

The shear gradient,  $du/dz$ , is frequently called  $G$ .  $A_{ij} = (a_i + a_j)$ , which is the collision radius for particles  $i$  and  $j$ , can be re-written in terms of the particle volume of a primary particle.  $A_{ij}$  then becomes  $a_1(c_i^{1/3} + c_j^{1/3})^3$ , where  $a_1$  is the radius of the primary particle and  $i$  and  $j$  are the number concentration of  $c_i$  and  $c_j$  size

particles respectively. Laminar shear flocculation is then described by an equation of the following form:

$$dc_k/dt = [2G/3] \sum_{\substack{i=1 \\ j=k-i}}^{i=k-1} c_i c_j (a_i + a_j)^3 - 2 \sum_{i=1}^{\infty} c_i c_k (a_i + a_k)^3$$

Once again, the first term represents particles growing into the k size class, and the second term represents particles growing out of the k class and into another size class. Without a breakup term in the model, as time approaches infinity, all of the particles will form a single macro-floc. In a situation where the bulk flow is driving the flocculation this will not happen, the floc will reach a maximum size and then break. The maximum size of the floc will be determined by the strength of the particle bonds in the floc and the stress exerted on the floc by the bulk flow. The breakup terms will be the same as the two terms just presented, except that the sign on them will be reversed. That is particles will be growing into the class size due to breakage of larger floc, and particles will be leaving the class size due to break up to smaller floc. Because these models assume a mono-dispersed suspension, neither of them include a differential sedimentation term.

Researchers that followed Smoluchowski assumed that the shear and brownian terms were additive. Swift and Friedlander (1964) developed the population balance equations again from a rigorous theoretical

base, and achieved results which were consistent with those of Smoluchoski. They then showed experimentally that:

- o Brownian and shear flocculation appeared additive
- o Between  $G = 1$  to  $80 \text{ sec}^{-1}$  and time = 0 to 100 minutes, the theory does an excellent job of predicting the coagulation kinetics of a  $2 \times 10^8$  particles/cm<sup>3</sup> suspension of DOW polystyrene latex spheres in a laminar shear flow.

From the brief discussion of Brownian and laminar shear flow flocculation in Schowalter's paper (1982) it is obvious that even these relatively well defined systems are very complex. The difficulty in solving the equations describing the physical system are enormous when more than one of the following factors are included:

- o poly-dispersed particle size distribution
- o hydrodynamic forces
- o colloidal interactions
- o change of the floc structure with floc diameter.

Van den Ven and Mason (1977) went a step further and included hydrodynamic and interparticle forces in the shear flocculation model. Based on their work, they reinterpreted Swift and Friedlander's (1964) data and concluded that Brownian and shear flocculation are not additive. They showed theoretically that the perikinetic flocculation rate was independent of  $G$  and a constant. The orthokinetic flocculation capture efficiency ( $\alpha$ ), due to

hydrodynamic interaction, is not constant, but is a function of  $G$ , and decreases as  $G$  increases. Their interpretation of Swift and Friedlanders data showed  $\alpha$  decreasing by 10 % with an increase of  $G$  from 20 to 80  $\text{sec}^{-1}$ . Theory predicted a reduction in efficiency of 20 percent.

Speilman (1978) brings out a number of interesting characteristics of the Smuluchoski type model by including hydrodynamic and interparticle effects. It is pure serendipity that these two effects tend to cancel each other out. Because of this the perikinetic model gives a very good description of doublet formation. In orthokinetic shear flocculation the situation is more complex, and there are some interesting results:

- o Theoretical results show the frequency of doublet formation not strictly proportional to  $G$ , as predicted by Smuluchowski in the absence of repulsion, but is proportional to  $G^{0.82}$ .
- o When both attraction and repulsion are important, i.e., partially destabilized particles, the possibility exists of a suspension which will flocculate at high (primary minimum flocculation) and low (secondary minimum flocculation) shear rates, and be stable at medium shear rates
- o and, once again, the assumption of additivity of Brownian and shear flocculation are in disagreement with rigorous results.

The effect of hydrodynamic forces on shear flocculation have also been considered by Goren (1971), Honig, Roeberson, and Wiersema (1971), and Adler (1981). Honig, Roeberson, and Wiersema's results

completely agree with those of Speilman. They found that the hydrodynamic interaction reduced the rate of rapid coagulation by a factor of 0.4 to 0.6, depending on the assumed Hamakers Constant.  $G$  values of 3 to  $810 \text{ sec}^{-1}$  were considered. Adler's (1981) work was more theoretical, and more general in nature, but it substantially agreed with the earlier work of Speilman (1978).

Gregory (1986) provided a recent discussion of hydrodynamic effects in shear flocculation, including the following points of interest. For equal size particles, the magnitude of the interaction depends on the particle size and the shear rate. This interaction may result in a factor of 10 reduction in the actual flocculation rate as compared to the rate predicted by the Smuluchowski equation. For unequal sized particles this effect is even more significant. For a  $10 \mu\text{m}$  and a  $1 \mu\text{m}$  particle under shear, the distance of closest approach is predicted by theory to be  $1.4 \mu\text{m}$ . Over this distance normal colloidal forces would not cause flocculation. This  $1.4 \mu\text{m}$  assumes no Brownian motion, solid spheres, and no surface roughness. Relaxing any of these assumptions will reduce the  $1.4 \mu\text{m}$ . Nevertheless, this "hydrodynamic gap" is probably always significant in shear flocculation.

In the turbulent flow environment there is an added degree of difficulty, because the flow field which is driving the flocculation is poorly defined in the mathematical sense. In other words if one



attempts to write a set of equations to define the flow field, one ends up with more unknowns than equations. Since it is not possible to write a closed set of equations which describe the flow field, it is necessary to make some type of simplifying assumption. For instance, it is common to assume that Taylor's hypothesis is valid to facilitate the solving of the coagulation equations. Taylor's hypothesis says that the velocity fluctuations at a single point in space can be imagined to be caused by the whole turbulent flow field passing that point as a "frozen" field (Hinze, 1975). This provides a means of sampling a single point over time and then estimating the turbulence over space. It is also wrong, particularly in the non-homogeneous flow field of a laboratory scale mixed reactor. This is unfortunate since it is a convenient assumption and we do need some means of getting a handle on the flow field.

Camp and Stein (1943) were early leaders in the effort to extend Smoluchowski's work into the turbulent flow region. They took Smoluchowski's solution for the well defined laminar shear flow, and replaced the velocity gradient ( $du/dz$ ) with a root mean square velocity gradient, and called the rms velocity gradient  $G$  for the turbulent flow field. They did this by defining an absolute velocity gradient at a point,  $G_p$ .

$$G_p = [ (du/dy + dv/dx)^2 + (du/dz + dw/dx)^2 + (dv/dz + dw/dy)^2 ]^{1/2}$$

where  $u, v, w$  are velocity components in the  $x, y,$  and  $z$  directions respectively. For a Newtonian fluid this can be reduced to

$$G = (\epsilon/\nu)^{1/2}$$

where  $\epsilon$  is the total energy dissipated/unit time/unit mass, and  $\nu$  is the kinematic viscosity. This expression for  $G$  is then placed directly into the model previously given for laminar shear flocculation to yield a model for turbulent flocculation.

The results of Camp and Stein (1943) are still widely used in flocculator design, and it is noted that they give results which are adequate for design purposes. However, this approach does not provide an adequate tool for pursuing basic research. The main problem with the model is that it does not specifically include many important phenomena which could have an impact on the rate and efficiency of flocculation. Consider for instance some of the following:

- o eddy size distribution and the relationship between eddy size and the transport of floc of various sizes
- o DVOL forces, and the impact of primary minimum flocculation vs secondary minimum flocculation
- o effect of coagulant chemistry and precipitate surface chemistry
- o effect of coagulant and system chemistry on floc strength
- o non-isotropic, non-homogeneous nature of the flow field (ie spatial variation in the flow field)

- o Mechanisms involved in breakup (surface erosion vs fracture), and the dependence of the dominant breakup mechanism on floc size and flowfield characteristics
- o particle and floc size distributions are usually poly-dispersed and frequently multi-nodal
- o particle and floc structure
- o hydrodynamic forces.

Since these effects are not included explicitly in the model, they are all lumped into whatever parameters are used to fit the model to the observed data, such as a sticking factor, and a breakup factor. Because of this it is difficult to determine the importance of the individual phenomenon in flocculation process.

Many attempts have been made to improve on Camp and Stein's generalization of Smoluchowski's model. The following paragraphs will touch on a few of these just to demonstrate the breadth of the research since Camp and Stein.

Speilman (1978) noted that there existed no rigorous analysis accounting for hydrodynamic interactions between particle encounters in turbulent flocculation. He then suggested that his results for laminar shear flow can be used as a first approximation. Even this, however, is non-trivial.

Saffman and Turner (1956) developed a model for turbulent flocculation of rain drops in a cloud. Interestingly enough, even though their model was much more rigorously derived, their model differed from Camp and Stein's model by only a constant. Camp and Stein's model contained a constant 1.333, and theirs contained a constant 1.294. One of the fundamental assumptions made in developing their model was that the particles being flocculated were much smaller than the Kolmogorov micro-scale of turbulence. That would mean that at 25 °C the particles must meet the criteria shown in Table 18 for the model to be valid.

Table 18. G-value and corresponding limiting particle size for the Saffman and Turner model; this size is the Kolmogorov Microscale of Turbulence

G-value	Limiting Size in $\mu\text{m}$
10 $\text{sec}^{-1}$	300
50 $\text{sec}^{-1}$	134
100 $\text{sec}^{-1}$	77

In the context for which the model was developed the particles of interest were one or two orders of magnitude smaller than the Kolmogorov micro-scale. In water treatment the energy input is usually tapered from 100  $\text{sec}^{-1}$  to 20  $\text{sec}^{-1}$ , and the floc can easily be larger than the corresponding micro-scale. The primary particles found in water treatment will usually fulfill this criteria, since they are usually less than 10  $\mu\text{m}$ . This model may have a region of applicability, before large floc have been formed in the reactor.

Delichatsios and Probstein (1975) addressed the issue of floc larger than the microscale, but in order to do so they assumed the existence of the inertial subrange of turbulence. As is pointed out by Spielman (1978), it is very unlikely that the inertial subrange exists in a flocculation system, since it is stirred very gently, and an eddy Reynolds number in the range of  $10^5$  to  $10^6$  is necessary for the existence of the inertial subrange. Delichatsios and Probstein (1975) also compared theoretical flocculation rates for monodispersed and polydispersed suspensions with the same floc volumes, and showed that polydisperseness results in a decrease in the coagulation rate. This means that flocculation models which assume monodisperse suspensions will over-estimate the flocculation rate in most natural systems. It is also noted that in comparing the flocculation rates of the mono- and poly-dispersed suspension, these authors did not consider differential sedimentation. This omission may be very important to the validity of their results.

Lawler et al. (1980) also investigated the difference in treatment plant efficiency between monodispersed and polydispersed systems with the same floc volume. These authors performed a simulation using a Smoluchowski type model assuming additivity of Brownian and shear flocculation. They concluded that the process performance was worse for the homogeneous suspension than for the suspension with a broad particle size distribution.

Hudson (1965), starting from the work of Camp and Stein (1943), made the assumption that the diameter of the floc ( $d_2$ ) are so large that the primary particle diameter ( $d_1$ ) can be safely ignored. From this assumption he then derived a model in which total particle reduction is a function of floc volume.

$$N_t/N_0 = e^{-\phi V G t / \pi}$$

$V$  - Volume of floc/unit volume of water

$N_0$  - suspended matter originally present

$N_t$  - free or unflocculated matter at time "t"

$\phi$  - sticking factor

In Hudson's words "The most significant point is that the rate of entrapment of suspended matter in flocs is dependent upon the volume of the floc, not on the number or size of the floc particles.

Since Hudson developed this model a number of investigators have used it (Camp, 1968; Francois, 1988). It appears that for flocculation in the sweep floc region this model produces good results. In the sweep floc region large metal hydroxide precipitates form early in the flocculation process, and these precipitates tend to dominate the kinetics of the flocculation process. However, in flocculation in the A/D region, the fundamental assumptions upon which this model are based are violated for a significant length of time. For the early

portion of the flocculation process, the number concentration of larger floc is too small to have an impact on the flocculation kinetics. Francois's (1988; Francois and Van Haute, 1983) work is entirely in sweep floc, so it will not be discussed further.

Lawler, Izurieta, and Kao (1983) proposed a model which accounted for flocculation by differential sedimentation as well as by shear and Brownian mechanisms. However, it is hard to know how to interpret the results since the flocculation conditions were quite unusual. Monodispersed latex spheres in extremely high concentrations (200 to 600 mg/L) were flocculated at modest flocculation rates ( $G = 25$  to  $44 \text{ sec}^{-1}$ ) for very long times (15 hours). Due to the unusual materials and conditions, it is hard to know what to make of the end results. Lawler (1989) presented theoretical work comparing the flocculation of mono- and poly-dispersed systems using a similar model. This model also accounted for hydrodynamic interactions and intermolecular forces. Based on theoretical considerations, Lawler demonstrated that, in a poly-dispersed suspension, differential sedimentation becomes the dominant mechanism in many practical systems. He also showed that the shear flocculation mechanism is much less important than traditionally believed.

**Breakup** It is noted that none of the investigators to this point have included breakup in their models. Kim and Glasgow (1986) noted that since neither aggregation or disintegration can be

disregarded in a flocculation tank, both phenomena must be considered by any modeling procedure striving for physical realism. They also asserted that floc susceptibility to hydrodynamic stress effects is largely dependent upon the nature of the coagulant. Lawler, Izurieta, and Kao (1983) considered breakup briefly and then left it out of their model. Speilman (1978) discussed it, and developed the frame work for including it, but took it no further. In Speilman's words:

"The difficult task is to determine the specific form that the breakup function will have in a given situation."

Harris (1966), and Harris, Kaufman, and Krone (1966) presented a really nice piece of work on flocculation modeling including breakup. Unfortunately in order to produce a useable model, it was once again necessary to make a number of simplifying assumptions. The final product looked very much like Hudson's (1965) model, and the verification was all carried out in the sweep floc region. Some of the problems which Harris found insurmountable in solving the general model were:

- o lack of information on the floc breakup mechanism
- o lack of information on the floc structure
- o inability to account for the non-homogeneity of the turbulent flow field in the general rate equation
- o inability to measure the number concentration of the unflocculated primary particles.



The mechanism of floc breakup has long eluded researchers, and in the past 20 years a great deal of effort has been put into this topic.

Hinze (1955) dealt with the fundamental mechanisms involved in the splitting of a liquid droplet in a dispersion process. Hinze discussed three types of deformation mechanisms (e.g., lenticular, cigar-shaped, and bulgy deformation) and their application to 5 different types of flow fields. In lenticular deformation the droplet is flattened forming the shape of a contact lens. The breakup depends on the magnitude and duration of the force applied to the drop. If the magnitude and force are sufficient, the drop forms a torus which then breaks into many small drops. Cigar-shaped deformation forms a prolate ellipsoid, then a long cylindrical thread, and finally the structure breaks up into droplets. Bulgy deformation takes place when the surface of the droplet is deformed locally, due to local pressure differences at the interface. Bulges and protuberances occur, and parts of the drop finally separate. In droplet breakup the effect of surface tension is important. If the deformation is not too large the surface tension restores the drop to its spherical shape. This restorative mechanism is not present in a floc, so some of the concepts presented by Hinze need to be tempered with this consideration. It is none the less important to be aware of Hinze's work, because it provides the basis for much of the work that followed. The dominant mechanism in droplet formation in a

turbulent flow field is a function of droplet size. In droplets equal to or larger than the Kolmogorov microscale, the dynamic pressure forces of the turbulent motion are the factor determining the size of the largest drops. It also appears from the discussion that below the Kolmogorov microscale, the viscous stresses will be the dominant breakup mechanism. This last idea is never explicitly stated by Hinze.

Thomas (1964) studied the turbulent disruption of floc in small particle size suspensions. This work was performed at solid concentrations in excess of 5 percent solids by weight. Thomas mentions the following floc deformation modes which may lead to floc disruption:

- o elongation into prolate spheroids under the action of simple shear (Cigar-shaped deformation),
- o bulbous distortion by irregular dynamic pressures (bulgy deformation),
- o for sufficiently large ratios of floc viscosity(?) to suspending medium viscosity the floc might retain a roughly spherical shape while undergoing rotation and particle rearrangement.

In this last case, according to Thomas, rupture could only occur through the imposition of shear stress across the floc which would exceed the yield stress. The first two cases may work together in a turbulent flow field. The velocity gradient may extend the floc, while simultaneously applied dynamic pressure differences will tend

to disrupt the extended floc. Thomas noted that, floc characteristics must be precisely defined to discuss floc breakup. Thomas's experimental work was performed at such high solids concentrations and velocity gradients that it is doubtful we in water treatment flocculation can draw much insight from his experimental work.

Michaels and Bolger (1962) worked with kaolinite suspensions, and found that floc yield stress was a function of solids concentration. At less than 5 percent solids by weight, the yield stress increased as a function of the solids concentration squared, while at greater concentrations it increased at an even faster rate. The high solids concentrations used in this work probably make the experimental results reported of little value in the current study, but it does point out that floc strength may be a function of solids concentration.

Hannah, Cohen, and Robeck (1967a) performed floc strength measurements using a Coulter counter to break the floc. They flocculated 5, 15, and 50 mg/L kaolinite suspensions with 15 mg/L alum. The dilution water used was distilled water, buffered with 50 mg/L sodium bicarbonate. The floc were formed by mixing the suspension for one hour in a modified couette flow reactor at a G of  $50 \text{ sec}^{-1}$ . The typical pH for this work is given as 7.6, which would indicate sweep floc. They based their strength comparisons on the

particle size remaining after the flocculated suspension was passed through the Coulter counter orifice. The results are as follows:

Alum Dose mg/L as Alum	Kaolinite mg/L	Modal Size ( $\mu\text{m}$ )	Maximum Size ( $\mu\text{m}$ )
15	0	6	9
15	5	8	11
15	15	11	14
15	50	11	14

They also compared the results of holding the clay constant and varying the alum dose; 5, 15, and 25 mg/L. The 5 mg/L dosage (the lowest alum to solids ratio that was tested) formed the largest number of large floc and formed floc better able to resist fragmentation, but the formation rate was quite slow. Floc strength was also a function of pH. Floc were grown at pH values of 7.2, 7.6, and 8.1. The floc grown at 7.2 were the strongest, but took a relatively long time to grow. The floc grown at pH = 7.6 were considered optimal because, although they were weaker, they grew much faster. There was very little flocculation at pH = 8.1. The authors listed some relative forces of attraction which are of interest; Chemical bonds = 50 to 100 kcal/mole, hydrogen bonds = 3 to 10 kcal/mole, and van der Waals forces = 1 to 2 kcal/mole.

Camp (1968) reported on the strength of iron hydroxide floc formed in the sweep floc region (15 mg/L ferric sulfate @ pH = 6.0), in the absence of other particles. The floc were formed and then exposed to

an increased velocity gradient. The size of the particles remaining, as measured using a microscope, indicated the relative strength of the floc. The strength of the floc was quantified by assuming that the surface energy of the floc could be equated with the shearing energy in the water volume occupied by the floc at the point of impending destruction. Camp found that in a blender with a G of  $12,500 \text{ sec}^{-1}$  it was possible to prevent formation of floc larger than  $3 \mu\text{m}$ , and to breakup preformed floc to particles smaller than  $3 \mu\text{m}$ . Camp estimated that the floc strength of the flocs interparticle bonding was on the order of  $4.8 \times 10^{-8} \text{ kcal/mole}$ . If one assumes that the van der Waals attraction is on the order of  $1 \text{ kcal/mole}$ , then we are dealing with a bond 100,000,000 times weaker than a van der Waals bond. He notes that the particle bond strength is probably underestimated due to the non-homogeneous nature of the turbulent flow field, nevertheless, the estimate will serve as an indicator. Assuming spherical floc and a constant value of interfacial tension, the maximum floc size should vary inversely with the mean velocity gradient in the reactor. The theoretical and actual data are presented below:

G Sec <sup>-1</sup>	Theoretical Max Floc Size ( $\mu\text{m}$ )	Actual Max Floc Size ( $\mu\text{m}$ )
500	240	160
3,800	31	<3
12,500	9	<3

Camp suggested that the deviation of the actual from the theoretical was due to the decrease in interfacial tension as the floc become larger and trap more water. This would suggest that the effects of floc structure are significant.

Tomi and Bagster (1977) looked at the theoretical considerations in turbulent agitation. They note that floc rupture by instantaneous pressure differences on opposite sides of the floc is only theoretically valid for floc in the size range where inertial effects dominate. That is for floc larger than the Kolmogorov microscale. For smaller aggregates, viscous effects are significant, and breakup may be due to local velocity gradient effects at the floc surface. The results for turbulent breakup in this size range are analogous to the results for simple shear flow. He also noted that floc disruption due to the interstitial flow is not reasonable because interstitial flows have been found to be very small by other workers.

Boadway (1978), working with alum and clay, noted that if the strength of the bonds between particles is independent of size, and the equilibrium floc size is shear rate dependent, then there must be structural differences in the larger floc. Their photographic evidence shows that the larger the floc, the more tenuous the bonds become, with evidence of weak spots.

Tambo and Hozumi (1979) plotted log of max floc diameter vs log energy dissipation, in a clay-aluminum floc system. These plots were linear over the pH range investigated; pH = 6.5 to 8, exhibiting increasing size with decreasing energy dissipation. The Kolmogorov microscale was also plotted. As the pH increased the maximum floc size also increased. At a pH level of 6.5, the maximum floc size was below the microscale over most of the mixing intensity range. All of the maximum floc diameters were close to the microscale, so the authors assumed that the conditions of the viscous subrange of isotropic turbulence held. According to previously reviewed work, this would imply failure due to viscous forces.

Matsuo and Unno (1981) performed a theoretical study of forces acting on floc and then verified the results using alum and clay at a pH of

7. They drew the following conclusions:

- o surface shear is the predominant floc rupture mechanism, not density differences between the floc and the surrounding fluid.
- o based on floc strength analysis, the optimum coagulant dosage is smaller than the dosage which produces minimum residual turbidity.

Pandya and Speilman (1983) studied the breakup characteristics of a kaolinite and ferric hydroxide floc system over a range of G values (60 to 400  $\text{sec}^{-1}$ ). Over this range, the average number of daughter

floc resulting from a floc breakup was 2.5. It was hypothesized that this number would increase slowly as the floc diameter increases.

Glasgow and Hsu (1984) performed a breakup study using kaolinite and a polyacrylamide. The system was flocculated for 20 minutes at a  $G$  of  $53 \text{ sec}^{-1}$ , then for three minutes the flocculation intensity was increased to  $224 \text{ sec}^{-1}$ . The increase in mixing intensity did not cause an increase in the number of primary particles, but it did cause a decrease in the number of large particles. Based on this, the authors concluded that the floc has a multi-level structure, and rather than being broken down to primary particles it is being reduced to first or second level aggregates.

Francois and van Haute (1983), working in an alum-kaolinite system, determined that the floc had a four level structure. The structure consisted of primary particles, flocculi (small floc), flocs (made of aggregate flocculi), and floc aggregates. Each level above the primary particles is a little bit weaker. When the mixing intensity in the reactor is increased the flocculated material will break until a floc structure is reached which has sufficient strength to stand the stress.

Clark (1985a), working in an idealized liquid-liquid system, presented evidence that breakup occurs only in the near region behind the impeller, and does not occur in the bulk of the flowfield.



Models including breakup      A number of investigators have attempted to include breakup concepts in their modeling efforts.

Argaman and Kaufman (1968,1970) sought to include breakup in their model through the surface erosion mechanism. Their data did suggest that the breakup experienced was consistent with the viscous dissipation subrange. This, however, does not necessarily imply surface erosion. They also tried to incorporate the effect of the turbulent structure in their model by relating the turbulent energy spectrum to an effective turbulent diffusion coefficient for the particles. The experimental verification was performed in the sweep floc region using 25 mg/L of alum and 25 mg/L of kaolinite.

Ives (1978) and Ives and Bhole (1973) introduced breakup by floc rupture into their flocculation model. They arbitrarily limited the floc diameter to 49 units, and then using computer simulation explored the impact of various breakup rules. The following breakup rules were considered:

- 1      growth beyond 49 restricted by not allowing collisions to occur which would result in a combined size greater than 49
- 2      aggregates which form and exceed 49 are immediately broken into two equal parts and returned to the flocculation process
- 3      same as 2 but broken into 3 equal parts
- 4      same as 2 but broken into 4 equal parts.

It is interesting that the different breakup rules had a major impact on the equilibrium particle size distribution and on the process kinetics. The various breakup rules lead to the following limiting sizes (by limiting size Ives refers to the mode of the PSD):

Breakup Rule	Limiting Size (units)
1	49
2	36
3	21
4	18

Ives could give no explanation for these limiting values. The breakup rules not only provided progressively smaller sizes, but also provided progressively better primary particle removal. The kinetics of a polydispersed (trimodal) system, were also simulated and showed very little difference from the monodispersed system. A simulation was also done in which contacts were restricted to a particles of similar size;  $0.8 < r_i/r_j < 1.25$ . This resulted in poorer flocculation, with an increase in the number of particles remaining in the  $i-1$  to  $10 \mu\text{m}$  size range.

Ives and Dibouni (1979) attempted to verify experimentally the simulation results of Ives and Bhole. They presented a number of interesting results. Up to a  $G$  of  $10 \text{ sec}^{-1}$  both perikinetic and orthokinetic flocculation are important. The perikinetic data fit the theoretical model well. The orthokinetic data are qualitatively

in agreement with the theory; higher velocity gradients and more time produce more flocculation. The authors, however, felt that quantitative comparisons would have to wait for better data on floc structure, specifically porosity relationships.

Flow field homogeneity Tambo and Hozumi (1979) stated that because of the uneven energy distribution in the reactor, referring to the high energy dissipation rate in the vicinity of the impeller, only 10 to 20 percent of the energy put into the reactor is available for flocculation. They accounted for this in their modeling by multiplying  $\epsilon$  by 0.10 to 0.20, and calling it the "effective mean rate of energy dissipation".

Koh, Andrews, and Uhlherr (1984) addressed the non-homogeneous nature of the turbulent flow field in modeling orthokinetic flocculation. They did this by modeling the flocculation of a fully destabilized suspension in a compartmentalized reactor. The reactor was divided into a number of compartments and a volume averaged shear rate was used to model the flocculation process. Using energy dissipation values from the literature, they considered 2, 3, and 30 compartment models. The various multi-compartment models all gave very similar results, therefore it was concluded that there was little advantage in considering more than two compartments (impeller region and bulk flow region). The authors made a number of noteworthy points. In general, the collisions of particles from 1 to 20  $\mu\text{m}$  are invariably

caused by laminar shear mechanisms, even though the general flow field may be turbulent. Perikinetic flocculation is only significant for particles less than  $1 \mu\text{m}$  in size (S.G.=2.5) in a shear field with a  $G$  of less than  $10 \text{ sec}^{-1}$ . The effective mean shear rate for flocculation is not the same as the mean value obtained from power dissipation per unit mass ( $\epsilon$ ), but is equal to the volume average value obtained from the first moment of the shear rate distribution. This quantity is highly dependent on the system geometry. Experimental results indicate flocculation efficiency in a couette flow reactor and in a stirred tank reactor are comparable if the effective mean shear rates are used.

Koh (1984) took the compartmentalization concept a step further by considering partially destabilized suspensions. These partially destabilized suspensions require some minimum shear rate ( $G_{\text{crit}}$ ) before flocculation can occur. In a compartmentalized stirred tank, there will be areas where the shear rate is high enough to cause flocculation even though  $G_{\text{ave}}$  is less than  $G_{\text{crit}}$ . Flocculation rate data for the couette flow and stirred tank reactors deviate at low  $G$  values. The deviation is the result of high shear rate regions, near the impeller of the stirred tank, which exceed  $G_{\text{crit}}$ . These regions are absent in the couette flow reactor.

Kim and Glasgow (1986) also used a two compartment model. They assumed that flocculation occurred in the total tank volume, but breakup only occurred in the impeller region.

### Structural Models

All of the models previously discussed have been modifications of the kinetic model proposed by Smoluchowski. Each of the researchers has fine tuned the coagulation kernel to account for some aspect of physical reality. The fact that the kernel in this model contains all of the physics leads to some problems. Jullien and Botet (1987) state:

" The main problem with Smoluchowski's formalism is that all of the physics is entirely contained within the  $K_{ij}$ , and thus, as long as we do not get any precise idea on their  $i$ - and  $j$ - dependence, we will certainly play with very interesting mathematical games, but without any obvious link to reality."

By 'their  $i$ - and  $j$ - dependence' the author is referring to the transport and structural interaction relationships between the  $i$  and  $j$  size entities. Thus, it is necessary to go beyond simple kinetic relationships based on conservation of volume and the mean field theory approximation. It is necessary to incorporate transport mechanisms and floc structure into our thinking.

It is noted that in all of the attempts to fine tune the population balance model for turbulent flocculation, mentioned above, it was

necessary to make simplifying assumptions, or somehow compromise the equations to achieve a solution. These compromises and simplifications are probably inevitable as long as the problem is being attacked using the population balance approach.

I believe that the analytical approach to population balance modeling will continue to yield valuable information, but it needs to be supplemented by additional research tools. The kinetic models assume that the flocculating particles are spheres which, upon sticking, coalesce to form a larger sphere. This denies the importance of the floc structure, and yet we know that the structure is important. If the density of the floc changes with size, or the ability of the particles to penetrate the floc changes with size, the process kinetics can be greatly effected. Gregory (1986) noted that these structural considerations can have a large influence on the processes which follow flocculation, i.e., sedimentation and filtration. A number of researchers (Koh, Andrews, and Uhlherr, 1987; Tambo and Watanabe, 1979a, and 1979b; Lagvankar and Gemell, 1968; Boadway, 1978) have recognized that floc structure needs to be considered. These authors attempted to incorporate floc structure into their models by identifying a mathematical relationship which would relate floc density and floc radius.

Early attempts Lagvankar and Gemell (1968), early pioneers in this attempt to incorporate structural information into the

Smoluchowski model, used the Vold model. This model gave qualitatively reasonable results, but wasn't ideal. A three level floc structure was observed in the laboratory, and the Vold model wasn't capable of accounting for more than a single level structure. The authors recognized that the Sutherland model, which could accommodate the multi-level structure, was probably superior to the Vold model, but at that time it did not have a functional form which allowed easy inclusion into the kinetic model. Boadway (1978) followed Lagvankar and Gemmell's lead and incorporated the Vold model into the kinetic equations.

Tambo and Watanabe (1979a, and 1979b) also recognized the superiority of the Sutherland model, but had difficulty in formulating a convenient mathematical expression. They responded to this by formulating a primitive cluster-cluster aggregation model, which is conceptually similar to the more sophisticated models of Meakin (1986a, 1986b, 1985, 1984, 1983a, and 1983b), Kolb (1986), Kolb et al. (1986, and 1983). In verifying their diameter density relationship they concluded that floc density (alum/kaolinite system) was independent of the following factors:

- o type of aluminum coagulant used; alum vs polyaluminum chloride @ 20 °C
- o agitation intensity (40 to 80 rpm in a non-standard reactor; breakup was not dominant)
- o alkalinity

o flocculant aids

From this one must conclude that the floc structure is dominated by the particle transport mechanism. The alum dose did have a significant impact on the floc strength.

Present Modeling Efforts      These attempts at including aggregate structure were performed without knowledge of the veritable explosion of structure information being generated by the theoretical physics community. Mandelbrot (1983) really kicked the whole thing off by making the world aware of fractals, or perhaps more specifically, fractal geometry. This is really what Lagvankar, Gemell, and the others were looking for. They were equipped with all of the tools needed to deal with Euclidian concepts, but floc are by their very nature non-Euclidian. They are instead random fractals.

Let's step back a moment and define some terms. The Smoluchowski model assumes that when two spheres of sizes  $i$  and  $j$  contact, they form a single sphere of size  $k$ , and volume is conserved. This is what the theoretical physicists call a compact or non-fractal structure. The density of the object is constant at all scales. What exactly is a fractal? Mandelbrot (1983) defines a fractal as a set "whose Hausdorff dimension is a fraction or otherwise exceeds their topological dimension". This exact definition is of little practical use to an engineer. La Brecque (1987) states "the fractal



dimension of an object, usually a non-integer or fractional value, is a measure of the extent to which it (the object) fills the space in which it is embedded." This is a friendlier definition, but it still makes it difficult to see the power of the concept.

Let's look at a more intuitive definition. Consider (Gregory, 1986) a plot on a log-log scale of a characteristic length (diameter; x-axis) of an aggregate versus the number of particles in the aggregate (floc mass; y-axis). The slope of this log-log plot represents the fractal dimension of the aggregates. If the floc is a perfect sphere, the fractal dimension and the Euclidian dimension will be equal, and both dimensions are 3. However, for an aggregate, a plot of this type typically yields a slope substantially less than 3, which indicates that the objects density decreases as the diameter increases. Thus the fractal dimension will be less than the Euclidian dimension.

Gregory calculated the fractal dimension for some of the alum floc data of Tambo and Watanabe (1979a). The fractal dimension ( $d$ ) of these floc was 1.7 in 3 dimensional space. Feder (1988) reports the fractal dimensions of a number of real life aggregate systems including; gold colloids with  $d=1.71$  in 3 dimensions; silica clusters with  $d=2.12$  in 3 dimensions. We can tell a little something about the geometry of the floc by simply looking at their fractal dimension. Two of the natural systems mentioned have a fractal

dimension of less than 2 in a 3 dimensional space. Feder (1988) states that, if a fractal object has a 3 dimensional fractal dimension  $>2$  and it is projected in 2 dimensions, it will appear compact. If an object has a three dimensional fractal dimension  $<2$  and it is projected in 2 dimensions, its projected image will have an open or non-compact structure. Thus, if the floc have a fractal structure, we should be able to inspect the floc, and look at the simulated floc produced by the various models and determine which of the simulation models appears most appropriate. Gregory (1986) has suggested that applying these concepts to modify the Smoluchowski theory would be worthwhile.

Let's review some of the simulation models and see how they compare to what we know about orthokinetic flocculation.

There is a great deal of work on this topic from the area of theoretical physics. The interested reader is referred to: Meakin (1985); Kolb, Botet, and Jullien (1983); Meakin (1983a and b); Meakin (1984); Meakin (1986a and b); Kolb et al. (1986). The information presented here reflects material presented in the above references, but follows most closely the presentation by Jullien and Botet (1987).

All of the structural models are based on computer simulation techniques. These computer simulations can be broken down into two

main classes; particle-cluster aggregation (PCA) and cluster-cluster aggregation (CCA).

The PCA models are conceptually similar to the Smoluchowski model in that they have a fixed collector and stick irreversibly. The mechanism involved in the particle approaching the collector dictates the structure of the aggregate.

The PCA models most frequently used are given in Table 19 along with their aliases and the type of particle trajectory used in the model.

Table 19. Common particle-cluster aggregation models

Model Name	Alias	Trajectory
Witten-Sanders	Diffusion limited aggregation (DLA)	Brownian
Eden	Chemical	Brownian W/ limited prob- ability of sticking
Vold	Ballistic	Linear W/ random impact parameter Linear W/O random impact parameter

Because each of the PCA models currently in use can be viewed as a variant of the DLA model, the DLA model will be discussed first. The DLA model assumes a fixed collector particle which is approached by other particles driven by Brownian motion. If the particles come in

contact with the collector particle, the probability of sticking irreversibly is 1. The Brownian motion is simulated using a random walk. Figure 58 illustrates the mechanics of a typical random walk simulation (Meakin, 1986a). A particle is released from a randomly selected point on the middle ring of the three rings in the figure, this is sometimes referred to as the launch ring. The particle is then moved in randomly selected directions until one of two things happens. The particle may move outside of the outer ring. If it does this, it is considered infinitely far away with a zero probability of coming in contact with the collector, and is "killed". This other ring is sometimes called the kill ring. The other alternative is for the particle to land on or occupy a site adjacent to the collector particle. If this happens, the two are irreversibly bonded, and the collector particle becomes a collector cluster. This process simulates the Brownian diffusion of a particle in water. Many of these particles are released during the course of a simulation.

If the random walk trajectory is kept, and we change the probability of sticking from 1 to something approaching 0, we get the Eden model. This model is also called the chemical model because it acts as if there is a barrier to sticking. This barrier to sticking can be thought of as a partial screening, similar to an activation energy in some chemical reactions. Physically, in terms of flocculation, one can think of the DLA model as representing perikinetic

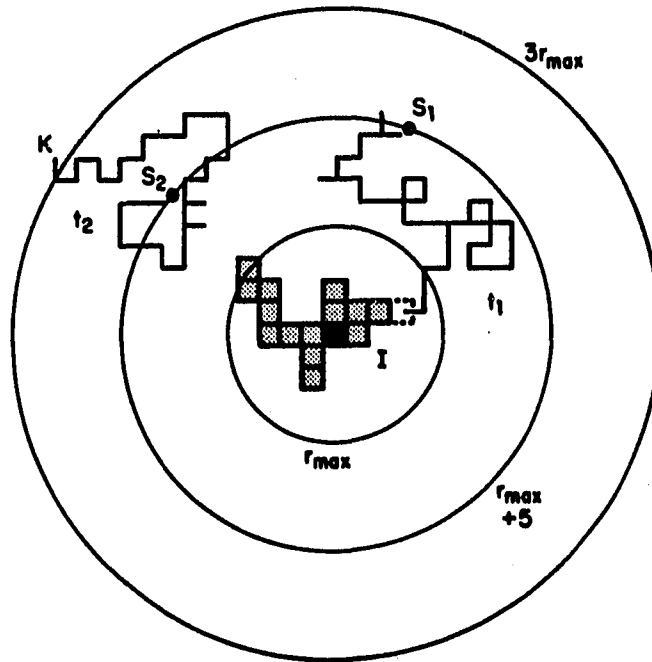


Figure 58. Simulation of a two-dimensional Witten-Sander aggregate using a square lattice. The two particle trajectories ( $t_1$  and  $t_2$ ) start at random points on the "launching circle" which has a radius of  $r_{\max} + 5$  lattice units where  $r_{\max}$  is the maximum radius for the cluster. Trajectory  $t_1$  reaches an unoccupied interface site and growth occurs into this site. Trajectory  $t_2$  reaches the  $3r_{\max}$  "kill ring" and is retired from the simulation

flocculation with little or no repulsive barrier, and the Eden model as representing a large repulsive barrier.

In the Vold model (Ballistic) the probability of sticking is again set at 1, but the trajectory is now linear. A particle is launched from a randomly selected point on the launch ring and follows a randomly oriented linear path. If the particle comes in contact with the collector, it sticks irreversibly. The randomly selected angle of launch is called the impact parameter. In a linear trajectory without impact parameter, all trajectories must pass through the origin. It is noted that the collector particle is located at the origin.

The 2 and 3 dimensional structures which result from these PCA models are shown in Figures 59 and 60. It is noted that, if the simulation is carried out long enough, all of the models presented here except the DLA will produce a compact structure, i.e., non-fractal. The Vold model, due to small scale simulations, was originally thought to have a 3 dimensional fractal dimension of 2.3. It is now known to have a fractal dimension greater than 2.8, and it is probably equal to 3 (Meakin, 1986b; Jullien and Botet, 1987).

La Brecque (1987) Quotes Paul Meakin:

"It is clear that the Witten-Sanders model is just not the way real colloids aggregate. Rather than occurring at a single growth site to which particles are added one at a

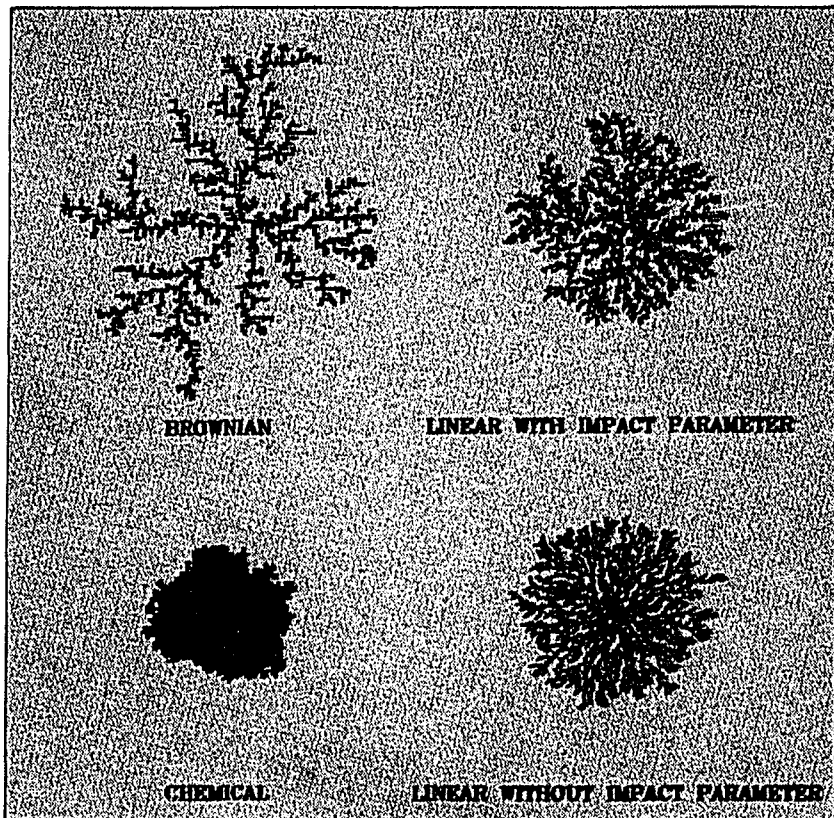


Figure 59. This is an illustration of the influence the particle trajectory has on the resulting shapes of the clusters obtained by particle-cluster aggregation processes in two dimensions. To give an idea of their relative size, all of the aggregates have the same number of equal sized particles (4,096). Only the Witten-Sanders (Brownian) aggregate is fractal

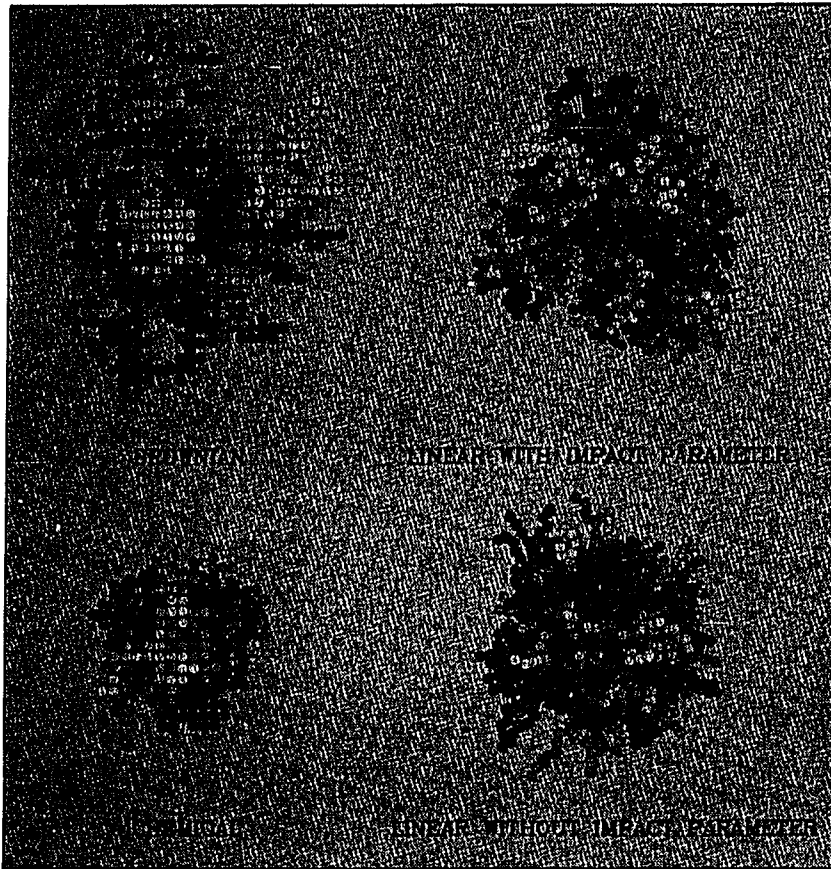


Figure 60. This is an illustration of the influence the particle trajectory has on the resulting shapes of the clusters obtained by particle-cluster aggregation processes in three dimensions. To give an idea of their relative size, all of the aggregates have the same number of equal sized particles (4,096). As in two-dimensions, only the Witten-Sanders (Brownian) aggregate is fractal. However, since its fractal dimension is larger than two ( $D \approx 2.5$ ), it looks compact in projection



time, the aggregation process is going on all over the place. You start to form small clusters, and the small clusters combine to form larger clusters and they combine to form still larger ones."

This is the essence of simulating cluster-cluster aggregation (CCA). The first CCA model was developed in 1957 by Sutherland (Meakin, 1986a), but without the unifying concept of fractal geometry it lay virtually unused until 1983. In 1983 two research groups, Meakin (1983a) and Kolb, Botet, and Jullien (1983), rediscovered the model independently of each other and of Sutherland. The model starts with an ensemble of single particles. Pairs of the particles are launched from the launching ring. If they aggregate before one of them passes the kill ring, the aggregate is placed into the ensemble as an entity to be launched. If the particles do not aggregate, they are placed back into the ensemble to be selected again as primary particles. Eventually one ends up aggregating aggregates. This is the original CCA model, and is referred to as a hierarchial aggregation model. All of the trajectories and sticking probability combinations discussed under the PCA models also apply here.

A CCA box model was also developed (Meakin, 1986), in which all of the particles are placed randomly on a lattice. The particles are then selected at random and moved. The aggregation process is carried out as long as desired, or until all of the particles are contained in a single aggregate. The two CCA techniques produce the same aggregate characteristics.

Figures 61 and 62 show the structures formed by the different CCA models. Their fractal dimensions are shown in Table 20.

Allowing clusters to rotate as well as translate has no measurable impact on the fractal dimension, as long as the rate of rotation is within realistic bounds.

The simulation models discussed above are comparable to the Smoluchowski type models for Brownian motion and shear flocculation

Table 20. Common cluster-cluster aggregation models and their fractal dimensions

Model Name	2-Dimensional	3-Dimensional
Brownian	1.44	1.78
Chemical	1.55	2.04
Ballistic	1.51	1.91
Ballistic W/O		
Impact Parameter	1.56	2.06

without a breakup term. All of these simulation models have assumed that the aggregation is irreversible. As previously mentioned this is not a valid assumption for flocculation in a turbulent flow field.

Meakin (1985, 1986b) and Kolb (1986) have both carried out simulation studies dealing with the effect of reversibility on the nature of the

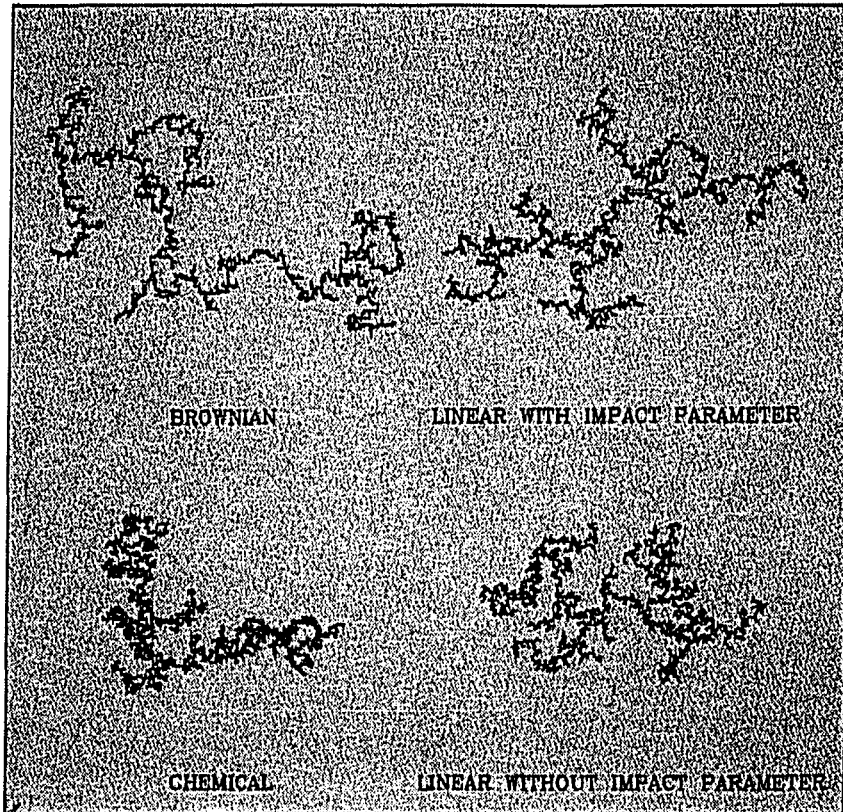


Figure 61. This is an illustration of the influence the cluster trajectories on the resulting shapes of the clusters obtained by cluster-cluster aggregation processes in two dimensions. To give an idea of their relative size, all of the aggregates have the same number of equal sized particles (4,096)



Figure 62. This is an illustration of the influence the cluster trajectories on the resulting shapes of the clusters obtained by cluster-cluster aggregation processes in three dimensions. To give an idea of their relative size, all of the aggregates have the same number of equal sized particles (4,096)

structures formed during CCA. They both incorporated reversibility by allowing bonds to break after a set time with some probability. Allowing reversibility of this type produces a 3 dimensional fractal dimension of 1.56. The only way that this type of reversibility is pertinent to flocculation, is if the time scale for breakage were related to the time scale for floc exposure to the impeller region. It is suggested that it would be more meaningful to fracture the aggregate at it's weak point, i.e., point of fewest bonds, when a certain shear stress is exceeded. This is an area where there is currently a large amount of work going on (Jullien and Botet, 1987).

It is interesting that the PCA, DLA aggregate is symmetrical around its center, and all of the PCA models produce a structure which is spherical in their overall shape. The CCA models on the other hand produce a structure which is distinctly anisotropic. Intuitively this is expected. Since the CCA floc are formed by two clusters of roughly the same size, one would expect a shape which is on the average oblong or ellipsoidal (Jullien and Botet, 1987).

Boadway (1978), working with an alum floc, reported that small floc appeared as dense spheroids, and the large floc were loose aggregates of the small dense particles. The large floc were irregular in shape, but on the average were a prolate spheroid with the length twice the width.

Reed and Mery (1986), working with alum floc, found that the particles at optimum alum dose were generally irregular in shape and tended to have discontinuities. The floc at non-optimum dosages of alum were smaller and tended to be spheroids.

The descriptions given in these two references sound a lot like the structure of a CCA aggregate. It is proposed that if one observes the floc produced in the laboratory, and selects a CCA model which produces a similar structure, it would be possible to incorporate this information into a kinetic model. There are currently a number of groups in the theoretical physics area who are working on this very problem (Leyvraz, 1986; Kolb, Botet, Jullien, and Herrmann, 1986; Family, 1986; Feder and Jossang, 1986; Ernst, 1986; Racz, 1986). However, these researchers have yet to produce anything the average engineer can apply to the orthokinetic flocculation problem.

All of the orthokinetic flocculation modeling studies discussed above have relied on the viscosity term in  $G$  to correct for the temperature at which the flocculation is carried out. There are two places where  $G$  has frequently been found in the models used in the previously mentioned studies; the aggregation term, and the breakup term, if the model has one. All of the studies discussed, except 2, have simply used  $G$  in the aggregation term. Speilman (1978), and van den Ven and Mason (1977) both used  $G^{0.82}$ . Changes in  $G$  cause changes in the flocculation rate which are directly proportional to  $G$  and inversely

proportional to  $\mu^{1/2}$ . Thus changing the temperature from 20 °C to 5 °C, one would expect a change in the rate of primary particle disappearance on the order of  $(\mu_{20}/\mu_5)^{1/2}$ . If  $\epsilon$  is kept constant, this would result in a 18 percent reduction in the rate. Assuming the relationship is  $G^{0.82}$ , a 16 percent decrease in rate would result.

All of the studies which included a breakup term, except two, also assumed that the breakup term is directly proportional to  $G$ . The two exceptions are Hinze (1955) and Camp (1968). Assuming that breakup is proportional to  $G$  would indicate that as the viscosity went up (colder temperature), for the same  $\epsilon$ , the breakup would go down. Hinze (1955) assumed that breakup would be directly proportional to  $\mu$ , this would yield a 1.5x increase in breakup in going from 20 to 5 °C. Camp said  $T = \mu * G$ , where  $T$  is surface stress. This yields  $\mu^{1/2}$  or an increase in breakup of 1.22x for the same temperature change. If breakup is proportional to  $G$ , one would expect to see larger floc at 5 degrees than at 20 degrees for constant  $\epsilon$ , given enough time, because although the kinetics are slower the breakup is less. However, if Hinze or Camp is correct, the colder temperature should produce a smaller floc.

## METHODS SECTION

### Introduction

The first portion of this methods section, i.e., the Introduction, is an overview of the experimental portion of the work being reported herein. The second portion contains detailed information regarding materials preparation and equipment.

The work being reported here is an experimental study. The main objective is to determine the effect of low temperature on flocculation in a turbulent flow field. Experiments were conducted at three temperatures, 20 °, 5 °, and one experiment at 2 °C. The effects of temperature were measured by changing the flow field characteristics and the system chemistry and measuring the impact of these changes on the flocculation process. This required the performance and monitoring of flocculation experiments in a controlled temperature setting. The controlled temperature conditions were achieved using a walk-in constant temperature room. The temperature in the room was monitored and controlled using a personal computer (PC) based data acquisition and control system.

Kaolinite clay was used as the primary particle system. The suspension water was buffered Ames, IA tap water. Alum, ferric sulfate, and a high molecular weight cationic polymer (MagniFloc 573C) were used as coagulants in this work.



The flocculation work was performed in a bench scale batch reactor similar to the reactor used by Argaman and Kaufman (1968). Both stator and turbine impellers, shown in Figure 27, were used. The physical and chemical conditions in the flocculation reactor were monitored using the forementioned data acquisition system. The following process control parameters were monitored:

- o reactor pH
- o reactor temperature
- o impeller rpm
- o energy input.

The impeller rpm was used as the operational control parameter. The  $G$  for the reactor was estimated from  $G$  versus rpm curves published by Argaman and Kaufman (1968). The other turbulent flow field parameters, i.e.,  $\epsilon$  and  $\eta$ , were calculated based on the  $G$  value given in these calibration curves.

Samples were collected during each flocculation experiment at the following times:

- o homogenized sample
- o immediately following rapid mixing with the coagulant
- o 1, 3, 5, 10, ..., 30 minutes after slow mixing began
- o 45 minutes after slow mixing began (discretionary)

After a settling period, each of these samples was analyzed. The particle size distributions were determined using automatic image analysis (Lemont OASYS), coupled directly to a microscope. In addition, a permanent photographic record was made of each sample.

Initial suspension turbidity, initial suspension zeta potential, and zeta potential following rapid mixing, were used as quality control parameters.

#### Materials Preparation

##### Clay

Kaolinite clay was used as the primary particle system. The kaolinite had a log mean diameter of 1.8  $\mu\text{m}$ . Figure 63 contains the log mean diameter  $\pm$  1 standard deviation for 28 of the homogenized samples. It is clear from these data that the stock suspension was quite consistent. For evaluation purposes, a primary particle has been defined as a particle with an equivalent circular diameter smaller than 2.5  $\mu\text{m}$ . Based on a 25 mg/L suspension, a 1.8  $\mu\text{m}$  diameter, a specific gravity (S.G.) of 2.65, and an assumption of spherical geometry, one can calculate 3 million primary particles per mL. The particle counting technique used in this project consistently counted around 6 million primary particles per mL in the homogenized sample. In Figure 64, for example, the total particle count in the homogenized sample was approximately 7.1 million particles/mL, and the primary particle count is approximately 6.5

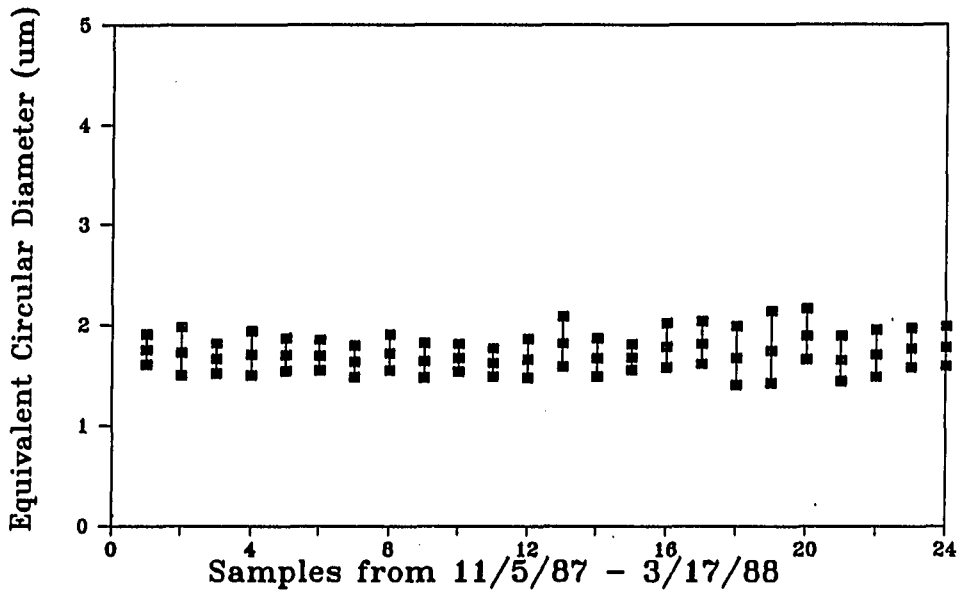


Figure 63. Primary particle size distribution stability; log-mean equivalent spherical diameter +/- one standard deviation for 28 arbitrarily selected homogenized samples

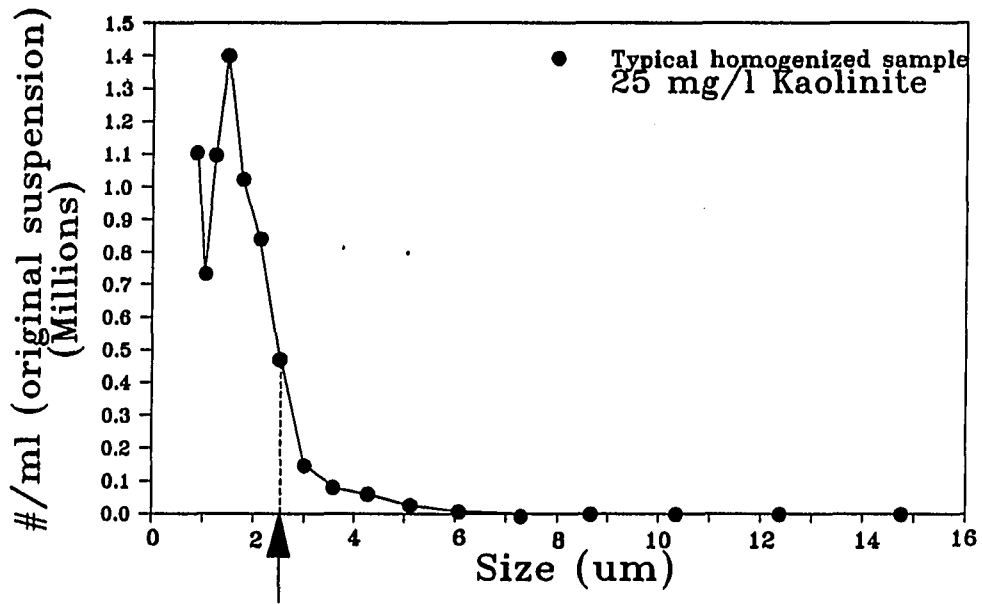


Figure 64. Typical primary particle size distribution (PSD)

million particles/mL. This is good agreement when one considers that the particles are actually plate-like material rather than spheres. A 12 channel HIAC PC-320, with a 1-60 sensor, was also used to count many of the samples, it consistently counted around 200 thousand particles/mL.

The major problem encountered in using clay as the primary particle system was dispersion of the clay. Three methods of achieving uniform dispersion were tested. These were:

- o intense mixing of the dry powder into tap water for 5 minutes using a homogenizer,
- o pre-wetting the clay by soaking it overnight, followed by intense mixing for 5 minutes using a homogenizer, and
- o adding the clay to water circulating through a centrifugal pump, circulation was continued for at least an hour, and then repeated periodically (total of 3-6 hours of recirculation) for a day prior to use.

Neither of the first two techniques provided adequate dispersion of the clay. The third technique provided complete dispersion. Figure 65, is a schematic representation of the clay dispersion and mixing system. This system has a number of advantages, including:

- o 45 liters of 800 mg/l suspension can be prepared at a time. This minimizes suspension variability. Errors due to measuring the clay and clay loss in sample transfer were reduced in significance because a fairly large mass of solid material (36 grams) is added to a large volume (45 liters) of Ames, Iowa tap water,

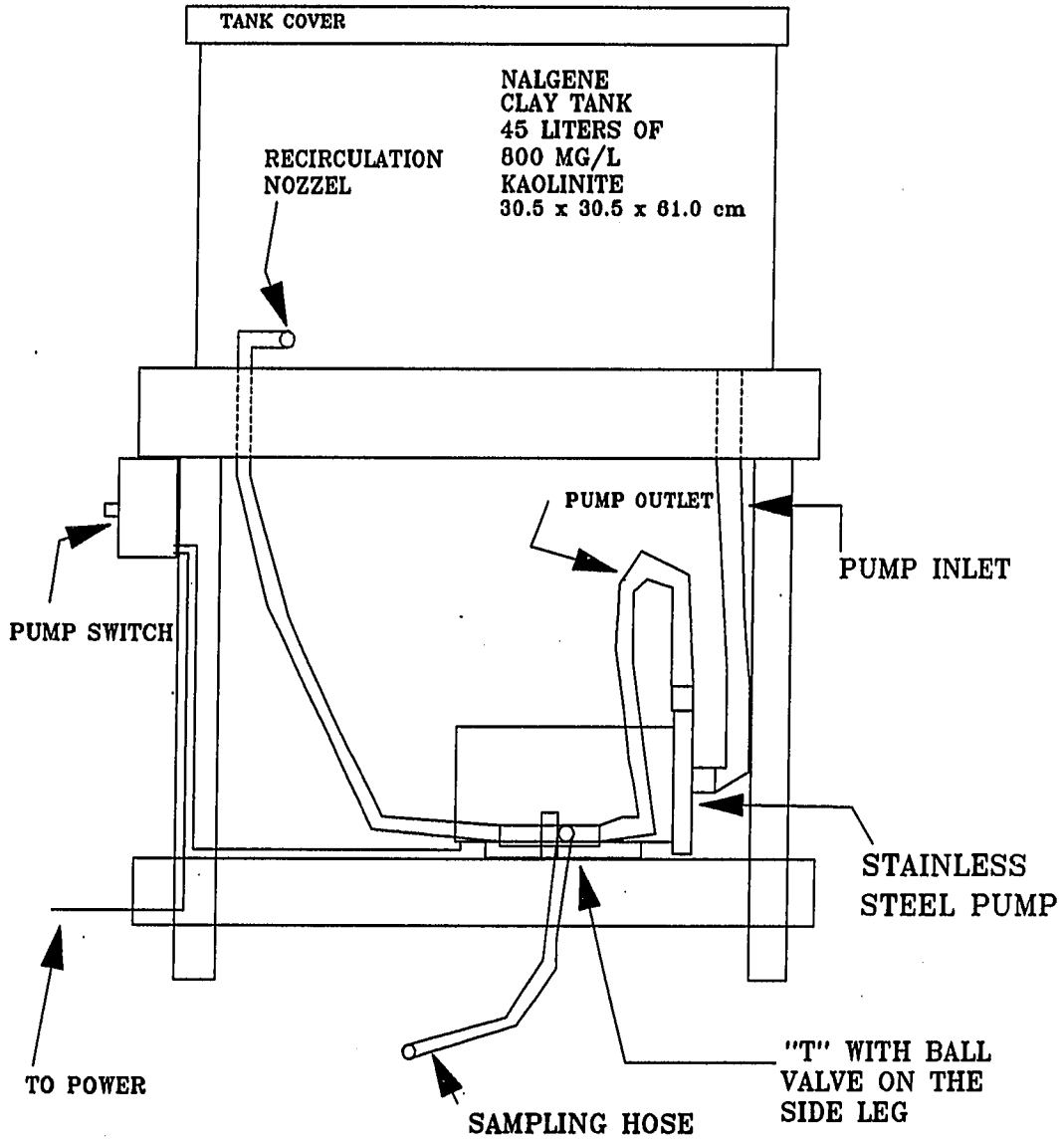


Figure 65. Schematic of the clay dispersion and mixing system

- o the 45 liters of stock solution provided primary particles for a large number of experiments, providing continuity from one set of experimental conditions to another, and
- o the recirculation system made it easy to get a representative sample of the stock solution.

The following method was used to add the primary particles to the reactor. Approximately 15-16 liters of water were placed in the reactor, and the impeller was turned on at a rate of 100 rpm ( $G=80 \text{ sec}^{-1}$ ). The clay recirculation system was turned on and run for 10+ minutes to insure complete homogeneity in the clay tank. It is noted that the clay recirculation nozzle enters the tank parallel to the tank floor and about 3/4" above the floor. This jet scours the floor clean of settled material. The sample hose was also used to scour out the corners and insure that all of the settled clay was in suspension. Once the clay suspension was completely mixed, the sample hose was purged briefly to waste, and a 500 mL sample of the 800 mg/l stock clay suspension was measured into a 500 mL graduated cylinder. The recirculation was shut down immediately after the sample was drawn. The 500 mL of stock suspension was added to the reactor, and the mixing increased to 250 rpm ( $G=550 \text{ sec}^{-1}$ ). The volume of liquid in the reactor was then brought up to 18 liters for all turbine runs and 17 liters for all stake and stator runs.

The 45 liters of stock solution were never used completely. After a period of time, usually about 2 weeks, the suspension color would start to change from off-white to white with a tinge of orange or

brown. When this change was detectable with the eye the remaining clay was discarded. The initial turbidity and the zeta potential in the reactor were measured as quality control parameters, and neither of these exhibited significant change during the course of the study. Based on this, it is believed that the change noticed in the clay color did not impact the character of the clay significantly.

#### Buffered dilution water

The suspension dilution water was Ames, IA tap water buffered with 100 mg/L  $\text{NaHCO}_3$ . The buffer stock solution was 1 molar  $\text{NaHCO}_3$ , that is 84.01 g/l or 84 mg/mL  $\text{NaHCO}_3$ . An analysis of the tap water used in this study, with the buffer added, is shown in Table 21. The dilution water was made up as follows:

- o the large stainless steel tank was rinsed thoroughly,
- o about 150 liters of tap water were run into the tank,
- o the buffer was added; 357 mL of the buffer described above was added to the tap water,
- o the water level was brought up to the 300 liter mark,
- o the water was then mixed thoroughly and let stand overnight,
- o after standing overnight the water was placed in rinsed, 18 liter carboys, and the carboys are placed in constant temperature storage.

Table 21. Dilution water chemical analysis summary

Parameter	Units	Dilution Water Batch					
		1	2	3	4	5	6
HCO3-	mg/L	114	114	116.6	119	114	139
CO3--	mg/L	3.5	7.4	6.3	11.8	16.4	---
PH	-log[H+]	8.54	8.8	8.75	8.89	8.95	8.3
NO3+NO2-N	mg/L as N	0.61	0.45	0.78	0.63	0.33	0.2
TOTAL-P	mg/L as PO4	0.097	0.32	0.1	0.075	0.15	0.14
SULFATE	mg/L as SO4	129	121	119	121	114	111
CHLORIDE	mg/L	44.4	31	29.6	31.2	33.4	32
Na	mg/L	48.5	47	47.7	46.2	44.7	52.1
K	mg/L	2.43	2.65	2.73	2.56	2.48	2.56
Ca	mg/L	56.9	50.4	62.4	60.9	58.4	59.5
Mg	mg/L	10.5	11	6.11	7.94	9.88	4.56
Mn	mg/L	0.0018	0.004	0.012	0.004	0.004	0.001
Fe	mg/L	0.017	0.083	0.132	0.054	0.056	0.015
Al	mg/L		0.03	0.06	0.03	0.038	0.02
NPOC	mg/L	1.54			0.6	1.5	1.88
Batch		1	2	3	4	5	6
Date		11/04/87; 12/02/87; 01/28/88; 02/26/88; 5/27/88; 8/18/88					



Coagulant

Alum, ferric sulfate, and a high molecular weight cationic polymer (MagniFloc 573C) were used as coagulants in this work. The metal salts were stored as 0.25 molar stock solutions. The pH of the stock solutions were checked periodically to insure that the integrity of the solution was maintained. The pH of the iron stayed below 2.2, and the pH of the alum stayed below 3.2. The metal salt dosing solutions were prepared volumetrically from the stock solution the day before they were used. This was done to insure consistent speciation in the coagulant. If there was an aging of the solution, it would have a few hours to take place before the solution was used. 10 mg/mL dosing solutions were used for the metal coagulants.

The polymer, which is a polyquaternary amine (MW approx. 100,000 grams/mole), was also made up the day before it was used. The polymer was prepared by weighing one gram of polymer into a weighing boat, followed by dilution to 1 liter. The final working solution for the polymer was a 0.1 mg/mL solution. This final working solution was prepared approximately 1/2 hour prior to use by a 10:1 volumetric dilution of the 1 gram/L solution.

All of the coagulant solutions were stored at room temperature until they were to be used. The coagulant was loaded into a syringe and

taken into the constant temperature room just prior to injection into the reactor.

### Acid

All pH adjustments were made using reagent grade HCl diluted volumetrically to 0.1 N with distilled water. The acid used for pH adjustment was not standardized.

## Equipment and Methods

### pH adjustment and monitoring

The acid was added to the reactor using a 60 mL syringe with a #13 gauge needle. The acid was added through the sample port on the side of the reactor, and was discharged into the impeller stream. The pH of the system was continuously monitored using a 12 mm diameter pH probe (pHeonix Electrode Company of Houston, TX), and a Fisher Accumet #610 pH meter. The pH meter was standardized using first a 7 buffer, and then a 4 buffer. It was then checked again with the 7 buffer. The 4 buffer has a pH = 4.05 and the 7 buffer has a pH=7.11 at 5 °C. The pH meter was checked at both the beginning and the end of each experiment.

The pH adjustment for the first six experiments, carried out at 20 °C, were performed as follows. The pH was lowered to approximately 7.5 to 7.2 prior to rapid mixing. The alum was injected at the beginning

of rapid mixing, and the pH was fine tuned to pH = 6.8 during rapid mixing.

At 5 °C fine tuning the pH during the rapid mix was not possible. The addition of the alum suppressed the pH and it did not recover until the rapid mix was over. The difference in pH recovery at 20 and 5 °C is shown in Figure 66. This phenomenon lead to a number of questions:

- o What caused the slow recovery? Slow pH probe? Poor mixing efficiency? Carbonate chemistry?
- o Why was the pH depression consistently larger in magnitude at a pH of 7.4 than at a pH of 6.8?
- o Did the slow recovery cause the reduction in flocculation efficiency noted at 5 °C?

A pH probe with a fast response time was purchased. The pH probe response time was verified using various buffers at low temperature, and the probe was eliminated as a potential source of the problem. Figures 67 and 68 illustrate the impact of mixing time and intensity on the pH recovery rate. The low energy condition represents a G of  $450 \text{ sec}^{-1}$  (250 rpm), and the high energy condition represents a G of  $1020 \text{ sec}^{-1}$  (500 rpm). It is apparent from these figures that neither duration nor intensity have a large impact on the recovery rate.

Having considered the probe and the mixing regime, the next obvious thing to consider was the buffer system. The carbonate system

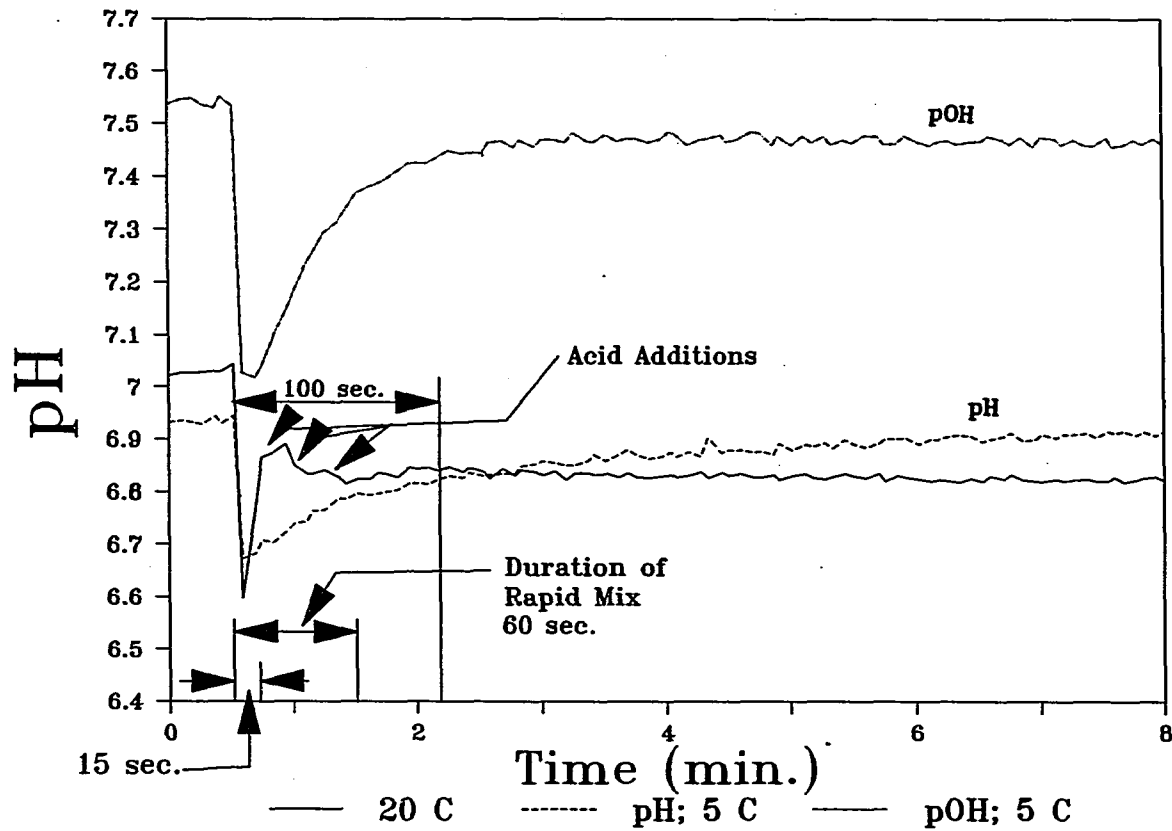


Figure 66. The effect of temperature on the pH recovery time after alum addition; the carbonate buffer system is used

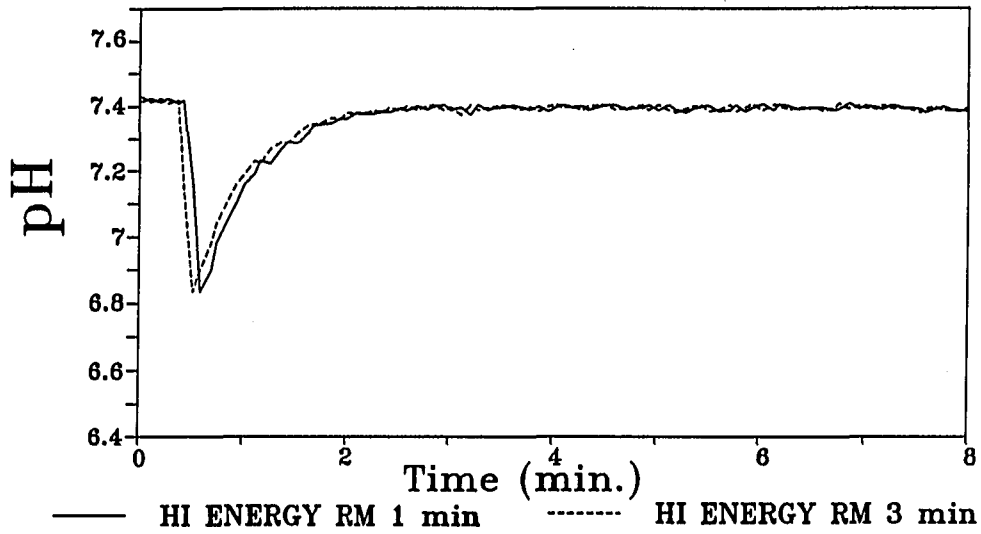


Figure 67. The effect of rapid mixing intensity on the pH recovery time after alum addition at 5 °C; the carbonate buffer system is used

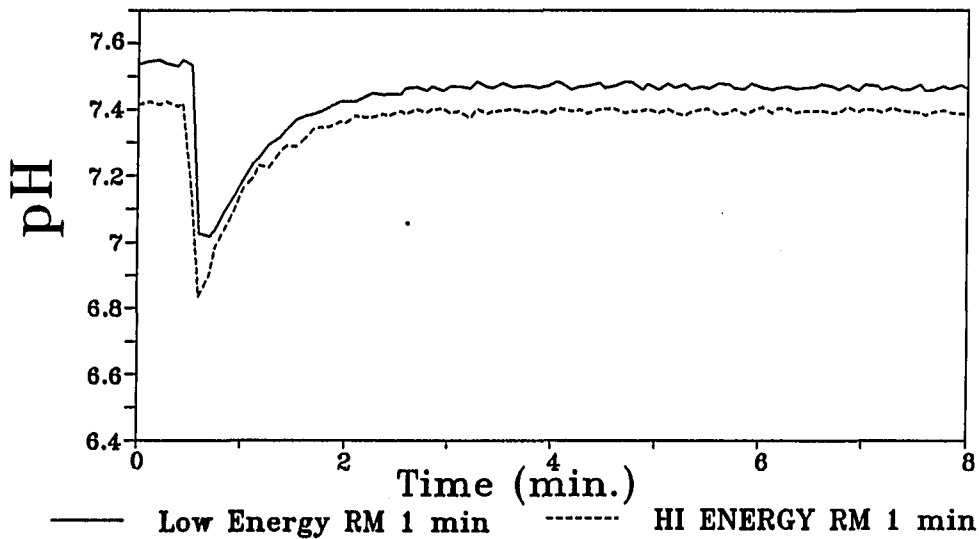
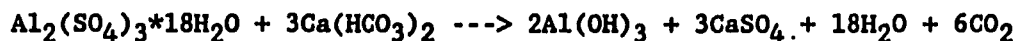
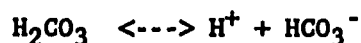


Figure 68. The effect of rapid mixing time on the pH recovery time after alum addition at 5 °C; the carbonate buffer system is used

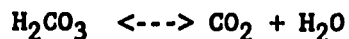
consists of 4 major species;  $\text{CO}_3^{--}$ ,  $\text{HCO}_3^-$ ,  $\text{CO}_2$ , and  $\text{H}_2\text{CO}_3$ . In the range of pH values of interest the  $\text{CO}_3^{--}$  is negligible, so we will only consider the partitioning of the others. When alum ( $\text{Al}_2(\text{SO}_4)_3 \cdot 18\text{H}_2\text{O}$ ) is added to water the following overall reaction takes place.



This is actually a composite reaction which gives a simple description of a more complex series of reactions. It is suggested that the actual sequence of events is more like this. The alum is added and quickly forms  $\text{Al}(\text{OH})_3$  precipitate. This leaves an excess of  $\text{H}^+$  ions in solution, because each of the aluminum has tied up three hydroxides. The carbonic acid-bicarbonate reaction:



is quick, on the order of 0.05 to 0.10 seconds at 25 °C (Stumm and Morgan, 1981). However, the carbonic acid-carbon dioxide reaction:



is slow, on the order of 24 to 40 seconds at 25 °C (Stumm and Morgan, 1981).

If we assume a temperature correction of the form  $K = A e^{(-E_a/RT)}$ , then  $K_1/K_2 = 2.5$  for a temperature change from 25 °C to 5 °C. The reaction times at the two temperatures are shown below.

Reaction	Reaction Time (Seconds)	
	25 °C	5 °C
$\text{H}_2\text{CO}_3/\text{HCO}_3^-$	0.01-0.05	0.25-0.13
$\text{H}_2\text{CO}_3/\text{CO}_2$	25-40	62.5-100

Looking at Figure 66 we see that at 20 °C, it took about 15 seconds for the pH to recover about 1/2 way out of its depression. At that point acid was added to adjust the pH to 6.8. However, it appears that it would have achieved equilibrium in about 30-40 seconds. We also see that the recovery, at 5 °C, takes about 120 seconds at both pH values. It appears that the slow pH recovery agrees very well with what carbonate chemistry would lead us to expect, and the slow recovery may indeed be due to the slow equilibrium time of the  $\text{H}_2\text{CO}_3/\text{CO}_2$  reaction.

It is interesting to note that the magnitude of the depression is about the same for both the 5 and 20 °C samples near a pH of 7, and is considerably larger for the test run at pH of 7.5. This demonstrates two things. First, the change in the magnitude of the depression with pH is a nice demonstration of the change in the carbonate system buffer capacity with pH. Figure 50 shows the buffer intensity decreasing rapidly between pH=6.2 and pH=8.0. Thus, one would anticipate that the magnitude of the depression would be larger at a pH of 7.4 than at a pH of 6.8. Second, the similarity in the magnitude of the depression between the 20 °C and the 5 °C

demonstrates that the carbonate chemistry in this pH range is insensitive to temperature changes of this magnitude. Theory would lead us to expect this, as is shown in the curves in Figure 49 and 50 in the Literature Review.

Comparing data for 20 and 5 °C at a pH of 6.8, one sees that the rate at which the pH drops and lowest pH reached is very similar. These two things give an indication of the rapidity and extent of the aluminum hydroxide reaction. Based on this it is suggested that the changes in the carbonate buffer system kinetics does not seem to inhibit the alum reaction measurably, and one must look else where to explain any measured effect of temperature on flocculation.

A number of hardware comments are appropriate at this point. A 9 mm diameter combination pH electrode was used during the initial 20 °C work. However, at 5 °C the 9 mm electrode was erratic. Replacement of the 9 mm electrode with a 12 mm electrode solved the problem. It is noted that the 9 mm electrode continued to work well at 20 °C, and the slope of the electrode was well within specifications, thus the problems were apparently related to the temperature conditions. The pH meter, along with the other equipment, was originally housed in the constant temperature room. Because of the problems with the pH probe at 5 °C it was deemed best to move all of the electronics out of the constant temperature room. Only the sensors were left in the



constant temperature room. The sensor cables were approximately 6 feet in length.

There were two other major interferences with the pH monitoring system. The type "T" thermocouple used to measure the temperature in the reactor interfered with pH measurement because of the voltage produced at the junction on the bi-metallic thermocouple. This voltage, which is above the ground state, induces a voltage across the pH probe membrane which is unrelated to the hydrogen ion concentration in the solution. However, the pH meter could not tell the difference, and therefore, gave results which were incorrect. The problem was solved by sealing the end of a small diameter glass tube, and placing the thermocouple inside the glass tube. The top of the glass tube was sealed with shrink tape to minimize moisture accumulation inside the protective sheath. As long as the inside of the tube remained dry, the thermocouple was isolated from the pH probe and there were no further problems.

The second interference problem with the pH meter was caused by the mixing motor. It appears that the collapsing field around the windings on the AC motor induced a current, which needed to be isolated from the reactor solution. Once a non-metallic coupler (Lexan) was used to connect the motor to the impeller, the interference was removed. On very humid days there continued to be a minor problem, even with the non-metallic coupler. This may have

been due to moisture in the coupler. This interference was readily identifiable because as the motor rpm was increased or decreased, the pH meter reading also increased or decreased. It is also noted that this motor interference problem was experienced with the Phipps and Bird jar test apparatus. Either plastic impellers and shafts or an isolation transformer placed between the building circuit and the mixer should be used if it is necessary to measure pH values while the jar tester is running.

#### Sample collection

During the flocculation work, samples were collected at the following times for analysis of the particle size distributions:

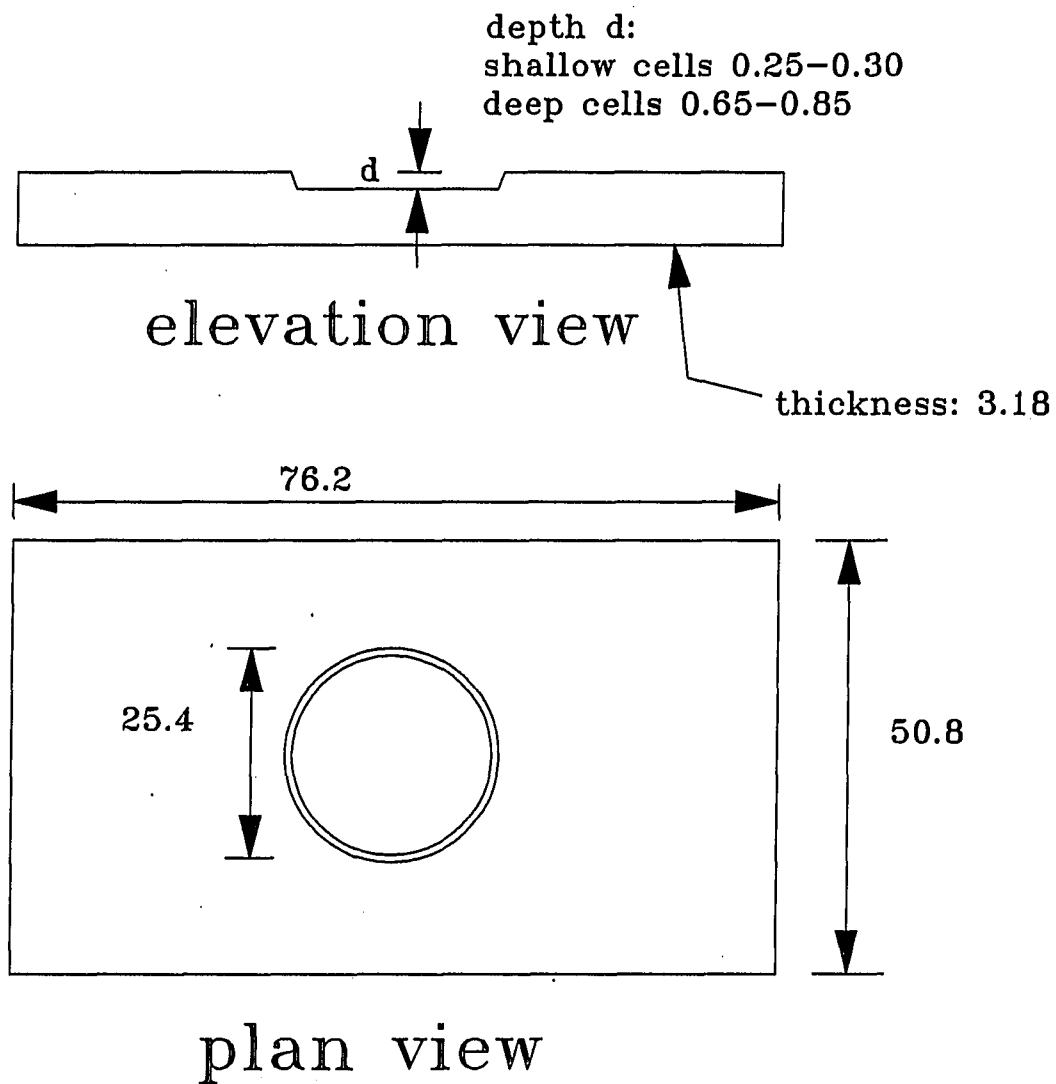
- o prior to coagulant addition, homogenized sample
- o immediately following rapid mixing, time zero
- o 1, 3, 5, 10, ..., 30 minutes after slow mixing began
- o 45 minutes after slow mixing began (this sample was not taken during the first 6 experiments).

The samples were withdrawn from the reactor through a side port using a 1 mL disposable syringe with a #13 gauge Perfectum PS 13 Hospiluer 4-1/2 stainless steel hypodermic needle. Popper & Sons, Inc. of New Hyde Park, New York manufactured the needles. The sampling port consisted of a 3/8" brass hose fitting threaded into the wall of the reactor at the centerline of the turbine impeller blade. The port was fitted with a septum. Sample collection was initiated 5 seconds

prior to the sampling time, and a total of 15 seconds was used to draw a 1 mL sample. The sample was immediately placed in a specially constructed counting cell, which is shown in Figure 69. The 0.65-0.85 mm deep cells were used in these flocculation experiments. Each sample cell was covered with 45x50 mm Number 1-1/2 (0.16--0.19 mm thick) Fisher brand Microscope Cover Glass. The slip covers are manufactured by Allied Fisher Scientific, of Pittsburgh, Pennsylvania.

The sample cell was filled as follows. The slip cover was placed at the far edge of the sample well. The tip of the needle was rested upon the edge of the slip cover, and the sample was slowly discharged from the syringe. As the sample was discharged it was slowly drawn under the slip cover and filled the sample well. The slip cover was drawn across the sample well at a rate which was just fast enough to keep the sample from piling up in front of the slip cover. When this was done properly, the resulting sample was free from bubbles and could be stored intact for 24 hours or more. It is important that the slip covers not be stored sitting over the sample well. This deforms the glass slip cover and they do not seal properly.

Once the sample cell was loaded it was allowed to sit for 2 hours or longer. This curing period was to allow the particles time to settle to the bottom of the cell which is also the focal plane of the microscope. At the beginning of this project a series of



COUNTING CELL FOR  
USE WITH AIA  
ALL DIMENSIONS IN MM

Figure 69. Schematic of the sample counting cell used with the AIA

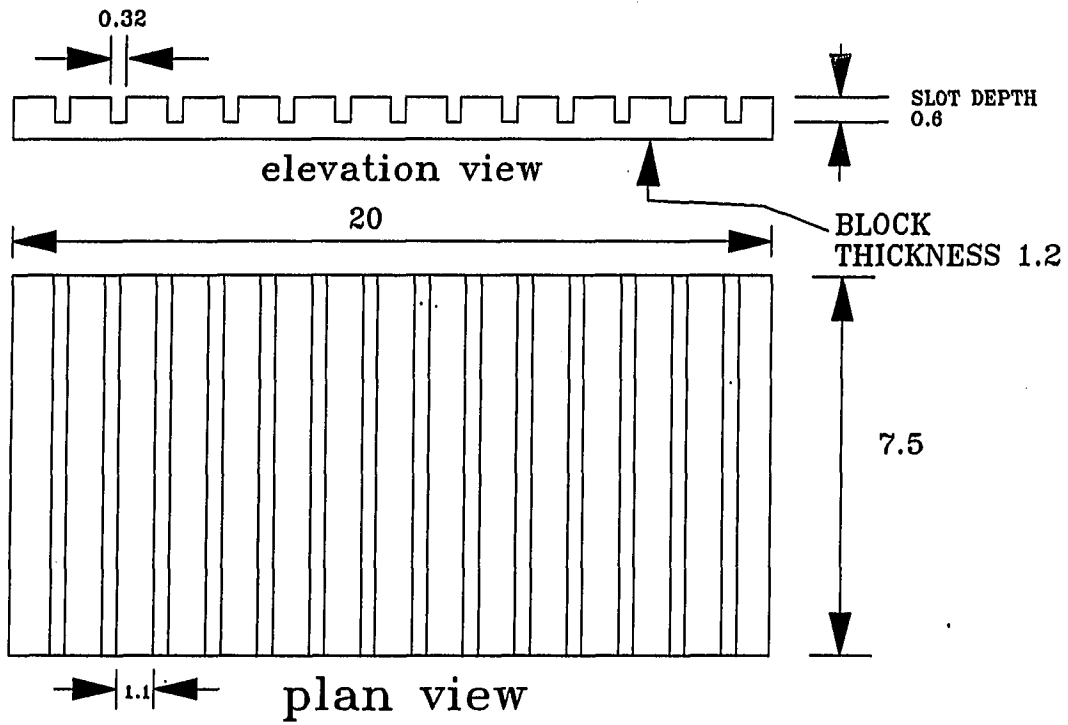
photographic studies were performed over time to establish an appropriate sample curing time. The purpose of the curing time was two fold; to insure that the settling period was sufficiently long, and that no flocculation was taking place in the counting cells. From the photographic study the minimum acceptable curing time at 20°C was 40-60 minutes. From this it was assumed that 2 hours would be more than adequate at 5°C. It should be noted that in the 24 hour period over which photographs were taken, no further flocculation was detected within the counting cell. Once a particle reached the bottom of the cell it ceased to move regardless of its size. Because of the large size of some of the floc present in the suspension, it was possible to have the floc in crisp focus, and have the primary particles out of focus to the point of being nearly invisible. It was very important to focus the microscope on the primary particles and not on the floc, because the flocculation progress was being based on the disappearance of the primary particles.

Construction of the sample cells was a two step process. The sample well was first machined. In machining the plexiglass, it was necessary to use a new tool, and to turn the tool fast with a slow feed rate. These conditions were used to minimize tearing of the plexiglass material. Once the depression was formed it was necessary to buff it smooth. The buffing was performed using first a coarse grit to abrade away all tears and scratches. Then progressively finer abrasives were used until a smooth finish was produced. It is

noted that the plexiglass is very soft and the needles easily put deep scratches in the floor of the cell.

#### Counting cell cleaning

Cleaning the counting cells and slip covers was a multiple step procedure. The loaded cell was first placed under a large volume low pressure stream of tap water at about a 45° angle with the slip cover side up. This lifted the slip cover off from the cell hydraulically, and the slip cover must be caught or it will shatter upon impact with the sink. Once the slip cover was lifted, it was placed in a soaking solution of distilled water and "Micro" laboratory cleaning solution. The cleaning solution "Micro" is manufactured by International Products Corp. of Trenton NJ. The counting cell was then rinsed; first with tap water, and then with high pressure water from the distilled water tap. After rinsing the cells were placed on edge in the cell holder, which is shown in Figure 70. The cells, in the cell holder, were placed in an ultrasonic bath and vibrated for at least 20 minutes. The ultrasonic bath used to clean the counting cells was a Bransonic Model 220 manufactured by Branson Ultrasonic Corp. of Danbury, CT. The ultrasonic bath contained a mixture of distilled water and "Micro" laboratory cleaning solution. Every 5 minutes the ultrasonic bath was shutoff and the cells were lifted up and down to flush the face of the cells. If the cleaning period was shortened, the micro not used, or if the 5 minute rinses were not performed, the cell cleaning was inadequate. The dirt tended to pile up in windrows



COUNTING CELL STAND  
FOR CLEANING IN THE ULTRASONIC  
ALL DIMENSIONS IN CM

Figure 70. Schematic of the cell holder used in cleaning the sample cells

of particles which caused severe problems when the next set of samples were being analyzed.

Once the cells had been washed in the ultrasonic bath, they were again rinsed with a high pressure jet of distilled water. After rinsing, the cells are placed between lint free paper towels, and a weight was placed on top of them. This encouraged the wicking away of water droplets and prevented the formation of water spots. Upon drying the cells were ready for re-use.

The slip covers were cleaned in much the same manner. There were, however, additional steps required with the slip covers. Despite the best efforts made, the slip covers inevitably had visible contamination, which would have interfered with viewing of the samples if it were not removed. The final cleaning was accomplished by breathing on the slip cover and then buffing the slip cover with a cleaning tissue. This process was repeated until either the slip cover was clean or until it broke.

#### Reactor cleaning

The reactor was cleaned immediately following each experiment. The suspension in the reactor was first subject to intense mixing to re-suspend any material which may have settled during the experiment. The mixing also caused the breakup of any large floc, which had



formed during flocculation, into small slowly settling aggregates.

After the mixing the reactor was:

- o completely drained,
- o rinsed with cold tap water and then drained completely (this was done twice),
- o scrubbed down with a clean sponge,
- o rinsed with cold tap water a final time and drained, and
- o dried completely with a clean towel.

#### Turbidity measurement

The turbidity of the initial suspension was checked on a Hach Model 18900 Ratio Turbidimeter before the experiment and recorded.

Turbidity was used as a quick, surrogate check of the kaolinite primary particle concentration, which is an indication of the primary particle concentration. Figure 71 is a calibration curve indicating the approximate relationship between kaolinite concentration and the suspension turbidity. The turbidity test was intended to detect gross variations in the character of the primary particle suspension. Since the test was not used as an absolute standard, a variation of  $\pm 2$  NTU in the initial suspension turbidity was considered acceptable. Initial turbidities for all of the experiments are shown in Figure 72. The run number shown is an arbitrary value, this figure is intended to demonstrate the range of values measured.

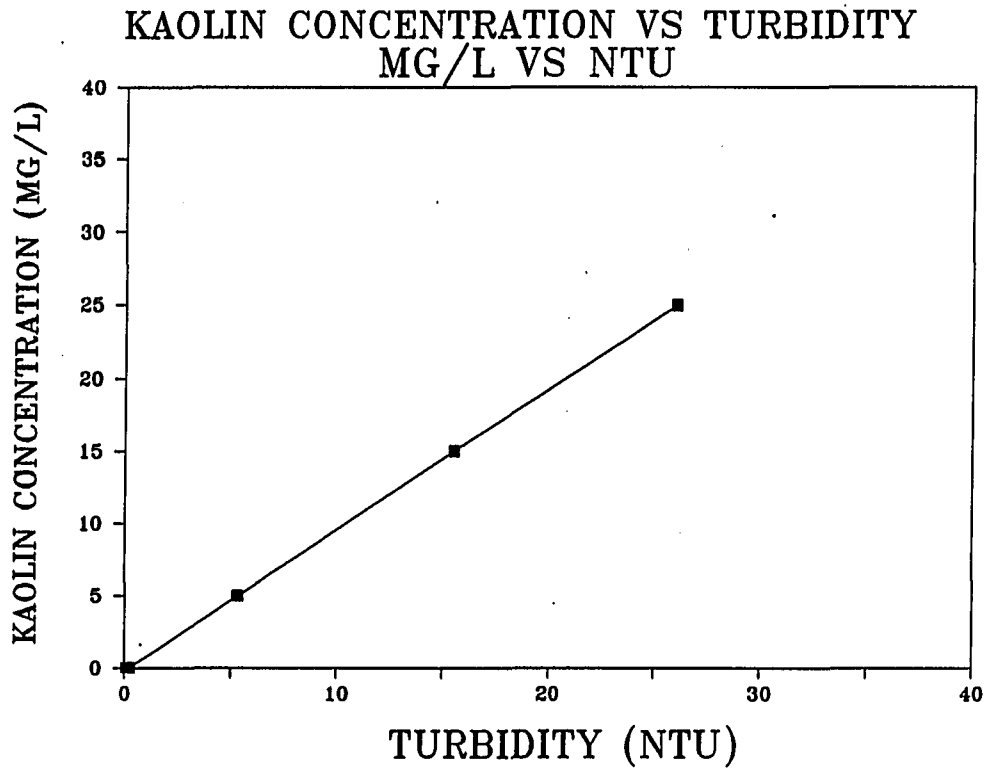


Figure 71. Calibration curve for kaolinite concentration versus turbidity

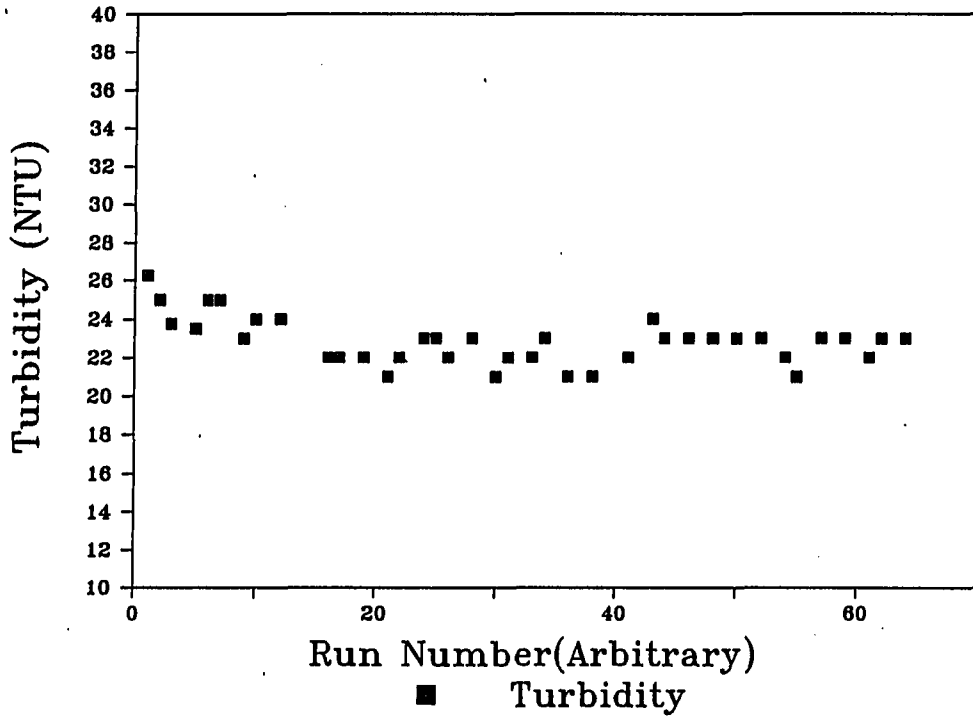


Figure 72. Quality control chart showing the consistency of the homogenized sample turbidity measurements

The turbidimeter was calibrated as per the manufacturers recommendations. The sample turbidity to be analyzed was drawn from the reactor sampling port and measured prior to coagulant addition. The sample was loaded directly into a sample cuvette, and was inverted several times prior to measurement. The outside of the sample cuvette was wiped clean with a tissue just as the sample was placed in the instrument. Water tended to condense on the cold samples, however, this did not appear to effect the measurements, which were in the 20 NTU range. It was noted that all samples needed 0.5 to 1 minute to produce a stable reading.

#### Zeta potential

A Model 102 Lazer Zee Meter, manufactured by Pen-Kem, Inc. of Croton-on-Hudson, NY, was used to measure zeta potential. The electronics in the zeta meter have been upgraded to Model 104 electronics, but the optics are still original. Zeta potential (ZP) was used as a quality control parameter. ZPs were measured on both the homogenized sample and on the coagulated sample immediately following rapid mixing. It was intended that maintaining a constant ZP would insure that the surface charge of the clay would be maintained constant. The measurement techniques detailed in the manufacturers literature were followed closely.

The calibration of the instrument was checked using a standard suspension provided by the instrument manufacturer. The instrument

performed very well measuring the standard colloid. The location of the ZP cells stationary layer was checked daily.

The sample to be measured was drawn from the reactor and allowed to come to room temperature. This was done because the cold temperature samples frequently formed gas bubbles during ZP measurement and these gas bubbles made the measurements unreliable. In retrospect, this practice probably made the cold temperature ZP measurements completely useless. It is very likely that the surface charge induced by the hydroxide precipitate is temperature sensitive.

#### Jar test technique

The standard jar test was used to determine the optimal coagulant dose for the batch reactor experiments. The jar tests were conducted using a Model 7790-300 Phipps & Bird 6 Paddle Stirrer. Both coagulant dose and system pH were controlled variables during the jar test experiments. A titration technique was used to deduce the amount of this acid to be used to achieve a specific target pH. The actual pH was always verified at the end of the jar test. The dilution water and the primary particle system were identical to those used in the batch reactor. The pH adjustment was performed prior to the rapid mix process. It was verified that the pH correction could be performed up to 1/2 hour prior to rapid mixing, and the target pH was still consistently achieved.

The particle suspension was produced by adding the appropriate amount of buffered tap water to each jar using a 2 liter graduated cylinder. The stock particle suspension was then measured into a 60 mL syringe and injected into the 2 liter glass beakers. Round glass beakers with baffles were used (Hudson, 1981). The volume of the suspension was corrected for the volume of acid and coagulant to be added to the jar. The final volume was 2 liters of fluid. Acid and coagulant additions were dosed with disposable plastic syringes with #13 gauge needles.

The jar tests were run as follows. The coagulant syringes were filled and laid along-side the appropriate jars. The mixer was set at 300 rpm, which corresponds to a G value of  $\sim 1000 \text{ sec}^{-1}$ . The coagulant syringes were injected into the jars in rapid sequence. Typically this would take approximately 15-20 seconds for 6 syringes. The coagulant was injected below the first baffle, above the impeller, and near the tip of the impeller. As soon as the last syringe was emptied the stop watch was started, and rapid mixing continued for 1 minute. At the end of the rapid mixing time, the mixer was set at 50 rpm, which corresponds to a G of  $\sim 50 \text{ sec}^{-1}$ , and flocculation continued for 30 minutes. ZP samples were collected immediately following rapid mixing, during the first minute of flocculation. After 30 minutes of flocculation, the suspension was allowed to settle for 30 minutes. Optimum coagulant dose was based on settled turbidities. The settled turbidity sample was taken

midway between the end of the upper baffle and the impeller shaft. Figures 73, 74, and 75 are typical jar test results for alum, ferric sulfate, and MagniFloc 573C respectively. In these Figures, alum dosage is expressed as mg/L of  $\text{Al}_2(\text{SO}_4)_3 \cdot 18\text{H}_2\text{O}$ , and ferric sulfate dosage is expressed as mg/L of  $\text{Fe}_2(\text{SO}_4)_3 \cdot 7\text{H}_2\text{O}$ .

#### Temperature measurement

Routine temperature measurements were all performed using a type "T" thermocouple. The thermocouple consists of a pair of wires (copper/constantine), which form a bi-metallic junction. The junction produces a voltage which varies directly as the temperature varies. The data acquisition card is equipped with a cold block (junction), and is internally calibrated to convert the voltage produced by the thermocouple to a temperature reading. The internal calibration of the card was checked using an ice bath, and was found to be correct at the ice point. The thermocouple was encased in a glass sheath to prevent interference with the pH measurements. The glass sheath caused a minor lag in the response time of the probe, but it was not long enough to warrant concern, on the order of seconds.

#### Tachometer

The mixing speed was measured using an Ametek Model 1736 tachometer with an encoder type sensor. This instrument was obtained from Cole-Parmer Instrument Company of Chicago, IL.

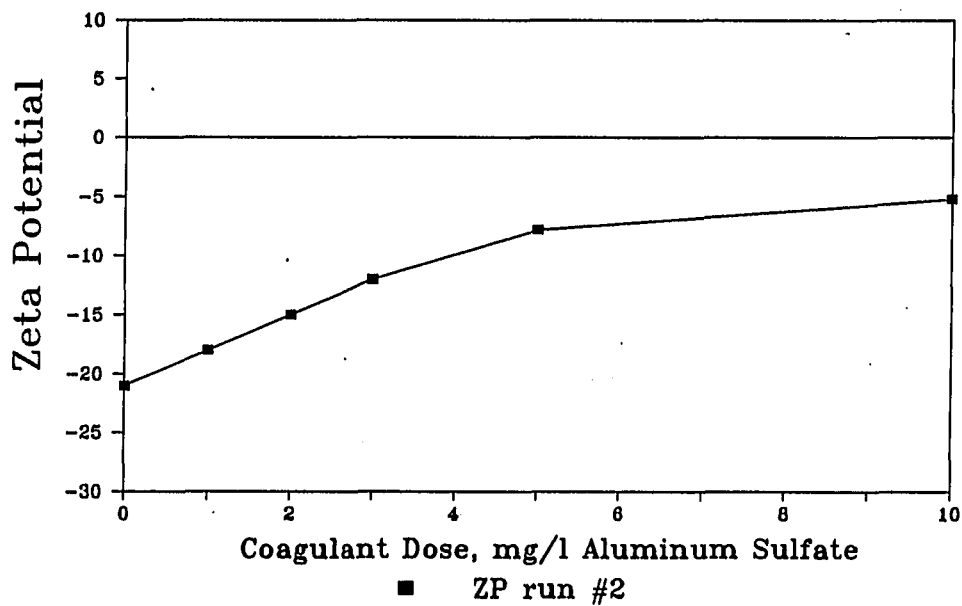
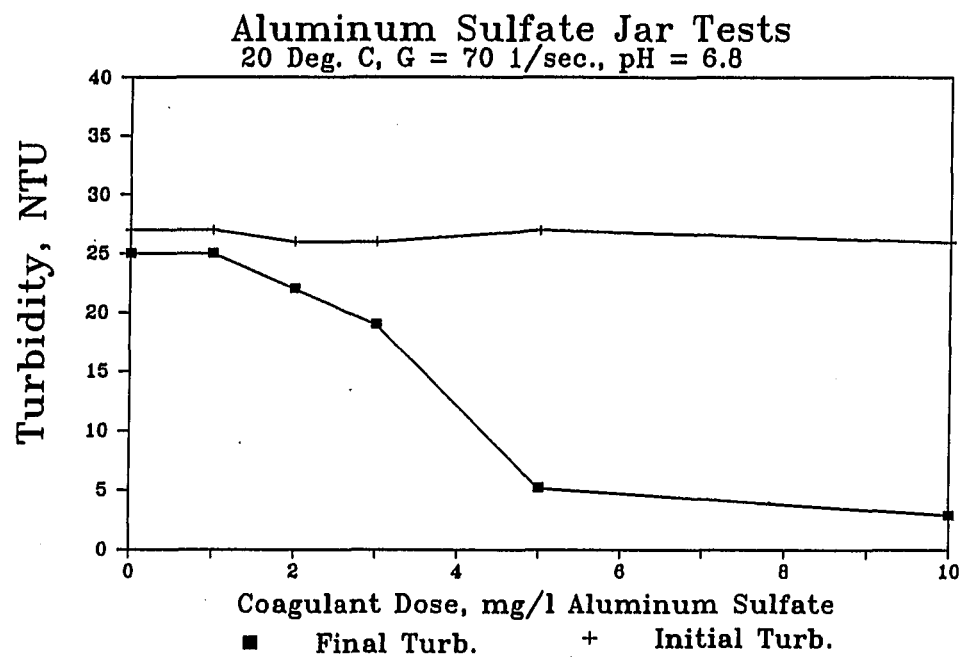


Figure 73. Typical alum jar test results and ZP measurements



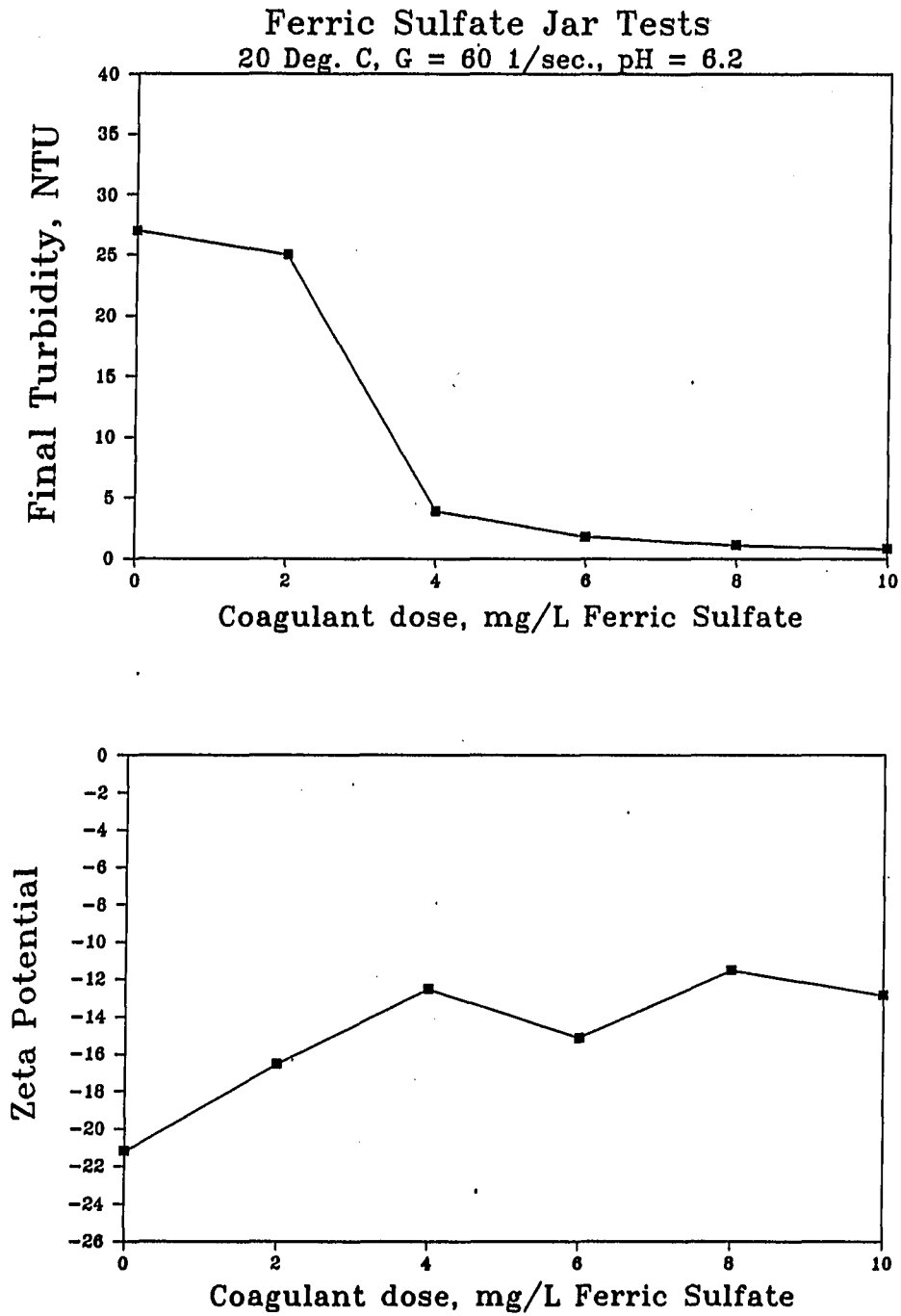


Figure 74. Typical ferric sulfate jar test results and ZP measurements

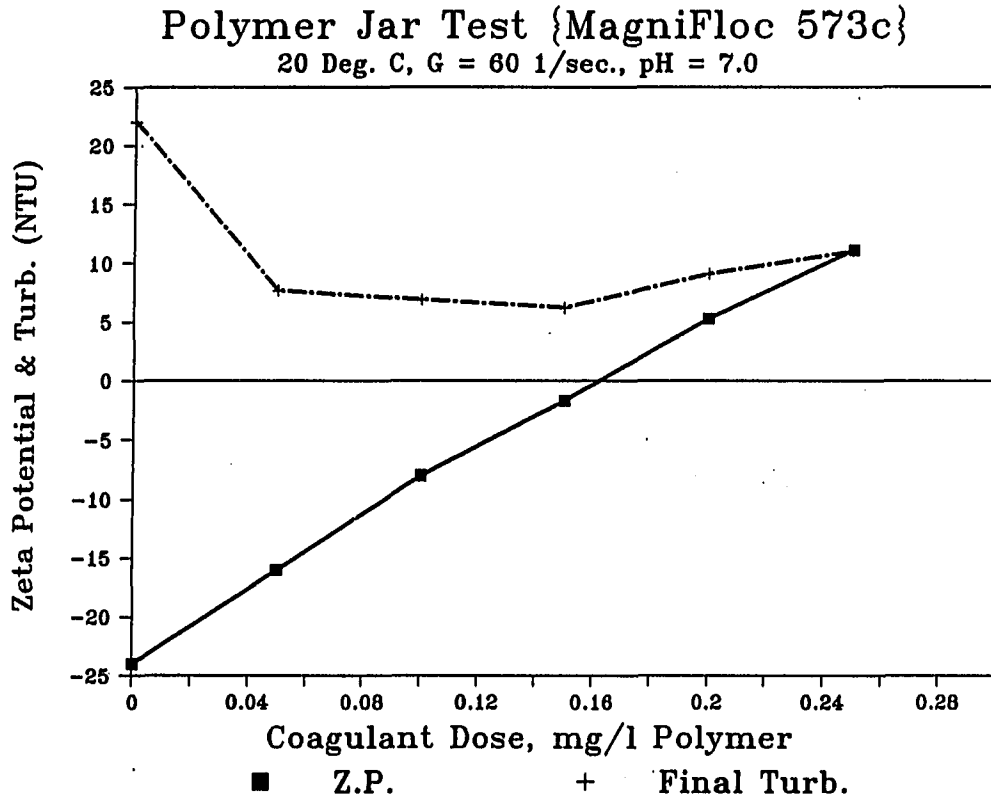


Figure 75. Typical cationic polymer (MagniFloc 573c) jar test results and ZP measurements

### Motor controller

The Master Servodyne motor and motor controller, manufactured by Cole-Parmer Instrument Company of Chicago, IL., was used to mix the batch reactor and monitor the energy put into the reactor. This system was used to control the speed at which the motor was rotating as well as hold the rotational speed constant. The Servodyne also measured (in DC millivolts) the torque being exerted on the motor. This measurement was used to monitor the relative rate at which energy was being applied to the contents of the reactor, and insure that it remained constant during each experiment and was reproducible from one experiment to another.

### Data acquisition and control

The data acquisition system was used to monitor the flocculation reactor. The following process control parameters were monitored:

- o reactor pH
- o reactor temperature
- o impeller rpm
- o energy input

The tachometer, servodyne, pH meter and thermocouple were attached to a terminal panel which was connected to the analog card of the ACPC-16 Analog Connection PC personal computer based data acquisition/control system (Strawberry Tree Computers; Sunnyvale, Ca)

(STC). The data acquisition and control card was housed in a Z-159 Zenith Desktop Personal Computer System, which is an XT clone. During each experiment the STC collected the data and read it to a file on a 5 1/4 inch floppy disk. Graphs produced from this file were later plotted to provide a permanent record of the flocculation conditions. Figure 76 is an example of the data plots produced.

The constant temperature conditions were achieved using a walk-in constant temperature room. The temperature in the room was also monitored and controlled using the STC PC based data acquisition and control system.

#### Control of mixing intensity

The impeller rpm was used as the operational control parameter. The  $G$  for the reactor was estimated from  $G$  versus rpm curves published by Argaman and Kaufman (1968); see Figures 77 and 78. The other turbulent flow field parameters, i.e.,  $\epsilon$  and  $\eta$ , were calculated based on the  $G$  value given in these calibration curves; see Figures 79 and 80. The formulas used to calculate these values are given in the turbulence section of the Literature Review.

The energy put into the reactor was monitored for quality control purposes, but not for process control purposes. The ideal situation would have been to measure this energy directly, and to use this as

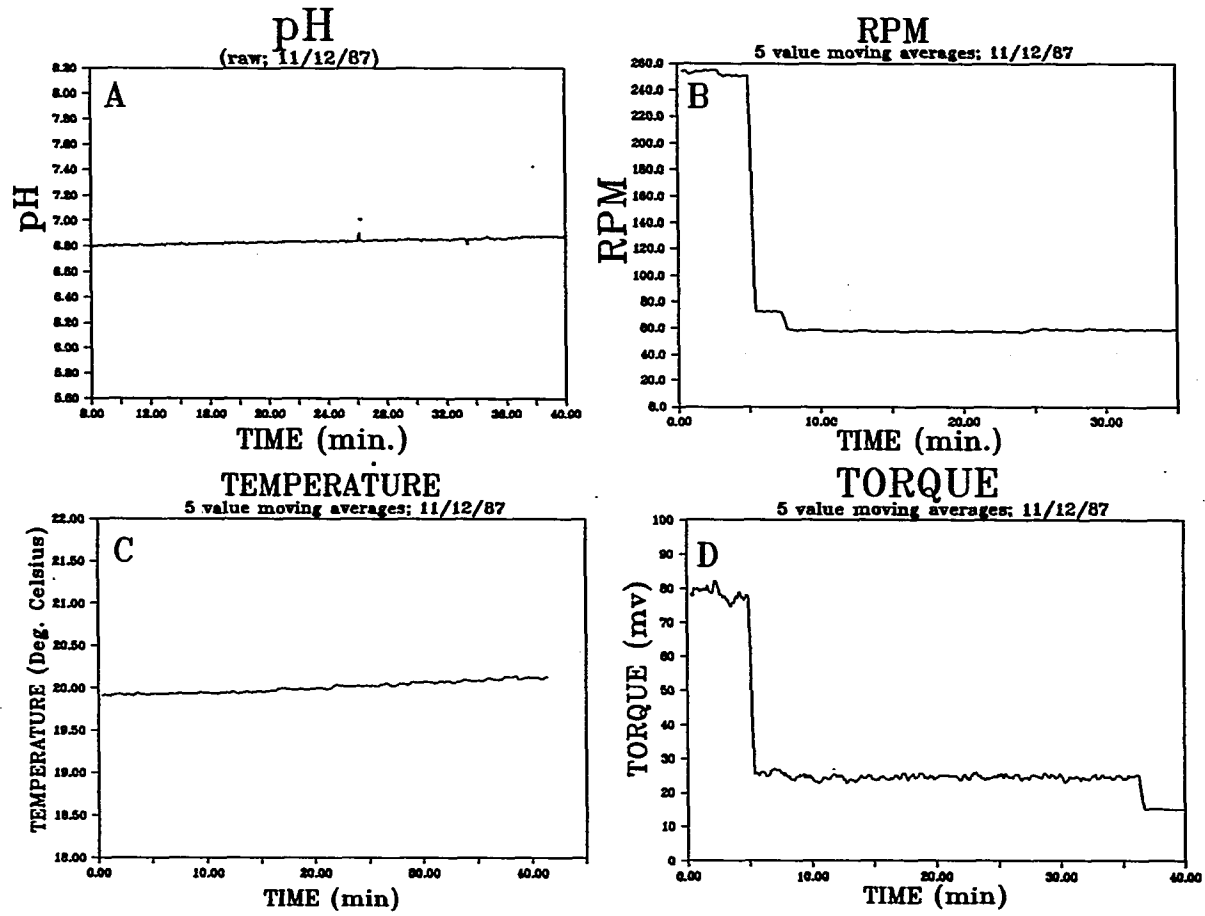


Figure 76. Typical data collected by the data acquisition system in monitoring the flocculation reactor

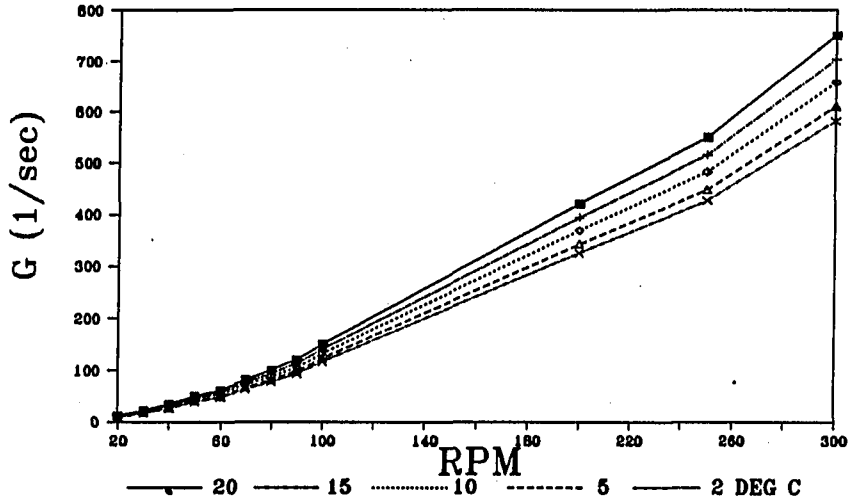


Figure 77. Variation in G produced by the turbine impeller with temperature and rpm; 20 °C values based on Argaman and Kaufman's data (1968)

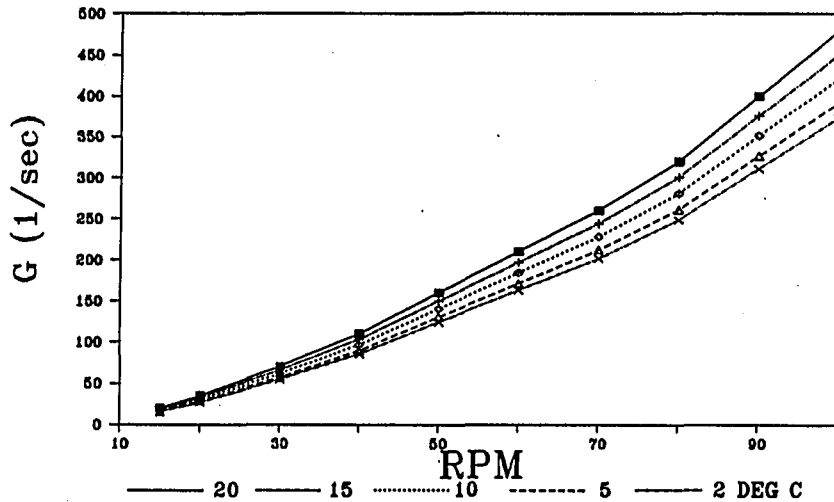


Figure 78. Variation in G produced by the stake and stator impeller with temperature and rpm; 20 °C values based on Argaman and Kaufman's data (1968)

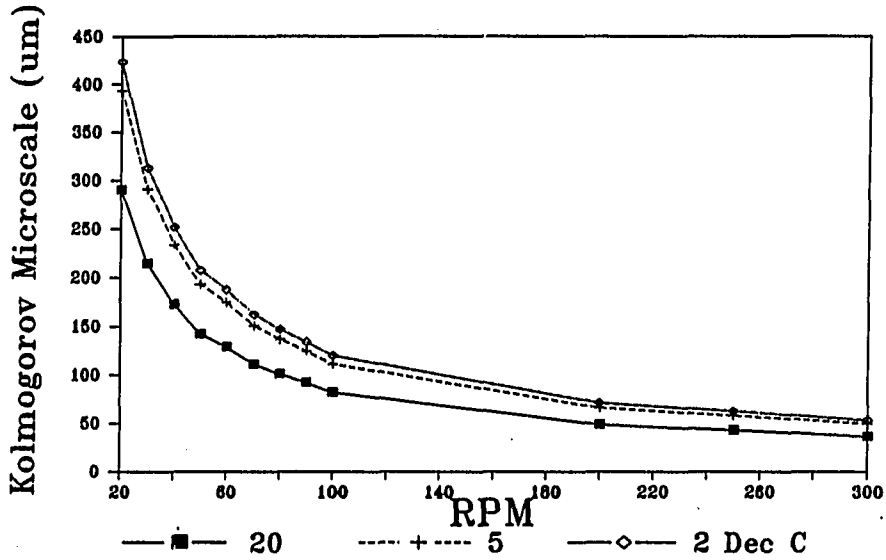


Figure 79. Variation in  $\eta$ , Kolmogorov microscale of turbulence, produced by the turbine impeller with temperature and rpm; Calculated based on 20 °C values for G from Argaman and Kaufman's data (1968)

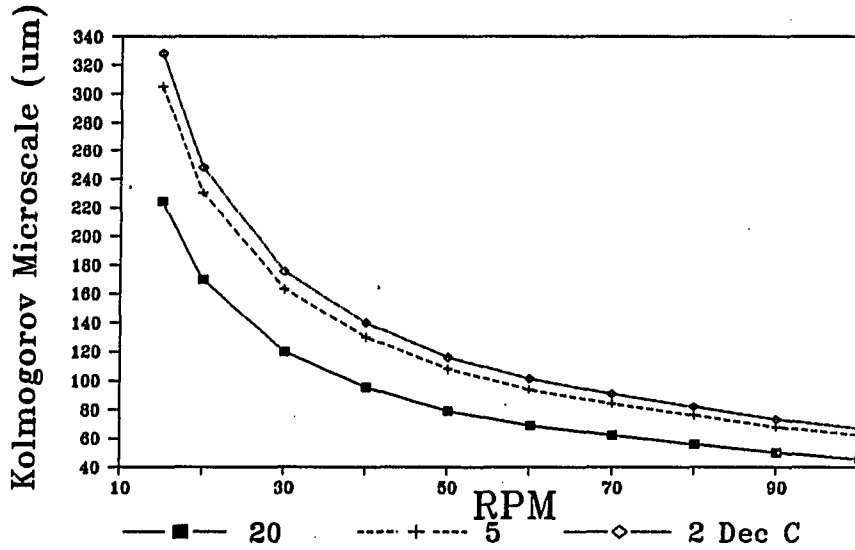


Figure 80. Variation in  $\eta$ , Kolmogorov microscale of turbulence, produced by the stake and stator impeller with temperature and rpm; Calculated based on 20 °C values for G from Argaman and Kaufman's data (1968)

the basis for process control. However this was not possible for a number of reasons:

- o the linear factory calibration for the Master Servodyne was performed at 1500 rpm and the linearity assumption was not valid at the impeller speeds used in this study,
- o the on-site calibration, performed using a home-made prony brake, proved woefully inaccurate,
- o If either of the above mentioned calibration techniques had been successful the Master servodyne output signal would have proved inadequate. The output had a high noise/signal ratio, which made the energy input measurement unsuitable as a primary control parameter.

The system rpm on the other hand can be monitored and controlled very precisely, therefore it was selected as the process control parameter.

Using rpm as the control parameter raises the question, how does constant rpm relate to constant  $\epsilon$ , as temperature changes? The response is that maintaining a constant rpm as the temperature varies is equivalent to maintaining a constant  $\epsilon$ . This is because the system is inertially dominated, and viscous forces can be neglected. This was verified experimentally, by measuring the energy output of the mixing system at various mixing speeds while operating at both 5 and 20°C. A data point was collected every 15 seconds for 5 minutes at each rpm and temperature condition. The average of this data set was then used as the energy output under the specified conditions. The result of this is shown in Figure 81, and it can be seen that the



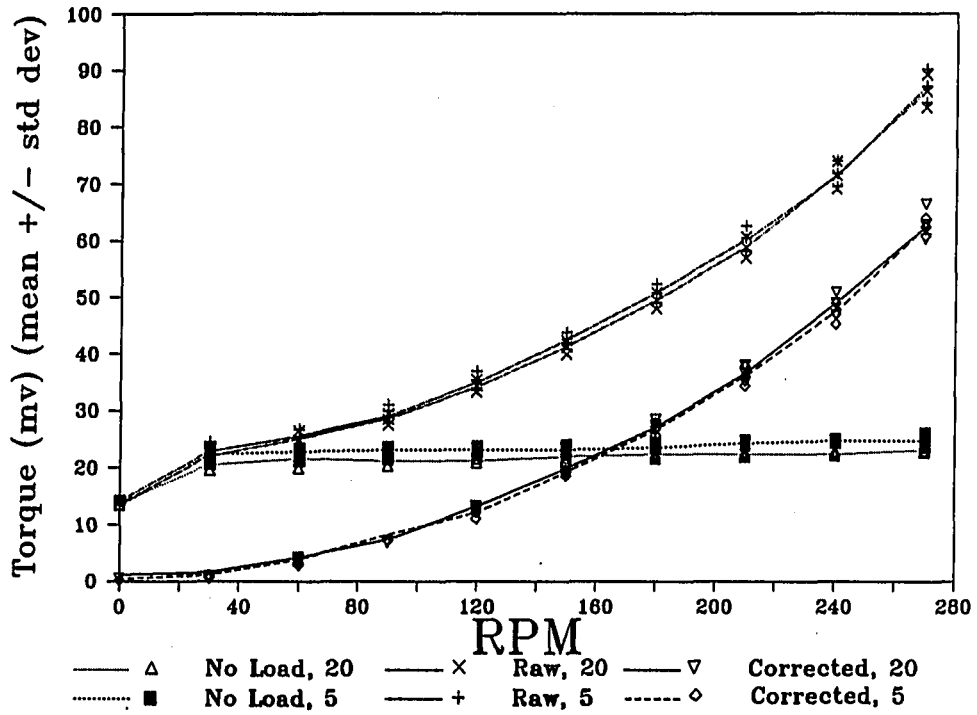


Figure 81. Experimental evidence that the  $\epsilon$  versus rpm relationship is inertially controlled

curves for 5 and 20°C are nearly identical. There are three symbols plotted for each data point. The middle symbol with the line through it is the average value. The symbols above and below the average represent  $\pm$  one standard deviation. Each of the final energy output curves is in reality a composite of 2 individual curves. Data were collected with the reactor full, and with the reactor empty. The reactor empty data were subtracted from the reactor full data to correct for any temperature induced changes not caused by the water. From Figure 81 it is obvious that the system is inertia controlled. This conclusion is also supported by the impeller Reynolds number, which is given for the turbine impeller in Table 22. The following formula was used to calculate the impeller Reynolds number.

$$Re = (10.754 * N * D^2 * \rho) / \mu$$

Where:

- Re - impeller Reynolds number
- N - impeller speed in rpm
- D - impeller diameter in inches
- $\rho$  - fluid density, gm/cm<sup>3</sup>
- $\mu$  - absolute viscosity in cp
- 10.754 - dimensional constant to correct for mixed units

Based on the Reynolds numbers presented in Table 22, it is not really surprising that the relationship between rpm and  $\epsilon$  is independent of viscosity. Re is the ratio of inertial forces to viscous forces, thus the Reynolds number tells us that the inertial forces are about

$10^4$  to  $10^5$  times as important as the viscous forces, and we should expect an inertially dominated system.

Table 22. Impeller Reynolds number for the turbine impeller

Temperature °C		20	5	2	
RPM	30	Re	7982	5310	4818
	60		15964	10621	9636
	250		66515	44253	40150

The impeller Reynolds number for the stake and stator impeller was not calculated, but it would obviously not be operating in the region where viscosity was dominant.

### Reactor

The work presented in this paper was carried out in a bench scale batch reactor similar to the reactor used by Argaman and Kaufman. Both stake and stator and turbine impellers, shown in Figure 27 of the Literature Review, were used. Essential features of the plexiglass reactor used in the study are shown in Figure 82. The electric mixing motor was mounted on a wooden support which was rigidly attached to the top of the reactor. The tachometer encoder was attached to the shaft of the electric motor, and the encoder sensor was attached to the wooden support. The wooden support for the motor also held the pH probe and the thermocouple.

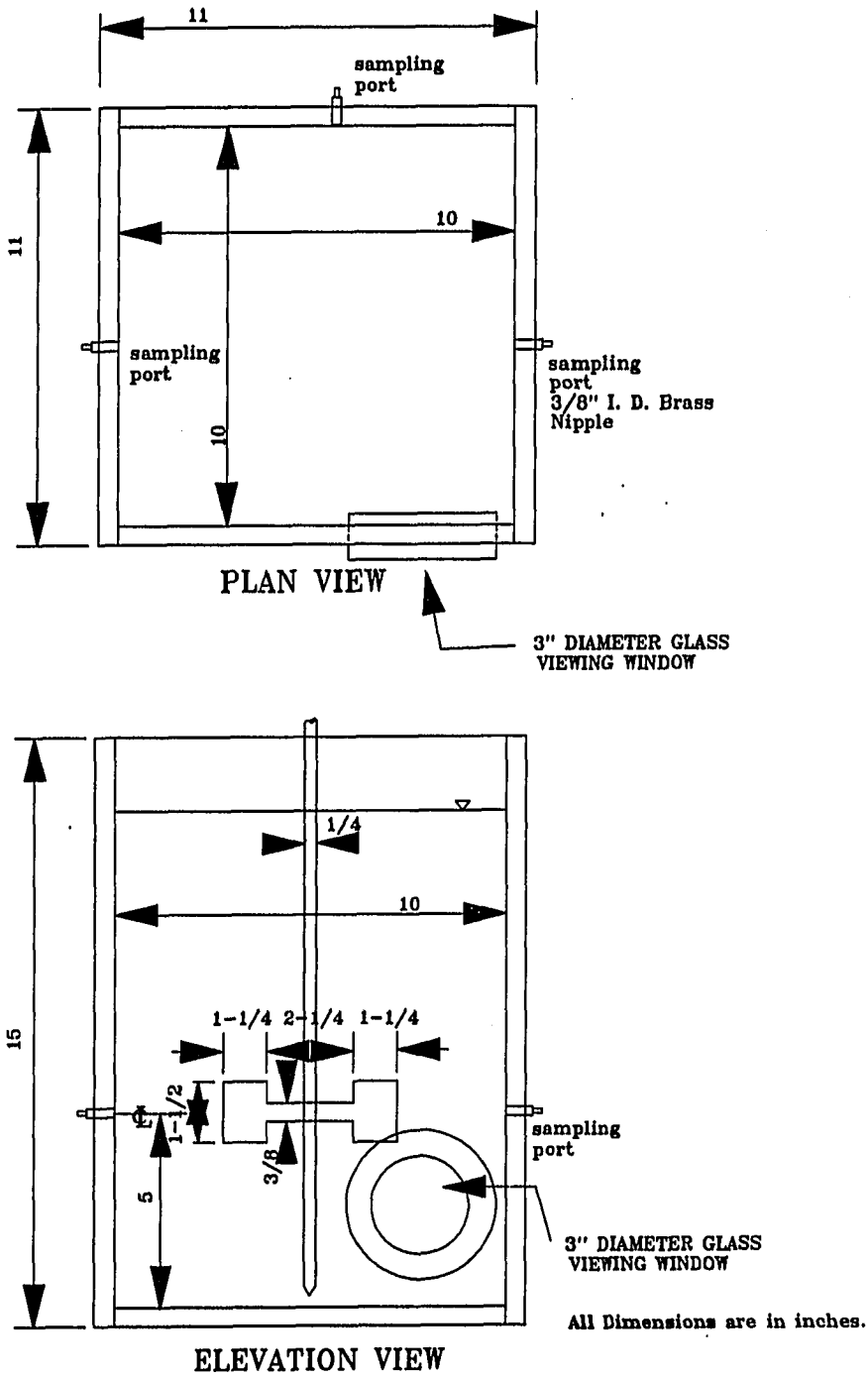


Figure 82. Schematic of the batch reactor

### Lemont OASYS fully automatic image analysis

The particle size measurements were performed using automatic image analysis (Lemont OASYS), coupled directly to a microscope. This system is shown schematically in Figure 55 of the Literature Review. The AIA was coupled directly to an Olympus BH-2S upright, transmitted light microscope with research quality optics (S Plan Achromat Objectives). Phase contrast, Nomarski DIC, and dark-field optics were available for the microscope.

In using this system, the operator selects a field to be counted, and adjusts the image focus and contrast on the live image. The image analyzer takes the live image from the microscope, and digitizes the image. This digitized image is the basis for all of the analyses performed by the image analyzer. Based on the information from the digitized image, the image analysis software estimates such things as the particles projected area, equivalent circular diameter, perimeter, angle of repose, length to width ratio, etc., and then divides the particles into classes based on this information.

There are two parts of the system which are potentially limiting. The first potential limitation is the light microscope itself. Table 16 and Table 17 of the Literature Review list some pertinent information on the optics of the light microscope. Remember, that the resolution of the system is dependent on the magnification of the

objective used, and is not a function of the total magnification of the system. It is also noted that regardless of the objective lens in use, if a particle is smaller than  $0.22 \mu\text{m}$ , the particle is too small to be resolved by the system. This constraint is the result of the nature of light. The highest frequency components of visible light have a wavelength of approximately  $0.44 \mu\text{m}$ . This wavelength sets the lower resolution limit for most light microscope systems. It is also held as a general guideline that, if the particle is  $>0.22 \mu\text{m}$  but  $<0.5 \mu\text{m}$ , the system will resolve the particle but quantitative measurements of the particles will be difficult.

It would be ideal to work at a magnification which would provide the maximum technical resolution of the microscope all of the time. Although this would be desirable it is also probably unreasonable to expect, because although it is technically possible to work at the systems maximum resolution all of the time, it would be cost prohibitive. At the magnifications necessary to achieve  $0.22 \mu\text{m}$  resolution there are very few particles in each microscope field to be analyzed. This means many fields would need to be analyzed, and therefore extensive image analysis time and higher expense. Striving for this level of resolution is probably not warranted considering the other potential sources of variability involved in the flocculation process. Rather than striving for the highest resolution that can be achieved, the lowest resolution which gave, reasonable and reproducible data, was used in this research.

The following sequence of steps was used in selecting an acceptable combination of optics system and counting cell for use with the AIA. The first step was selection of the optimal optics system. Phase contrast was rejected after a brief qualitative comparison with dark field and Nomarski. This rejection was based on the bright phase ring which appeared around objects. A series of counts was then performed to determine the appropriate optical system, sample cell depth, and objective lens magnification. This was done to minimize analysis costs and operator time, while still producing reliable results. Deepening the cell has two competing effects. A deeper cell means more particles to count per unit area after the particles have settled to the bottom (the focal plane). However, as the cell is deepened the water column is also deepened which degrades the image. A lower magnification means more area per field, and thus a higher number of particles counted per field. A lower magnification also means a reduction in optical resolution. If the cell used is too deep, or the magnification is too low the counts will be inaccurate and erratic. The following options were considered:

- o optics: Nomarski and dark field,
- o system magnification: 238x (10x obj.) and 474.6x (20x obj.),
- o cell depth: deep (~0.75 mm) and shallow (~0.27 mm).

From stage micrometer measurements and the AIA software, the area per field for the 238x and 474.6x was determined to be  $1.19 \times 10^{-3} \text{ cm}^2$  and  $2.73 \times 10^{-4} \text{ cm}^2$  respectively. The lower magnification field has 4.36x the area, and therefore, 4.36x the particle count of the higher magnification field. If the deep cell at low magnification is compared to the shallow cell at high magnification, there is approximately 9.45x more volume per field measured, and there should be 9.45x more particles. Using this line of reasoning, all of the field counts were adjusted to a common basis, and the optics systems were compared. The results of the comparison are shown in Table 23. Based on these data and the image quality perceived by the operator, it was decided that it was best to use dark field optics, a magnification of 474.6x, and the deep cells.

The second potential limitation is the LEMONT itself. Ideally the LEMONT resolution limitations should be less restrictive than the light microscope limitations. Figure 54, from the Literature Review, and Figure 83, are distilled from information given in the LEMONT documentation (Lemont Scientific Inc., 1984). These figures show the digitized step size of the OASYS system as a function of magnification. The OASYS creates a 512 x 480 pixel digitized image. The resolution of this image is limited by the magnification of the object which was digitized. The graphs presented here show the dimensions of the individual pixels at the various magnifications. Figure 83 demonstrates nicely the fact that there is a diminishing



Table 23. Optics, magnification, and cell depth comparison

Sample Name	Optics and Cell Combination				
	Deep Cell				Shallow Cell
	Nomarski		Dark Field (DF)		DF
	Hi	Lo	Hi	Lo	Hi
	Counts	per Field			
Homog.	359	216	550	500	569
RM			597	491	485
3 min.			512	395	
10 min.	324	129	343	239	
15 min.			271	142	
20 min.			155	115	
25 min.			126	69	
30 min.			115	61	

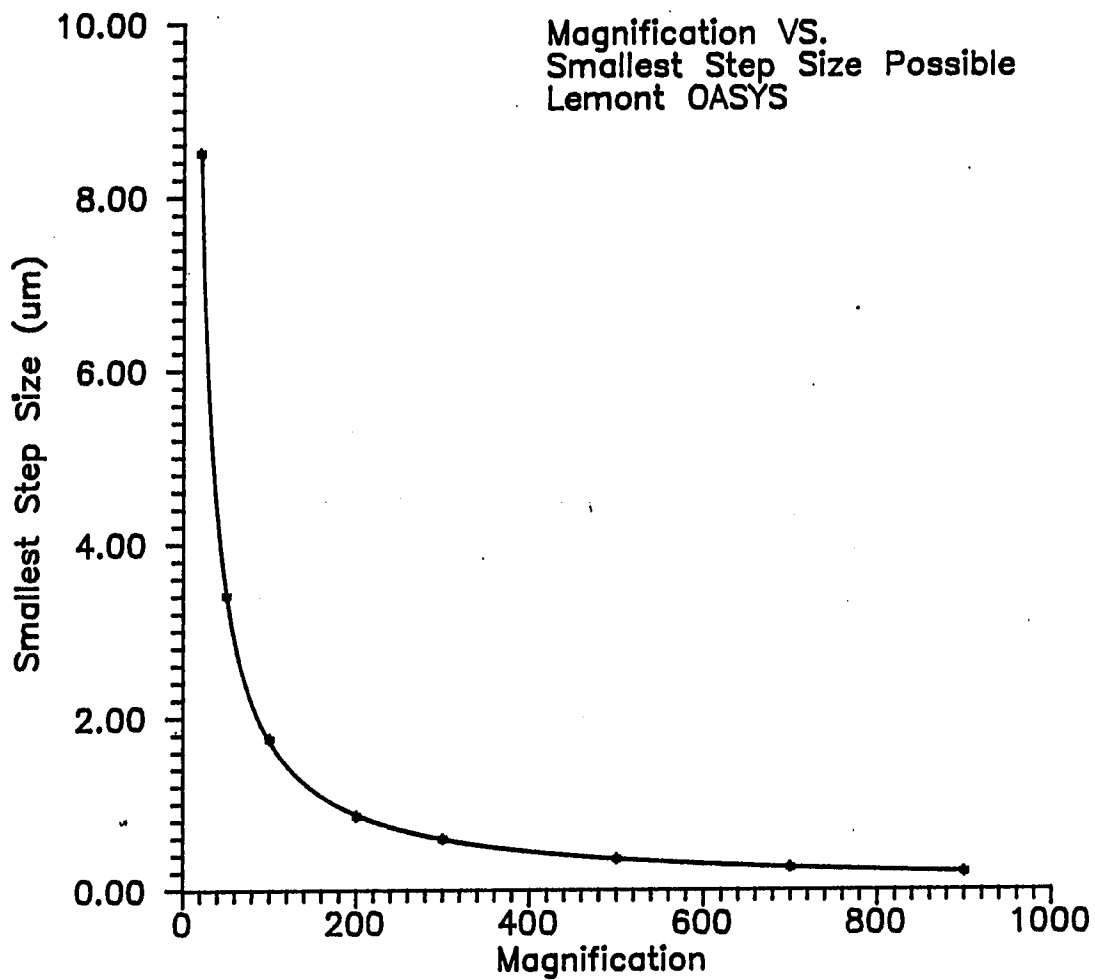


Figure 83. Magnification versus the smallest increment the Lemont AIA can measure, which is roughly equivalent to the smallest feature resolved; linear plot

return in increasing magnification after a certain point. Somewhere near 350x the increase in resolution for an increase in magnification becomes minimal. Figure 54 allows for rapid estimates the minimum step size.

The Table 24 lists the magnifications available using the Olympus BH-2S with Nomarski on the OASYS. The data for the dark field optics are identical to the data in this Table 24. This is because the portion of the Nomarski optics which affects system magnification was left in place during the use of the dark field. In the last column of the table is listed the smallest step the LEMONT OASYS is capable of taking at each magnification. The NFK lens shown in Table 24 is a lens between the microscope and the video camera, which the operator may change.

The previous discussion dealt strictly with resolution in two dimensions (i.e., the x-y plan). Since we are working in a three dimensional system, there is also another dimension which is of interest, and we should really consider this dimension. It is desirable to have a clear crisp image, to perform quantitative image analysis. This requires that the depth of field available must be larger than the z dimension of the object to be measured. Table 17 lists the depth of field for a number of objectives. It is obvious from this table that, if the floc are in excess of 50  $\mu\text{m}$  it will not be possible to provide enough depth of field to provide a crisp

Table 24. System magnification for the Olympus BH-2S microscope, with the Nomarski in place, coupled with the OASYS AIA

---

NFK Lens = 2.5x			
Objective	Magnification	Field of View Video Monitor( $\mu\text{m}$ )	Smallest Step ( $\mu\text{m}$ )
10	79.61x	1260.93	2.16
20	159.53x	626.86	1.08
40	317.71x	314.75	0.55

NFK Lens = 5x			
Objective	Magnification	Field of View Video Monitor( $\mu\text{m}$ )	Smallest Step ( $\mu\text{m}$ )
10	158.85x	629.51	1.09
20	320.31x	312.20	0.54
40	635.42x	157.38	0.28

NFK Lens = 15x			
Objective	Magnification	Field of View Video Monitor( $\mu\text{m}$ )	Smallest Step ( $\mu\text{m}$ )
10	239.26x	417.96	0.72
20	474.61x	210.70	0.37
40	953.125	104.918	0.18

---

image. In fact, the maximum practical depth of field is actually closer to 10  $\mu\text{m}$  than to 50  $\mu\text{m}$ . This means that, with very large particles, it is necessary to work with an image which is always defocused to some degree. There is really no solution to this problem if we are to work with an optical microscope.

Another concern is the number of features which must be counted on the AIA to give a statistically sound sample. During the first few experiments the counts were considered adequate when a total of 250 features had been counted with 100 features in the mode and a minimum of 10 features in each class of importance. Figure 84(A) illustrates the degree of scatter that this set of guidelines yielded. It was believed that the quality of data could be greatly improved with little additional effort. Based on this belief, the following revised guide lines were adopted to determine when enough particles have been counted:

- o a goal of a minimum of 1000 features measured, if they can be measured in less than 20 frames,
- o a goal of a minimum of 500 features measured, if they can be measured in 30 frames,
- o an absolute minimum of 250 particles measured.
- o a minimum of 100 particles in the particle class which represents the mode of the distribution,
- o a minimum of 10 particles in any particle class important to the shape of the distribution curve.

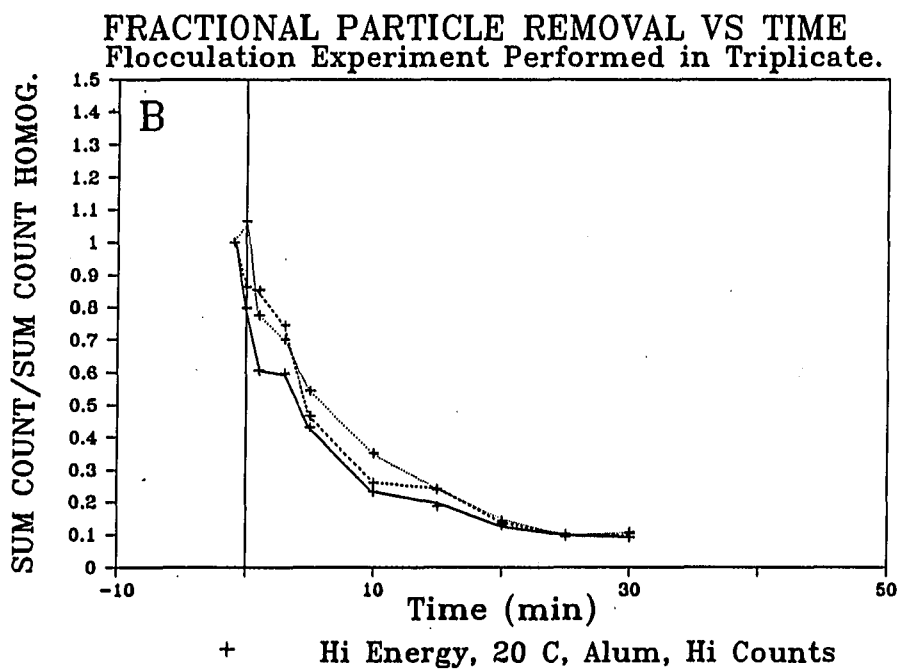
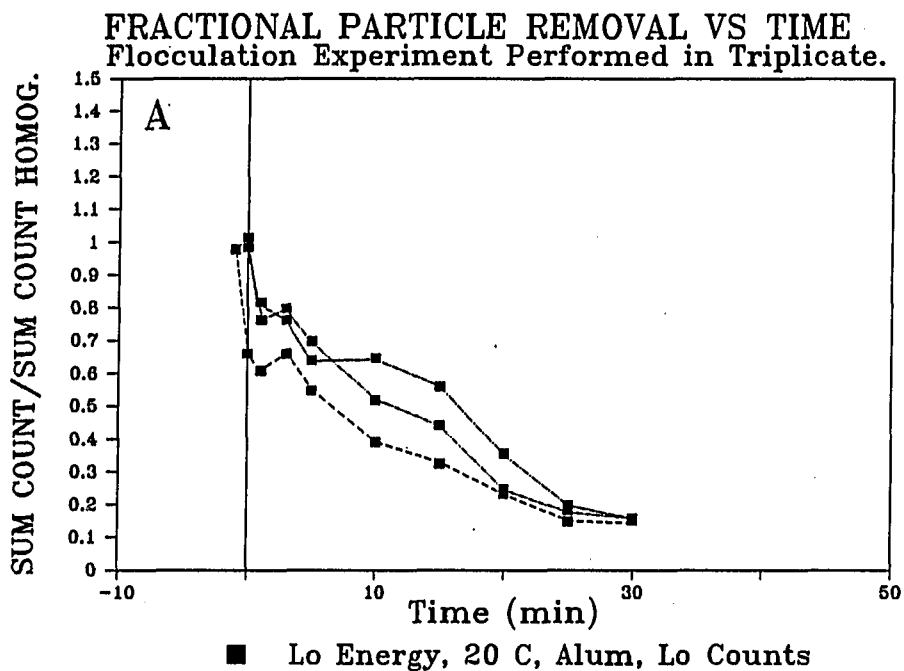


Figure 84. The effect of total features counted on the reproducibility of the AIA analysis data

Figure 84(B) is an example of the reproducibility experienced with the new guidelines.

When analyzing the samples it was important to eliminate operator bias as much as possible. There is a temptation for the operator to select sample fields which represent the operators view of "the way the sample should be". For example, in early samples there might be a temptation to select fields with large particle counts, in the later samples there might be a temptation to select fields with few primary particles and with a large floc in them. This problem was avoided by dividing the sample cell into randomized fields and analyzing the fields as they were selected. The random fields were selected based on the x-y coordinates provided by the verniers on the microscope stage. The range of x values and y values on the verniers corresponding to the sample well area on the sample cell were randomized, using a random number generator, and paired. The fields corresponding to these coordinate pairs were then analyzed until an acceptable number of features had been measured.

The analysis of a typical field of particles would be as follows. The random field is selected. Once the field is selected the image is focused, the condenser is focused, the camera brightness and contrast are optimized, and the light intensity is optimized. It is very important to optimize the image prior to digitization of the image, since editing the image to enhance contrast always has the

potential of destroying information. After the image is optimized it is collected, or digitized. In this step the computer scans the image and assigns a gray level to every pixel on the screen, the image analyzer software groups the screen pixels into a 256 x 256 pixel matrix. Every pixel in this 256 x 256 matrix has an x and y location and a gray level varying from 0 (black) to 256 (white). It is possible, and usually necessary, to edit the digitized image to enhance the contrast. The purpose of the editing is to be sure that the computer actually sees what is really in the image. The image is edited by applying various digital filters, i.e., mathematical algorithms, to the digitized image. It is important that the operator maintain an original image to compare the edited image against. This is to guard against unwittingly corrupting the image. Intermediate images are also maintained in case a specific filter happens to destroy the image, and all of the previous work is lost. This is a concern because an image which contains fairly complex floc structures may take an experienced operator in excess of 5 minutes to prepare for analysis. This is balanced on the other extreme by simple fields which can be prepared and analyzed in as little as 40 seconds. The final image is analyzed by the image analyzer and the raw information is stored to disk. During the analysis of the image the operator selects another random field, and the process begins again. This continues until an adequate total number of features have been analyzed.



Once all of the samples have been analyzed, the raw data are then processed, or played back. In this part of the analysis the operator sets up the analysis parameters and the size classes of interest. The processed data are sent from the image analyzer to a microcomputer via the telephone lines, and the final data processing is all accomplished on a microcomputer.

## EXPERIMENTAL DESIGN

The experimental design section is intended to act as a road map for the Results and Discussion Section of the Dissertation. The first portion of the Results and Discussion Section deals with the selection of a particle sizing and counting system. The second part represents the main thrust of the research, the effect of temperature on flocculation. Both the particle counter evaluation and the flocculation studies were performed simultaneously.

### Particle Counter Evaluation

The particle counter evaluation contains the results of a comparison of the HIAC PC-320 particle counter, equipped with a 1-60  $\mu\text{m}$  sensor, and the Lemont OASYS fully automatic image analysis system. This work was performed early in the research project in making a decision as to the optimal particle counting system for the flocculation work. Figure 85 summarizes the experiments which were performed in evaluating the two systems.

### Flocculation Experiments

There are two areas in which we might expect the flocculation process to be effected by temperature. The characteristics of the turbulent flow field may change as the temperature changes, and the system chemistry may change with temperature. The tests performed to measure the relative importance of these areas are described in the

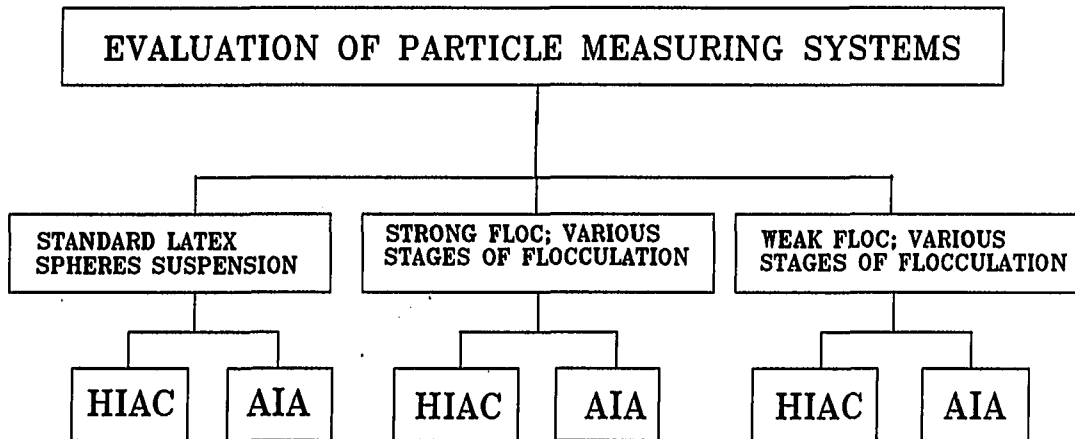


**Figure 85. Experimental plan for evaluation of particle measuring systems**

next two sections. Table 25 is a summary of the experimental conditions used during the testing.

#### Changes in the flow field

Figures 86-89 show the testing performed in studying the impact of temperature induced changes in the turbulent flow field on the flocculation process. Two major parameters were changed in this testing, the impeller geometry and the mixing energy being put into the reactor.

The sensitivity of the system to changes in the structure of the small scale eddies was addressed by changing the energy input into the system. Two energy regimes were tested at 20 °C;  $G = 22$  and  $60 \text{ sec}^{-1}$ . This established a base line for low temperature comparisons. Once a baseline was established, the suitability of various parameters for predicting the nature of the turbulent flow field at the lower temperature was tested. The assumption being that, if the character of the flow field was identical, then the flocculation performance should also be identical. There are a number of parameters commonly used to characterize a turbulent flow field, including:

- o  $\epsilon$ , the energy/unit mass-time
- o  $\eta$ , the Kolmogorov microscale of turbulence
- o  $G$ , the RMS velocity gradient.

Table 25. Summary of experimental conditions

Primary Particles: Kaolin (Kentucky Ball Clay) 1.88  $\mu\text{m}$  dia.  
 Particle Concentration: 25 mg/L, 24 NTU,  $5.8 \times 10^6$  particles/mL  
 Dilution Water: Ames, IA tap water buffered with 100 mg/L  $\text{Na}(\text{HCO}_3)$

Coagulant: Alum as  $\text{Al}_2(\text{SO}_4)_3 \cdot 18 \text{H}_2\text{O}$ ; 10 mg/mL aged at room temperature overnight.

Coagulant Dose: 5 mg/L as  $\text{Al}_2(\text{SO}_4)_3 \cdot 18 \text{H}_2\text{O}$  Base pH: 6.8 at 20 °C

Coagulant: Ferric Sulfate as  $\text{Fe}_2(\text{SO}_4)_3 \cdot 6 \text{H}_2\text{O}$ ; 10 mg/mL aged at room temperature overnight.

Coagulant Dose: 4 mg/L as  $\text{Fe}_2(\text{SO}_4)_3 \cdot 6 \text{H}_2\text{O}$  Base pH: 5.5 at 20 °C

Coagulant: MagniFloc 573; 0.1 mg/mL aged at room temperature overnight.

Coagulant Dose: 0.1 mg/L as MagniFloc 573C Base pH: 7.0

Rapid Mixing: 60 seconds

#### Turbulent Parameters

Temperature (°C)	Turbine RPM	Energy Input per Unit Mass ( $\text{cm}^2/\text{sec}^3$ )	RMS Velocity Gradient ( $\text{sec}^{-1}$ )	Kolmogorov Microscale ( $\mu\text{m}$ )
20	250	$3.03 \times 10^3$	550	43
5	250	$3.03 \times 10^3$	448	58

Flocculation: 30 minutes @ 20 °C; 45 minutes @ 5 °C

#### Turbulent Parameters

Temperature (°C)	Turbine RPM	Energy / Unit Mass ( $\text{cm}^2/\text{sec}^3$ )	G-RMS Vel. Grad. ( $\text{sec}^{-1}$ )	Kolmog. Micro. Scale ( $\mu\text{m}$ )	Turbulent Parameter Held Const.
20	30	4.89	22	214	Baseline
20	60	37.60	60	129	Baseline
5	30	4.89	18	291	Const. $\epsilon$
5	45	18.47	34	214	Const. $\eta$
5	34	7.86	22	266	Const. G
5	60	37.6	50	175	Const. $\epsilon$
5	86	129.6	92	129	Const. $\eta$
5	67	55.74	60	161	Const. G

In this research, the mixing energy put into the reactor was adjusted at low temperature so that each of these parameters was held constant one at a time. The full range of testing, shown in Figure 86, was done, in the A/D flocculation region using alum as the coagulant; the conditions were:

- o at 20 °C, alum dose = 5 mg/l as alum\*18H<sub>2</sub>O, G = 22 and 60 sec<sup>-1</sup>, pH = 6.8, Turbine geometry.
- o at 5 °C, alum dose = 5 mg/l as alum\*18H<sub>2</sub>O, pOH constant,  $\epsilon$ ,  $\eta$ , and G constant, Turbine geometry.

Additional testing was done using ferric sulfate (Figure 87), and a cationic polymer (Figure 88) flocculated at constant  $\epsilon$ . The polymer testing was done under the presumption that the polymer should be insensitive to changes in system chemistry. Thus, if the initial mixing is adequate to disperse the polymer, any differences should be due to changes in the fluid dynamics of the system. The rapid mixing of the polymer was found to be very sensitive to temperature induced changes. The effect of temperature on rapid mixing is discussed in Srivastava (1988). Only the results under optimal rapid mixing of cationic polymer are presented here.

The sensitivity of the batch flocculation process to large scale turbulence, and to the locally variable nature of the flow field was tested by using two dissimilar impeller geometries (Figure 89). If the floc in the reactor are much smaller than the production scale

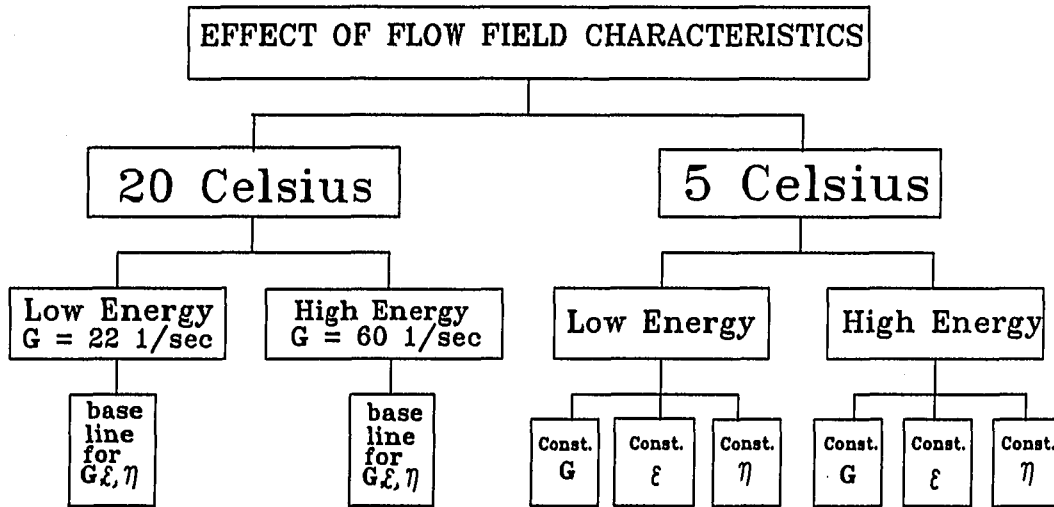


Figure 86. Experimental plan for evaluating the effect of turbulent flow field characteristics on flocculation efficiency with varying temperature

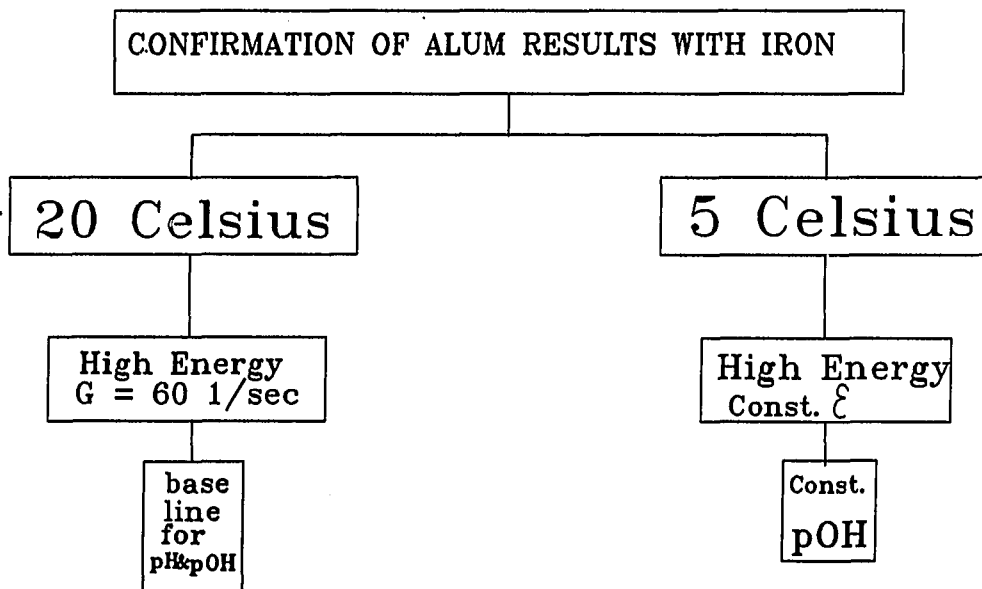


Figure 87. Experimental plan for the confirmation of the turbulence results using iron as the primary coagulant

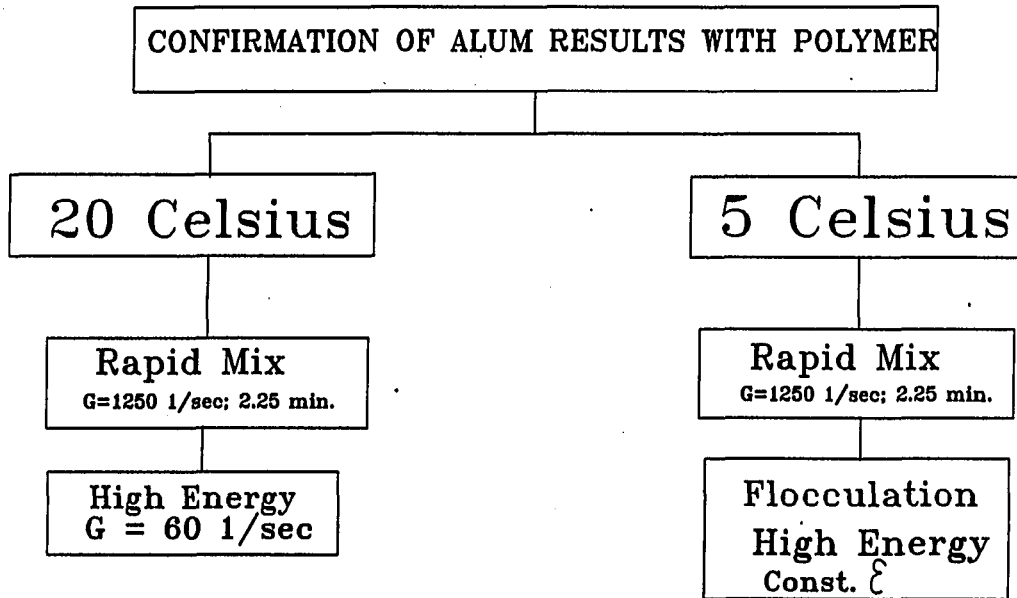


Figure 88. Experimental plan for the confirmation of the turbulence results using cationic polymer as the primary coagulant

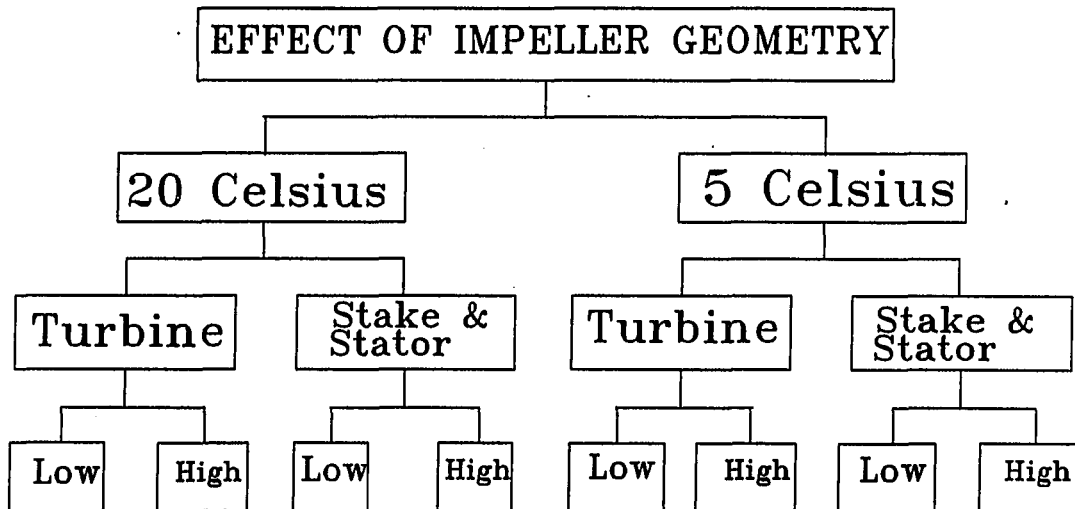


Figure 89. Experimental plan for evaluating the effect of impeller geometry on flocculation efficiency with varying temperature



eddies, then any variability introduced by the geometry change is due to the non-homogeneous, anisotropic nature of the flow field. If the floc are similar in size to the production scale eddies, the variability may be due to either the change in the eddy distribution at the production scale, or it may be due to the non-homogeneous, anisotropic nature of the flow field. The testing was again done using alum, in A/D flocculation under the following conditions:

- o at 20 °C, alum dose = 5 mg/l as alum\*18H<sub>2</sub>O, G = 22 and 60 sec<sup>-1</sup>, pH = 6.8, Stake and Stator geometry, and the Turbine geometry.
- o at 5 °C, alum dose = 5 mg/l as alum\*18H<sub>2</sub>O, pOH constant, ε constant, Stake and Stator geometry and the Turbine geometry.

#### Changes in system chemistry

It is commonly assumed that the metal coagulants form various soluble hydroxyl species or a hydroxide precipitate. This would indicate that if one desires to keep flocculation conditions constant as the temperature drops, it will be necessary to maintain the pOH constant. However, it is the pH which is frequently cited as the variable of importance. Figure 90 shows the tests which have been performed in establishing the effect of system chemistry on flocculation with respect to making temperature adjustments. A base line was established at 20 °C, and then experiments were performed at 5 °C maintaining constant pH and constant pOH. Most of the testing was performed using alum; then a number of tests were performed with

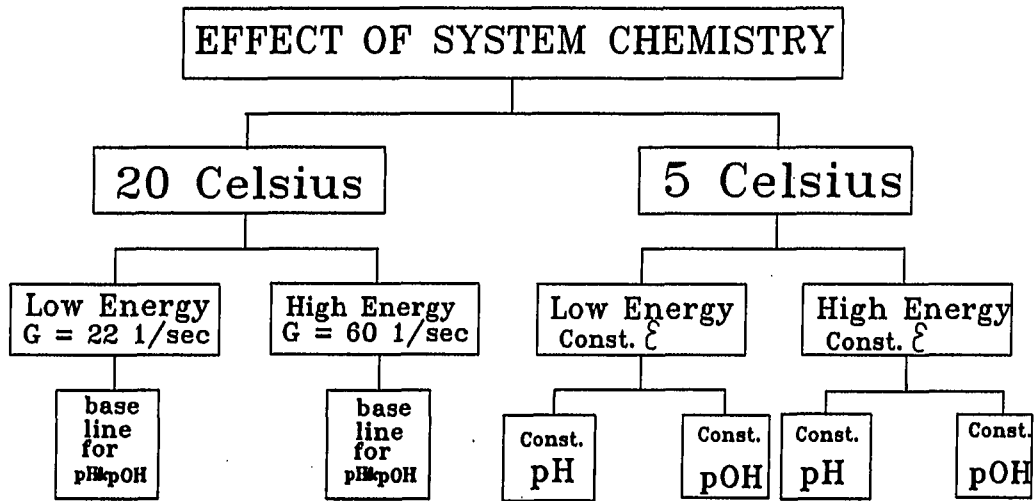


Figure 90. Experimental plan for evaluating the effect of system chemistry on flocculation efficiency with metal salts as the coagulant and varying temperature

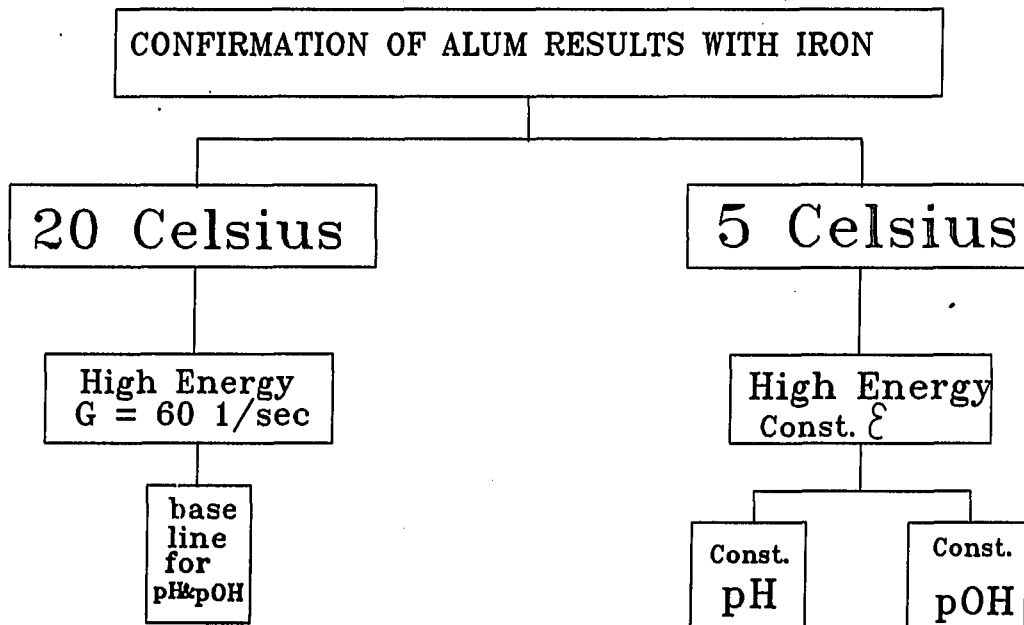


Figure 91. Experimental plan for the confirmation of the system chemistry results using iron as the primary coagulant

iron to confirm the alum work. The iron tests are shown in Figure 91.

It is likely that the system chemistry not only affects the flocculation efficiency, but also the floc strength. This was tested with both the alum and the iron coagulants, by measuring the resistance of the floc to breakup (Figure 92).

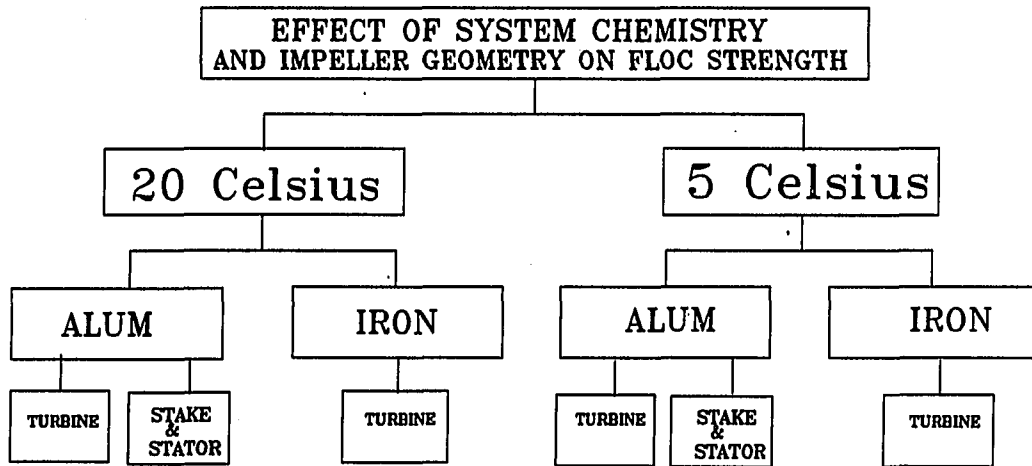


Figure 92. Experimental plan for evaluating the effect of impeller geometry and system chemistry on floc break up

## RESULTS AND DISCUSSION

A summary of the experimental conditions was presented earlier in Table 25. The experimental results are presented in a graphical format, under two major groupings: data on particle counting and data on the effects of temperature on flocculation. The flocculation data will be divided into 4 sections: turbulence effects, system chemistry effects, breakup, and miscellaneous data.

Figure 93 is a typical example of the raw data collected during each experiment. Each particle size distribution (psd) in this figure represents a sample taken from the flocculation reactor at a different point in time. The y-axis is number of particles per mL in each size class, and the x-axis is the equivalent circular diameter of each size class. Some of the samples have been omitted from this graph for the sake of clarity. Data of this type were then evaluated using a number of data presentation techniques.

Most of the comparisons presented herein are based on a normalized rate of change of the primary particle number concentration. Primary particles have been defined as particles with an equivalent circular diameter less than 2.5  $\mu\text{m}$ . Flocculation efficiency data will be presented as  $n_t/n_0$  versus diameter, where  $n_t$  is the primary particle number concentration/mL at time "t",  $n_0$  is the particle number concentration/mL at time zero, and diameter is the equivalent

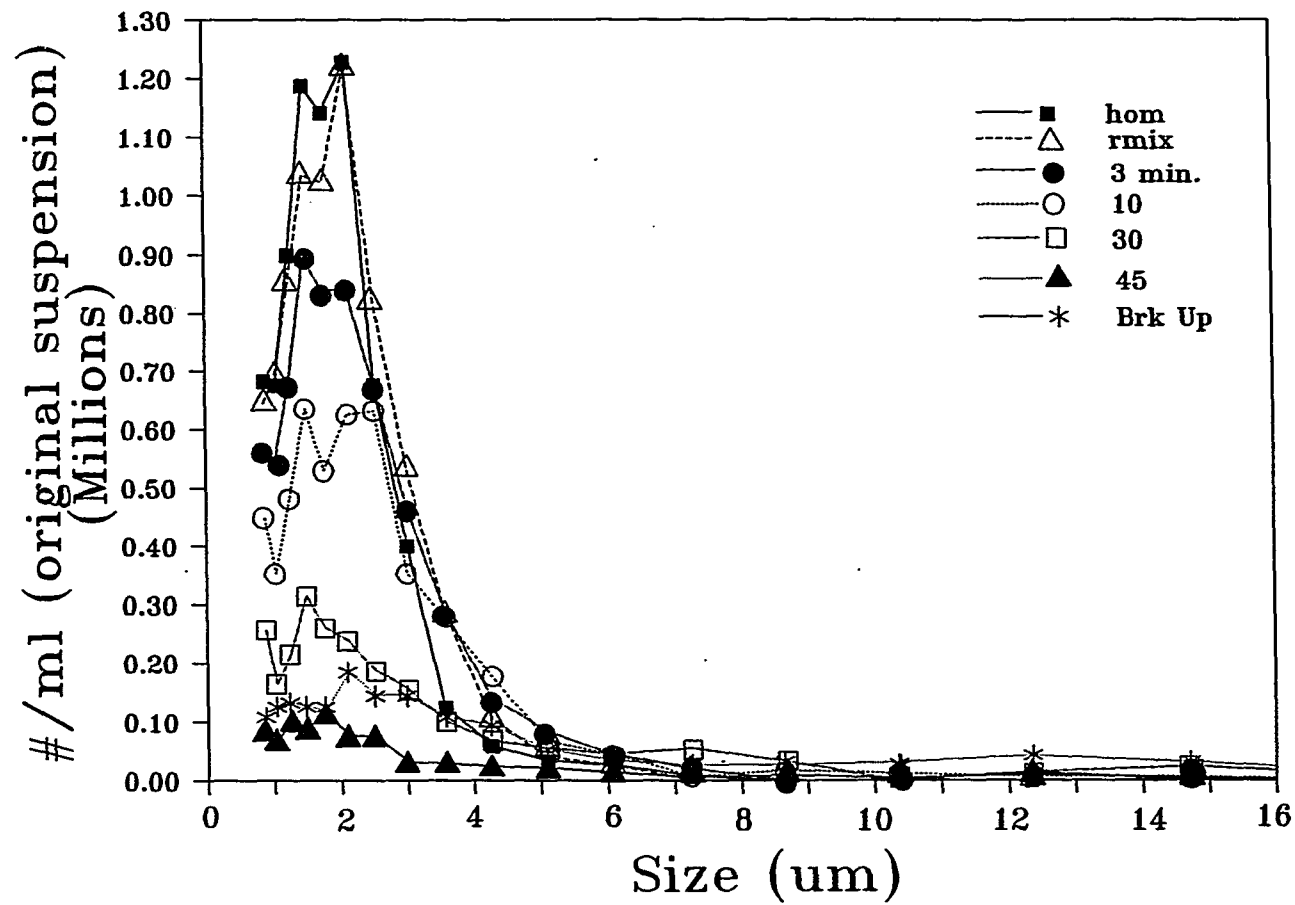


Figure 93. Particle size distribution data as flocculation proceeds; 5 mg/l alum, pH=6.8,  $G=22 \text{ sec}^{-1}$ , Stake and Stator

circular diameter in  $\mu\text{m}$ . The ratio  $n_t/n_0$  is the fraction of primary particles remaining in suspension at any time. Note that this ratio is always one for the homogenized sample. The zero coordinate on the time scale in this type of graph is defined as the end of rapid mixing. Because of this, the homogenized sample is always reported as negative time.

The floc strength data will be presented as  $n_t$  versus diameter, where  $n_t$  is the particle number concentration/mL at time "t" in each size class, and diameter is the equivalent circular diameter in  $\mu\text{m}$ .

In addition to these commonly used graphs the particle counter comparison data sets contain a graph showing the actual number concentration per mL of original sample at any given time. These graphs show both the total number of particles/mL in the suspension and the total number of primary particles/mL in suspension.

Almost all of the experiments were performed in duplicate. The exceptions are as follows. The baseline conditions for alum at 20 °C with the turbine impeller were performed in triplicate. Alum flocculated with the turbine impeller at high energy, constant pOH, constant  $\epsilon$ , at 5 °C was performed in triplicate. The 2 °C test with alum was performed once. All constant G experiments at 5 °C were performed once. The 5 °C, high energy iron experiment was performed once. The polymer tests reported here were performed once. When

multiple experiments have been performed, the average value for the experiments has been presented in the graphical comparisons.

#### Particle Counter Evaluation

In performing this comparison it was assumed that the light microscope/AIA system would provide the highest quality data. This comparison would actually be better termed an evaluation of the HIAC PG-320 12 channel particle counter equipped with a 60  $\mu\text{m}$  sensor, using the AIA. Time was invested in this comparison for two reasons.

First, the water treatment industry accepts and uses the HIAC particle counter in monitoring the flocculation process, and the reason for this acceptance is not obvious. There has never been a well thought out and controlled study reported in the literature which would demonstrate that the industries faith in this technology is warranted. The HIAC was designed for counting discrete particles, as opposed to flocculated material. It is possible, perhaps even likely, that breakup of floc in the counting cell is severe. It is also possible that severe breakup of floc in the counting cell may not affect the usefulness of the instrument in monitoring flocculation, if we define flocculation as the disappearance of primary particles. The impact of breakup on the instruments usefulness will depend upon the breakup mechanism. In other words, are the floc broken down to second level floc structures, or are the floc broken down to primary particles.



Second, if the HIAC is a suitable instrument for monitoring the flocculation process, it is much more convenient to use than the AIA. A problem inherent in the use of the AIA, and other microscopic techniques, is the small sample size. The HIAC can easily count 60,000 particles in the half the time it takes to count 1,000 particles on the AIA.

The following suspensions were used to evaluate the HIAC:

- o standard latex sphere suspension containing a combination of discrete sphere sizes (Figure 94),
- o well defined clay suspension (25 mg/l kentucky ball clay kaolinite) (Homogenized sample for the flocculation tests),
- o a flocculated suspension containing strong floc (Figures 95 and 96), and
- o a flocculated suspension containing weak floc (Figure 97).

In Figure 94, the HIAC PC-320 was evaluated using a latex spheres in water suspension provided by the manufacturer. The sensor is rated by the manufacturer for 1 to 60  $\mu\text{m}$ . The purpose of this experiment was to establish the low end sensitivity of the sensor. The primary particles used in the flocculation experiments were 1.8  $\mu\text{m}$  in diameter. If the disappearance of primary particles was to be the measure of flocculation efficiency, then it was important that the instrument be capable of reliably resolving and measuring particles smaller than the primary particles. Figure 94 shows that it would be

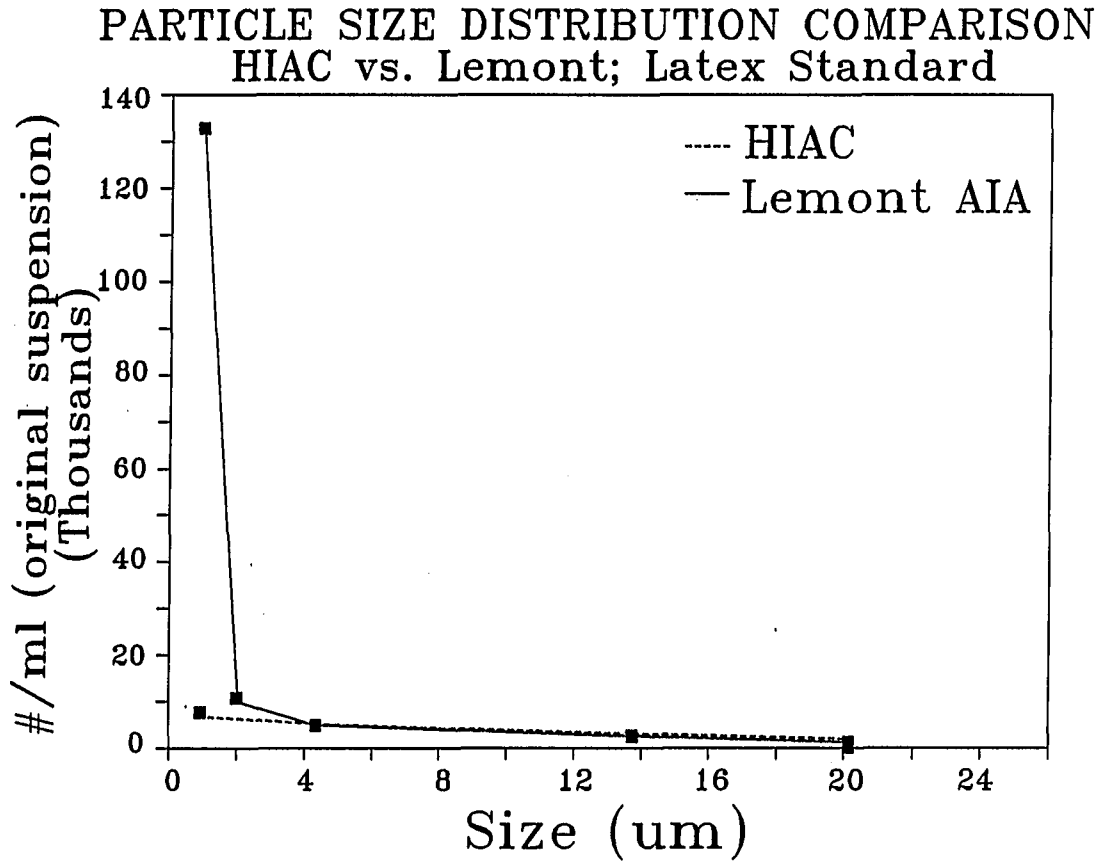


Figure 94. Comparison of the HIAC and the AIA using a standard latex sphere suspension

more accurate to consider the sensor completely reliable for the measurement of particles larger than 4  $\mu\text{m}$ . The particle size class representing the sensors lower limit (1  $\mu\text{m}$ ), based on the manufacturers literature, exhibits a tremendous discrepancy. This is a definite indication that the HIAC may have some shortcomings, but this is not necessarily proof that the HIAC is useless. The latex spheres are translucent and the HIAC works on a light blockage principle, it is possible that the HIAC may count natural material in the 1  $\mu\text{m}$  range more effectively than it counts the latex spheres.

Figure 95 is a composite figure in which the HIAC and the AIA have both been used to evaluate the changes in particle numbers of different size categories at several times in the flocculation process. The kaolinite clay being flocculated in these tests is representative of many naturally occurring colloids. The homogenized sample is dispersed clay, or, in other words, the primary particles used in all of the flocculation experiments. The flocculation conditions are given in the upper right hand corner of Figure 95B, and a strong floc was produced under these conditions. Note that this floc was formed in a low energy environment.

Figure 95A and 95B show the actual particle size distributions measured. Note that the vertical axis on the HIAC graph is in thousands and the vertical axis in the AIA graph is in millions. Note also the total count/mL shown in 95C, and recall that, based on

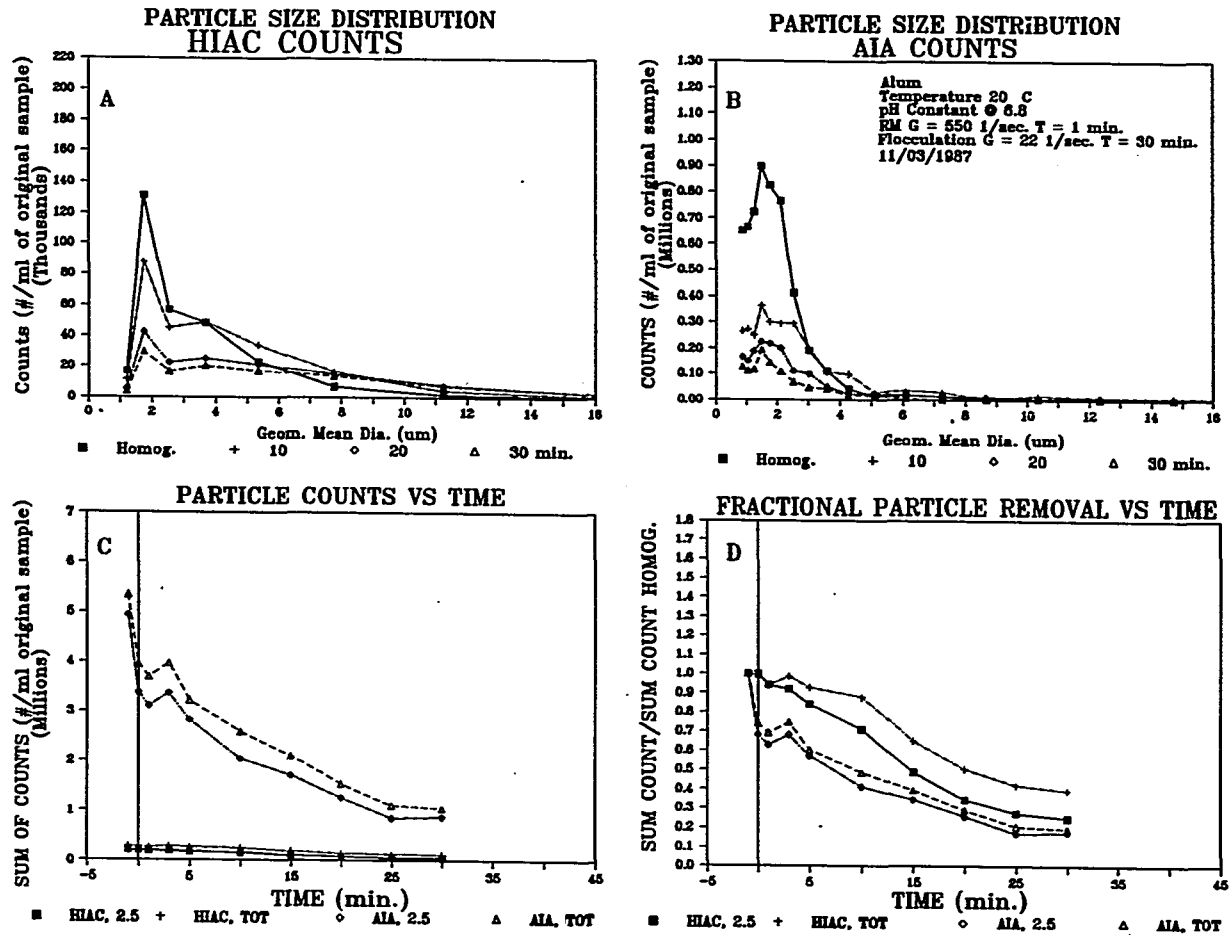


Figure 95. Comparison of the HIAC and the AIA using a strong alum floc suspension aggregated at 20 °C and a  $G = 22 \text{ sec}^{-1}$

a spherical geometry, a theoretical primary particle concentration of 3 million particles/mL was calculated. This is another indication of the HIAC's inability to reliably measure particles smaller than 4  $\mu\text{m}$ , with a 60  $\mu\text{m}$  sensor.

It is obvious from the preceding data that, although the HIAC does not measure all of the particles smaller than 4  $\mu\text{m}$ , it does measure some of the particles smaller than 4  $\mu\text{m}$ . Figure 95C is the particle concentration/mL versus time during flocculation. There are two pairs of lines on this plot, the upper pair are the AIA numbers the lower pair are the HIAC numbers. The upper line of each pair represents the total number of particles/mL at the time specified. The bottom line of the two represents the total number of particles/mL smaller than 2.5  $\mu\text{m}$ . From this graph one can see that, even though the HIAC is not reliably counting all of the particles smaller than 4  $\mu\text{m}$ , the small particles still account for the majority of the particles counted. Because this is the case, the HIAC data can be normalized and flocculation trends measured if the floc are a robust floc. Figure 95D demonstrates that even if the absolute numbers obtained by the HIAC are incorrect, the flocculation trend established maybe useful. Figure 95D represents the HIAC and AIA data both normalized by dividing the particle count data by the particle count numbers in the homogenized sample. For this system with strong floc, the flocculation rate information is remarkably

good considering the poor quality of the absolute number count data for the HIAC instrument.

Figure 96 is confirmation of the results shown in Figure 95. The floc grown in Figure 96 were grown under high energy conditions. A total of six tests were performed with the strong floc, and all six revealed the same general trends shown in Figures 95 and 96.

These HIAC data must be viewed cautiously, because even with the strong floc, there were occasional anomalies in the data. These anomalies were usually single data points which had extremely high counts when compared to the other HIAC data for the same experiment. None of the anomalies which occurred in the HIAC data occurred in the AIA data, the AIA data produced relatively smooth, well behaved, curves. Based on this, one must conclude that even in a system of strong floc, it would be necessary to continually check the HIAC results with a microscope.

Figure 97 is similar to Figures 95 and 96, but the data in Figure 97 were collected from a weak floc system. The trends measured by the HIAC no longer mimic the trends measured by the AIA. The AIA shows a significant decrease in the number of particles over time, but the HIAC shows virtually no change in the particles less than 3  $\mu\text{m}$ , and actually shows an increase in the number of particles larger than 3  $\mu\text{m}$ . Figure 97D, the normalized counts make the source of the problem

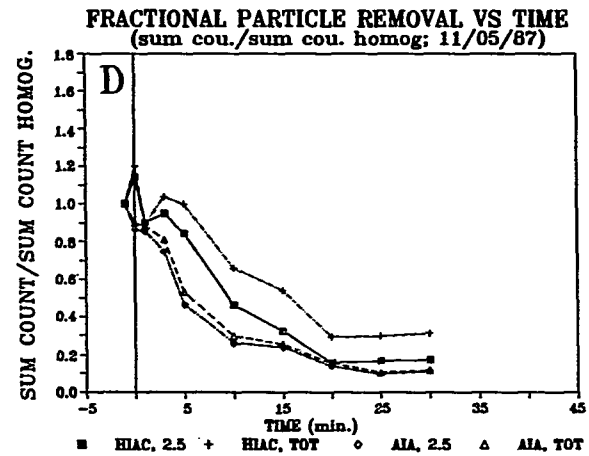
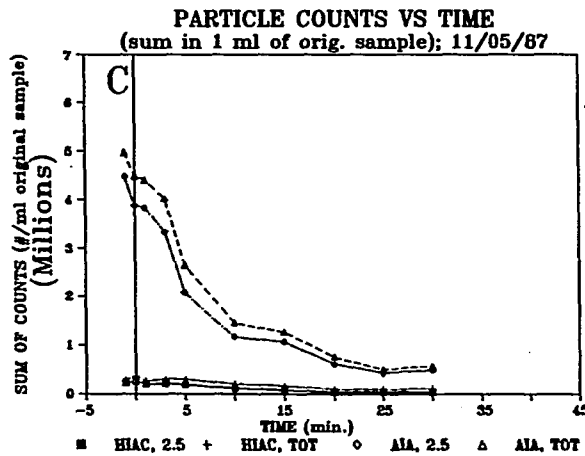
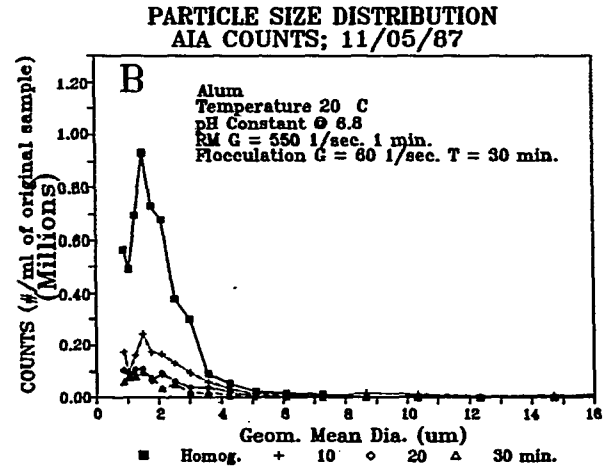
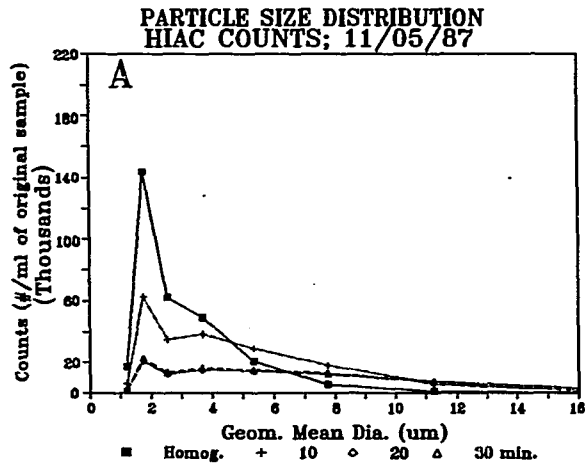


Figure 96. Comparison of the HIAC and the AIA using a strong alum floc suspension aggregated at 20 °C and a  $G = 60 \text{ sec}^{-1}$

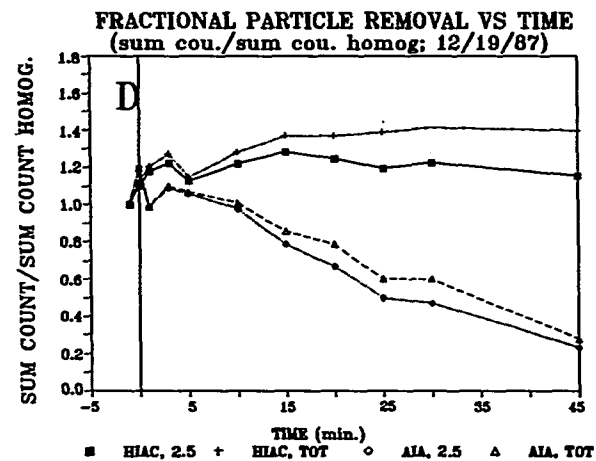
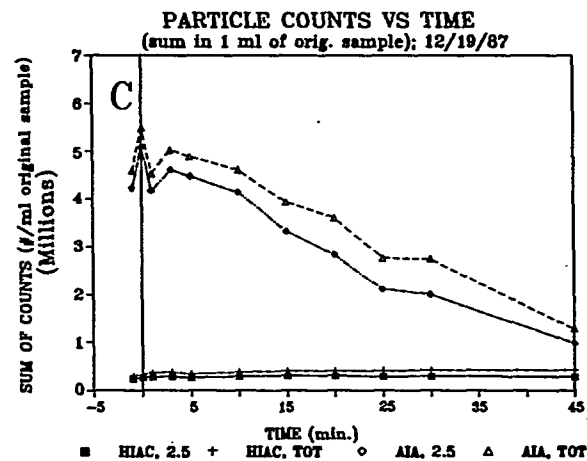
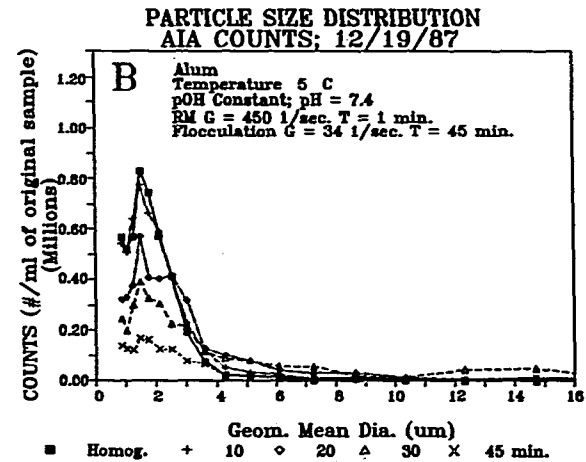
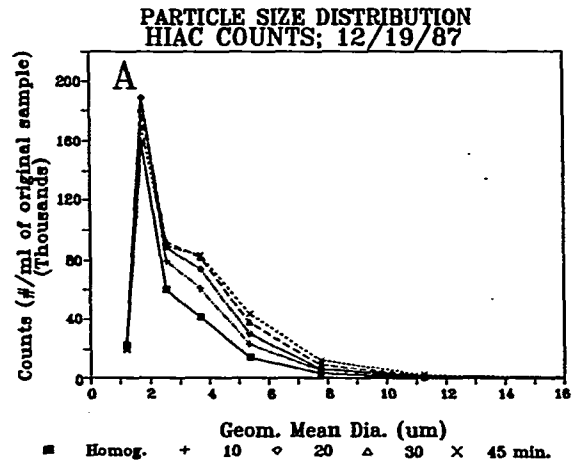


Figure 97. Comparison of the HIAC and the AIA using a weak alum floc suspension aggregated at 5 °C and a  $G = 34 \text{ sec}^{-1}$



obvious. The floc which have grown are not structurally strong enough to withstand the shear induced by transfer from the bulk liquid to the sensor and are being broken up in the sampling tube or in the sensor itself. As a result of the flocculation and then subsequent breakup, the number of particles being counted on the HIAC is not only not being reduced, but is actually being increased. Particles are growing into the 4+  $\mu\text{m}$  size and thus into the size range where the ability of the HIAC instrument to reliably count particles is good. Again, there were 6 tests performed with the weak floc, which showed the same general trends. Anomalies in the HIAC data were once again present.

It appears that counting flocculated materials with the HIAC is perhaps possible with some floc systems, but the researcher must be extremely careful. Because it was necessary to use a weak floc system in some portions of this work, and because the HIAC did not reliably count the primary particles used in this work, the results produced by the HIAC were unacceptable for use in the work reported herein.

#### Effect of Temperature on Flocculation

##### Turbulence results

Figures 98-101 contain the comparisons used to explore the effects of modifying the flow field characteristics,  $G$ ,  $\eta$ , and  $\epsilon$ , as the temperature was changed.

Figures 98 and 99 represent flocculation of kaolinite with alum under high and low energy conditions in the A/D flocculation region, at 5 °C and constant pOH, compared with 20 °C. The 5 °C experiments were conducted at constant  $G$ ,  $\eta$ , and  $\epsilon$ , each of these parameters was held equal to the values at 20 °C. Constant  $G$  (root mean square velocity gradient) is the traditional means used in sanitary engineering for correcting the turbulent mixing intensity for temperature effects. Constant  $\eta$  (Kolmogorov microscale of turbulence) produces a flow field in which the size of the eddy with an eddy Reynolds number of 1 is the same. In practical terms, the lower bound of the turbulent flow field is in the same place. Constant  $\epsilon$  is equivalent to making no attempt to correct for temperature effects. The system is inertially dominated, so keeping  $\epsilon$  constant means keeping impeller rpm constant. The hope was that, by holding these various turbulent flow field parameters constant at the cold temperature, a parameter would be identified which did a superior job of producing identical transport conditions in the flow field at the length scales equal to the primary particle size. In both the high and low energy environments,  $G$ ,  $\eta$ , and  $\epsilon$  all did a comparable job of correcting for the temperature induced changes. None of the three energy parameters was able to eliminate the effect of temperature on alum flocculation.

The constant  $\epsilon$  at 5 °C in the high energy test is almost identical to the low energy results at 20 °C. One is tempted to rationalize this

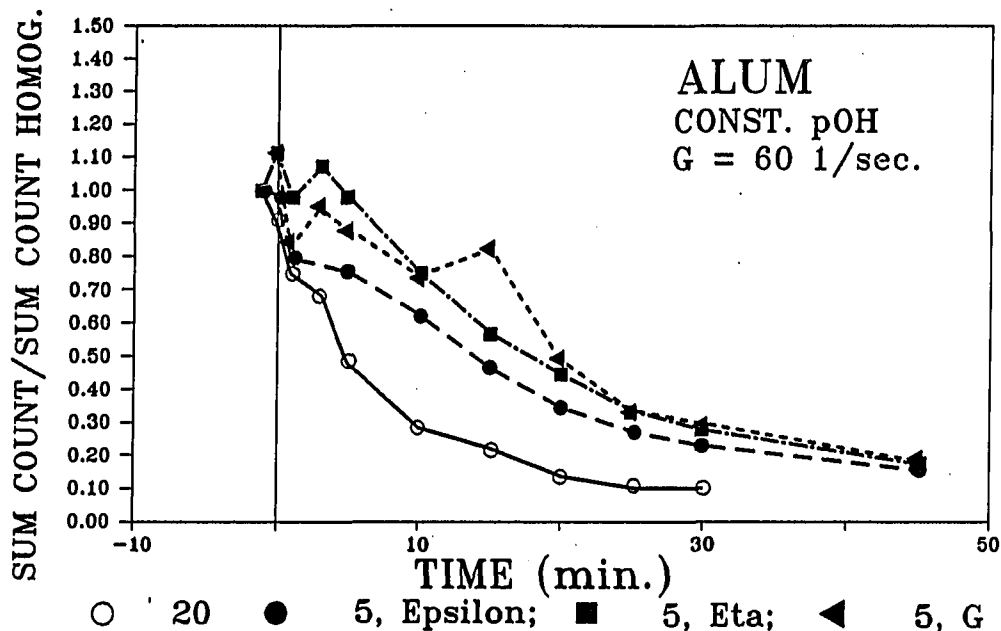


Figure 98. Effect of turbulent flow field parameters on flocculation; Constant pOH,  $G = 60 \text{ sec}^{-1}$  @ 20 °C

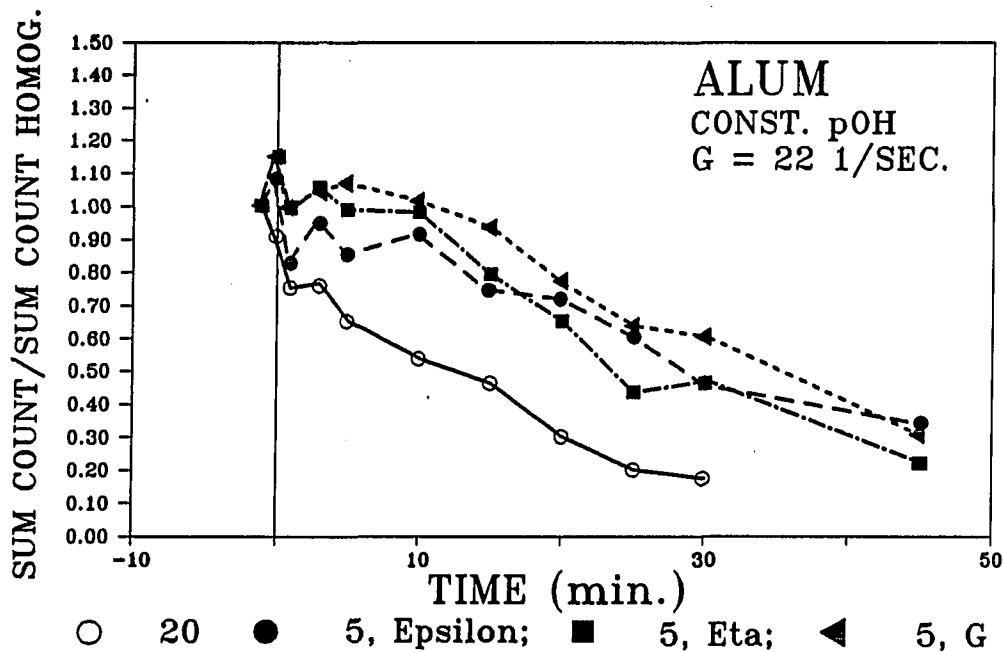


Figure 99. Effect of turbulent flow field parameters on flocculation; Constant pOH,  $G = 22 \text{ sec}^{-1}$  @ 20 °C

by analyzing the various turbulent flow field parameters. However, further work, yet to be presented, using ferric sulfate, work with a cationic polymer, and breakup studies lead to the conclusion that much of the difference seen between the 20 °C and 5 °C alum floc is related to floc strength, and not to turbulent flow field characteristics. The floc strength data will be discussed later, for now it is sufficient to say that the alum floc formed at low temperature is extremely weak.

Figure 100 presents experiments performed with ferric sulfate to confirm the alum results. Figure 100 presents flocculation data with ferric sulfate at 20 and 5 °C, holding pOH and  $\epsilon$  constant. The experiments were conducted without correcting the mixing intensity for temperature effects, that is, the energy input to the reactor was held constant as the temperature was varied. Under these conditions the results at 5 °C are very close to the results at 20 °C. There is a measurable difference between the 5 °C and the 20 °C data, but the difference is small especially when compared to the differences exhibited by the alum.

Figure 101 presents a confirming experiment performed with cationic polymer (MagniFloc 573C) to confirm the alum work. Figure 101 is for flocculation at 20 °C and 5 °C, holding pH and  $\epsilon$  constant. Again, one can see that although there is a measurable difference between the flocculation efficiencies at the two temperatures, the difference

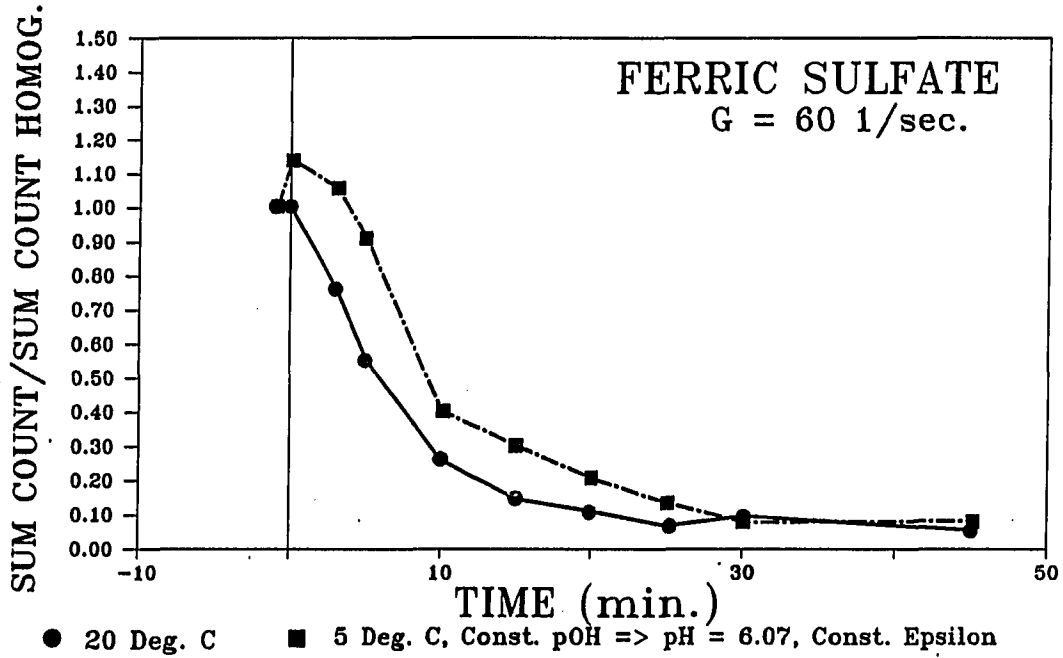


Figure 100. Confirmation: effect of constant epsilon ( $\epsilon$ ) on flocculation using ferric sulfate, turbine

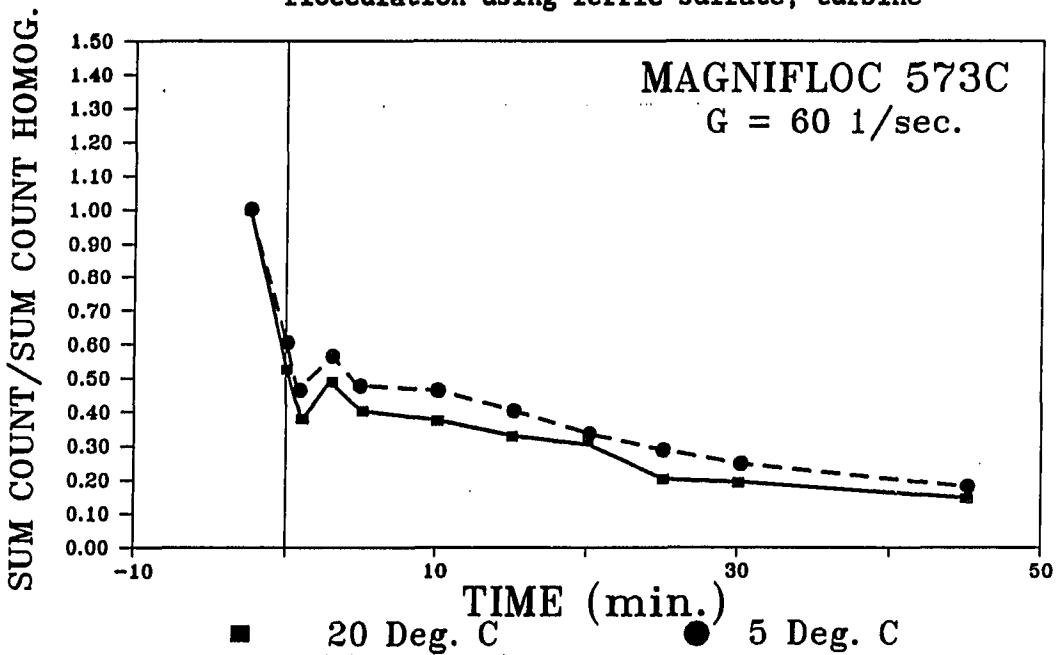


Figure 101. Confirmation: effect of constant epsilon ( $\epsilon$ ) on flocculation using MagniFloc 573C, turbine

is small compared to the differences exhibited by the alum. It is noted that the rapid mix conditions for the polymer were quite different than for the alum. A  $G$  of  $1250 \text{ sec}^{-1}$  for 2.25 minutes was used at  $20 \text{ }^\circ\text{C}$ . At  $5 \text{ }^\circ\text{C}$ , the rapid mix  $\epsilon$  was held constant, resulting in a  $G$  of approximately  $1000 \text{ sec}^{-1}$ . The rapid mixing of the polymer was quite sensitive to temperature effects, however, there is not sufficient space here to discuss this phenomenon. Optimization of the rapid mixing step for the polymer is presented in Srivastava (1988).

Figures 102-107 present the comparisons between the turbine impeller and the stake and stator impeller. The fundamental question of interest in these experiments deals with the homogeneity of the turbulent flow field in the tank. How important is it to distribute  $\epsilon$  evenly over 80 % of the tank, as opposed to 5 % of the tank? All of the turbulent flow field parameters commonly used, i.e.,  $G$ ,  $\eta$ , and  $\epsilon$ , assume a volume averaged  $\epsilon$ . This assumption implies that the energy input to the reactor is evenly distributed over 100 percent of the reactor volume. Figure 102 gives an indication of the non-homogeneity of  $\epsilon$  in the reactor flow field. Figure 102 shows that the turbine impeller must turn quite rapidly to put the same energy into the water as the S&S.

Figure 103 and 104 are comparisons of the flocculation efficiency at a  $G = 22 \text{ sec}^{-1}$  and  $G = 60 \text{ sec}^{-1}$ , at  $20 \text{ }^\circ\text{C}$ , using the turbine impeller

### EFFECT OF IMPELLER GEOMETRY ON THE RPM VERSUS ENERGY RELATIONSHIP

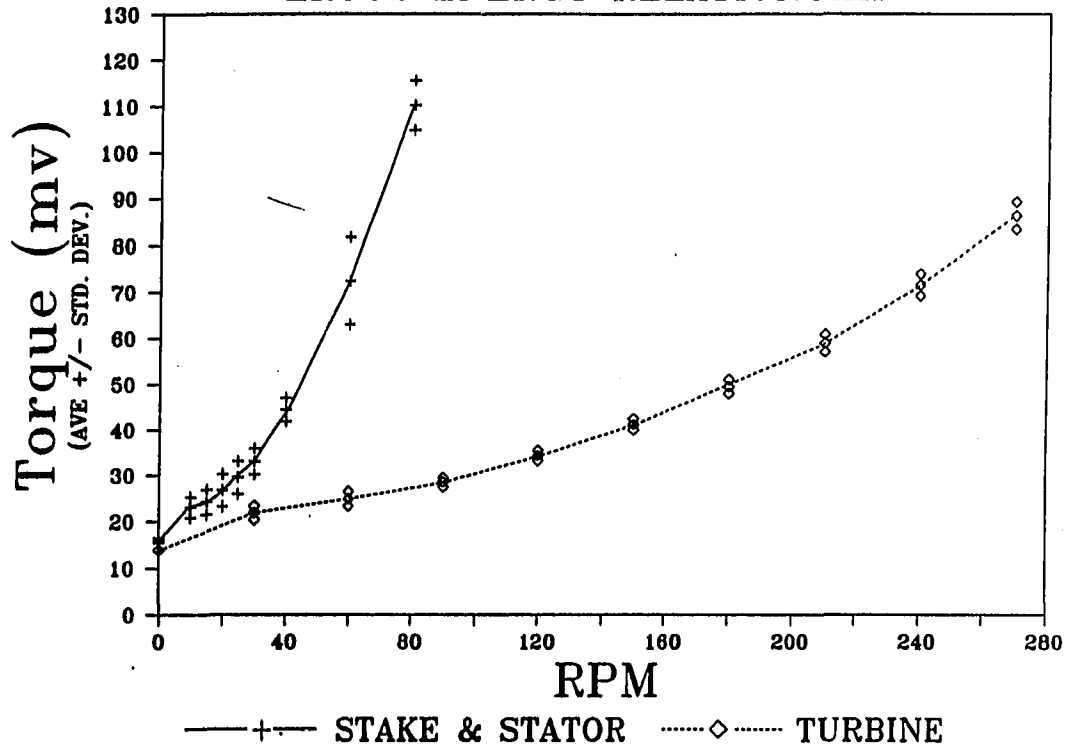


Figure 102.  $\epsilon$  versus RPM relationship for the two impeller geometries

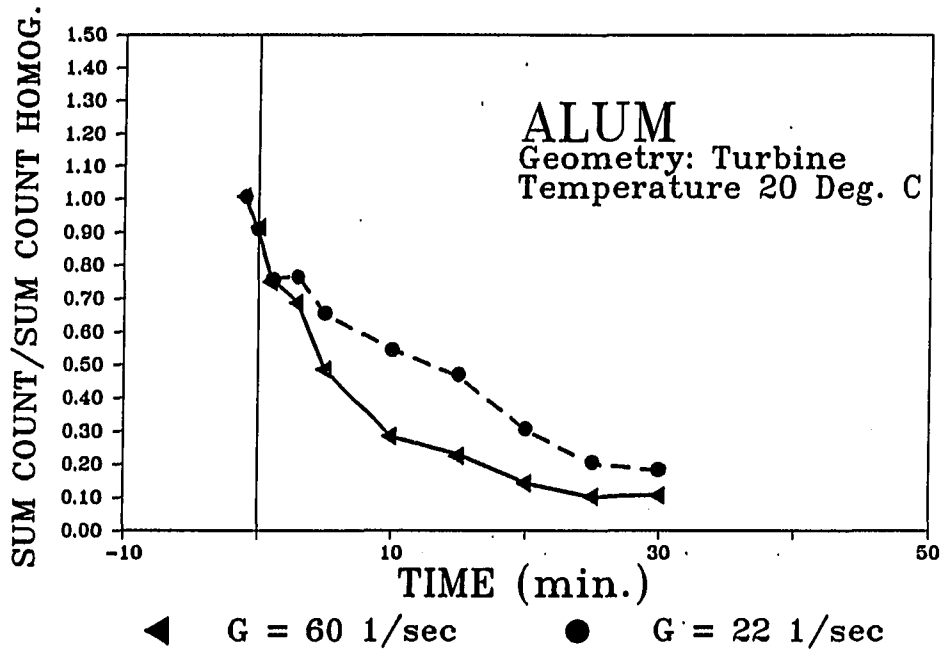


Figure 103. Effect of mixing intensity,  $G$ , on flocculation efficiency using the turbine impeller with alum as the coagulant

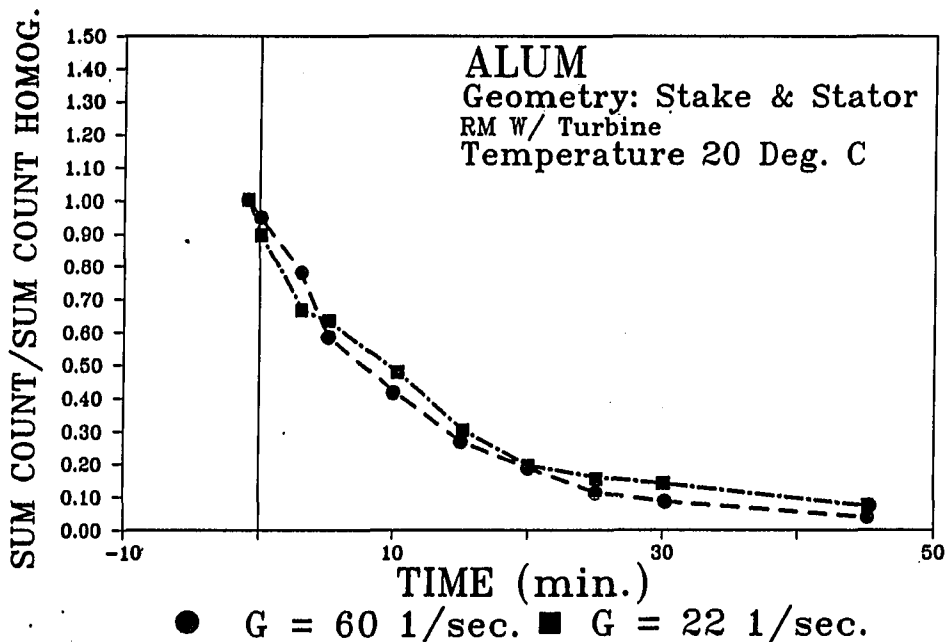


Figure 104. Effect of mixing intensity,  $G$ , on flocculation efficiency using the stake and stator impeller with alum as the coagulant



and the stake and stator impeller respectively. It is interesting to note that while there is a measurable difference between the primary particle removals produced by the turbine impeller, the difference in removal rate is not as great as one would have expected if primary particle reduction is a linear function of  $G$ . The results produced by the S&S impeller at the high and low energy conditions are nearly identical. It is suspected that the reason there is so little difference between the high and low energy flocculation conditions is related to the wide separation in length scales between the primary particles and  $\eta$ .

The impeller geometry comparisons may shed more light on this. Note that the volume averaged Kolmogorov microscale is 214 and 129  $\mu\text{m}$  at low and high  $G$  respectively (Table 25). Figure 105 is a comparison of alum flocculation at  $G = 60 \text{ sec}^{-1}$  at 20 °C and 5 °C, with constant  $\text{pOH}$  and  $\epsilon$ , using both the turbine and the stake and stator (S&S). At 5 °C, the S&S starts out at a lower rate of flocculation, and then it eventually overtakes the turbine and passes it. There is a lag of approximately 10 minutes before the S&S impeller produces any noticeable change, but once it becomes effective, it performs very well. By 45 minutes, it has also done as well as the 20 °C S&S run. Keep this lag and subsequent catch-up in mind.

Figure 106 is similar to Figure 105 except it is the low energy conditions. Note that once again the 20 °C S&S data are very similar

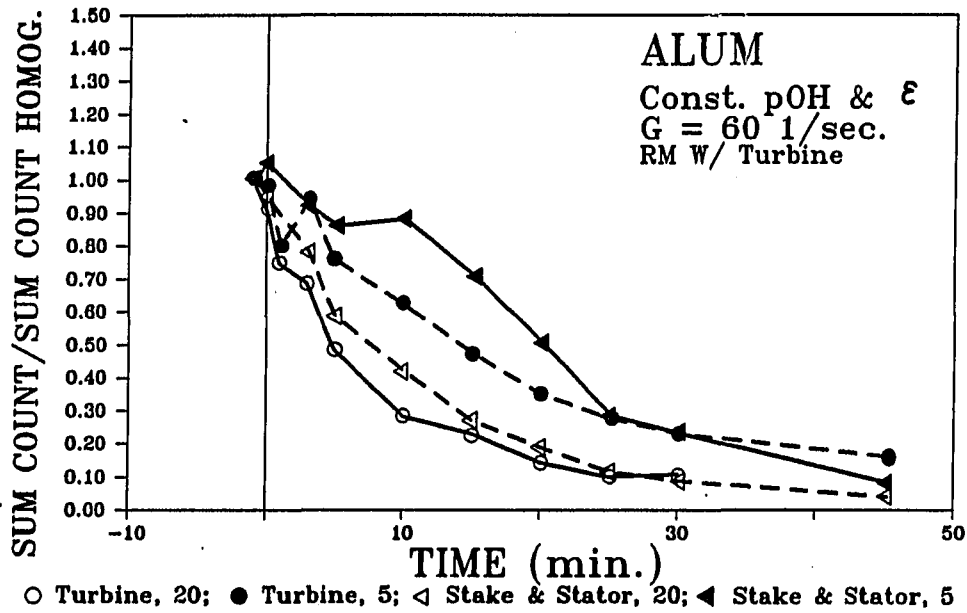


Figure 105. Effect of impeller geometry on flocculation; Constant pOH and  $\epsilon$ ,  $G = 60 \text{ sec}^{-1}$  @  $20^\circ \text{C}$

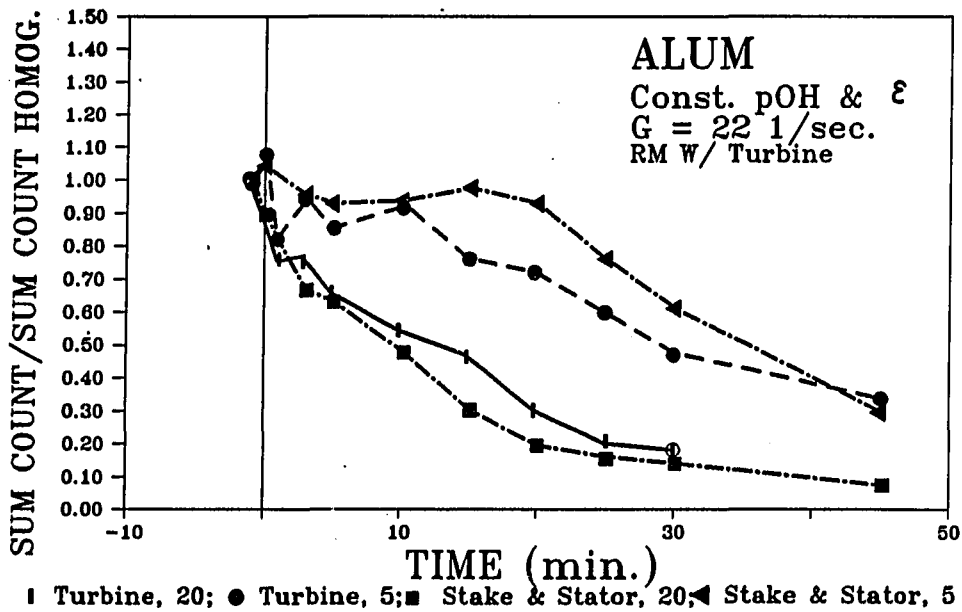


Figure 106. Effect of impeller geometry on flocculation; Constant pOH and  $\epsilon$ ,  $G = 22 \text{ sec}^{-1}$  @  $20^\circ \text{C}$

to the 20 °C turbine data. Also, once again the lag is evident at 5 °C, and this time the lag is evident for both the turbine and the S&S. For the first 10 minutes of the turbine data very little is happening, and then flocculation takes off. Looking back at Figure 99 this lag is evident in all of the low energy low temperature turbine data. The first 20 minutes of the S&S data exhibit very little measurable flocculation taking place, and then once again it takes off and overtakes the turbine impellers performance. It does not duplicate the performance at 20 °C even after 45 minutes, but there is every indication that with a little more time it would have. It is suggested that the lag represents particles which were below the resolution limit of the particle counting system growing into the countable size range as rapidly as particles are leaving the primary particle range. Thus, no net change is observed. At 20 °C, with flocculation at a  $G$  of  $60 \text{ sec}^{-1}$ , the primary particles leave the small sizes rapidly enough so that there is a net loss from the beginning, and the lag is not noticed. The cause of the slow growth is discussed further later.

Figure 107 is a comparison of the S&S at two temperatures and at high and low energy conditions. The  $pOH$  and  $\epsilon$  were held constant as the temperature was changed. Note that at 20 °C, the performance is once again almost identical at  $G = 22$  and  $60 \text{ sec}^{-1}$ . Once again at 5 °C, the lag is evident at both low and high energy, and is almost 2x as long at the low energy.

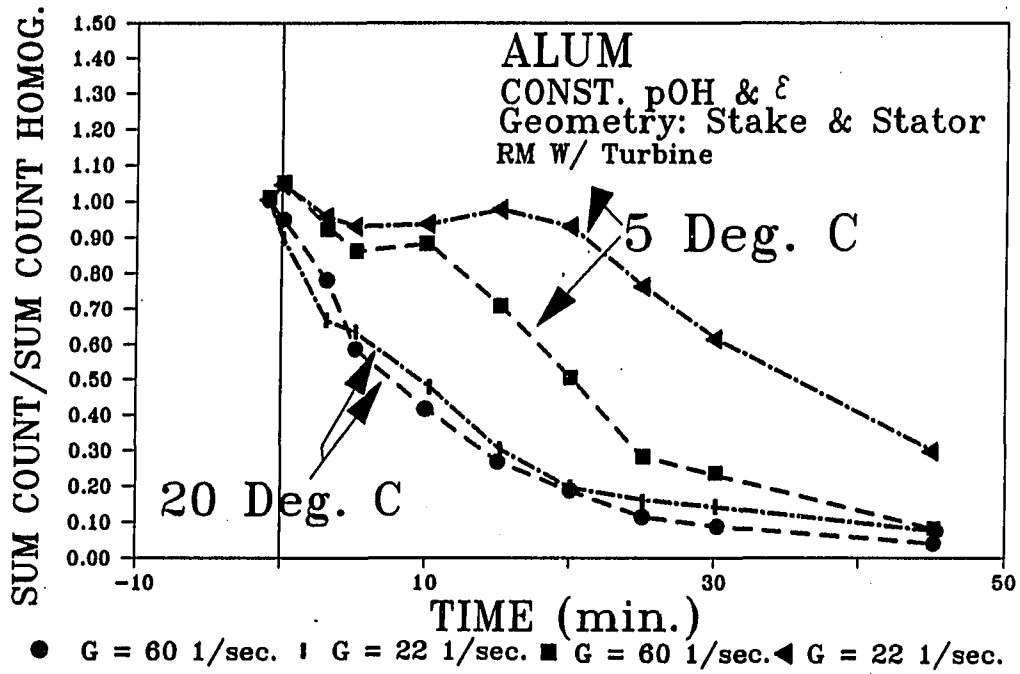


Figure 107. Effect of mixing intensity and temperature on flocculation efficiency using the S&S impeller; constant pOH and  $\epsilon$

As part of each experimental run, the floc size in the reactor was observed through a photographic quality glass window in the reactor. A general estimate of the maximum floc size was obtained using a 30x hand-held microscope with an optical micrometer. It was noted that, regardless of the impeller geometry, the average floc size in the reactor was smaller at cold temperature than at warm temperature. For alum, the maximum floc sizes with the turbine impeller at 20 °C, were approximately 100 and 200  $\mu\text{m}$  for the G of 60 and 22  $\text{sec}^{-1}$  respectively. For the 5 °C, constant pH, and high energy, the maximum floc size was <50  $\mu\text{m}$ , and for constant pOH it was around 75  $\mu\text{m}$ . The maximum floc size for the 5 °C low energy experiments, was about 75  $\mu\text{m}$  for both constant pH and constant pOH. The maximum floc size for the S&S impeller was a little larger at 20 °C, than the maximum floc size for the turbine impeller. However, at 5 °C, regardless of conditions the max floc size produced by the S&S impeller also appeared to be the average floc size. The floc were extremely uniform, and were approximately 50  $\mu\text{m}$  in size. This is in sharp contrast to the floc formed by the turbine, which appeared to cover a fairly large range of sizes.

#### System chemistry results

Figures 108-110 contain the comparisons used to explore the effects, on flocculation efficiency, of altering the system chemistry with temperature. The system pH is the control parameter most frequently

used in flocculation. However, one must ask whether pH or pOH is the appropriate control parameter to use under varying temperature conditions. Table 26 is used to convert from a specified pH at 20 °C, to the appropriate pH for a constant pOH at another temperature. Figure 108 shows high energy alum flocculation results at 20 °C and 5 °C, holding  $\epsilon$  constant, and varying the system pH to produce either constant pH or pOH with changing temperature. Figure 109 is the same for the low energy flocculation conditions. In both cases constant pOH significantly out performed constant pH. It is noted that alum at 5 °C does not perform as well as alum at 20 °C, even with the pOH held constant. It is not obvious why this is the case. It may be because the half-time of water molecules in the water sheath associated with the aluminum ion is lengthened as the temperature is lowered. If the half-time were nsec, as it is with the iron ion, this might not be a concern. However, with aluminum the time scale is more on the order of seconds, and doubling the length of the association time may significantly change the reactions which dominate in the system. The first thought that came to mind, was that the reaction kinetics no longer favored surface adsorption of the positively charged species, and small hydroxide precipitates were forming in suspension. These hydroxide precipitates, if they exist, would form more primary particles and would be less effective at neutralizing the surface charges on the clay particles. The data, at first glance, seem to lend credence to this hypothesis. Most of the alum experiments and the iron experiments at 5 °C showed an increase

Table 26. Conversion from pH at a specified temperature to the appropriate pH for constant pOH at another temperature. The purpose of this table is to allow the user to maintain a constant pOH as the temperature is varied

pOH	Temperature (°C)							
	30 pH	25	20	15	10	5	2	0
8.67	5.17	5.33	5.5	5.68	5.87	6.07	6.21	6.28
8.57	5.27	5.43	5.6	5.78	5.97	6.17	6.31	6.38
8.47	5.37	5.53	5.7	5.88	6.07	6.27	6.41	6.48
8.37	5.47	5.63	5.8	5.98	6.17	6.37	6.51	6.58
8.27	5.57	5.73	5.9	6.08	6.27	6.47	6.61	6.68
8.17	5.67	5.83	6.0	6.18	6.37	6.57	6.71	6.78
8.07	5.77	5.93	6.1	6.28	6.47	6.67	6.81	6.88
7.97	5.87	6.03	6.2	6.38	6.57	6.77	6.91	6.98
7.87	5.97	6.13	6.3	6.48	6.67	6.87	7.01	7.08
7.77	6.07	6.23	6.4	6.58	6.77	6.97	7.11	7.18
7.67	6.17	6.33	6.5	6.68	6.87	7.07	7.21	7.28
7.57	6.27	6.43	6.6	6.78	6.97	7.17	7.31	7.38
7.47	6.37	6.53	6.7	6.88	7.07	7.27	7.41	7.48
7.37	6.47	6.63	6.8	6.98	7.17	7.37	7.51	7.58
7.27	6.57	6.73	6.9	7.08	7.27	7.47	7.61	7.68
7.17	6.67	6.83	7.0	7.18	7.37	7.57	7.71	7.78
7.07	6.77	6.93	7.1	7.28	7.47	7.67	7.81	7.88
6.97	6.87	7.03	7.2	7.38	7.57	7.77	7.91	7.98
6.87	6.97	7.13	7.3	7.48	7.67	7.87	8.01	8.08
6.77	7.07	7.23	7.4	7.58	7.77	7.97	8.11	8.18
6.67	7.17	7.33	7.5	7.68	7.87	8.07	8.21	8.28
6.57	7.27	7.43	7.6	7.78	7.97	8.17	8.31	8.38
6.47	7.37	7.53	7.7	7.88	8.07	8.27	8.41	8.48
6.37	7.47	7.63	7.8	7.98	8.17	8.37	8.51	8.58
6.27	7.57	7.73	7.9	8.08	8.27	8.47	8.61	8.68
6.17	7.67	7.83	8.0	8.18	8.37	8.57	8.71	8.78
6.07	7.77	7.93	8.1	8.28	8.47	8.67	8.81	8.88
5.97	7.87	8.03	8.2	8.38	8.57	8.77	8.91	8.98
5.87	7.97	8.13	8.3	8.48	8.67	8.87	9.01	9.08

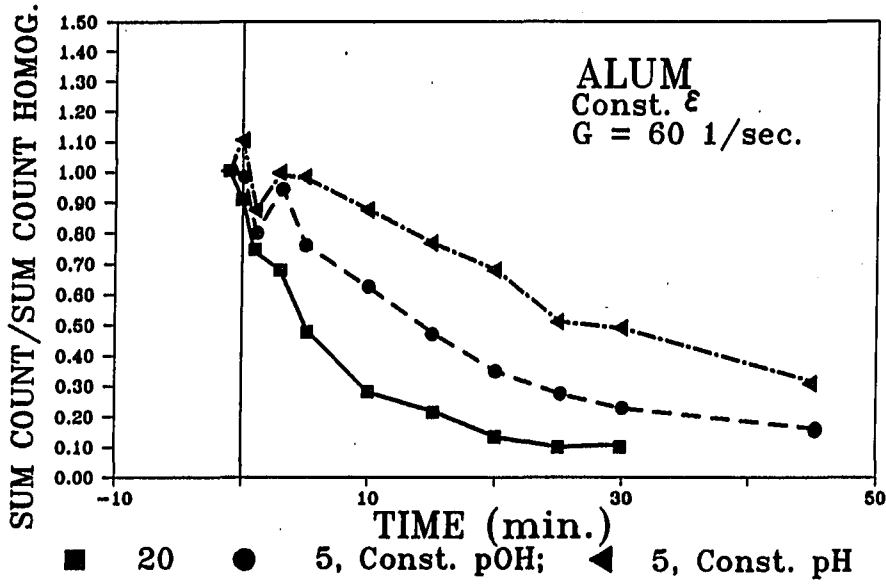


Figure 108. Effect of system chemistry on alum flocculation; high energy, turbine

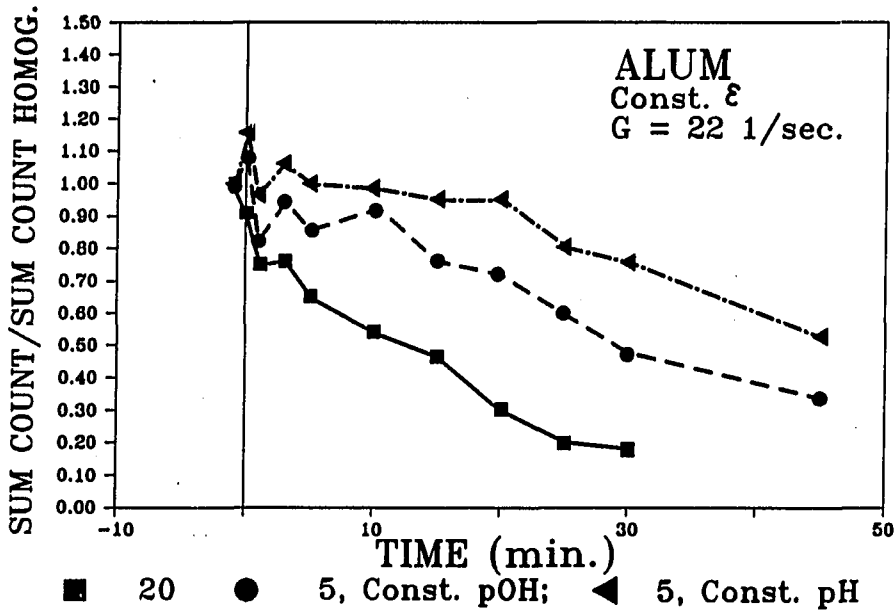


Figure 109. Effect of system chemistry on alum flocculation; low energy, turbine



in the number of primary particles at the end of rapid mixing. However, the hypothesis doesn't really fit the iron system, since the half-time for water associating with the iron ions is in the nsec range, and the iron experiments exhibited an increase in particles at the end of the rapid mix. To explore this issue further the following set of experiments were performed to isolate the reason that the number of primary particles increased early in the low temperature flocculation experiments.

It is suggested that there are two potential causes for the increase in the number of particles in the rapid mixed sample. First, it is possible that when the alum is added, it precipitates and the precipitates show up as an increase in primary particles. It is also possible that the aluminum does not form visible precipitates, but that submicron clay particles grow into a measurable size. In an effort to determine which of these mechanisms was most likely, two experiments were conducted.

If the cause of the particles is simply aluminum precipitation, then the aluminum should precipitate whether the clay is present or not. The solution without the clay will be significantly more supersaturated than the solution with the clay, because when the surface of the clay is present it competes for the aluminum and removes it from solution. Thus, with the clay present the aluminum would tend to precipitate on the surface of the clay and not as free

particles in suspension. Therefore, if the particles do not appear in the absence of the clay, then submicron clay particles are also involved in the particle growth. In the two experiments, only the rapid mix phase of the coagulation/flocculation process was run. This is because the particles are noticed at the end of the rapid mix cycle, and appear to be associated with the rapid mix.

The following experimental conditions were used:

- o mixing intensity 250 RPM;  $G = 450 \text{ sec}^{-1}$
- o temperature = 5 °C
- o alum dose 5 mg/l as alum
- o dilution water was tap water buffered with carbonate
- o constant pH and pOH conditions were both tested

The kaolinite clay particles were absent, and the rapid mix was extended to five minutes, instead of the usual one minute rapid mix, to allow ample time for reactions to take place. First, the constant pOH (pH = 7.41) results. The thin sample cells were loaded with homogenized, 1, 3, and 5 minute samples. The cells were viewed at 474.609x, and there were no differences between any of the cells viewed. This indicates that no precipitates were formed which could be resolved by the microscope. The following turbidity changes were measured during the 5 minutes of rapid mixing.

Initial Turbidity	0.18 NTU
1 min Turbidity	0.23 NTU

5 min Turbidity                      0.26 NTU

This would indicate that something did happen when the alum was added. However, the changes which took place were at a scale smaller than the microscope could resolve.

During the constant pH (pH = 6.8) experiment, the cells were not filled, since it is unlikely that there would be visible precipitates at pH=6.8, if there were none at pH=7.41. The following turbidity changes were measured.

Initial Turbidity	0.15 NTU
1 Min Turbidity	0.17 NTU
3 Min Turbidity	0.24 NTU
5 Min Turbidity	0.28 NTU

Again, it appears that there is an effect, but it is difficult to determine what is causing the effect. It seems that at this pH the change which occurs may take place more slowly than it did at pH=7.41.

It appears that no measurable primary particles are formed due to aluminum precipitation. Any increase in number concentration which is measured is probably caused by small clay particles interacting with the alum and growing into the visible range. This phenomenon is probably also occurring at 20 °C, but at 5 °C the particles are growing into the visible range faster than they are growing out of

it. At 20 °C the particles are leaving the primary particle size range fast enough so there is no measurable net increase in particles. Having said all of this, it is still not clear why the 5 °C, constant pOH, alum experiments did not reproduce the flocculation efficiencies measured at 20 °C.

Figure 110 contains confirmation of the alum results with ferric sulfate. Again, the constant pOH outperformed the constant pH. The performance at constant pOH at 5 °C was almost as good as the performance at 20 °C. Based on the data presented one would have to conclude that, when using metal salt coagulants in the flocculation process, constant pOH is the process control parameter of choice to minimize temperature effects.

#### Breakup data

Another measure of the optimal system chemistry control strategy is resulting floc strength. Figures 111, 112, and 113 contain evidence of floc strength at two temperatures, with two coagulants, with two impeller geometries, at constant pH and pOH with temperature. As mentioned previously Figures 111 and 112 present particle size distributions of various alum floc samples after breakup. The floc were formed by flocculating the suspension for 45 minutes in the high energy environment. The floc were then broken up by subjecting them to the same volume averaged  $\epsilon$ , that was used during rapid mixing. In Figure 111 the turbine impeller was used to breakup the floc, and in

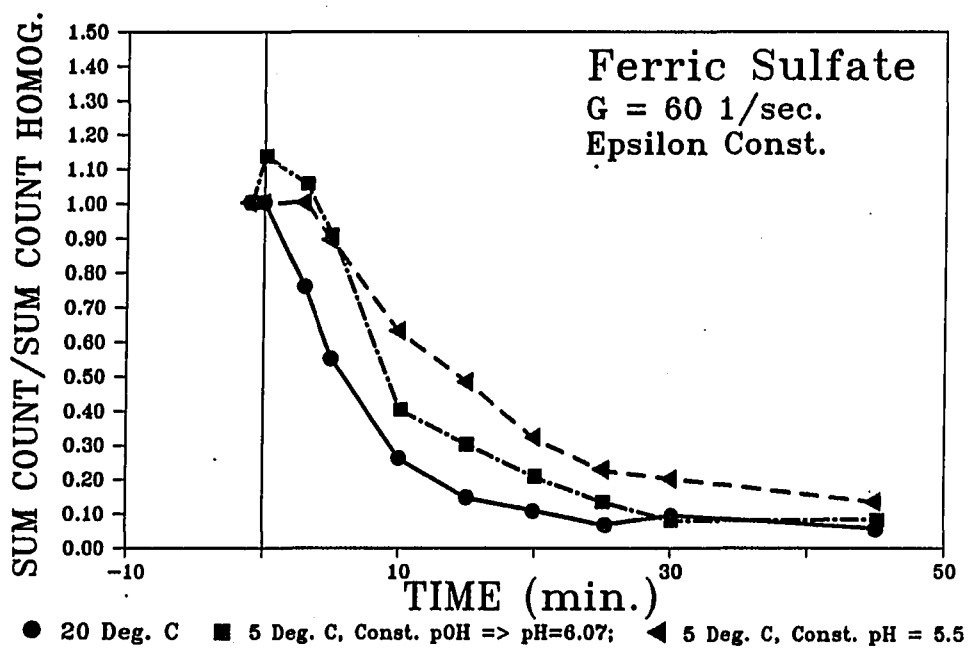


Figure 110. Confirmation: effect of system chemistry on iron flocculation; high energy, turbine

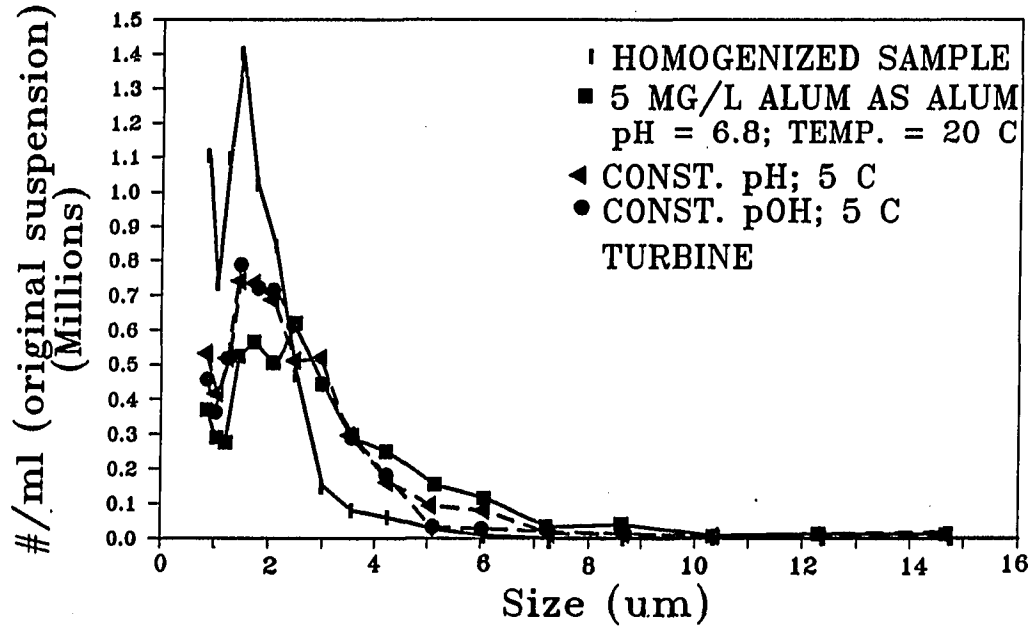


Figure 111. Primary particles produced by breakup of alum floc; turbine

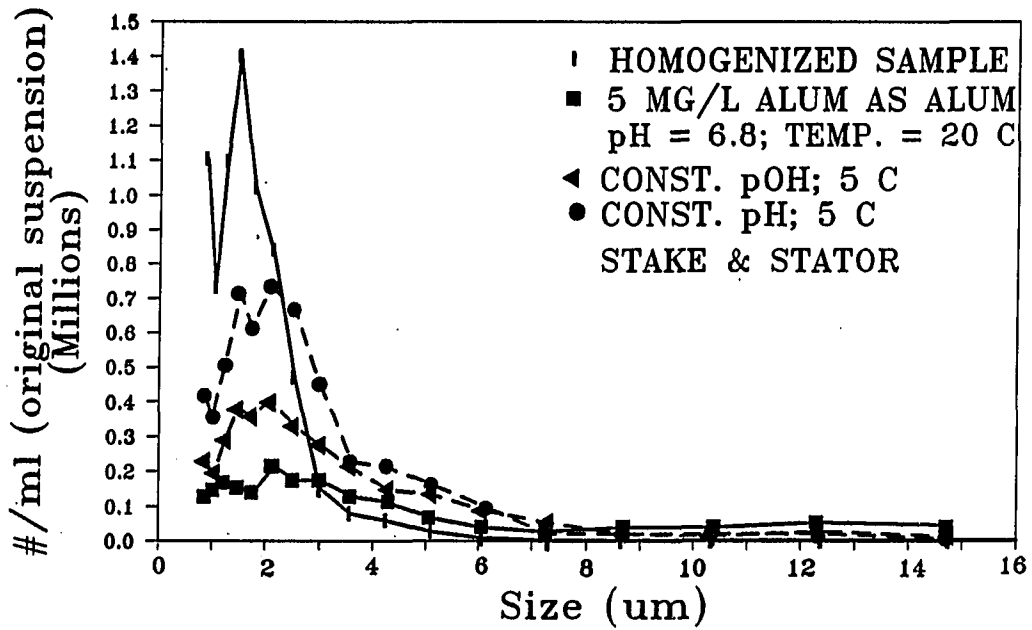


Figure 112. Primary particles produced by breakup of alum floc; S&S

Figure 112 the S&S impeller was used to breakup the floc. Note in Figure 111 that, when the breakup was performed with the turbine impeller, neither of the two alum floc formed at cold temperatures was capable of withstanding the stress. This is evidenced by the fact that the number of primary particles was very large after breakup. Also note that it was not possible to detect any differences in the strength of the two cold temperature alum floc using the turbine impeller, the number of primary particles formed during breakup was nearly identical at both constant pH and pOH. The floc formed at 20 °C were slightly stronger than the cold temperature floc, but it also experienced significant breakup.

When the breakup was performed with the S&S (Figure 112), very few primary particles were produced from the floc formed at 20 °C. The particle size distribution (psd) data in Figure 93, is from the 20 °C S&S experiment, and indicates the magnitude of the primary particle increase caused by the breakup. The 45 minute sample in Figure 93 represents the psd in the tank immediately prior to breakup. Figure 112 shows that the alum floc formed at 5 °C and at constant pOH was not as strong as the floc formed at 20 °C, but it was much stronger than the floc formed at 5 °C constant pH. This is evidenced by the relative number of primary particles after breakup shown in Figure 112. The breakup of the 5 °C alum floc formed at constant pH was as severe with the S&S impeller as with the turbine impeller, indicating an extremely fragile floc.

This also confirms what was already expected, the localized shear field produced by the turbine is much more intense than the localized shear fields produced by the S&S at the same  $G$  or same  $\epsilon$ .

Figure 113 presents breakup data for floc formed using ferric sulfate as the coagulant. Only the turbine impeller was used with the ferric floc. It is noted that the floc formed with the ferric sulfate is much stronger than the floc formed with the alum. The number of primary particles generated by the breakup routine was very small, and nearly equal, at 20 °C and at 5 °C with constant pOH. Both the alum floc and the iron floc were formed in what should have been the optimal A/D region for the two coagulants. The constant pH floc formed with iron and broken up with the turbine, is almost identical to the 20 °C alum floc broken up with the turbine. It is seen that even the weakest iron floc studied is as strong as the strongest alum floc studied. Table 27 reports the visual appearance of the reactor following the breakup test.

The smoke referred to in the Table 27 is the iridescent Tyndall cloud which indicates the presence of high concentrations of colloidal particles. The table entry which says "some smoke", actually had very little smoke. It was also the only test which had clearly visible floc remaining. The fact that the floc were clearly visible means that they were at least 50-75  $\mu\text{m}$  in size.



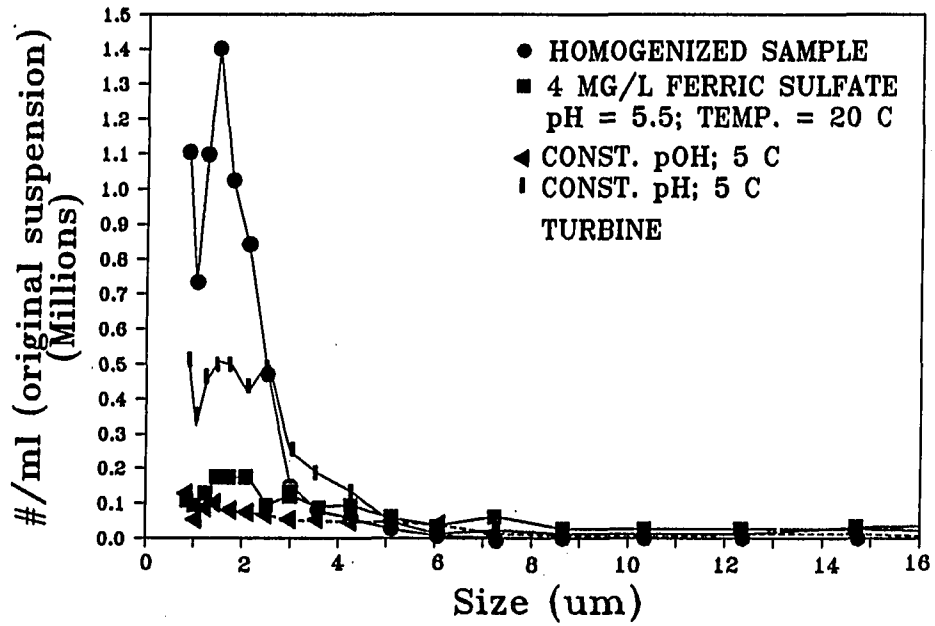


Figure 113. Primary particles produced by breakup of iron floc; turbine

Table 27. Appearance of the reactor following breakup

Geometry	Test Conditions					
	Alum			Ferric Sulfate		
	20 °C	5 °C		20 °C	5 °C	
		pH	pOH		pH	pOH
Turbine	no smoke	smoke	smoke	no smoke	smoke	smoke
S&S	no smoke	smoke	some smoke			

The macroscopic observations in Table 27 agree well with the particle size distribution data presented. Again, the breakup observations indicate that constant pOH appears to be the process control parameter of choice.

Figure 114 is a photograph of a large floc. This floc was in the 15 minute sample of a 20 °C, low energy, turbine impeller, alum experiment. The size bar on the photograph represents 50 $\mu$ m. Since the floc is  $\approx$ 250  $\mu$ m across, the photograph actually represents a cross section of the floc. This photograph is included for the following reasons:

- o this two dimensional cross section hints at the actual complexity of the three dimensional structure,

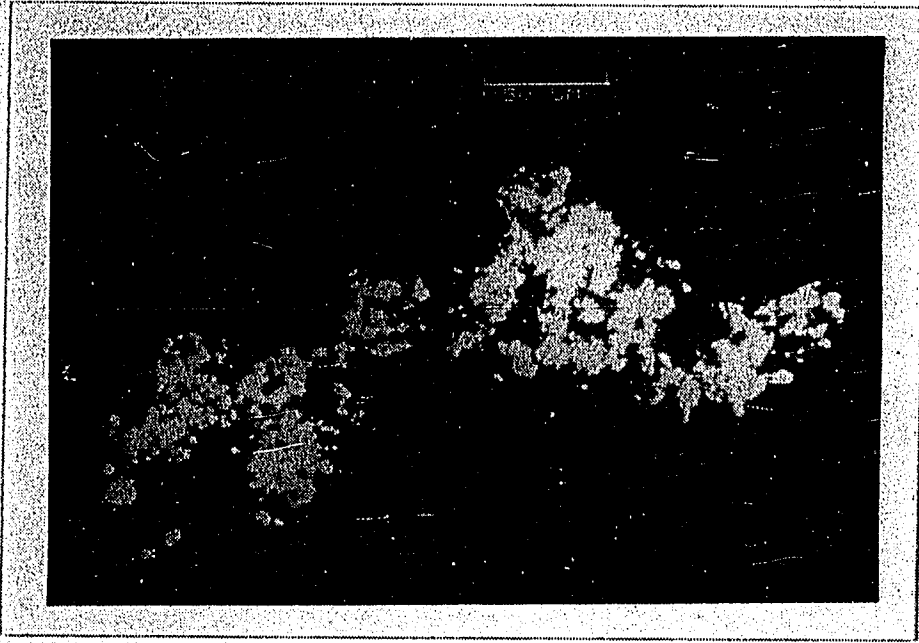


Figure 114. 2-Dimensional projection of a typical large kaolinite floc; the coagulant is alum in A/D, Z.P. $\approx$ 10 mV

- o it highlights the difficulty of trying to monitor the large floc, with either the HIAC or the AIA, and demonstrates the necessity of monitoring primary particle removal, and
- o to provide insight into the actual floc growth mechanism, and the floc breakup mechanism.

The appearance of this floc is representative of the larger floc at both high and low temperature. The low temperature floc were, in general, smaller, but they still were highly complex. Under a stereo scope it was possible to inspect the entire floc and the structure of the larger floc was universally reminiscent of the cluster-cluster aggregation (CCA) discussed in the literature review. Recall Figures 61 and 62 from the Literature Review section on flocculation modeling studies. The structure of the floc in Figure 114, inspite of the poor image quality, is strikingly similar to the cluster-cluster aggregation (CCA) images. It is possible to say that the CCA model produces a structure much closer to this floc than the particle-cluster (PCA) model. It is not possible to say conclusively that a specific CCA model appears to describe the structure of the floc in Figure 114 better than another model. However, it does appear that the chemical model (see Figure 62) is the least appropriate.

Observations made during the analysis of many samples throughout this study lead to the observation that early in the flocculation process the PCA mechanism dominates the floc growth process. Later in the flocculation process the dominant mechanism appears to become CCA.

It appears from Figure 114, that the floc consists of at least three levels of floc structure. The large floc, a second level floc which is 20-40  $\mu\text{m}$  in diameter, and the primary particles. Table 31 contains observations from the photographic record of the breakup experiments regarding maximum floc size prior to breakup and after breakup. The first number in each entry is the largest floc observed in the photographic record. The second value reported is the size of the large aggregates remaining after the reactor has been subjected to the increased mixing intensity to cause breakup. No values have been reported for the alum experiment at 20°C using the turbine impeller. This photographic record was not available.

Note that earlier a maximum floc size observed in the reactor was reported. These two numbers are not necessarily the same, since the value reported in Table 28 represents a single floc in a sample cell, and the value reported earlier was the observed "average" maximum floc size in the reactor. "Average" in this case implies that there were enough of this maximum size class of floc in the 18 liter reactor to be noticeable.

The floc which produced smoke in the earlier breakup table were also the floc which broke up into aggregates which were smaller than 20  $\mu\text{m}$ . This agrees, intuitively, with what we expect looking at Figure 114.

Table 28. Maximum floc size observed in photographic record prior to floc breakup and size of larger aggregates remaining after breakup

Geometry	Test Conditions					
	Alum			Ferric Sulfate		
	20 °C	5 °C		20 °C	5 °C	
		pH	pOH		pH	pOH
Turbine		75 <20	100 <20	200 20-50	100 <20	150 20-50
S&S	300 20-50	50 <20	100 30-50			

In the literature review it was pointed out that a floc continues to rupture until it reaches a floc level which can withstand the shear being imposed upon it. If this is the case, one would expect that a generation of a large number of primary particles would be accompanied by a maximum remaining floc size which is quite small. One would also anticipate that if the floc ceased to break when the remaining floc reached the 20-50  $\mu\text{m}$  size, very few primary particles would be produced. The data presented agree well with both of these expectations.

The fact that the floc in this study are structured as shown in Figure 114, in addition to the breakup data in Table 28 and the breakup mode just described, lead one to wonder again about the

maximum floc sizes measured by Morris (1983) and Morris and Knocke (1984). These authors report particle size distributions for floc formed with both alum and iron at low temperatures. In all cases, the maximum floc size did not exceed 40  $\mu\text{m}$ . They also reported floc size distributions for a series of tests performed at pH=7 and 1 °C, where alum doses of 1, 5, 10 mg/L as Al were used to flocculate turbidity. The maximum floc sizes reported for these tests were:

Alum dose	Floc Size ( $\mu\text{m}$ )
1	42
5	35
10	22

In addition to discussing the particle size distributions, the authors also discussed the size of the floc observed in the reactor. Based on the fact that the resolution limit of the human eye is probably about 50-75  $\mu\text{m}$ , one might speculate that, what has been reported here is not the size of the aggregates in the suspension, but is the size of the second level aggregates in the suspension. Perhaps, as the floc were counted, the shear in the counting cell disrupted the aggregates to a level which was strong enough to withstand the shear. Thus, the values given above may actually be more indicative of floc strength at the various dosages, than of the maximum floc size in the reactor.

### Miscellaneous results

Figure 115 contains a comparison of results from three high energy alum flocculation runs at 20 °C, 5 °C, and 2 °C. The pOH, and  $\epsilon$  have been held constant. This comparison was inspired by the case study reported by Morris and Knocke (1984), in which flocculation efficiency deteriorated dramatically at temperatures less than 4.5 °C. It is seen from this figure that under the present test conditions, constant pOH and constant  $\epsilon$ , there was no detectable difference between 5 °C and 2 °C.

Figure 116 is a comparison of A/D and sweep floc at 20 °C, with ferric sulfate as the coagulant. This test was performed out of pure curiosity. The industry, for the most part, coagulates and flocculates water in the sweep floc region. This experiment illustrates a key difference between the sweep floc and A/D regions: process kinetics. The kinetics of the sweep floc mechanism are much faster than the kinetics of A/D mechanism. The sweep floc experiment was approaching steady state at 5 minutes, as opposed to 15 minutes in A/D experiment. The hump in the sweep floc curve appeared to be restructuring of the floc.

Figure 117 is a comparison of two coagulants; alum in the A/D region of coagulation, and MagniFloc 573C. The alum appears to do a much better job of sweeping up the primary particles. This phenomenon was seen regularly. The polymer formed large, strong floc, but was less



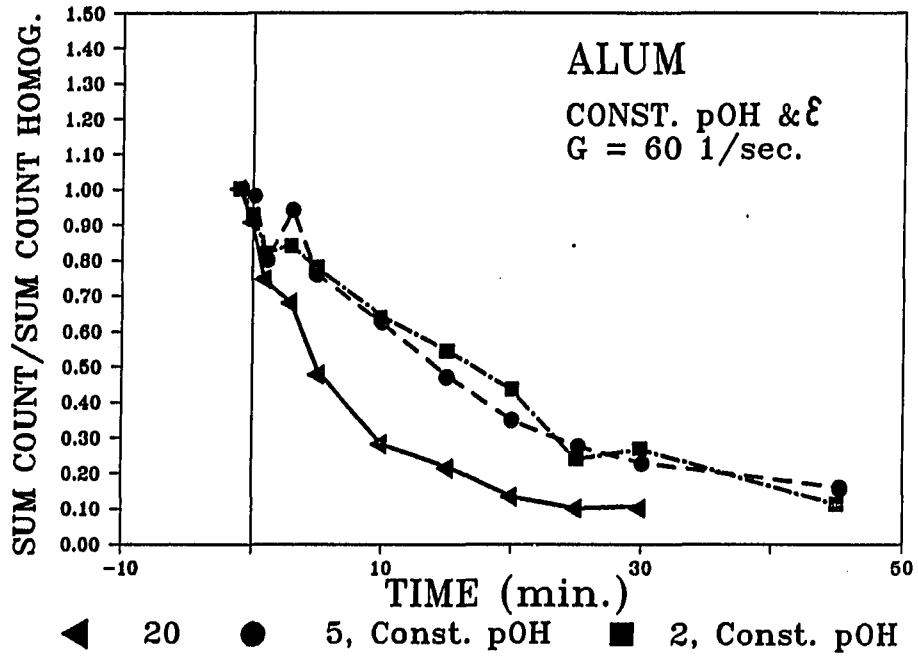


Figure 115. Effect of temperatures near 0 °C on flocculation efficiency, turbine

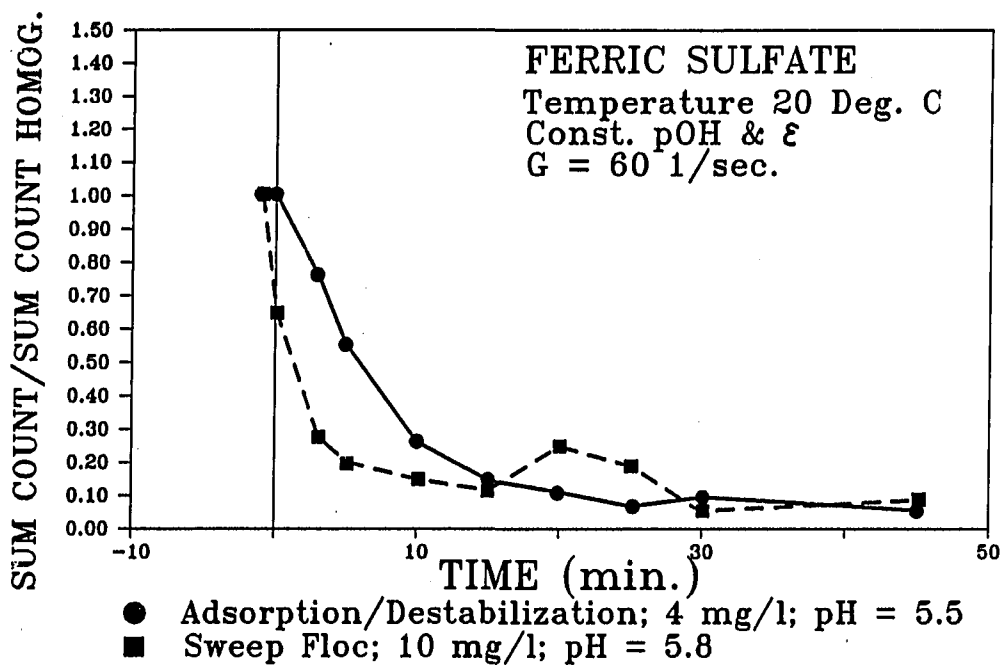


Figure 116. Effect of sweep floc versus A/D flocculation, turbine

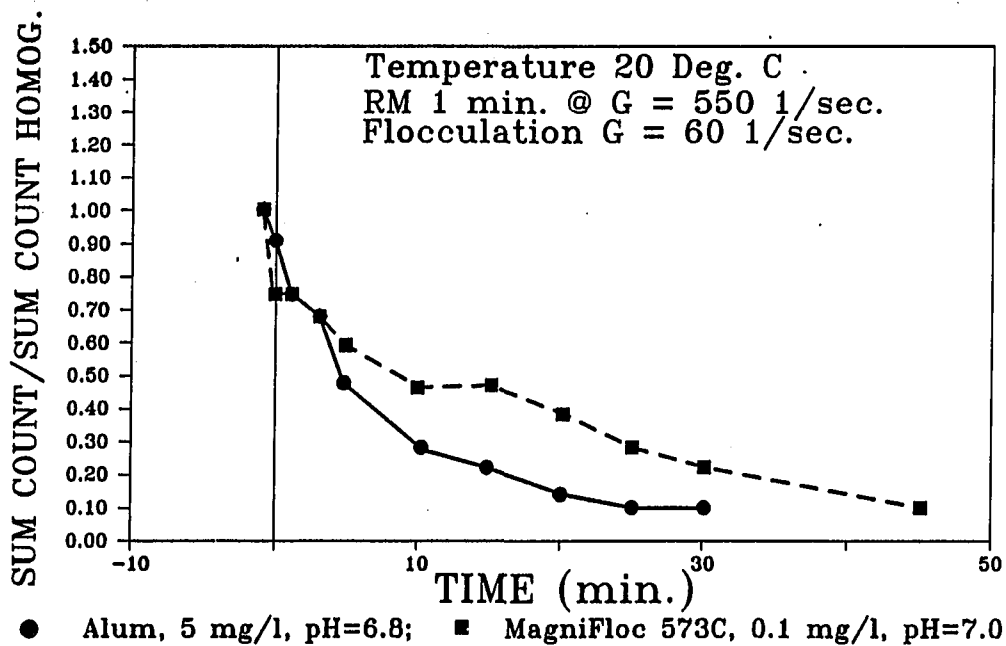


Figure 117. Alum versus cationic polymer (MagniFloc 573c), turbine

efficient at picking up the primary particles. The alum on the other hand, formed a fairly weak floc, but did a good job of picking up the primary particles. Hudson (1980) in a personal communication to Cleasby reported having good luck adding 0.1-0.2 mg/L of cationic polymer 1 minute before the alum was added. It is suggested that it might make sense to apply cationic polymer first, and rapid mix long (2+ minutes) and hard ( $G = 1250 \text{ sec}^{-1}$ ). Then apply alum to destabilize the remaining particles and rapid mix short (1 minute) and easy ( $G = 500 \text{ sec}^{-1}$ ), followed by flocculation. The polymer will provide a strong base structure for the floc, and the alum will help pick up the remaining primary particles. The rapid mix for the alum will actually act as an intense flocculation stage for the polymer.

### Musings

Dissertations frequently end with a section titled future research needs or some such. This section is really such a section. An attempt will be made to look at some of the uglier questions raised by the data which has been collected, and to consider some of the apparent inconsistencies. The following paragraphs must really be labeled musings rather than discussion, the evidence presented is far from conclusive, and the system is so complex that it becomes difficult to sort things out and isolate cause and effect. Many of the questions raised in this section would be interesting to address in a future modeling study, the data presented herein would provide a basis for model verification.

Let's go back and sharpen our mental picture of mass transport in the turbulent flow field, starting with the phenomena of turbulence.

Recall the picture of vortex stretching presented in Figure 20. The diameter of the initial vortex can be considered to be roughly the same size as the impeller blade width. This vortex is stretched by interacting with other vortices around it, and the smallest diameter it stretches to is approximately the size of the Kolmogorov microscale. At the microscale, the vortex is bound by viscosity and the energy dissipates. Below the microscale, flocculation is the result of localized shear fields induced by the vortex stretching process. The smaller the microscale of turbulence, the more intense the localized velocity gradients, i.e., localized shear fields.

Also recall from Figure 21, that the stretching process tends to be space filling, but, from Figure 25, most of the energy dissipation tends to occur where the turbulence is created in the reactor. So, although the process is locally space filling, there can also be spacial variability within the reactor.

Below the microscale of turbulence, viscosity tends to be the great equalizer. Regardless of how much energy is put into the system at the production scale, it is quickly dissipated below the microscale. Recall from Figure 17, that energy dissipation is a function of  $\epsilon k^2$  where  $k$  is the wave number. If  $\epsilon_A$  is 3 times as large, at a specific

wave number  $k_1$ , in a flow field A, as  $\epsilon_B$  in flow field B, then the energy in flow field A will be dissipated 3 times as fast at  $k_1$ . Thus, at some distance in wave space below  $k_1$  the difference between  $\epsilon_A$  and  $\epsilon_B$  will be less than a factor of 3. As long as  $\epsilon_A$  is greater than  $\epsilon_B$ , it will dissipate energy at a faster rate than  $\epsilon_B$ . Given sufficient time, and assuming that the energy doesn't go to zero first, one would expect them to approach the same value.

In thinking about the flocculation process, there is a fixed point of reference which is important, and that is the energy environment at the size scale of the primary particles. The question of interest is, how do such factors as impeller geometry, temperature, and  $\epsilon$  affect the amount of energy present at the size scale of the particles. As noted earlier, a crude estimate of  $\eta$  for the various flow fields at 20 °C would be:

	$G = 60 \text{ sec}^{-1}$	$G = 20 \text{ sec}^{-1}$
	$\eta =$	$\eta =$
Turbine	40 $\mu\text{m}$	71 $\mu\text{m}$
Stake & Stator	129 $\mu\text{m}$	214 $\mu\text{m}$

One can see that in terms of wave space the energy is crossing into the viscosity dominated region a long way from the size of the primary particles.

At 5 °C the difference between  $\eta$  and the primary particle size becomes even greater. For instance, if we assume again that the  $\eta$  calculated based on the volume averaged  $\epsilon$ , is representative of the "true"  $\eta$  for the stake and stator flow field, the following result is produced:

	$G = 50 \text{ sec}^{-1}$	$G = 18 \text{ sec}^{-1}$ (Constant $\epsilon$ )
Stake & Stator	$\eta = 175 \mu\text{m}$	$\eta = 291 \mu\text{m}$

In addition to moving the point in wave space where the energy is crossing into the viscosity dominated region further from the size of the primary particles, the cold also increases the fluid viscosity. Thus, the energy which crosses the microscale is going to be dissipated quicker.

Now, lets think about the flocculation process in terms of some specific questions. Why does varying  $G$  have such a weak impact on flocculation efficiency (Figures 103 and 104)? Note that in both high and low energy flocculation the primary particles are a long way in size from the microscale. If we assume that in the turbine the  $\epsilon$  of the impeller region is 10x as high as in the rest of the tank, then  $\eta$  in this region would be 40  $\mu\text{m}$  for a  $G$  of 60  $\text{sec}^{-1}$  and about 71  $\mu\text{m}$  for a  $G$  of 20  $\text{sec}^{-1}$ . This brings the lower bound of turbulence closer to the particles, but still not down to the scale of the particles. The collision frequency in the impeller region of the

turbine would be higher but the collision frequency in the bulk of the reactor would be lower.

The reason that a three fold change in  $G$  does not produce a larger change in flocculation efficiency may be related to a couple of things. First, the models which show a strong correlation between the rate of reduction in primary particle number concentration and  $G$ , all assume a particle suspension which is mono-dispersed, and in which differential sedimentation is assumed to be negligible. As flocculation proceeds this assumption becomes false, and we obviously need to reassess how we view the relationship between  $G$  and  $dn_1/dt$ .

The S&S results at 20 °C were nearly identical at the two energy levels (Figure 104). This leads one to consider another factor which is really accentuated by the S&S geometry. This factor is the difference in length scales between the primary particles and the lower scale of turbulence. As has been shown earlier, the energy cascades below  $\eta$  where viscosity dominates, and the relationship between viscosity and the energy that reaches the primary particles may be non-linear. The only suggestion I can make is that at 20 °C there is the same amount of energy actually reaching the primary particles under both mixing conditions. This suggestion may be true, to some extent for both impeller geometries.

A second obvious question is why do both impellers perform nearly the same at 20 °C, when they behave differently at 5 °C? Figures 98, 99, and 100 indicate the impact of temperature on the turbine impeller. Figure 107 indicates the effect of temperature on the stake and stator impeller. Figures 105 and 106 show both impeller geometries at 5 ° and 20 °C. It is possible that the reason the flocculation performance of both impellers is the same at 20 °C under both energy conditions, is a combination of the effects of fluid dynamics and floc strength. The turbine reactor is acting as three reactors of different size and energy input in parallel. In the region of the impeller, the energy is effectively driven to very small length scales. As long as the floc is strong enough so that it is not immediately broken, the volume of the reactor in the impeller region will produce rapid flocculation. The same is true of the impeller discharge area. The bulk flow region of the tank, which represents the majority of the tank volume, will produce less flocculation, but will provide volume for differential sedimentation and will not disrupt the floc. In the cold temperature setting the alum floc is weaker, and the breakup process near the impeller dominates reducing the efficiency of the flocculation.

The S&S reactor is acting as a single reactor with a the same volume and energy input as the three reactors in parallel. However, the energy is distributed more uniformly throughout the reactor. See Figure 107. At 20 °C, the entire reactor volume is producing a



measurable, but relatively low level of flocculation. At 5 °C the energy is dissipated more rapidly and much less of the energy is reaching the length scale of the primary particles. Because there is so little energy still available at the length scale of the primary particles, the flocculation proceeds very slowly. After a lag time some aggregates are formed which are large enough to be moved effectively by the energy available, and/or differential sedimentation. Once some minimum number of these aggregates are formed, the flocculation proceeds at a measurable rate. The lower the energy input to the system the less energy that reaches the small length scales. The less energy that reaches the small length scales the longer it takes for aggregates to form that are large enough to perform efficient flocculation by differential sedimentation, thus the longer observed lag period. With the turbine impeller at 5 °C there is very little lag for the high energy flocculation (Figure 98), and roughly a 10 minute lag for the low energy flocculation (Figure 99). Using the S&S impeller at 5 °C, there is a 10 minute lag with the high energy flocculation and a 20 minute lag with the low energy flocculation (Figure 107). The concept of differential sedimentation was brought up by Lawler (1989). According to Lawler (1989) as the suspension becomes poly-dispersed, differential sedimentation becomes an important flocculation mechanism. In many practical systems, differential sedimentation becomes equal to or more important than shear flocculation. Because the range of shear gradients is large in the flow field generated by the turbine

impeller, it may produce a system which is poly-dispersed more quickly. This would allow the differential sedimentation mechanism to become important more quickly and produce a high rate of flocculation early in the test.

The S&S impeller consistently out performs the turbine impeller late in the flocculation run (Figures 105 and 106). The cause of this may be two fold. First, the turbine impeller becomes breakup dominated much quicker than the S&S impeller does. Second, the S&S impeller produces a more uniform floc. This means that the number concentration of moderate size floc is quite high, rather than having a few big floc which are periodically broken up. Since flocculation is a function of number concentration and particle diameter, a large number of moderate size floc will continue removing primary particles more effectively than a few large particles. These impeller characteristics indicate that there might be benefits in using turbine impellers in the early flocculation stages, and S&S impellers in the later stages of flocculation. It is interesting that some of the older water treatment plants were designed that way.

Based on the preceding comments, one would expect that, at low temperature, high energy and low energy flocculation tests would again be nearly identical. This is obviously not entirely the case for either the turbine (Figures 98, 99) or for the stake and stator (Figure 107). The differences exhibited by the turbine are very

likely the result of increased breakup, which is probably the result of reduced floc strength. The alum floc in Figures 98 and 99 are much weaker than the iron floc in Figure 100, as shown the breakup comparisons in Figures 111, 112, and 113. It is also probable that the polymer floc are much stronger than the alum floc. Therefore, if the floc is sufficiently strong, the expectation voiced earlier is realized with the turbine impeller, because the localized Kolmogorov microscale is quite small. Thus, with a  $\Delta T = 15$  °C, the energy environment in the vicinity of the particles has not changed significantly. It is, perhaps, the fact that the energy environment has not changed and the alum floc has gotten weaker, which causes the problems with the alum floc.

I believe that breakup is not causing the differences noted with the S&S impeller (Figure 107). There are a number of things which might be happening, but I believe the most important is the effect of the increased viscosity of the flow field structure. The Kolmogorov microscale has moved further from the primary particles in wave space, this means that the localized velocity gradient is reduced in magnitude. In addition, due to the increased viscosity, more of the turbulence is being dissipated in the immediate region of the impeller. This will effectively reduce the volume of the reactor which is active in the flocculation process. When the process finally accelerates it may be because the system has become

sufficiently poly-dispersed for differential sedimentation to become an important mechanism.

All of the preceding comments could be explored, and perhaps verified, using a population balance model which compartmentalized the reactor into three segments, and contained the following terms:

- o a Brownian flocculation term,
- o a shear flocculation term,
- o a differential sedimentation flocculation term,
- o a breakup term, and
- o which accounted for the change in floc density with floc growth.

## CONCLUSIONS

The following conclusions are drawn from the research.

1. When alum is added to water at low temperature the pH of the system remains depressed much longer than when the solution is warm. This appears to be due to the kinetics of the carbonic acid-CO<sub>2</sub> reaction, and not to the kinetics of the Al(OH)<sub>3</sub> formation. This does not imply that the rate of Al(OH)<sub>3</sub> formation is not slower at the low temperature. It simply implies that the time scales of the carbonic acid partitioning reaction are so much longer than the time scales involved in the Al(OH)<sub>3</sub> reaction, that the buffer system reaction controls the pH depression phenomena.
2. The HIAC particle counter, using the 1-60 μm sensor, consistently under-counted the number of particles smaller than 2.5 μm. This under-counting is evident in both the standard latex spheres suspensions and in the clay suspensions.
3. Under strong floc conditions, the normalized HIAC flocculation data for primary particle disappearance during

flocculation correlated reasonably well with the AIA flocculation data. This leads one to believe that the HIAC may be a useful tool for optimizing the flocculation process if the floc system is robust.

4. Under weak floc conditions, the normalized HIAC flocculation data correlated very poorly with the AIA data, probably because of floc breakup in the HIAC counting cell area. This indicates that although the HIAC may be useful under some circumstances, it is not universally useful for studying flocculation. The user must be very careful, and should check the HIAC data against optical microscope data.
5. Flocculation efficiency at 20 °C, as measured by the removal of primary particles, was not sensitive to the geometry of the impeller used in the flocculator.
6. At 5 °C the geometry of the impeller was much more important. Very likely, this observation is because of the primary particle size with respect to the size of the local Kolmogorov microscale of turbulence,  $\eta$ .
7. Impeller geometry is particularly important, because of its impact on breakup of the floc. The turbine impeller caused much more floc breakup than the stake and stator impeller.

8. It was not possible to demonstrate that one measure of turbulent intensity is better than another, i.e.,  $G$ ,  $\eta$ , and  $\epsilon$ , when attempting to correct mixing intensity for temperature effects.
  
9. With metallic coagulants, the use of constant pOH is the appropriate parameter, as opposed to constant pH, to use in correcting system chemistry for temperature effects. This is, in effect, maintaining the hydroxyl ion concentration constant as the temperature changes. With iron as the primary coagulant, the flocculation results at 20 °C & 5 °C were nearly identical when the pOH was held constant. The flocculation efficiency was markedly decreased at cold temperature when the pH was held constant. With alum as the coagulant, flocculation at 5 °C with constant pOH yielded much better efficiency than constant pH conditions, but the flocculation efficiency was still not as good as the efficiency at 20 °C.
  
10. The alum floc was significantly weaker than the iron floc under all conditions tested. The iron floc at 20 °C and at 5 °C with constant pOH showed similar strengths, but the iron floc at 5 °C with constant pH was much weaker than the iron floc formed at 20 °C. The alum floc at 20 °C was

considerably stronger than the alum floc formed at 5 °C. Of the alum floc formed at 5 °C, the floc formed at constant pOH was stronger than the floc formed at constant pH.

11. As a final overall conclusion, the system chemistry was found to be much more important than the choice of energy input parameter on flocculation kinetics at different water temperatures. With appropriate system chemistry, the effect of cold water temperature on flocculation kinetics was eliminated using ferric sulfate or cationic polymer as the primary coagulant.



## BIBLIOGRAPHY

- Abramowitz, M. Microscope Basics and Beyond. Volume 1. Olympus Corp., Lake Success N.Y., 1985.
- Adler, P. M. Heterocoagulation in Shear Flow. *J. Colloid and Interface Science*, 83, No. 1 (September, 1981): 106-115.
- Akers, R. J. Experimental Methods. pp. 131-163. In K. J. Ives, ed. The Scientific Basis of Flocculation. Nato Advanced Study Institute Series, Series E, Applied Science - No. 27. Sijthoff & Noorhoff, Netherlands, 1978.
- Al-Ani, M., J. M. McElroy, C. P. Hibbler, and D. W. Hendricks. Filtration of Giardia Cysts and Other Substances. Volume 3. Rapid-Rate Filtration, Project Summary, EPA-600-S2-85-027, September, 1985.
- Al-Layla, M. A., E. J. Middlebrooks, and D. B. Porcella. Effect of Temperature on Algal Removal by Alum Coagulation. Research Report # PRWG139-1. Utah Water Research Laboratory, College of Engineering, Utah State University, Logan, Utah, July, 1974.
- Allen, T. Particle Size Measurement. Third Edition. Powder Technology Series. Chapman and Hall, New York, 1981.
- Ambegaonkar, A. S., A. S. Dhruv, and L. L. Tavlarides. Fluid-Particle Hydrodynamics in Agitated Vessels. *Can. J. Chem. Eng.*, 55 (August, 1977): 414-420.
- Amirtharajah, A. Rapid Mixing and Coagulation Processes. pp. 19-30. In AWWA Seminar Proceedings: Influence of Coagulation on the Selection, Operation, and Performance of Water Treatment Facilities. AWWA, Denver, June, 1987.
- Amirtharajah, A. Research at Montana State University into Coagulation, Flocculation, and Mixing. Presented at CH<sub>2</sub>M-Hill Cold Water Coagulation Seminar, Denver, Colo., July 13, 1984.
- Amirtharajah, A. Initial Mixing. pp. 1-22. In AWWA Seminar Proceedings: Coagulation Filtration: Back to the Basics. AWWA, Denver, June, 1981.
- Argaman, Y. A. Pilot-Plant Studies of Flocculation. *JAWWA*, 63, No. 12 (December, 1971): 775-777.
- Argaman, Y., and W. J. Kaufman. Turbulence in Orthokinetic

- Flocculation.** SERL Report No. 68-5. Sanitary Engineering Research Laboratory, University of California, Berkeley, Calif., July, 1968.
- Argaman, Y., and W. J. Kaufman. Turbulence and Flocculation. J. Sanitary Engineering Division Proceedings of the American Society of Civil Engineers, 96, SA 2 (April, 1970): 223-241.
- ASTM. Designation F312-69 (Re-approved 1980). Microscopical Sizing and Counting Particles From Aerospace Fluids on Membrane Filters. In Annual Book of ASTM Standards, Vol. 15.03. American Society for Testing and Materials, Philadelphia, Penn., 1986.
- ASTM. Designation E 20-85. Standard Practice for Particle Analysis of Particulate Substances in the Range of 0.2 to 0.75 Micrometers by Optical Microscope. In Annual Book of ASTM Standards, Vol. 14.02. American Society for Testing and Materials, Philadelphia, Penn., 1985.
- Baes, C. F., and R. E. Mesmer. The Hydrolysis of Cations. John Wiley and Sons, New York, 1976.
- Baylis, J. R. Silicates as Aids to Coagulation. JAWWA, 28, No. 7 (July, 1936): 1355-1396.
- Beard II, J. D., and T. S. Tanaka. A Comparison of Particle Counting and Nephelometry. JAWWA, 69, No. 10 (October, 1977): 533-538.
- Beck, C. The Microscope. D. Van Nostrand Co., New York, 1924.
- Bendek, A., and J. J. Bancsi. Laboratory Evaluation of Polymeric Flocculants. JEED, 102, No. EE1 (February, 1976): 17-28.
- Bennett, R. H., and M. H. Hulbert. Clay Microstructure. D. Reidel Publishing Company, Boston, 1986.
- Bhole, A. G., and P. Limaye. Effect of Shape of Paddle and Container on Flocculation Process. IE (I) Journal-EN, 57 (February, 1977): 52-57.
- Birkner, F. B., and J. J. Morgan. Polymer Flocculation Kinetics of Dilute Colloidal Suspensions. JAWWA, 60, No. 1 (February, 1968): 175-191.
- Black, A. P., and C. Chen. Electrokinetic Behavior of Aluminum Species in Dilute Dispersed Kaolinite Systems. JAWWA, 59, No. 9 (September, 1967): 1173-1183.
- Boadway, J. D. Dynamics of Growth and Breakage of Alum Floc in the

- Presence of Fluid Shear. JEED, 104, No. EE5 (October, 1978): 901-915.
- Botet, R., R. Jullien, and M. Kolb. Cluster Aggregation. pp. 255-258. In L. Pietronero, and E. Tosatti, eds. Fractals in Physics. Elsevier Science Publishers, Netherlands, 1986.
- Brace, R., and E. Matejevic. Aluminum Hydrous Oxide Sols. I. Spherical Particles of Narrow Size Distribution. J. Inorg. Nucl. Chem., 35 (1973): 3691-3705.
- Bradshaw, P. An Introduction to Turbulence and its Measurement. Pergamon Press, New York, 1971.
- Brink, D. R., S. Choi, M. Al-Ani, and D. W. Hendricks. Bench Scale Evaluation of Coagulants for Low Turbidity Water. JAWWA, 80, No. 4 (April, 1988): 199-204.
- British Standard 3406. Part 4, Methods for Determination of Particle Size Distribution; Optical Microscope Method. British Standards House, London, 1984.
- Brochard, F., and P. G. DiGennes. Kinetics of Polymer Dissolution. Physico Chemical Hydrodynamics (PCH), 4, No. 4 (1983): 313-322.
- Brodkey, R. S. The Phenomena of Fluid Motion. Addison-Wesley Series in Chemical Engineering. Addison-Wesley, Reading, Massachusetts, 1967.
- Burgess, J. Ions in Solution: Basic Principles of Chemical Interactions. Ellis-Horwood Limited, Chichester, John Wiley & Sons, New York, 1988.
- Calbrese, R. V. , and C. M. Stoots. Flow in the Impeller Region of a Stirred Tank. Chemical Engineering Progress, 85, No. 5 (May, 1989): 43-50.
- Camp T. R. Floc Volume Concentration. JAWWA, 60, No. 6 (June, 1968): 656-673.
- Camp, T. R., and Stein, P. C. Velocity Gradients and Internal Work in Fluid Motion. J. Boston Society of Civil Engineers, 30, No. 4 (October, 1943): 219-237.
- Camp, T. R., B. A. Root, and B. V. Bhoota. Effects of Temperature on the Rate of Floc Formation. JAWWA, 32, No. 11 (November, 1940): 1913-1927.
- Clark, M. M. Drop Break-up in a Turbulent Flow. Doctoral

- Dissertation. Johns Hopkins University, 1985a.
- Clark, M. M. Critique of Camp and Stein's RMS Velocity Gradient. JEED, 111, No. 6 (December, 1985b): 741-754.
- Cleasby, J. L. Is Velocity Gradient a Valid Turbulent Flocculation Parameter? JEED, 110, No. 5 (October, 1984): 875-897.
- Cleasby, J. L., G. Sindt, H. Dharmarajah, E. R. Baumann. Design and Operation Guidelines for Optimization of the High Rate Filtration Process. Quarterly Report Number 2 for period between November 1-February 1, 1988. ERI, Iowa State University.
- Cohen, J., Z. Priel, and Y. Rabin. Viscosity of Dilute Polyelectrolyte Solutions. J. Chem. Phys., 88, No. 11 (June, 1988): 7111-7116.
- Corrsin, S. Turbulent Flow. American Scientist, 49, (1961): 300-325.
- Corrsin, S. Outline of Some Topics in Homogeneous Turbulent Flow. J. Geophys. Res., 64, No. 12 (December, 1959): 2134-2150.
- Cutter, L. A. Flow and Turbulence in a Stirred Tank. A. I. Ch. E. J., 12, No. 1 (January, 1966): 35-44.
- Dann, R. Ferric Chloride Favored Over Alum for Cost Saving Coagulation. Waterworld News, (March/April, 1988): 16-17.
- Davis, K. S., and J. A. Day. Water the Mirror of Science. Science Study Series S-18. Anchor Books, Doubleday and Company, Inc., Garden City, New York, 1961.
- Deer, W. A., R. A. Howie, and J. Zussman. An Introduction to Rock-forming Minerals. Longman Group Limited, London, 1966.
- Delichatsios, M. A., and Probstein, R. F. Coagulation in Turbulent Flow: Theory and Experiment. J. Colloid and Interface Science, 51, No. 3 (June, 1975): 394-405.
- Dempsey, B.A. Chemistry of Coagulants. pp. 19-30. In AWWA Seminar Proceedings: Influence of Coagulation on the Selection, Operation, and Performance of Water Treatment Facilities. AWWA, Denver, June, 1987.
- Dentel, S. K. Optimizing Coagulant Additions From Laboratory and Field Test Methods. pp. 49-88. In AWWA Seminar Proceedings: Influence of Coagulation on the Selection, Operation, and

- Performance of Water Treatment Facilities. AWWA, Denver, June, 1987.
- Dentel, S. K., and J. N. Gossett. Mechanisms of Coagulation with Aluminum Salts. JAWWA, 80, No. 4 (April, 1988): 187-198.
- Dentel, S. K., J. J. Resta, P. V. Shetty, and T. A. Bober. Simulation of Organic Polyelectrolyte Effects in Water Treatment. pp. 1621-1649. In AWWA Annual Conference Proceedings, Denver, Colorado. AWWA, Denver, 1986.
- Drobny, N. L. Effect of Paddle Design on Flocculation. J. Sanitary Engineering Division ASCE, 89, No. SA2 (April, 1963): 17-30.
- Duluth Water Utility. Personal Communication. Unpublished flocculation system operations control data from Duluth, Minnesota water treatment plant, treating Lake Superior Water. These data were obtained during a plant visit in 1987.
- Edzwald, J. K. Coagulation. pp. 23-44. In AWWA Seminar Proceedings: Coagulation and Filtration. Back to the Basics. AWWA, Denver, June, 1981.
- Eilbeck, W. J., and G. Mattock. Chemical Processes in Wastewater Treatment. Ellis-Horwood Limited, Chichester, 1987.
- Ernst, M. H. Kinetics of Clustering in Irreversible Aggregation. pp. 289-302. In L. Pietronero, and E. Tosatti, eds. Fractals in Physics. Elsevier Science Publishers, Netherlands, 1986.
- Family, F. Dynamics of Aggregation Processes. pp. 231-236. In H. E. Stanley, and N. Ostrowsky, eds. On Growth and Form Fractal and Non-fractal Patterns in Physics. Martinus Nijhoff Publishers, Netherlands, 1986.
- Farinato, Ray. Personal communication with technical representative. Letter, 6/24/88. American Cyanamid, Stamford, Conn. 06904.
- Farinato, Ray. Personal communication with technical representative. Telephone conversation, 6/20/88. American Cyanamid, Stamford, Conn. 06904.
- Feder, J. Fractals. Plenum Press, New York, 1988.
- Feder, J., and T. Jossang. Aggregation Kinetics of Immunoglobulin. pp. 33-42. In G. Grimvall, ed. Physica Scripta, Vol T13, The General Conference of the Condensed Matter Division of the European Physical Society. Royal Swedish Academy of Sciences, Stockholm, Sweden, 1986.

- Francois, R. J. Growth Kinetics of Hydroxide Floccs. *JAWWA*, 80, No. 6 (June, 1988): 92-96.
- Francois, R. J., and A. A. Van Haute. Floc Strength Measurements Giving Experimental Support for a Four Level Hydroxide Floc Structure. pp. 221-234. In Pawlowski, Verdier, and Lacey, eds. *Proceedings of an International Conference - Chemistry for Protection of the Environment*. September 19-25, Toulouse, France. Elsevier, 1983.
- Franks, F. Water. The Royal Society of Chemistry, London, 1983.
- Franks, F. Water, a Comprehensive Treatise: Volume 1. The Physics and Physical Chemistry of Water. Plenum Press, New York, 1972.
- Friedlander, S. K. Smoke, Dust, and Haze. John Wiley & Sons, New York, 1977.
- Frost, W., and T. H. Moulden. Handbook of Turbulence: Volume 1: Fundamentals and Applications. Plenum Press, New York, 1977.
- Gallegos, C. L., and R. G. Menzel. Submicron Size Distribution of Inorganic Suspended Solids in Turbid Waters by Photon Correlation Spectroscopy. *Water Research*, 23, No. 4 (April, 1987): 596-602.
- Ghosh, M. M., C. D. Cox, and T. M. Prakash. Polyelectrolyte Selection for Water Treatment. *JAWWA*, 77, No. 3 (March, 1985): 67-73.
- Gibbs, R. J. Floc Breakage During HIAC Light-blocking Analysis. *Environmental Science and Technology*, 16, No. 5 (May, 1982): 298-299.
- Glaberson, W. I., and K. W. Schwarz. Quantized Vortices in Superfluid Helium-4. *Physics Today*, 40, No. 2 (February, 1987): 54-60.
- Glasgow, L. A., Personal communication. Correspondence with Dr. J. L. Cleasby. Iowa State University, Kansas State University Chemical Engineering Dept., Manhattan, Kansas, February 7, 1985.
- Glasgow, L. A., and J. Hsu. Floc Characteristics in Water and Wastewater Treatment. pp. 285-303. In *Particulate Science and Technology*, 2. Hemisphere Publishing Company, 1984.
- Glasgow, L. A., and Y. H. Kim. Characterization of Agitation

- Intensity in Flocculation Processes. JEED, 112, No. 6 (December, 1986): 1158-1163.
- Goren, S. L. The Hydrodynamic Forces on Touching Spheres Along the Line of Centers Exerted by a Shear Field. J. Colloid and Interface Science, 36, No. 1 (May, 1971): 94-96
- Graf, J. Sizing with Modern Image Analyzers. In Stockham and Fochtman, eds. Particle Size Analysis. Ann Arbor Science Publishers, Ann Arbor, Mich., 1977.
- Grasso, D., and W. J. Weber. Ozone-induced Particle Destabilization. JAWWA, 80, No. 8 (August, 1988): 73-81.
- Gregory, J. Flocculation by Polymers and Polyelectrolytes. pp. 163-181. In Th. F. Tadros, ed. Solid/Liquid Dispersions. Academic Press, Orlando, Fl., 1987.
- Gregory, J. Flocculation by Inorganic Salts. pp. 89-100. In K. J. Ives, ed. The Scientific Basis of Flocculation. Nato Advanced Study Institute Series, Series E, Applied Science - No. 27. Sijthoff & Noorhoff, Netherlands, 1978a.
- Gregory, J. Effects of Polymers on Colloid Stability. pp. 101- 130. In K. J. Ives, ed. The Scientific Basis of Flocculation. Nato Advanced Study Institute Series, Series E, Applied Science - No. 27. Sijthoff & Noorhoff, Netherlands, 1978b.
- Gregory, J. Flocculation. pp. 55-99. In R. Wakeman, ed. Progress in Filtration and Separation 4. Elsevier, Amsterdam, 1986.
- Groves, M.J. Particle Size Characterization in Dispersions. J. Dispersion Science and Technology, 1, No. 1 (1980): 97-124.
- Gunkel, A. A., and M. E. Weber. Flow Phenomena in a Stirred Tank. Part I: The Impeller Stream. A.I.Ch.E. J., 21, No. 5 (September, 1975): 931-948.
- Haarhoff, J. Direct Filtration of Chlorella and Scenedesmus Suspensions for Potable Water Treatment. Doctoral Dissertation. Iowa State University, Ames, Iowa, 1988.
- Haarhoff, J., and J. L. Cleasby. Comparing Aluminum and Iron Coagulants for In-line Filtration of Cold Water. JAWWA, 80, No. 4 (April, 1988): 168-175.
- Hahn, H. H., and W. Stumm. Coagulation by Al(III); the Role of Adsorption of Hydrolyzed Aluminum in the Kinetics of Coagulation. Chapter 9. In Adsorption from Aqueous Solution. Advances in

- Chemistry Series no. 79. American Chemical Society, Washington, D. C., 1968a.
- Hahn, H. H., and W. Stumm. Kinetics of Coagulation with Hydrolyzed Al(III). *J. Colloid and Interface Science*, 28, No. 1 (September, 1968b): 134-144.
- Hall, E. S. The Zeta Potential of Aluminum Hydroxide in Relation to Water Treatment Coagulation. *J. Appl. Chem.*, 15 (May, 1965): 197-205.
- Hannah, S. A., J. M. Cohen, and G. G. Robeck. Measurement of Floc Strength by Particle Counting. *JAWWA*, 59, No. 7 (July, 1967a): 843-858.
- Hannah, S. A., J. M. Cohen, and G. G. Robeck. Control Techniques for Coagulation-Filtration. *JAWWA*, 59, No. 9 (September, 1967b): 1149-1163.
- Harris, H., W. J. Kaufman, and R. B. Krone. Orthokinetic Flocculation in Water Treatment. *JEED*, 92, No. SA6 (December, 1966): 95-111.
- Harris, H. S. Orthokinetic Flocculation of Polydispersed Systems. Doctoral Dissertation. University of California-Berkeley, 1966.
- Harwood, C. F. Problems in Particle Sizing-The Effect of Particle Shape. In Stockham, and Fochtman, eds. Particle Size Analysis. Ann Arbor Science Publishers, Ann Arbor, Mich., 1977.
- Hayden, P. L., and A. J. Rubin. Systematic Investigation of the Hydrolysis and Precipitation of Aluminum (III). pp. 317-381. In A. J. Rubin, ed. Aqueous-Environmental Chemistry of Metals. Ann Arbor Science Publishers, Inc., Ann Arbor, Michigan, 1974.
- Herdan, G., and M. L. Smith. Small Particle Statistics. Elsevier Publishing Company, New York, 1963.
- Hiemenz, P. C. Principles of Colloid and Surface Chemistry. Second edition. Marcel Dekker Inc., New York, 1986.
- Hinze, J.O. Turbulence. McGraw - Hill Series in Mechanical Engineering. Second edition. McGraw - Hill, Inc., New York, 1975.
- Hinze, J.O. Fundamentals of the Hydrodynamic Mechanisms of Splitting in the Dispersion Process. *A.I.Ch.E. J.*, 1, No. 1 (September, 1955): 289-295.



- Hirtzel, C. S., and R. Rajagopalan. Colloidal Phenomena: Advanced Topics. Noyes Publications, Park Ridge, NJ, 1985.
- Hong-Xiao, T., and W. Stumm. The Coagulating Behavior of Fe (III) Polymeric Species-II; Preformed Polymers in Various Concentrations. *Water Research*, 21, No. 1 (1987a): 123-128.
- Hong-Xiao, T., and W. Stumm. The Coagulating Behavior of Fe (III) Polymeric Species-I; Preformed Polymers by Base Addition. *Water Research*, 21, No. 1 (1987b): 115-121.
- Honig, E. P., G. J. Roeberson, and P. H. Wiersema. Effect of Hydrodynamic Interaction on the Coagulation Rate of Hydrophobic Colloids. *J. Colloid and Interface Science*, 36, No. 1 (May, 1971): 97-109.
- Honig, E. P., and P. M. Mul. Tables and Equations of the Diffuse Double Layer Repulsion at Constant Potential and at Constant Charge. *J. Colloid and Interface Science*, 36, No. 2 (June, 1971): 258-272.
- Hudson Jr., H. E. Physical Aspects of Flocculation. *JAWWA*, 57, No. 7 (July, 1965): 885-892.
- Hudson Jr., H. E. Water Clarification Processes. Practical Design and Evaluation. Van Nostrand and Reinhold Company, New York, 1981.
- Hudson, H. Personal communication to Dr. J. L. Cleasby. Dept. of Civil and Construction Engineering. Iowa State University Ames, Iowa, July, 15, 1980.
- Hutchinson, C.W. On-Line Particle Counting Improves Filter Efficiency. In Proceedings of ISA International Conference and Exhibit, Instrument Society of America, Research Triangle Park, N. C., 1984.
- Hutchinson, W. and P. D. Foley. Operational and Experimental Results of Direct Filtration. *JAWWA*, 66, No. 2 (February, 1974): 79-87.
- Hynes, H. B. N., The Ecology of Running Water. University of Toronto Press, Toronto, Canada, 1970.
- Israelachvili, J. N., Intermolecular and Surface Forces: with Applications to Colloidal and Biological Systems. Academic Press, Orlando, Fl., 1985.
- Ives, K. J. Experiments in Orthokinetic Flocculation. pp. 196-220.

- In J. Gregory, ed. Solid-Liquid Separation. Ellis Horwood limited, Chichester, England, 1984.
- Ives, K. J. Rate Theories. pp. 37-61 In K. J. Ives, ed. The Scientific Basis of Flocculation. Nato Advanced Study Institute Series, Series E, Applied Science - No. 27. Sijthoff & Noorhoff, Netherlands, 1978.
- Ives, K. J., and A. G. Bhole. Theory of Flocculation for Continuous Flow System. JEED, 99, No. EE1 (February, 1973): 17-34.
- Ives, K. J., and M. A. Dibouni. Orthokinetic Flocculation of Latex Microspheres. Chem Eng. Sci. 34 (1979): 983-991.
- James, J. Light Microscope Techniques in Biology and Medicine. Martinus Nijhoff Medical Division, Netherlands, 1976.
- Johnson, P. N., and A. Amirtharajah. Ferric Chloride and Alum as Single and Dual Coagulants. JAWWA, 75, No. 5 (May, 1983): 232-239.
- Jullien, R., and R. Botet. Aggregation and Fractal Aggregates. World Scientific, Singapore, 1987.
- Kavanau, J. L. Water and Solute Interactions. Holden-Day, Inc., San Francisco, 1964.
- Kavanaugh, M. C., C. H. Tate, A. R. Trussell, R. R. Trussell, and G. Treweek. Use of Particle Size Distribution Measurements for Selection and Control of Solid/Liquid Separation Processes. Chapter 14. In Kavanaugh and Leckie, ed. Particulates in Water. Advances in Chemistry Series 189. American Chemical Society Publishers, Washington, D. C., 1980.
- Kim, Y. H., and L. A. Glasgow. Simulation of Aggregation and Breakage in Flocculation Processes. pp. 82-85. In Proceedings of World Congress III of Chemical Engineering. Tokyo, Japan, 1986.
- Knocke, W. R., S. West, and R. C. Hoehn. Effects of Low Temperature on the Removal of Trihalomethane Precursors by Coagulation. JAWWA, 78, No. 4 (April, 1986): 189-195.
- Koh, P. T. L. Compartmental Modelling of a Stirred Tank for Flocculation Requiring a Minimum Critical Shear Rate. Chemical Engineering Science, 39, No. 12 (1984): 1759-1764.
- Koh, P. T. L., J. R. G. Andrews, and P. H. T. Uhlherr. Modeling

- Shear Flocculation by Population Balances. *Chemical Engineering Science*, 42, No. 2 (1987): 353-362.
- Koh, P.T.L., Andrews, J.R.G., Uhlherr, P.H.T. Flocculation in Stirred Tanks. *Chemical Engineering Science*, 39, 6 (June, 1984): 975-985.
- Kolb, M., R. Botet, and R. Jullien. Scaling Kinetically Growing Clusters. *Physical Review Letters*, 51, No. 13 (September, 1983): 1123-1126.
- Kolb, M. Reversibility in Cluster Aggregation. pp. 263-266. In L. Pietronero, and E. Tosatti, eds. Fractals in Physics. Elsevier Science, Netherlands, 1986.
- Kolb, M., R. Botet, R. Jullien, and H. J. Herrmann. Flocculation and Gelation in Cluster Aggregation. pp. 222-226. In H. E. Stanley, and N. Ostrowsky, eds. On Growth and Form Fractal and Non-fractal Patterns in Physics. Martinus Nijhoff, Netherlands, 1986.
- La Brecque, M. Fractals in Physics; Part II of a Special Report. *Mosaic*, 18, No. 2 (1987): 23-41.
- Lagvankar, A. L., and R. S. Gemmill. A Size Distribution Relationship for Floccs. *JAWWA*, 60, No. 9 (September, 1968): 1040-1046.
- Lawler, D. F. Particle Size Distributions: Measurement in Flocculation. pp. 19-30. In AWWA Seminar Proceedings: Influence of Coagulation on the Selection, Operation, and Performance of Water Treatment Facilities. AWWA, Denver, June, 1987.
- Lawler, D. F. The Relative Insignificance of G. In AWWA Annual Conference Proceedings, Los Angeles, Calif. AWWA, Denver, June, 1989.
- Lawler, D. F., E. Izurieta, and C. Kao. Changes in Particle Size Distribution in Batch Flocculation. *JAWWA*, 75, No. 12 (December, 1983): 604-611.
- Lawler, D. F., C. R. O'Melia, and J. E. Tobiason. Integral Water Treatment Plant Design: From Particle Size to Plant Performance. Chapter 16. In Kavanaugh, and Leckie, eds. Particulates in Water. Advances in Chemistry Series 189. American Chemical Society Publishers, Washington, D. C., 1980

- Leibovich, S., and J. L. Lumley. Complex Fluid Motion: Models and Metaphors. *Chaos and Physical Systems, Engineering Cornell Quarterly*, 20, No. 3 (1986): 27-36.
- Leipold, C. Mechanical Agitation and Alum Flocc Formation. *JAWWA*, 26, No. 8 (August, 1934): 1070-1084.
- Lemont Scientific Inc. DB-10 Manual: Version 1984.6 (85B) (With Update Material for the OASYS System). Lemont Scientific Inc., Science Park, Penn., 1984.
- Letterman, R. D., and S. G. Vanderbrook. Effects of Solution Chemistry on Coagulation with Al(III); Significance of the Sulfate Ion and pH. *Water Research*, 17 (1983): 195-204.
- Letterman, R.D., M. Tabatabaie, and R. S. Ames, Jr. The Effect of the Bicarbonate Ion Concentration on Flocculation with Aluminum Sulfate. *JAWWA*, 71, No. 8 (August, 1979): 467-472.
- Letterman, R. D., S. G. Vanderbrook, and P. Sricharoenchaikit. Electrophoretic Mobility Measurements in Coagulation with Aluminum Salts. *JAWWA*, 76, No. 1 (January, 1982): 44-51.
- Leu, R., and M. M. Ghosh. Polyelectrolyte Characteristics and Flocculation. *JAWWA*, 80, No. 4 (April, 1988): 159-167.
- Leyvraz, F. Rate Equation Approach to Aggregation Phenomena. pp. 136-144. In H. E. Stanley, and N. Ostrowsky, eds. On Growth and Form Fractal and Non-fractal Patterns in Physics. Martinus Nijhoff, Netherlands, 1986.
- Lieberman, A. Fine Particle Characterization Methods in Liquid Suspensions. In J. K. Bedow, ed. Particle Characterization in Technology. Volume 1: Applications and Microanalysis. CRC Press, Inc., Boca Raton, Florida, 1984.
- Lyklema, J. Structure of the Solid/Liquids Interface and the Double Layer. In Th. F. Tadros, ed. Solid/Liquid Dispersions. Academic Press, Orlando, Fl., 1987.
- Mandelbrot, B. B. The Fractal Geometry of Nature. Revised. W. H. Freeman and Company, New York, 1983.
- Mangravite, F. J. Synthesis and Properties of Polymers Used in Water Treatment. pp. 1-16. In AWWA Seminar Proceedings: Use of Organic Polyelectrolytes in Water Treatment. AWWA, Denver, 1983.
- Matijevic, E., and P. Scheiner. Ferric Hydrous Oxide Sols: III.

Preparation of Uniform Particles by Hydrolysis of Fe (III) - Chloride, -Nitrate, -Perchlorate Solutions. *J. Colloid and Interface Science*, 63, No. 3 (March, 1978): 509-524.

Matijevic, E., and B. Tezak. Coagulation Effects of Aluminum Nitrate and Aluminum Sulfate on Aqueous Sols of Silver Halide *In Statu Nascendi*. Detection of Polynuclear Complex Aluminum Ions by Means of Coagulation Measurements. *J. Physical Chemistry*, 57 (December, 1953): 951-954.

Matijevic, E., R. S. Sapiesyko, and J. B. Melville. Ferric Hydrrous Oxide Sols: I. Mono-dispersed Basic Iron (III) Sulfate Particles. *J. Colloid and Interface Science*, 50, No. 3 (March, 1975): 567-581.

Mathews, B. A., and C. T. Rhodes. The Use of the Coulter Counter for Investigating the Coagulation of Mixed Monodisperse Particulate Systems. *J. Coll. Sci.*, 28, No. 1 (1968): 71-81.

Matsuo, T., H. Unno. Forces Acting on Floc and Strength of Floc. *JEED*, 107, No. EE3 (June, 1981): 527-545.

McTigue, N. and K. Berman. The Use of Particle Counters for Utilities. Presented at AWWA Water Quality Technology Conference, 1988.

McTigue, N. and D. A. Cornwell. The Use of Particle Counting for the Evaluation of Filter Performance. In AWWA Annual Conference Proceedings. AWWA, Denver, 1988.

McTigue, N., H. Dunn, and K. Berman. Particle Counting and Sizing. In Coagulation Control. To be published AWWA, Denver.

Meakin, P. Computer Simulation of Growth and Aggregation Processes. pp. 111-135. In H. E. Stanley, and N. Ostrowsky, eds. On Growth and Form Fractal and Non-fractal Patterns in Physics. Martinus Nijhoff, Netherlands, 1986a.

Meakin, P. The Effects of Reorganization Processes on Two Dimensional Cluster-Cluster Aggregation. *J. Colloid and Interface Science*, 112, No. 1 (July, 1986b): 187-194.

Meakin, P. Two Dimensional Simulation of Cluster-Cluster Aggregation and Deposition onto a Surface. *J. Colloid and Interface Science*, 104, No. 1 (March, 1985): 282-284.

Meakin, P. Computer Simulation of Cluster-Cluster Aggregation Using Linear Trajectories: Results from Three Dimensional Simulations and a Comparison with Aggregates Formed Using Brownian

- Trajectories. *J. Colloid and Interface Science*, 102, No. 2 (December, 1984): 505-512.
- Meakin, P. Formation of Fractal Clusters and Networks by Irreversible Diffusion Limited Aggregation. *Physical Review Letters*, 51, No. 13 (September, 1983a): 1119-1122.
- Meakin, P. The Vold-Sutherland and Eden Models of Cluster Formation. *J. Colloid and Interface Science*, 96, No. 2 (December, 1983b): 415-424.
- Michaels, A. S., and J. C. Bolger. Plastic Flow Behavior of Flocculated Kaolin Suspensions. *Ind. Eng. Chem. Fundam.*, 1, No. 3 (August, 1962): 153-162.
- Miller, L. B. A Study of the Effects of Anions upon the Properties of Alum Floc. *Public Health Reports*, 40 (1925): 351-367.
- Mitchell, J. K. Fundamentals of Soil Behavior. John Wiley and Sons, New York, 1976.
- Moffett, J. W. The Chemistry of High Rate Water Treatment. *JAWWA*, 60, No. 11 (November, 1968): 1255-1270.
- Morris, J. K. Temperature Effects on Turbidity Removal Using Metal Ion Coagulants. Master's Thesis. Virginia Polytechnic Institute and State University, Blacksburg, Virginia, 1983.
- Morris, J. K., and W. R. Knocke. Temperature Effects on the Use of Metal-ion Coagulants for Water Treatment. *JAWWA*, 76, No. 3 (March, 1984): 74-79.
- Morrow, J. J., and E. G. Rausch. Colloid Destabilization with Cationic Polyelectrolytes as Affected by Velocity Gradients. *JAWWA*, 66, No. 11 (November, 1974): 646-653.
- Murphy, C. M. Handbook of Particle Sampling and Analysis Methods. Verlag Chemie International, Deerfield Beach, Florida, 1984.
- Needham, G. H. The Practical Use of the Microscope. Charles C. Thomas, Springfield, Ill., 1958.
- Newman, A. C. D. The Interaction of Water with Clay Mineral Surfaces. Chapter 5. In A. C. D. Newman, ed. Chemistry of Clay and Clay Minerals; Mineralogical Society Monograph No. 6. Longman Scientific and Technical, Harlow, Essex, England, 1987.
- Nimtz, G. Magic Numbers of Water Molecules Bound Between Lipid

- Layers. pp. 259-256. In G. Grimvall, ed. *Physica Scripta*, Vol T13, The General Conference of the Condensed Matter Division of the European Physical Society. Royal Swedish Academy of Science, Stockholm, Sweden, 1986.
- O'Melia, C. R. Coagulation in Waste Water Treatment. In K. J. Ives, ed. The Scientific Basis of Flocculation. Nato Advanced Study Institute Series, Series E, Applied Science - No. 27. Sijthoff & Noorhoff, Netherlands, 1978.
- Okamoto, Y. M., M. Nishikawa, and K. Hashimoto. Energy Dissipation Rate Distribution in Mixing Vessels and its Effect on Liquid-Liquid Mass Transfer, *Int. Chem. Eng.*, 21, No. 1 (January, 1981): 88-94.
- Oldshue, J. Y. Fluid Mixing Technology. McGraw-Hill, New York, 1983.
- Oldshue, J. Y., and O. B. Mady. Flocculator Impellers, a Comparison. *C. E. P.* (May, 1979): 72-75.
- Oldshue, J. Y., and O. B. Mady. Flocculation Performance of Mixing Impellers. *C. E. P.* (August, 1978): 103-108.
- Olympus Corp. Olympus System Microscope Instruction Manual. Model BHS. Olympus Optical Co. LTD., Tokyo, 1985.
- Ottweill, R. H. Properties of Concentrated Dispersions. In Th. F. Tadros, ed. Solid/Liquid Dispersions. Academic Press, New York, 1987.
- Packham, R. F. Some Studies of the Coagulation of Dispersed Clays with Hydrolyzing Salts. *J. Colloid Science*, 20, No. 1 (January, 1965): 81-92.
- Paladin, G., and A. Vulpiani. Fractals for Two and Three Dimensional Turbulence. pp. 255-258. In L. Pietronero, and E. Tosatti, eds. Fractals in Physics. Elsevier Science, Netherlands, 1986.
- Pandya, J. D., and L. A. Spielman. Floc Breakage in Agitated Suspensions: Effect of Agitation Rate. *Chem. Eng. Sci.*, 38, No. 12 (1983): 1983-1992.
- Parthasarathy, N, and J. Buffle. Study of Polymeric Aluminum (III) Hydroxide Solutions for Application in Waster Water Treatment. Properties of the Polymer and Optimal Conditions of Preparation. *Water Research*, 19, No. 1 (1985): 25-36.
- Patwardham, S.V. and A. G. Mirajgaonkar. *Hydraulics of Flocculation*

- and Paddle Characteristics. I. E. (I) J.-PH, 50 (February, 1970): 60-64.
- Placek, J., L. L. Tavlarides, and G. W. Smith. Turbulent Flow in Stirred Tanks, Part II: A Two Scale Model of Turbulence. A. I. CH. E. J., 32, No. 11 (November, 1986): 1771-1786.
- Placek, J., and L. L. Tavlarides. Turbulent Flow in Stirred Tanks, Part I: Turbulent Flow in the Turbine Impeller Region. A. I. CH. E. J., 31, No. 7 (July, 1985): 1113-1120.
- Rabin, Y. Viscosity of Polyelectrolyte Solutions - the Generalized Fuose Law. J. Polymer Science: Part C: Polymer Letters, 26 (1988): 397-399.
- Rabin, A. J., and H. Blockside. Coagulation of Montmorillinite Suspensions with Aluminum Sulfate. JAWWA, 60, No. 2 (February, 1979): 102-108.
- Racz, Z. Scaling Generalization of the Smoluchowski Equation. pp. 263-266. In L. Pietronero, and E. Tosatti, eds. Fractals in Physics. Elsevier Science, Netherlands, 1986.
- Rahman, A., and F. H. Stillinger. Molecular Dynamics Study of Liquid Water. J. Chemical Physics, 55, No. 7 (October, 1971): 330-354, Reprinted In G. Ciccotti, D. Frenkel, and I. R. Mc Donald, eds. Simulations of Liquids and Solids. Molecular Dynamics and Monte Carlo Methods in Statistical Mechanics. North-Holland Publishing Company, Amsterdam, 1987.
- Rajagopalan, R., and J. S. Kim. Adsorption of Brownian Particles in the Presence of Potential Barriers: Effect of Different Modes of Double Layer Interaction. J. Colloid and Interface Science, 83, No. 2 (October, 1981): 428-449.
- Rao, M. A., and R. S. Brodkey. Continuous Flow Stirred Tank Turbulence Parameters in the Impeller Stream. Chemical Engineering Science, 27 (1972): 137-156.
- Reed, G. D., and P. C. Mery. Influence of Floc Size Distribution on Clarification. JAWWA, 78, No. 8 (August, 1986): 75-80.
- Reynolds, A. J. Turbulent Flows in Engineering. John Wiley and Sons, New York, 1974.
- Riddick, T. M. Zeta Potential and its Application to Difficult Waters. JAWWA, 53, No. 8 (August, 1961): 1007-1030.
- Rigby, M., E. B. Smith, W. A. Wakeham, and G. C. Maitland.



- The Forces Between Molecules. Clarendon Press, Oxford, 1986.
- Ross, S., and I. D. Morrison. Colloidal Systems and Interfaces. John Wiley and Sons, New York, 1988.
- Rossauer, E. A. Instruments for Material Analysis. Iowa State University Press, Ames, 1981.
- Russel, W. B. The Dynamics of Colloidal Systems. University of Wisconsin Press, Madison, 1987.
- Saffman, P. G., Turner, J. S. On the Collision of Drops in Turbulent Clouds, *J. Fluid Mechanics*, 1 (January, 1956): 16-30.
- Saatci, A. M., and M. Halilsoy. Critique of Camp and Steins RMS Velocity Gradient. Discussion. *JEED*, 113, No. 3 (June, 1987): 675-678.
- Schenkel, J. H., and J. A. Kitchener. A Test of Derjaguin-Verwey-Overbeck Theory with a Colloidal Suspension. *Transactions Faraday Society*, 56, No. 1 (1960): 161-173.
- Schowalter, W.R. The Effect of Bulk Motion on Coagulation Rates of Colloidal Dispersions. *Advances in Colloid and Interface Science*, 17 (1982): 129-147.
- Schertzer, D., and S. Lovejoy. Generalized Scale Invariance and Anisotropic Inhomogeneous Fractals in Turbulence. In L. Pietronero, and E. Tosatti, eds. Fractals in Physics. Elsevier Science, Netherlands, 1986.
- Skyluk, W. P., and F. S. Stow Jr. Aging and Loss of Flocculation Activity of Aqueous Polyacrylamide Solution. *J. Applied Polymer Science*, 13 (1969): 1023-1036.
- Slayter, E. Optical Methods in Biology. Wiley-Interscience, New York, 1970.
- Snodgrass, W. J., M. M. Clark, and C. R. O'Melia. Particle Formation and Growth in Dilute Aluminum(III) Solutions: Characterization of Particle Size Distributions at a pH of 5.5. *Water Research*, 18, No. 4 (1984): 479-488.
- Sonntag, R. C., and W. B. Russel. Structure and Breakup of Floccs Subjected to Fluid Stress. *J. Colloid and Interface Science*, 113, No. 2 (October, 1986): 399-413.
- Speilman, L. A. Hydrodynamic Aspects of Flocculation. pp. 63-88.

- In K. J. Ives, ed. The Scientific Basis of Flocculation. Sijthoff & Noordhoff, Netherlands, 1978.
- Sricharoenchaikit, P., and R. D. Letterman. Effect of Al(III) and Sulfate Ion on Flocculation Kinetics. *JEED*, 113, No. 5 (October, 1987): 1120-1138.
- Srivastava, R. M. Impact of Rapid Mixing and Temperature on Flocculation of Clay Suspensions in Water. Master's Thesis. Iowa State University, Ames, Iowa, 1988.
- Stockham, J. D. What is Particle Size: The Relationship Among Statistical Diameters. In Stockham and Fochtman, ed. Particle Size Analysis. Ann Arbor Science Publishers, Ann Arbor, Mich. 1977.
- Stumm, W., and C. R. O'Melia. Stoichiometry of Coagulation. *JAWWA*, 60, No. 5 (May, 1968): 514-539.
- Stumm, W., and J. J. Morgan. Chemical Aspects of Coagulation, *JAWWA*, 56, No. 8 (August, 1962): 971-994.
- Stumm, W., and J. J. Morgan. Aquatic Chemistry. 2nd edition. John Wiley and Sons, New York, 1981.
- Stump, V. L., and J. T. Novak. Mixing of Polyelectrolytes for Direct Filtration. pp. 14A-2. In AWWA Annual Conference Proceedings, Part 1 of 2, Anaheim, Ca. AWWA, Denver, 1976.
- Sullivan Jr., J. H., and J. E. Singley. Reactions of Metal Ions in Dilute Aqueous Solution: Hydrolysis of Aluminum. *JAWWA*, 60, No. 11 (November, 1968): 1280-1287.
- Swift, D. L., and S. K. Friedlander. The Coagulation of Hydrosols by Brownian Motion and Laminar Shear Flow. *J. Colloid Science*, 19 (1964): 621-647.
- Tambo, N., and H. Hozumi. Physical Characteristics of Floccs - II. Strength of Floc. *Water Research*, 13 (1979): 421-427.
- Tambo, N., and Y. Watanabe. Physical Characteristics of Floccs - I. The Floc Density Function and Aluminum Floc. *Water Research*, 13 (1979a): 409-419.
- Tambo, N., and Y. Watanabe. Physical Aspect of Flocculation Process-I. Fundamental Treatise. *Water Research*, 13 (1979b): 429-439.
- Tekippe, R. J., and R. K. Ham. Apparatus to Examine Floc Forming

- Processes. JAWWA, 62, No. 4 (April, 1970): 260-268.
- Tennekes, H., J. L. Lumley. A First Course in Turbulence. MIT Press, Cambridge, Mass., 1972.
- Thomas, D. G. Turbulent Disruption of Flocs in Small Particle Size Suspensions. A. I. Ch. E. J., 10, No. 4 (July, 1964): 517-523.
- Thomas, I. L., and K. H. Mc Corkel. Theory of Orientational Flocculation. J. Colloid and Interface Science, 36, No. 1 (May, 1971): 110-118.
- Tomi, D. T., and D. F. Bagster. The Behavior of Aggregates in Stirred Vessels: Part I - Theoretical Considerations on the Effects of Agitation. Transactions Institution of Chemical Engineers, 56, No. 1 (1977): 1-8.
- Trace Inorganic Substances Committee. A Review of Solid-Solution Interactions and Implications for the Control of Trace Inorganic Materials in Water Treatment. JAWWA, 80, No. 10 (October, 1988): 56-64.
- Treweek, G. P. Optimization of Flocculation Time Prior to Direct Filtration. JAWWA, 71, No. 2 (February, 1979): 96-101.
- Treweek, G. P., and J. J. Morgan. Prediction of Suspension Turbidities from Aggregate Size Distribution. Chapter 15. In Kavanaugh, and Leckie, eds. Particulates in Water. American Chemical Society Publishers, Washington, D. C., 1980
- Treweek, G. P., and J. J. Morgan. Size Distribution of Flocculated Particles: Application of Electric Particle Counters. Environmental Science & Technology, 11, No. 7 (July, 1977): 707-714.
- Turski, L. A. Possible Freezing Scenarios for Classical Liquids. pp. 259-256. In G. Grimvall, ed. Physica Scripta, Vol T13, The General Conference of the Condensed Matter Division of the European Physical Society. Royal Swedish Academy of Science, Stockholm, Sweden, 1986.
- van Olphen, H. An Introduction to Clay Colloid Chemistry. 2nd edition. John Wiley and Sons, New York, 1977.
- van Olphen, H. Dispersion and Flocculation. pp. 203-208. In A. C. D. Newman, ed. Chemistry of Clay and Clay Minerals; Mineralogical Society Monograph No. 6. Longman Scientific and Technical, Harlow, Essex, England, 1987.

- van den Ven, T. G. M., and S. G. Mason. The Microrheology of Colloidal Dispersions VII. Orthokinetic Doublet Formation of Spheres. *Colloid and Polymer Science*, 255, No. 5 (1977): 468-479.
- Van't Reit, K., W. Brijn, and J. M. Smith. Real and Pseudo-turbulence in the Discharge Stream from a Rushton Turbine. *Chemical Engineering Science*, 31 (1976): 407-412.
- Van't Reit, K., and J. M. Smith. The Trailing Vortex System Produced by Rushton Turbine Agitators. *Chemical Engineering Science*, 30 (1975): 1093-1105.
- Velz, C. J., Influence of Temperature on Coagulation. *Civil Engineering*, 4, No. 7 (July, 1934): 345-349.
- Voke, P. E., M. W. Collins. Large Eddy Simulation: Retrospect and Prospect. *Physico Chemical Hydrodynamics*, 4, No. 2 (1983): 119-161.
- Weber, W. J., and W. Stumm. Mechanisms of Hydrogen Ion Buffering in Natural Waters. *JAWWA*, 55, No. 12 (December, 1963): 1553-1578.
- Wetzel, R. G. Limnology. W. B. Saunders Company, Philadelphia, Penn., 1975.
- Yamate, G., and J. D. Stockham. Sizing Particles Using the Microscope. Chapter 3. In Stockham and Fochtman, Particle Size Analysis. Ann Arbor Science Publishers, Ann Arbor, Mich. 1977.
- Yao, K. M., M. T. Habian, and C. O'Melia. Water and Wastewater Filtration: Concepts and Applications. *Environmental Science & Technology*, 5 (1971): 1105-1112.
- Yeh, H., and M. M. Ghosh. Selecting Polymers for Direct Filtration. *JAWWA*, 73, No. 4 (April, 1981): 211-218.
- Zabrusky, N. J. Grappling with Complexity. *Physics Today*, 40, No. 10 (October, 1987): 25-27.
- Zeta-Meter, Inc. Promotional Literature. 1720 First Ave, New York, New York, 10028, 1986.

## APPENDIX A

This is a summary of the operating commands needed to use the automatic image analyzer(AIA) in direct imaging from the light microscope. The software for this instrument is continually being updated and changed. Therefore, this can not be considered a cookbook. It will, however, give the reader a starting point from which the reader may begin to explore the AIA system.

This is a summary of the operating commands needed to use the automatic image analyzer(AIA) in direct imaging from the light microscope. This document will be divided into the following subsets:

- o Starting the software with the machine turned on
- o collecting the image
- o setting the color levels
- o analyzing the image
- o exporting information to the IBM XT
- o exiting from the system
- o Starting the software with the machine shutoff, or hung

Each of these topics will be dealt with separately.

### I. Hot Start

If the screen is dark press the return key; <CR>. This will reactivate the monitor screen if the main computer has shut it down.

If the screen prompt "." is on the screen (this means the RT-11 operating system is running), then type "LEMSET" <CR>, to initiate the operation of the OASYS software. If the aforementioned prompt is not on the screen you can either type menu, and see if the menu comes up, or you can follow directions and type "LEMSET". As a last resort you can always go to the cold start-up procedure.

Log the starting time into the Lemont logbook.

The screen prompt will ask which system you want to work with; respond  
"OA" <CR> to perform image analysis.

Enter the password. The password appears on the screen immediately above the prompt where the password is to be entered. The first menu (Lemont Public Program OASYS and X-ray) will now appear. You need to perform two tasks in this menu, these are:

- o initialize the hardware ("31" <CR>)
- o enter image analysis mode ("1" <CR>)

#### Initializing the Hardware

Initializing the hardware insures that any bizarre instrument settings left by the previous user will be removed. This is important, and the problem is real. Don't skip this step, it

literally takes 2 seconds, and may save you from a severe headache. Type "31" <CR>.

### Entering Image Analysis

This puts you in the specific part of the program which will allow you to collect an image from the light microscope.

Now to enter the image analysis mode type "1" <CR>.

The screen prompt at the top of the screen is asking for a file known as the answer file. This file takes care of a large number of house keeping chores. If you simply hit return the default file (INP:OASYS.ANS) will be put in place.

You are now in the second menu (Lemont OASYS Menu). You will see this menu periodically during the acquisition and analysis of an image. Enter "1" <CR> to acquire an image, or calibrate a lens combination.

### II. Collect an Image

The third menu (Image Selection Commands) will now have appeared, and you will need to do two things on this menu. These are:

- o calibrate the system optics ("C" <CR>)
- o collect an optical image for analysis. ("0" <CR>)

### Calibrating the System Optics

If you are using the BH-2S up-right Olympus scope with Nomarski optics, and are willing to trust someone else's calibration numbers, there are values presented later in this document. If you are on a different light scope or don't trust the numbers presented here, place a stage micrometer on the microscope stage and proceed.

The first step in the calibration is to collect an image of the stage micrometer, for instructions on doing this see the next section "Collecting an Optical Image".

Type "C" <CR> this will put you in the subroutine for checking the systems total magnification using a stage micrometer.

Note: Check the video monitor switch, it must be set to "RGB" in order to perform calibration.

Using the arrow keys move the "+" to the starting point on the stage micrometer image which appears on the video monitor screen and <CR>, then move the "+" to the ending point and <CR>. The step size used in moving the "+" can be adjusted by entering 0-5, 0 yields the finest step. Setting the step size at 0, allows you to get the "+" exactly on the point of interest. The screen prompt will then ask you for the actual length measured on the stage micrometer. Once you have entered the actual length measured, the monitor will report the magnification. Write this down you will need it later. The calibration operation can be carried out a number of times and the results averaged.

When you are done with the calibration, type "N" to return to the previous menu. You are now ready to collect an image.

#### Collecting an Optical Image

The first step in collecting the image is to place the specimen on the microscope stage and focus the scope. If the video monitor is off turn it on. There is a panel on the bottom front of the monitor. Open the panel and press the Line 'A' button, this puts the live image on the video monitor screen.

Now with the hardware and the specimen setup, type "0" <CR>. You have selected optical imaging, this allows one to use the light microscope as the primary sensor for the AIA system. At this point you should have a live image visible on the video monitor. If not there are a number of things which can be checked:

- o is the tri-nocular head on the scope sending light to the camera?
- o is the light level on the scope too high or low? It is actually more common for the light level to be too high and be overloading the camera than for it to be too low. Turn the light all of the way down and let the thing sit for 30 sec., then adjust up from there slowly.
- o Take the little black box, set it on manual and adjust with the contrast and brightness.
- o Go get Glen Oren ( This is a last resort, Glen feeds people to the hard drive who do this first instead of last).

Note: It is important that the image on the video monitor be in crisp focus, it is not necessary that the image seen through the eyepieces be crisp, so focus the image while looking at the screen.

The screen prompt will ask how many times the image should be averaged. You can fiddle with the live image to your hearts content, until you answer this prompt. Once you answer this prompt the live



image will be gone and you will actually be looking at the digitized image. A response of 1 - 3 is reasonable. Example: "2" <CR>

Note: If you don't know the magnification of the lens combination and camera which you are using you must go to "Calibration" and find out before you collect an image.

Once you have collected the image type "x"<CR> to return to the previous menu for color selection and image analysis.

### III. Setting the Image Color Levels

In this section we adjust the digitized image so the computer is analyzing the features which are of interest to us. This is done by defining specific shades of gray or contrast levels on the image (grey levels) as discrete bands. The computer will then analyze the features within a defined band as features of interest. A specific band is assigned a color so that humans can also see what is going on, since we are not as sensitive to gray levels as the computer. There are files stored which contain approximate gray level assignments, these files need to be imported and fine tuned for the specific sample on the scope.

This is done in Menu option 2 - Set Levels For Analysis

Note: Switch the monitor from Line "A" to the "RGB" setting using the push-buttons in the front panel on the video monitor.

Type "2" <CR>.

At this point the screen prompt will ask for a color file name. This file defines the color levels of interest in this particular analysis. For instance for the analysis of flocculated clay the color file "clay" is used.

Once the file has been selected you optimize the file, using option "C" <CR> and the arrow keys. To check how accurately the color bar represents the actual image of interest, alternate between "V" <CR> and "T" <CR>. This switches back and forth between the original image and the colored image. Once the color bar looks good type "x" <CR>. At this point you will be asked if you want to name and save the modified file. In general you don't save every file.

To leave this portion of the program type "x" (Note: Do not type <CR> this time) and you will return to the previous menu.

### IV. Analyzing the Image

Now we are ready to analyze the image using menu option 3 -"Analyze Frame"

Occasionally at this point you will get a screen prompt which says "Need Thresholds". When this screen prompt shows up enter, the color file name. If you don't enter the color file name, the computer gets really ugly.

Example: "clay" <CR>

The screen prompt will ask if you would like to "Change Block Data Constants". This is where size discriminators can be entered.

"0" <CR> will give you no change in the constants

If you want to change any of the constants type in the number of the option which you want to change (1 - 13), then enter the new value (see LEMONT manual).

The screen prompt ask if you want to locate particles with a JOY BOX, type "-1" <CR> for yes.

At the next screen prompt enter "0" <CR> to analyze composite structures(i.e., Whole floc).

This screen prompt asks for the Magnification. This is the magnification which was determined in the calibration routine. If you are using the Olympus BH-2S with Nomarski, you can use the following magnification values.

**NFK Lens = 2.5x**

<u>Objective</u>	<u>Magnification</u>	<u>Field of View (Video</u>
<u>Monitor)(um)</u>		
10	79.61x	1260.93
20	159.53x	626.86
40	317.71x	314.75

**NFK Lens = 5x**

<u>Objective</u>	<u>Magnification</u>	<u>Field of View (Video</u>
<u>Monitor)(um)</u>		
10	158.85x	629.51
20	320.31x	312.20
40	635.42x	157.38

NFK Lens = 15x

<u>Objective</u>	<u>Magnification</u>	<u>Field of View (Video Monitor)(um)</u>
10	239.26x	417.96
20	474.61x	210.70
40	953.125x	104.918

This screen prompt asks if you want information printed out on each particle encountered. Unless you have a very good reason for doing otherwise, always type in "0" <CR>, for no. Any other response will generate just a TON of worthless paper.

The screen prompt "specify a guard ring" sets a guard ring around the JOY BOX. This is a little weird, because we still have not assigned the joy box, it will be defined down two paragraphs. This guard ring prevents particles which are mostly outside of the joy box from being measured as smaller particles within the box. The guard ring is a band around the joy box. If the center of a particle is outside of the joy box the particle is not included in the analysis. A suggested value to be entered here is approx. one-half the size of the larger particles expected in the sample (i.e., if the particles will be 20 um set the guard ring at 10 um). This is so the guard ring is wide enough to allow the computer to discriminate against large particles which are mostly outside the joy box.

The screen prompt is now asking you to designate a file name. This is a temporary file where the data being generated will be stored for the LEMONT to manipulate it. This is the same file you may want to export later so give it a reasonable name, and write it down on the submittal forms provided for this purpose. If the file is not logged on the appropriate submittal form, MARL personnel may destroy the file in routine house cleaning. A typical file name would be DL2:RM7987. This is a file which is on device DL2 (a virtual disc on the hard drive). The name tells us that it was a rapid mixed sample from the test run on 7/9/1987.

This screen prompt is simply a sample ID of 50 characters or less, use your imagination.

This section is to set the JOY BOX around the particles to be analyzed. The joy box restricts the area which the AIA will analyze. If the guard ring is used but the joy box is not, the AIA will analyze the entire frame, and will reject the particles whose centers are outside the guard ring. If the joy box is used the AIA will only analyze the area within the joy box plus the guard ring, which is a specified distance outside the joy box, and then will reject any

particles whose centers are not inside of the joy box. In situations where the entire frame is not of interest, the joy box saves a great deal of analysis time.

Typing "H" or "V" will tell the computer that you are adjusting the horizontal or vertical dimension of the box. Then "+" or "-" will expand or reduce the respective dimensions. The arrow keys are used to position the box on the screen. The step size used in adjusting and moving the joy box can be adjusted by entering 0-5, 0 yields the finest step. Once the location and size of the joy box are satisfactory type "x" (Note: Typing <CR> here is fatal DO NOT <CR> HERE if you do it is stored in the keyboard buffer and a 0 is entered at the next screen prompt. The result is that you can only enter one frame/file.) Once you have typed "x" the analysis of the frame will begin immediately.

After the analysis of the frame is complete, the screen prompt will indicate the number of this frame in the analysis and the number of features which were encountered in this analysis. It will then give the following options:

- 0 - No more frames
- 1 - New frame
- 2 - Print intermediate results
- R - Return to restart options

"0"<CR> tell the computer that this is the last information to be placed in the present file, the file will be closed after the final results are printed. The screen prompt will now ask if you want plot options this is pretty much self explanatory. The monitor will display the following menu:

```
plot options
-1 finished
1 more plots
```

If you don't ask for more plots ("1" <CR>), you won't get any plots at all.

If you type "-1" CR the screen prompt will ask some non-fatal questions and then you will go back to menu 3 and you can collect another image or exit the program.

"1" <CR> keeps the current data file open, and sends you right back to menu 3, where you can either collect another image(the usual thing to do), or you can modify the joy box on the current image and analyze a new field on the current image.

"2" <CR> will print the results for just this frame. This is usually not done. However, if it is, the basic results will be printed as described above. The monitor will display the following menu:

```
plot options
-1 finished
1 more plots
```

Remember, if you don't ask for more plots ("1" <CR>), you won't get any plots at all.

If you tell it you are finished, by typing "-1" <CR>, the screen prompt will ask if you want more frames. If you type "1" <CR>, you will be taken back two menus. This is just fine. If you want to analyze more frames on the current image type "3" <CR>, and you will find yourself back on the current image and able to move the joy box to another place on the image. If you want to collect a new image but continue to add the information to the same file type "1" <CR>, and go collect a new image.

If you type "R" <CR>, you again close the current file and open a new file. This means, if you wanted to merge the information together, you will have to do it manually, based on the areas analyzed in the two files. However, if you were done with that specimen, either this or 0 is the appropriate option, since it allows you to start the next sample fresh.

#### V. Collecting Output and Exporting Files to the IBM XT

Collect your paper output from the printer. Use only the formfeed button to advance the paper!

#### VI. Exiting From the System

If at any time you want to exit from the Lemont system, type Control "C" twice. The first Control "C" gets you back to the main menu. The second Control "C", gets you back to the operating system.

Turn off the video monitor.

When ever you are exiting a session remember to "LOGOFF" from the session, and to enter the exiting time in the Lemont logbook.

Remember to clean up the light microscope after each session. This includes:

- o place the light intensity on 0 and then shut off the light
- o remove the video camera(\$8,000.00) from the scope and reinstall it on the macro-table, if you won't be using it for a while (Don't drop it!)
- o remove any specimens from the scope and clean the cell
- o cover and/or put away all optics, this includes;
  - cover the scope(\$10,000.00)
  - put away the NFK lenses properly(\$135.00)
  - put away the video camera adapter(\$175.00)

In general, clean up your mess, you are a guest here!

### VII. Cold Start

If the system is turned off, check that the following equipment is on:

- those normally on
  - o main power switch for the computer system
  - o computer panel power switch
  - o operators console
  - o digitizer tablet (ie. plug it in if you need it)
- those probably on
  - o video camera
  - o film recorder
- those probably off
  - o video color monitor
  - o microscope light source

When the DEC computer is turned on, but the operating system is not available press the "Run" button on the DEC. If the monitor is dark but the computer is on, press return on the terminal keyboard, the DEC shuts off the monitor if the keyboard sits idle for any extended period. Upon start-up the system will request information on the date and time, the information should take the following form:

- o 20-JUL-87
- o 16:00:00

This will get the operating system to a point where the hot start procedure can be followed.

Playback Analysis Summary

This document assumes that the files to be played back are on 8 inch floppies, and that the user desires to transfer the output to 5 1/4 inch floppies on the IBM XT.

The first step is to set the DEC up so that it sends everything to the IBM instead of to the line printer.

Type .Assign AM LP

(NOTE: If you want to display results to the screen instead of sending them to the line printer or the IBM you can use an .ASSIGN TT LP)

Then be sure that Cable AH goes to Cable A at the LEMONT, and Cable IBM goes to Cable A at the IBM.

Boot the IBM, and, once the SHELL comes up, type K <CR> to get into kermit.

At this point go to the LEMONT and get it set up. This is AIA below.

The next series of steps are repeated for each file that is analyzed and transferred from the AIA.

MS> LOG File.Name (e.g., A:FLOG5MIN.PRN)

MS> CONNECT <CR> (The IBM is now set up to log any thing which comes to it from the DEC into a file on the 5 1/4 inch disc. It will continue to do this until it is told to quit.)

MS>CONTROL ] C (This will tell the IBM to quit logging to the open file.)

MS>CLOSE <CR> (This will close the file which was opened.)

These four steps can be repeated as often as desired. When you desire to leave kermit simply type;

MS>EXIT

Don't forget to reassign the line printer before you leave the DEC;

.ASSIGN LS LP

## AIA

Type LEMSET to enter the Lemont programs.

Type ll <CR> for OASYS Playback.

Type <CR> for the default answer file.

Type N <CR>

The block data change prompt is now on the screen. This is the point at which discriminators can be set, and histogram classes are changed.

To set histogram classes:

Type 13 <CR> to enter misc. prog. variables.

III FFFFFFFF (The screen will display this line)

2 31.1 <CR> (Type this line to set an upper limit of 31.1

histogram class intervals.)

Type 0 <CR> to exit misc. variables.

Type 1 <CR> to set histogram class coordinates.

Type 2 <CR> to select a log scale;

Y-Beg FFFFFFFFFF Y-End FFFFFFFFFF (The screen will display this.)

0.5 20,000 <CR> (Type this in response)

Type 30 <CR>

This sets up a log scale histogram with 30 classes beginning at 0.5  $\mu\text{m}^2$  (Diameter = 0.79  $\mu\text{m}$ ) and ending at 20,000  $\mu\text{m}^2$  (Diameter = 160  $\mu\text{m}$ ).

Type 0 <CR>

General Notes to Self:

Double control C gets us back to the system

Up to 30 size categories can set up, and these can be distributed in the areas of interest.

SHO will get a list of how different pieces of physical and logical hardware are assigned.

DIR: will get the directory.



## APPENDIX B

This appendix contains the data used to create the graphs presented in the body of the text. The reader is reminded that the experimental conditions are detailed in Table 25. Specific information on such things as G-values corresponding to a specific rpm can be found on that table. Neither the data from HIAC particle counter nor the data from the breakup experiments is included in this table. A number of the experiments which have been included have not been discussed in the results section.

FLOCCULATION EXPERIMENT MATRIX  
TURBINE GEOMETRY

RUN DATE	RM RPM	RM TIME (MIN)	COAG. TYPE	FLOC. MIXING ENERGY	TEMP. °C	PARAMETERS HELD CONSTANT				
						pH	pOH	$\epsilon$	$\eta$	G
5/2/88	500	2.25	POLYMER	HI	20	1	1	1	1	1
4/14/88	500	2.25	POLYMER	HI	5	1		1		
4/26/88	250	1	POLYMER	LO	20	1	1	1	1	1
4/28/88	250	1	POLYMER	HI	20	1	1	1	1	1
3/3/88	250	1	POLYMER	LO	5	1		1		
3/1/88	250	1	POLYMER	LO	5	1		1		
2/23/88	250	1	POLYMER	HI	5	1		1		
2/25/88	250	1	POLYMER	HI	5	1		1		
5/4/88	500	1	ALUM	HI	20	1	1	1	1	1
3/17/88	500	1	ALUM	LO	5		1	1		
3/29/88	500	1	ALUM	LO	5		1	1		
4/12/88	500	1	ALUM	HI	5		1	1		
4/7/88	500	3	ALUM	LO	5		1	1		

FLOCCULATION EXPERIMENT MATRIX  
TURBINE GEOMETRY

RUN DATE	RM RPM	RM COAG. TIME TYPE (MIN)	FLOC. MIXING ENERGY	TEMP. °C	PARAMETERS HELD CONSTANT				
					pH	pOH	$\epsilon$	$\eta$	G
4/21/88	250	5 ALUM	LO	20	1	1	1	1	1
4/19/88	250	5 ALUM	LO	20	1	1	1	1	1
2/1/88	250	5 ALUM	LO	5		1	1		
2/5/88	250	5 ALUM	LO	5		1	1		
2/9/88	250	5 ALUM	HI	5		1	1		
10/22/87	250	1 ALUM	LO	20	1	1	1	1	1
11/3/87	250	1 ALUM	LO	20	1	1	1	1	1
10/24/87	250	1 ALUM	LO	20	1	1	1	1	1
11/5/87	250	1 ALUM	HI	20	1	1	1	1	1
11/10/87	250	1 ALUM	HI	20	1	1	1	1	1
11/12/87	250	1 ALUM	HI	20	1	1	1	1	1
11/19/87	250	1 ALUM	LO	5	1		1		
12/1/87	250	1 ALUM	LO	5	1		1		
1/14/88	250	1 ALUM	HI	5	1		1		
1/19/88	250	1 ALUM	HI	5	1		1		

**FLOCCULATION EXPERIMENT MATRIX  
TURBINE GEOMETRY**

RUN DATE	RM RPM	RM COAG. TIME TYPE (MIN)	FLOC. MIXING ENERGY	TEMP. °C	PARAMETERS HELD CONSTANT					
					pH	pOH	$\epsilon$	$\eta$	G	
12/15/87	250	1 ALUM	LO	5		1				1
12/8/87	250	1 ALUM	LO	5		1	1			
12/31/87	340	1 ALUM	LO	5		1			2	
12/22/87	250	1 ALUM	LO	5		1			1	
12/19/87	250	1 ALUM	LO	5		1			1	
1/21/88	250	1 ALUM	HI	5		1	1			
1/2/88	250	1 ALUM	HI	5		1	1			
1/5/88	250	1 ALUM	HI	5		1	1			
1/7/88	250	1 ALUM	HI	5		1				1
1/26/88	250	1 ALUM	HI	5		1			1	
1/28/88	250	1 ALUM	HI	5		1			1	
2/11/88	250	1 ALUM	HI	2		1	1			

A 2 IN COLUMN "N" INDICATES THAT THE KOLMOGOROV MICROSCALE WAS HELD CONSTANT DURING BOTH RAPID MIXING AND SLOW MIXING.

FLOCCULATION EXPERIMENT MATRIX  
STAKE & STATOR GEOMETRY

RUN DATE	RM RPM	RM TIME (MIN)	COAG. TYPE	FLOC. MIXING ENERGY	TEMP. °C	PARAMETERS HELD CONSTANT				
						pH	pOH	$\epsilon$	$\eta$	G
6/23/88	250	1	ALUM	LO	20	1	1	1	1	1
8/9/88	250	1	ALUM	LO	20	1	1	1	1	1
6/21/88	250	1	ALUM	HI	20	1	1	1	1	1
7/28/88	250	1	ALUM	HI	20	1	1	1	1	1
6/27/88	250	1	ALUM	LO	5		1	1		
8/15/88	250	1	ALUM	LO	5		1	1		
6/29/88	250	1	ALUM	HI	5		1	1		
8/17/88	250	1	ALUM	HI	5		1	1		

FLOCCULATION EXPERIMENT MATRIX  
TURBINE GEOMETRY

RUN DATE	RM RPM	RM TIME (MIN)	COAG. TYPE	FLOC. MIXING ENERGY	TEMP. °C	PARAMETERS HELD CONSTANT				
						pH	pOH	$\epsilon$	$\eta$	G
9/16/88	250	1	FERRIC	HI	20	1	1	1	1	1
9/12/88	250	1	FERRIC	HI	20	1	1	1	(Sweep)	
9/20/88	250	1	FERRIC	HI	5	1		1		
9/30/88	250	1	FERRIC	HI	5		1	1		
9/23/88	250	1	FERRIC	HI	5		1	1		

The data presented on this page is representative of the data which accompanied each AIA analysis.

Mar. 3, 1988 DARKFIELD, Objective Mag. = 20X;  
System Mag. = 474.61X

area anal (sq cm)	cell name	cell depth (mm)	sample volume (mm <sup>3</sup> )
0.00289	hom N	0.680	0.1965
0.00289	rmix B	0.685	0.1980
0.00289	1 min C	0.831	0.2402
0.00289	3 min D	0.696	0.2011
0.00289	5 min E	0.775	0.2240
0.00289	10 min F	0.706	0.2040
0.00289	15 min G	0.642	0.1855
0.00289	20 min X	0.645	0.1864
0.00321	25 min H	0.694	0.2228
0.00449	30 min O	0.681	0.3058
0.00449	45 min A	0.758	0.3403

The first column above represents the total area of the sample cell which has been analyzed by the AIA. The second column is the sample name. The third column is the sample cell identification. The fourth column is the average depth of the sample cell. The last column is the total sample volume which has been measured. This is calculated based on the area in column 1 and the and the cell depth in column 4. The numbers in the following pages are number concentration/mL, in the original sample, of particles in each size class. This number concentration is based on the calculated volume, as shown in column five above. As explained previously, the experimental conditions for the various experiments are given in Table 26 of the text and the table at the beginning of this appendix. Using the two tables and this data, it should be possible to completely reconstruct how the experiments were performed and the results of the experiments.



	15 min 15	20 min 20	25 min 25	30 min 30	45 min 45
dia.					
0.87	1.94E+05	2.54E+05	1.44E+05	1.96E+05	9.75E+04
1.04	2.47E+05	2.17E+05	1.35E+05	1.11E+05	9.53E+04
1.24	2.77E+05	2.46E+05	1.73E+05	1.34E+05	9.75E+04
1.48	3.49E+05	3.30E+05	2.25E+05	2.19E+05	1.65E+05
1.77	3.25E+05	2.74E+05	2.12E+05	1.83E+05	1.49E+05
2.11	2.23E+05	2.34E+05	1.09E+05	1.37E+05	1.13E+05
2.51	1.70E+05	1.65E+05	1.06E+05	6.21E+04	8.02E+04
3.00	1.31E+05	1.09E+05	5.13E+04	8.83E+04	4.55E+04
3.58	7.28E+04	5.64E+04	3.21E+04	3.92E+04	1.30E+04
4.27	6.31E+04	3.22E+04	1.60E+04	2.94E+04	1.30E+04
5.10	1.94E+04	3.62E+04	2.57E+04	1.31E+04	1.08E+04
6.08	1.94E+04	1.21E+04	2.25E+04	9.81E+03	8.67E+03
7.26	1.46E+04	1.61E+04	6.42E+03	3.27E+03	2.17E+03
8.66	4.85E+03	8.05E+03	9.63E+03	3.27E+03	2.17E+03
10.33	9.70E+03	4.03E+03	0.00E+00	0.00E+00	0.00E+00
12.33	0.00E+00	0.00E+00	0.00E+00	0.00E+00	2.17E+03
14.71	9.70E+03	0.00E+00	0.00E+00	0.00E+00	0.00E+00
17.55	1.46E+04	4.03E+03	3.21E+03	3.27E+03	0.00E+00
20.94	4.85E+03	4.03E+03	3.21E+03	3.27E+03	0.00E+00
24.98	4.85E+03	0.00E+00	0.00E+00	3.27E+03	0.00E+00
29.81	4.85E+03	8.05E+03	0.00E+00	3.27E+03	0.00E+00
35.56	0.00E+00	0.00E+00	0.00E+00	0.00E+00	0.00E+00
42.43	4.85E+03	0.00E+00	3.21E+03	0.00E+00	0.00E+00
50.63	0.00E+00	0.00E+00	0.00E+00	3.27E+03	0.00E+00
60.41	0.00E+00	4.03E+03	0.00E+00	0.00E+00	2.17E+03
72.08	0.00E+00	0.00E+00	0.00E+00	0.00E+00	2.17E+03
86.00	0.00E+00	4.03E+03	0.00E+00	0.00E+00	0.00E+00
102.62	0.00E+00	0.00E+00	0.00E+00	0.00E+00	2.17E+03
122.44	0.00E+00	0.00E+00	0.00E+00	0.00E+00	0.00E+00





	15 min 15	20 min 20	25 min 25	30 min 30	45 min 45
dia.					
0.87	2.49E+05	2.20E+05	1.76E+05	1.45E+05	1.08E+05
1.04	2.37E+05	1.89E+05	1.76E+05	1.33E+05	1.27E+05
1.24	3.16E+05	2.77E+05	2.07E+05	2.06E+05	1.36E+05
1.48	3.47E+05	3.73E+05	2.73E+05	2.78E+05	1.90E+05
1.77	3.35E+05	2.20E+05	2.49E+05	2.14E+05	1.36E+05
2.11	2.86E+05	2.28E+05	2.04E+05	1.83E+05	9.81E+04
2.51	2.49E+05	1.76E+05	1.59E+05	9.15E+04	9.49E+04
3.00	1.10E+05	6.59E+04	5.87E+04	8.77E+04	5.06E+04
3.58	6.69E+04	6.59E+04	5.18E+04	2.67E+04	1.58E+04
4.27	3.04E+04	2.64E+04	2.42E+04	4.20E+04	6.33E+03
5.10	1.83E+04	3.95E+04	1.04E+04	2.67E+04	6.33E+03
6.08	6.08E+03	1.32E+04	1.04E+04	7.63E+03	3.16E+03
7.26	1.22E+04	1.76E+04	3.46E+03	3.81E+03	3.16E+03
8.66	6.08E+03	8.78E+03	0.00E+00	0.00E+00	3.16E+03
10.33	0.00E+00	0.00E+00	3.46E+03	3.81E+03	0.00E+00
12.33	1.22E+04	2.20E+04	2.07E+04	1.14E+04	6.33E+03
14.71	6.08E+03	0.00E+00	0.00E+00	0.00E+00	0.00E+00
17.55	0.00E+00	0.00E+00	0.00E+00	3.81E+03	0.00E+00
20.94	0.00E+00	4.39E+03	3.46E+03	0.00E+00	0.00E+00
24.98	0.00E+00	0.00E+00	0.00E+00	0.00E+00	0.00E+00
29.81	0.00E+00	0.00E+00	0.00E+00	3.81E+03	0.00E+00
35.56	6.08E+03	0.00E+00	0.00E+00	0.00E+00	0.00E+00
42.43	6.08E+03	4.39E+03	0.00E+00	0.00E+00	3.16E+03
50.63	0.00E+00	0.00E+00	3.46E+03	0.00E+00	3.16E+03
60.41	0.00E+00	0.00E+00	0.00E+00	0.00E+00	0.00E+00
72.08	0.00E+00	0.00E+00	0.00E+00	3.81E+03	0.00E+00
86.00	0.00E+00	4.39E+03	0.00E+00	3.81E+03	0.00E+00
102.62	0.00E+00	0.00E+00	3.46E+03	0.00E+00	0.00E+00
122.44	0.00E+00	0.00E+00	0.00E+00	0.00E+00	0.00E+00



	15 min	20 min	25 min	30 min	45 min
	15	20	25	30	45
dia.					
0.87	5.55E+05	5.36E+05	4.63E+05	4.16E+05	2.72E+05
1.04	4.74E+05	3.27E+05	3.54E+05	3.13E+05	1.89E+05
1.24	3.83E+05	3.49E+05	3.22E+05	2.59E+05	2.28E+05
1.48	6.14E+05	4.83E+05	5.08E+05	3.62E+05	2.69E+05
1.77	4.64E+05	4.35E+05	3.41E+05	3.74E+05	2.06E+05
2.11	3.88E+05	4.02E+05	1.99E+05	3.17E+05	2.11E+05
2.51	2.53E+05	3.17E+05	1.22E+05	1.98E+05	1.18E+05
3.00	1.78E+05	1.82E+05	1.03E+05	1.22E+05	7.95E+04
3.58	1.08E+05	7.51E+04	7.72E+04	9.92E+04	4.94E+04
4.27	1.02E+05	1.02E+05	4.50E+04	4.20E+04	5.49E+04
5.10	2.69E+04	2.15E+04	3.22E+04	3.81E+04	1.65E+04
6.08	5.39E+04	1.07E+04	1.93E+04	1.91E+04	8.23E+03
7.26	1.62E+04	3.22E+04	1.93E+04	7.63E+03	8.23E+03
8.66	1.08E+04	2.15E+04	1.93E+04	1.14E+04	1.65E+04
10.33	1.08E+04	1.61E+04	6.43E+03	0.00E+00	8.23E+03
12.33	3.23E+04	5.36E+03	6.43E+03	7.63E+03	8.23E+03
14.71	5.39E+03	1.07E+04	6.43E+03	7.63E+03	2.74E+03
17.55	0.00E+00	5.36E+03	1.29E+04	3.81E+03	2.74E+03
20.94	1.08E+04	5.36E+03	6.43E+03	0.00E+00	2.74E+03
24.98	0.00E+00	5.36E+03	0.00E+00	3.81E+03	0.00E+00
29.81	0.00E+00	0.00E+00	0.00E+00	0.00E+00	2.74E+03
35.56	0.00E+00	0.00E+00	0.00E+00	3.81E+03	0.00E+00
42.43	0.00E+00	0.00E+00	0.00E+00	0.00E+00	0.00E+00
50.63	0.00E+00	0.00E+00	0.00E+00	0.00E+00	2.74E+03
60.41	0.00E+00	0.00E+00	0.00E+00	0.00E+00	0.00E+00
72.08	0.00E+00	0.00E+00	0.00E+00	0.00E+00	0.00E+00
86.00	0.00E+00	0.00E+00	0.00E+00	0.00E+00	0.00E+00
102.62	0.00E+00	0.00E+00	0.00E+00	0.00E+00	0.00E+00
122.44	0.00E+00	0.00E+00	0.00E+00	0.00E+00	0.00E+00



	15 min 15	20 min 20	25 min 25	30 min 30	45 min 45
dia.					
0.87	6.04E+05	4.59E+05	3.14E+05	3.24E+05	9.59E+04
1.04	4.69E+05	3.19E+05	2.57E+05	2.32E+05	9.59E+04
1.24	3.93E+05	3.77E+05	2.61E+05	1.98E+05	9.13E+04
1.48	4.26E+05	3.77E+05	3.76E+05	2.75E+05	1.00E+05
1.77	4.85E+05	3.96E+05	2.53E+05	1.89E+05	1.10E+05
2.11	3.29E+05	2.75E+05	2.04E+05	9.16E+04	7.76E+04
2.51	2.53E+05	2.22E+05	1.31E+05	7.63E+04	6.39E+04
3.00	1.40E+05	1.79E+05	6.12E+04	5.50E+04	5.93E+04
3.58	5.39E+04	7.24E+04	4.49E+04	2.75E+04	3.65E+04
4.27	4.31E+04	2.90E+04	2.04E+04	2.14E+04	9.13E+03
5.10	2.16E+04	3.86E+04	2.86E+04	1.22E+04	1.37E+04
6.08	2.16E+04	1.93E+04	2.04E+04	6.11E+03	1.37E+04
7.26	1.62E+04	4.83E+03	4.08E+03	6.11E+03	0.00E+00
8.66	2.69E+04	4.83E+03	4.08E+03	3.05E+03	0.00E+00
10.33	1.08E+04	0.00E+00	0.00E+00	0.00E+00	0.00E+00
12.33	1.62E+04	9.66E+03	4.08E+03	3.05E+03	4.56E+03
14.71	5.39E+03	9.66E+03	4.08E+03	0.00E+00	0.00E+00
17.55	0.00E+00	0.00E+00	8.16E+03	3.05E+03	0.00E+00
20.94	5.39E+03	0.00E+00	0.00E+00	3.05E+03	0.00E+00
24.98	0.00E+00	0.00E+00	4.08E+03	0.00E+00	0.00E+00
29.81	0.00E+00	0.00E+00	8.16E+03	0.00E+00	0.00E+00
35.56	0.00E+00	0.00E+00	0.00E+00	0.00E+00	0.00E+00
42.43	0.00E+00	0.00E+00	0.00E+00	0.00E+00	0.00E+00
50.63	0.00E+00	0.00E+00	4.08E+03	3.05E+03	0.00E+00
60.41	0.00E+00	0.00E+00	8.16E+03	3.05E+03	0.00E+00
72.08	0.00E+00	4.83E+03	0.00E+00	0.00E+00	0.00E+00
86.00	0.00E+00	0.00E+00	0.00E+00	3.05E+03	0.00E+00
102.62	0.00E+00	0.00E+00	0.00E+00	0.00E+00	9.13E+03
122.44	0.00E+00	0.00E+00	0.00E+00	0.00E+00	0.00E+00



	15 min 15	20 min 20	25 min 25	30 min 30	45 min 45
dia.					
0.87	5.55E+05	5.04E+05	5.19E+05	4.03E+05	3.16E+05
1.04	4.96E+05	5.10E+05	4.09E+05	2.79E+05	3.16E+05
1.24	5.17E+05	5.74E+05	6.23E+05	4.62E+05	3.66E+05
1.48	7.44E+05	8.15E+05	7.33E+05	6.77E+05	5.22E+05
1.77	7.76E+05	7.14E+05	6.43E+05	6.36E+05	4.89E+05
2.11	7.33E+05	6.92E+05	4.64E+05	5.21E+05	3.45E+05
2.51	5.01E+05	5.04E+05	4.34E+05	3.71E+05	2.22E+05
3.00	3.34E+05	2.20E+05	2.04E+05	2.06E+05	1.60E+05
3.58	1.46E+05	1.18E+05	1.10E+05	1.78E+05	1.19E+05
4.27	8.08E+04	1.02E+05	4.49E+04	1.19E+05	4.11E+04
5.10	4.85E+04	2.15E+04	1.50E+04	6.86E+04	3.29E+04
6.08	2.69E+04	1.07E+04	1.99E+04	2.29E+04	2.05E+04
7.26	5.39E+03	2.68E+04	4.99E+03	1.37E+04	4.11E+03
8.66	5.39E+03	1.07E+04	0.00E+00	9.15E+03	1.23E+04
10.33	2.69E+04	5.36E+03	4.99E+03	1.83E+04	4.11E+03
12.33	0.00E+00	0.00E+00	0.00E+00	9.15E+03	4.11E+03
14.71	0.00E+00	0.00E+00	0.00E+00	9.15E+03	0.00E+00
17.55	0.00E+00	0.00E+00	4.99E+03	0.00E+00	4.11E+03
20.94	0.00E+00	0.00E+00	0.00E+00	4.57E+03	0.00E+00
24.98	0.00E+00	0.00E+00	0.00E+00	0.00E+00	0.00E+00
29.81	0.00E+00	0.00E+00	0.00E+00	0.00E+00	0.00E+00
35.56	0.00E+00	0.00E+00	0.00E+00	0.00E+00	0.00E+00
42.43	0.00E+00	0.00E+00	0.00E+00	0.00E+00	0.00E+00
50.63	0.00E+00	0.00E+00	0.00E+00	0.00E+00	0.00E+00
60.41	0.00E+00	0.00E+00	0.00E+00	0.00E+00	0.00E+00
72.08	0.00E+00	0.00E+00	0.00E+00	0.00E+00	0.00E+00
86.00	0.00E+00	0.00E+00	0.00E+00	0.00E+00	0.00E+00
102.62	0.00E+00	0.00E+00	0.00E+00	0.00E+00	0.00E+00
122.44	0.00E+00	0.00E+00	0.00E+00	0.00E+00	0.00E+00





	15 min 15	20 min 20	25 min 25	30 min 30	45 min 45
dia.					
0.87	4.26E+05	3.97E+05	4.04E+05	3.96E+05	2.94E+05
1.04	4.04E+05	3.97E+05	4.40E+05	3.17E+05	2.47E+05
1.24	4.85E+05	4.72E+05	4.04E+05	4.94E+05	3.85E+05
1.48	7.76E+05	6.06E+05	6.19E+05	5.46E+05	4.70E+05
1.77	7.38E+05	6.54E+05	5.61E+05	4.61E+05	3.97E+05
2.11	6.31E+05	5.85E+05	5.25E+05	4.87E+05	3.82E+05
2.51	4.47E+05	4.45E+05	4.08E+05	3.73E+05	2.53E+05
3.00	2.80E+05	2.68E+05	2.06E+05	2.09E+05	1.47E+05
3.58	9.16E+04	1.98E+05	7.18E+04	1.24E+05	9.40E+04
4.27	1.29E+05	5.90E+04	8.53E+04	7.19E+04	6.46E+04
5.10	6.47E+04	4.83E+04	4.04E+04	4.58E+04	1.76E+04
6.08	3.23E+04	2.68E+04	1.35E+04	3.60E+04	1.18E+04
7.26	5.39E+03	2.68E+04	1.80E+04	1.64E+04	2.94E+03
8.66	1.08E+04	5.36E+03	4.49E+03	6.54E+03	8.81E+03
10.33	0.00E+00	0.00E+00	4.49E+03	0.00E+00	1.18E+04
12.33	0.00E+00	0.00E+00	4.49E+03	3.27E+03	0.00E+00
14.71	0.00E+00	0.00E+00	0.00E+00	9.81E+03	0.00E+00
17.55	0.00E+00	0.00E+00	4.49E+03	6.54E+03	0.00E+00
20.94	0.00E+00	0.00E+00	0.00E+00	3.27E+03	0.00E+00
24.98	0.00E+00	0.00E+00	4.49E+03	3.27E+03	0.00E+00
29.81	0.00E+00	0.00E+00	0.00E+00	0.00E+00	0.00E+00
35.56	0.00E+00	0.00E+00	0.00E+00	0.00E+00	0.00E+00
42.43	0.00E+00	0.00E+00	0.00E+00	0.00E+00	0.00E+00
50.63	0.00E+00	0.00E+00	0.00E+00	0.00E+00	0.00E+00
60.41	0.00E+00	0.00E+00	0.00E+00	0.00E+00	0.00E+00
72.08	0.00E+00	0.00E+00	0.00E+00	0.00E+00	0.00E+00
86.00	0.00E+00	0.00E+00	0.00E+00	0.00E+00	0.00E+00
102.62	0.00E+00	0.00E+00	0.00E+00	0.00E+00	0.00E+00
122.44	0.00E+00	0.00E+00	0.00E+00	0.00E+00	0.00E+00



	15 min	20 min	25 min	30 min	45 min
	15	20	25	30	45
dia.					
0.87	2.85E+05	3.21E+05	2.65E+05	3.11E+05	2.35E+05
1.04	2.92E+05	2.42E+05	2.24E+05	3.29E+05	2.03E+05
1.24	3.82E+05	3.39E+05	3.37E+05	2.38E+05	2.29E+05
1.48	5.77E+05	4.18E+05	3.32E+05	4.16E+05	2.67E+05
1.77	4.38E+05	4.36E+05	3.14E+05	3.29E+05	2.59E+05
2.11	5.08E+05	3.51E+05	2.15E+05	3.52E+05	2.09E+05
2.51	2.64E+05	2.12E+05	2.29E+05	1.51E+05	1.73E+05
3.00	1.25E+05	1.64E+05	1.57E+05	1.05E+05	8.81E+04
3.58	1.11E+05	7.27E+04	5.39E+04	8.69E+04	5.58E+04
4.27	5.56E+04	6.06E+04	5.39E+04	5.03E+04	3.23E+04
5.10	4.17E+04	3.63E+04	1.80E+04	1.37E+04	5.88E+03
6.08	3.48E+04	3.03E+04	2.69E+04	9.15E+03	1.47E+04
7.26	2.09E+04	1.82E+04	4.49E+03	2.29E+04	5.88E+03
8.66	0.00E+00	0.00E+00	8.98E+03	0.00E+00	2.94E+03
10.33	6.95E+03	6.06E+03	0.00E+00	1.37E+04	0.00E+00
12.33	0.00E+00	6.06E+03	0.00E+00	0.00E+00	0.00E+00
14.71	0.00E+00	6.06E+03	8.98E+03	0.00E+00	2.94E+03
17.55	0.00E+00	0.00E+00	1.80E+04	0.00E+00	2.94E+03
20.94	0.00E+00	0.00E+00	4.49E+03	4.57E+03	5.88E+03
24.98	0.00E+00	0.00E+00	0.00E+00	0.00E+00	0.00E+00
29.81	0.00E+00	6.06E+03	8.98E+03	9.15E+03	0.00E+00
35.56	0.00E+00	0.00E+00	0.00E+00	0.00E+00	5.88E+03
42.43	0.00E+00	0.00E+00	0.00E+00	0.00E+00	0.00E+00
50.63	0.00E+00	0.00E+00	4.49E+03	0.00E+00	0.00E+00
60.41	0.00E+00	0.00E+00	0.00E+00	0.00E+00	0.00E+00
72.08	0.00E+00	0.00E+00	0.00E+00	0.00E+00	0.00E+00
86.00	0.00E+00	0.00E+00	0.00E+00	0.00E+00	0.00E+00
102.62	0.00E+00	0.00E+00	0.00E+00	0.00E+00	0.00E+00
122.44	0.00E+00	0.00E+00	0.00E+00	0.00E+00	0.00E+00



	15 min 15	20 min 20	25 min 25	30 min 30	45 min 45
dia.					
0.87	4.20E+05	3.80E+05	2.60E+05	2.35E+05	1.23E+05
1.04	3.99E+05	2.90E+05	2.28E+05	2.81E+05	1.21E+05
1.24	4.20E+05	3.69E+05	3.43E+05	3.17E+05	2.22E+05
1.48	6.68E+05	5.14E+05	4.69E+05	4.19E+05	3.18E+05
1.77	5.61E+05	5.14E+05	3.88E+05	3.17E+05	2.55E+05
2.11	6.74E+05	5.04E+05	3.34E+05	3.63E+05	2.03E+05
2.51	4.74E+05	2.56E+05	2.09E+05	1.70E+05	1.26E+05
3.00	2.59E+05	2.11E+05	1.44E+05	1.28E+05	4.39E+04
3.58	1.56E+05	7.25E+04	8.02E+04	7.52E+04	3.84E+04
4.27	1.08E+05	5.52E+04	3.85E+04	4.25E+04	2.47E+04
5.10	6.47E+04	4.83E+04	1.60E+04	1.96E+04	8.23E+03
6.08	1.62E+04	1.38E+04	6.42E+03	2.94E+04	2.74E+03
7.26	3.77E+04	1.38E+04	9.63E+03	3.27E+03	1.10E+04
8.66	5.39E+03	6.91E+03	9.63E+03	1.31E+04	5.49E+03
10.33	1.08E+04	0.00E+00	3.21E+03	3.27E+03	2.74E+03
12.33	0.00E+00	1.04E+04	1.28E+04	6.54E+03	0.00E+00
14.71	0.00E+00	1.04E+04	0.00E+00	6.54E+03	0.00E+00
17.55	0.00E+00	0.00E+00	3.21E+03	6.54E+03	2.74E+03
20.94	0.00E+00	1.38E+04	9.63E+03	1.31E+04	0.00E+00
24.98	0.00E+00	6.91E+03	6.42E+03	3.27E+03	0.00E+00
29.81	0.00E+00	0.00E+00	0.00E+00	0.00E+00	0.00E+00
35.56	0.00E+00	0.00E+00	0.00E+00	3.27E+03	2.74E+03
42.43	0.00E+00	0.00E+00	0.00E+00	0.00E+00	0.00E+00
50.63	0.00E+00	0.00E+00	0.00E+00	0.00E+00	0.00E+00
60.41	0.00E+00	0.00E+00	0.00E+00	0.00E+00	0.00E+00
72.08	0.00E+00	0.00E+00	0.00E+00	0.00E+00	2.74E+03
86.00	0.00E+00	0.00E+00	0.00E+00	0.00E+00	0.00E+00
102.62	0.00E+00	0.00E+00	0.00E+00	0.00E+00	0.00E+00
122.44	0.00E+00	0.00E+00	0.00E+00	0.00E+00	0.00E+00



	15 min 15	20 min 20	25 min 25	30 min 30	45 min 45
dia.					
0.87	1.99E+05	1.35E+05	1.38E+05	6.41E+04	6.59E+04
1.04	2.23E+05	1.16E+05	7.38E+04	6.19E+04	2.47E+04
1.24	1.84E+05	1.35E+05	9.63E+04	6.87E+04	4.94E+04
1.48	2.57E+05	1.55E+05	1.22E+05	8.93E+04	4.94E+04
1.77	2.14E+05	8.21E+04	1.06E+05	4.35E+04	4.53E+04
2.11	1.89E+05	1.11E+05	1.16E+05	5.73E+04	4.53E+04
2.51	1.75E+05	8.21E+04	5.46E+04	2.98E+04	2.68E+04
3.00	1.07E+05	4.35E+04	4.81E+04	3.67E+04	8.23E+03
3.58	6.31E+04	1.93E+04	4.49E+04	1.83E+04	1.65E+04
4.27	6.79E+04	2.90E+04	6.42E+03	2.29E+03	4.12E+03
5.10	2.91E+04	3.38E+04	1.28E+04	9.16E+03	4.12E+03
6.08	1.94E+04	0.00E+00	6.42E+03	9.16E+03	2.06E+03
7.26	3.40E+04	1.45E+04	1.28E+04	2.29E+03	2.06E+03
8.66	9.70E+03	9.66E+03	6.42E+03	2.29E+03	0.00E+00
10.33	1.94E+04	1.45E+04	0.00E+00	2.29E+03	0.00E+00
12.33	1.94E+04	4.83E+03	3.21E+03	4.58E+03	8.23E+03
14.71	3.40E+04	0.00E+00	3.21E+03	2.29E+03	0.00E+00
17.55	4.85E+03	9.66E+03	6.42E+03	2.29E+03	6.17E+03
20.94	0.00E+00	0.00E+00	0.00E+00	4.58E+03	6.17E+03
24.98	1.46E+04	9.66E+03	3.21E+03	1.37E+04	6.17E+03
29.81	0.00E+00	1.93E+04	1.28E+04	4.58E+03	4.12E+03
35.56	0.00E+00	0.00E+00	0.00E+00	0.00E+00	2.06E+03
42.43	0.00E+00	0.00E+00	9.63E+03	6.87E+03	2.06E+03
50.63	0.00E+00	0.00E+00	0.00E+00	0.00E+00	2.06E+03
60.41	0.00E+00	0.00E+00	0.00E+00	0.00E+00	0.00E+00
72.08	0.00E+00	0.00E+00	0.00E+00	0.00E+00	0.00E+00
86.00	0.00E+00	0.00E+00	0.00E+00	2.29E+03	0.00E+00
102.62	0.00E+00	0.00E+00	0.00E+00	0.00E+00	0.00E+00
122.44	0.00E+00	0.00E+00	0.00E+00	0.00E+00	0.00E+00





	15 min 15	20 min 20	25 min 25	30 min 30	45 min 45
dia.					
0.87	6.02E+05	4.30E+05	3.67E+05	3.45E+05	2.65E+05
1.04	4.87E+05	4.35E+05	3.51E+05	2.83E+05	1.68E+05
1.24	6.27E+05	4.01E+05	4.49E+05	3.54E+05	2.69E+05
1.48	9.25E+05	6.81E+05	7.27E+05	5.57E+05	4.11E+05
1.77	7.54E+05	6.96E+05	5.39E+05	5.91E+05	3.44E+05
2.11	6.63E+05	6.28E+05	5.88E+05	4.33E+05	2.73E+05
2.51	4.56E+05	4.97E+05	4.04E+05	3.16E+05	1.94E+05
3.00	2.80E+05	2.95E+05	2.49E+05	2.66E+05	1.57E+05
3.58	1.10E+05	1.64E+05	1.63E+05	1.83E+05	6.35E+04
4.27	6.69E+04	2.90E+04	1.02E+05	8.74E+04	4.11E+04
5.10	3.04E+04	1.45E+04	4.90E+04	7.90E+04	1.87E+04
6.08	1.22E+04	1.45E+04	3.27E+04	5.82E+04	2.99E+04
7.26	0.00E+00	0.00E+00	2.04E+04	2.50E+04	0.00E+00
8.66	6.08E+03	0.00E+00	2.04E+04	3.74E+04	0.00E+00
10.33	0.00E+00	0.00E+00	8.16E+03	1.25E+04	0.00E+00
12.33	0.00E+00	4.83E+03	8.16E+03	8.32E+03	1.49E+04
14.71	0.00E+00	0.00E+00	4.08E+03	0.00E+00	7.47E+03
17.55	0.00E+00	0.00E+00	0.00E+00	4.16E+03	1.49E+04
20.94	0.00E+00	0.00E+00	8.16E+03	4.16E+03	7.47E+03
24.98	0.00E+00	0.00E+00	0.00E+00	4.16E+03	3.74E+03
29.81	0.00E+00	0.00E+00	0.00E+00	0.00E+00	0.00E+00
35.56	0.00E+00	0.00E+00	0.00E+00	0.00E+00	0.00E+00
42.43	0.00E+00	0.00E+00	0.00E+00	0.00E+00	0.00E+00
50.63	0.00E+00	0.00E+00	0.00E+00	0.00E+00	0.00E+00
60.41	0.00E+00	0.00E+00	0.00E+00	0.00E+00	0.00E+00
72.08	0.00E+00	0.00E+00	0.00E+00	0.00E+00	0.00E+00
86.00	0.00E+00	0.00E+00	0.00E+00	0.00E+00	0.00E+00
102.62	0.00E+00	0.00E+00	0.00E+00	0.00E+00	0.00E+00
122.44	0.00E+00	0.00E+00	0.00E+00	0.00E+00	0.00E+00



	15 min 15	20 min 20	25 min 25	30 min 30	45 min 45
dia.					
0.87	4.90E+05	3.53E+05	3.14E+05	2.06E+05	7.35E+04
1.04	3.61E+05	3.53E+05	2.86E+05	1.78E+05	9.40E+04
1.24	3.93E+05	4.15E+05	4.04E+05	3.11E+05	1.79E+05
1.48	7.17E+05	4.93E+05	4.86E+05	4.57E+05	2.17E+05
1.77	5.87E+05	6.09E+05	4.33E+05	3.93E+05	2.12E+05
2.11	5.17E+05	4.40E+05	4.41E+05	4.03E+05	2.29E+05
2.51	4.74E+05	3.38E+05	2.78E+05	2.97E+05	1.47E+05
3.00	3.18E+05	1.84E+05	1.92E+05	1.46E+05	1.12E+05
3.58	1.72E+05	3.86E+04	8.16E+04	1.42E+05	4.41E+04
4.27	8.08E+04	9.18E+04	6.53E+04	5.95E+04	3.82E+04
5.10	3.23E+04	4.35E+04	1.63E+04	1.83E+04	1.76E+04
6.08	2.69E+04	9.66E+03	1.63E+04	9.15E+03	5.88E+03
7.26	1.62E+04	9.66E+03	8.16E+03	2.29E+04	2.06E+04
8.66	5.39E+03	9.66E+03	4.08E+03	9.15E+03	1.18E+04
10.33	5.39E+03	4.83E+03	4.08E+03	0.00E+00	5.88E+03
12.33	0.00E+00	0.00E+00	8.16E+03	9.15E+03	2.94E+03
14.71	0.00E+00	0.00E+00	4.08E+03	4.57E+03	2.94E+03
17.55	0.00E+00	0.00E+00	0.00E+00	0.00E+00	0.00E+00
20.94	0.00E+00	0.00E+00	0.00E+00	0.00E+00	1.47E+04
24.98	0.00E+00	0.00E+00	0.00E+00	0.00E+00	1.18E+04
29.81	0.00E+00	0.00E+00	0.00E+00	0.00E+00	0.00E+00
35.56	0.00E+00	0.00E+00	0.00E+00	0.00E+00	0.00E+00
42.43	0.00E+00	0.00E+00	0.00E+00	0.00E+00	0.00E+00
50.63	0.00E+00	0.00E+00	0.00E+00	0.00E+00	2.94E+03
60.41	0.00E+00	0.00E+00	0.00E+00	0.00E+00	0.00E+00
72.08	0.00E+00	0.00E+00	0.00E+00	0.00E+00	0.00E+00
86.00	0.00E+00	0.00E+00	0.00E+00	0.00E+00	0.00E+00
102.62	0.00E+00	0.00E+00	0.00E+00	0.00E+00	0.00E+00
122.44	0.00E+00	0.00E+00	0.00E+00	0.00E+00	0.00E+00



	15 min 15	20 min 20	25 min 25	30 min 30	45 min 45
dia.					
0.87	2.80E+05	2.18E+05	1.76E+05	1.79E+05	9.11E+04
1.04	2.74E+05	2.85E+05	2.16E+05	1.37E+05	8.23E+04
1.24	4.20E+05	3.15E+05	2.53E+05	1.87E+05	8.52E+04
1.48	6.15E+05	3.57E+05	3.27E+05	2.58E+05	1.38E+05
1.77	4.69E+05	2.54E+05	3.10E+05	2.20E+05	8.23E+04
2.11	4.56E+05	3.69E+05	3.27E+05	2.00E+05	9.70E+04
2.51	3.59E+05	3.63E+05	2.57E+05	1.16E+05	7.64E+04
3.00	2.37E+05	2.18E+05	2.33E+05	1.37E+05	7.35E+04
3.58	1.83E+05	1.09E+05	1.18E+05	5.82E+04	4.11E+04
4.27	1.03E+05	1.09E+05	8.16E+04	7.49E+04	1.18E+04
5.10	7.91E+04	7.27E+04	4.49E+04	4.58E+04	1.47E+04
6.08	1.83E+04	1.82E+04	3.27E+04	5.41E+04	1.47E+04
7.26	2.43E+04	6.66E+04	3.67E+04	2.50E+04	1.76E+04
8.66	1.22E+04	3.03E+04	1.63E+04	1.66E+04	5.88E+03
10.33	6.08E+03	2.42E+04	2.04E+04	4.16E+03	1.18E+04
12.33	6.08E+03	1.82E+04	2.45E+04	1.25E+04	5.88E+03
14.71	0.00E+00	0.00E+00	2.04E+04	1.25E+04	1.76E+04
17.55	0.00E+00	0.00E+00	4.08E+03	4.16E+03	5.88E+03
20.94	0.00E+00	0.00E+00	0.00E+00	4.16E+03	2.94E+03
24.98	0.00E+00	0.00E+00	0.00E+00	0.00E+00	2.94E+03
29.81	0.00E+00	0.00E+00	0.00E+00	0.00E+00	2.94E+03
35.56	0.00E+00	0.00E+00	0.00E+00	0.00E+00	0.00E+00
42.43	0.00E+00	0.00E+00	0.00E+00	0.00E+00	2.94E+03
50.63	0.00E+00	0.00E+00	0.00E+00	0.00E+00	0.00E+00
60.41	0.00E+00	0.00E+00	0.00E+00	0.00E+00	0.00E+00
72.08	0.00E+00	0.00E+00	0.00E+00	0.00E+00	0.00E+00
86.00	0.00E+00	0.00E+00	0.00E+00	0.00E+00	0.00E+00
102.62	0.00E+00	0.00E+00	0.00E+00	0.00E+00	0.00E+00
122.44	0.00E+00	0.00E+00	0.00E+00	0.00E+00	0.00E+00



	15 min 15	20 min 20	25 min 25	30 min 30	45 min 45
dia.					
1.04	3.35E+05	4.00E+05	2.93E+05	2.06E+05	1.09E+05
1.24	4.20E+05	3.27E+05	3.32E+05	2.52E+05	1.32E+05
1.48	5.78E+05	4.00E+05	3.83E+05	3.75E+05	1.88E+05
1.77	6.27E+05	6.84E+05	5.74E+05	4.21E+05	2.50E+05
2.11	6.08E+05	4.60E+05	4.45E+05	4.67E+05	2.17E+05
2.51	5.96E+05	6.54E+05	4.95E+05	3.80E+05	1.97E+05
3.00	4.38E+05	5.09E+05	4.33E+05	2.20E+05	1.15E+05
3.58	2.62E+05	2.54E+05	3.04E+05	1.83E+05	1.12E+05
4.27	1.70E+05	1.82E+05	1.97E+05	1.14E+05	6.46E+04
5.10	9.13E+04	8.48E+04	8.44E+04	6.86E+04	2.94E+04
6.08	3.04E+04	5.45E+04	5.63E+04	4.57E+04	1.18E+04
7.26	0.00E+00	3.63E+04	3.38E+04	3.66E+04	1.47E+04
8.66	0.00E+00	2.42E+04	2.25E+04	2.29E+04	8.81E+03
10.33	6.08E+03	1.21E+04	5.63E+03	3.20E+04	8.81E+03
12.33	6.08E+03	1.21E+04	5.63E+03	2.29E+04	5.88E+03
13.46	0.00E+00	6.06E+03	1.13E+04	1.83E+04	1.18E+04
14.71	0.00E+00	0.00E+00	1.69E+04	4.57E+03	0.00E+00
17.55	0.00E+00	0.00E+00	5.63E+03	1.83E+04	2.94E+03
20.94	0.00E+00	0.00E+00	0.00E+00	0.00E+00	2.94E+03
24.98	0.00E+00	0.00E+00	0.00E+00	0.00E+00	8.81E+03
29.81	0.00E+00	0.00E+00	0.00E+00	0.00E+00	5.88E+03
35.56	0.00E+00	0.00E+00	0.00E+00	0.00E+00	5.88E+03
42.43	0.00E+00	0.00E+00	0.00E+00	0.00E+00	0.00E+00
50.63	0.00E+00	0.00E+00	0.00E+00	0.00E+00	0.00E+00
60.41	0.00E+00	0.00E+00	0.00E+00	0.00E+00	0.00E+00
72.08	0.00E+00	0.00E+00	0.00E+00	0.00E+00	0.00E+00
86.00	0.00E+00	0.00E+00	0.00E+00	0.00E+00	0.00E+00
102.62	0.00E+00	0.00E+00	0.00E+00	0.00E+00	0.00E+00
122.44	0.00E+00	0.00E+00	0.00E+00	0.00E+00	0.00E+00





	15 min 15	20 min 20	25 min 25	30 min 30	45 min 45
dia.					
0.87	2.13E+05	1.52E+05	1.16E+05	7.85E+04	7.20E+04
1.04	1.16E+05	1.10E+05	8.99E+04	6.54E+04	4.73E+04
1.24	1.38E+05	1.52E+05	1.03E+05	8.18E+04	4.94E+04
1.48	2.05E+05	2.21E+05	1.22E+05	1.14E+05	7.20E+04
1.77	1.53E+05	1.45E+05	6.42E+04	7.85E+04	8.44E+04
2.11	1.64E+05	1.69E+05	1.12E+05	5.89E+04	4.94E+04
2.51	1.49E+05	1.10E+05	6.74E+04	4.91E+04	4.32E+04
3.00	1.12E+05	8.63E+04	7.06E+04	4.58E+04	2.68E+04
3.58	8.59E+04	6.91E+04	4.49E+04	4.25E+04	1.03E+04
4.27	6.35E+04	4.49E+04	3.21E+04	1.96E+04	1.03E+04
5.10	3.74E+04	5.18E+04	1.93E+04	3.27E+04	8.23E+03
6.08	2.61E+04	2.42E+04	9.63E+03	6.54E+03	1.44E+04
7.26	2.99E+04	3.45E+03	6.42E+03	0.00E+00	4.12E+03
8.66	2.99E+04	1.73E+04	9.63E+03	3.27E+03	2.06E+03
10.33	1.49E+04	1.73E+04	6.42E+03	6.54E+03	2.06E+03
12.33	2.24E+04	6.91E+03	9.63E+03	0.00E+00	0.00E+00
14.71	1.12E+04	3.45E+03	0.00E+00	0.00E+00	0.00E+00
17.55	1.12E+04	3.45E+03	3.21E+03	6.54E+03	4.12E+03
20.94	3.74E+03	3.45E+03	3.21E+03	3.27E+03	0.00E+00
24.98	1.12E+04	3.45E+03	0.00E+00	0.00E+00	2.06E+03
29.81	0.00E+00	0.00E+00	9.63E+03	0.00E+00	0.00E+00
35.56	0.00E+00	6.91E+03	0.00E+00	0.00E+00	2.06E+03
42.43	3.74E+03	0.00E+00	3.21E+03	9.81E+03	0.00E+00
50.63	0.00E+00	3.45E+03	3.21E+03	0.00E+00	2.06E+03
60.41	0.00E+00	0.00E+00	3.21E+03	0.00E+00	0.00E+00
72.08	0.00E+00	0.00E+00	6.42E+03	0.00E+00	2.06E+03
86.00	0.00E+00	0.00E+00	0.00E+00	6.54E+03	2.06E+03
102.62	0.00E+00	0.00E+00	0.00E+00	3.27E+03	0.00E+00
122.44	0.00E+00	0.00E+00	0.00E+00	0.00E+00	2.06E+03



	15 min 15	20 min 20	25 min 25	30 min 30	45 min 45
dia.					
0.87	1.94E+05	1.88E+05	1.17E+05	1.41E+05	7.62E+04
1.04	1.50E+05	1.01E+05	1.05E+05	9.81E+04	6.59E+04
1.24	1.81E+05	2.17E+05	1.29E+05	1.80E+05	6.59E+04
1.48	2.82E+05	1.74E+05	1.26E+05	1.54E+05	1.07E+05
1.77	2.16E+05	2.66E+05	1.20E+05	1.83E+05	7.20E+04
2.11	2.96E+05	1.88E+05	1.02E+05	1.18E+05	5.35E+04
2.51	2.56E+05	1.59E+05	9.59E+04	7.85E+04	4.73E+04
3.00	1.50E+05	1.21E+05	7.49E+04	6.21E+04	2.88E+04
3.58	6.62E+04	1.01E+05	2.70E+04	4.58E+04	8.23E+03
4.27	7.50E+04	5.31E+04	4.79E+04	1.64E+04	1.23E+04
5.10	5.30E+04	3.38E+04	2.40E+04	1.31E+04	6.17E+03
6.08	2.21E+04	1.93E+04	1.20E+04	6.54E+03	8.23E+03
7.26	4.41E+03	4.83E+03	1.20E+04	1.31E+04	2.06E+03
8.66	4.41E+03	0.00E+00	8.99E+03	6.54E+03	4.12E+03
10.33	8.83E+03	9.66E+03	3.00E+03	0.00E+00	0.00E+00
12.33	8.83E+03	0.00E+00	0.00E+00	0.00E+00	0.00E+00
14.71	4.41E+03	4.83E+03	0.00E+00	0.00E+00	0.00E+00
17.55	0.00E+00	4.83E+03	5.99E+03	0.00E+00	0.00E+00
20.94	4.41E+03	9.66E+03	0.00E+00	3.27E+03	0.00E+00
24.98	4.41E+03	4.83E+03	0.00E+00	0.00E+00	0.00E+00
29.81	0.00E+00	0.00E+00	3.00E+03	0.00E+00	0.00E+00
35.56	4.41E+03	0.00E+00	3.00E+03	6.54E+03	0.00E+00
42.43	0.00E+00	0.00E+00	3.00E+03	3.27E+03	2.06E+03
50.63	0.00E+00	4.83E+03	5.99E+03	0.00E+00	0.00E+00
60.41	0.00E+00	0.00E+00	0.00E+00	3.27E+03	4.12E+03
72.08	0.00E+00	4.83E+03	0.00E+00	0.00E+00	2.06E+03
86.00	0.00E+00	0.00E+00	3.00E+03	0.00E+00	0.00E+00
102.62	0.00E+00	0.00E+00	0.00E+00	0.00E+00	0.00E+00
122.44	0.00E+00	0.00E+00	0.00E+00	6.57E+03	0.00E+00

02/01/88

Time----->

homog 0 min 1 min 3 min 5 min 10 min

dia.

0.87	6.38E+05	4.73E+05	4.09E+05	4.15E+05	3.62E+05	3.68E+05
1.04	7.87E+05	4.90E+05	4.47E+05	4.71E+05	2.81E+05	3.77E+05
1.24	6.78E+05	4.73E+05	4.79E+05	5.00E+05	4.29E+05	4.36E+05
1.48	1.00E+06	7.81E+05	6.96E+05	7.18E+05	6.70E+05	6.47E+05
1.77	8.04E+05	6.90E+05	6.96E+05	5.95E+05	5.31E+05	5.78E+05
2.11	6.84E+05	6.27E+05	6.25E+05	6.12E+05	5.58E+05	5.24E+05
2.51	4.94E+05	4.68E+05	4.14E+05	4.71E+05	4.51E+05	4.51E+05
3.00	3.56E+05	3.36E+05	3.10E+05	2.97E+05	3.21E+05	3.19E+05
3.58	2.13E+05	2.22E+05	1.50E+05	1.40E+05	9.82E+04	2.40E+05
4.27	1.09E+05	5.13E+04	7.99E+04	4.49E+04	6.25E+04	1.13E+05
5.10	4.60E+04	2.28E+04	2.82E+04	1.68E+04	6.25E+04	3.43E+04
6.08	2.30E+04	0.00E+00	9.40E+03	1.12E+04	2.23E+04	1.96E+04
7.26	5.74E+03	5.70E+03	0.00E+00	0.00E+00	1.34E+04	9.80E+03
8.66	0.00E+00	5.70E+03	0.00E+00	0.00E+00	0.00E+00	1.47E+04
10.33	5.74E+03	0.00E+00	0.00E+00	0.00E+00	0.00E+00	0.00E+00
12.33	0.00E+00	1.14E+04	4.70E+03	0.00E+00	0.00E+00	0.00E+00
14.71	0.00E+00	0.00E+00	0.00E+00	0.00E+00	0.00E+00	0.00E+00
17.55	0.00E+00	0.00E+00	0.00E+00	0.00E+00	0.00E+00	0.00E+00
20.94	0.00E+00	0.00E+00	0.00E+00	0.00E+00	0.00E+00	0.00E+00
24.98	0.00E+00	0.00E+00	0.00E+00	0.00E+00	0.00E+00	0.00E+00
29.81	0.00E+00	0.00E+00	0.00E+00	0.00E+00	0.00E+00	0.00E+00
35.56	0.00E+00	0.00E+00	0.00E+00	0.00E+00	0.00E+00	0.00E+00
42.43	0.00E+00	0.00E+00	0.00E+00	0.00E+00	0.00E+00	0.00E+00
50.63	0.00E+00	0.00E+00	0.00E+00	0.00E+00	0.00E+00	0.00E+00
60.41	0.00E+00	0.00E+00	0.00E+00	0.00E+00	0.00E+00	0.00E+00
72.08	0.00E+00	0.00E+00	0.00E+00	0.00E+00	0.00E+00	0.00E+00
86.00	0.00E+00	0.00E+00	0.00E+00	0.00E+00	0.00E+00	0.00E+00
102.62	0.00E+00	0.00E+00	0.00E+00	0.00E+00	0.00E+00	0.00E+00
122.44	0.00E+00	0.00E+00	0.00E+00	0.00E+00	0.00E+00	0.00E+00

	15 min 15	20 min 20	25 min 25	30 min 30	45 min 45
dia.					
0.87	3.40E+05	2.04E+05	9.97E+04	1.25E+05	8.23E+04
1.04	2.96E+05	1.77E+05	6.98E+04	1.46E+05	1.02E+05
1.24	3.13E+05	4.13E+05	2.89E+05	1.58E+05	1.86E+05
1.48	4.15E+05	3.92E+05	2.69E+05	1.91E+05	2.23E+05
1.77	3.67E+05	3.97E+05	2.04E+05	2.66E+05	1.33E+05
2.11	4.04E+05	3.81E+05	2.44E+05	1.91E+05	1.40E+05
2.51	2.86E+05	3.33E+05	2.74E+05	2.16E+05	7.50E+04
3.00	2.75E+05	2.04E+05	1.60E+05	1.12E+05	8.23E+04
3.58	1.08E+05	1.13E+05	9.47E+04	5.82E+04	3.39E+04
4.27	1.46E+05	6.97E+04	4.99E+04	4.99E+04	2.42E+04
5.10	7.01E+04	4.83E+04	3.49E+04	3.74E+04	7.26E+03
6.08	2.16E+04	2.15E+04	3.49E+04	2.50E+04	7.26E+03
7.26	2.69E+04	2.15E+04	1.50E+04	4.16E+03	9.68E+03
8.66	2.16E+04	1.07E+04	1.99E+04	8.32E+03	0.00E+00
10.33	1.08E+04	1.07E+04	4.99E+03	8.32E+03	0.00E+00
12.33	5.39E+03	2.15E+04	9.97E+03	4.16E+03	4.84E+03
14.71	5.39E+03	0.00E+00	4.99E+03	1.25E+04	2.42E+03
17.55	0.00E+00	5.36E+03	4.99E+03	0.00E+00	2.42E+03
20.94	0.00E+00	5.36E+03	0.00E+00	4.16E+03	2.42E+03
24.98	0.00E+00	0.00E+00	0.00E+00	8.32E+03	4.84E+03
29.81	0.00E+00	0.00E+00	4.99E+03	4.16E+03	2.42E+03
35.56	0.00E+00	5.36E+03	0.00E+00	4.16E+03	0.00E+00
42.43	0.00E+00	0.00E+00	0.00E+00	0.00E+00	0.00E+00
50.63	0.00E+00	0.00E+00	0.00E+00	4.16E+03	4.84E+03
60.41	0.00E+00	0.00E+00	0.00E+00	0.00E+00	0.00E+00
72.08	0.00E+00	0.00E+00	0.00E+00	0.00E+00	2.42E+03
86.00	0.00E+00	0.00E+00	0.00E+00	0.00E+00	0.00E+00
102.62	0.00E+00	0.00E+00	0.00E+00	0.00E+00	0.00E+00
122.44	0.00E+00	0.00E+00	0.00E+00	0.00E+00	0.00E+00



	15 min 15	20 min 20	25 min 25	30 min 30	45 min 45
dia.					
0.87	2.91E+05	1.84E+05	1.55E+05	8.74E+04	7.93E+04
1.04	2.29E+05	1.41E+05	1.35E+05	1.25E+05	6.17E+04
1.24	3.49E+05	2.68E+05	2.61E+05	1.66E+05	1.62E+05
1.48	4.72E+05	3.91E+05	2.65E+05	2.37E+05	1.44E+05
1.77	3.93E+05	2.64E+05	2.73E+05	2.16E+05	1.53E+05
2.11	4.32E+05	3.47E+05	3.06E+05	2.00E+05	1.53E+05
2.51	3.57E+05	2.24E+05	1.88E+05	1.66E+05	6.46E+04
3.00	2.03E+05	2.33E+05	1.31E+05	1.21E+05	6.17E+04
3.58	1.10E+05	1.14E+05	4.90E+04	3.74E+04	3.23E+04
4.27	6.62E+04	7.47E+04	2.86E+04	3.74E+04	1.76E+04
5.10	8.38E+04	5.71E+04	2.45E+04	3.33E+04	8.81E+03
6.08	4.85E+04	2.64E+04	8.16E+03	8.32E+03	1.18E+04
7.26	1.32E+04	1.76E+04	1.22E+04	2.50E+04	5.88E+03
8.66	1.32E+04	4.39E+03	8.16E+03	8.32E+03	1.76E+04
10.33	0.00E+00	2.20E+04	0.00E+00	4.16E+03	2.94E+03
12.33	4.41E+03	4.39E+03	2.04E+04	8.32E+03	2.94E+03
14.71	4.41E+03	0.00E+00	4.08E+03	8.32E+03	5.88E+03
17.55	0.00E+00	0.00E+00	1.63E+04	1.25E+04	0.00E+00
20.94	4.41E+03	8.78E+03	8.16E+03	0.00E+00	5.88E+03
24.98	0.00E+00	0.00E+00	4.08E+03	4.16E+03	8.81E+03
29.81	0.00E+00	0.00E+00	4.08E+03	0.00E+00	8.81E+03
35.56	0.00E+00	0.00E+00	0.00E+00	4.16E+03	0.00E+00
42.43	0.00E+00	0.00E+00	0.00E+00	1.25E+04	0.00E+00
50.63	0.00E+00	0.00E+00	0.00E+00	0.00E+00	0.00E+00
60.41	0.00E+00	0.00E+00	0.00E+00	0.00E+00	2.94E+03
72.08	0.00E+00	0.00E+00	0.00E+00	0.00E+00	0.00E+00
86.00	0.00E+00	0.00E+00	0.00E+00	0.00E+00	0.00E+00
102.62	0.00E+00	0.00E+00	0.00E+00	0.00E+00	0.00E+00
122.44	0.00E+00	0.00E+00	0.00E+00	0.00E+00	0.00E+00





	15 min 15	20 min 20	25 min 25	30 min 30	45 min 45
dia.					
0.87	1.72E+05	9.66E+04	2.07E+04	3.60E+04	3.72E+04
1.04	1.19E+05	1.19E+05	4.49E+04	2.62E+04	4.12E+04
1.24	2.29E+05	1.58E+05	1.11E+05	1.21E+05	5.49E+04
1.48	3.35E+05	1.58E+05	1.07E+05	1.14E+05	8.63E+04
1.77	2.74E+05	1.80E+05	7.95E+04	7.52E+04	6.86E+04
2.11	1.94E+05	1.58E+05	9.33E+04	1.11E+05	6.86E+04
2.51	1.94E+05	1.36E+05	1.00E+05	6.21E+04	4.90E+04
3.00	1.24E+05	7.47E+04	5.87E+04	4.25E+04	2.94E+04
3.58	9.27E+04	5.27E+04	3.80E+04	3.27E+04	1.57E+04
4.27	1.15E+05	2.20E+04	6.91E+03	1.64E+04	7.84E+03
5.10	4.41E+04	6.59E+04	1.38E+04	1.64E+04	5.88E+03
6.08	5.30E+04	2.64E+04	1.38E+04	9.81E+03	3.92E+03
7.26	3.09E+04	8.78E+03	6.91E+03	1.96E+04	0.00E+00
8.66	2.21E+04	8.78E+03	3.46E+03	9.81E+03	3.92E+03
10.33	1.77E+04	1.76E+04	1.38E+04	1.96E+04	5.88E+03
12.33	1.77E+04	0.00E+00	6.91E+03	6.54E+03	0.00E+00
14.71	0.00E+00	0.00E+00	6.91E+03	0.00E+00	0.00E+00
17.55	8.83E+03	4.39E+03	1.73E+04	1.96E+04	5.88E+03
20.94	0.00E+00	1.32E+04	3.46E+03	1.31E+04	1.96E+03
24.98	0.00E+00	0.00E+00	6.91E+03	6.54E+03	1.96E+03
29.81	0.00E+00	0.00E+00	3.46E+03	3.27E+03	1.96E+03
35.56	0.00E+00	0.00E+00	3.46E+03	3.27E+03	3.92E+03
42.43	0.00E+00	0.00E+00	0.00E+00	3.27E+03	1.96E+03
50.63	0.00E+00	0.00E+00	0.00E+00	0.00E+00	0.00E+00
60.41	0.00E+00	0.00E+00	0.00E+00	3.27E+03	0.00E+00
72.08	0.00E+00	0.00E+00	0.00E+00	3.27E+03	1.96E+03
86.00	0.00E+00	0.00E+00	0.00E+00	0.00E+00	0.00E+00
102.62	0.00E+00	0.00E+00	0.00E+00	0.00E+00	0.00E+00
122.44	0.00E+00	0.00E+00	0.00E+00	0.00E+00	0.00E+00



	15 min 15	20 min 20	25 min 25	30 min 30
dia.				
0.87	3.76E+05	1.88E+05	1.68E+05	1.18E+05
1.04	2.71E+05	1.23E+05	1.68E+05	1.30E+05
1.24	3.62E+05	1.72E+05	1.80E+05	1.49E+05
1.48	4.45E+05	2.58E+05	1.68E+05	2.02E+05
1.77	4.03E+05	2.52E+05	1.50E+05	1.22E+05
2.11	3.13E+05	2.25E+05	1.27E+05	1.07E+05
2.51	2.29E+05	1.77E+05	9.36E+04	1.03E+05
3.00	1.39E+05	1.29E+05	7.86E+04	6.10E+04
3.58	1.74E+05	6.97E+04	4.49E+04	2.67E+04
4.27	9.74E+04	4.83E+04	3.74E+04	2.29E+04
5.10	4.17E+04	1.61E+04	1.87E+04	1.14E+04
6.08	2.09E+04	1.07E+04	0.00E+00	1.14E+04
7.26	6.95E+03	1.07E+04	1.12E+04	3.81E+03
8.66	4.87E+04	1.07E+04	1.12E+04	7.63E+03
10.33	2.09E+04	1.07E+04	3.74E+03	7.63E+03
12.33	6.95E+03	0.00E+00	3.74E+03	0.00E+00
14.71	6.95E+03	1.07E+04	3.74E+03	3.81E+03
17.55	1.39E+04	5.36E+03	0.00E+00	3.81E+03
20.94	6.95E+03	5.36E+03	0.00E+00	3.81E+03
24.98	6.95E+03	0.00E+00	0.00E+00	0.00E+00
29.81	6.95E+03	0.00E+00	3.74E+03	3.81E+03
35.56	6.95E+03	5.36E+03	0.00E+00	0.00E+00
42.43	0.00E+00	0.00E+00	0.00E+00	0.00E+00
50.63	0.00E+00	0.00E+00	0.00E+00	0.00E+00
60.41	0.00E+00	0.00E+00	0.00E+00	0.00E+00
72.08	0.00E+00	0.00E+00	0.00E+00	0.00E+00
86.00	0.00E+00	0.00E+00	0.00E+00	0.00E+00
102.62	0.00E+00	0.00E+00	0.00E+00	0.00E+00
122.44	0.00E+00	0.00E+00	0.00E+00	0.00E+00

11/03/87

Time-----&gt;

	homog	0 min	1 min	3 min	5 min
dia.	-1	0	1	3	5
0.87	6.51E+05	3.02E+05	3.82E+05	4.07E+05	3.29E+05
1.04	6.64E+05	3.64E+05	3.49E+05	4.03E+05	2.70E+05
1.24	7.24E+05	4.59E+05	4.31E+05	4.88E+05	4.97E+05
1.48	8.98E+05	6.33E+05	5.92E+05	6.02E+05	6.03E+05
1.77	8.25E+05	5.87E+05	5.85E+05	5.49E+05	4.24E+05
2.11	7.65E+05	5.83E+05	4.46E+05	5.01E+05	4.24E+05
2.51	4.12E+05	4.38E+05	3.22E+05	4.11E+05	2.67E+05
3.00	1.92E+05	2.48E+05	2.55E+05	2.56E+05	1.68E+05
3.58	1.10E+05	1.57E+05	1.65E+05	1.10E+05	6.58E+04
4.27	4.12E+04	6.62E+04	5.62E+04	9.77E+04	7.31E+04
5.10	1.37E+04	4.14E+04	4.87E+04	6.11E+04	2.19E+04
6.08	1.83E+04	3.31E+04	1.87E+04	3.26E+04	1.83E+04
7.26	1.37E+04	2.48E+04	1.87E+04	2.04E+04	2.19E+04
8.66	0.00E+00	0.00E+00	7.50E+03	2.04E+04	1.10E+04
10.33	4.58E+03	4.14E+03	3.75E+03	0.00E+00	7.31E+03
12.33	0.00E+00	4.14E+03	0.00E+00	0.00E+00	0.00E+00
14.71	0.00E+00	4.14E+03	0.00E+00	0.00E+00	1.46E+04
17.55	0.00E+00	0.00E+00	0.00E+00	4.07E+03	3.66E+03
20.94	0.00E+00	0.00E+00	0.00E+00	0.00E+00	0.00E+00
24.98	0.00E+00	0.00E+00	0.00E+00	0.00E+00	0.00E+00
29.81	0.00E+00	0.00E+00	0.00E+00	0.00E+00	0.00E+00
35.56	0.00E+00	0.00E+00	0.00E+00	0.00E+00	0.00E+00
42.43	0.00E+00	0.00E+00	0.00E+00	0.00E+00	0.00E+00
50.63	0.00E+00	0.00E+00	0.00E+00	0.00E+00	0.00E+00
60.41	0.00E+00	0.00E+00	0.00E+00	0.00E+00	0.00E+00
72.08	0.00E+00	0.00E+00	0.00E+00	0.00E+00	0.00E+00
86.00	0.00E+00	0.00E+00	0.00E+00	0.00E+00	0.00E+00
102.62	0.00E+00	0.00E+00	0.00E+00	0.00E+00	0.00E+00
122.44	0.00E+00	0.00E+00	0.00E+00	0.00E+00	0.00E+00

	15 min 15	20 min 20	25 min 25	30 min 30
dia.				
0.87	2.22E+05	1.65E+05	1.48E+05	1.27E+05
1.04	2.19E+05	1.51E+05	1.11E+05	1.10E+05
1.24	2.52E+05	1.91E+05	1.22E+05	1.16E+05
1.48	3.16E+05	2.25E+05	1.43E+05	1.94E+05
1.77	2.67E+05	2.19E+05	1.30E+05	1.43E+05
2.11	2.49E+05	2.02E+05	1.00E+05	1.08E+05
2.51	1.85E+05	1.11E+05	9.52E+04	7.01E+04
3.00	1.09E+05	9.96E+04	8.46E+04	4.85E+04
3.58	5.47E+04	5.12E+04	4.49E+04	4.31E+04
4.27	6.98E+04	2.28E+04	3.70E+04	1.89E+04
5.10	3.34E+04	2.28E+04	2.12E+04	1.62E+04
6.08	3.04E+04	1.99E+04	1.32E+04	8.08E+03
7.26	1.21E+04	1.14E+04	7.93E+03	0.00E+00
8.66	3.64E+04	1.14E+04	1.06E+04	5.39E+03
10.33	1.21E+04	5.69E+03	0.00E+00	2.69E+03
12.33	6.07E+03	8.53E+03	5.29E+03	2.69E+03
14.71	6.07E+03	0.00E+00	2.64E+03	5.39E+03
17.55	3.04E+03	2.84E+03	2.64E+03	5.39E+03
20.94	6.07E+03	2.84E+03	2.64E+03	0.00E+00
24.98	3.04E+03	8.53E+03	0.00E+00	0.00E+00
29.81	6.07E+03	0.00E+00	2.64E+03	0.00E+00
35.56	3.04E+03	2.84E+03	2.64E+03	0.00E+00
42.43	0.00E+00	8.53E+03	5.29E+03	0.00E+00
50.63	0.00E+00	0.00E+00	7.93E+03	0.00E+00
60.41	0.00E+00	0.00E+00	0.00E+00	2.69E+03
72.08	0.00E+00	0.00E+00	0.00E+00	5.39E+03
86.00	0.00E+00	0.00E+00	2.64E+03	2.69E+03
102.62	0.00E+00	0.00E+00	0.00E+00	0.00E+00
122.44	0.00E+00	0.00E+00	0.00E+00	0.00E+00



	15 min 15	20 min 20	25 min 25	30 min 30
dia.				
0.87	4.62E+05	2.42E+05	2.08E+05	1.47E+05
1.04	4.56E+05	2.60E+05	2.00E+05	1.44E+05
1.24	5.42E+05	2.79E+05	2.16E+05	1.44E+05
1.48	6.15E+05	4.06E+05	2.53E+05	1.86E+05
1.77	5.48E+05	3.82E+05	1.96E+05	1.73E+05
2.11	4.44E+05	3.88E+05	1.22E+05	1.50E+05
2.51	3.83E+05	2.91E+05	1.06E+05	1.14E+05
3.00	2.43E+05	9.08E+04	1.18E+05	7.19E+04
3.58	7.91E+04	6.06E+04	5.31E+04	5.23E+04
4.27	7.91E+04	2.42E+04	3.27E+04	3.60E+04
5.10	9.13E+04	2.42E+04	2.45E+04	9.81E+03
6.08	9.74E+04	3.63E+04	8.16E+03	1.31E+04
7.26	4.87E+04	0.00E+00	4.08E+03	9.81E+03
8.66	1.83E+04	1.82E+04	1.22E+04	1.31E+04
10.33	3.04E+04	6.06E+03	4.08E+03	6.54E+03
12.33	3.65E+04	6.06E+03	0.00E+00	0.00E+00
14.71	1.22E+04	1.82E+04	0.00E+00	3.27E+03
17.55	0.00E+00	1.21E+04	0.00E+00	6.54E+03
20.94	1.22E+04	0.00E+00	4.08E+03	3.27E+03
24.98	0.00E+00	0.00E+00	0.00E+00	3.27E+03
29.81	0.00E+00	6.06E+03	4.08E+03	0.00E+00
35.56	0.00E+00	6.06E+03	0.00E+00	0.00E+00
42.43	0.00E+00	0.00E+00	0.00E+00	3.27E+03
50.63	0.00E+00	0.00E+00	0.00E+00	0.00E+00
60.41	0.00E+00	0.00E+00	0.00E+00	3.27E+03
72.08	0.00E+00	0.00E+00	4.08E+03	3.27E+03
86.00	0.00E+00	0.00E+00	0.00E+00	0.00E+00
102.62	0.00E+00	0.00E+00	0.00E+00	0.00E+00
122.44	0.00E+00	0.00E+00	0.00E+00	0.00E+00



11/05/87

Time-----&gt;

	homog	0 min	1 min	3 min	5 min
dia.	-1	0	1	3	5
0.87	5.67E+05	4.51E+05	4.81E+05	3.78E+05	2.79E+05
1.04	4.92E+05	4.47E+05	4.34E+05	3.78E+05	2.66E+05
1.24	6.96E+05	5.17E+05	5.03E+05	4.96E+05	3.03E+05
1.48	9.33E+05	7.36E+05	7.91E+05	5.50E+05	3.89E+05
1.77	7.33E+05	6.62E+05	6.41E+05	5.47E+05	3.19E+05
2.11	6.79E+05	6.12E+05	5.84E+05	5.18E+05	3.11E+05
2.51	3.79E+05	4.51E+05	3.91E+05	4.70E+05	2.20E+05
3.00	3.00E+05	2.81E+05	2.72E+05	2.53E+05	1.90E+05
3.58	9.17E+04	1.28E+05	1.66E+05	1.79E+05	1.48E+05
4.27	5.42E+04	1.03E+05	8.44E+04	1.15E+05	6.97E+04
5.10	2.50E+04	5.38E+04	2.19E+04	5.44E+04	4.02E+04
6.08	1.67E+04	3.31E+04	1.25E+04	3.52E+04	1.88E+04
7.26	1.25E+04	0.00E+00	3.13E+03	1.92E+04	2.15E+04
8.66	0.00E+00	8.27E+03	9.38E+03	9.60E+03	2.15E+04
10.33	0.00E+00	4.14E+03	9.38E+03	6.40E+03	1.88E+04
12.33	0.00E+00	0.00E+00	0.00E+00	6.40E+03	1.34E+04
14.71	0.00E+00	0.00E+00	3.13E+03	3.20E+03	1.07E+04
17.55	0.00E+00	0.00E+00	0.00E+00	0.00E+00	5.37E+03
20.94	0.00E+00	0.00E+00	0.00E+00	0.00E+00	0.00E+00
24.98	0.00E+00	0.00E+00	0.00E+00	0.00E+00	0.00E+00
29.81	0.00E+00	0.00E+00	0.00E+00	3.20E+03	0.00E+00
35.56	0.00E+00	0.00E+00	0.00E+00	0.00E+00	0.00E+00
42.43	0.00E+00	0.00E+00	0.00E+00	0.00E+00	0.00E+00
50.63	0.00E+00	0.00E+00	0.00E+00	0.00E+00	0.00E+00
60.41	0.00E+00	0.00E+00	0.00E+00	0.00E+00	0.00E+00
72.08	0.00E+00	0.00E+00	0.00E+00	0.00E+00	0.00E+00
86.00	0.00E+00	0.00E+00	0.00E+00	0.00E+00	0.00E+00
102.62	0.00E+00	0.00E+00	0.00E+00	0.00E+00	0.00E+00

	15 min	20 min	25 min	30 min
	15	20	25	30
dia.				
0.87	1.31E+05	1.05E+05	6.07E+04	6.26E+04
1.04	9.96E+04	7.52E+04	5.84E+04	7.78E+04
1.24	2.04E+05	1.07E+05	6.97E+04	8.24E+04
1.48	2.04E+05	1.10E+05	9.44E+04	9.92E+04
1.77	1.65E+05	6.72E+04	7.19E+04	7.63E+04
2.11	1.31E+05	9.40E+04	4.72E+04	3.66E+04
2.51	1.34E+05	6.18E+04	2.70E+04	5.19E+04
3.00	7.78E+04	4.03E+04	2.25E+04	1.98E+04
3.58	4.37E+04	4.03E+04	2.25E+04	1.83E+04
4.27	1.22E+04	2.15E+04	8.99E+03	9.16E+03
5.10	1.70E+04	2.69E+03	6.74E+03	1.22E+04
6.08	1.22E+04	2.69E+03	0.00E+00	3.05E+03
7.26	7.29E+03	8.06E+03	2.25E+03	1.53E+03
8.66	2.43E+03	0.00E+00	0.00E+00	1.53E+03
10.33	4.86E+03	5.37E+03	0.00E+00	0.00E+00
12.33	2.43E+03	2.69E+03	0.00E+00	0.00E+00
14.71	2.43E+03	2.69E+03	2.25E+03	0.00E+00
17.55	4.86E+03	5.37E+03	0.00E+00	0.00E+00
20.94	4.86E+03	0.00E+00	0.00E+00	0.00E+00
24.98	2.43E+03	1.07E+04	0.00E+00	0.00E+00
29.81	0.00E+00	2.69E+03	0.00E+00	3.05E+03
35.56	0.00E+00	0.00E+00	2.25E+03	6.11E+03
42.43	2.43E+03	0.00E+00	8.99E+03	3.05E+03
50.63	0.00E+00	0.00E+00	2.25E+03	1.53E+03
60.41	0.00E+00	0.00E+00	0.00E+00	0.00E+00
72.08	0.00E+00	0.00E+00	0.00E+00	1.53E+03
86.00	0.00E+00	0.00E+00	0.00E+00	0.00E+00
102.62	0.00E+00	0.00E+00	0.00E+00	1.53E+03



	15 min	20 min	25 min	30 min
dia.	15	20	25	30
0.87	1.33E+05	7.94E+04	5.70E+04	4.89E+04
1.04	8.95E+04	5.42E+04	6.74E+04	6.16E+04
1.24	1.41E+05	8.90E+04	5.87E+04	7.26E+04
1.48	1.69E+05	1.35E+05	1.09E+05	1.01E+05
1.77	1.46E+05	8.71E+04	5.87E+04	7.74E+04
2.11	1.05E+05	8.13E+04	6.39E+04	8.21E+04
2.51	8.44E+04	7.36E+04	3.97E+04	3.79E+04
3.00	4.35E+04	3.48E+04	2.07E+04	2.05E+04
3.58	3.32E+04	1.94E+04	1.38E+04	1.42E+04
4.27	2.05E+04	7.74E+03	8.64E+03	4.74E+03
5.10	2.30E+04	9.68E+03	8.64E+03	1.58E+03
6.08	1.02E+04	3.87E+03	5.18E+03	1.58E+03
7.26	7.67E+03	5.81E+03	1.73E+03	0.00E+00
8.66	2.56E+03	3.87E+03	1.73E+03	7.89E+03
10.33	2.56E+03	3.87E+03	0.00E+00	0.00E+00
12.33	2.56E+03	0.00E+00	1.73E+03	3.16E+03
14.71	0.00E+00	0.00E+00	1.73E+03	3.16E+03
17.55	7.67E+03	0.00E+00	0.00E+00	1.58E+03
20.94	0.00E+00	0.00E+00	0.00E+00	1.58E+03
24.98	0.00E+00	0.00E+00	0.00E+00	1.58E+03
29.81	2.56E+03	1.94E+03	1.73E+03	0.00E+00
35.56	0.00E+00	3.87E+03	5.18E+03	0.00E+00
42.43	5.12E+03	3.87E+03	0.00E+00	3.16E+03
50.63	0.00E+00	1.94E+03	1.73E+03	1.58E+03
60.41	0.00E+00	1.94E+03	1.73E+03	0.00E+00
72.08	0.00E+00	0.00E+00	0.00E+00	1.58E+03
86.00	0.00E+00	1.94E+03	0.00E+00	1.58E+03
102.62	0.00E+00	0.00E+00	0.00E+00	0.00E+00
122.44	0.00E+00	3.28E+03	0.00E+00	3.28E+03



	15 min 15	20 min 20	25 min 25	30 min 30
dia.				
0.87	1.53E+05	7.94E+04	5.30E+04	6.11E+04
1.04	1.40E+05	8.29E+04	5.62E+04	4.58E+04
1.24	1.53E+05	9.50E+04	8.02E+04	4.43E+04
1.48	1.73E+05	1.14E+05	8.99E+04	8.70E+04
1.77	1.65E+05	9.15E+04	5.94E+04	6.56E+04
2.11	1.46E+05	8.46E+04	6.58E+04	6.56E+04
2.51	1.09E+05	7.94E+04	3.85E+04	3.82E+04
3.00	6.07E+04	3.80E+04	2.41E+04	2.14E+04
3.58	3.47E+04	1.55E+04	2.25E+04	1.07E+04
4.27	3.30E+04	1.38E+04	1.28E+04	9.16E+03
5.10	2.60E+04	1.04E+04	1.60E+03	4.58E+03
6.08	5.20E+03	5.18E+03	0.00E+00	6.11E+03
7.26	1.04E+04	0.00E+00	3.21E+03	3.05E+03
8.66	1.04E+04	6.91E+03	0.00E+00	0.00E+00
10.33	6.94E+03	1.73E+03	0.00E+00	0.00E+00
12.33	3.47E+03	1.73E+03	0.00E+00	1.53E+03
14.71	3.47E+03	1.73E+03	1.60E+03	0.00E+00
17.55	3.47E+03	0.00E+00	0.00E+00	0.00E+00
20.94	5.20E+03	3.45E+03	0.00E+00	0.00E+00
24.98	3.47E+03	0.00E+00	1.60E+03	0.00E+00
29.81	1.73E+03	5.18E+03	0.00E+00	3.05E+03
35.56	3.47E+03	5.18E+03	0.00E+00	3.05E+03
42.43	0.00E+00	3.45E+03	1.60E+03	1.53E+03
50.63	0.00E+00	0.00E+00	0.00E+00	1.53E+03
60.41	0.00E+00	1.73E+03	1.60E+03	1.53E+03
72.08	0.00E+00	0.00E+00	0.00E+00	1.53E+03
86.00	0.00E+00	1.73E+03	1.60E+03	3.05E+03
102.62	0.00E+00	0.00E+00	0.00E+00	0.00E+00
122.44	0.00E+00	0.00E+00	0.00E+00	0.00E+00



	15 min 15	20 min 20	25 min 25	30 min 30	45 min 45
dia.					
0.87	3.66E+05	4.96E+05	3.78E+05	3.33E+05	2.70E+05
1.04	4.68E+05	4.08E+05	3.71E+05	2.87E+05	2.14E+05
1.24	5.52E+05	4.79E+05	5.28E+05	4.12E+05	2.88E+05
1.48	7.68E+05	6.41E+05	7.41E+05	6.49E+05	3.97E+05
1.77	7.10E+05	6.02E+05	5.69E+05	5.37E+05	3.50E+05
2.11	6.80E+05	6.85E+05	5.61E+05	4.66E+05	3.26E+05
2.51	4.85E+05	5.97E+05	3.93E+05	4.04E+05	2.53E+05
3.00	4.28E+05	4.35E+05	2.32E+05	2.08E+05	1.91E+05
3.58	1.68E+05	1.54E+05	1.05E+05	1.83E+05	7.64E+04
4.27	1.10E+05	1.58E+05	6.36E+04	9.15E+04	4.70E+04
5.10	5.30E+04	5.71E+04	3.74E+04	7.49E+04	2.35E+04
6.08	2.21E+04	2.20E+04	2.99E+04	3.74E+04	2.94E+04
7.26	2.21E+04	2.64E+04	2.25E+04	3.74E+04	8.81E+03
8.66	8.83E+03	8.78E+03	2.25E+04	1.25E+04	1.76E+04
10.33	0.00E+00	0.00E+00	1.12E+04	8.32E+03	2.06E+04
12.33	0.00E+00	0.00E+00	0.00E+00	8.32E+03	8.81E+03
14.71	0.00E+00	0.00E+00	0.00E+00	4.16E+03	2.94E+03
17.55	0.00E+00	0.00E+00	0.00E+00	8.32E+03	2.94E+03
20.94	0.00E+00	0.00E+00	0.00E+00	0.00E+00	2.94E+03
24.98	0.00E+00	0.00E+00	0.00E+00	0.00E+00	2.94E+03
29.81	0.00E+00	0.00E+00	0.00E+00	0.00E+00	2.94E+03
35.56	0.00E+00	0.00E+00	0.00E+00	0.00E+00	5.88E+03
42.43	0.00E+00	0.00E+00	0.00E+00	0.00E+00	0.00E+00
50.63	0.00E+00	0.00E+00	0.00E+00	0.00E+00	0.00E+00
60.41	0.00E+00	0.00E+00	0.00E+00	0.00E+00	0.00E+00
72.08	0.00E+00	0.00E+00	0.00E+00	0.00E+00	0.00E+00
86.00	0.00E+00	0.00E+00	0.00E+00	0.00E+00	0.00E+00
102.62	0.00E+00	0.00E+00	0.00E+00	0.00E+00	0.00E+00
122.44	0.00E+00	0.00E+00	0.00E+00	0.00E+00	0.00E+00



12/01/87

Time----->

homog	0 min	1 min	3 min	5 min	10 min
-1					

pla.

0.87	6.67E+05	6.16E+05	5.16E+05	6.07E+05	6.40E+05	5.49E+05
1.04	6.33E+05	7.07E+05	5.08E+05	6.76E+05	5.54E+05	5.69E+05
1.24	7.46E+05	8.13E+05	7.41E+05	7.81E+05	6.70E+05	8.04E+05
1.48	9.42E+05	1.10E+06	7.54E+05	9.79E+05	1.03E+06	1.01E+06
1.77	8.21E+05	9.19E+05	7.50E+05	9.40E+05	8.57E+05	8.23E+05
2.11	6.58E+05	7.27E+05	6.62E+05	7.51E+05	6.25E+05	6.96E+05
2.51	4.75E+05	5.15E+05	4.83E+05	3.63E+05	4.64E+05	3.97E+05
3.00	2.33E+05	2.42E+05	2.37E+05	2.73E+05	2.82E+05	2.45E+05
3.58	7.08E+04	1.11E+05	9.58E+04	1.34E+05	8.57E+04	8.82E+04
4.27	5.83E+04	2.53E+04	1.67E+04	4.97E+04	4.03E+04	5.39E+04
5.10	1.25E+04	5.05E+03	2.50E+04	2.49E+04	2.02E+04	4.41E+04
6.08	4.17E+03	1.01E+04	1.25E+04	1.49E+04	1.01E+04	4.90E+03
7.26	8.33E+03	0.00E+00	8.33E+03	0.00E+00	5.04E+03	9.80E+03
8.66	4.17E+03	5.05E+03	4.16E+03	0.00E+00	0.00E+00	0.00E+00
10.33	0.00E+00	0.00E+00	0.00E+00	0.00E+00	5.04E+03	0.00E+00
12.33	0.00E+00	0.00E+00	0.00E+00	0.00E+00	5.04E+03	0.00E+00
14.71	0.00E+00	0.00E+00	0.00E+00	0.00E+00	5.04E+03	0.00E+00
17.55	0.00E+00	0.00E+00	0.00E+00	0.00E+00	0.00E+00	0.00E+00
20.94	0.00E+00	0.00E+00	0.00E+00	0.00E+00	0.00E+00	0.00E+00
24.98	0.00E+00	0.00E+00	0.00E+00	0.00E+00	0.00E+00	0.00E+00
29.81	0.00E+00	0.00E+00	0.00E+00	0.00E+00	0.00E+00	0.00E+00
35.56	0.00E+00	0.00E+00	0.00E+00	0.00E+00	0.00E+00	0.00E+00
42.43	0.00E+00	0.00E+00	0.00E+00	0.00E+00	0.00E+00	0.00E+00
50.63	0.00E+00	0.00E+00	0.00E+00	0.00E+00	0.00E+00	0.00E+00
60.41	0.00E+00	0.00E+00	0.00E+00	0.00E+00	0.00E+00	0.00E+00
72.08	0.00E+00	0.00E+00	0.00E+00	0.00E+00	0.00E+00	0.00E+00
86.00	0.00E+00	0.00E+00	0.00E+00	0.00E+00	0.00E+00	0.00E+00
102.62	0.00E+00	0.00E+00	0.00E+00	0.00E+00	0.00E+00	0.00E+00
122.44	0.00E+00	0.00E+00	0.00E+00	0.00E+00	0.00E+00	0.00E+00

	15 min	20 min	25 min	30 min	45 min
	15	20	25	30	45
dia.					
0.87	5.11E+05	5.47E+05	4.54E+05	4.94E+05	3.33E+05
1.04	6.25E+05	6.17E+05	4.44E+05	4.53E+05	3.78E+05
1.24	6.41E+05	7.24E+05	5.78E+05	5.17E+05	4.27E+05
1.48	9.49E+05	9.28E+05	7.48E+05	6.68E+05	4.97E+05
1.77	6.90E+05	8.64E+05	7.13E+05	7.73E+05	5.59E+05
2.11	8.52E+05	8.32E+05	6.43E+05	6.68E+05	3.66E+05
2.51	6.49E+05	5.58E+05	4.24E+05	4.67E+05	3.04E+05
3.00	3.57E+05	2.74E+05	2.59E+05	3.02E+05	2.67E+05
3.58	1.87E+05	1.39E+05	1.30E+05	1.51E+05	1.44E+05
4.27	8.11E+04	8.58E+04	3.49E+04	8.23E+04	6.58E+04
5.10	2.43E+04	3.22E+04	3.99E+04	5.95E+04	3.29E+04
6.08	1.62E+04	2.68E+04	1.50E+04	2.29E+04	1.64E+04
7.26	8.11E+03	0.00E+00	1.50E+04	1.83E+04	3.29E+04
8.66	0.00E+00	1.61E+04	9.97E+03	4.57E+03	2.88E+04
10.33	0.00E+00	0.00E+00	4.99E+03	4.57E+03	1.64E+04
12.33	0.00E+00	0.00E+00	0.00E+00	0.00E+00	1.23E+04
14.71	0.00E+00	0.00E+00	0.00E+00	0.00E+00	4.11E+03
17.55	0.00E+00	0.00E+00	0.00E+00	0.00E+00	0.00E+00
20.94	0.00E+00	0.00E+00	0.00E+00	0.00E+00	4.11E+03
24.98	0.00E+00	0.00E+00	0.00E+00	0.00E+00	0.00E+00
29.81	0.00E+00	0.00E+00	0.00E+00	0.00E+00	0.00E+00
35.56	0.00E+00	0.00E+00	0.00E+00	0.00E+00	0.00E+00
42.43	0.00E+00	0.00E+00	0.00E+00	0.00E+00	0.00E+00
50.63	0.00E+00	0.00E+00	0.00E+00	0.00E+00	0.00E+00
60.41	0.00E+00	0.00E+00	0.00E+00	0.00E+00	0.00E+00
72.08	0.00E+00	0.00E+00	0.00E+00	0.00E+00	0.00E+00
86.00	0.00E+00	0.00E+00	0.00E+00	0.00E+00	0.00E+00
102.62	0.00E+00	0.00E+00	0.00E+00	0.00E+00	0.00E+00
122.44	0.00E+00	0.00E+00	0.00E+00	0.00E+00	0.00E+00



	15 min	20 min	25 min	30 min	45 min
	15	20	25	30	45
dia.					
0.87	5.29E+05	4.00E+05	3.27E+05	3.29E+05	2.39E+05
1.04	4.93E+05	4.12E+05	3.18E+05	3.12E+05	1.91E+05
1.24	4.56E+05	5.94E+05	3.92E+05	3.08E+05	2.28E+05
1.48	7.61E+05	6.54E+05	6.04E+05	5.08E+05	3.29E+05
1.77	7.42E+05	6.42E+05	4.53E+05	3.95E+05	3.06E+05
2.11	6.69E+05	6.72E+05	3.80E+05	4.87E+05	2.62E+05
2.51	5.42E+05	5.27E+05	3.14E+05	4.28E+05	2.47E+05
3.00	4.44E+05	3.69E+05	2.49E+05	2.79E+05	1.61E+05
3.58	2.13E+05	2.42E+05	2.00E+05	2.00E+05	1.27E+05
4.27	9.13E+04	1.51E+05	1.51E+05	1.37E+05	1.08E+05
5.10	8.52E+04	1.03E+05	7.76E+04	7.90E+04	5.61E+04
6.08	2.43E+04	3.63E+04	4.08E+04	7.07E+04	4.11E+04
7.26	1.83E+04	1.82E+04	2.04E+04	2.91E+04	4.86E+04
8.66	6.08E+03	2.42E+04	4.08E+03	4.16E+04	4.11E+04
10.33	0.00E+00	0.00E+00	1.22E+04	1.66E+04	1.49E+04
12.33	0.00E+00	0.00E+00	0.00E+00	4.16E+03	1.87E+04
14.71	0.00E+00	0.00E+00	0.00E+00	0.00E+00	3.74E+03
17.55	0.00E+00	0.00E+00	0.00E+00	0.00E+00	7.47E+03
20.94	0.00E+00	0.00E+00	0.00E+00	0.00E+00	0.00E+00
24.98	0.00E+00	0.00E+00	0.00E+00	0.00E+00	0.00E+00
29.81	0.00E+00	0.00E+00	0.00E+00	0.00E+00	0.00E+00
35.56	0.00E+00	0.00E+00	0.00E+00	0.00E+00	0.00E+00
42.43	0.00E+00	0.00E+00	0.00E+00	0.00E+00	0.00E+00
50.63	0.00E+00	0.00E+00	0.00E+00	0.00E+00	0.00E+00
60.41	0.00E+00	0.00E+00	0.00E+00	0.00E+00	0.00E+00
72.08	0.00E+00	0.00E+00	0.00E+00	0.00E+00	0.00E+00
86.00	0.00E+00	0.00E+00	0.00E+00	0.00E+00	0.00E+00
102.62	0.00E+00	0.00E+00	0.00E+00	0.00E+00	0.00E+00
122.44	0.00E+00	0.00E+00	0.00E+00	0.00E+00	0.00E+00



	15 min 15	20 min 20	25 min 25	30 min 30	45 min 45
dia.					
0.87	3.64E+05	3.73E+05	2.94E+05	2.70E+05	1.80E+05
1.04	3.64E+05	3.03E+05	3.22E+05	2.08E+05	1.83E+05
1.24	4.85E+05	4.44E+05	2.78E+05	3.54E+05	2.18E+05
1.48	7.18E+05	6.02E+05	4.69E+05	3.58E+05	2.21E+05
1.77	5.87E+05	4.83E+05	4.25E+05	3.87E+05	1.77E+05
2.11	6.65E+05	4.70E+05	3.96E+05	4.12E+05	2.09E+05
2.51	5.39E+05	4.08E+05	2.86E+05	2.95E+05	1.80E+05
3.00	4.61E+05	2.24E+05	2.08E+05	2.45E+05	1.33E+05
3.58	1.89E+05	1.54E+05	1.18E+05	1.46E+05	9.81E+04
4.27	1.21E+05	7.91E+04	8.57E+04	7.90E+04	5.38E+04
5.10	4.85E+04	5.71E+04	4.08E+04	8.32E+04	5.38E+04
6.08	1.46E+04	2.64E+04	2.04E+04	4.99E+04	2.53E+04
7.26	1.94E+04	2.20E+04	2.04E+04	2.50E+04	2.85E+04
8.66	0.00E+00	1.32E+04	1.22E+04	1.66E+04	2.21E+04
10.33	0.00E+00	4.39E+03	4.08E+03	8.32E+03	6.33E+03
12.33	0.00E+00	0.00E+00	0.00E+00	8.32E+03	2.21E+04
14.71	0.00E+00	8.78E+03	0.00E+00	0.00E+00	0.00E+00
17.55	0.00E+00	0.00E+00	0.00E+00	0.00E+00	9.49E+03
20.94	0.00E+00	0.00E+00	0.00E+00	0.00E+00	0.00E+00
24.98	0.00E+00	0.00E+00	0.00E+00	0.00E+00	0.00E+00
29.81	0.00E+00	0.00E+00	0.00E+00	0.00E+00	0.00E+00
35.56	0.00E+00	0.00E+00	0.00E+00	0.00E+00	0.00E+00
42.43	0.00E+00	0.00E+00	0.00E+00	0.00E+00	0.00E+00
50.63	0.00E+00	0.00E+00	0.00E+00	0.00E+00	0.00E+00
60.41	0.00E+00	0.00E+00	0.00E+00	0.00E+00	0.00E+00
72.08	0.00E+00	0.00E+00	0.00E+00	0.00E+00	0.00E+00
86.00	0.00E+00	0.00E+00	0.00E+00	0.00E+00	0.00E+00
102.62	0.00E+00	0.00E+00	0.00E+00	0.00E+00	0.00E+00
122.44	0.00E+00	0.00E+00	0.00E+00	0.00E+00	0.00E+00



	15 min 15	20 min 20	25 min 25	30 min 30	45 min 45
dia.					
0.87	4.19E+05	4.04E+05	2.69E+05	3.37E+05	1.67E+05
1.04	3.84E+05	4.35E+05	2.57E+05	2.58E+05	1.62E+05
1.24	4.50E+05	4.66E+05	3.55E+05	3.24E+05	1.85E+05
1.48	8.07E+05	5.80E+05	5.47E+05	3.83E+05	2.44E+05
1.77	6.13E+05	4.66E+05	4.69E+05	3.74E+05	1.79E+05
2.11	5.65E+05	4.13E+05	3.51E+05	4.24E+05	1.91E+05
2.51	4.24E+05	2.81E+05	2.69E+05	2.70E+05	9.70E+04
3.00	2.16E+05	1.84E+05	1.76E+05	1.62E+05	1.12E+05
3.58	1.46E+05	1.05E+05	4.90E+04	1.12E+05	4.70E+04
4.27	8.38E+04	9.22E+04	4.49E+04	4.99E+04	4.41E+04
5.10	6.18E+04	3.07E+04	2.04E+04	4.16E+04	2.06E+04
6.08	2.21E+04	1.76E+04	2.86E+04	5.41E+04	2.35E+04
7.26	4.41E+03	1.32E+04	1.63E+04	8.32E+03	1.47E+04
8.66	1.32E+04	8.78E+03	8.16E+03	1.66E+04	1.76E+04
10.33	4.41E+03	4.39E+03	4.08E+03	4.16E+03	1.18E+04
12.33	4.41E+03	0.00E+00	0.00E+00	8.32E+03	5.88E+03
14.71	0.00E+00	0.00E+00	0.00E+00	4.16E+03	2.94E+03
17.55	0.00E+00	0.00E+00	4.08E+03	0.00E+00	1.47E+04
20.94	0.00E+00	0.00E+00	0.00E+00	0.00E+00	2.94E+03
24.98	0.00E+00	0.00E+00	0.00E+00	0.00E+00	0.00E+00
29.81	0.00E+00	0.00E+00	0.00E+00	0.00E+00	2.94E+03
35.56	0.00E+00	0.00E+00	0.00E+00	0.00E+00	2.94E+03
42.43	0.00E+00	0.00E+00	0.00E+00	0.00E+00	0.00E+00
50.63	0.00E+00	0.00E+00	0.00E+00	0.00E+00	0.00E+00
60.41	0.00E+00	0.00E+00	0.00E+00	0.00E+00	0.00E+00
72.08	0.00E+00	0.00E+00	0.00E+00	0.00E+00	0.00E+00
86.00	0.00E+00	0.00E+00	0.00E+00	0.00E+00	0.00E+00
102.62	0.00E+00	0.00E+00	0.00E+00	0.00E+00	0.00E+00
122.44	0.00E+00	0.00E+00	0.00E+00	0.00E+00	0.00E+00





	15 min 15	20 min 20	25 min 25	30 min 30	45 min 45
dia.					
0.87	4.90E+05	4.92E+05	3.55E+05	3.36E+05	1.97E+05
1.04	5.44E+05	4.39E+05	3.80E+05	2.75E+05	2.77E+05
1.24	6.31E+05	5.62E+05	3.76E+05	3.85E+05	2.41E+05
1.48	7.65E+05	6.81E+05	5.76E+05	4.40E+05	3.37E+05
1.77	5.82E+05	5.80E+05	5.02E+05	4.03E+05	2.96E+05
2.11	5.23E+05	5.31E+05	4.82E+05	3.72E+05	2.08E+05
2.51	3.99E+05	4.26E+05	4.33E+05	2.14E+05	1.87E+05
3.00	2.91E+05	2.68E+05	2.65E+05	2.17E+05	1.37E+05
3.58	1.19E+05	1.27E+05	1.35E+05	1.10E+05	9.87E+04
4.27	7.01E+04	8.34E+04	7.76E+04	6.72E+04	7.13E+04
5.10	5.93E+04	5.27E+04	4.08E+04	3.97E+04	3.02E+04
6.08	1.08E+04	3.51E+04	1.22E+04	3.66E+04	2.47E+04
7.26	5.39E+03	8.78E+03	2.04E+04	2.14E+04	1.37E+04
8.66	0.00E+00	4.39E+03	4.08E+03	1.53E+04	1.10E+04
10.33	5.39E+03	4.39E+03	4.08E+03	1.53E+04	1.10E+04
12.33	0.00E+00	8.78E+03	1.22E+04	0.00E+00	1.10E+04
14.71	0.00E+00	0.00E+00	0.00E+00	0.00E+00	8.23E+03
17.55	0.00E+00	0.00E+00	0.00E+00	0.00E+00	8.23E+03
20.94	0.00E+00	0.00E+00	0.00E+00	3.05E+03	8.23E+03
24.98	0.00E+00	0.00E+00	0.00E+00	0.00E+00	2.74E+03
29.81	0.00E+00	0.00E+00	4.08E+03	3.05E+03	0.00E+00
35.56	0.00E+00	0.00E+00	0.00E+00	0.00E+00	0.00E+00
42.43	0.00E+00	0.00E+00	0.00E+00	0.00E+00	0.00E+00
50.63	0.00E+00	0.00E+00	0.00E+00	0.00E+00	0.00E+00
60.41	0.00E+00	0.00E+00	0.00E+00	0.00E+00	0.00E+00
72.08	0.00E+00	0.00E+00	0.00E+00	0.00E+00	0.00E+00
86.00	0.00E+00	0.00E+00	0.00E+00	0.00E+00	0.00E+00
102.62	0.00E+00	0.00E+00	0.00E+00	0.00E+00	0.00E+00
122.44	0.00E+00	0.00E+00	0.00E+00	0.00E+00	0.00E+00



	15 min 15	20 min 20	25 min 25	30 min 30	45 min 45
dia.					
0.87	4.85E+05	2.77E+05	2.37E+05	3.04E+05	8.52E+04
1.04	3.97E+05	3.12E+05	2.33E+05	3.20E+05	1.23E+05
1.24	5.12E+05	4.48E+05	3.14E+05	4.12E+05	9.70E+04
1.48	7.02E+05	5.71E+05	4.25E+05	4.45E+05	1.59E+05
1.77	5.82E+05	4.39E+05	2.86E+05	3.70E+05	1.65E+05
2.11	6.44E+05	4.74E+05	3.67E+05	3.66E+05	1.50E+05
2.51	5.38E+05	4.30E+05	2.69E+05	2.54E+05	8.23E+04
3.00	3.18E+05	2.90E+05	1.55E+05	1.54E+05	7.05E+04
3.58	1.41E+05	1.71E+05	1.02E+05	1.12E+05	4.11E+04
4.27	1.15E+05	1.10E+05	6.94E+04	4.16E+04	3.23E+04
5.10	7.06E+04	7.47E+04	4.08E+04	4.99E+04	1.18E+04
6.08	3.97E+04	3.07E+04	2.86E+04	1.66E+04	1.18E+04
7.26	2.21E+04	3.95E+04	2.04E+04	1.25E+04	1.76E+04
8.66	4.41E+03	1.76E+04	4.08E+03	1.25E+04	8.81E+03
10.33	1.32E+04	1.32E+04	8.16E+03	8.32E+03	5.88E+03
12.33	0.00E+00	4.39E+03	4.08E+03	8.32E+03	0.00E+00
14.71	0.00E+00	0.00E+00	4.08E+03	1.25E+04	5.88E+03
17.55	0.00E+00	0.00E+00	0.00E+00	1.66E+04	5.88E+03
20.94	0.00E+00	0.00E+00	0.00E+00	0.00E+00	5.88E+03
24.98	0.00E+00	0.00E+00	8.16E+03	4.16E+03	2.94E+03
29.81	0.00E+00	0.00E+00	0.00E+00	4.16E+03	8.81E+03
35.56	0.00E+00	0.00E+00	0.00E+00	0.00E+00	0.00E+00
42.43	0.00E+00	0.00E+00	0.00E+00	0.00E+00	0.00E+00
50.63	0.00E+00	0.00E+00	0.00E+00	0.00E+00	0.00E+00
60.41	0.00E+00	0.00E+00	0.00E+00	0.00E+00	0.00E+00
72.08	0.00E+00	0.00E+00	0.00E+00	0.00E+00	0.00E+00
86.00	0.00E+00	0.00E+00	0.00E+00	0.00E+00	0.00E+00
102.62	0.00E+00	0.00E+00	0.00E+00	0.00E+00	0.00E+00
122.44	0.00E+00	0.00E+00	0.00E+00	0.00E+00	0.00E+00

12/22/87

Time----->

homog -1  
0 min 0  
1 min 1  
3 min 3  
5 min 5  
10 min 10

dia.

0.87	6.21E+05	5.91E+05	5.69E+05	4.52E+05	4.64E+05	4.73E+05
1.04	5.79E+05	5.29E+05	5.56E+05	5.05E+05	4.75E+05	4.57E+05
1.24	6.33E+05	6.70E+05	6.24E+05	5.86E+05	6.32E+05	5.66E+05
1.48	7.67E+05	8.77E+05	8.69E+05	8.26E+05	8.22E+05	7.70E+05
1.77	7.17E+05	7.90E+05	7.30E+05	8.06E+05	6.32E+05	7.14E+05
2.11	6.12E+05	7.49E+05	5.52E+05	6.92E+05	5.45E+05	6.82E+05
2.51	2.75E+05	5.05E+05	3.85E+05	4.92E+05	3.36E+05	5.22E+05
3.00	1.37E+05	2.69E+05	1.94E+05	1.79E+05	2.23E+05	3.25E+05
3.58	5.83E+04	4.55E+04	7.50E+04	6.51E+04	8.77E+04	1.48E+05
4.27	2.50E+04	3.31E+04	1.70E+04	4.48E+04	3.29E+04	4.01E+04
5.10	2.08E+04	8.27E+03	1.02E+04	1.22E+04	2.19E+04	2.41E+04
6.08	4.17E+03	8.27E+03	1.36E+04	2.04E+04	3.66E+03	2.01E+04
7.26	0.00E+00	8.27E+03	3.41E+03	0.00E+00	7.31E+03	1.20E+04
8.66	4.17E+03	4.14E+03	0.00E+00	8.14E+03	3.66E+03	4.01E+03
10.33	0.00E+00	0.00E+00	3.41E+03	0.00E+00	1.10E+04	0.00E+00
12.33	0.00E+00	0.00E+00	0.00E+00	0.00E+00	3.66E+03	0.00E+00
14.71	0.00E+00	0.00E+00	0.00E+00	0.00E+00	3.66E+03	0.00E+00
17.55	0.00E+00	0.00E+00	0.00E+00	0.00E+00	0.00E+00	0.00E+00
20.94	0.00E+00	0.00E+00	0.00E+00	0.00E+00	3.66E+03	0.00E+00
24.98	0.00E+00	0.00E+00	0.00E+00	0.00E+00	0.00E+00	0.00E+00
29.81	0.00E+00	0.00E+00	0.00E+00	0.00E+00	0.00E+00	0.00E+00
35.56	0.00E+00	0.00E+00	0.00E+00	0.00E+00	0.00E+00	0.00E+00
42.43	0.00E+00	0.00E+00	0.00E+00	0.00E+00	0.00E+00	0.00E+00
50.63	0.00E+00	0.00E+00	0.00E+00	0.00E+00	0.00E+00	0.00E+00
60.41	0.00E+00	0.00E+00	0.00E+00	0.00E+00	0.00E+00	0.00E+00
72.08	0.00E+00	0.00E+00	0.00E+00	0.00E+00	0.00E+00	0.00E+00
86.00	0.00E+00	0.00E+00	0.00E+00	0.00E+00	0.00E+00	0.00E+00
102.62	0.00E+00	0.00E+00	0.00E+00	0.00E+00	0.00E+00	0.00E+00
122.44	0.00E+00	0.00E+00	0.00E+00	0.00E+00	0.00E+00	0.00E+00

	15 min 15	20 min 20	25 min 25	30 min 30	45 min 45
dia.					
0.87	3.31E+05	2.94E+05	2.04E+05	2.41E+05	1.38E+05
1.04	3.79E+05	2.50E+05	1.76E+05	2.25E+05	1.26E+05
1.24	4.77E+05	3.29E+05	2.29E+05	2.83E+05	1.47E+05
1.48	5.91E+05	4.79E+05	3.22E+05	3.70E+05	1.88E+05
1.77	6.22E+05	5.01E+05	2.78E+05	3.04E+05	1.53E+05
2.11	6.05E+05	5.45E+05	2.53E+05	3.16E+05	8.81E+04
2.51	4.10E+05	3.25E+05	1.96E+05	2.12E+05	8.81E+04
3.00	3.35E+05	2.37E+05	1.39E+05	2.29E+05	6.76E+04
3.58	1.90E+05	1.58E+05	8.16E+04	1.29E+05	2.94E+04
4.27	1.32E+05	1.32E+05	6.53E+04	9.57E+04	2.94E+04
5.10	4.85E+04	5.27E+04	2.45E+04	3.74E+04	1.76E+04
6.08	3.53E+04	3.51E+04	3.27E+04	1.66E+04	8.81E+03
7.26	2.65E+04	1.32E+04	2.04E+04	3.33E+04	1.18E+04
8.66	2.21E+04	8.78E+03	3.67E+04	1.25E+04	8.81E+03
10.33	8.83E+03	8.78E+03	1.22E+04	1.66E+04	5.88E+03
12.33	0.00E+00	1.32E+04	0.00E+00	8.32E+03	0.00E+00
14.71	0.00E+00	0.00E+00	1.22E+04	0.00E+00	8.81E+03
17.55	0.00E+00	4.39E+03	0.00E+00	1.66E+04	2.94E+03
20.94	0.00E+00	0.00E+00	0.00E+00	0.00E+00	2.94E+03
24.98	0.00E+00	0.00E+00	4.08E+03	0.00E+00	5.88E+03
29.81	0.00E+00	0.00E+00	0.00E+00	4.16E+03	0.00E+00
35.56	0.00E+00	0.00E+00	0.00E+00	0.00E+00	5.88E+03
42.43	0.00E+00	0.00E+00	0.00E+00	0.00E+00	0.00E+00
50.63	0.00E+00	0.00E+00	0.00E+00	0.00E+00	0.00E+00
60.41	0.00E+00	0.00E+00	0.00E+00	0.00E+00	0.00E+00
72.08	0.00E+00	0.00E+00	0.00E+00	0.00E+00	0.00E+00
86.00	0.00E+00	0.00E+00	0.00E+00	0.00E+00	0.00E+00
102.62	0.00E+00	0.00E+00	0.00E+00	0.00E+00	0.00E+00
122.44	0.00E+00	0.00E+00	0.00E+00	0.00E+00	0.00E+00



	15 min 15	20 min 20	25 min 25	30 min 30	45 min 45
dia.					
0.87	4.02E+05	3.25E+05	2.29E+05	2.45E+05	1.41E+05
1.04	3.66E+05	3.34E+05	2.49E+05	2.00E+05	1.29E+05
1.24	4.10E+05	3.78E+05	3.35E+05	3.00E+05	1.23E+05
1.48	5.65E+05	5.71E+05	3.10E+05	3.91E+05	1.70E+05
1.77	6.31E+05	4.08E+05	3.59E+05	3.29E+05	1.65E+05
2.11	5.38E+05	4.04E+05	3.71E+05	3.08E+05	1.26E+05
2.51	4.10E+05	4.17E+05	2.57E+05	2.25E+05	1.26E+05
3.00	2.38E+05	3.21E+05	2.20E+05	2.16E+05	7.64E+04
3.58	1.63E+05	1.32E+05	1.14E+05	1.16E+05	6.46E+04
4.27	1.06E+05	1.01E+05	1.14E+05	8.74E+04	2.06E+04
5.10	3.53E+04	7.91E+04	5.31E+04	7.90E+04	1.76E+04
6.08	3.09E+04	3.95E+04	4.49E+04	5.41E+04	1.76E+04
7.26	1.32E+04	3.07E+04	3.27E+04	5.41E+04	1.18E+04
8.66	8.83E+03	3.07E+04	2.04E+04	1.66E+04	1.18E+04
10.33	0.00E+00	1.32E+04	2.04E+04	1.25E+04	5.88E+03
12.33	0.00E+00	4.39E+03	8.16E+03	4.16E+04	2.94E+03
14.71	0.00E+00	8.78E+03	8.16E+03	4.58E+04	1.18E+04
17.55	0.00E+00	0.00E+00	8.16E+03	8.32E+03	1.18E+04
20.94	0.00E+00	0.00E+00	0.00E+00	8.32E+03	1.47E+04
24.98	0.00E+00	0.00E+00	0.00E+00	0.00E+00	1.18E+04
29.81	0.00E+00	0.00E+00	0.00E+00	4.16E+03	5.88E+03
35.56	0.00E+00	0.00E+00	0.00E+00	0.00E+00	8.81E+03
42.43	0.00E+00	0.00E+00	0.00E+00	0.00E+00	2.94E+03
50.63	0.00E+00	0.00E+00	0.00E+00	0.00E+00	0.00E+00
60.41	0.00E+00	0.00E+00	0.00E+00	0.00E+00	0.00E+00
72.08	0.00E+00	0.00E+00	0.00E+00	0.00E+00	0.00E+00
86.00	0.00E+00	0.00E+00	0.00E+00	0.00E+00	0.00E+00
102.62	0.00E+00	0.00E+00	0.00E+00	0.00E+00	0.00E+00
122.44	0.00E+00	0.00E+00	0.00E+00	0.00E+00	0.00E+00





	15 min 15	20 min 20	25 min 25	30 min 30	45 min 45
dia.					
0.87	3.18E+05	2.81E+05	1.92E+05	1.26E+05	1.04E+05
1.04	2.87E+05	1.71E+05	1.59E+05	1.03E+05	7.68E+04
1.24	4.19E+05	3.12E+05	1.96E+05	1.87E+05	9.05E+04
1.48	4.68E+05	4.35E+05	2.49E+05	2.33E+05	1.40E+05
1.77	3.75E+05	2.55E+05	1.96E+05	1.83E+05	8.78E+04
2.11	3.93E+05	3.03E+05	3.27E+05	2.10E+05	9.60E+04
2.51	3.75E+05	2.85E+05	1.35E+05	1.56E+05	1.12E+05
3.00	2.82E+05	2.68E+05	1.71E+05	1.03E+05	6.03E+04
3.58	1.50E+05	1.71E+05	1.06E+05	6.48E+04	7.95E+04
4.27	1.28E+05	1.23E+05	9.80E+04	5.34E+04	4.11E+04
5.10	4.85E+04	6.59E+04	4.49E+04	4.96E+04	3.84E+04
6.08	4.85E+04	7.91E+04	2.86E+04	4.20E+04	3.29E+04
7.26	2.21E+04	2.20E+04	2.45E+04	1.91E+04	2.19E+04
8.66	4.41E+03	3.07E+04	4.49E+04	4.20E+04	1.92E+04
10.33	0.00E+00	4.39E+03	1.22E+04	7.63E+03	1.92E+04
12.33	0.00E+00	0.00E+00	2.04E+04	2.67E+04	2.19E+04
14.71	4.41E+03	4.39E+03	0.00E+00	1.14E+04	1.10E+04
17.55	0.00E+00	0.00E+00	4.08E+03	7.63E+03	2.74E+03
20.94	0.00E+00	0.00E+00	4.08E+03	3.81E+03	0.00E+00
24.98	0.00E+00	0.00E+00	0.00E+00	3.81E+03	2.74E+03
29.81	4.41E+03	0.00E+00	0.00E+00	0.00E+00	2.74E+03
35.56	0.00E+00	0.00E+00	0.00E+00	0.00E+00	0.00E+00
42.43	0.00E+00	0.00E+00	0.00E+00	0.00E+00	2.74E+03
50.63	0.00E+00	0.00E+00	0.00E+00	0.00E+00	2.74E+03
60.41	0.00E+00	0.00E+00	0.00E+00	0.00E+00	0.00E+00
72.08	0.00E+00	0.00E+00	0.00E+00	0.00E+00	0.00E+00
86.00	0.00E+00	0.00E+00	0.00E+00	0.00E+00	0.00E+00
102.62	0.00E+00	0.00E+00	0.00E+00	0.00E+00	0.00E+00
122.44	0.00E+00	0.00E+00	0.00E+00	0.00E+00	0.00E+00



	15 min 15	20 min 20	25 min 25	30 min 30	45 min 45
dla.					
0.87	3.09E+05	1.93E+05	1.55E+05	1.79E+05	1.32E+05
1.04	2.07E+05	1.84E+05	1.63E+05	1.29E+05	1.18E+05
1.24	2.34E+05	2.50E+05	2.29E+05	1.21E+05	1.41E+05
1.48	3.97E+05	3.51E+05	2.73E+05	2.50E+05	1.53E+05
1.77	4.15E+05	2.77E+05	2.61E+05	1.41E+05	1.35E+05
2.11	3.31E+05	2.68E+05	2.20E+05	9.98E+04	1.03E+05
2.51	2.91E+05	1.49E+05	1.55E+05	9.15E+04	1.03E+05
3.00	1.77E+05	1.36E+05	1.02E+05	2.08E+04	2.35E+04
3.58	1.37E+05	7.03E+04	7.76E+04	3.33E+04	2.64E+04
4.27	6.62E+04	3.07E+04	2.45E+04	2.08E+04	2.64E+04
5.10	3.09E+04	2.20E+04	1.63E+04	1.66E+04	8.81E+03
6.08	2.65E+04	2.20E+04	1.22E+04	4.16E+03	5.88E+03
7.26	2.65E+04	1.76E+04	2.04E+04	0.00E+00	2.94E+03
8.66	1.77E+04	1.32E+04	8.16E+03	8.32E+03	8.81E+03
10.33	2.21E+04	8.78E+03	8.16E+03	0.00E+00	2.94E+03
12.33	8.83E+03	4.39E+03	1.63E+04	4.16E+03	0.00E+00
14.71	1.32E+04	1.32E+04	4.08E+03	0.00E+00	5.88E+03
17.55	4.41E+03	4.39E+03	1.22E+04	1.25E+04	5.88E+03
20.94	8.83E+03	4.39E+03	1.22E+04	8.32E+03	2.94E+03
24.98	0.00E+00	0.00E+00	4.08E+03	8.32E+03	5.88E+03
29.81	0.00E+00	8.78E+03	8.16E+03	4.16E+03	2.94E+03
35.56	0.00E+00	0.00E+00	4.08E+03	8.32E+03	2.94E+03
42.43	0.00E+00	0.00E+00	0.00E+00	0.00E+00	2.94E+03
50.63	0.00E+00	0.00E+00	0.00E+00	4.16E+03	2.94E+03
60.41	0.00E+00	0.00E+00	0.00E+00	0.00E+00	5.88E+03
72.08	0.00E+00	0.00E+00	0.00E+00	0.00E+00	0.00E+00
86.00	0.00E+00	0.00E+00	0.00E+00	0.00E+00	0.00E+00
102.62	0.00E+00	0.00E+00	0.00E+00	0.00E+00	0.00E+00
122.44	0.00E+00	0.00E+00	0.00E+00	0.00E+00	0.00E+00



	15 min	20 min	25 min	30 min	45 min
dia.	15	20	25	30	45
0.87	2.34E+05	1.93E+05	1.02E+05	1.29E+05	1.06E+05
1.04	2.47E+05	1.76E+05	1.22E+05	1.21E+05	8.22E+04
1.24	2.07E+05	2.42E+05	1.14E+05	1.41E+05	1.34E+05
1.48	3.40E+05	2.46E+05	2.41E+05	1.83E+05	1.47E+05
1.77	3.18E+05	2.24E+05	1.55E+05	1.54E+05	9.59E+04
2.11	3.00E+05	2.28E+05	1.71E+05	1.41E+05	8.22E+04
2.51	1.99E+05	1.19E+05	6.94E+04	1.21E+05	1.13E+05
3.00	2.07E+05	1.49E+05	7.35E+04	4.99E+04	6.51E+04
3.58	1.06E+05	7.03E+04	6.12E+04	4.99E+04	4.80E+04
4.27	6.62E+04	5.71E+04	3.27E+04	4.16E+04	3.08E+04
5.10	3.53E+04	3.95E+04	2.45E+04	1.66E+04	2.40E+04
6.08	2.21E+04	2.20E+04	8.16E+03	8.32E+03	1.37E+04
7.26	3.53E+04	2.20E+04	8.16E+03	2.50E+04	1.03E+04
8.66	2.21E+04	8.78E+03	8.16E+03	1.25E+04	1.37E+04
10.33	8.83E+03	1.76E+04	1.22E+04	2.50E+04	3.43E+03
12.33	8.83E+03	4.39E+03	4.08E+03	1.25E+04	1.03E+04
14.71	1.77E+04	8.78E+03	1.22E+04	4.16E+03	3.43E+03
17.55	4.41E+03	8.78E+03	4.08E+03	8.32E+03	3.43E+03
20.94	4.41E+03	1.76E+04	4.08E+03	1.66E+04	3.43E+03
24.98	0.00E+00	0.00E+00	0.00E+00	0.00E+00	6.85E+03
29.81	0.00E+00	0.00E+00	4.08E+03	4.16E+03	0.00E+00
35.56	0.00E+00	0.00E+00	0.00E+00	0.00E+00	0.00E+00
42.43	0.00E+00	0.00E+00	0.00E+00	4.16E+03	0.00E+00
50.63	0.00E+00	0.00E+00	0.00E+00	0.00E+00	0.00E+00
60.41	0.00E+00	0.00E+00	0.00E+00	0.00E+00	0.00E+00
72.08	0.00E+00	0.00E+00	0.00E+00	0.00E+00	0.00E+00
86.00	0.00E+00	0.00E+00	0.00E+00	0.00E+00	0.00E+00
102.62	0.00E+00	0.00E+00	0.00E+00	0.00E+00	0.00E+00
122.44	0.00E+00	0.00E+00	0.00E+00	0.00E+00	0.00E+00



	15 min 15	20 min 20	25 min 25	30 min 30	45 min 45
dia.					
0.87	6.18E+05	2.72E+05	2.25E+05	1.79E+05	1.44E+05
1.04	4.99E+05	2.59E+05	1.63E+05	2.08E+05	1.38E+05
1.24	6.31E+05	4.04E+05	2.33E+05	2.25E+05	1.35E+05
1.48	7.99E+05	4.88E+05	3.10E+05	2.50E+05	1.65E+05
1.77	6.66E+05	3.86E+05	2.65E+05	2.50E+05	1.62E+05
2.11	6.40E+05	4.57E+05	2.98E+05	2.50E+05	1.35E+05
2.51	4.24E+05	3.21E+05	2.49E+05	1.91E+05	9.70E+04
3.00	3.31E+05	3.25E+05	2.16E+05	1.75E+05	9.99E+04
3.58	1.99E+05	1.36E+05	1.10E+05	1.25E+05	6.46E+04
4.27	1.32E+05	1.19E+05	1.22E+05	5.82E+04	2.35E+04
5.10	5.30E+04	8.34E+04	4.49E+04	2.50E+04	2.64E+04
6.08	2.21E+04	3.51E+04	4.90E+04	5.82E+04	2.35E+04
7.26	1.32E+04	2.20E+04	3.67E+04	2.08E+04	1.18E+04
8.66	4.41E+03	1.76E+04	2.86E+04	3.33E+04	2.35E+04
10.33	4.41E+03	8.78E+03	2.04E+04	3.74E+04	1.18E+04
12.33	4.41E+03	4.39E+03	1.22E+04	1.66E+04	8.81E+03
14.71	4.41E+03	0.00E+00	0.00E+00	4.16E+03	1.47E+04
17.55	0.00E+00	4.39E+03	1.63E+04	4.16E+03	1.18E+04
20.94	0.00E+00	0.00E+00	0.00E+00	0.00E+00	2.94E+03
24.98	0.00E+00	0.00E+00	0.00E+00	0.00E+00	2.94E+03
29.81	0.00E+00	0.00E+00	0.00E+00	0.00E+00	5.88E+03
35.56	0.00E+00	0.00E+00	0.00E+00	0.00E+00	0.00E+00
42.43	0.00E+00	0.00E+00	0.00E+00	0.00E+00	0.00E+00
50.63	0.00E+00	0.00E+00	0.00E+00	0.00E+00	0.00E+00
60.41	0.00E+00	0.00E+00	0.00E+00	0.00E+00	0.00E+00
72.08	0.00E+00	0.00E+00	0.00E+00	0.00E+00	0.00E+00
86.00	0.00E+00	0.00E+00	0.00E+00	0.00E+00	0.00E+00
102.62	0.00E+00	0.00E+00	0.00E+00	0.00E+00	0.00E+00
122.44	0.00E+00	0.00E+00	0.00E+00	0.00E+00	0.00E+00





	15 min	20 min	25 min	30 min	45 min
dia.	15	20	25	30	45
0.87	2.47E+05	2.37E+05	1.76E+05	1.37E+05	1.26E+05
1.04	3.04E+05	2.59E+05	1.51E+05	1.18E+05	1.15E+05
1.24	2.87E+05	3.12E+05	2.25E+05	2.03E+05	1.41E+05
1.48	4.46E+05	3.07E+05	3.22E+05	2.85E+05	1.32E+05
1.77	3.66E+05	2.72E+05	1.76E+05	1.90E+05	1.26E+05
2.11	3.09E+05	2.24E+05	2.29E+05	1.41E+05	1.38E+05
2.51	3.62E+05	2.46E+05	2.00E+05	1.73E+05	6.17E+04
3.00	2.74E+05	1.98E+05	1.27E+05	1.08E+05	8.52E+04
3.58	1.59E+05	1.49E+05	7.76E+04	1.05E+05	6.17E+04
4.27	1.28E+05	1.19E+05	5.71E+04	8.50E+04	5.58E+04
5.10	1.01E+05	7.91E+04	7.76E+04	8.50E+04	3.82E+04
6.08	5.74E+04	1.76E+04	3.67E+04	3.92E+04	3.23E+04
7.26	3.53E+04	5.71E+04	1.63E+04	2.94E+04	2.35E+04
8.66	8.83E+03	2.20E+04	4.08E+03	1.31E+04	2.35E+04
10.33	1.32E+04	4.83E+04	1.22E+04	3.60E+04	1.76E+04
12.33	4.41E+03	8.78E+03	8.16E+03	2.62E+04	2.06E+04
14.71	0.00E+00	0.00E+00	1.22E+04	9.81E+03	8.81E+03
17.55	4.41E+03	0.00E+00	0.00E+00	0.00E+00	2.35E+04
20.94	0.00E+00	0.00E+00	0.00E+00	0.00E+00	0.00E+00
24.98	0.00E+00	0.00E+00	0.00E+00	0.00E+00	0.00E+00
29.81	0.00E+00	0.00E+00	4.08E+03	0.00E+00	5.88E+03
35.56	0.00E+00	0.00E+00	0.00E+00	0.00E+00	0.00E+00
42.43	0.00E+00	0.00E+00	0.00E+00	0.00E+00	0.00E+00
50.63	0.00E+00	0.00E+00	0.00E+00	0.00E+00	0.00E+00
60.41	0.00E+00	0.00E+00	0.00E+00	0.00E+00	0.00E+00
72.08	0.00E+00	0.00E+00	0.00E+00	0.00E+00	0.00E+00
86.00	0.00E+00	0.00E+00	0.00E+00	0.00E+00	0.00E+00
102.62	0.00E+00	0.00E+00	0.00E+00	0.00E+00	0.00E+00
122.44	0.00E+00	0.00E+00	0.00E+00	0.00E+00	0.00E+00

01/28/88

Time----->

homog	0 min	1 min	3 min	5 min	10 min
-1	0	1	3	5	10

dia.

0.87	6.03E+05	6.73E+05	5.45E+05	4.94E+05	4.89E+05	4.26E+05
1.04	5.40E+05	7.07E+05	5.78E+05	6.34E+05	3.88E+05	3.77E+05
1.24	7.98E+05	6.90E+05	7.00E+05	6.62E+05	5.49E+05	5.15E+05
1.48	8.85E+05	9.64E+05	8.13E+05	9.54E+05	8.77E+05	6.22E+05
1.77	7.93E+05	8.15E+05	7.62E+05	6.68E+05	6.91E+05	5.78E+05
2.11	5.69E+05	6.96E+05	6.25E+05	7.30E+05	5.90E+05	5.54E+05
2.51	3.16E+05	5.13E+05	3.95E+05	4.43E+05	4.59E+05	3.68E+05
3.00	1.61E+05	2.45E+05	1.65E+05	1.96E+05	2.22E+05	3.23E+05
3.58	1.15E+05	1.14E+05	9.40E+04	1.29E+05	1.26E+05	1.67E+05
4.27	4.60E+04	9.12E+04	4.70E+03	5.61E+04	9.07E+04	7.84E+04
5.10	3.45E+04	1.14E+04	2.35E+04	3.37E+04	3.53E+04	2.45E+04
6.08	0.00E+00	5.70E+03	0.00E+00	1.68E+04	2.52E+04	2.94E+04
7.26	0.00E+00	5.70E+03	0.00E+00	0.00E+00	5.04E+03	9.80E+03
8.66	0.00E+00	5.70E+03	0.00E+00	5.61E+03	0.00E+00	4.90E+03
10.33	0.00E+00	0.00E+00	0.00E+00	0.00E+00	0.00E+00	0.00E+00
12.33	0.00E+00	0.00E+00	0.00E+00	0.00E+00	0.00E+00	0.00E+00
14.71	0.00E+00	0.00E+00	0.00E+00	0.00E+00	0.00E+00	0.00E+00
17.55	0.00E+00	0.00E+00	0.00E+00	0.00E+00	0.00E+00	0.00E+00
20.94	0.00E+00	0.00E+00	0.00E+00	0.00E+00	0.00E+00	0.00E+00
24.98	0.00E+00	0.00E+00	0.00E+00	0.00E+00	0.00E+00	0.00E+00
29.81	0.00E+00	0.00E+00	0.00E+00	0.00E+00	0.00E+00	0.00E+00
35.56	0.00E+00	0.00E+00	0.00E+00	0.00E+00	0.00E+00	0.00E+00
42.43	0.00E+00	0.00E+00	0.00E+00	0.00E+00	0.00E+00	0.00E+00
50.63	0.00E+00	0.00E+00	0.00E+00	0.00E+00	0.00E+00	0.00E+00
60.41	0.00E+00	0.00E+00	0.00E+00	0.00E+00	0.00E+00	0.00E+00
72.08	0.00E+00	0.00E+00	0.00E+00	0.00E+00	0.00E+00	0.00E+00
86.00	0.00E+00	0.00E+00	0.00E+00	0.00E+00	0.00E+00	0.00E+00
102.62	0.00E+00	0.00E+00	0.00E+00	0.00E+00	0.00E+00	0.00E+00
122.44	0.00E+00	0.00E+00	0.00E+00	0.00E+00	0.00E+00	0.00E+00

	15 min 15	20 min 20	25 min 25	30 min 30	45 min 45
dia.					
0.87	3.18E+05	2.81E+05	1.92E+05	1.26E+05	1.04E+05
1.04	2.87E+05	1.71E+05	1.59E+05	1.03E+05	7.68E+04
1.24	4.19E+05	3.12E+05	1.96E+05	1.87E+05	9.05E+04
1.48	4.68E+05	4.35E+05	2.49E+05	2.33E+05	1.40E+05
1.77	3.75E+05	2.55E+05	1.96E+05	1.83E+05	8.78E+04
2.11	3.93E+05	3.03E+05	3.27E+05	2.10E+05	9.60E+04
2.51	3.75E+05	2.85E+05	1.35E+05	1.56E+05	1.12E+05
3.00	2.82E+05	2.68E+05	1.71E+05	1.03E+05	6.03E+04
3.58	1.50E+05	1.71E+05	1.06E+05	6.48E+04	7.95E+04
4.27	1.28E+05	1.23E+05	9.80E+04	5.34E+04	4.11E+04
5.10	4.85E+04	6.59E+04	4.49E+04	4.96E+04	3.84E+04
6.08	4.85E+04	7.91E+04	2.86E+04	4.20E+04	3.29E+04
7.26	2.21E+04	2.20E+04	2.45E+04	1.91E+04	2.19E+04
8.66	4.41E+03	3.07E+04	4.49E+04	4.20E+04	1.92E+04
10.33	0.00E+00	4.39E+03	1.22E+04	7.63E+03	1.92E+04
12.33	0.00E+00	0.00E+00	2.04E+04	2.67E+04	2.19E+04
14.71	4.41E+03	4.39E+03	0.00E+00	1.14E+04	1.10E+04
17.55	0.00E+00	0.00E+00	4.08E+03	7.63E+03	2.74E+03
20.94	0.00E+00	0.00E+00	4.08E+03	3.81E+03	0.00E+00
24.98	0.00E+00	0.00E+00	0.00E+00	3.81E+03	2.74E+03
29.81	4.41E+03	0.00E+00	0.00E+00	0.00E+00	2.74E+03
35.56	0.00E+00	0.00E+00	0.00E+00	0.00E+00	0.00E+00
42.43	0.00E+00	0.00E+00	0.00E+00	0.00E+00	2.74E+03
50.63	0.00E+00	0.00E+00	0.00E+00	0.00E+00	2.74E+03
60.41	0.00E+00	0.00E+00	0.00E+00	0.00E+00	0.00E+00
72.08	0.00E+00	0.00E+00	0.00E+00	0.00E+00	0.00E+00
86.00	0.00E+00	0.00E+00	0.00E+00	0.00E+00	0.00E+00
102.62	0.00E+00	0.00E+00	0.00E+00	0.00E+00	0.00E+00
122.44	0.00E+00	0.00E+00	0.00E+00	0.00E+00	0.00E+00



	15 min 15	20 min 20	25 min 25	30 min 30	45 min 45
dia.					
0.87	3.61E+05	2.04E+05	3.67E+04	1.53E+05	5.49E+04
1.04	2.96E+05	2.09E+05	5.71E+04	1.37E+05	5.21E+04
1.24	3.77E+05	3.00E+05	2.29E+05	2.36E+05	7.41E+04
1.48	4.90E+05	3.33E+05	2.29E+05	2.71E+05	1.01E+05
1.77	4.96E+05	3.54E+05	2.12E+05	2.02E+05	1.10E+05
2.11	4.20E+05	4.29E+05	2.69E+05	1.79E+05	1.12E+05
2.51	3.77E+05	4.13E+05	1.96E+05	1.91E+05	6.03E+04
3.00	2.59E+05	2.79E+05	1.22E+05	1.56E+05	4.39E+04
3.58	1.62E+05	1.45E+05	1.02E+05	1.07E+05	4.66E+04
4.27	8.08E+04	9.66E+04	8.16E+04	6.48E+04	3.02E+04
5.10	6.47E+04	6.97E+04	4.90E+04	4.20E+04	3.02E+04
6.08	2.16E+04	2.68E+04	4.90E+04	6.87E+04	1.65E+04
7.26	2.69E+04	3.22E+04	2.45E+04	2.29E+04	1.92E+04
8.66	5.39E+03	3.22E+04	2.04E+04	3.43E+04	1.37E+04
10.33	0.00E+00	5.36E+03	1.22E+04	2.29E+04	8.23E+03
12.33	1.08E+04	5.36E+03	1.63E+04	3.81E+04	1.65E+04
14.71	0.00E+00	0.00E+00	1.22E+04	7.63E+03	1.10E+04
17.55	1.62E+04	5.36E+03	1.63E+04	7.63E+03	1.10E+04
20.94	2.16E+04	2.68E+04	2.04E+04	3.81E+03	0.00E+00
24.98	0.00E+00	0.00E+00	0.00E+00	0.00E+00	5.49E+03
29.81	0.00E+00	0.00E+00	0.00E+00	0.00E+00	2.74E+03
35.56	0.00E+00	0.00E+00	0.00E+00	3.81E+03	0.00E+00
42.43	0.00E+00	0.00E+00	0.00E+00	0.00E+00	0.00E+00
50.63	0.00E+00	0.00E+00	0.00E+00	0.00E+00	0.00E+00
60.41	0.00E+00	0.00E+00	0.00E+00	0.00E+00	0.00E+00
72.08	0.00E+00	0.00E+00	0.00E+00	0.00E+00	0.00E+00
86.00	0.00E+00	0.00E+00	0.00E+00	0.00E+00	0.00E+00
102.62	0.00E+00	0.00E+00	0.00E+00	0.00E+00	0.00E+00
122.44	0.00E+00	0.00E+00	0.00E+00	0.00E+00	0.00E+00

06/23/88

Time-----&gt;

	homog	0 min	3 min	5 min	10 min
dia.	-1	0	3	5	10
0.87	6.96E+05	4.82E+05	4.03E+05	4.11E+05	2.94E+05
1.04	5.91E+05	5.28E+05	3.68E+05	3.53E+05	2.11E+05
1.24	9.78E+05	6.39E+05	5.72E+05	4.87E+05	4.21E+05
1.48	1.08E+06	1.06E+06	8.05E+05	5.54E+05	4.85E+05
1.77	8.86E+05	8.80E+05	5.47E+05	4.69E+05	3.48E+05
2.11	6.76E+05	6.91E+05	5.42E+05	5.85E+05	4.26E+05
2.51	4.14E+05	4.89E+05	3.03E+05	4.78E+05	3.33E+05
3.00	2.95E+05	3.65E+05	2.39E+05	2.86E+05	2.45E+05
3.58	8.53E+04	1.37E+05	1.09E+05	1.34E+05	1.76E+05
4.27	6.57E+04	1.17E+05	7.46E+04	1.29E+05	1.23E+05
5.10	2.63E+04	2.61E+04	2.98E+04	5.36E+04	7.35E+04
6.08	1.31E+04	2.61E+04	4.97E+03	3.13E+04	7.35E+04
7.26	0.00E+00	6.52E+03	1.49E+04	1.79E+04	2.45E+04
8.66	6.57E+03	0.00E+00	0.00E+00	4.46E+03	1.96E+04
10.33	6.57E+03	0.00E+00	0.00E+00	4.46E+03	4.90E+03
12.33	0.00E+00	0.00E+00	0.00E+00	0.00E+00	4.90E+03
14.71	0.00E+00	0.00E+00	0.00E+00	0.00E+00	1.47E+04
17.55	3.28E+04	6.52E+03	4.97E+03	4.46E+03	3.43E+04
20.94	0.00E+00	0.00E+00	0.00E+00	0.00E+00	0.00E+00
24.98	0.00E+00	0.00E+00	0.00E+00	0.00E+00	0.00E+00
29.81	0.00E+00	0.00E+00	0.00E+00	0.00E+00	0.00E+00
35.56	0.00E+00	0.00E+00	0.00E+00	0.00E+00	0.00E+00
42.43	0.00E+00	0.00E+00	0.00E+00	0.00E+00	0.00E+00
50.63	0.00E+00	0.00E+00	0.00E+00	0.00E+00	0.00E+00
60.41	0.00E+00	0.00E+00	0.00E+00	0.00E+00	0.00E+00
72.08	0.00E+00	0.00E+00	0.00E+00	0.00E+00	0.00E+00
86.00	0.00E+00	0.00E+00	0.00E+00	0.00E+00	0.00E+00
102.62	0.00E+00	0.00E+00	0.00E+00	0.00E+00	0.00E+00
122.44	0.00E+00	0.00E+00	0.00E+00	0.00E+00	0.00E+00

	15 min 15	20 min 20	25 min 25	30 min 30	45 min 45
dia.					
0.87	1.99E+05	8.98E+04	1.54E+05	9.81E+04	4.12E+04
1.04	1.59E+05	1.17E+05	8.02E+04	1.05E+05	4.84E+04
1.24	2.12E+05	1.80E+05	1.28E+05	8.83E+04	7.75E+04
1.48	2.91E+05	1.97E+05	1.12E+05	1.41E+05	6.29E+04
1.77	2.25E+05	1.42E+05	1.25E+05	1.08E+05	7.26E+04
2.11	2.43E+05	1.80E+05	1.09E+05	9.48E+04	3.87E+04
2.51	2.60E+05	1.24E+05	8.34E+04	8.18E+04	3.39E+04
3.00	1.99E+05	7.25E+04	5.13E+04	5.89E+04	7.26E+03
3.58	1.10E+05	7.60E+04	2.57E+04	3.92E+04	7.26E+03
4.27	1.01E+05	4.14E+04	3.21E+04	4.25E+04	7.26E+03
5.10	6.18E+04	4.49E+04	1.93E+04	9.81E+03	4.84E+03
6.08	5.30E+04	1.38E+04	1.28E+04	3.27E+04	2.42E+03
7.26	3.97E+04	1.38E+04	2.25E+04	1.96E+04	9.68E+03
8.66	2.65E+04	2.76E+04	6.42E+03	1.64E+04	4.84E+03
10.33	2.21E+04	1.04E+04	3.21E+03	6.54E+03	1.45E+04
12.33	0.00E+00	6.91E+03	3.21E+03	9.81E+03	4.84E+03
14.71	1.32E+04	1.04E+04	0.00E+00	3.27E+03	2.42E+03
17.55	1.77E+04	2.76E+04	1.28E+04	1.64E+04	4.84E+03
20.94	8.83E+03	1.04E+04	6.42E+03	0.00E+00	2.42E+03
24.98	0.00E+00	6.91E+03	0.00E+00	0.00E+00	7.26E+03
29.81	0.00E+00	6.91E+03	6.42E+03	0.00E+00	2.42E+03
35.56	0.00E+00	0.00E+00	6.42E+03	0.00E+00	0.00E+00
42.43	0.00E+00	0.00E+00	6.42E+03	0.00E+00	0.00E+00
50.63	0.00E+00	0.00E+00	0.00E+00	0.00E+00	0.00E+00
60.41	0.00E+00	0.00E+00	0.00E+00	0.00E+00	2.42E+03
72.08	0.00E+00	0.00E+00	0.00E+00	0.00E+00	0.00E+00
86.00	0.00E+00	0.00E+00	0.00E+00	0.00E+00	2.42E+03
102.62	0.00E+00	0.00E+00	0.00E+00	0.00E+00	0.00E+00
122.44	0.00E+00	0.00E+00	0.00E+00	0.00E+00	0.00E+00



08/09/88

Time-----&gt;

	homog	0 min	3 min	5 min	10 min
dia.	-1	0	3	5	10
0.87	6.83E+05	6.45E+05	5.64E+05	4.03E+05	4.48E+05
1.04	6.76E+05	6.91E+05	5.45E+05	4.49E+05	3.54E+05
1.24	8.99E+05	8.54E+05	6.80E+05	5.44E+05	4.81E+05
1.48	1.19E+06	1.04E+06	8.98E+05	6.25E+05	6.36E+05
1.77	1.14E+06	1.02E+06	8.34E+05	5.09E+05	5.31E+05
2.11	1.23E+06	1.22E+06	8.47E+05	6.55E+05	6.25E+05
2.51	6.76E+05	8.21E+05	6.73E+05	5.24E+05	6.31E+05
3.00	4.00E+05	5.34E+05	4.68E+05	3.83E+05	3.54E+05
3.58	1.25E+05	2.87E+05	2.89E+05	2.47E+05	2.77E+05
4.27	5.91E+04	1.04E+05	1.41E+05	2.37E+05	1.77E+05
5.10	3.28E+04	3.91E+04	8.34E+04	6.55E+04	6.64E+04
6.08	2.63E+04	2.61E+04	4.49E+04	6.05E+04	4.43E+04
7.26	6.57E+03	0.00E+00	1.92E+04	1.01E+04	5.53E+03
8.66	0.00E+00	0.00E+00	0.00E+00	1.51E+04	1.66E+04
10.33	0.00E+00	0.00E+00	0.00E+00	0.00E+00	1.11E+04
12.33	0.00E+00	0.00E+00	1.28E+04	1.51E+04	5.53E+03
14.71	0.00E+00	0.00E+00	0.00E+00	5.04E+03	5.53E+03
17.55	0.00E+00	0.00E+00	0.00E+00	0.00E+00	0.00E+00
20.94	0.00E+00	0.00E+00	0.00E+00	0.00E+00	0.00E+00
24.98	0.00E+00	0.00E+00	0.00E+00	0.00E+00	0.00E+00
29.81	0.00E+00	0.00E+00	0.00E+00	0.00E+00	0.00E+00
35.56	0.00E+00	0.00E+00	0.00E+00	0.00E+00	0.00E+00
42.43	0.00E+00	0.00E+00	0.00E+00	0.00E+00	0.00E+00
50.63	0.00E+00	0.00E+00	0.00E+00	0.00E+00	0.00E+00
60.41	0.00E+00	0.00E+00	0.00E+00	0.00E+00	0.00E+00
72.08	0.00E+00	0.00E+00	0.00E+00	0.00E+00	0.00E+00
86.00	0.00E+00	0.00E+00	0.00E+00	0.00E+00	0.00E+00
102.62	0.00E+00	0.00E+00	0.00E+00	0.00E+00	0.00E+00
122.44	0.00E+00	0.00E+00	0.00E+00	0.00E+00	0.00E+00

	15 min 15	20 min 20	25 min 25	30 min 30	45 min 45
dia.					
0.87	2.67E+05	1.69E+05	9.36E+04	2.56E+05	8.49E+04
1.04	2.96E+05	1.89E+05	1.05E+05	1.65E+05	6.69E+04
1.24	3.49E+05	3.02E+05	1.95E+05	2.15E+05	1.03E+05
1.48	4.51E+05	4.03E+05	2.73E+05	3.16E+05	8.74E+04
1.77	4.37E+05	2.82E+05	1.87E+05	2.61E+05	1.16E+05
2.11	5.48E+05	2.54E+05	2.36E+05	2.38E+05	7.71E+04
2.51	4.37E+05	2.58E+05	1.68E+05	1.88E+05	7.46E+04
3.00	3.01E+05	2.82E+05	1.57E+05	1.56E+05	3.09E+04
3.58	2.62E+05	1.21E+05	1.46E+05	1.01E+05	2.83E+04
4.27	1.84E+05	1.13E+05	8.61E+04	6.86E+04	2.31E+04
5.10	1.21E+05	5.24E+04	6.74E+04	5.49E+04	2.06E+04
6.08	3.88E+04	7.25E+04	4.12E+04	4.57E+04	1.29E+04
7.26	2.43E+04	3.62E+04	4.49E+04	5.49E+04	5.14E+03
8.66	2.43E+04	4.43E+04	2.99E+04	3.20E+04	7.71E+03
10.33	2.43E+04	2.82E+04	7.49E+03	0.00E+00	2.57E+03
12.33	3.88E+04	1.21E+04	2.25E+04	1.37E+04	1.03E+04
14.71	9.70E+03	8.05E+03	1.87E+04	2.29E+04	2.57E+03
17.55	0.00E+00	8.05E+03	1.50E+04	9.15E+03	0.00E+00
20.94	0.00E+00	4.03E+03	1.50E+04	4.57E+03	0.00E+00
24.98	0.00E+00	4.03E+03	1.12E+04	0.00E+00	0.00E+00
29.81	0.00E+00	0.00E+00	0.00E+00	4.57E+03	0.00E+00
35.56	0.00E+00	0.00E+00	3.74E+03	9.15E+03	0.00E+00
42.43	0.00E+00	0.00E+00	0.00E+00	0.00E+00	0.00E+00
50.63	0.00E+00	0.00E+00	0.00E+00	0.00E+00	2.57E+03
60.41	0.00E+00	0.00E+00	0.00E+00	0.00E+00	0.00E+00
72.08	0.00E+00	0.00E+00	0.00E+00	0.00E+00	0.00E+00
86.00	0.00E+00	0.00E+00	0.00E+00	0.00E+00	0.00E+00
102.62	0.00E+00	0.00E+00	0.00E+00	0.00E+00	0.00E+00
122.44	0.00E+00	0.00E+00	0.00E+00	0.00E+00	0.00E+00

06/21/88

Time-----&gt;

	homog	0 min	3 min	5 min	10 min
	-1	0	3	5	10
dia.					
0.87	6.96E+05	6.65E+05	6.54E+05	3.28E+05	2.40E+05
1.04	8.34E+05	5.80E+05	5.20E+05	3.34E+05	3.14E+05
1.24	8.21E+05	9.91E+05	7.95E+05	6.16E+05	3.68E+05
1.48	1.27E+06	1.24E+06	8.40E+05	6.91E+05	5.29E+05
1.77	1.05E+06	8.93E+05	8.27E+05	6.97E+05	4.12E+05
2.11	9.98E+05	9.91E+05	7.18E+05	6.39E+05	4.41E+05
2.51	7.42E+05	6.97E+05	6.16E+05	4.09E+05	3.58E+05
3.00	4.40E+05	3.13E+05	3.72E+05	2.76E+05	3.33E+05
3.58	1.44E+05	1.56E+05	1.35E+05	1.56E+05	2.30E+05
4.27	9.19E+04	3.91E+04	8.34E+04	1.32E+05	1.37E+05
5.10	3.28E+04	2.61E+04	3.21E+04	8.06E+04	1.13E+05
6.08	2.63E+04	6.52E+03	2.57E+04	2.30E+04	7.84E+04
7.26	6.57E+03	6.52E+03	1.92E+04	1.15E+04	4.41E+04
8.66	3.28E+04	1.96E+04	6.41E+03	0.00E+00	2.94E+04
10.33	1.31E+04	2.61E+04	0.00E+00	1.15E+04	4.90E+03
12.33	0.00E+00	0.00E+00	0.00E+00	5.76E+03	9.80E+03
14.71	0.00E+00	0.00E+00	0.00E+00	0.00E+00	0.00E+00
17.55	0.00E+00	0.00E+00	1.28E+04	2.88E+04	2.94E+04
20.94	6.57E+03	0.00E+00	1.92E+04	3.46E+04	3.43E+04
24.98	0.00E+00	0.00E+00	0.00E+00	0.00E+00	0.00E+00
29.81	0.00E+00	0.00E+00	0.00E+00	0.00E+00	0.00E+00
35.56	0.00E+00	0.00E+00	0.00E+00	0.00E+00	0.00E+00
42.43	0.00E+00	0.00E+00	0.00E+00	0.00E+00	0.00E+00
50.63	0.00E+00	0.00E+00	0.00E+00	0.00E+00	0.00E+00
60.41	0.00E+00	0.00E+00	0.00E+00	0.00E+00	0.00E+00
72.08	0.00E+00	0.00E+00	0.00E+00	0.00E+00	0.00E+00
86.00	0.00E+00	0.00E+00	0.00E+00	0.00E+00	0.00E+00
102.62	0.00E+00	0.00E+00	0.00E+00	0.00E+00	0.00E+00
122.44	0.00E+00	0.00E+00	0.00E+00	0.00E+00	0.00E+00

	15 min 15	20 min 20	25 min 25	30 min 30	45 min 45
dia.					
0.87	1.99E+05	1.37E+05	1.12E+05	6.87E+04	3.09E+04
1.04	1.46E+05	1.49E+05	1.06E+05	8.18E+04	3.60E+04
1.24	2.23E+05	1.73E+05	1.35E+05	8.83E+04	4.89E+04
1.48	3.49E+05	2.30E+05	9.95E+04	1.11E+05	4.37E+04
1.77	2.86E+05	1.45E+05	1.09E+05	6.54E+04	3.09E+04
2.11	2.72E+05	2.05E+05	6.42E+04	5.56E+04	2.57E+04
2.51	2.04E+05	1.33E+05	7.38E+04	5.23E+04	1.80E+04
3.00	1.55E+05	8.86E+04	5.13E+04	2.29E+04	5.14E+03
3.58	1.50E+05	5.64E+04	2.89E+04	2.62E+04	1.03E+04
4.27	1.07E+05	6.04E+04	3.21E+04	2.29E+04	1.03E+04
5.10	5.82E+04	3.62E+04	1.60E+04	6.54E+03	1.03E+04
6.08	6.79E+04	2.82E+04	3.21E+04	1.31E+04	0.00E+00
7.26	3.88E+04	1.21E+04	1.28E+04	9.81E+03	0.00E+00
8.66	2.43E+04	2.42E+04	3.21E+03	3.27E+03	0.00E+00
10.33	1.94E+04	2.01E+04	1.93E+04	0.00E+00	0.00E+00
12.33	0.00E+00	8.05E+03	1.60E+04	6.54E+03	0.00E+00
14.71	1.46E+04	2.01E+04	1.28E+04	9.81E+03	2.57E+03
17.55	2.43E+04	3.22E+04	2.57E+04	9.81E+03	5.14E+03
20.94	2.91E+04	1.21E+04	1.60E+04	3.27E+04	2.57E+03
24.98	0.00E+00	8.05E+03	6.42E+03	6.54E+03	0.00E+00
29.81	0.00E+00	0.00E+00	3.21E+03	9.81E+03	5.14E+03
35.56	0.00E+00	0.00E+00	0.00E+00	1.31E+04	5.14E+03
42.43	0.00E+00	0.00E+00	3.21E+03	0.00E+00	0.00E+00
50.63	0.00E+00	0.00E+00	3.21E+03	0.00E+00	1.03E+04
60.41	0.00E+00	0.00E+00	0.00E+00	0.00E+00	2.57E+03
72.08	0.00E+00	0.00E+00	0.00E+00	0.00E+00	2.57E+03
86.00	0.00E+00	0.00E+00	0.00E+00	0.00E+00	0.00E+00
102.62	0.00E+00	0.00E+00	0.00E+00	0.00E+00	0.00E+00
122.44	0.00E+00	0.00E+00	0.00E+00	0.00E+00	0.00E+00

07/28/88

Time-----&gt;

	homog	0 min	3 min	5 min	10 min
dia.	-1	0	3	5	10
0.87	5.91E+05	6.00E+05	6.03E+05	3.83E+05	3.04E+05
1.04	5.51E+05	5.67E+05	4.55E+05	3.78E+05	3.00E+05
1.24	7.22E+05	5.93E+05	6.09E+05	5.75E+05	3.66E+05
1.48	9.52E+05	8.86E+05	8.08E+05	6.65E+05	4.50E+05
1.77	8.40E+05	8.54E+05	6.93E+05	5.70E+05	4.59E+05
2.11	6.04E+05	7.43E+05	6.29E+05	5.75E+05	4.63E+05
2.51	4.27E+05	6.52E+05	4.87E+05	5.70E+05	3.35E+05
3.00	2.30E+05	3.06E+05	3.14E+05	3.68E+05	3.00E+05
3.58	9.85E+04	2.28E+05	1.54E+05	1.92E+05	2.03E+05
4.27	5.25E+04	1.30E+05	1.09E+05	1.21E+05	1.32E+05
5.10	1.31E+04	3.26E+04	4.49E+04	4.54E+04	9.71E+04
6.08	6.57E+03	1.30E+04	6.41E+03	1.51E+04	5.74E+04
7.26	1.97E+04	6.52E+03	1.28E+04	1.01E+04	4.41E+04
8.66	1.31E+04	6.52E+03	6.41E+03	5.04E+03	2.65E+04
10.33	6.57E+03	0.00E+00	0.00E+00	5.04E+03	1.32E+04
12.33	0.00E+00	0.00E+00	1.28E+04	0.00E+00	1.77E+04
14.71	0.00E+00	0.00E+00	0.00E+00	0.00E+00	0.00E+00
17.55	6.57E+03	1.30E+04	1.28E+04	1.51E+04	1.77E+04
20.94	0.00E+00	0.00E+00	0.00E+00	0.00E+00	0.00E+00
24.98	0.00E+00	0.00E+00	0.00E+00	0.00E+00	0.00E+00
29.81	0.00E+00	0.00E+00	0.00E+00	0.00E+00	0.00E+00
35.56	0.00E+00	0.00E+00	0.00E+00	0.00E+00	0.00E+00
42.43	0.00E+00	0.00E+00	0.00E+00	0.00E+00	0.00E+00
50.63	0.00E+00	0.00E+00	0.00E+00	0.00E+00	0.00E+00
60.41	0.00E+00	0.00E+00	0.00E+00	0.00E+00	0.00E+00
72.08	0.00E+00	0.00E+00	0.00E+00	0.00E+00	0.00E+00
86.00	0.00E+00	0.00E+00	0.00E+00	0.00E+00	0.00E+00
102.62	0.00E+00	0.00E+00	0.00E+00	0.00E+00	0.00E+00
122.44	0.00E+00	0.00E+00	0.00E+00	0.00E+00	0.00E+00

	15 min 15	20 min 20	25 min 25	30 min 30	45 min 45
dia.					
0.87	1.98E+05	1.29E+05	7.79E+04	6.87E+04	4.29E+04
1.04	1.12E+05	1.10E+05	8.69E+04	7.33E+04	3.77E+04
1.24	2.24E+05	1.39E+05	1.26E+05	9.62E+04	6.35E+04
1.48	2.28E+05	1.97E+05	1.68E+05	9.39E+04	6.86E+04
1.77	1.64E+05	1.68E+05	9.29E+04	6.41E+04	5.15E+04
2.11	1.87E+05	1.45E+05	8.69E+04	6.87E+04	2.57E+04
2.51	2.17E+05	9.03E+04	9.29E+04	4.35E+04	4.12E+04
3.00	1.23E+05	8.38E+04	5.39E+04	2.75E+04	1.37E+04
3.58	1.23E+05	2.26E+04	3.30E+04	2.29E+04	1.20E+04
4.27	7.10E+04	3.55E+04	4.19E+04	2.52E+04	1.03E+04
5.10	6.35E+04	2.58E+04	2.10E+04	6.87E+03	5.15E+03
6.08	2.61E+04	2.90E+04	0.00E+00	9.16E+03	6.86E+03
7.26	2.99E+04	1.61E+04	1.20E+04	6.87E+03	6.86E+03
8.66	2.61E+04	9.67E+03	3.00E+03	6.87E+03	0.00E+00
10.33	1.49E+04	1.93E+04	8.99E+03	4.58E+03	0.00E+00
12.33	1.49E+04	3.22E+03	5.99E+03	2.29E+03	0.00E+00
14.71	1.87E+04	3.22E+03	3.00E+03	2.29E+03	0.00E+00
17.55	2.61E+04	1.29E+04	5.99E+03	6.87E+03	6.86E+03
20.94	7.47E+03	1.29E+04	3.00E+03	0.00E+00	1.72E+03
24.98	3.74E+03	9.67E+03	0.00E+00	0.00E+00	0.00E+00
29.81	0.00E+00	9.67E+03	3.00E+03	2.29E+03	0.00E+00
35.56	0.00E+00	3.22E+03	3.00E+03	0.00E+00	5.15E+03
42.43	0.00E+00	0.00E+00	3.00E+03	2.29E+03	0.00E+00
50.63	0.00E+00	0.00E+00	0.00E+00	0.00E+00	1.72E+03
60.41	0.00E+00	0.00E+00	0.00E+00	4.58E+03	3.43E+03
72.08	0.00E+00	0.00E+00	0.00E+00	2.29E+03	0.00E+00
86.00	0.00E+00	0.00E+00	0.00E+00	0.00E+00	0.00E+00
102.62	0.00E+00	0.00E+00	0.00E+00	0.00E+00	0.00E+00
122.44	0.00E+00	0.00E+00	0.00E+00	0.00E+00	0.00E+00

06/27/88

Time----->

homog	0 min	3 min	5 min	10 min
-1	0	3	5	10

dia.

0.87	6.43E+05	7.04E+05	7.63E+05	5.70E+05	5.06E+05
1.04	6.37E+05	6.45E+05	6.03E+05	5.82E+05	4.49E+05
1.24	7.22E+05	7.89E+05	7.83E+05	8.18E+05	8.98E+05
1.48	1.06E+06	1.19E+06	9.11E+05	9.22E+05	8.98E+05
1.77	8.67E+05	9.38E+05	7.38E+05	8.64E+05	7.46E+05
2.11	8.34E+05	8.28E+05	7.63E+05	6.45E+05	8.09E+05
2.51	5.51E+05	4.24E+05	5.07E+05	5.24E+05	6.64E+05
3.00	3.09E+05	2.74E+05	2.63E+05	3.00E+05	2.34E+05
3.58	1.25E+05	1.43E+05	8.98E+04	1.50E+05	1.33E+05
4.27	1.05E+05	4.56E+04	3.21E+04	5.18E+04	8.85E+04
5.10	3.28E+04	6.52E+03	4.49E+04	2.30E+04	1.26E+04
6.08	2.63E+04	6.52E+03	6.41E+03	1.73E+04	1.90E+04
7.26	1.97E+04	6.52E+03	6.41E+03	0.00E+00	1.26E+04
8.66	0.00E+00	0.00E+00	0.00E+00	0.00E+00	0.00E+00
10.33	0.00E+00	0.00E+00	0.00E+00	0.00E+00	0.00E+00
12.33	0.00E+00	0.00E+00	0.00E+00	0.00E+00	6.32E+03
14.71	0.00E+00	0.00E+00	0.00E+00	0.00E+00	0.00E+00
17.55	0.00E+00	0.00E+00	0.00E+00	0.00E+00	0.00E+00
20.94	0.00E+00	0.00E+00	0.00E+00	0.00E+00	0.00E+00
24.98	0.00E+00	0.00E+00	0.00E+00	0.00E+00	0.00E+00
29.81	0.00E+00	0.00E+00	0.00E+00	0.00E+00	0.00E+00
35.56	0.00E+00	0.00E+00	0.00E+00	0.00E+00	0.00E+00
42.43	0.00E+00	0.00E+00	0.00E+00	0.00E+00	0.00E+00
50.63	0.00E+00	0.00E+00	0.00E+00	0.00E+00	0.00E+00
60.41	0.00E+00	0.00E+00	0.00E+00	0.00E+00	0.00E+00
72.08	0.00E+00	0.00E+00	0.00E+00	0.00E+00	0.00E+00
86.00	0.00E+00	0.00E+00	0.00E+00	0.00E+00	0.00E+00
102.62	0.00E+00	0.00E+00	0.00E+00	0.00E+00	0.00E+00
122.44	0.00E+00	0.00E+00	0.00E+00	0.00E+00	0.00E+00

	15 min 15	20 min 20	25 min 25	30 min 30	45 min 45
dla.					
0.87	7.23E+05	5.26E+05	5.27E+05	4.27E+05	1.92E+05
1.04	5.35E+05	4.98E+05	3.92E+05	3.35E+05	2.10E+05
1.24	8.27E+05	8.17E+05	5.73E+05	5.13E+05	2.42E+05
1.48	8.97E+05	9.34E+05	6.75E+05	6.76E+05	3.01E+05
1.77	8.14E+05	7.96E+05	5.79E+05	5.13E+05	2.42E+05
2.11	8.00E+05	7.61E+05	7.59E+05	4.67E+05	2.24E+05
2.51	5.84E+05	5.88E+05	5.21E+05	3.25E+05	1.37E+05
3.00	2.99E+05	3.18E+05	3.73E+05	2.64E+05	1.00E+05
3.58	1.46E+05	2.35E+05	2.19E+05	2.03E+05	1.00E+05
4.27	1.18E+05	7.61E+04	1.03E+05	1.22E+05	1.05E+05
5.10	4.17E+04	6.23E+04	6.43E+04	8.64E+04	3.20E+04
6.08	6.95E+03	6.92E+03	5.15E+04	8.13E+04	1.83E+04
7.26	1.39E+04	2.08E+04	1.29E+04	3.56E+04	2.74E+04
8.66	6.95E+03	6.92E+03	6.43E+03	2.03E+04	3.65E+04
10.33	1.39E+04	6.92E+03	1.29E+04	5.08E+03	3.20E+04
12.33	0.00E+00	0.00E+00	6.43E+03	2.54E+04	2.28E+04
14.71	0.00E+00	0.00E+00	0.00E+00	5.08E+03	1.37E+04
17.55	6.95E+03	0.00E+00	0.00E+00	1.52E+04	4.56E+03
20.94	0.00E+00	0.00E+00	0.00E+00	0.00E+00	0.00E+00
24.98	0.00E+00	0.00E+00	0.00E+00	0.00E+00	0.00E+00
29.81	0.00E+00	0.00E+00	0.00E+00	0.00E+00	0.00E+00
35.56	0.00E+00	0.00E+00	0.00E+00	0.00E+00	0.00E+00
42.43	0.00E+00	0.00E+00	0.00E+00	0.00E+00	0.00E+00
50.63	0.00E+00	0.00E+00	0.00E+00	0.00E+00	0.00E+00
60.41	0.00E+00	0.00E+00	0.00E+00	0.00E+00	0.00E+00
72.08	0.00E+00	0.00E+00	0.00E+00	0.00E+00	0.00E+00
86.00	0.00E+00	0.00E+00	0.00E+00	0.00E+00	0.00E+00
102.62	0.00E+00	0.00E+00	0.00E+00	0.00E+00	0.00E+00
122.44	0.00E+00	0.00E+00	0.00E+00	0.00E+00	0.00E+00



08/15/88

Time-----&gt;

	homog	0 min	3 min	5 min	10 min
dia.	-1	0	3	5	10
0.87	1.10E+06	6.45E+05	8.21E+05	6.97E+05	7.02E+05
1.04	7.35E+05	8.02E+05	6.22E+05	6.16E+05	6.07E+05
1.24	1.10E+06	9.32E+05	1.02E+06	7.83E+05	8.41E+05
1.48	1.40E+06	1.40E+06	1.15E+06	9.85E+05	1.09E+06
1.77	1.02E+06	1.21E+06	1.03E+06	8.47E+05	9.17E+05
2.11	8.40E+05	8.73E+05	8.60E+05	8.01E+05	8.22E+05
2.51	4.73E+05	4.56E+05	4.11E+05	4.49E+05	6.39E+05
3.00	1.51E+05	3.26E+05	3.27E+05	2.65E+05	2.72E+05
3.58	7.88E+04	1.24E+05	1.41E+05	1.21E+05	1.45E+05
4.27	5.91E+04	7.17E+04	7.06E+04	5.76E+04	7.59E+04
5.10	2.63E+04	3.91E+04	5.77E+04	2.88E+04	2.53E+04
6.08	6.57E+03	6.52E+03	1.92E+04	2.30E+04	1.26E+04
7.26	0.00E+00	1.30E+04	6.41E+03	1.15E+04	6.32E+03
8.66	0.00E+00	0.00E+00	6.41E+03	0.00E+00	6.32E+03
10.33	0.00E+00	6.52E+03	1.28E+04	0.00E+00	0.00E+00
12.33	0.00E+00	0.00E+00	0.00E+00	0.00E+00	0.00E+00
14.71	0.00E+00	0.00E+00	0.00E+00	0.00E+00	0.00E+00
17.55	0.00E+00	0.00E+00	0.00E+00	0.00E+00	0.00E+00
20.94	0.00E+00	0.00E+00	0.00E+00	0.00E+00	0.00E+00
24.98	0.00E+00	0.00E+00	0.00E+00	0.00E+00	0.00E+00
29.81	0.00E+00	0.00E+00	0.00E+00	0.00E+00	0.00E+00
35.56	0.00E+00	0.00E+00	0.00E+00	0.00E+00	0.00E+00
42.43	0.00E+00	0.00E+00	0.00E+00	0.00E+00	0.00E+00
50.63	0.00E+00	0.00E+00	0.00E+00	0.00E+00	0.00E+00
60.41	0.00E+00	0.00E+00	0.00E+00	0.00E+00	0.00E+00
72.08	0.00E+00	0.00E+00	0.00E+00	0.00E+00	0.00E+00
86.00	0.00E+00	0.00E+00	0.00E+00	0.00E+00	0.00E+00
102.62	0.00E+00	0.00E+00	0.00E+00	0.00E+00	0.00E+00
122.44	0.00E+00	0.00E+00	0.00E+00	0.00E+00	0.00E+00

	15 min	20 min	25 min	30 min	45 min
dia.	15	20	25	30	45
0.87	6.51E+05	5.15E+05	4.04E+05	4.57E+05	2.34E+05
1.04	5.35E+05	5.09E+05	4.58E+05	3.81E+05	2.96E+05
1.24	8.94E+05	6.78E+05	5.48E+05	5.13E+05	3.62E+05
1.48	1.23E+06	9.02E+05	8.39E+05	7.27E+05	4.93E+05
1.77	8.09E+05	8.30E+05	6.60E+05	6.66E+05	3.62E+05
2.11	9.07E+05	8.54E+05	5.52E+05	6.71E+05	4.32E+05
2.51	6.02E+05	6.84E+05	4.00E+05	4.17E+05	3.70E+05
3.00	3.10E+05	3.39E+05	3.28E+05	3.56E+05	2.18E+05
3.58	1.58E+05	2.91E+05	1.80E+05	2.13E+05	1.56E+05
4.27	1.52E+05	1.27E+05	1.30E+05	1.63E+05	1.11E+05
5.10	6.69E+04	8.48E+04	3.59E+04	6.61E+04	6.16E+04
6.08	6.08E+03	4.84E+04	4.94E+04	9.15E+04	6.58E+04
7.26	6.08E+03	2.42E+04	4.04E+04	4.06E+04	6.16E+04
8.66	0.00E+00	2.42E+04	2.69E+04	3.05E+04	2.88E+04
10.33	6.08E+03	0.00E+00	8.98E+03	1.02E+04	2.05E+04
12.33	6.08E+03	6.06E+03	4.49E+03	5.08E+03	8.22E+03
14.71	0.00E+00	0.00E+00	8.98E+03	1.02E+04	1.23E+04
17.55	0.00E+00	0.00E+00	0.00E+00	5.08E+03	1.23E+04
20.94	0.00E+00	0.00E+00	0.00E+00	0.00E+00	0.00E+00
24.98	0.00E+00	0.00E+00	0.00E+00	0.00E+00	0.00E+00
29.81	0.00E+00	0.00E+00	0.00E+00	0.00E+00	0.00E+00
35.56	0.00E+00	0.00E+00	0.00E+00	0.00E+00	0.00E+00
42.43	0.00E+00	0.00E+00	0.00E+00	0.00E+00	0.00E+00
50.63	0.00E+00	0.00E+00	0.00E+00	0.00E+00	0.00E+00
60.41	0.00E+00	0.00E+00	0.00E+00	0.00E+00	0.00E+00
72.08	0.00E+00	0.00E+00	0.00E+00	0.00E+00	0.00E+00
86.00	0.00E+00	0.00E+00	0.00E+00	0.00E+00	0.00E+00
102.62	0.00E+00	0.00E+00	0.00E+00	0.00E+00	0.00E+00
122.44	0.00E+00	0.00E+00	0.00E+00	0.00E+00	0.00E+00

06/29/88

Time-----&gt;

	homog	0 min	3 min	5 min	10 min
dia.	-1	0	3	5	10
0.87	8.93E+05	7.30E+05	5.58E+05	5.82E+05	6.07E+05
1.04	7.94E+05	7.23E+05	5.39E+05	5.13E+05	4.30E+05
1.24	8.21E+05	8.86E+05	7.50E+05	7.72E+05	6.45E+05
1.48	1.25E+06	1.10E+06	1.19E+06	8.76E+05	9.86E+05
1.77	8.21E+05	9.91E+05	8.85E+05	8.70E+05	8.28E+05
2.11	7.48E+05	8.93E+05	7.89E+05	6.97E+05	8.54E+05
2.51	3.09E+05	5.87E+05	4.81E+05	5.18E+05	6.01E+05
3.00	1.44E+05	3.98E+05	2.18E+05	2.82E+05	3.79E+05
3.58	1.05E+05	1.24E+05	1.54E+05	1.44E+05	2.02E+05
4.27	5.25E+04	5.21E+04	3.21E+04	9.22E+04	8.22E+04
5.10	3.28E+04	1.96E+04	3.21E+04	1.15E+04	1.26E+04
6.08	1.31E+04	6.52E+03	0.00E+00	0.00E+00	1.26E+04
7.26	1.97E+04	0.00E+00	0.00E+00	0.00E+00	1.26E+04
8.66	6.57E+03	6.52E+03	0.00E+00	0.00E+00	0.00E+00
10.33	6.57E+03	0.00E+00	0.00E+00	5.76E+03	0.00E+00
12.33	0.00E+00	0.00E+00	0.00E+00	0.00E+00	0.00E+00
14.71	0.00E+00	0.00E+00	0.00E+00	0.00E+00	6.32E+03
17.55	6.57E+03	6.52E+03	1.28E+04	1.15E+04	0.00E+00
20.94	2.63E+04	3.26E+04	2.57E+04	3.46E+04	3.79E+04
24.98	0.00E+00	0.00E+00	0.00E+00	0.00E+00	0.00E+00
29.81	0.00E+00	0.00E+00	0.00E+00	0.00E+00	0.00E+00
35.56	0.00E+00	0.00E+00	0.00E+00	0.00E+00	0.00E+00
42.43	0.00E+00	0.00E+00	0.00E+00	0.00E+00	0.00E+00
50.63	0.00E+00	0.00E+00	0.00E+00	0.00E+00	0.00E+00
60.41	0.00E+00	0.00E+00	0.00E+00	0.00E+00	0.00E+00
72.08	0.00E+00	0.00E+00	0.00E+00	0.00E+00	0.00E+00
86.00	0.00E+00	0.00E+00	0.00E+00	0.00E+00	0.00E+00
102.62	0.00E+00	0.00E+00	0.00E+00	0.00E+00	0.00E+00
122.44	0.00E+00	0.00E+00	0.00E+00	0.00E+00	0.00E+00

	15 min 15	20 min 20	25 min 25	30 min 30	45 min 45
dia.					
0.87	4.73E+05	2.95E+05	1.50E+05	1.63E+05	5.88E+04
1.04	3.96E+05	3.27E+05	1.89E+05	1.52E+05	6.46E+04
1.24	5.49E+05	4.67E+05	2.39E+05	2.08E+05	7.35E+04
1.48	7.23E+05	5.36E+05	3.09E+05	2.34E+05	6.76E+04
1.77	6.68E+05	4.99E+05	1.75E+05	1.98E+05	7.93E+04
2.11	6.61E+05	4.08E+05	2.59E+05	2.34E+05	5.29E+04
2.51	5.01E+05	2.84E+05	2.49E+05	1.22E+05	4.41E+04
3.00	3.20E+05	2.09E+05	1.45E+05	8.64E+04	2.94E+04
3.58	1.95E+05	1.72E+05	1.15E+05	9.65E+04	2.94E+04
4.27	1.04E+05	1.34E+05	5.98E+04	6.10E+04	1.18E+04
5.10	4.87E+04	6.97E+04	4.49E+04	2.03E+04	1.76E+04
6.08	5.56E+04	2.68E+04	6.48E+04	2.03E+04	1.47E+04
7.26	2.78E+04	3.22E+04	2.49E+04	3.05E+04	8.81E+03
8.66	1.39E+04	3.22E+04	1.50E+04	3.05E+04	1.18E+04
10.33	0.00E+00	5.36E+03	1.50E+04	2.03E+04	1.18E+04
12.33	0.00E+00	1.61E+04	4.49E+04	2.03E+04	0.00E+00
14.71	0.00E+00	5.36E+03	1.50E+04	1.02E+04	2.94E+03
17.55	2.09E+04	1.07E+04	3.99E+04	1.52E+04	1.18E+04
20.94	2.78E+04	4.29E+04	2.49E+04	2.03E+04	5.88E+03
24.98	0.00E+00	0.00E+00	0.00E+00	0.00E+00	2.06E+04
29.81	0.00E+00	0.00E+00	0.00E+00	0.00E+00	8.81E+03
35.56	0.00E+00	0.00E+00	0.00E+00	0.00E+00	0.00E+00
42.43	0.00E+00	0.00E+00	0.00E+00	0.00E+00	0.00E+00
50.63	0.00E+00	0.00E+00	0.00E+00	0.00E+00	0.00E+00
60.41	0.00E+00	0.00E+00	0.00E+00	0.00E+00	0.00E+00
72.08	0.00E+00	0.00E+00	0.00E+00	0.00E+00	0.00E+00
86.00	0.00E+00	0.00E+00	0.00E+00	0.00E+00	0.00E+00
102.62	0.00E+00	0.00E+00	0.00E+00	0.00E+00	0.00E+00
122.44	0.00E+00	0.00E+00	0.00E+00	0.00E+00	0.00E+00

08/17/88

Time-----&gt;

	homog	0 min	3 min	5 min	10 min
dia.	-1	.0	3	5	10
0.87	6.50E+05	7.91E+05	7.86E+05	7.09E+05	5.82E+05
1.04	6.76E+05	6.31E+05	6.51E+05	5.93E+05	4.93E+05
1.24	7.02E+05	1.03E+06	8.23E+05	7.60E+05	6.89E+05
1.48	1.04E+06	1.32E+06	1.17E+06	8.29E+05	1.05E+06
1.77	6.50E+05	1.03E+06	8.16E+05	8.41E+05	8.28E+05
2.11	4.99E+05	1.05E+06	7.48E+05	7.55E+05	6.32E+05
2.51	2.82E+05	5.70E+05	4.12E+05	4.32E+05	4.11E+05
3.00	1.38E+05	3.12E+05	1.95E+05	2.02E+05	2.78E+05
3.58	4.60E+04	1.52E+05	1.12E+05	8.64E+04	9.49E+04
4.27	5.91E+04	9.12E+04	4.49E+04	8.06E+04	3.79E+04
5.10	6.57E+03	2.28E+04	4.49E+04	2.30E+04	8.22E+04
6.08	1.31E+04	7.60E+03	7.48E+03	5.76E+03	0.00E+00
7.26	6.57E+03	0.00E+00	0.00E+00	0.00E+00	6.32E+03
8.66	1.31E+04	0.00E+00	0.00E+00	5.76E+03	6.32E+03
10.33	0.00E+00	0.00E+00	0.00E+00	5.76E+03	0.00E+00
12.33	0.00E+00	0.00E+00	0.00E+00	0.00E+00	6.32E+03
14.71	0.00E+00	0.00E+00	0.00E+00	0.00E+00	0.00E+00
17.55	0.00E+00	0.00E+00	0.00E+00	0.00E+00	0.00E+00
20.94	0.00E+00	0.00E+00	0.00E+00	0.00E+00	0.00E+00
24.98	0.00E+00	0.00E+00	0.00E+00	0.00E+00	0.00E+00
29.81	0.00E+00	0.00E+00	0.00E+00	0.00E+00	0.00E+00
35.56	0.00E+00	0.00E+00	0.00E+00	0.00E+00	0.00E+00
42.43	0.00E+00	0.00E+00	0.00E+00	0.00E+00	0.00E+00
50.63	0.00E+00	0.00E+00	0.00E+00	0.00E+00	0.00E+00
60.41	0.00E+00	0.00E+00	0.00E+00	0.00E+00	0.00E+00
72.08	0.00E+00	0.00E+00	0.00E+00	0.00E+00	0.00E+00
86.00	0.00E+00	0.00E+00	0.00E+00	0.00E+00	0.00E+00
102.62	0.00E+00	0.00E+00	0.00E+00	0.00E+00	0.00E+00
122.44	0.00E+00	0.00E+00	0.00E+00	0.00E+00	0.00E+00

	15 min 15	20 min 20	25 min 25	30 min 30	45 min 45
dia.					
0.87	5.28E+05	4.30E+05	3.01E+05	2.65E+05	1.93E+05
1.04	4.66E+05	3.33E+05	2.24E+05	2.01E+05	1.36E+05
1.24	6.26E+05	4.66E+05	3.32E+05	2.33E+05	2.30E+05
1.48	7.44E+05	6.06E+05	4.53E+05	4.62E+05	2.30E+05
1.77	8.14E+05	4.24E+05	3.37E+05	3.20E+05	2.22E+05
2.11	6.75E+05	5.57E+05	3.73E+05	3.52E+05	2.30E+05
2.51	5.28E+05	4.00E+05	2.33E+05	2.42E+05	1.89E+05
3.00	3.76E+05	3.33E+05	2.29E+05	1.83E+05	1.44E+05
3.58	2.92E+05	1.64E+05	1.80E+05	1.56E+05	1.03E+05
4.27	1.67E+05	1.03E+05	1.08E+05	8.69E+04	6.58E+04
5.10	8.34E+04	6.66E+04	1.21E+05	1.01E+05	6.16E+04
6.08	4.87E+04	4.84E+04	4.49E+04	6.40E+04	3.29E+04
7.26	6.95E+03	3.03E+04	1.80E+04	4.12E+04	2.88E+04
8.66	1.39E+04	1.82E+04	4.04E+04	3.20E+04	3.29E+04
10.33	0.00E+00	0.00E+00	2.69E+04	3.20E+04	2.88E+04
12.33	0.00E+00	6.06E+03	1.35E+04	4.57E+03	8.22E+03
14.71	0.00E+00	6.06E+03	1.80E+04	1.37E+04	4.11E+03
17.55	0.00E+00	0.00E+00	4.49E+03	9.15E+03	1.64E+04
20.94	0.00E+00	0.00E+00	0.00E+00	4.57E+03	0.00E+00
24.98	0.00E+00	0.00E+00	0.00E+00	0.00E+00	0.00E+00
29.81	0.00E+00	0.00E+00	0.00E+00	0.00E+00	0.00E+00
35.56	0.00E+00	0.00E+00	0.00E+00	0.00E+00	0.00E+00
42.43	0.00E+00	0.00E+00	0.00E+00	0.00E+00	0.00E+00
50.63	0.00E+00	0.00E+00	0.00E+00	0.00E+00	0.00E+00
60.41	0.00E+00	0.00E+00	0.00E+00	0.00E+00	0.00E+00
72.08	0.00E+00	0.00E+00	0.00E+00	0.00E+00	0.00E+00
86.00	0.00E+00	0.00E+00	0.00E+00	0.00E+00	0.00E+00
102.62	0.00E+00	0.00E+00	0.00E+00	0.00E+00	0.00E+00
122.44	0.00E+00	0.00E+00	0.00E+00	0.00E+00	0.00E+00

09/16/88

Time-----&gt;

	homog	0 min	3 min	5 min	10 min
dia.	-1	0	3	5	10
0.87	7.04E+05	7.04E+05	5.33E+05	4.08E+05	1.99E+05
1.04	6.78E+05	6.78E+05	4.94E+05	3.02E+05	1.90E+05
1.24	8.21E+05	8.21E+05	7.02E+05	4.28E+05	2.16E+05
1.48	1.15E+06	1.15E+06	7.35E+05	6.50E+05	3.22E+05
1.77	9.19E+05	9.19E+05	6.96E+05	5.54E+05	1.90E+05
2.11	8.60E+05	8.60E+05	6.40E+05	4.18E+05	1.90E+05
2.51	5.21E+05	5.21E+05	5.00E+05	3.63E+05	1.59E+05
3.00	3.19E+05	3.19E+05	3.09E+05	2.92E+05	1.01E+05
3.58	8.47E+04	8.47E+04	1.91E+05	2.02E+05	7.94E+04
4.27	5.87E+04	5.87E+04	9.54E+04	1.26E+05	5.30E+04
5.10	0.00E+00	0.00E+00	6.73E+04	9.07E+04	7.94E+04
6.08	1.96E+04	1.96E+04	2.24E+04	3.02E+04	4.85E+04
7.26	0.00E+00	0.00E+00	1.12E+04	2.02E+04	1.32E+04
8.66	0.00E+00	0.00E+00	0.00E+00	1.51E+04	2.21E+04
10.33	0.00E+00	0.00E+00	0.00E+00	1.51E+04	2.65E+04
12.33	0.00E+00	0.00E+00	0.00E+00	0.00E+00	1.32E+04
14.71	0.00E+00	0.00E+00	0.00E+00	0.00E+00	8.83E+03
17.55	0.00E+00	0.00E+00	0.00E+00	0.00E+00	4.41E+03
20.94	0.00E+00	0.00E+00	0.00E+00	1.51E+04	1.77E+04
24.98	0.00E+00	0.00E+00	0.00E+00	0.00E+00	8.83E+03
29.81	0.00E+00	0.00E+00	0.00E+00	0.00E+00	0.00E+00
35.56	0.00E+00	0.00E+00	0.00E+00	0.00E+00	0.00E+00
42.43	0.00E+00	0.00E+00	0.00E+00	0.00E+00	0.00E+00
50.63	0.00E+00	0.00E+00	0.00E+00	0.00E+00	0.00E+00
60.41	0.00E+00	0.00E+00	0.00E+00	0.00E+00	0.00E+00
72.08	0.00E+00	0.00E+00	0.00E+00	0.00E+00	0.00E+00
86.00	0.00E+00	0.00E+00	0.00E+00	0.00E+00	0.00E+00
102.62	0.00E+00	0.00E+00	0.00E+00	0.00E+00	0.00E+00
122.44	0.00E+00	0.00E+00	0.00E+00	0.00E+00	0.00E+00

	15 min 15	20 min 20	25 min 25	30 min 30	45 min 45
dia.					
0.87	9.27E+04	6.91E+04	4.81E+04	7.85E+04	3.53E+04
1.04	9.71E+04	6.22E+04	4.81E+04	6.21E+04	6.17E+04
1.24	1.37E+05	1.00E+05	6.74E+04	8.83E+04	5.58E+04
1.48	1.72E+05	1.24E+05	7.06E+04	8.83E+04	5.29E+04
1.77	1.01E+05	1.17E+05	6.74E+04	9.16E+04	3.82E+04
2.11	1.15E+05	5.52E+04	4.49E+04	7.52E+04	3.23E+04
2.51	1.10E+05	8.98E+04	3.21E+04	5.23E+04	3.23E+04
3.00	7.94E+04	7.60E+04	2.25E+04	1.96E+04	1.18E+04
3.58	1.77E+04	2.76E+04	1.28E+04	3.27E+04	5.88E+03
4.27	2.21E+04	2.07E+04	3.21E+03	2.29E+04	8.81E+03
5.10	3.53E+04	6.91E+03	1.28E+04	3.27E+03	2.94E+03
6.08	2.65E+04	6.91E+03	3.21E+03	3.27E+03	0.00E+00
7.26	8.83E+03	6.91E+03	0.00E+00	3.27E+03	2.94E+03
8.66	1.32E+04	6.91E+03	3.21E+03	3.27E+03	2.94E+03
10.33	0.00E+00	0.00E+00	0.00E+00	0.00E+00	0.00E+00
12.33	1.32E+04	3.45E+03	0.00E+00	0.00E+00	5.88E+03
14.71	0.00E+00	3.45E+03	0.00E+00	0.00E+00	2.94E+03
17.55	0.00E+00	0.00E+00	0.00E+00	0.00E+00	0.00E+00
20.94	1.32E+04	1.04E+04	0.00E+00	0.00E+00	0.00E+00
24.98	8.83E+03	0.00E+00	0.00E+00	0.00E+00	0.00E+00
29.81	0.00E+00	3.45E+03	0.00E+00	3.27E+03	0.00E+00
35.56	0.00E+00	0.00E+00	3.21E+03	0.00E+00	2.94E+03
42.43	8.83E+03	6.91E+03	3.21E+03	0.00E+00	0.00E+00
50.63	0.00E+00	3.45E+03	3.21E+03	3.27E+03	0.00E+00
60.41	0.00E+00	0.00E+00	3.21E+03	0.00E+00	2.94E+03
72.08	0.00E+00	3.45E+03	0.00E+00	0.00E+00	2.94E+03
86.00	0.00E+00	0.00E+00	0.00E+00	0.00E+00	0.00E+00
102.62	0.00E+00	0.00E+00	0.00E+00	0.00E+00	0.00E+00
122.44	0.00E+00	0.00E+00	0.00E+00	0.00E+00	0.00E+00



09/12/88

Time-----&gt;

	homog	0 min	3 min	5 min	10 min
dia.	-1	0	3	5	10
0.87	6.67E+05	3.55E+05	1.54E+05	1.17E+05	7.06E+04
1.04	4.73E+05	2.82E+05	1.14E+05	1.00E+05	6.62E+04
1.24	7.17E+05	3.73E+05	1.49E+05	1.45E+05	1.01E+05
1.48	8.40E+05	4.78E+05	1.69E+05	1.29E+05	1.37E+05
1.77	6.26E+05	4.32E+05	1.74E+05	8.84E+04	5.30E+04
2.11	4.07E+05	3.73E+05	1.49E+05	9.65E+04	7.94E+04
2.51	2.70E+05	2.77E+05	1.74E+05	9.25E+04	6.18E+04
3.00	1.32E+05	2.87E+05	1.09E+05	3.62E+04	1.32E+04
3.58	5.60E+04	2.27E+05	8.45E+04	4.02E+04	2.21E+04
4.27	3.56E+04	1.50E+05	1.99E+04	1.61E+04	0.00E+00
5.10	2.54E+04	1.14E+05	1.99E+04	1.61E+04	4.41E+03
6.08	0.00E+00	7.73E+04	3.48E+04	8.04E+03	0.00E+00
7.26	0.00E+00	3.64E+04	1.49E+04	0.00E+00	0.00E+00
8.66	0.00E+00	3.18E+04	1.49E+04	8.04E+03	0.00E+00
10.33	0.00E+00	9.10E+03	1.49E+04	4.02E+03	0.00E+00
12.33	0.00E+00	3.64E+04	4.97E+03	4.02E+03	0.00E+00
14.71	0.00E+00	0.00E+00	9.94E+03	8.04E+03	0.00E+00
17.55	0.00E+00	0.00E+00	9.94E+03	4.02E+03	0.00E+00
20.94	0.00E+00	0.00E+00	4.97E+03	0.00E+00	0.00E+00
24.98	0.00E+00	0.00E+00	0.00E+00	0.00E+00	4.41E+03
29.81	0.00E+00	0.00E+00	0.00E+00	0.00E+00	0.00E+00
35.56	0.00E+00	0.00E+00	4.97E+03	0.00E+00	4.41E+03
42.43	0.00E+00	0.00E+00	0.00E+00	4.02E+03	4.41E+03
50.63	0.00E+00	0.00E+00	4.97E+03	4.02E+03	4.41E+03
60.41	0.00E+00	0.00E+00	0.00E+00	0.00E+00	0.00E+00
72.08	0.00E+00	0.00E+00	0.00E+00	4.02E+03	0.00E+00
86.00	0.00E+00	0.00E+00	0.00E+00	0.00E+00	0.00E+00
102.62	0.00E+00	0.00E+00	0.00E+00	0.00E+00	0.00E+00
122.44	0.00E+00	0.00E+00	0.00E+00	0.00E+00	0.00E+00

	15 min 15	20 min 20	25 min 25	30 min 30	45 min 45
dia.					
0.87	7.50E+04	1.29E+05	7.79E+04	2.11E+04	5.38E+04
1.04	6.62E+04	1.10E+05	8.69E+04	1.76E+04	4.43E+04
1.24	6.18E+04	1.39E+05	1.26E+05	2.82E+04	5.69E+04
1.48	5.30E+04	1.97E+05	1.68E+05	4.23E+04	7.59E+04
1.77	1.01E+05	1.68E+05	9.29E+04	2.82E+04	6.01E+04
2.11	4.85E+04	1.45E+05	8.69E+04	2.46E+04	2.53E+04
2.51	4.41E+04	9.03E+04	9.29E+04	3.17E+04	6.33E+03
3.00	2.65E+04	8.38E+04	5.39E+04	2.46E+04	1.27E+04
3.58	2.21E+04	2.26E+04	3.30E+04	1.41E+04	6.33E+03
4.27	8.83E+03	3.55E+04	4.19E+04	0.00E+00	6.33E+03
5.10	1.32E+04	2.58E+04	2.10E+04	0.00E+00	0.00E+00
6.08	8.83E+03	2.90E+04	0.00E+00	7.04E+03	3.16E+03
7.26	8.83E+03	1.61E+04	1.20E+04	0.00E+00	3.16E+03
8.66	0.00E+00	9.67E+03	3.00E+03	3.52E+03	0.00E+00
10.33	0.00E+00	1.93E+04	8.99E+03	0.00E+00	3.16E+03
12.33	0.00E+00	3.22E+03	5.99E+03	0.00E+00	0.00E+00
14.71	0.00E+00	3.22E+03	3.00E+03	0.00E+00	0.00E+00
17.55	4.41E+03	1.29E+04	5.99E+03	0.00E+00	0.00E+00
20.94	0.00E+00	1.29E+04	3.00E+03	3.52E+03	0.00E+00
24.98	0.00E+00	9.67E+03	0.00E+00	0.00E+00	3.16E+03
29.81	4.41E+03	9.67E+03	3.00E+03	0.00E+00	0.00E+00
35.56	0.00E+00	3.22E+03	3.00E+03	0.00E+00	0.00E+00
42.43	0.00E+00	0.00E+00	3.00E+03	3.52E+03	0.00E+00
50.63	4.41E+03	0.00E+00	0.00E+00	0.00E+00	0.00E+00
60.41	0.00E+00	0.00E+00	0.00E+00	0.00E+00	0.00E+00
72.08	0.00E+00	0.00E+00	0.00E+00	7.04E+03	0.00E+00
86.00	0.00E+00	0.00E+00	0.00E+00	0.00E+00	3.16E+03
102.62	4.41E+03	0.00E+00	0.00E+00	3.52E+03	0.00E+00
122.44	0.00E+00	0.00E+00	0.00E+00	0.00E+00	0.00E+00

09/20/88

Time-----&gt;

	homog	0 min	3 min	5 min	10 min
dia.	-1	0	3	5	10
0.87	6.91E+05	6.91E+05	7.57E+05	7.09E+05	4.55E+05
1.04	6.06E+05	6.06E+05	5.77E+05	5.76E+05	4.68E+05
1.24	7.82E+05	7.82E+05	8.40E+05	7.37E+05	4.62E+05
1.48	1.16E+06	1.16E+06	1.06E+06	1.00E+06	6.89E+05
1.77	9.25E+05	9.25E+05	8.40E+05	7.26E+05	5.37E+05
2.11	7.43E+05	7.43E+05	8.08E+05	6.28E+05	4.93E+05
2.51	4.95E+05	4.95E+05	5.32E+05	4.49E+05	2.97E+05
3.00	2.15E+05	2.15E+05	3.34E+05	3.00E+05	1.96E+05
3.58	9.78E+04	9.78E+04	1.41E+05	1.21E+05	1.20E+05
4.27	4.56E+04	4.56E+04	5.13E+04	5.76E+04	9.49E+04
5.10	2.61E+04	2.61E+04	1.92E+04	1.15E+04	3.79E+04
6.08	0.00E+00	0.00E+00	6.41E+03	5.76E+03	2.53E+04
7.26	0.00E+00	0.00E+00	6.41E+03	1.15E+04	0.00E+00
8.66	0.00E+00	0.00E+00	0.00E+00	0.00E+00	6.32E+03
10.33	0.00E+00	0.00E+00	6.41E+03	0.00E+00	0.00E+00
12.33	0.00E+00	0.00E+00	0.00E+00	0.00E+00	0.00E+00
14.71	0.00E+00	0.00E+00	0.00E+00	0.00E+00	0.00E+00
17.55	0.00E+00	0.00E+00	0.00E+00	0.00E+00	0.00E+00
20.94	0.00E+00	0.00E+00	0.00E+00	0.00E+00	0.00E+00
24.98	0.00E+00	0.00E+00	0.00E+00	0.00E+00	0.00E+00
29.81	0.00E+00	0.00E+00	0.00E+00	0.00E+00	0.00E+00
35.56	0.00E+00	0.00E+00	0.00E+00	0.00E+00	0.00E+00
42.43	0.00E+00	0.00E+00	0.00E+00	0.00E+00	0.00E+00
50.63	0.00E+00	0.00E+00	0.00E+00	0.00E+00	0.00E+00
60.41	0.00E+00	0.00E+00	0.00E+00	0.00E+00	0.00E+00
72.08	0.00E+00	0.00E+00	0.00E+00	0.00E+00	0.00E+00
86.00	0.00E+00	0.00E+00	0.00E+00	0.00E+00	0.00E+00
102.62	0.00E+00	0.00E+00	0.00E+00	0.00E+00	0.00E+00
122.44	0.00E+00	0.00E+00	0.00E+00	0.00E+00	0.00E+00

	15 min 15	20 min 20	25 min 25	30 min 30	45 min 45
dia.					
0.87	3.16E+05	1.93E+05	1.39E+05	1.74E+05	1.40E+05
1.04	3.47E+05	2.03E+05	2.06E+05	1.33E+05	7.81E+04
1.24	3.59E+05	2.80E+05	1.98E+05	1.46E+05	1.19E+05
1.48	4.62E+05	3.77E+05	2.33E+05	2.33E+05	1.40E+05
1.77	4.38E+05	2.51E+05	1.71E+05	1.78E+05	9.04E+04
2.11	4.14E+05	2.08E+05	1.53E+05	1.37E+05	1.07E+05
2.51	2.74E+05	2.03E+05	1.08E+05	8.69E+04	4.11E+04
3.00	1.95E+05	1.55E+05	7.18E+04	8.23E+04	2.88E+04
3.58	1.89E+05	8.21E+04	4.04E+04	5.95E+04	3.70E+04
4.27	1.10E+05	8.21E+04	8.08E+04	5.03E+04	1.64E+04
5.10	7.91E+04	5.31E+04	3.59E+04	3.20E+04	0.00E+00
6.08	4.87E+04	7.24E+04	1.35E+04	9.15E+03	1.23E+04
7.26	4.26E+04	5.31E+04	1.35E+04	4.57E+03	4.11E+03
8.66	1.22E+04	1.45E+04	4.04E+04	1.37E+04	8.22E+03
10.33	1.83E+04	1.93E+04	1.35E+04	0.00E+00	0.00E+00
12.33	6.08E+03	9.66E+03	1.35E+04	4.57E+03	2.05E+04
14.71	1.22E+04	4.35E+04	2.24E+04	9.15E+03	1.23E+04
17.55	0.00E+00	9.66E+03	3.14E+04	1.83E+04	1.64E+04
20.94	0.00E+00	9.66E+03	4.49E+03	9.15E+03	1.64E+04
24.98	0.00E+00	0.00E+00	4.49E+03	1.83E+04	4.11E+03
29.81	0.00E+00	0.00E+00	0.00E+00	9.15E+03	1.64E+04
35.56	0.00E+00	0.00E+00	0.00E+00	0.00E+00	8.22E+03
42.43	0.00E+00	0.00E+00	0.00E+00	0.00E+00	0.00E+00
50.63	0.00E+00	0.00E+00	0.00E+00	0.00E+00	0.00E+00
60.41	0.00E+00	0.00E+00	0.00E+00	0.00E+00	0.00E+00
72.08	0.00E+00	0.00E+00	0.00E+00	0.00E+00	0.00E+00
86.00	0.00E+00	0.00E+00	0.00E+00	0.00E+00	0.00E+00
102.62	0.00E+00	0.00E+00	0.00E+00	0.00E+00	0.00E+00
122.44	0.00E+00	0.00E+00	0.00E+00	0.00E+00	0.00E+00

09/20/88

Time-----&gt;

	homog	0 min	3 min	5 min	10 min
dia.	-1	0	3	5	10
0.87	5.45E+05	7.89E+05	5.52E+05	5.18E+05	2.38E+05
1.04	6.24E+05	7.43E+05	6.61E+05	4.95E+05	1.99E+05
1.24	7.29E+05	7.89E+05	7.57E+05	6.62E+05	3.15E+05
1.48	8.99E+05	9.19E+05	9.11E+05	7.20E+05	2.71E+05
1.77	8.34E+05	8.80E+05	6.93E+05	6.62E+05	2.77E+05
2.11	5.12E+05	5.15E+05	7.25E+05	5.36E+05	2.55E+05
2.51	2.69E+05	3.91E+05	3.66E+05	4.15E+05	2.21E+05
3.00	1.31E+05	2.15E+05	2.50E+05	2.59E+05	1.49E+05
3.58	5.25E+04	1.04E+05	9.62E+04	1.09E+05	1.11E+05
4.27	1.31E+04	4.56E+04	7.06E+04	4.61E+04	1.05E+05
5.10	1.31E+04	6.52E+03	1.92E+04	1.73E+04	3.87E+04
6.08	6.57E+03	1.96E+04	0.00E+00	1.15E+04	4.98E+04
7.26	1.31E+04	0.00E+00	0.00E+00	0.00E+00	1.66E+04
8.66	0.00E+00	0.00E+00	0.00E+00	0.00E+00	1.66E+04
10.33	6.57E+03	6.52E+03	6.41E+03	0.00E+00	2.77E+04
12.33	0.00E+00	0.00E+00	0.00E+00	5.76E+03	1.11E+04
14.71	0.00E+00	6.52E+03	0.00E+00	0.00E+00	2.21E+04
17.55	0.00E+00	0.00E+00	0.00E+00	0.00E+00	1.66E+04
20.94	0.00E+00	0.00E+00	0.00E+00	0.00E+00	0.00E+00
24.98	0.00E+00	0.00E+00	0.00E+00	0.00E+00	1.11E+04
29.81	0.00E+00	0.00E+00	0.00E+00	0.00E+00	0.00E+00
35.56	0.00E+00	0.00E+00	0.00E+00	0.00E+00	0.00E+00
42.43	0.00E+00	0.00E+00	0.00E+00	0.00E+00	0.00E+00
50.63	0.00E+00	0.00E+00	0.00E+00	0.00E+00	0.00E+00
60.41	0.00E+00	0.00E+00	0.00E+00	0.00E+00	0.00E+00
72.08	0.00E+00	0.00E+00	0.00E+00	0.00E+00	0.00E+00
86.00	0.00E+00	0.00E+00	0.00E+00	0.00E+00	0.00E+00
102.62	0.00E+00	0.00E+00	0.00E+00	0.00E+00	0.00E+00
122.44	0.00E+00	0.00E+00	0.00E+00	0.00E+00	0.00E+00

	15 min 15	20 min 20	25 min 25	30 min 30	45 min 45
dia.					
0.87	1.64E+05	9.66E+04	9.43E+04	7.17E+04	6.17E+04
1.04	1.40E+05	1.21E+05	9.43E+04	5.30E+04	6.76E+04
1.24	2.19E+05	1.50E+05	1.17E+05	5.92E+04	5.29E+04
1.48	2.37E+05	1.74E+05	1.08E+05	7.17E+04	5.29E+04
1.77	1.95E+05	1.50E+05	7.18E+04	4.36E+04	4.99E+04
2.11	2.01E+05	1.01E+05	6.28E+04	3.43E+04	5.29E+04
2.51	1.70E+05	1.11E+05	4.04E+04	1.56E+04	2.64E+04
3.00	1.28E+05	8.21E+04	3.59E+04	2.18E+04	2.64E+04
3.58	4.87E+04	3.86E+04	1.80E+04	3.12E+03	1.18E+04
4.27	6.69E+04	9.66E+03	2.24E+04	6.24E+03	0.00E+00
5.10	3.65E+04	9.66E+03	4.49E+03	0.00E+00	0.00E+00
6.08	3.04E+04	0.00E+00	4.49E+03	3.12E+03	5.88E+03
7.26	6.08E+03	1.45E+04	4.49E+03	0.00E+00	2.94E+03
8.66	6.08E+03	0.00E+00	4.49E+03	0.00E+00	0.00E+00
10.33	6.08E+03	9.66E+03	0.00E+00	3.12E+03	0.00E+00
12.33	1.22E+04	4.83E+03	0.00E+00	0.00E+00	0.00E+00
14.71	1.22E+04	4.83E+03	0.00E+00	0.00E+00	0.00E+00
17.55	3.04E+04	4.83E+03	0.00E+00	0.00E+00	0.00E+00
20.94	0.00E+00	4.83E+03	0.00E+00	3.12E+03	0.00E+00
24.98	0.00E+00	0.00E+00	4.49E+03	0.00E+00	0.00E+00
29.81	0.00E+00	0.00E+00	0.00E+00	0.00E+00	0.00E+00
35.56	0.00E+00	0.00E+00	0.00E+00	3.12E+03	0.00E+00
42.43	6.08E+03	4.83E+03	0.00E+00	0.00E+00	0.00E+00
50.63	0.00E+00	4.83E+03	0.00E+00	3.12E+03	0.00E+00
60.41	0.00E+00	0.00E+00	4.49E+03	0.00E+00	2.94E+03
72.08	0.00E+00	0.00E+00	0.00E+00	0.00E+00	2.94E+03
86.00	0.00E+00	0.00E+00	0.00E+00	0.00E+00	0.00E+00
102.62	0.00E+00	0.00E+00	0.00E+00	0.00E+00	0.00E+00
122.44	0.00E+00	0.00E+00	0.00E+00	0.00E+00	0.00E+00

09/23/88

Time-----&gt;

	homog	0 min	3 min	5 min	10 min
dia.	-1	0	3	5	10
0.87	8.67E+05	7.30E+05	6.93E+05	5.24E+05	1.72E+05
1.04	6.50E+05	6.45E+05	4.23E+05	3.63E+05	1.72E+05
1.24	9.39E+05	6.84E+05	6.41E+05	4.72E+05	1.94E+05
1.48	1.08E+06	9.84E+05	6.48E+05	5.99E+05	2.52E+05
1.77	8.34E+05	5.67E+05	6.03E+05	5.65E+05	1.59E+05
2.11	5.78E+05	5.47E+05	4.62E+05	5.59E+05	1.90E+05
2.51	2.69E+05	3.26E+05	2.50E+05	3.57E+05	1.59E+05
3.00	1.25E+05	1.37E+05	1.41E+05	2.25E+05	8.83E+04
3.58	5.91E+04	4.56E+04	7.70E+04	1.09E+05	8.83E+04
4.27	4.60E+04	1.96E+04	2.57E+04	5.18E+04	7.50E+04
5.10	1.31E+04	0.00E+00	1.92E+04	4.61E+04	3.09E+04
6.08	0.00E+00	6.52E+03	6.41E+03	3.46E+04	5.30E+04
7.26	6.57E+03	0.00E+00	0.00E+00	1.73E+04	3.97E+04
8.66	0.00E+00	0.00E+00	0.00E+00	0.00E+00	3.97E+04
10.33	0.00E+00	0.00E+00	0.00E+00	0.00E+00	1.32E+04
12.33	0.00E+00	0.00E+00	0.00E+00	5.76E+03	4.41E+03
14.71	0.00E+00	0.00E+00	0.00E+00	0.00E+00	1.32E+04
17.55	0.00E+00	0.00E+00	0.00E+00	0.00E+00	4.41E+03
20.94	0.00E+00	0.00E+00	0.00E+00	0.00E+00	0.00E+00
24.98	0.00E+00	0.00E+00	0.00E+00	0.00E+00	0.00E+00
29.81	0.00E+00	0.00E+00	0.00E+00	0.00E+00	0.00E+00
35.56	0.00E+00	0.00E+00	0.00E+00	0.00E+00	0.00E+00
42.43	0.00E+00	0.00E+00	0.00E+00	0.00E+00	0.00E+00
50.63	0.00E+00	0.00E+00	0.00E+00	0.00E+00	0.00E+00
60.41	0.00E+00	0.00E+00	0.00E+00	0.00E+00	0.00E+00
72.08	0.00E+00	0.00E+00	0.00E+00	0.00E+00	0.00E+00
86.00	0.00E+00	0.00E+00	0.00E+00	0.00E+00	0.00E+00
102.62	0.00E+00	0.00E+00	0.00E+00	0.00E+00	0.00E+00
122.44	0.00E+00	0.00E+00	0.00E+00	0.00E+00	0.00E+00

	15 min 15	20 min 20	25 min 25	30 min 30	45 min 45
dia.					
0.87	1.41E+05	7.73E+04	8.98E+04	5.56E+04	7.64E+04
1.04	1.31E+05	1.35E+05	6.36E+04	8.18E+04	4.41E+04
1.24	1.99E+05	7.24E+04	9.73E+04	6.87E+04	9.11E+04
1.48	1.60E+05	1.35E+05	9.73E+04	7.85E+04	6.76E+04
1.77	1.36E+05	9.18E+04	8.98E+04	8.18E+04	7.35E+04
2.11	1.21E+05	7.24E+04	7.49E+04	5.23E+04	3.82E+04
2.51	9.22E+04	4.83E+04	3.74E+04	3.27E+04	3.53E+04
3.00	6.31E+04	2.90E+04	2.25E+04	2.29E+04	5.88E+03
3.58	5.82E+04	1.93E+04	2.25E+04	1.31E+04	2.94E+03
4.27	2.91E+04	1.93E+04	1.12E+04	6.54E+03	0.00E+00
5.10	4.85E+03	1.45E+04	3.74E+03	3.27E+03	0.00E+00
6.08	4.85E+03	1.45E+04	7.49E+03	6.54E+03	0.00E+00
7.26	9.70E+03	0.00E+00	7.49E+03	0.00E+00	0.00E+00
8.66	1.46E+04	9.66E+03	0.00E+00	3.27E+03	0.00E+00
10.33	0.00E+00	0.00E+00	3.74E+03	0.00E+00	0.00E+00
12.33	9.70E+03	0.00E+00	0.00E+00	0.00E+00	0.00E+00
14.71	0.00E+00	0.00E+00	3.74E+03	0.00E+00	2.94E+03
17.55	0.00E+00	4.83E+03	0.00E+00	0.00E+00	0.00E+00
20.94	4.85E+03	4.83E+03	3.74E+03	0.00E+00	0.00E+00
24.98	0.00E+00	0.00E+00	0.00E+00	0.00E+00	0.00E+00
29.81	9.70E+03	0.00E+00	0.00E+00	0.00E+00	2.94E+03
35.56	0.00E+00	0.00E+00	0.00E+00	0.00E+00	5.88E+03
42.43	0.00E+00	4.83E+03	0.00E+00	0.00E+00	0.00E+00
50.63	0.00E+00	0.00E+00	0.00E+00	0.00E+00	2.94E+03
60.41	0.00E+00	0.00E+00	0.00E+00	3.27E+03	0.00E+00
72.08	0.00E+00	0.00E+00	3.74E+03	3.27E+03	0.00E+00
86.00	0.00E+00	0.00E+00	0.00E+00	0.00E+00	0.00E+00
102.62	0.00E+00	0.00E+00	0.00E+00	0.00E+00	0.00E+00
122.44	0.00E+00	0.00E+00	0.00E+00	0.00E+00	0.00E+00